Alma Mater Studiorum · Università di Bologna

Dottorato di Ricerca in Fisica
Ciclo XXXIII

Settore concorsuale di afferenza: 02/A2
Settore scientifico disciplinare: Fis/02

Axion-like particles and inflation from String Theory

Presentata da:
Veronica Guidetti

Relatore:
Prof. Michele Cicoli

Coordinatore Dottorato:
Prof. Michele Cicoli

Esame finale anno 2021

Ma sedendo e mirando,
interminati spazi
. . . e sovrumani silenzi, e
profondissima quiete
io nel pensier mi fingo, ove per
poco il cor non si spaura.

L'infinito *Giacomo Leopardi*

Abstract

This thesis is focused on cosmological applications of the 4D Effective Field Theory (EFT) coming from type IIB string theory. We focus in particular on model building in inflation, dark matter and dark radiation using Kähler moduli and axion-like fields which are ubiquitous features of type IIB flux compactifications. These fields enjoy effective approximate symmetries which can protect their potential against quantum corrections. This property makes both of them good inflaton candidates and implies that axion-like particles from string theory tend naturally to be very light with intriguing applications to dark radiation and dark matter. We first consider a class of type IIB inflationary models called "Fibre Inflation" where the inflaton is a Kähler modulus. We provide a consistent global embedding of these models into Calabi-Yau orientifolds with D-branes, fluxes and a chiral visible sector. We also analyse the multi-field dynamics of this class of models, including both Kähler moduli and axion-like particles which give rise to isocurvature perturbations. We then focus on different applications of axion-like particles coming from string theory. Depending on the value of their mass and decay constant, together with their production mechanism, these particles can drive inflation or can represent a non-negligible component of dark matter and dark radiation. We provide a string embedding of a model that explains the 3.5 keV line recently detected from galaxy clusters by exploting axion-photon conversion in astrophysical magnetic fields. Finally, we analyse the mechanisms of electro-magnetic dissipation in models where the inflaton is an axion, finding a new resonant behaviour in the gauge field production that affects the shape of the cosmological parameters.

Declaration

This thesis is based on results presented in the following papers

[1] 2017, October

M. Cicoli, V. A. Diaz, V. Guidetti and M. Rummel,
"The 3.5 keV Line from Stringy Axions,"
JHEP **10** (2017), 192, arXiv:1707.02987 [hep-th].

[2] 2017, November

M. Cicoli, D. Ciupke, V. A. Diaz, V. Guidetti, F. Muia and P. Shukla,
"Chiral Global Embedding of Fibre Inflation Models,"
JHEP **11** (2017), 207, arXiv:1709.01518 [hep-th].

[3] 2018, December

M. Cicoli, V. Guidetti, F. G. Pedro and G. P. Vacca,
"A geometrical instability for ultra-light fields during inflation?,"
JCAP **12** (2018), 037, arXiv:1807.03818 [hep-th].

[4] 2019, March

M. Cicoli, V. Guidetti and F. G. Pedro,
"Geometrical Destabilisation of Ultra-Light Axions in String Inflation,"
JCAP **05** (2019), 046, arXiv:1903.01497 [hep-th].

[5] 2020, February

V. Domcke, V. Guidetti, Y. Welling and A. Westphal,
"Resonant backreaction in axion inflation,"
JCAP **09** (2020), 009, arXiv:2002.02952 [astro-ph.CO]].

2020 (work in progress)

M. Cicoli, V. Guidetti, F. Muia, F. G. Pedro, and G. P. Vacca
"Ultra-light axions in string inflation: geometrical destabilisation with vanishing relative entropy?".

Acknowledgements

I would like to thank all the collaborators who made the realisation of this Thesis possible: Michele Cicoli, Francisco Gil Pedro, Gian Paolo Vacca, Francesco Muia, Victor Alfonso Diaz, Markus Rummel, David Ciupke, Pramod Shukla, Valerie Domcke, Alexander Westphal and Yvette Welling.

I'm particularly grateful to Michele who taught me how to do research in a good mood and with a sense of optimism.

Contents

Part I

Introduction

One of the most fascinating topics on which the research in theoretical physics is focused today is related to the origin and evolution of the Universe. Currently, the simplest cosmological model that fits experimental observations is the ΛCDM model, according to which spacetime is described by the Friedmann-Robertson-Walker metric, while the gravitational field is generated by dark energy, cold dark matter (DM) and a small quantity of ordinary matter. Despite its great success, in order to explain the observed large scale structure, the theory must be completed by an initial period of accelerated expansion called inflation. During this phase the space expands quasi-exponentially, and therefore it is also possible to explain the overall homogeneity and flatness of the Universe.

Particle physics, on the other hand, is successfully described in the context of the Standard Model (SM), augmented by neutrino masses, which is in excellent agreement with experimental data. However, unfortunately, it represents only an Effective Field Theory (EFT) whose cut-off can be pushed at most up to the Planck scale where a full theory of quantum gravity should emerge. In addition, it fails to address several issues like the hierarchy problem for the Higgs mass, gauge coupling unification and the strong CP problem. Finally, it is not able to explain the origin of DM, baryogenesis and dark energy.
Several theories have been proposed for fundamental physics beyond current understanding. Here we will focus on string theory which is at present the most promising candidate for a consistent theory of gravity that can also incorporate all known interactions and matter in an elegant unified framework. In this thesis, we consider inflationary models in the context of the 4D EFT coming from type IIB string theory. Given the high sensitivity of the inflationary dynamics to UV physics, finding a string embedding of inflation would provide a powerful tool to overcome many of the standard issues related to the usual EFT approach. String theory does not only provide a consistent quantisation of gravity, but it also allows us to derive the inflationary Lagrangian from a top-down perspective. Moreover, working in its perturbative regime, all corrections to the inflationary potential arising form higher dimensional operators, can be in principle computed. This would give an unprecedented theoretical control on model building. String theory contains a single parameter, the string length ℓ_s, and the structure of the 4D theory is completely determined by the topology of the extra dimensions and the presence of local objects as Dp-branes and Op-planes. This reduces the arbitrariness of the 4D Lagrangian and, moreover, allows us to point out which fields appear in the low-energy theory, equipped with symmetries that can protect their potential against dangerous quantum corrections. We focus in particular on Kähler moduli that feature a non-compact symmetry, the so-called extended no-scale structure, and axion-like particles (ALPs), that feature at tree-level a compact continuous shift-symmetry. We will work in the context of Large Volume Scenario (LVS) com-

pactifications that provide a hierarchy between the relevant energy scales which is suitable for 4D descriptions of inflation.

The first part of this thesis gives an overview of the current knowledge of high energy physics that will be relevant throughout this work. In Chapter 1 we briefly review the state of the art of particle physics and cosmology. As already mentioned, the main pillars are given by the SM of particle physics and the ΛCDM model of cosmology. These two theories have been tested to high precision and have an outstanding accordance with experimental results. Nevertheless, they feature some fundamental problems that suggest evidence of new particles and force us to search for UV extensions of these models.
In Chapter 2 we introduce high energy theories that try to solve the main problems of the SM and the ΛCDM model. We begin introducing cosmic inflation that provides a working mechanism to overcome the initial condition problems of standard Big Bang cosmology and can lead to successful large structure formation. After that, we briefly review the main features of axions and ALPs, whose existence was firstly theorised for explaining the CP symmetry conservation of QCD. According to their production mechanism, their mass and their coupling to SM degrees of freedom, these particles can also represent a significant part of both DM and dark radiation, or can play the role of the inflaton field. Finally, we introduce some basic concepts of string theory, focusing on type IIB, and we list the conditions under which it is possible to get low energy 4D theories that can reproduce the basic ingredients of SM physics, such as chiral matter, gauge theories and Yukawa couplings. Throughout this thesis we will use a bottom-up approach, analysing 4D string vacua equipped with sets of local sources as Dp-branes and Op-planes. This approach is less general than starting from the full 10D theory but it may be more efficient in trying to identify promising string vacua which can reproduce all the features of the SM. We then conclude this chapter discussing moduli stabilisation and inflationary models form string theory.

Moduli are scalar fields that parametrise continuous deformations of the extra-dimensional metric that do not change the topology of the compact extra-dimensional space. These fields appear as massless and testify the presence of extra dimensions in the 4D theory. We need to find dynamical ways to develop a potential for the moduli and avoid the presence of undetected fifth-forces. This goes under the name of moduli stabilistion and is a crucial step in concrete model building. Indeed, moduli vacuum expectation values (VEVs) set all the couplings between different particles, including the string coupling. These fields can be either heavy or light and their presence can affect the primordial and present history of the Universe. Given the plethora of possible string vacua (the number of known Calabi Yau manifolds is of order 10^6) and considering that each 4D theory implies the presence of a large number of moduli (which can be as large as $\mathcal{O}(10^3)$), it is

mandatory to understand which kind of mass spectrum and couplings are typical of these fields. During the inflationary epoch, fields that are much heavier than the Hubble scale H can be safely integrated out. On the other hand, fields having masses below H can drive inflation, while other fields much lighter than H can affect the cosmological parameters through their quantum perturbations. Given the high level of complexity of inflationary systems involving a large number of fields and the sensitivity of inflation to UV physics, it is nearly impossible to treat moduli stabilisation and inflation independently. This makes string cosmology a highly non trivial research area.

The second part of this thesis contains some applications of the aforementioned topics that I analysed during my PhD. In Chapter 3 we study the global embedding of a class of Kähler moduli inflation models called *Fibre inflation*. These are first introduced in Sec. 2.4.1. We construct explicit examples of Fibre inflation models which are globally embedded in type IIB orientifolds with chiral matter on D7-branes and full closed string moduli stabilisation. We perform a consistent choice of orientifold involution, brane setup and gauge fluxes which leads to chiral matter and a moduli-dependent Fayet-Iliopoulos term. Using LVS we are able to perform moduli stabilisation step by step. The inflationary potential is generated by suitable string loop corrections in combination with higher derivative effects. We analyse the inflationary dynamics both in the single-field approximation and by numerically deriving the full multi-field evolution in detail. Interestingly, we find that the Kähler cone conditions set strong constraints on the allowed inflaton field range. In particular, we see that in some cases it is not easy to get the correct normalisation of the power spectrum using inflaton density perturbations. This motivates the study of other possible ways of producing the correct amplitude of the scalar power spectrum.

We then study in Chapter 4 the role played by light fields during inflation, focusing on ALPs. These always appear in string theory compactifications and tend to be naturally very light. Indeed, the presence of light spectator fields during inflation leads to the production of isocurvature perturbations that can be converted into density perturbations through the curvaton mechanism. This can help to circumvent the issues mentioned in Chapter 3. On the other hand, the bosonic Lagrangian of 4D supergravity coming from dimensional reduction, is given by a non-linear sigma model. This means that the field space is curved. The analysis of cosmological perturbations points out that, in case of negative scalar curvature, isocurvature pertubations may show a tachyonic mass that seems to quickly lead the system out of the perturbative regime. We analyse general systems composed by the inflaton and a light or heavy spectator field. We conclude that geometrical destabilisation cannot occur in the case of heavy spectator fields. On the other hand, systems with light spectator fields may be plagued by a tachyonic

instability of isocurvature perturbations. After that, we focus on concrete examples coming from string compactifications and in particular on Fibre inflation models. We study the dynamics of both the background and the perturbations. Choosing a wide range of initial conditions for inflation, we show that the background evolution is stable. Despite that, the equation of motion for the isocurvature perturbations seems to show an instability. We will however point out that this instability is unphysical (in agreement with the fact that the background evolution is stable) since it is just an artifact due to the use of gauge invariant variables which in our case turn out to be ill-defined.

In Chapter 5 we give an example of axionic DM coming from type IIB string compactifications. This work is based on the recent detection of an unexplained 3.5 keV line from galaxy clusters. A promising model which can explain the morphology of the signal and other experimental evidences, namely its non-observation in dwarf spheroidal galaxies, involves a 7 keV DM particle decaying into a pair of ultra-light axions that convert into photons in the magnetic field of the clusters. Given that light axions naturally emerge in 4D string vacua, we present a microscopic realisation of this model within the framework of type IIB flux compactifications, where the DM particle is an open string axion. After describing the Calabi-Yau geometry and the brane set-up, we discuss in depth moduli stabilisation, the resulting mass spectrum and the strength of all relevant couplings.

Finally, in Chapter 6, we study some features of axion inflation models. Axion inflation entails a coupling of the inflaton to gauge fields through the Chern-Simons term. This results in a strong gauge field production during inflation which backreacts on the inflaton equation of motion. These effects have been previously studied using analytical methods. In this Chapter, performing a full numerical analysis, we show that this strongly non-linear system generically experiences a resonant enhancement of the gauge field production. This gives rise to oscillatory features in the inflaton velocity as well as in the gauge field spectrum. The gauge fields source a strongly enhanced scalar power spectrum at small scales, exceeding previous estimates and leading the system out of the perturbative regime. For appropriate parameter choices, the collapse of these over-dense regions can lead to a large population of (light) primordial black holes, with remarkable phenomenological consequences.

Chapter 1

State of the Art

1.1 Standard Model of particle physics

Over the past 4 decades the joint collaboration between theorists and experimentalists brought us to a new and well posed conception of matter. Indeed, using the tool of quantum field theory they were able to enclose three kinds of fundamental interactions in a single theory: the Standard Model (SM) of particle physics. Except from some (non-negligible) exceptions that we will describe later on in this Chapter, the Standard Model turned out to be in excellent accordance with all to date experimental data for what concerns both low and high energy Physics phenomena. The fermion field content of SM can be summarised as follows:

- **leptons**: electron e, muon μ, τ-lepton, electron neutrino, ν_e, muon neutrino, ν_μ, $\tau-$ neutrino, ν_τ. The first three particles carry electrical charge while the others are neutral;
- **quarks**: up u, down d, strange s, charme c, bottom b and top t quarks.

These particles transform as spinors under the Lorentz group and represent the matter content of the theory. On the other hand we have bosons:

- **gauge fields**: photon, γ, gluon, g, $W^{\pm}-$bosons and $Z-$ boson. These are the mediators of gauge interactions and transform as vectors under gauge group.
- **Higgs boson**: neutral scalar field, its vacuum expectation value gives a mass to all massive SM particles and it participates in the Yukawa interactions.

The Standard Model gauge group is given by:

$$SU(3)_c \times SU(2)_L \times U(1)_y \tag{1.1}$$

where $SU(3)_c$ describes strong interactions via Quantum Chomodynamics (QCD) while $SU(2)_L \times U(1)_y$ describes electro-weak interactions. Matter particles are organised into three generations (or families) of quarks and leptons:

$$\begin{array}{rl} 1_{st} \text{ family} : & u,\, d,\, \nu_e,\, e \\ 2_{nd} \text{ family} : & c,\, s,\, \nu_\mu,\, \mu \\ 3_{rd} \text{ family} : & t,\, b,\, \nu_\tau,\, \tau. \end{array} \tag{1.2}$$

Particles belonging to the same generation have different quantum numbers which mean different gauge interactions, while correspondent particles in different generations, i.e. columns in (1.2), share the same quantum numbers but show different masses and different Yukawa couplings to the Higgs boson. From the point of view of strong interaction both left and right quarks transform under the fundamental representation (triplets), this means that in order to describe strong interaction we do not need to separate quarks into left and right components. The most interesting peculiarities about strong interaction are given by *color confinement* and *asymptotic freedom*. In order to give a hint about these two properties let us introduce the Lagrangian of QCD

$$\mathcal{L} = \bar{\psi}(i\gamma^\mu \mathcal{D}_\mu - m)\psi - \frac{1}{2} Tr[G_{\mu\nu} G^{\mu\nu}] \tag{1.3}$$

where the spinor field ψ is given by a color triplet

$$\psi = \begin{pmatrix} q_{red} \\ q_{green} \\ q_{blue} \end{pmatrix}, \tag{1.4}$$

indeed every single quark can exist in three different color states. The covariant derivative is

$$\mathcal{D}_\mu = \partial_\mu + i\, g_S\, G_\mu\,, \tag{1.5}$$

where g_S is the strong coupling constant and B_μ is a 3×3 dimensional matrix in color space given by the product of the eight color gauge fields g^i_μ and the generators $\frac{\lambda^i}{2}$ of $SU(3)$ written in terms of the Gell-Mann matrices λ^i. The gluon field-strength is given by

$$G_{\mu\nu} = \frac{1}{2} G^i_{\mu\nu} \lambda^i = (i g_S)^{-1} [\mathcal{D}_\mu, \mathcal{D}_\nu] = \partial_\nu G_\mu - \partial_\mu G_\nu + i\, g_S\, [G_\nu, G_\mu]. \tag{1.6}$$

where the last term takes into account the non-abelian nature of the interaction accounting for three- and fourth-gluon self-interactions. With the introduction of color hypothesis the number of quarks gets multiplied by three, in particular we should have that some proton $p = uud$ may be given by quarks having different

	quark		antiquark	
	Y_c	I_{3c}	Y_c	I_{3c}
r:	$\frac{1}{2}$	$\frac{1}{3}$	$-\frac{1}{2}$	$-\frac{1}{3}$
g:	$-\frac{1}{2}$	$\frac{1}{3}$	$\frac{1}{2}$	$-\frac{1}{2}$
b:	0	$-\frac{2}{3}$	0	$\frac{2}{3}$

Table 1.1: Quark and antiquark color isospin and hypercharge quantum numbers.

colors. From the experimental point of view no colored hadron has ever been observed and one can postulate that all free hadrons observed in nature should be either colorless or white, that is the color confinement hypothesis. The direct consequences of this statement can be summarised as follows. We can pick out two generators of $SU(3)$ that have color spinors as eigenstates, i.e. they are diagonal matrices, these are λ_3 and λ_8, then we define two new operators called *color isospin*, I_{3c}, and *color hypercharge* Y_c

$$I_{3c} = \frac{1}{2}\lambda_3 = \frac{1}{2}\begin{pmatrix} 1 & 0 & 0 \\ 0 & -1 & 0 \\ 0 & 0 & 0 \end{pmatrix} \qquad Y_c = \frac{1}{\sqrt{3}}\lambda_8 = \frac{1}{3}\begin{pmatrix} 1 & 0 & 0 \\ 0 & 1 & 0 \\ 0 & 0 & -2 \end{pmatrix} \tag{1.7}$$

The quantum numbers associated with color isospin and hypercharge are listed in Table 1.1. This means that mesons $M \equiv q\bar{q}$ and baryons $B \equiv qqq$ must be described by colour-singlet combinations

$$B = \frac{1}{\sqrt{6}}|q_{\alpha\beta\gamma}\rangle, \qquad M = \frac{1}{\sqrt{3}}\delta^{\alpha\beta}|q_{\alpha\beta}\rangle \qquad \alpha = r, g, b \tag{1.8}$$

satisfying $Y_c = 0$ and $I_{3c} = 0$. In order to see that color-singlet states are the preferred configurations we should focus on the quark-gluon interaction term in the Lagrangian:

$$\mathcal{L}_{qg} = -\frac{g_S}{2} g^i_\mu \bar{\psi}\gamma^\mu \lambda^i \psi \tag{1.9}$$

from which the Feynman rule for the $\bar{\psi}\psi q$ vertex is

$$-\,i\, g_S \lambda^i_{\alpha\beta}\gamma_\mu \tag{1.10}$$

where i and μ are the gluon color and Lorentz index respectively, while α and β are the quark and antiquark color indices. Therefore the 1-gluon exchange force between quarks in the transition $\alpha + \beta \to \delta + \gamma$ is proportional to

$$\mathcal{E} = \frac{(g_S)^2}{4}\sum_a \lambda^i_{\alpha\beta}\lambda^i_{\delta\gamma}. \tag{1.11}$$

System	$\sum_{i<j}\langle \boldsymbol{T}^{(i)} \cdot \boldsymbol{T}^{(j)} \rangle$
$\langle q\bar{q} \rangle_{\mathbf{1}}$	$-\frac{4}{3}$
$\langle q\bar{q} \rangle_{\mathbf{8}}$	$+\frac{1}{6}$
$\langle qq \rangle_{\mathbf{3^*}}$	$-\frac{2}{3}$
$\langle qq \rangle_{\mathbf{6}}$	$+\frac{1}{3}$
$\langle qqq \rangle_{\mathbf{1}}$	-2
$\langle qqq \rangle_{\mathbf{8}}$	$-\frac{1}{2}$
$\langle qqq \rangle_{\mathbf{10}}$	$+1$
$\langle qqqq \rangle_{\mathbf{3}}$	-2

Table 1.2: Interaction energy of low-dimensional quark systems

Then we can perform a toy calculation assuming that we can trust perturbation theory at lowest order, neglecting multiple gluon exchanges, and the effects related to the creation of a isolated colored state. In order to estimate Eq.(1.11) we need to evaluate the expectation value of the squared generators $\langle \boldsymbol{T}^2 \rangle = \frac{1}{4}\langle \boldsymbol{\lambda}^2 \rangle$. In particular for $SU(N)$ theories this is equivalent to average the square of any generator over a representation, here we choose I_{3c}. This implies that in representations with dimension d we have [6]

$$\langle \boldsymbol{T}^2 \rangle_d = (N^2-1) \sum_{rep.d} \frac{I_{3c}^2}{d} \,. \tag{1.12}$$

Then the single gluon exchange force can be estimated to be $\mathcal{E} = g_S^2 \langle \boldsymbol{T}^{(1)} \cdot \boldsymbol{T}^{(2)} \rangle$ and we can easily extend the calculation to multi-body systems, being the interaction given by the sum of two-body interactions:

$$\mathcal{E} = g_S^2 \sum_{i<j} \langle \boldsymbol{T}^{(i)} \cdot \boldsymbol{T}^{(j)} \rangle = \frac{\langle \boldsymbol{T}^2 \rangle - \sum_i \langle \boldsymbol{T}^{(i)2} \rangle}{2} \,. \tag{1.13}$$

We list in Table 1.2 the results of the binding energies for few-body systems in our toy calculation. It is easy to see that for two- and three-quark systems the color singlet is the most attractive setup. The four quarks triplet can be interpreted as as a baryon+quark system and there is no difference between its binding energy and that of a single baryon: adding a quark to a baryon is not convenient and the fourth quark can be considered as a free particle. Despite being experimentally verified, a rigorous proof for color confinement is still lacking. Lattice QCD, albeit

good for certain qualitative and quantitative predictions, also does not allows us to prove something on a fundamental level. Furthermore, there is the AdS/CFT correspondence, which allows us to describe theories which are similar to QCD in many respects, but a description of QCD itself is not accessible at this point.

In order to understand asymptotic freedom, we write down the energy dependence of the strong coupling constant $\alpha_S = g_S/4\pi$:

$$\frac{1}{\alpha_S(Q^2)} = \frac{11N_c - 2n_f}{12\pi} \ln\left(\frac{Q^2}{\Lambda_{QCD}}\right) \tag{1.14}$$

where N_c is the number of colors and n_f is the number of active quark flavours. We see that at high energies the theory is weakly coupled and for $Q^2 \to \infty$ we have $\alpha_S(Q^2) \to 0$, so we find asymptotic freedom. At small energies the theory is strongly coupled and quarks are confined in colorless or white hadrons such as mesons and baryons. We need to consider that if we want Eq. (1.14) to be continuous at flavour threshold (when the number of kinematically accessible quark flavours changes), then Λ_{QCD} must depend on n_f: $\Lambda_{QCD} = \Lambda^{n_f}$. In addition its value also depends on the selected renormalisation scheme, the canonical choice that is usually made is the modified minimal subtraction scheme $\bar{M}S$: $\Lambda_{QCD} = \Lambda^{n_f}_{\bar{M}S}$. For instance, if we consider the case $Q = M_Z$ and $n_f = 5$ we have

$$\Lambda^5_{\bar{M}S} \simeq 210MeV \tag{1.15}$$

and

$$\alpha_S(M_Z^2) = 0.1184 \pm 0.0007. \tag{1.16}$$

Asymptotic freedom comes from the non-abelian nature of $SU(3)$, where gluons that couple to the colour charges do carry a colour charge too so they can couple among themselves giving rise to 3- and 4-gluon vertices.

Electroweak interactions need to be described in a more complex way. We know that weak force, as suggested by its name, is the weakest force described in SM and it acts on short distances. This implies that the vector bosons that mediate this force need to be massive. In addition we know that leptons and quarks are massive particles but, in order to preserve $SU(2)_L \times U(1)$ gauge invariance, no explicit fermion mass is allowed to appear in the Lagrangian. Moreover the low-energy experimental results on energy and angular momentum distribution in β decays, e.g. $\mu^- \to e^-\bar{\nu}_e\nu_\mu$ or $n \to pe^-\bar{\nu}_e$, revealed that only left-handed (right-handed) fermion (anti-fermion) chiralities contribute in weak transitions and the strength of such interaction appears to be universal. The study of processes like $\pi^- \to e^-\bar{\nu}_e$ showed that neutrinos appear with only left-handed chirality (anti-neutrinos with only right-handed chirality). They also found that it was possible to distinguish neutrinos from anti-neutrinos requiring lepton number conservation ($\bar{\nu}_e p \to e^+ n$

while $\nu_e p \nrightarrow e^+ n$). These low energy information, together with the absence of flavour-changing neutral current transitions and the requirements related to unitarity (in order to have a proper energy behaviour), led to the construction of electroweak theory. Leptons and quarks have to be grouped into left-handed doublet and right-handed singlets as follows

$$\begin{aligned} Q_1 &= \begin{pmatrix} u \\ d \end{pmatrix}_L , \qquad Q_2 = \begin{pmatrix} c \\ s \end{pmatrix}_L , \qquad Q_3 = \begin{pmatrix} t \\ b \end{pmatrix}_L , \\ L_1 &= \begin{pmatrix} \nu_e \\ e \end{pmatrix}_L , \qquad L_2 = \begin{pmatrix} \nu_\mu \\ \mu \end{pmatrix}_L , \qquad L_3 = \begin{pmatrix} \nu_\tau \\ \tau \end{pmatrix}_L , \\ U_i &= \{u_R,\, c_R,\, t_R\} \\ D_i &= \{d_R,\, s_R,\, b_R\} \\ E_i &= \{e_R,\, \mu_R,\, \tau_R\} \qquad i = 1, 2, 3; \end{aligned} \tag{1.17}$$

In order to write the structure of the required Lagrangian let us focus on a single quark family so that we can write the free Lagrangian as:

$$\begin{aligned} \mathcal{L}_{free} &= i\bar{u}(x)\gamma^\mu \partial_\mu u(x) + i\bar{d}(x)\gamma^\mu \partial_\mu d(x) \\ &= i\bar{Q}_1(x)\gamma^\mu \partial_\mu Q_1(x) + i\bar{U}_1(x)\gamma^\mu \partial_\mu U_1(x) + i\bar{D}_1(x)\gamma^\mu \partial_\mu D_1(x) \end{aligned} \tag{1.18}$$

This is invariant under global G transformation in flavour space:

$$\begin{aligned} Q_1(x) &\xrightarrow{G} Q_1'(x) \equiv \exp\{iy_{Q_1}\beta\}\, U_L\, Q_1(x) \\ U_1(x) &\xrightarrow{G} U_1'(x) \equiv \exp\{iy_{U_1}\beta\}\, U_1(x) \\ D_1(x) &\xrightarrow{G} D_1'(x) \equiv \exp\{iy_{D_1}\beta\}\, D_1(x) \end{aligned} \tag{1.19}$$

where

$$U_L \equiv \exp\left\{iT_W^i \alpha^i\right\} , \qquad i = 1, 2, 3 \tag{1.20}$$

is a $SU(2)$ transformation that only acts on the doublet made of left-handed fermions, $T_W^i = \frac{\sigma_i}{2}$ are the generators of $SU(2)$ and σ_i are the Pauli matrices. As always in order to have a theory which is invariant under local (or gauge) transformations ($\alpha_i(x)$, $\beta(x)$) we need to introduce a number of gauge bosons equal to the number of the group degrees of freedom (in this case 3 bosons for $SU(2)$ and a boson for the hypercharge) and to convert standard fermion derivatives into covariant derivatives. Denoting the general spinor element with ψ, we

end up with

$$\mathcal{L} = \sum_{\psi=Q_1,U_1,D_1} i\bar{\psi}(x)\gamma^\mu \mathcal{D}_\mu \psi(x) - \frac{1}{4}B_{\mu\nu}B^{\mu\nu} - \frac{1}{2}Tr[W_{\mu\nu}W^{\mu\nu}] \tag{1.21}$$

where

$$\begin{aligned} \mathcal{D}_\mu Q_1 &= \left(\partial_\mu - ig_w T_W^i W_\mu^i - ig_Y \tfrac{Y_{Q_1}}{2} B_\mu\right) Q_1 \,, \\ \mathcal{D}_\mu U_1 &= \left(\partial_\mu - ig_Y \tfrac{Y_{U_1}}{2} B_\mu\right) U_1 \,, \end{aligned} \tag{1.22}$$

g_w and g_Y are the weak and the hypercharge coupling constant respectively. The strength tensors of the theory are given by

$$\begin{aligned} B_{\mu\nu} &\equiv \partial_m u B_\nu - \partial_\nu B_\mu \\ W_{\mu\nu} &\equiv \partial_m u W_\nu - \partial_\nu W_\mu - ig_w[W_\mu, W_\nu] \end{aligned} \tag{1.23}$$

and $W_\nu = \frac{\sigma_i}{2} W_\mu^i$. Already at this stage we can see that the theory predicts two charged currents and two neutral currents. Indeed if we look at the interacting piece of the Lagrangian

$$g_w \bar{Q}_1 \gamma^\mu W_\mu Q_1 + g_Y B_\mu \sum_{\psi=Q_1,U_1,D_1} y_\psi \bar{\psi}\gamma^\mu \psi \tag{1.24}$$

in the first term we have

$$W_\mu = \frac{\sigma_i}{2} W_\mu^i = \frac{1}{\sqrt{2}} \begin{pmatrix} \sqrt{2}W_\mu^3 & W^+ \\ W_\mu^- & -\sqrt{2}W_\mu^3 \end{pmatrix} \tag{1.25}$$

where $W^\pm = (W_\mu^1 \mp i W_\mu^2)$, the off diagonal terms are related to charged currents, while the diagonal terms together with the second term of Eq. (1.24) are related to neutral currents. It is important to notice that the previous formulas are valid for each family of quarks and leptons. It is apparent to see that the Lagrangian we wrote still shows a fundamental problem: the gauge boson and the fermion fields are still massless. As already said introducing an explicit term for fermion masses would explicitly break the electroweak gauge symmetry so a new mechanism should be found. In order to solve these problems we need to introduce a doublet of complex scalars that is a singlet under the group of strong interactions, doublet under $SU(2)_L$ and carries a $U(1)_Y$ charge, this is the Higgs field ϕ:

$$\phi(x) \equiv \begin{pmatrix} \phi^+(x) \\ \phi^0(x)\,. \end{pmatrix} \tag{1.26}$$

Renormalisability and gauge invariance require the gauged Lagrangian related to the Higgs field to be

$$\mathcal{L}_\phi = (\mathcal{D}\phi)^\dagger D^\mu \phi - \mu^2 \phi^\dagger \phi + \lambda(\phi^\dagger \phi)^2 \,, \qquad \mu^2 > 0 \quad \lambda > 0 \,; \tag{1.27}$$

$$D_\mu \phi = (\partial_\mu - i g_w W_\mu - i g_Y Y_\phi B_\mu)\, \phi \,, \qquad y_\phi = Q_\phi - T_3 = \frac{1}{2} \,. \tag{1.28}$$

We need to fix the value of the scalar hypercharge so that we have the right coupling between A_μ and ϕ: the photon should not couple to ϕ^0 and ϕ^+ needs to have the right electric charge. The minimum of the potential gives an infinite number of continuous possible vacuum expectation values all satisfying

$$\phi^\dagger \phi = \frac{\mu^2}{2\lambda} \equiv v^2 \,. \tag{1.29}$$

Among all the possible vacua we set

$$\langle 0|\phi(x)|0\rangle = \frac{1}{\sqrt{2}} \begin{pmatrix} 0 \\ v \end{pmatrix} \tag{1.30}$$

and since, due to the electric charge conservation, only a neutral scalar field can acquire a non vanishing VEV, we see that ϕ^0 has to be interpreted as the neutral ϕ component with $Q_{\phi^0} = 0$. Once we choose a particular ground state the gauge symmetry gets spontaneously broken

$$SU(2)_L \times U(1)_Y \to U(1)_{QED} \tag{1.31}$$

and three massless Goldstone bosons should appear. We can then fix the gauge in order to get rid of these spurious degrees of freedom. Using unitary gauge we get:

$$\phi(x) = \frac{1}{\sqrt{2}} \begin{pmatrix} 0 \\ v + H(x) \end{pmatrix} . \tag{1.32}$$

Expanding the double covariant derivative term in Eq. (1.27) it is easy to see that it contains gauge boson masses

$$\mathcal{L}_H \supset \frac{v^2}{8} \left[g_w^2 ((W_\mu^1)^2 + (W_\mu^2)^2) + (g_w W_\mu^3 - g_Y B_\mu)^2 \right] . \tag{1.33}$$

We can immediately read the mass term for $W^\pm$ gauge bosons

$$\frac{1}{2} m_W^2 W_\mu^\dagger W^\mu \,, \qquad \text{where} \qquad m_W = \left(\frac{v g_w}{2} \right) . \tag{1.34}$$

Moreover, assuming that A_μ and the Z_μ are related to B_μ and W_μ^3 through a unitary rotation

$$\begin{pmatrix} W_\mu^3 \\ B_\mu \end{pmatrix} \equiv \begin{pmatrix} \cos(\theta_w) & \sin(\theta_w) \\ -\sin(\theta_w) & \cos(\theta_w) \end{pmatrix} \begin{pmatrix} Z_\mu \\ A_\mu \end{pmatrix} \tag{1.35}$$

and looking at the combination of B_μ and W^3_μ that gets a mass in Eq. (1.33), we can conclude that the photon and the Z-boson can be expressed as

$$A_\mu \equiv \frac{1}{\sqrt{g_w^2+g_Y^2}}(g_Y W^3_\mu + g_w B_\mu)\,, \qquad Z_\mu \equiv \frac{1}{\sqrt{g_w^2+g_Y^2}}(g_w W^3_\mu - g_Y B_\mu) \tag{1.36}$$

and have the following masses

$$m_A = 0\,, \qquad m_Z = \frac{v}{2}\sqrt{g_w^2+g_Y^2}. \tag{1.37}$$

In order to understand how we can get mass terms for fermions we need to consider that introducing the Higgs field in the theory implies that new lagrangian terms may be allowed, we refer to these terms as the Yukawa lagrangian, $\mathcal{L}_y$:

$$\mathcal{L}_y = Y^l_{mn}\bar{L}_m\tilde{\phi}E_m + Y^d_{mn}\bar{Q}_m\phi D_n + Y^u_{mn}\bar{Q}_m\tilde{\phi}U_n + \ h.c. \tag{1.38}$$

indeed it is easy to see that these terms are gauge invariant as the combination $\bar{L}\phi R$ is a $SU(2)$ singlet[1]. After spontaneous symmetry breaking these terms give a mass to all fermions except for neutrinos that in SM do not have right-handed counter-parties and so we are not allowed to write down their Yukawa interactions.

We conclude this brief introduction putting all the the pieces together and writing the full SM lagrangian:

$$\begin{aligned}\mathcal{L}_{SM} = \ & -\tfrac{1}{2}Tr[G_{\mu\nu}G^{\mu\nu}] - \tfrac{1}{2}Tr[W_{\mu\nu}W^{\mu\nu}] - \tfrac{1}{4}B_{\mu\nu}B^{\mu\nu} \\ & + i\textstyle\sum_{\psi=L,E,Q,U,D}\bar{\psi}_n\mathcal{D}^\mu\gamma_\mu\psi_n \\ & - \left(Y^l_{mn}\bar{L}_m\tilde{\phi}E_m + Y^d_{mn}\bar{Q}_m\phi D_n + Y^u_{mn}\bar{Q}_m\tilde{\phi}U_n + \ h.c\right) \\ & + \mathcal{D}_\mu\phi^\dagger\mathcal{D}^\mu\phi - \lambda\left(\phi^\dagger\phi - \tfrac{v^2}{2}\right)^2 .\end{aligned} \tag{1.39}$$

Despite its astonishing accordance with experimental results there are many physical issues that SM cannot explain. The main problems concern the fact that SM does not accommodate gravitation and it can not explain the nature of dark matter and dark radiation. Indeed there is no known way of describing general relativity, the canonical theory of gravitation, within quantum field theory. Furthermore, according to experimental measurements on the mass and energy content of the universe it seems that SM is able to describe just 5% of them.
We can also find a long list of minor but fundamental observational and conceptual problems related to SM. We list some of them below.

[1]Since the mass terms should be hypercharge-less we need to use 2 representation of the Higgs field, the first one is the same as in Eq.(1.26) and has $y_\phi = 1/2$, the other one is given by $\bar{\phi} = \epsilon_{ij}\phi^*_j$ and has $y_\phi = -1/2$, they transform under $SU(2)$ in the same way.

The existence of **neutrino oscillations** implies that neutrinos are not massless, they have very small mass differences and violate the conservation of individual leptonic numbers.
Another problem is given by CP conservation in strong interaction. Indeed QCD lagrangian allows for the presence of a term proportional to $\theta G_{\mu\nu}\tilde{G}^{\mu\nu}$, where $\tilde{G}^{\mu\nu} = \frac{1}{2}\epsilon^{\mu\nu\alpha\beta}G_{\alpha\beta}$ is the gluon dual field strength and θ is a parameter. This term can contribute to physical processes through instanton effects and is CP-violating. Despite this term is allowed in the theory and naturally comes out from the study of QCD vacuum structure, experiments on neutron electric dipole model suggest that CP is actually conserved in strong interaction constraining $\theta < 10^{-10}$. The huge amount of fine-tuning required to match the experimental results goes under the name of **strong CP problem**.
Moreover, accepting that SM can be interpreted as an effective field theory it still shows a **naturalness problem**, i.e. the requirement that theories should be able to describe physics at low energies in ways that do not invoke a sensitive dependence on those theories' descriptions of physics at much higher energies [7]. One of the most widely known manifestations of it is the hierarchy problem related to the mass of the Higgs field. Indeed it turns out to be quadratically sensitive to the effective field theory scale or to the heavy fermion masses (depending on the regularisation scheme), thus revealing that we do not have a clear distinction between physical phenomena belonging to different energy scales:

$$m_h^2 = m_{h,0}^2 + \frac{Y_t^2}{8\pi}\left[\Lambda^2 + m_t^2 + m_{h\,0}^2 \ln\left(\frac{\Lambda}{m_t}\right) + \mathcal{O}\left(\frac{m_t^4}{\Lambda^4}\right)\right] \tag{1.40}$$

where $m_{h,0}$ is the Higgs bare mass, Λ is the UV cutoff scale of the effective field theory, m_t and Y_t are the the mass and the Yukawa coupling related to the top quark. The scale at which SM breaks down is not known, however assuming that it is valid at least till $\mathcal{O}(1)$ TeV (LHC run II), we get a mass correction to the Higgs field that is several orders of magnitude larger than its measured value. The reason why this happens is that in general scalar fields are not protected against quantum corrections by any symmetry, thus they can receive arbitrarily large quantum corrections to their masses. If we want to solve this puzzle avoiding to introduce any symmetry property or matter content in the theory we incur into a fine-tuning problem. Assuming that $\Lambda = M_P$, if we want to keep the Higgs mass light, we need to fine-tune the 0-th order dimensionless coupling of the effective field theory down to $m_\phi^2/\Lambda^2 \sim 10^{-34}$.
Furthermore, it has been seen that the running of the renormalisation group predicts that the gauge coupling constants related to $SU(3)_S$, $SU(2)_L$ and $U(1)_Y$ become approximately equal around 10^{16} GeV. However SM can not provide a deep reason that justifies **gauge coupling unification** and the energy scale at

which it takes place. In addition within SM this mechanism is not sufficiently precise and it can be interpreted as accidental.
The last problem that we want to mention is that, also in its minimal formulation (massless neutrinos), SM involves a lot of parameters, 10 mass parameters related to leptons, quarks, gauge bosons and the Higgs field, 3 parameters related to the coupling constants, 1 parameter related to the VEV of the Higgs field and 4 parameters related to the CKM matrix which describes cross-generational mixing of weak interaction. Moreover we also need to insert by hand the required number of families in SM. In addition since we now have good experimental evidence that neutrinos have small but non-vanishing masses this introduces 3 more mass inputs and 4 parameters related to neutrino oscillations giving a total of **25 input parameters**. Despite the great accordance with data, this huge amount of arbitrariness stresses the effective field theory nature of SM and call for research into UV completed models that can embed SM, giving a deeper explanation of these parameters in terms of dynamical mechanisms which can fix their values to the physical ones.

1.2 Standard Model of Cosmology

During the last three decades technological advances in observational cosmology brought us to a new conception of the universe. Large galaxy surveys which collected data from all visible galaxies confirmed that the universe is homogeneous and isotropic on large spatial scales. This means that if we look at large spatial regions of the universe we will see a translational and rotational invariance. In addition it has been proved that the universe is expanding with increasing speed, i.e. the relative distance between non-gravitationally bounded objects (different galaxies) is increasing in time at higher and higher rate. All these experimental results, together with the success of SM in the context of particle physics, led a formulation of the theory of the early universe that involves SM together with classical general relativity. In this theory the metric for an expanding universe has the *Friedmann-Robertson-Walker (FRW)* form:

$$ds^2 = dt^2 - a^2(t)\gamma_{ij}dx^i dx^j \,, \tag{1.41}$$

where $a(t)$ is the scale factor which takes into account the universe expansion rate and γ_{ij} is the spatial metric. We can parametrise the spatial manifold as a unit 3-sphere, a unit 3-hyperboloid or a 3-plane with spatial curvatures $\kappa = 1$, $\kappa = -1$ and $\kappa = 0$ respectively. It is important to notice that Eq. (1.41) implies that the space is the same at each moment of time and assumes that we are in a comoving frame, i.e. particles at rest follow a geodesic motion and can be considered as free particles. Experimental results suggest that the metric of the universe is essentially

flat $\kappa \sim 0$ [8]. For a spatially flat universe the scale factor $a(t)$ is dimensionless and does not have any physical meaning since at any time it can be set equal to any number rescaling the spatial coordinates. What is meaningful is the ratio of the scale factor computed at different times and the parameter which shows how the scale factor evolves in time, i.e. the Hubble parameter H:

$$H(t) \equiv \frac{\dot{a}(t)}{a(t)} \,. \tag{1.42}$$

Another way of parametrising the expansion of the universe is considering the wavelength variation of a photon, that is produced at a given time t_e in some point of the universe (through a known process, so that we know λ_e), once it is detected at time t_0 on Earth:

$$\lambda_0 = \lambda_e \frac{a_0}{a(t_e)} \equiv \lambda_e[1 + z(t_e)] \,, \tag{1.43}$$

where $z(t)$ is called redshift

$$z(t) = \frac{a_0}{a(t)} - 1 \,. \tag{1.44}$$

Throughout this section all quantities with sub-index 0 are referred to present time. Since the universe is expanding, $a_0 > a(t_e)$, we see that detection wavelength is always smaller than emission wavelength, this is the reason why it is said that the universe expansion induces a redshift effect. Expanding the previous equation at linear order we obtain the Hubble law for small redshift:

$$v = H_0 \, r \qquad v \ll 1 \tag{1.45}$$

where H_0 is the present value of the Hubble parameter. Recent measurements coming CMB observations made by the Planck satellite suggest [8][2]

$$H_0 = (67.36 \pm 0.54) \, \frac{\text{km}}{\text{s} \cdot \text{Mpc}} . \tag{1.47}$$

Hubble law can be interpreted as a sort of cosmological Doppler effect: redshift is induced by the expansion of the universe which causes the radial motion of galaxies from the Earth with velocities that increase at increasing distances. The

[2]There is tension between the Hubble parameter measurement coming from CMB observations, Eq. (1.47), and that one coming from low redshift objects, such as supernovae and cepheids, that gives [9]

$$H_0 = (73.5 \pm 0.5) \, \frac{\text{km}}{\text{s} \cdot \text{Mpc}} \,. \tag{1.46}$$

This tension represents a problem for the standard cosmological model, as these two values should coincide, and it might be a hint in favour of BSM physics.

inverse of H_0 gives a rough estimate of the age of the universe: $t_0 = H_0^{-1} \simeq 1.4 \times 10^{19}$ yrs.

The dynamics of the universe can be studied starting from the *Einstein-Hilbert action*

$$\mathcal{S}_{EH} = \frac{M_p^2}{2} \int d^4x \sqrt{-g}\, R \tag{1.48}$$

where $g = \det(g_{\mu\nu})$ is the metric determinant, R is the curvature scalar associated to $g_{\mu\nu}$ and $M_p = 2.435 \times 10^{18}$ GeV is the reduced Planck mass that is related to the universal gravitational constant through $M_p = 1/\sqrt{8\pi G}$. From Eq. (1.48) it is possible to derive the law of cosmological expansion, this is given by the *Einstein equations*

$$R_{\mu\nu} - \frac{g_{\mu\nu}}{2} R = \frac{T_{\mu\nu}}{M_p^2}\,, \tag{1.49}$$

where $R_{\mu\nu}$ is the Ricci tensor and $T_{\mu\nu}$ is the stress energy-tensor. If we consider the universe as an isotropic and homogeneous fluid, with energy density $\rho(t)$ and pressure $p(t)$, its energy momentum tensor is given by

$$T^{\mu\nu} = (p + \rho) u^\mu u^\nu - p\, g^{\mu\nu}\,, \tag{1.50}$$

where u^μ is the 4-velocity that satisfies $u_\mu u^\nu = 1$. Since we are working in a comoving frame, the fluid is at rest, the only non vanishing component of the 4-velocity is $u^0 = 1$ and the non vanishing components of the energy momentum tensor are

$$T_{00} = \rho\,, \qquad T_{ij} = -\gamma_{ij} p\,. \tag{1.51}$$

The 00-component of Eq. (1.49) gives us the relation between the energy density of the universe, the expansion rate and the spatial curvature:

$$H^2 = \frac{\rho}{3M_p^2} - \frac{\kappa}{a^2}\,, \tag{1.52}$$

this is called *Friedmann equation*. Considering the Universe as a closed system we have that the covariant conservation of the energy-momentum tensor, $D_\mu T^{\mu\nu} = 0$, can be written as:

$$\dot{\rho} + 3H(\rho + p) = 0\,. \tag{1.53}$$

In order to explicitly solve the dynamical equations for an expanding universe we need a last ingredient that does not follow from general relativity, this is the equation of state of the matter content of the universe $p = p(\rho)$. Assuming that the equation of state can take the perfect fluid form,

$$p = \omega \rho\,, \tag{1.54}$$

	ω	$a(t)$	$H(t)$	$\rho(a)$
dust	0	$\propto t^{2/3}$	$\propto t^{-1}$	$\propto a^{-3}$
radiation	$\frac{1}{3}$	$\propto t^{1/2}$	$\propto t^{-1}$	$\propto a^{-4}$
vacuum	-1	$\propto e^{H_{dS}t}$	H_{dS} (const.)	ρ_{vac} (const.)

Table 1.3: Behaviour of $a(t)$ and H and $\rho(a)$ in case of flat space, i.e. $\kappa = 0$. We consider the cases in which the universe is dominated by non-relativistic matter (dust), relativistic matter (radiation) and vacuum energy. In case of vacuum energy domination we have that both $H = H_{dS}$ and $\rho = \rho_{vac}$ are constant, they are related by $H_{dS} = \sqrt{\frac{\rho_{vac}}{3M_p^2}}$.

we can identify 3 main kinds of behaviour: non-relativistic matter is associated with the "dust" equation $p = 0$, relativistic matter follows radiation equation $p = \rho/3$ and vacuum contribution follows $p = -\rho$. If we have different kinds of matter characterised by different equations of state that do not interact with each other, every single component must satisfy $D_\mu T_i^{\mu\nu} = 0$ and Eq. (1.53) independently. On the other hand Eq. (1.52) must contain the sum of all the energy density contributions. We list in Table 1.3 the behaviour of $a(t)$, $H(t)$ and $\rho(a)$ in case of flat space, i.e. $\kappa = 0$, for the 3 main simplified scenarios of dust, relativistic and vacuum energy content. The general solution for $p = \omega\rho$ with $\omega > -1$ is given by:

$$\rho \propto \frac{1}{a^{3(1+\omega)}}\,; \qquad \rho \propto t^{-2}\,; \qquad a \propto t^{\alpha} \qquad \text{where} \quad \alpha = \frac{2}{3}\frac{1}{1+\omega} > 0\,. \tag{1.55}$$

The acceleration of the universe is parametrised by $\ddot{a}$ and is given by

$$\ddot{a} \propto \alpha(\alpha - 1)t^{\alpha-2}\,, \tag{1.56}$$

so we see that for $\omega < -1/3$ we have an accelerated expansion while for $\omega > -1/3$ the universe expansion decelerate.

This kind of solution is not realistic since we know that the universe contains several forms of matter having different properties. The present energy density of the spatially flat universe is given by the critical density today:

$$\rho_c = \frac{3}{8\pi} H_0^2\, M_p^2 \sim 0.52 \times 10^{-2}\, \frac{\text{GeV}}{\text{cm}^3}\,. \tag{1.57}$$

We can express the current fraction of energy density carried by each single component as

$$\Omega_i = \frac{\rho_{0,i}}{\rho_c}\,. \tag{1.58}$$

The main relative contribution to non-relativistic matter coming from known particles is related to baryons Ω_B, while that one associated to relativistic matter comes from photons Ω_γ:

$$\Omega_B \equiv \frac{\rho_B}{\rho_c} = 0.048\,, \qquad \Omega_\gamma \equiv \frac{\rho_\gamma}{\rho_c} = 5 \times 10^{-5}. \tag{1.59}$$

All the other known and stable particles give negligible contributions to matter and radiation energy density, e.g. light neutrino contribution is negligible compared to Ω_γ and electron contribution gives $\Omega_e \sim \frac{m_e}{m_p}\Omega_B \simeq 2.5 \times 10^{-5}$. So we can conclude that our current understanding in particle physics covers less than 5% of the universe content.

In realistic models the other contributions to the universe energy density come from non-relativistic dark matter ρ_{DM}, dark energy ρ_Λ and the spatial curvature ρ_κ. In particular this last contribution can be written as:

$$\rho_\kappa = -\frac{3\kappa}{a^2 M_p^2}\,, \tag{1.60}$$

but observations of CMB anisotropy imply that κ is either zero or very small and the bound on Ω_κ is

$$|\Omega_\kappa| < 0.02\,. \tag{1.61}$$

The major part of the universe is therefore composed by dark matter and dark radiation, two unknown energy sources that represent more than 95% of the energy content [8]:

$$\Omega_\Lambda \simeq 0.68\,, \qquad \Omega_{DM} \simeq 0.31\,. \tag{1.62}$$

Despite we can not give a clear and unambiguous description of these two quantities, observations tell us which kind of properties these two components need to show.
We can safely say that dark energy behaves as vacuum energy and it is responsible for the acceleration of the universe. Different models have been developed in order to describe dark energy, we can group them into two main categories: if the energy density does not depend on time we talk about cosmological constant models, while if it does have a time dependence we call them quintessence models. This last case would imply the existence of a new form of matter in nature, this is usually given by a scalar field that satisfies $\frac{1}{2}\dot{\phi}^2 \ll V(\phi)$ so that $p_\phi \sim -\rho_\phi$.

On the other hand dark matter can create clusters and it is probably made out of non-relativistic particles that can interact with ordinary particles only through gravitational couplings. The nature of DM is not clear yet but it is a common belief that it must be composed by particles that do not appear in SM. A common assumption is that DM is made out of matter particles that were in thermal

equilibrium with usual matter in the early Universe. At some time these particles decouple, they get out of equilibrium and start to freely propagate through the universe. We talk about cold dark matter if the decoupling temperature is lower than the DM particle mass, $T_d < m_{DM}$, in this case DM particles decouple being non-relativistic. If this condition is not satisfied we can have two different possibilities: if $m_{DM} < 1$ eV the particles remain relativistic at matter-radiation equality ($T_e \sim 1$eV) and we call it hot dark matter, while if $m_{DM} > 1$ eV DM is non-relativistic by equality epoch it is called warm dark matter. The presence of DM in the early universe is crucial in getting large structure formation. In order to reproduce structure formation we need primordial density perturbations that start growing at radiation-matter equality, giving rise to gravitationally bounded regions. Without DM, density perturbation would start to grow too late (after recombination) and no structure would have been formed in the universe yet. In order for this mechanism to work we need that DM becomes non-relativistic at early stages of the universe evolution. This is a hint in favour of cold DM, the studies of structure with size larger than 0.1 Mpc give a lower bound on the mass of DM particle: $m_{DM} \gtrsim 1$ keV. This bound only applies if DM was in kinetic equilibrium with usual matter at early stages of the universe.

A spatially flat cosmological model with cold dark matter and dark energy with energy densities close to Eq. (1.62) is called *ΛCDM model*. In these models the role of dark energy is played by the cosmological constant whose contribution ρ_Λ is constant over time. Knowing how dust, radiation and vacuum energy densities evolve in time we can relate present results with relative contributions at any given time using Friedmann equation:

$$H^2 = \frac{\rho_c}{3M_p^2}\left[\Omega_M\left(\frac{a_0}{a}\right)^3 + \Omega_{rad}\left(\frac{a_0}{a}\right)^4 + \Omega_\Lambda + \Omega_{curv}\left(\frac{a_0}{a}\right)^2\right], \tag{1.63}$$

where Ω_M contains DM and SM non relativistic degrees of freedom, while Ω_{rad} contains relativistic degrees of freedom.

The fact that the Universe is expanding determines that it was denser and warmer in the past. In what follows we briefly sum up the main stages of the universe evolution according to ΛCDM model:

- **Photon last scattering** $T_{ls} = 0.26$ **eV**: it is the moment after which photon decouple from cosmic plasma and can freely propagate through the universe. After this time the universe becomes transparent. These photons can be observed today as the Cosmic Microwave Background (CMB), their spectrum is the same as that one of a black body with temperature

$$T = 2.726 \pm 0.001\text{K}\,,$$

while their angular anisotropy is of order $\delta T/T \sim 10^{-4} - 10^{-5}$. This measure tells us that the universe at photon decoupling was almost perfectly homogeneous and isotropic.

- **Recombination ($T_r \sim$ 0.33 eV)**: it determines the transition from plasma to gas. At higher energies the binding energy was insufficient to keep electrons in atoms, the matter was made of a plasma containing baryons, photons and electrons. Electrons were coupled to the cosmic plasma through Thomson scattering $e^- + p^+ \rightarrow H + \gamma$. At recombination the equilibrium abundances of free protons and hydrogen atoms are equal.

- **Matter-radiation equality ($T_{mre} = 0.7$ eV)**: time at which the Universe moved from a stage where its energy content was mainly given by relativistic particles into a stage of non-relativistic matter domination.

- **Big Bang Nucleosynthesis - BBN ($T_{BBN} \sim$ MeV)**: it represents the time when neutrons got captured into nuclei. At $T > T_{BBN}$ protons and neutrons were free in cosmic plasma while at $T \lesssim T_{BBN}$ light nuclei get formed, e.g. hydrogen and helium.

- **Neutrino decoupling ($T_\nu \sim 2 - 3$ MeV)**: it represents the temperature at which neutrinos decoupled from the cosmic plasma. At $T > T_\nu$ neutrinos were in thermal equilibrium with the other particles while at $T \lesssim T_\nu$ they could freely propagate in the universe.

- **QCD transition ($T_{QCS} \sim 200$ MeV)**: at higher temperatures quarks and gluons behaved as individual particles while at $T \lesssim T_{QCS}$ they got confined into colourless hadrons.

- **EW transition ($T_{EW} \sim 100$ GeV)**: at higher temperatures there is no Higgs condensate, $W^\pm$ and Z bosons and all the fermionic particles are massless. At $T \lesssim T_{EW}$ Higgs mechanism takes place, we have SSB of $SU(2)_w \times U(1)_Y \rightarrow U(1)_{em}$ and $W^\pm$, Z and all the fermions (except neutrinos if we just consider SM physics) acquire a mass.

Despite the huge success in reproducing the history of the universe back to BBN, ΛCDM model still suffers from some theoretical and experimental problems. As already discussed, the most prominent one is given by the lack of an explicit description of the nature of dark matter and dark energy. We list below other minor but fundamental issues that need to be addressed in order to provide a natural UV-complete model of cosmology:

- **baryon asymmetry.** The present universe contains baryons and practically no anti-baryon. The study of Big Bang nucleosynthesis and CMB gives that the ratio between baryon and photon number density (n_B and n_γ respectively) is

$$\eta_B \equiv \frac{n_B}{n_\gamma} \simeq 6 \times 10^{-10}. \tag{1.64}$$

  The baryon number is conserved at low energies and η_B was of the same order also in the early Universe. Indeed at $T > 100$ MeV, before QCD transition, there were a lot of quarks and antiquarks in the cosmic plasma that annihilated and were created in pairs. The number of quark-antiquark pairs at that epoch was the same as the number of photons and the baryon asymmetry was given by

$$\frac{n_q - n_{\bar{q}}}{n_q + n_{\bar{q}}} \sim \eta_B \sim 10^{-10}\,. \tag{1.65}$$

  This tiny baryon asymmetry is responsible for the abundance of baryonic matter that we currently see in the present universe. It is extremely unlikely that this small baryon excess was present in the Universe from the very beginning and it was probably created at high energies though baryon number non-conserving processes. There is still no unique answer to this problem and it cannot be found a solution within the framework of SM of particle physics.

- **Cosmological constant problem.** While in quantum field theory the vacuum energy can be ignored and subtracted from the theory through renormalisation techniques, in general relativity this can not be done since, as any other kinds of energy, vacuum energy gravitates. If the universe is approximately isotropic and homogeneous the vacuum energy is the same everywhere anytime and it represents a good candidate for dark energy. If we assume naturalness, giving that energy density has dimensions M^4, we may think that it needs to be related to the proper energy (mass) scales of fundamental interactions: 1 GeV for strong interactions, 10^2 GeV for electroweak interactions and $M_P \sim 10^{19}$ GeV for gravitational interactions. The actual dark energy density is given by

$$\rho_\Lambda \sim 10^{-46}\,\mathrm{GeV}^4 \tag{1.66}$$

  and is easy to see that it is several orders of magnitude below any theoretical estimates. The value of ρ_Λ is crucial for reproducing the history of the universe: different ρ_Λ may lead to recollapsing universe or do not allow for large scale structure formation. There is still not a clear answer to this problem that can be considered as one of the most important missing milestones in fundamental physics.

- **Initial singularity.** Realistic cosmological models predict the existence of a singularity at the initial moment of time (Big Bang), when the scale factor vanishes while energy and pressure become infinite. This singularity is not related to homogeneity and isotropic assumptions, it is a general property of expanding cosmological solutions. The presence of a singularity shows that we cannot apply classical field theory at the very beginning of the evolution. Therefore we need a quantum theory of gravity that can be valid at energies higher than M_p. Indeed this is the only dimensionful parameter that appears in GR, so it is quite natural to think that classical field theory should break down at that scale.

- **Horizon problem.** Let us define the cosmological horizon, $l_H(t)$, as the maximum length a photon emitted at Big Bang travels by time t:

$$l_H(t) = a(t) \int_{t_p}^{t} \frac{dt}{a(t)} \,, \tag{1.67}$$

,it gives the size of causally connected regions in the universe at time t. Since the universe expands, the actual size of $l_H(t)$ is stretched to $l_H(t)_0 = l_H(t)a(t_0)/a(t)$. Within Hot Big Bang theories the scale factor increases in time as $a \propto t^\alpha$ where $\alpha = 1/2, 2/3$ during radiation and matter domination respectively. It is therefore easy to see that $l_H(t)_0 \ll l_H(t_0)$ when $t < t_0$. Indeed, neglecting the recent accelerated expansion and comparing the size of the sphere of last scattering, seen via CMB, with the actual size of cosmological horizon at recombination, we get that the number of causally disconnected regions in CMB is of order

$$\left(\frac{l_H(t_0)}{l_H(t_r)_0} \right)^2 \sim 10^3 \,. \tag{1.68}$$

These regions have never been in causal contact before photon decoupling, but they show an extremely high level of homogeneity and isotropy: $\delta T/T \lesssim 10^{-4}$. Hot Big Bang theory can not give the reason why causally disconnected regions should show a thermal equilibrium spectrum.

- **Flatness problem.** As already said, the only dimensionful parameter in the theory in given by M_p and one would naively think that at $t_p = M_p^{-1}$ the energy density of the universe is equally distributed among its component. Therefore the spatial curvature should to be of order M_p^{-2}:

$$|\Omega_\kappa(t_p)| = \frac{|\rho_\kappa(t_p)|}{\rho_c(t_p)} \sim 1 \,. \tag{1.69}$$

Nevertheless we saw that the present value is given by $|\Omega_\kappa(t_0)| \sim 0.02$ and this quantity changes in time as

$$\Omega_\kappa(t) \propto \frac{1}{a^2(t)H^2(t)} \,. \tag{1.70}$$

This means that tracing back the current value to Planck epoch we get

$$\frac{\Omega_\kappa(t)}{\Omega_\kappa(t_0)} = \frac{a^2(t_0)H^2(t_0)}{a^2(t_p)H^2(t_p)} \sim 10^{-60} \,. \tag{1.71}$$

The spatial curvature has to be 60 orders of magnitude smaller than the a priori natural estimate.

- **CMB anisotropy.** Despite CMB has a nearly black body spectrum, it shows density fluctuations of order $\delta\rho/\rho \lesssim 10^{-4}$, whose spectrum is close to flat. These primordial fluctuations and their precise value are at the origin of structure formation in universe as we currently see it. Hot Big Bang theory does not provide a mechanism for generating these fluctuations and they must be put in "by hand".

- **Coincidence problem.** A coincidence that requires an explanation is that in the present universe the different energy contributions, i.e. dark energy, dark matter and baryons, are of the same order of magnitude. Having different origins, a priori they may have contributions of different orders of magnitude. From Hot Big Bang theory it seems that fine tuned initial conditions lead to a sort of equipartition of energy at late times.

Chapter 2

Beyond Standard Models

2.1 Inflation

As pointed out in the previous section, Big Bang cosmology suffers from initial condition problems, such as horizon and flatness problems, and it is not able to motivate the initial value of density perturbations needed to efficiently reproduce large structure formation in the present universe. These problems are naturally solved by Cosmological Inflation theory, this is one of most famous extensions of ΛCDM models that in addition shows an outstanding accordance with current cosmological experiments. We saw that the cosmological particle horizon is given by

$$l_H(t) = a(t) \int_{t_p}^{t} \frac{dt}{a(t)} = a(t) \int_{a(t_p)}^{a} (t) \frac{d \ln a'}{a' H(a')} \,. \tag{2.1}$$

The horizon and flatness problems arise from the fact that aH in Hot Big Bang theory is a monotonically decreasing quantity. Inflation is able to solve these problems introducing an epoch where the comoving Hubble radius, $a(t)H(t)$, increases, this can happen if the scale factor increases in time faster than t and the Universe undergoes an accelerated expansion rate. In particular it can happen that causally disconnected patches at current time were in causal connection at earlier times. Indeed if we call t_{end} the time when inflation ends, the present size of cosmological horizon at t_{end} is given by

$$l_H(t_{end})_0 = a(t_0) \int_{a(t_p)}^{a(t_{end})} \frac{da}{a^2 H} \simeq \frac{a_0}{a(t_p) H(t_p)} \,, \tag{2.2}$$

where we assumed that, being aH increasing during inflation, the main part of the integral comes from its lower bound. The ratio between this size and the current

Hubble length can be larger than one:

$$\frac{l_H(t_{end})_0}{l_H(t_0)} = \frac{a_0 H_0}{a(t_p)H(t_p)} \gtrsim 1\,. \tag{2.3}$$

It is immediate to see that this relation also provides a natural solution to the flatness problem of Eq. (1.71). We know that in order to have a period of accelerated expansion we need the universe to be dominated by a kind of matter which shows negative pressure, i.e $\omega < -1/3$, and we may ask ourselves how much time this stage need to last to solve standard cosmological problems. Let us assume that, after the end of inflation, the universe instantaneously reheats at t_{end} and the hot stage begins at a temperature

$$T_{reh} \sim \sqrt{M_p H(t_{end})}\,. \tag{2.4}$$

In order to solve horizon and flatness problems we need Eq. (2.3) to be satisfied, this implies

$$\frac{a(t_{end})H(t_{end})}{a(t_p)H(t_p)} \gtrsim \frac{a(t_{end})H(t_{end})}{a_0 H_0} \sim \frac{T_0}{T_{reh}}\frac{H(t_{end})}{H_0}\,. \tag{2.5}$$

We can define the number of e-foldings required between Planck time and the end of inflation as

$$N_{end} = \ln\left(\frac{a(t_{end})}{a(t_p)}\right) \tag{2.6}$$

and from Eq.(2.5) we immediately find a lower bound for N_{end}:

$$N_{end} \gtrsim \ln\left(\frac{T_0}{H_0}\right) + \ln\left(\frac{H(t_{end})}{T_{reh}}\right) \sim 68 + \ln\left(\frac{H(t_{end})}{T_{reh}}\right)\,. \tag{2.7}$$

We see that the second part of the previous equation is model dependent but, in general, it requires N_{end} to be larger than 70. Considering a reheating temperature in the range $T_{reh} = 1\,\mathrm{TeV} - M_p$ the previous bound in terms of cosmic time becomes:

$$\Delta t_{end} > 10^{-42} - 10^{-9}\,\mathrm{s}\,. \tag{2.8}$$

Inflation predicts that within an extremely small fraction of a second the universe grows exponentially at an accelerating rate. In realistic models the reheating period is not instantaneous and can last many Hubble times, this relaxes the bound to be

$$N_{end} \gtrsim 60\,, \tag{2.9}$$

of course the precise value of the lower bound depends on the details of the model under study.

2.1.1 Background evolution

The simplest model of inflation relies on adding to the theory a single scalar field that is called the *inflaton*. It plays the role of an order parameter that accounts for the time evolution of the inflationary energy density. The classical dynamics of inflation requires that the inflaton field is initially displaced from its true vacuum and its rolling motion to the bottom of its potential causes the exponential expansion of the universe.

The dynamics of a scalar field minimally coupled to gravity is governed by the following action:

$$S = \int d^4x\sqrt{-g}\left[\frac{1}{2}R + \frac{1}{2}g^{\mu\nu}\partial_\mu\phi\partial_\nu\phi - V(\phi)\right] \tag{2.10}$$

where $V(\phi)$ is the potential associated to the inflaton. The energy momentum tensor is given by

$$T_{\mu\nu} = \partial_\mu\phi\partial_\nu\phi - g_{\mu\nu}\left(\frac{1}{2}\partial_\alpha\phi\partial^\alpha\phi + V(\phi)\right) \tag{2.11}$$

and the field equation of motion is

$$\frac{1}{\sqrt{-g}}\partial_\mu\left(\sqrt{-g}\partial^\mu\phi\right) + \frac{\partial V(\phi)}{\partial\phi} = 0\,. \tag{2.12}$$

We assume that we are dealing with FRW metric with flat space and that we are allowed to separate the field ϕ into a homogeneous and a non-homogeneous part, we call them ϕ_0 and $\delta\phi$ respectively:

$$\phi(t,\vec{x}) = \phi_0(t) + \delta\phi(t,\vec{x})\,. \tag{2.13}$$

The energy momentum tensor related to ϕ_0 take the perfect fluid form with energy and pressure given by

$$\rho_{\phi_0} = \frac{1}{2}\dot{\phi}_0^2 + V(\phi_0)\,, \qquad p_{\phi_0} = \frac{1}{2}\dot{\phi}_0^2 - V(\phi_0) \tag{2.14}$$

that imply the following equation of state

$$\omega_{\phi_0} = \frac{p_{\phi_0}}{\rho_{\phi_0}} = \frac{\frac{1}{2}\dot{\phi}_0^2 - V(\phi_0)}{\frac{1}{2}\dot{\phi}_0^2 + V(\phi_0)} \tag{2.15}$$

In case this field dominates the energy density of the universe and if the potential energy is much larger than the kinetic one, we have $\omega_\phi < 0$ and the scalar field motion can lead to an epoch of negative pressure and accelerated expansion (if

$\omega_\phi < -1/3$). Considering only the contributions coming from the homogeneous field, the field equation of motion and the FRW equations become

$$\ddot{\phi}_0 + 3H\dot{\phi}_0 + V_{\phi_0} = 0\,, \qquad H^2 = \frac{\rho_{\phi_0}}{3}\,, \qquad \frac{\ddot{a}}{a} = H^2\left(1 - \frac{\dot{\phi_0}^2}{2H^2}\right)\,. \tag{2.16}$$

Having accelerated expansion requires

$$\dot{\phi}_0^2 \ll V(\phi_0) \tag{2.17}$$

so that $\omega_\phi \sim -1$ and we have a slow-roll motion, in addition in order to have a long lasting period of accelerated expansion we need that

$$|\ddot{\phi}| \ll |3H\dot{\phi}|\,,\, |V_\phi|\,. \tag{2.18}$$

We introduce the Hubble slow roll parameters ϵ and η that parametrise the validity of slow-roll approximation:

$$\epsilon = -\frac{\dot{H}}{H^2} = \frac{\dot{\phi}^2}{H^2}\,, \qquad \eta = -\frac{\ddot{\phi}}{H\dot{\phi}}\,, \tag{2.19}$$

these are two dimensionless parameters that satisfy the condition that, if ϵ and η are much less than 1, slow-roll motion is realised and inflation takes place. Inflation ends when $\epsilon \sim 1$. Under slow-roll conditions the universe undergoes a phase of exponentially fast expansion and the space-time is almost de Sitter:

$$a(t) \propto e^{H_{dS}t}\,, \qquad H^2 \sim \frac{V(\phi)}{3} \sim H_{dS}^2\,(\text{constant})\,. \tag{2.20}$$

It is possible to rephrase slow-roll condition with equivalent parameters that are referred to the inflaton potential, these are ϵ_V and η_V:

$$\epsilon_V = \frac{1}{2}\left(\frac{V_\phi}{V}\right)^2\,, \qquad \eta_V = \frac{V_{\phi\phi}}{V}\,. \tag{2.21}$$

Under slow-roll approximation we have $\epsilon_V \approx \epsilon$ and $\eta_V \approx \eta$. If slow-roll conditions are satisfied, the number of e-foldings before inflation ends allows us to find an implicit bound on the inflation field initial conditions, ϕ_{in}

$$N_{end}(\phi_{in}) = \ln\left(\frac{a_{end}}{a_{in}}\right) = \int_{t_{in}}^{t_{end}} H dt \approx \int_{\phi_{end}}^{\phi_{in}} \frac{d\phi}{\sqrt{2\epsilon_V}} \gtrsim 60\,. \tag{2.22}$$

2.1.2 Cosmological perturbations and CMB

The primordial density fluctuations that we can observe in the CMB have a quantum origin and can not be described using just the homogeneous part of the inflaton. In particular, as we have already done for the inflaton field in Eq. (2.13), we need to divide the space-time metric into its classical part and linear perturbations:

$$g_{\mu\nu} = \bar{g}_{\mu\nu}(t) + \delta g_{\mu\nu}(t, \vec{x}) \,. \tag{2.23}$$

Quantum perturbations must be present in the theory and metric and inflaton perturbations are tightly coupled to each other. An easy way to see this is to look at the equation of motion for $\delta\phi$, neglecting metric perturbations:

$$\ddot{\delta\phi} + 3H\dot{\delta\phi} - \frac{\nabla^2\delta\phi}{a^2} + V_{\phi\phi}\delta\phi = 0 \,. \tag{2.24}$$

Indeed, if we focus for simplicity on far sub-horizon modes ($k/aH \ll 1$) and we consider de Sitter expansion (constant H), we find that Eq. (2.24) is the same that has to be satisfied by $\dot{\phi}_0$. Since $\delta\phi$ and $\dot{\phi}_0$ satisfy the same differential equation in time, they need to be related by a constant of proportionality which depends on space coordinates, i.e. $\delta\phi = -\dot{\phi}_0\delta t(x)$. Under these conditions, the split of the inflaton field into background value and perturbations can be seen as a Taylor expansion of

$$\phi(t\vec{x}) = \phi_0(t - \delta t(\vec{x}), \vec{x}) \,. \tag{2.25}$$

The inflaton field does not acquire the same value in any given space point at a given time, i.e. it can not be considered as a homogeneous field, and the relation between its physical value and the background approximation can be interpreted as a local change of coordinates.

Metric perturbations can be decomposed according to their spin with respect to a local rotation of the spatial coordinates on hypersurfaces of constant time, they can be either scalar (spin 0), vector (spin 1) or tensor perturbations (spin 2). The true symmetric, traceless and transverse degrees of freedom are $\frac{1}{2}(n-2)(n+1)$, where n is the number of space dimensions, in our case $n = 3$. We have 2 scalar, 2 vector and 2 tensor degrees of freedom. Vector perturbations are not exited during inflation since there is no rotational velocity in the inflationary stage, tensor perturbations are responsible for gravitational waves production. Since we are interested in density perturbations generation, let us focus on scalar degrees of freedom. At linear order, scalar, vector and tensor perturbations evolve independently and we are allowed to analyse them separately. Focusing on scalar degrees of freedom, the most generic perturbed metric is

$$\begin{aligned} ds^2 &= g_{\mu\nu}dx^\mu dx^\nu \\ &= -(1-2\Phi)dt^2 + 2aB_i dx^i dt + a^2[(1-2\Psi)\delta_{ij} + E_{ij}]dx^i dx^j \,, \end{aligned} \tag{2.26}$$

where $E_{ij} = (\partial_i\partial_j - \frac{1}{3}\delta_{ij}\nabla^2)E$. Perturbations in the metric give rise to connection, Riemann tensor, Ricci scalar and scalar curvature perturbations: $\delta\Gamma^{\alpha}_{\beta\gamma}$, $\delta R^{\alpha}_{\beta\gamma\delta}$, $\delta R_{\alpha\beta}$ and δR respectively. On the other hand the combination between metric and inflaton perturbations lead to the perturbed stress-energy tensor. The dynamics of the system can be studied solving the perturbed Klein-Gordon equation for the inflaton field and the perturbed Einstein equations:

$$\delta\left[\frac{1}{\sqrt{-g}}\partial_\mu\left(\sqrt{-g}g^{\mu\nu}\partial_\nu\phi\right)\right] = V_{\phi\phi}\delta\phi\,, \qquad \delta T_{\mu\nu} = \frac{1}{M_p^2}\left(\delta R_{\mu\nu} - \frac{1}{2}\delta R\right)\,. \tag{2.27}$$

Before we can look at the results of perturbation theory in case on single field inflation, we need to understand how to work with physical quantities. Performing the metric expansion we want to study small perturbations away from the homogeneous and isotropic FRW flat space-time. The aim of perturbation theory is to give at linear level the difference between the real physical space-time and its unperturbed background approximation . In order to do it properly these two quantities need to be computed at the same space-time point. On the other hand, being general relativity a gauge theory, where gauge transformation are given by local coordinate changes, we need to find a map that univocally identifies the same space-time points in the two different geometries. Changing the map corresponds to perform a gauge transformation, while choosing a map (coordinate choice) is fixing the gauge.
Scalar perturbations in Eq. (2.26) are not gauge invariant, indeed, under a local coordinate change as

$$\begin{aligned} t &\to t + \alpha\,, \\ x^i &\to x^i + +\delta^{ij}\beta_{,j}\,, \end{aligned} \tag{2.28}$$

the spin 0 degrees of freedom transform as

$$\begin{aligned} \Phi &\to \Phi - \dot{\alpha}\,, \\ \Psi &\to \Psi + H\alpha\,, \\ B &\to B + \frac{\alpha}{a} - a\dot{\beta}\,, \\ E &\to E - \beta\,. \end{aligned} \tag{2.29}$$

A change of the map implies a variation of perturbations and working in a fixed gauge may lead to spurious gauge artifacts. It is therefore useful to construct gauge-invariant scalars that allow us to work with only physical quantities. Among them, we cite the *comoving curvature perturbation* $\mathcal{R}$. It measures the spatial

curvature of comoving hypersurfaces and in single field inflation has the following form:

$$\mathcal{R} \equiv \Psi + \frac{H}{\dot{\phi}_0}\delta\phi\,. \tag{2.30}$$

It can be proven that on super-horizon scales, this quantity does not evolve and can be related to the dimensionless density perturbations. Therefore its primordial value gives the seed for CMB fluctuations and large structure formation. In single field inflation $\mathcal{R}$ can be safely considered as a gaussian variable, non gaussianities are predicted to be small, and all the statistical information is encoded into the two-point correlation function:

$$\langle \mathcal{R}\mathcal{R}\rangle = \int_0^\infty \Delta^2_{\mathcal{R}}(k) d\ln k, \qquad \langle \mathcal{R}_{\vec{k}}\mathcal{R}_{\vec{k}'}\rangle = (2\pi)^3\delta(\vec{k}+\vec{k}')P_{\mathcal{R}}(k)\,, \tag{2.31}$$

where $\mathcal{R}_{\vec{k}}$ are the Fourier modes of $\mathcal{R}$, $\Delta^2_{\mathcal{R}} = \frac{k^3}{2\pi^2}P_{\mathcal{R}}$ is the dimensionless power spectrum and $P_{\mathcal{R}}$ is the power spectrum of $\mathcal{R}$. The scale dependence of the dimensionless power spectrum is measured by the scalar spectral index n_s

$$n_s \equiv 1 + \frac{d\ln\Delta^2_{\mathcal{R}}(k)}{d\ln k}\,, \tag{2.32}$$

current measurements set $n_s \simeq 0.96$ [10], pointing out that $\Delta^2_{\mathcal{R}}$ is almost scale invariant. In this context the scalar power spectrum can be approximated as

$$\Delta^2_{\mathcal{R}} = \mathcal{A}_s(k_*)\left(\frac{k}{k_*}\right)^{n_s-1+\frac{1}{2}\frac{dn_s}{dk}\ln(k/k_*)}\,, \tag{2.33}$$

where k_* is a pivot scale. The scalar power spectrum amplitude, $\mathcal{A}_s(k_*)$, can be constrained from CMB observations and it has been estimated to be $\mathcal{A}_s \simeq 2\times10^{-9}$ using the pivot scale $k_* = 0.05\,\mathrm{Mpc}^{-1}$ [10].

As already said, beside scalar perturbations, inflation excites tensor perturbations, h_{ij}, that can be expressed as

$$ds^2 = -dt^2 + a(t)^2\left[\delta_{ij} + h_{ij}\right]dx^i dx^j\,. \tag{2.34}$$

These are given by spin 2 degrees of freedom and are gauge invariant at linear order. The two physical polarisations, e^λ_{ij} where $\lambda = +,\times$, are usually composed by the eigenvalues of the spatial laplacian, $\Delta e_{ij} = -k^2 e_{ij}$, multiplied by a time dependent scalar amplitude $h(t)$

$$h_{ij} = h(t)e^{(+,\times)}_{ij}(\vec{x})\,, \tag{2.35}$$

where the two polarisations must be symmetric, transverse and traceless: $e^\lambda_{ij} = e^\lambda_{ji}$ and $e^\lambda_{ii} = k^i e_{ij} = 0$. Since in this setup the energy momentum tensor is diagonal,

the two canonically normalised tensor modes $a(t)h_{ij}^{\lambda}$ satisfy the equations of motion of two independent massless scalar fields. Being h_{ij}^{λ} physical quantities, we can then study the statistics associated to primordial tensor mode production as:

$$\langle hh \rangle = \int_0^\infty \Delta_h^2(k) d\ln k, \qquad \langle h_{\vec{k}} h_{\vec{k}'} \rangle = (2\pi)^3 \delta(\vec{k}+\vec{k}') P_h(k)\,, \tag{2.36}$$

where $P_h(k)$ is the tensor mode power spectrum and $\Delta_h^2(k)$ is its dimensionless counterpart. We define the dimensionless power spectrum of tensor perturbations $\Delta_t^2(k)$ as the sum of the contributions coming from the two polarisations: $\Delta_t^2(k) = 2\Delta_h^2(k)$. We can define the scale dependence of tensor power spectrum through the tensor spectral index: $n_t = \frac{d\ln\Delta_t^2(k)}{d\ln k}$. Using slow-roll approximation the two power spectra in case of single field inflation turn out to be

$$\Delta_{\mathcal{R}}^2(k) = \left.\frac{H^4}{(2\pi)^2\dot{\phi}_0^2}\right|_{k=aH}, \qquad \Delta_t^2(k) = \left.\frac{8}{M_p^2}\left(\frac{H}{(2\pi)}\right)^2\right|_{k=aH}. \tag{2.37}$$

The difference in magnitude between scalar and tensor power spectrum can be measured through the *tensor-to-scalar ratio*, r, whose experimental upper bound is [10]

$$r = \frac{\Delta_t^2(k)}{\Delta_{\mathcal{R}}^2(k)} \lesssim 0.1\,. \tag{2.38}$$

This parameter is extremely important since it allows to get an upper bound on the inflationary scale, being the relation between the inflaton potential and r given by

$$V^{1/4} \sim \left(\frac{r}{0.01}\right)^{1/4} 10^{16}\,\mathrm{GeV}\,. \tag{2.39}$$

Despite cosmological inflation theory has not been proved yet, its accordance with current experimental results, together with the ability of solving many of the theoretical problems related to standard cosmology, makes it the best candidate to extend hot big bang theory. Inflation is able to provide a natural dynamical solution to the flatness and horizon problems, adding to the theory a single scalar degree of freedom. Among the various achievements of this theory, the most striking hint in favour of inflation is the outstanding accordance between theoretical predictions and CMB spectrum. The shape of the primordial spectrum is easily reproduced by generic inflation models, the first acoustic peak appears at a scale that is consistent with flat universe, predicted by inflation, and the anisotropy spectrum of CMB shows peaks and troughs that can be explained only if all the Fourier modes of perturbations can be produced in a coherent way [11]. This last feature is the greatest success of inflation that naturally provides a mechanism for

coherent modes production. Modes deep inside the horizon during inflation oscillates with a frequency $k \ll 2\pi/k \ll aH$. However, during inflation, these modes get stretched to super-Hubble lengths, they get classical and their amplitude remains constant. When they re-enter the horizon, after the end of inflation, they start evolving very slowly, being $\dot{\mathcal{R}}$ very small at horizon crossing, and only coherent modes get excited. Since perturbations in $\mathcal{R}$ induce density perturbations and matter and radiation perturbations are strongly coupled in the early universe plasma, the coherent spectrum of Fourier modes that compose CMB power spectrum can be seen as a footprint of the primordial fluctuations in $\mathcal{R}$.

All the features listed above are already valid when we consider the simplest models, where we the inflaton is given by a single scalar field. Nevertheless, from Eq.(2.39) we see that the inflationary dynamics takes places at energies much higher than the scales at which SM has been tested in particles accelerators. Moreover, we know that the presence of dark matter and dark energy, together with all the theoretical problems related to SM, tell us that we may expect the existence of new kinds of particles that can extend SM. These observations suggest that inflation may be described in the context of beyond SM theories, such as supersymmetry or string theory, that usually predict the existence of a large number of new fields and some of them can be relevant for inflation. If this is the case, inflation may be driven by a combination of fields (multi-field inflation) or we may have light degrees of freedom, that are overdamped during inflation, which may leave imprints in the primordial spectrum through their quantum fluctuations (spectator fields). These models present a richer phenomenology and are usually characterised by isocurvature fluctuations production and a sizable amount of non-gaussianities in density perturbations that can be constrained or even detected in future experiments.

2.2 Axions and ALPs

As already discussed in the previous sections, SM can not be considered as a fundamental theory since it does not give a satisfactory explanation for the values of its underlying parameters, it is not a consistent quantum theory of gravity and it does not provide a model for dark energy and dark matter. Given that astrophysical observations show that dark matter represents nearly 30% of the energy content of the universe, looking for the existence of particles beyond the Standard Model seems to be a mandatory step.
Among the most prominent and widely-discussed candidates there are axions and axion-like particles (ALPs) which are often predicted by beyond-SM (BSM) theories and appear in many different forms in 4D effective fields theories coming from strings. These particles are particularly interesting since, depending on their mass

and on the mechanism related to their production, they can play both roles of cold dark matter (CDM) and dark radiation (DR).

2.2.1 Birth of Axions: the strong CP problem

Axion physics started in 1977 when Helen Quigg and Roberto Peccei proposed their solution to the strong CP problem postulating the existence of a new U(1) symmetry that leads to an extremely light and weakly interacting particle.
As already mentioned at the end of Section 1.1, quantum chromodynamics, the non abelian theory of strong interaction, allows for the presence of a CP-violating term in the lagrangian:

$$L_{CP} = \frac{g_S^2}{32\pi^2}\,\theta\; tr(G_{\mu\nu}\tilde{G}^{\mu\nu}) \tag{2.40}$$

where G is the gluonic field strength, $\tilde{G}^{\mu\nu} = \frac{1}{2}\epsilon^{\mu\nu\alpha\beta}G_{\alpha\beta}$ is its dual, g_S is the strong coupling constant and θ is a parameter which arises from the study of the QCD vacuum structure [12]. The above expression violates parity and time reversal but conserves charge, therefore it violates CP symmetry.
We can only determine the value of θ through experimental data; one of the main probes for it is the electric dipole moment of the neutron d_n, since it arises just from the CP-violating term (2.40). The experimental upper bound for its value is:

$$\mid d_n \mid \sim\; e\,\frac{m_q}{{m_n}^2}\,\theta \;\sim\; \theta\; 10^{-16}\,\text{ecm} \;< 10^{-26}\,\text{ecm}\,, \tag{2.41}$$

where m_q is a light-quark mass (u or d quark), m_n is the neutron mass and e is the electron charge; it is clear that the above relation implies $\theta < 10^{-10}$. If one adds to the QCD lagrangian the weak interaction contributions, $L_{qmass} = \bar{q}_{iR}M_{ij}q_{jL} + h.c.$, since the mass matrix is usually complex, one has to perform a transformation to diagonalise it and get a physical basis. As this transformation is chiral and chiral transformations change the QCD vacuum, the net effect of this calculation is to change the coefficient in front of the $G\tilde{G}$ term as

$$L_{CP} = \frac{g_S^2}{32\pi^2}\,\bar{\theta}\; tr(G_{\mu\nu}\tilde{G}^{\mu\nu}) := \frac{g_S^2}{32\pi^2}\,(\theta + Arg\;det\;M)\; tr(G_{\mu\nu}\tilde{G}^{\mu\nu})\,, \tag{2.42}$$

from which we see that the previous relation on θ now becomes $\bar{\theta} < 10^{-10}$.
A question arises spontaneously: why should this parameter be so small, or, similarly, why is CP conserved in strong interactions? These two questions are the core of what is called **strong CP problem**.
In 1977, Peccei and Quinn proposed a solution to this problem: they postulated

the existence of a global $U(1)_{PQ}$ chiral symmetry in the Lagrangian which is spontaneously broken. The axion is the Nambu-Goldstone boson of the broken $U(1)_{PQ}$ symmetry and its transformation rule under $U(1)_{PQ}$ is:

$$a(x) \to a(x) + \alpha\ f_a\,, \tag{2.43}$$

where f_a is the axion decay constant, which represents the order parameter associated with the breaking of $U(1)_{PQ}$.
The SM lagrangian must therefore be augmented by the axion kinetic terms and interactions:

$$\begin{aligned} L = \quad & L_{SM} + \tfrac{g_S^2}{32\pi^2}\ \bar{\theta}\ tr(G_{\mu\nu}\tilde{G}^{\mu\nu}) \\ & -\tfrac{1}{2}\partial^\mu a \partial_\mu a + L_{int}[\tfrac{\partial^\mu a}{f_a};\psi] + \xi\tfrac{a}{f_a}\tfrac{g_S^2}{32\pi^2} tr(G_{\mu\nu}\tilde{G}^{\mu\nu})\,, \end{aligned} \tag{2.44}$$

where ψ is a generic SM field and ξ is a model dependent parameter. The last term of the above equation is needed to give chiral anomaly to the $U(1)_{PQ}$ current and, at the same time, it also represents an effective potential for the axion field. The axion potential is generated by non perturbative effects of the QCD anomaly and looks like [12]:

$$V_{eff} \sim \cos(\bar{\theta} + \xi\frac{\langle a\rangle}{f_a})\,. \tag{2.45}$$

Its minimum with respect to $\langle a\rangle$ gives the Peccei-Quinn solution which sets dynamically the physical theta angle to zero:

$$\langle a\rangle = -\frac{f_a\bar{\theta}}{\xi}\,. \tag{2.46}$$

In fact, if we expand the axion field around its minimum we can see that its vacuum expectation value cancels out the $\bar{\theta}$ term. This provides a dynamical solution to the strong CP problem. The axion acquires a mass through instanton effects, this is given by:

$$(m^2)_a = \left\langle \frac{\partial^2 V_{eff}}{\partial a^2} \right\rangle |_{\langle a\rangle} = -\frac{\xi}{f_a}\frac{g_S^2}{32\pi^2}\frac{\partial}{\partial a}\langle G^{a\mu\nu}\tilde{G}^a_{\mu\nu}\rangle|_{\langle a\rangle}\,. \tag{2.47}$$

As we can see, the axion mass is a parametrically small quantity, it also depends on f_a which shows the energy scale of the $U(1)_{PQ}$ symmetry breakdown.
Using effective field theory techniques, the axion mass can be expressed in terms of the pion and up and down quarks as:

$$m_a = \frac{m_\pi f_\pi}{f_a}\frac{\sqrt{m_u m_d}}{m_u + m_d} \simeq 0.6\ \text{meV} \times \left(\frac{10^{10}\ GeV}{f_a}\right). \tag{2.48}$$

Looking at Eq.s (2.44) and (2.48), we see that for large decay constants the axion appears to be a weakly interacting, parametrically light particle. Models describing this kind of particles are called *invisible axion models*. These models introduce scalar fields which carry PQ charge and are $SU(2) \times U(1)$ singlets, this allows to have $U(1)$ symmetry breaking at high energies, decreasing the axion mass and the coupling strength.
There are two different benchmark models: the *Kim-Shifman-Vainshtein-Zakharov* (KSVZ) model and the *Dine-Fischler-Srednicki-Zhitnitsky* (DFSZ) model.
In the first one the axion is introduced as the phase of an additional EW singlet scalar field σ with $f_a = \langle\sigma\rangle \gg 250$ GeV. Since the known quarks cannot directly couple to such a field, as this would lead to unreasonably large quark masses, a new EW singlet heavy quark Q is introduced $M_Q \sim f_a$ and it couples to the new scalar field.
The second model (DFSZ) has two Higgs doublets and an EW singlet complex scalar ϕ, which acquires a non zero vacuum expectation value at the $U(1)_{PQ}$ symmetry breaking scale that must again satisfy $f_a = \langle\phi\rangle \gg 250$ GeV. This scalar couples only indirectly to the SM particles via its direct interaction with Higgs doublets. DFSZ models require that all fields appearing in the theory other than gauge bosons enjoy a Peccei-Quinn symmetry.

2.2.2 ALPs

Beyond the case of the strong CP problem, axions and axion-like particles (ALPs) appear in many models of physics beyond the Standard Model, such as string theory, as pseudo Nambu-Goldstone bosons associated to the breaking of U(1) symmetries. The properties of these particles are similar to that of axions but, in general, their mass and coupling to photons are not related, making the experimentally allowed parameter space very wide. Many extensions of the Standard Model contain extra $U(1)$ symmetries which are spontaneously broken. At energies below the spontaneous symmetry breaking scale, Nambu-Goldstone bosons come out representing the phase a of the complex scalar field ϕ charged under the $U(1)$ symmetry. If we call $\langle\phi\rangle = v_\sigma/\sqrt{2}$ the vacuum expectation value (VEV) of the field ϕ, we obtain, expanding it around its minimum:

$$\phi(x) = \frac{v_\sigma + \sigma(x)}{2}\, e^{i\frac{a(x)}{v_i}} \,. \tag{2.49}$$

The interaction of these particles with gluons, photons and SM matter fields (e.g. electrons) is suppressed by a large symmetry breaking scale, f_{a_i}, which must be higher than that one of the electroweak symmetry breaking $v = 246$ GeV, i.e. the Higgs VEV:

$$
\begin{aligned}
L = &\frac{1}{2}\partial_\mu a_i \partial^\mu a_i - \frac{\alpha_s}{8\pi}\Big(\sum_{i=1}^{n_{axions}} C_{ig}\frac{a_i}{f_{a_i}}\Big)\, G^b_{\mu\nu}\tilde{G}^{b,\mu\nu} \\
&- \frac{\alpha}{8\pi}\Big(\sum_{i=1}^{n_{axions}} C_{i\gamma}\frac{a_i}{f_{a_i}}\Big)\, F_{\mu\nu}\tilde{F}^{\mu\nu} + +\frac{1}{2}\Big(\sum_{i=1}^{n_{axions}} C_{ie}\frac{\partial_\mu a_i}{f_{a_i}}\Big)\bar{e}\gamma^\mu\gamma_5\, e + \dots ,
\end{aligned}
\tag{2.50}
$$

where C_{ig}, $C_{i\gamma}$ and C_{ie} represent the coupling to gluons, photons and electrons respectively.

We will focus on ALPs that come from string theory and string compactification in Section 2.3.10.

2.2.3 Axions and ALPs in cosmology

Axions as Cold DM Although DM has not be seen directly yet, its gravitational interaction with ordinary matter leaves unmistakable evidence for its existence. Cosmologists believe that DM is mostly comprised of cold slow moving particles that do not emit electromagnetic radiation or scatter light. The three most relevant features of particle candidates of cold DM (CDM), indirectly deduced from observations, are their feeble interactions with SM particles, their sufficiently non-relativistic momentum distribution during structure formation and their stability on cosmological time-scales.

A possible realisation of all these features are Weakly Interacting Massive Particles (WIMPs). In general WIMPs are supposed to be thermally produced in the early Universe and their large, of order TeV scale, mass ensures that by now they are non-relativistic. Their interactions are small due to the large mass of the mediator particles (such as W or Z bosons) and WIMP stability is ensured by the introduction of symmetries that conserve their particle number. A well-motivated WIMP candidate is the lightest supersymmetric particle which in most models is a neutralino. Although it is way too early to make a final judgment, it is nevertheless noteworthy that LHC measurements as well as direct WIMP searches have not given any clear indication of their existence. Because of these considerations, it is worthwhile to consider alternative ways to realise the essential features of DM. A possible alternative that can satisfy the observational constraints is given by Weakly Interacting Slim (very light) Particles (WISPs). In fact, sufficient stability of the DM particles can be achieved by combining the weakness of their interactions with a sufficiently small mass. This makes axions and ALPs good light CDM candidates. Indeed, despite them being so light, there are non-thermal means for producing sufficiently cold DM made of light particles. Among them, one of the most generic is the *vacuum misalignment mechanism* that we briefly summarise below.

We call ϕ and $E_{PQ} \sim f_\theta$ the field carrying the $U(1)_{PQ}$ symmetry and its SSB scale

respectively. We can parametrise ϕ as follows

$$\phi = |\phi(x)|e^{i\alpha(x)} = |\phi(x)|e^{i\theta(x)/f_\theta} \,.$$

The PQ symmetry is unbroken at early times and energies greater than E_{PQ}. Let us focus for simplicity on the case where SSB occurs at energies higher than the inflationary scale: $E_{PQ} > H_{inf}$. At energy $\sim E_{PQ}$, $U(1)_{PQ}$ breaks down spontaneously, $|\phi|$ acquires a non zero vacuum expectation value and the axion field $\theta(x)$, may have any value: $\theta(x)$ is still a flat direction of the potential. Going down to energy scales $E \sim \Lambda_{QCD} \sim 200$ MeV, where Λ_{QCD} is the confinement scale, QCD instantons effects generate an effective potential for the axion field. When these effects become significant, the axion field (randomly located in $\frac{\theta}{f_\theta} \in [-\pi;\pi]$) acquires a mass, rolls towards its minimum and starts oscillating around it. The temperature which sets the beginning of the oscillating regime T_{osc} is implicitly given by $m(T_{osc}) \sim H(T_{osc})$. For $T \gg T_{osc}$ the classical field is over-damped, $\theta \sim const$, and the energy density of θ contributes to the effective cosmological constant. On the other hand, when $T \ll T_{osc}$, the axion mass dominates over Hubble friction and the field undergoes damped harmonic motion behaving as non-relativistic matter: $\rho_\theta \propto a^{-3}$. For dark matter axions, oscillations must occur during radiation domination when the axion is a sub-dominant component of the total energy density. So we see that the oscillations of this "misaligned" classical axion field result in coherent field oscillations corresponding to a condensate of non-relativistic axions [13] that can contribute to the CDM content of the universe.

Axions as Dark Radiation Cold DM can be made of both stringy ALPs and the QCD axion. For a high decay constant, $10^9\,\text{GeV} < f_a < 10^{12}\,\text{GeV}$ the QCD axion can contribute significantly to cold DM, while ALPs can saturate the observed DM content for even larger decay constants (i.e. weaker couplings to gluons and photons). The most stringent experimental bound that these models need to satisfy comes from isocurvature bounds related to CMB measurements. Indeed, since these fields are present during inflation, they can develop isocurvature fluctuations that have been highly constrained by Planck experiment [10]. Indeed, the non-adiabatic fraction in the observed CMB temperature must satisfy:

$$\beta_{iso}(k_0) \equiv \left.\frac{|P_{\mathcal{SS}}|^2}{|P_{\mathcal{SS}}|^2 + |P_{\mathcal{RR}}|^2}\right|_{k_0} < 2.5 \times 10^{-2} \qquad \text{at} \quad 95\%\,\text{CL}\,, \tag{2.51}$$

where $|P_{\mathcal{RR}}|^2$ and $|P_{\mathcal{SS}}|^2$ are the adiabatic and isocurvature power spectra computed at a pivot scale $k_0 = 0.002$ Mpc^{-1}. In case of a single axion that plays the role of spectator field during inflation and has a natural value of the initial misalignment angle, $\Theta_{mi}^2 \sim \mathcal{O}(1)$, this bounds translates to

$$\alpha \simeq \frac{4}{\mathcal{A}_s}\left(\frac{\Omega_\theta}{\Omega_{DM}}\right)^2 \frac{\sigma_\theta^2}{\Theta_{mi}^2}\,, \tag{2.52}$$

where $\mathcal{A}_s$ is the total amount of scalar perturbations, $\sigma_\theta^2 = \left(\frac{H_{inf}}{2\pi f_\theta}\right)^2$ is the expectation value of the axion quantum fluctuations during inflation, while $\Omega_\theta/\Omega_{DM}$ represents the relative abundance of axionic DM. It is easy to see that Eq. (2.52) can be transformed into an upper bound for the inflationary scale of the model.

Being ALPs naturally very light, they can also represent good dark radiation candidates. Indeed, the straightforward way of getting relativistic axions and ALPs is given by direct decay. Focusing on string phenomenology, which will be the main topic of this thesis, a generic prediction of string compactifications is that reheating is driven by the late-time decay of the moduli, Φ. These are scalar fields that arise after dimensional reduction of the six extra dimensions space and will be introduced in Sec. 2.3.3. The typical moduli decay width is:

$$\Gamma \sim \frac{m_\Phi^3}{8\pi M_P^2}\,. \tag{2.53}$$

This leads to a reheating temperature which looks like:

$$T_\gamma \sim T_{reheating} \sim \sqrt{\Gamma M_P} \sim \frac{m_\Phi^{3/2}}{M_P^{1/2}}\,. \tag{2.54}$$

However, on top of SM particles, the moduli decay produces also hidden sector degrees of freedom such as very light ALPs which contribute to the radiation energy density of our universe. Therefore these relativistic ALPs behave as extra neutrino-like degrees of freedom ΔN_{eff} [14] which is defined as:

$$\rho_{rad} = \rho_\gamma + \rho_{rel\,d.o.f.} = \rho_\gamma\Big[1 + \Big(\frac{7}{8}\Big)\Big(\frac{4}{11}\Big)^{4/3}\Big(N_{eff,SM} + \Delta N_{eff}\Big)\Big]\,, \tag{2.55}$$

where ρ_γ is the photon energy density while $\rho_{rel\,d.o.f.}$ denotes the energy density of other relativistic degrees of freedom. The first two terms in the previous equation are related to SM physics, while the third one can be associated with extra ALP dark radiation proportional to ΔN_{eff}. Recent measurements of the Hubble constant H_0 [15] provide the following range of possible values for ΔN_{eff}: $\Delta N_{eff} \sim 0.4 - 1$ at 2σ. This can soften the tension between H_0 measurements of Eq.s (1.47) and (1.46), representing an interesting hint in favour of the existence of ALPs.

Thanks to their weak coupling to all ordinary particles, ALPs produced by direct decay of the moduli fields free-stream to the present days without thermalising and would form today a Cosmic Axion Background (CAB) [16]. The CAB energy density can be easily estimated by noticing that the ALP energy is:

$$E_{axion} = \frac{m_\Phi}{2}\,,$$

where m_Φ is the mass of the decaying modulus Φ. Using the reheating temperature above, we find that the ratio between the energies of ALPs and CMB photons today is:

$$\frac{E_{axion}}{T_\gamma} \sim \left(\frac{M_P}{m_\Phi}\right)^{1/2} \sim 10^6 \left(\frac{10^6 \text{ GeV}}{m_\Phi}\right)^{1/2},$$

where we used the fact that both ALPs and photons redshift as radiation from modulus decay till today. In order to avoid cosmological problems, the moduli need to have masses $m_\Phi \gtrsim 50$ TeV. For moduli masses $m \sim 10^6$ GeV, we have $E_{axion} \sim 10^6\ T_{CMB} \sim 200$ eV. Hence the CAB energy spectrum is expected to be located in the soft X-ray range $E \sim 0.1 - 1$ keV. This could have created, together with Primakoff process in the cluster magnetic field, the soft X-ray excess above the thermal emission of the intra-cluster medium detected from galaxy clusters as Coma [16]. We will discuss an explicit realisation of axionic DM in string theory in Chapter 5. There we describe how to perform a successful global embedding in type IIB string compactifications of the model of [17] for the 3.5 keV line that has been recently observed from galaxy clusters.

Axions as Inflaton Inflationary models are very sensitive to quantum corrections induced by higher dimensional operators that can spoil the flatness of the potential. These corrections can induce $\mathcal{O}(1)$ contributions to the slow-roll parameters, drastically shortening the duration of inflation to few e-foldings. This tells us that inflation is extremely sensitive to UV physics, so symmetries must be found that are able to protect the form of the inflationary potential, forbidding or suppressing the presence of such corrections. These considerations make axion-like particles good inflation candidates: they appear in the theory equipped with a continuous shift symmetry to all orders in perturbation theory, making the axion potential stable against quantum corrections. An extremely important parameter when studying axion inflation is the axion decay constant, f, that sets the magnitude of the least irrelevant shift-symmetric coupling with all the other fields, e.g. the dimension 5 operator that sets the coupling with gauge fields $\frac{\phi}{f} F\tilde{F}$. Moreover in case of embedding in UV complete theories, f sets the cutoff scale of the effective field field theory that should describe axion inflation: we need to integrate out all heavy modes having masses $m > f$. Historically the first model that was proposed is *natural inflation*, were a single axion plays the role on the inflaton, acquiring a mass through non-perturbative corrections. This leads to the following potential:

$$V(\phi) = \Lambda^4 \left[1 + \cos\left(\frac{\phi}{f}\right)\right], \tag{2.56}$$

where $\Lambda \ll M_P$ is the dynamically-generated energy scale of non-perturbative effects and ϕ is the canonically normalised axion. In order to give rise to prolonged

inflation and match experimental data this model requires $f > 10M_p$. Unfortunately, experimental bounds on the relation between scalar spectral index and tensor-to-scalar ratio tend to disfavour the validity of this model[10]. Since the birth of natural inflation, many extensions and other different models have been proposed. We discuss some of them together with their possible embedding in type IIB string theory in Section 2.4.2.

2.3 Type IIB string Phenomenology

The SM and many of its extensions, such as GUT theories or supersymmetric models like the MSSM, can be viewed as effective field theories, i.e. low-energy limits of some more fundamental theory. For instance, SM and GUT theories contain interactions that are not asymptotically free and lead to ultraviolet Landau poles. All these theories present a sick UV behaviour and leave as open problems many of the puzzles related to SM: number of families, flavour physics and others. In particular none of these theories provides a framework where general relativity can be reconciled with quantum field theory. On the other hand, the quantum version of Einstein's gravity is not renormalisable, therefore it should be seen as an effective field theory as well. String theory represents the more promising candidate to merge possible extensions of SM with a quantum theory of gravity that is free of quantum divergences. Indeed string theory provides a theory of gravity that can also describe non-abelian gauge interactions, fundamental scalars, charged chiral fermions appearing in different families and Yukawa couplings, all of which represent the building blocks of the SM.

One of the most revolutionary aspects of string theory is that elementary objects are not described by point-like particles but 1-dimensional strings whose typical length is l_s. Strings can be both open or closed and their dynamics is described by a 2-dimensional surface Σ that is called the *world-sheet*. An important feature of string theory is that l_s is the only free parameter in the theory, this implies that all the other SM parameters must be dynamically determined, drastically reducing the arbitrariness of the theory. The string scale $M_s = 1/l_s$, which represents the typical string interaction energy, can be constrained by particle accelerator experiments: the fact that no string effect has been detected in LHC yet sets a lower bound on M_s. At energy scales well below M_s it is not possible to feel the 1D structure of strings and their theory becomes a quantum field theory of point-like particles. Strings can vibrate and different string oscillations correspond to different particles having different masses, quantum numbers and Lorentz transformation properties. Depending on the number of exited oscillators, each string oscillation corresponds to an infinite tower of particles having different masses where the mass step is given by M_s.

In all string theories the quantisation procedure predicts the presence of a spin-2 particle in the closed string massless spectrum. This particle interacts as a graviton and its dynamics is invariant under the re-parametrisation of the space-time coordinates. Therefore string theory automatically incorporates a quantum version of gravity and provides a natural cutoff l_s that removes the UV divergences which appear in the straightforward quantisation of general relativity.

The building blocks of string theory are 2-dimensional bosons and fermions, $X^M(\tau,\sigma)$ and $\psi^M(\tau,\sigma)$, that represent the bosonic and fermionic coordinates of the string in a D-dimensional space-time, $M = 0,\ldots,D-1$. In particular $X^M(\tau,\sigma)$ represents the embedding of a 2-dimensional surface inside a D-dimensional space-time. Each point of the world-sheet is identified by two coordinates, τ and σ, that represent the time and the spatial extension of the string respectively. The motion of closed strings produces world-sheets with no boundary while open string world-sheets have boundaries. In order to point out some other features of string theory, let us write down the Polyakov action for a bosonic string [18, 19]:

$$S_P = -\frac{T}{2}\int_\Sigma d^2x\sqrt{-g}\, g^{ab}(\tau,\sigma)\,\partial_a X^M(\tau,\sigma)\,\partial_b X^N(\tau,\sigma)\,\eta_{MN} \tag{2.57}$$

where $T = 1/2\pi\alpha' = 2\pi/l_s^2$ is the string tension, g_{ab} is the world-sheet metric while η_{MN} is the D-dimensional Minkowski metric. This action shows different symmetries and some of them turn out to be redundancies that must be removed from the theory. In addition to D-dimensional Lorentz invariance, we have symmetries related to local invariance under local world-sheet coordinate re-parametrisation and rescaling (Weyl invariance). Since there are no graviton polarisation modes in 2-dimensions, the metric g_{ab} turns out to be trivial. Moreover, imposing invariance under local coordinate reparametrisation it turns out that the only physical oscillation modes are those transverse to the world-sheet plane. The resulting theory is then a 2-dimensional quantum field theory of $D-2$ non-interacting massless scalar fields on the world-sheet and the space of harmonic oscillators related to string oscillations represents the spectrum of space-time particles in string theory. The massless bosonic spectrum of closed and open strings contains the graviton, G_{MN}, an antisymmetric tensor B_{MN}, the dilaton ϕ and a gauge boson A_M. The dilaton ϕ is a scalar field whose vev is related to the string coupling constant as $g_s = e^{\langle\phi\rangle}$. If the dynamics allows for $g_s \ll 1$ we can treat string theory perturbatively. Indeed, despite the 2-dimensional world-sheet is non-interacting, we have non trivial interactions in the space-time theory and g_s represents the loop counting parameter. String scattering amplitude between asymptotic states in the perturbative regime can be computed similarly to QFT theories: they are computing using a path integral summing over all possible world-sheets (with different geometries) that interpolate between asymptotic states in the external legs. Indeed,

since the interacting objects are 1-dimensional the usual Feynman diagrams are replaced by scattering surfaces: world-sheets. If the interaction involves only closed strings, the perturbative expansion runs over surfaces showing different number of loops (handles) while in presence of open string external states we may have that world-sheets present boundaries. Each term in the perturbative expansion is characterised by a number of handles and boundaries, h and n_b, and is weighted by g_s^χ where

$$\chi = 2 - 2h - n_b \,. \tag{2.58}$$

is the genus or Euler characteristic of the world-sheet.

Knowing the massless spectrum of the bosonic string, we can extend the Polyakov action including background profiles for the massless excitations. This is known as 2-dimensional σ-model and its action is given by:

$$\begin{aligned} S_\sigma = -\tfrac{T}{2}\int_\sigma dx^2\sqrt{-g} \;\; & \left[\left(g^{ab}G_{MN}(X) + \epsilon^{ab}B_{MN}(X)\right)\partial_a X^M\,\partial_b X^N \right. \\ & \left. +\alpha'\phi R(g)\right] + \int_{\partial\Sigma} d\xi^a A_M(X)\partial_a X^M \end{aligned} \tag{2.59}$$

where ϵ^{ab} is the antisymmetric Levi-Civita tensor and $R(g)$ is the scalar curvature of the world-sheet metric. This action describes an interacting 2-dimensional field theory where the scalar fields parametrise the non trivial curved space. Indeed the background metric in the first term can be regarded as a superposition of a large number of graviton string states. The second term does not depend on the world-sheet metric, it is purely topological and tells us that the strings are charged under the field $B_2 = \frac{1}{2}B_{MN}\,dX^M \wedge dX^N$. The third term corresponds to the 2-dimensional Einstein Hilbert action for g_{ab} and the fourth term, that applies only to theories including open strings, sets the coupling between the string world-sheet and the background of the massless gauge boson A_M. This interacting theory may be studied perturbatively if the gradients associated background fields are small and when all curvatures are small in string units.

Thus string theory in a general background shows two perturbative expansions: the genus expansion, parametrised by g_s, that sums over all the possible topologies of the world-sheet connecting initial and final states and the α' expansion, whose expansion parameter is the curvature of the D-space-time in units of α', that for each world-sheet controls the appearance of higher dimensional operators related to the space-time curvature.

One of the most important properties of string theory is that the scattering amplitudes of the theory are unitary and finite order by order in perturbation theory. The scattering amplitudes show a well-behaved UV regime thanks to the natural cutoff scale M_s. Indeed, since the theory is characterised by Weyl symmetry and the vertices are delocalised, in case of large momentum transfer

$\gtrsim M_s$ it is possible to exchange long string states and the UV regime can be interpreted as the IR limit of a new diagram involving a dual channel. The tower of massive string modes acts as a UV regulator but the properties and the number of the massive string states depends on the number of space-time dimensions in which strings can oscillate. Requiring that UV divergences are appropriately cutoff we can fix the number of space-time dimensions to be equal to the *critical dimension* that can be found imposing that the quantum version of Weyl symmetry is not anomalous. For the bosonic string the critical dimension is $D = 26$.

In order to have fermionic degrees of freedom in the theory, we need to introduce a generalisation of the Polyakov action that shows a 2-dimensional supersymmetry on the world-sheet: superstring theory. This introduces a set of fermionic fields ψ^M that are superpartners of X^M but transforms as vectors under the space-time Lorentz group. Moreover, we have a supersymmetric partner of g_{ab} that is the world-sheet gravitino ψ_a. Superstring theory keeps the main properties of the Polyakov action that we described earlier in this section. On the other hand the field content changes: we have a 2-dimensional quantum field theory of $D-2$ free massless scalar fields and fermions and the critical dimension for superstring theory is $D = 10$. The action for the world-sheet fermions does not completely determine the space-time spectrum of the theory. Since 2-dimensional observables are quadratic in the fermion fields we can choose different fermionic boundary conditions on the world-sheet defining different sectors:

- Ramond sector: $\psi^M_\pm(\tau, \sigma + l_s) = \psi^M_\pm(\tau, \sigma)$
- Neveu-Schwarz sector: $\psi^M_\pm(\tau, \sigma + l_s) = -\psi^M_\pm(\tau, \sigma)$

where $\psi_\pm$ denote left and right movers respectively and $\psi^M \equiv \begin{pmatrix} \psi^M_- \\ \psi^M_+ \end{pmatrix}$. The choice of periodic or anti-periodic boundary conditions for fermions can be made for left and right movers independently so there are 4 possible sectors: NS-NS, R-R, NS-R, R-NS. The 10 dimensional EFT describing the interaction of the massless states of the superstring contains space-time bosons coming from NS-NS and R-R sectors and space-time fermions coming from NS-R and R-NS sectors. The construction of a consistent closed string theory with space-time fermions requires the sectors related to left and right movers to be glued together in a way that preserves modular invariance of the partition function. This step is called GSO projection and has to be done independently for NS-R and R-NS sectors. Choosing the same GSO projection for the two sectors leads to *type IIB string theory* whose low energy phenomenology will be the focus of the present work. This theory has a chiral spectrum, it contains only closed strings and since NS-R and R-NS sectors have the same spectrum it enjoys a world-sheet parity symmetry. The NS-NS sector contains the dilaton ϕ, the graviton G_{MN}, and a 2D symmetric form B_{MN}.

The R-R sector contains 0-, 2- and 4-forms: C_0, C_{MN} and C_{MNPQ}. Type IIB string theory contains two gravitinos and two dilatinos with same chirality and the massless spectrum features a ten-dimensional $\mathcal{N} = (2,0)$ supersymmetry.

Four other consistent superstring theories are known [20, 21]: *type IIA string theory*, $SO(32)$ and $E_8 \times E_8$ *heterotic string theories* and *type I string theory*. The five superstring theories are related to each other by dualities and can be interpreted as different limits of the same underlying theory: *M-theory* [22].

At energies well below M_s massive string modes cannot be exited and each superstring theory is described by a 10-dimensional supergravity theory. Focusing on the bosonic sector of type IIB string theory, the effective action can be decomposed into NS-NS, R-R, and Chern-Simon (CS) terms

$$S_{IIB} = S_{NSNS} + S_{RR} + S_{CS}\,. \tag{2.60}$$

The first contribution contains the space-time metric, the dilaton and the Kalb-Ramond two form B_2 [20, 21]:

$$S_{NSNS} = \frac{1}{2\kappa_{10}^2}\int dX^{10}\sqrt{-G}e^{-2\phi}\left(\boldsymbol{R}*\mathbf{1} + 4\partial_M\Phi\partial^M\Phi - \frac{1}{2}H_3\wedge *H_3\right)\,, \tag{2.61}$$

where $*$ stands for the Hodge operator, $\kappa_{10} = 8\pi^{7/2}\alpha'^2 = l_s^8/(4\pi)$ represents the 10-dimensional Newton constant and the three-form $H_3 = dB_2$ is the field strength related to B_2. The R-R and CS contribution additionally contains, C_0, C_2 and C_4 that are zero-, two- and four-forms respectively. They are given by

$$S_{RR} = -\frac{1}{4\kappa_{10}^2}\int d^{10}X\sqrt{-G}\sum_{p=1,3,5}\frac{1}{p!}F_p\wedge *F_p\,, \tag{2.62}$$

$$S_{CS} = -\frac{1}{4\kappa_{10}^2}\int C_4\wedge H_3\wedge F_3\,, \tag{2.63}$$

where

$$\begin{aligned} F_p &= \hat{F}_p - \textstyle\sum_{j=p-3,j>0} H_3\wedge C_j\,,\\ \hat{F}_p &= dC_{p-1}\,. \end{aligned} \tag{2.64}$$

F_p form fields are also called *fluxes* and the 5-form F_5 additionally satisfies the self-duality condition $F_5 = *_{10}\tilde{F}_5$. This 10d supergravity action is invariant under the following transformation for form fields

$$B_2 \to B_2 + d\lambda_1\,, \qquad C_p \to C_p + d\lambda_{p-1} - H_3\wedge\lambda_{p-3}\,, \tag{2.65}$$

where λ_k is a 10-dimensional k-form.

In the following sections we try to briefly sum up how to get 4D effective field theories from type IIB string theory. As we saw, in addition to the usual 4D space-time $\mathbb{R}^{1,3}$, string theory requires the existence of 6 extra spatial dimensions. In order to be able to separate the extra dimensions contribution from the low energy theory we need to require that these dimensions are compact and of very small size. Compactification of these dimensions is the way to link the 10D EFT of the massless string degrees of freedom with the low-energy physics of our real 4D world below the KK scale. One of the fundamental tasks of string phenomenology is to find a compactification whose low-energy EFT reproduces a suitable extension of the SM [20, 23]. The space-time manifold is decomposed as $\mathbb{R}^{1,3} \times Y_6$, where Y_6 is a compact 6D manifold.

The compactification is usually demanded to yield a $N = 1$ supersymmetric EFT that can describe chiral matter in 4D and the supersymmetry breaking scale is supposed to be low with respect to the KK scale in order to solve the Higgs hierarchy problem via low-energy supersymmetry. In addition a supersymmetric EFT simplifies the calculations thanks, for example, to the holomorphy of the superpotential and its non-renormalisation properties. If the 4D EFT is required to be a N=1 supergravity theory, Y_6 is forced to be a 'Calabi-Yau' space. This constraint put some limitations in model building but still allows for some freedom. Indeed, since the number of Calabi-Yau manifolds is in the order of 10^6, it is possible to choose among a huge number of compactification spaces. Given that the content of particles and forces of the resulting theory are determined by the topology of the extra dimensions, different theories arise from different choices of Y_6.

The generic properties of string compactifications are:

- Moduli fields which parametrise the size and the shape of the extra dimensions and correspond to uncharged 4D scalars;
- Antisymmetric tensors of different ranks which imply the existence of axion fields. It is also possible to turn on their fluxes in the extra dimensions giving rise to masses for the moduli. Moreover D-branes can couple to them and can host the SM;
- Chiral matter fields which appear as open string modes on stacks of D-branes.

In addition in order to study 4D models in the context of type IIB string compactification, two general approaches have been used so far:

- *Global string models*: This is a *top-down* approach where 10D string theory is compactified on 6D manifolds. The theory must be consistent at the global level. Gauge and matter fields live on D7-branes wrapped around internal

4-cycles or on D3-branes at singularities. Closed string moduli live instead in the bulk. A crucial issue to be addressed in these constructions is moduli stabilisation which is the process through which moduli become massive.

- *Local string models*: This is a *bottom-up* approach where one focuses on the detailed phenomenology of D-brane constructions in order to reproduce SM physics. The global aspects of the compactification are decoupled and the moduli are assumed to be stabilised by some unknown bulk dynamics. Eventually the configuration taken into account has to be embedded in a fully consistent global model. Even if a globally consistent compactification is more satisfactory, local configurations of D3- and D7-branes may be more efficient in trying to identify promising string vacua which can reproduce all the features of the SM independent of the details of the global theory.

Starting from Part II, we will mainly use the bottom-up approach, focusing on models that can give rise to a successful inflationary dynamics. In the rest of this section we outline the main ingredients that are needed to build realistic 4D models starting from 10D type IIB string theory.

2.3.1 Dp-branes

Dp-branes [24] are extended solitonic objects with p spatial dimensions that can appear in string theory and are charged under the gauge symmetries of R-R fields:

$$S_{CS} = \mu_p \int_{\Sigma_{p+1}} C_{p+1} \tag{2.66}$$

where μ_p is the electric charge of the brane and Σ_{p+1} is the brane world-volume. One of the most important aspects of Dp-brane is that open strings can end on their surfaces, their ending point satisfying Dirichlet conditions in the directions transverse to the brane surface and Neumann boundary conditions in the directions along the brane surface. This means that string edges cannot leave the brane but they can freely slide along the brane. These objects have p spatial dimensions and and have to fill 4-dimensional space-time in order not to break Poincarè invariance. Each Dp-brane comes with a $U(1)$ gauge theory that lives on its world-volume. Indeed the quantisation of the open strings ending on a single brane give rise to a massless spectrum containing scalar fields parametrising the Dp-brane position, ζ_a, a world-volume gauge field A_a with field strength F_{ab} and their supersymmetric partners. In order to understand the interactions between the light fields living on the Dp-brane and the background solution of type IIB string theory, let us write the Dirac-Born-Infeld (DBI) action:

$$S_{DBI} = -g_s T_p \int_{\sigma_{p+1}} d^{p+1}x e^{-\phi} \sqrt{-det\left(G_{ab} + \mathcal{F}_{ab}\right)} \tag{2.67}$$

where $T_p = \left[(2\pi)^p g_s (\alpha')^{(p+1)/2}\right]^{-1}$ is the brane tension, $G_{ab} = \frac{\partial X^M}{\partial x^a}\frac{\partial X^N}{\partial x^b} G_{MN}$ is the pull-back of the space-time metric onto the D-brane world-volume, $\mathcal{F}_{ab} = B_{ab} + 2\pi\alpha' F_{ab}$ is the gauge invariant field strength and B_{ab} is the pull-back of B_{MN} onto the brane world-volume. This action represents the combination between the generalisation of Polyakov actions and Maxwell's electromagnetism to higher dimensional objects. On the other hand the generalisation of CS action in presence of space-time and D-brane background fields becomes

$$S_{CS} = i\mu_p \sum_{n=0,2,4} \int_{\Sigma_{p+1}} C_n \wedge e^{\mathcal{F}} \,. \tag{2.68}$$

Stable Dp-branes are BPS objects that preserve half of the space-time symmetries. In order to preserve N=1 supersymmetry the brane tension must be equal to its RR-charge in appropriate units so that: $\mu_p = g_s T_p$. Adding the brane action to the type IIB bulk action may not vary the form of the 4D EFT theory that arises after KK reduction, but it always affects the definition of the 4-dimensional chiral coordinates and therefore the shape of Kähler potential and superpotential [25, 26]. In type IIB string theory we can have D3- and D7-branes. The presence of Dp-branes adds to the 4-dimensional spectrum p gauge neutral scalar moduli ζ^i that parametrise the the position of the Dp-brane and possible deformations of the extra dimension cycle wrapped by the brane. In case of D7-branes we have other field contributions coming from the 8-dimensional world-volume gauge field that give rise to a 4-dimensional $U(1)$ gauge field A_μ and to Wilson line moduli a_α.

As previously mentioned, the discovery of Dp-branes played a crucial role in type IIB string model building since their presence allows to have chiral matter in the 4D spectrum coming from open strings that live on the branes. Moreover they allow to reproduce gauge theories with chiral matter in localised areas of the spatial dimensions, thus decoupling the gauge theory form the details of the whole compact space. This enriches the model building landscape without providing additional problems to the compactification procedure.

2.3.2 String compactification and Calabi-Yau manifolds

In what follow we assume for simplicity that the 10-dimensional space-time $\mathcal{M}_{10}$ of superstring theory can be factorised as $\mathcal{M}_4 \times Y_6$ where $\mathcal{M}_4$ is the usual 4-dimensional space-time and Y_6 is the compact manifold associated to the extra dimensions:

$$\mathcal{M}_{10} = \mathcal{M}_4 \times Y_6 \tag{2.69}$$

this is called compactification of string theory. Let us first consider possible vacuum configurations that can lead to the description of 4D effective field theory. A

suitable ansatz for the metric decomposition in absence of energy sources is given by [1]

$$G_{MN}dX^M dX^N = \eta_{\mu\nu}dx^\mu dx^\nu + g_{mn}dy^n dy^m \tag{2.71}$$

where g_{mn} and y^m, $m = 1, \dots 6$ are the metric and the coordinates on Y_6. Such a decomposition is a valid vacuum solution if and only if the 10D metric solves the 10D Einstein equations. This requires that both $\mathcal{M}_4$ and Y_6 are Ricci flat manifolds, i.e. $R_{\mu\nu} = R_{mn} = 0$. A general class extra dimensions manifolds that satisfies this requirement is given by Calabi-Yau manifolds that we briefly introduce below.

For a general compactification manifold we have that the 10D Lorentz group decomposes into

$$SO(1,9) \to SO(1,3) \times SO(6)\,. \tag{2.72}$$

In order to study stable compactifications that do not contain tachyons and show a simple theoretical treatment we want to consider string compactifications that preserve a non-vanishing number of supersymmetries in 4 dimensions. This condition relies on the geometrical properties of Y_6. Indeed, the number of conserved supersymmetries in 4D is equivalent to the number of 6-dimensional spinors in Y_6, called Killing spinors, $\xi(y^m)$, that satisfy:

$$\nabla_{Y_6}\xi(y^m) = 0 \tag{2.73}$$

where $\nabla_{Y_6} = \partial_m + \frac{1}{4}\omega_m^{AB}\Gamma^{AB}$, ω_m^{AB} is the spin connection and Γ^{AB} is the generator of the spinor representation of SO(6). Indeed in type IIB string theory the 10D space-time has a set of 32 local 10D supercharges that transform as spinors of $SO(1,9)$. The number of supersymmetries in 4D is equal to the number of global supercharges of Y_6: being Y_6 a curved space, parallel transport would transform local supercharges under $SO(6)$ but, if Eq. (2.73) is satisfied, parallel transport of the spinor on a closed path does not rotate it , the spinor is covariantly constant in Y_6 and we have a global supercharge in Y_6.

This condition can be rephrased in terms of the holonomy group of Y_6. The group generated by all possible spinor rotations along closed paths in Y_6 defines the holonomy group of Y_6. The spinor decomposition induced by space-time splitting of Eq. (2.72) is given by:

$$\mathbf{16} \to (\mathbf{2},\mathbf{4}) \oplus (\bar{\mathbf{2}},\bar{\mathbf{4}}) \tag{2.74}$$

[1] It is important to notice that in concrete models the 10D metric does not represent the vacuum solution given in Eq. (2.71) and more general decompositions of space-time must be taken into account, e.g.

$$G_{MN}dX^m dX^N = e^{2A(y)}g_{\mu\nu}dx^\mu dx^\nu + e^{-2A(y)}g_{mn}dy^m dy^n \tag{2.70}$$

where $A(y)$ is called the warp factor and is a function of the extra dimensions coordinates. For instance this form may arise when we consider the presence of branes or background fluxes.

where $\mathbf{4}$ and $\bar{\mathbf{4}}$ are 6D Weyl spinors transforming under SO(6) while $\mathbf{2}$ and $\bar{\mathbf{2}}$ are 4D are the usual Weyl spinors transforming under $SL(2,\mathbb{C})$. For general extra-dimensions manifold the holonomy group is $SO(6)$ and no supersymmetry is preserved in 4D. Therefore we will be interested in finding Y_6 so that its holonomy group is a subgroup of $SO(6)$ that induces a decomposition of $\mathbf{4}$ that contains a singlet: a nowhere vanishing and globally well defined invariant spinor. This request is satisfied for instance by manifolds with holonomy group $SU(3) \subset SO(6)$ that preserve $\mathcal{N} = 1$ supersymmetry in 4 dimension. In this case the chiral 10D spinor is decomposed by space-time splitting and then by compactification into

$$\begin{array}{ccccc} SO(1,9) & \to & SO(6) \times SO(1,3) & \to & SU(3) \times SO(1,3) \\ \mathbf{16} & \to & (\mathbf{2},\mathbf{4}) \oplus (\bar{\mathbf{2}},\bar{\mathbf{4}}) & \to & (\mathbf{3},\mathbf{2}) \oplus (\bar{\mathbf{3}},\mathbf{2'}) \oplus (\mathbf{1},\mathbf{2}) \oplus (\mathbf{1},\mathbf{2'}) \end{array} \tag{2.75}$$

where $\mathbf{2}$ and $\mathbf{2'}$ represent left and right chiral spinors in 4d. Choices of Y_6 with smaller holonomy group lead to $\mathcal{N} > 1$ 4D supersymmetry. In type IIB, having $SU(3)$ holonomy group in the extra dimensions manifold leads to $\mathcal{N} = 2$ supersymmetries in 4 dimension. There is a wide class of manifold having $SU(N)$ holonomy group, that id called *Calabi-Yau manifolds*. These are N-dimensional complex and Kähler manifolds with vanishing first Chern class (Ricci flat). A complex N-dimensional manifold admits a (possibly non unique) globally defined *complex structure* that is a mixed tensor I_n^m satisfying $I_m^n I_n^p = -\delta_m^p$. This tensor can be used to define a local set of complex coordinates $dz^i = dx^i + iI_i^j dy^j$ starting from 2 sets of N real coordinates, dx^i and dy^i. Starting from a complex manifold we can find a metric that shows only mixed components $g_{i\bar{j}}$ through which we can define the following 2-form j

$$J = g_{i\bar{j}} dz^i d\bar{z}^j \tag{2.76}$$

If J is a closed form $dJ = 0$, the manifold is Kähler and J is called the Kähler form. Kähler manifolds are characterised by having at most $U(N)$ holonomy since parallel transport does not allow to mix holomorphic and anti-holomorphic coordinates. Imposing vanishing first Chern class further reduces holonomy group from $U(N) \simeq SU(N) \times U(1)$ to $SU(N)$. The number of Calabi-Yau (CY) manifold is of order $\mathcal{O}(10^6)$ and each of them defines a different vacuum theory, with different coupling constants, Yukawa couplings and energy scale hierarchy. This makes bottom-up model building highly non trivial and the best strategy to adopt is to find those phenomenological properties that are shared by a large number of compactifications. In order to do this, let us start by computing the number of degrees of freedom in a given CY three-fold. Since in Y_6 harmonic forms are in one-to one correspondence with the elements of the Dolbenault cohomology group, the number of possible choices in determining the $SU(N)$ holonomy metric can be easily computed. Indeed, the 3-cohomology group in a complex three-fold is given

by

$$H^3(Y_6) = H^{(3,0)}(Y_6) \oplus H^{(2,1)}(Y_6) \oplus H^{(1,2)}(Y_6) \oplus H^{(0,3)}(Y_6) \tag{2.77}$$

where $H^{(p,q)}$ are cohomology groups: the set of closed $(p,q)-$forms, having p holomorphic and q anti-holomorphic differentials, quotiented out by the number of exact $(p,q)-$forms. The dimensions of $H^{(p,q)}$ are topological invariants that are known as *Hodge numbers*, $h^{p,q} = \dim H^{(p,q)}(Y_6)$. Their sum gives the number of free parameters of a given $SU(3)$ holonomy metric related to a given CY manifold. Hodge numbers are usually arranged into the so called Hodge diamond

$$\begin{array}{ccccccc} & & h_{0,0} & & & & \\ & h_{1,0} & & h_{0,1} & & & \\ h_{2,0} & & h_{1,1} & & h_{0,2} & & \\ h_{3,0} & & h_{2,1} & & h_{1,2} & & h_{0,3} \\ & h_{3,1} & & h_{2,2} & & h_{1,3} & \\ & & h_{3,2} & & h_{2,3} & & \\ & & & h_{3,3} & & & \end{array} = \begin{array}{ccccccc} & & 1 & & & & \\ & 0 & & 0 & & & \\ 0 & & h_{1,1} & & 0 & & \\ 1 & & h_{2,1} & & h_{1,2} & & 1 \\ & 0 & & h_{2,2} & & 0 & \\ & & 0 & & 0 & & \\ & & & 1 & & & \end{array} . \tag{2.78}$$

that makes it easier to detect possible symmetries in Y_6 through line reflections in the diamond: complex conjugation (central vertical axis reflection), Hodge duality (central horizontal axis reflection) and mirror symmetry (diagonal axes reflection)[27].

From Eq. (2.78) we immediately see that the cohomology of a CY manifold is characterised by specifying the Hodge numbers $h_{1,1}$ and $h_{1,2}$. In addition, there is a single $(3,0)-$form, that we denote as $\Omega = \Omega_{ijk} dz^i dz^j dz^k$, which is nowhere vanishing and defines the complex structure of the CY. Since there are no harmonic 1- and 5-forms we have that $\Omega \wedge J = 0$. Moreover, being $h_{3,3} = 1$ we have that $J \wedge J \wedge J$ must be proportional to $\Omega \wedge \bar{\Omega}$. We briefly summarise their relation in the following lines. We already saw that $SU(3)$ holonomy in Y_6 corresponds to the existence of a 6-dimensional covariantly constant spinor in Y_6. Therefore there should be a bijection between the space of Y_6 metrics G_{Y_6} and spinors ξ and the space of possible complex structures Ω and Kähler metrics J

$$(G_{Y_6}, \xi) \leftrightarrow (\Omega, J) . \tag{2.79}$$

This map is given by

$$J_{i\bar{j}} = -i\xi^\dagger \Gamma_i \Gamma_{\bar{j}} \xi , \qquad \Omega_{ijk} = \xi^T \Gamma_i \Gamma_j \Gamma_k \xi , \tag{2.80}$$

where Γ_i are Dirac matrices. From certain properties of the Dirac matrices called Fierz identities we discover that

$$J \wedge J \wedge J = \frac{3i}{4}\Omega \wedge \bar{\Omega}\,. \tag{2.81}$$

The topological invariants, $h_{i,j}$ that are needed in order to uniquely determine the CY structure are tightly related to the field content in 4D. Indeed their value corresponds to the number of 4D scalar fields that appear after dimensional reduction, these are called moduli fields.

2.3.3 Moduli fields

As explained in the previous section, imposing $SU(3)$ holonomy in the extra dimensions manifold leads to Calabi-Yau manifolds. Nevertheless we saw that a CYs are a class of manifolds characterised by two free parameters, i.e. the Hodge numbers $h_{1,1}$ and $h_{1,2}$, that need to be specified in order to uniquely identify the geometry of extra dimensions. These parameters are tightly linked to the number of continuous background metric deformations that preserve supersymmetry and topology. These deformations can be interpreted as scalar fields in 4D and are called *moduli fields* [28].

The assumption of 10D compactification of Eq. (2.69) tells us that the Fourier transform of a 10D scalar field ϕ is given by

$$\phi(X^M) = \sum_{\boldsymbol{k}} \phi_6^{\boldsymbol{k}}(y^m)\phi_4^{\boldsymbol{k}}(x^\mu) \tag{2.82}$$

where $\phi_6^{\boldsymbol{k}}(y^m)$ are eigenfunctions of the six-dimensional laplacian of Y_6, Δ_{Y_6}, having eigenvalues $-\lambda^{(\boldsymbol{k})}$ (eigenvalues are negative for compact manifolds). If ϕ is massless in 10D, given that $\Box_{10} = \Delta_{Y_6} + \Box_4$, we have the following equation of motion for the 4D ϕ_4 field

$$\left(\Box_4 - \lambda^{(\boldsymbol{k})}\right)\phi_4^{\boldsymbol{k}}(x^\mu) = 0\,. \tag{2.83}$$

The eigenvalues of Δ_{Y_6} can be interpreted as masses of the 4D scalar fields. In particular, we see that each massless scalar field in 4D correspond to a harmonic form on Y_6, i.e. zero mode of Δ_{Y_6}. Given that there is a one-to-one correspondence between harmonic forms and the Dolbeault cohomology groups $H^{(p,q)}(Y_6)$, we immediately see that a Calabi-Yau compactification will give rise to $h_{1,1} + h_{1,2}$ massless moduli fields in 4D. The properties and the structure of these fields can be found analysing Y_6 metric deformations:

$$g_{m\bar{n}} \to g_{m\bar{n}} + \delta g_{m\bar{n}} \tag{2.84}$$

that preserve the Ricci-flatness condition

$$R_{m\bar{n}}(g_{m\bar{n}} + \delta g_{m\bar{n}}) = 0\,. \tag{2.85}$$

This requirement leads to differential equations for $\delta g_{m\bar{n}}$. Being CYs Kähler manifolds, the equations for mixed and pure components, $\delta g_{m\bar{n}}$ and δg_{mn}, decouple and can be studied separately.

- **Kähler moduli from** $\delta g_{n\bar{m}}$:
  The conservation of Ricci-flatness gives the following constraint

  $$\Delta \delta g_{n\bar{m}} = 0 \tag{2.86}$$

  which means that $\delta g_{n\bar{m}}$ must be a harmonic (1,1)-form. These deformations are closely related to deformations of the Kähler form

  $$J = -i g_{g\bar{n}} dy^m \wedge dy^{\bar{m}} \tag{2.87}$$

  and expanding J on a basis of $h_{1,1}$ (1,1)-harmonic forms $(\hat{D}_i)_{m\bar{n}}$ composing $H^{(1,1)}$ we get

  $$J = t^i (\hat{D}_i)_{m\bar{n}} \qquad i = 1, \ldots, h_{1,1} \tag{2.88}$$

  where t^i are called Kähler moduli and they can be interpreted as fields that control the size of the internal 2-cycles of Y_6. Since we want the perturbed metric to be positive definite we need to impose the following conditions:

  $$\int_\gamma J > 0\,, \qquad \int_\sigma J \wedge J > 0\,, \qquad \int_{Y_6} J \wedge J \wedge J > 0\,, \tag{2.89}$$

  for all complex curves γ and surfaces σ on the CY Y_6. In particular we have that the overall volume of the extra dimension manifold Y_6 is given by:

  $$\mathrm{Vol}(Y_6) = \frac{1}{3!}\int_{Y_6} J \wedge J \wedge J = \frac{1}{3!} t^i t^j t^k k_{ijk}\,. \tag{2.90}$$

  where $k_{ijk} = \int_{CY}(\hat{D}_i \wedge \hat{D}_j \wedge \hat{D}_k)$ are called intersection numbers. The conditions in Eq. (2.89) define the allowed Kähler moduli space that is also called Kähler cone: $\mathcal{M}^K_{h_{1,1}}$. In type IIB concrete model building the moduli space is usually complexified and J receives contributions coming from R-R sector 4-form C_4.

- **Complex structure moduli from** δg_{nm}:
  The conservation of Ricci-flatness gives the following constraint

  $$\Delta \delta g_{nm} = 0 \tag{2.91}$$

that implies that the allowed deformations are given by (2,0)-harmonic forms. We cannot expand δg_{nm} in such a basis since $h_{2,0} = h_{0,2} = 0$ in a CY manifold. On the other hand we can construct a (2,1)-form contracting Ω with the complex structure tensor, $\Omega_{ij\bar{k}} = \Omega_{ijl} I^l_{\bar{k}}$. This allows us to construct a one-to-one correspondence between (1,2)-forms and (2,0)-forms in the following way: we introduce a basis for (1,2)-forms of $H^{1,2}(Y_6)$, $(\chi_\alpha)_{i\bar{j}\bar{k}}$ where $\alpha = 1, \ldots, h_{1,2}$ and we decompose the metric perturbations as

$$\delta g_{ij} = \frac{i}{||\Omega||^2} U^\alpha \, (\bar{\chi}_\alpha)_{i\bar{k}\bar{l}} \Omega^{\bar{k}\bar{l}}_j \tag{2.92}$$

where $||\Omega||^2 = \Omega_{ijk}\Omega^{ijk}/3!$ and U^α are free parameters that are called complex structure moduli. These fields parametrise the sizes of internal 3-cycles and are related to deformations of the complex structure. We refer to the space of complex structure moduli as $\mathcal{M}^{cs}_{h_{1,2}}$.

At tree-level the space of moduli fields can de decomposed as

$$\mathcal{M} = \mathcal{M}^K_{h_{1,1}} \times \mathcal{M}^{cs}_{h_{1,2}} \, . \tag{2.93}$$

where the sub-index is referred to the space dimensionality. As already stated, moduli correspond to massless scalar fields in 4D and in order not to give rise to undetected fifth forces we will need to provide them a mass. This process goes under the name of *moduli stabilisation* and it is discussed in Sec. 2.3.8.

2.3.4 $\mathcal{N} = 2$ 4D supergravity

In this section we describe the 4D effective field theory that can be obtained starting from the $\mathcal{N} = 2$ ten-dimensional supergravity theory in type IIB given by Eq.s (2.60), (2.61), (2.62) , (2.63). We are going to give the results of string compactifications on a Calabi-Yau manifold,[18, 29, 30, 31]. As we already saw CY compactifications preserve the number of supersymmetries so through dimensional reduction we get a supergravity theory with $\mathcal{N} = 2$ (8 supercharges) in 4 dimensions. Despite this theory is not suitable for doing 4D phenomenology since it does not allow for the presence of chiral matter, it lays the foundation for realistic 4D theories that we will study in the next section.

The Ricci-flatness condition of CY manifolds allows to perform a Kaluza-Klein reduction of the 10D fields. This is done expanding each 10D field into eigenforms on Y_6 and keeping only the 0 modes. In order to be sure of the validity of this step, we need to be sure that the energy scale of physical phenomena appearing in the 4D theory is much lower than the KK energy scale. If the compactification manifold is isotropic the mass of KK modes is given by $m_n \sim nM_s/R = mM_P/\mathcal{V}^{2/3}$ where

R is the typical size of the extra dimensions $R = \mathcal{V}^{1/6}$ and $\mathcal{V}$ is the CY volume in string length. The 4D effective theory will be valid only at energies

$$E \ll M_{KK} \sim \frac{M_p}{\mathcal{V}^{2/3}}\,. \tag{2.94}$$

The reduction of the 10D theory gives rise to the following spectrum in 4 dimensions[2]. The reduction of the metric produces the 4 dimensional metric $g_{\mu\nu}$, $h_{1,1}$ Kähler moduli, $h_{1,2}$ complex structure moduli and a 1-form V^0 that is called the gravi-photon. From the NS-NS sector we get $h_{1,1}$ scalar fields, the dilaton ϕ and a 4D 2-form $B_2(x)$. Indeed, counting the number of degrees of freedom in the dimensional reduction we get:

Components	Degeneracy
$B_{\mu\nu}$	$h_{0,0} = 1$
$B_{\mu n}$	$h_{1,0} + h_{0,1} = 0$
B_{mn}	$h_{2,0} + h_{0,2} + h_{1,1} = h_{1,1}$

(2.95)

we can recast these degrees of freedom in a single 4D field as:

$$\phi = \phi(x)\,, \qquad B_2 = B_2(x) + b^i \hat{D}_i \qquad i = 1, \ldots, h_{1,1} \tag{2.96}$$

where again $\hat{D}_i$ represent a base of $H^{(1,1)}(Y_6)$. Through a similar decomposition procedure, we get the following forms from the NS-NS sector:

$$\begin{aligned} C_0 &= C_0(x)\,, \\ C_2 &= C_2(x) + c^i(x)\hat{D}_i\,, \qquad i = 1, \ldots, h_{1,1}\,, \\ C_4 &= V^a(x) \wedge \alpha_a + \rho_i(x)\tilde{D}^i\,, \quad a = 1, \ldots, h_{1,2} \end{aligned} \tag{2.97}$$

where C_0, c^i and ρ_i are scalar fields, V^a are 1-forms while $C_2(x)$ is a 2-form. $\hat{\tilde{D}}^i$ is the dual basis of $\hat{D}_i$ and α_a belongs to the the simplectic basis of $H^3(Y_6)$, (α_a, β^a), that satisfies

$$\int_{Y_6} \alpha_a \wedge \beta^b = \delta_a^b\,, \qquad \int_{Y_6} \alpha_a \wedge \alpha_b = \int_{Y_6} \beta^a \wedge \beta^b = 0\,. \tag{2.98}$$

In the expression for C_4 we used the fact that the field strength related to C_4 has to be self-dual, this conditions removes some degrees of freedom from the spectrum.

[2]All the following fields and forms are defined in 4 dimensions and do not have to be confused with the similar notation for 10 dimensional fields.

All the fields and forms listed so far belong to the bosonic sector of multiplets of 4D $\mathcal{N} = 2$ supergravity theory. The gravity multiplet contains $g_{\mu\nu}$ and V_0 while the double-tensor multiplet contains B_2, C_0, C_2 and the dilaton. In addition we have $h_{1,1}$ hypermultiplets containing t^i, b^i, c^i and ρ_i and $h_{1,2}$ vector multiplets that include V^a and U^a. Since this theory is not able to describe chiral matter in 4D, we need to find some way to halve the number of supersymmetries thus leading to a promising description of nature. This can be achieved through *orientifold involution* that we describe in the next section.

2.3.5 $\mathcal{N} = 1$ 4D supergravity from orientifold involution

An orientifold is a generalisation of orbifold, proposed by Sagnotti and Pradisi in 1987 [32, 33, 34]. In case of orientifolds the non trivial elements of the orbifold include the orientation reversal of the string [18]. The world-sheet parity Ω_p exchanges left and right movers through

$$\Omega_p : \sigma \leftrightarrow 2\pi - \sigma \tag{2.99}$$

where σ is the spatial coordinate on the world-sheet. Making an orientifold projection corresponds to gauging away this symmetry thus being left with unoriented world-sheets. In the context of Calabi-Yau compactifications this mechanisms has been generalised including the action of an isometric and holomorphic transformation that acts uniquely on Y_6: the involution σ_Y ($\sigma_Y^2 = 1$). In type IIB the action of σ_Y on the holomorphic 3-form Ω and Kähler form is given by the pull-back of the involution σ_Y^*:

$$\sigma_Y^*(\Omega) = (-1)^\epsilon \Omega\,, \qquad \sigma_Y^*(J) = J\,, \qquad \epsilon = 0, 1\,. \tag{2.100}$$

The orientifold involution in case of type IIB Calabi-Yau compactifications corresponds to gauging away the discrete symmetry

$$(-1)^{\epsilon F_L} \Omega_p \sigma_Y\,, \qquad \epsilon = 0, 1 \tag{2.101}$$

where F_L is the left moving fermion number. The hypersurface where the involution reduces to the change of string orientation is called *orientifold plane*. Since σ_Y does not act on $\mathcal{M}_4 = R^{(1,3)}$ the orientifold plane can have at least dimension 3 but, in case of $\sigma_Y(\Omega) = \Omega$, it is possible that all 4D space-time dimensions are left unchanged and an O9-plane can exist. Depending on the value of ϵ, we find two class of models: if $\epsilon = 0$ we have theories with O5/O9-planes, if $\epsilon = 1$ we have theories with O3/O7-planes. In general we can consider orientifold planes having as many dimensions as Dp-branes: this means that in what follows we choose $\epsilon = 1$ thus working with O3- and O7-planes. Beyond halving the number

4D supersymmetries, orientifold involution reduces the dimensionality of moduli space. Indeed harmonic (p,q)-forms can either be even or odd under the action of $\sigma*$. We can therefore split each cohomology class into two basis representing the eigenstates of σ^* with different parity

$$H_{p,q} = H^+_{p,q} \oplus H^-_{p,q}, . \tag{2.102}$$

We call $h^+_{p,q}$ and $h^-_{p,q}$ the dimensionality of $H^+_{p,q}$ and $H^-_{p,q}$ respectively. These are related through Eq.(2.102) by $h^+_{p,q} + h^-_{p,q} = h_{p,q}$. For CY manifolds we have that $h^\pm_{1,1} = h^\pm_{2,2}$ since they are related by Hodge duality that commutes with σ^*_Y, $h^\pm_{1,2} = h^\pm_{2,1}$ because of σ^*_Y holomorphy, $h^+_{3,0} = h^+_{0,3} = 0$ and $h^-_{3,0} = h^-_{0,3} = 1$ from Eq. (2.100) with $\epsilon = 1$ and $h^+_{3,3} = h^+_{0,0} = 1$ while $h^-_{3,3} = h^-_{0,0} = 0$ since the volume form should be invariant under σ^*_Y.

The dimensional reduction with orientifold involution proceeds as in Sec. 2.3.4 but in this case the KK expansion should keep only those fields that are invariant under the orientifold action. The parity properties of the 10-dimensional bosonic fields under the transformation $(-1)^{F_L}\Omega_p$ are given by

	ϕ	G	B_2	C_0	C_2	C_4
$(-1)^{F_L}$	+	+	+	−	−	−
Ω_p	+	+	−	−	+	−
$(-1)^{F_L}\Omega_p$	+	+	−	+	−	+

(2.103)

This implies that under the involution σ^* the fields need to obey:

	ϕ	G	B_2	C_0	C_2	C_4
σ^*	+	+	−	+	−	+

. (2.104)

We can then write down the bosonic invariant spectrum under orientifold involution as:

- **Kähler moduli t^{i_+}:** since both J and the complex structure are invariant under the action of σ_Y, we have that Kähler metric can be decomposed as:

$$J = t^{i_+}(x)\hat{D}^i_{i_+}\,, \qquad i_+ = 1, \ldots, h^+_{1,1} \tag{2.105}$$

  where $\hat{D}^i_{i_+}$ is a $H^+_{1,1}$ basis.

- **Complex structure moduli $U^{\alpha-}$:** since $\sigma^*_Y\Omega = -\Omega$ we have that only elements of $H^-_{1,2}$ correspond to complex structure moduli that can be kept in the spectrum. The metric deformation of Eq. (2.92) then becomes

$$\delta g_{ij} = \frac{i}{||\Omega||^2} U^{\alpha-}\,(\bar{\chi}_{\alpha-})_{i\bar{k}\bar{l}}\Omega^{\bar{k}\bar{l}}_j \tag{2.106}$$

where χ_{α_-} is a basis of $H^-_{1,2}$.

- C_0 **and dilaton:** since both C_0 and ϕ are invariant under orientifold involution they both remain in the spectrum.

- **Two-forms** B_2 C_2**:** Since both B_2 and C_2 need to be odd under σ_Y, their expansions look like

$$B_2 = b^{i_-}(x)\hat{D}_{i_-}\,, \qquad C_2 = c^{i_-}(x)\hat{D}_{i_-}\,, \qquad i = 1, \dots, h^-_{1,1} \tag{2.107}$$

  where $\hat{D}_{i_-}$ is a basis of $H^-_{1,1}$. The 4D 2-forms $B_2(x)$ and $C_2(x)$ that we found in the $\mathcal{N} = 2$ compactification are removed from the theory and we are left only with scalar fields $b^{i_-}(x)$ and $c^{i_-}(x)$.

- **Four-form** C_4**:** it must be even under the involution σ_Y and it expansion looks like

$$C_4 = V^{a_+}(x) \wedge \alpha_{a_+} + \rho_{i_+}(x)\tilde{D}^{i_+}\,, \qquad \begin{array}{l} a_+ = 1, \dots, h^+_{1,2}\,, \\ i_+ = 1, \dots, h^+_{1,1}\,, \end{array} \tag{2.108}$$

  where $\tilde{D}^{i_+}$ is a basis of $H^+_{2,2}$ that is dual to $\tilde{D}^{i_+}$ and α_{a_+} belongs to the real symplectic basis of H^+_3, $(\alpha_{a_+}, \beta^{a_+})$. We used the self duality condition on $F_5 = dC_4$ to remove redundant degrees of freedom.

These fields belong to 4D $\mathcal{N} = 1$ supersymmetric theory and they group together in different multiplets. Nevertheless the variables that appear in the KK reduction are not necessarily given by the bosonic components of the supersymmetric multiplets that represent the proper Kähler coordinate of the moduli space. Indeed these are given by [21, 20]:

- **Axio-dilaton:**

$$S = e^{-\phi} - iC_0\,; \tag{2.109}$$

- **2-form moduli:**

$$G_2 = G^{i_-}\hat{D}_{i_-} = \left(c^{i_-}(x) - Sb^{i_-}(x)\right)\hat{D}_{i_-} \qquad i_- = 1, \dots, h^-_{1,1,} \tag{2.110}$$

- **Complex structure moduli:**

$$U^{\alpha_-}\,, \qquad \alpha_- = 1, \dots, h^-_{1,2} \tag{2.111}$$

- **Kähler moduli:**[3]

$$T_{i_+} = \tau_{i_+} - \frac{k_{i_+ j_- k_-}}{Re(S)} G^{j_-} (G - \bar{G})^{k_-} + i\rho_{i_+} \qquad i_+ = 1, \ldots, h^+_{1,1}, \tag{2.112}$$

where

$$k_{i_+ j_- k_-} = \int_{Y_6} \hat{D}_{i_+} \wedge \hat{D}_{j_-} \wedge \hat{D}_{k_-} \tag{2.113}$$

while τ_{i_+} is related to t_{i_+} through

$$\tau_{i_+} = \frac{1}{2!} \int_{Y_6} J \wedge J \wedge \hat{D}_{i_+} = \frac{k_{i_+ k_{j_+} k_{k_+}}}{2!} t_{j_+} t_{k_+} = \frac{\partial \mathcal{V}}{\partial t^{i_+}} \,. \tag{2.114}$$

and the overall volume of extra dimensions $\mathcal{V}$ is given by

$$\mathcal{V} = \frac{1}{3!} \int_{Y_6} J \wedge J \wedge J = \frac{1}{3!} t_{i_+} t_{j_+} t_{k_+} \,. \tag{2.115}$$

In the models that we are going to analyse in the third part of this thesis we will consider orientifold projections such that $h^-_{1,1} = 0$, that means $h_{1,1} = h^+_{1,1}$. In this case the 2-form scalars b^{i-} and c^{i-} are projected out and the form of Kähler moduli becomes:

$$T_i = \tau_i + i\rho_i \,, \qquad i = 1, \ldots, h_{1,1} \,. \tag{2.116}$$

We can interpret τ_{i_+} as the volume of the divisor $D_{i_+} \in H_4(Y_6, \mathbb{Z})$ that is the Poincaré dual to $\hat{D}_{i_+}$ while the imaginary part of the Kähler field ρ_i is given by the component of the R-R 4-form C_4 along this cycle: $\rho_i = \int_{D_i} C_4$.

The supersymmetric multiplets coming from $O3/O7-$orientifold compactifications are then given by one gravity multiplet containing $g_{\mu\nu}$, $h^{2,1}_+$ vector multiplets containing V^{a_+} and $h^{2,1}_- + h^{1,1} + 1$ chiral multiplets containing T_{i_+}, $U^{\alpha-}$, G^{i-} and S.

The $\mathcal{N} = 1$ 4D supergravity action can be expressed in terms of the Kähler potential K, the holomorphic superpotential W and the holomorphic gauge kinetic couplings f as

$$S = -\int \frac{R}{2} * \mathbf{1} + K_{I\bar{J}} D\Phi^I \wedge * D\bar{\Phi}^{\bar{j}} + \frac{1}{2} \mathrm{Re}(f_{ab}) F^a \wedge * F^b + \frac{1}{2} \mathrm{Im}(f_{ab}) F^a \wedge F^b + V \tag{2.117}$$

[3]The Kähler coordinate T_i and the fields t_i in Eq. (2.105) are both called Kähler moduli. This can be a little confusing. In the rest of our work we will typically refer to Kähler moduli talking about the fields T_i that parametrise the size of 4-cycles in the extra dimensions.

where Φ represents all complex scalars in the theory, $F^a = dV^a$ is the field strength related to V^a, $a = 1, \ldots, h^{2,1}_+$, and $V = V_F + V_D$ is the scalar potential of the theory. The F-term scalar potential V_F arising from $\mathcal{N} = 1$ supergravity can be written as (here we use natural units, i.e. $M_p = 1$):

$$V_F = e^G\big((G^{-1})^{i\bar{j}}G_iG_{\bar{j}} - 3\big) = e^K\Big[K^{I\bar{J}}D_IWD_{\bar{J}}\bar{W} - 3|W|^2\Big] \tag{2.118}$$

where $G := K + \ln|W|^2$ is the Kähler function, $K^{I\bar{J}}$ is the inverse of Kähler metric $K_{I\bar{J}}$ and the covariant derivatives D_IW are given by

$$D_IW = \partial_IW + W\partial_IK\,. \tag{2.119}$$

On the other hand, the D-term scalar potential comes from the vector multiplet contributions and looks like:

$$V_D = \frac{1}{2}[Re(f)]^{ab}D_aD_b\,, \qquad D_a = ig\mathrm{Re}[(f^{-1})]^{ab}G_i(\mathcal{T}_b)^{ij}\phi_j \tag{2.120}$$

where g is the gauge coupling constant, $\mathcal{T}_a$ are the group generators in the same representation as the chiral matter fields and $(F^a)_{\mu\nu}$ is the gauge field strength. The tree level Kähler potential of the theory is given by:

$$K = -2\ln\mathcal{V}(T+\bar{T}) - \ln(S+\bar{S}) - \ln\Big(-i\int_{CY}\Omega(U)\wedge\bar{\Omega}(\bar{U})\Big) \tag{2.121}$$

where Ω is the holomorphic $(3,0)-$form of the CY that is a function of the complex moduli and $\mathcal{V}$ is the classical Calabi-Yau volume in string length natural units ($l_s = (2\pi\sqrt{\alpha'}) = 1$) that depends only on Kähler moduli. As we can see from equation (2.121), the Kähler potential gets factorised denoting that moduli space can be decomposed as:

$$\mathcal{M} = \mathcal{M}^K_{h^+_{1,1}+1} \times \mathcal{M}^{cs}_{h^-_{1,2}}\,. \tag{2.122}$$

where $\mathcal{M}^K_{h^+_{1,1}+1}$ is a Kähler manifold containing Kähler moduli and the dilaton while $\mathcal{M}^{cs}_{h^-_{1,2}}$ is a the special Kähler manifold related to complex structure moduli.

At tree level the superpotential is vanishing unless we switch on background fluxes. Therefore, without fluxes no scalar potential is generated and moduli remain exactly flat directions. This would give rise to unrealistic supersymmetric theories fulfilled with fifth forces mediators. In order to make contact with observations, we devote the next section to the study of the role played by background fluxes in type IIB Calabi-Yau orientifold compactification in presence of O3/O7-planes.

2.3.6 Background fluxes

If this section we allow for a background profile also for some of 10D p-forms in addition to the metric and we will briefly summarise flux compactifications on Calabi-Yau orientifolds [25, 35, 26, 36, 37]. We introduced fluxes for the 10D supergravity theory coming from type IIB string theory in Eq. (2.64). These need to satisfy the following Bianchi identities:

$$dH_3 = 0\,, \qquad dF_p - H_3 \wedge F_{p-2} = 0. \tag{2.123}$$

where, in presence of local sources like Dp-branes or Op-planes, the right hand side of the previous equations must replaced with a delta function with support on the sources world-volume. In order to preserve 4D Poincaré invariance, fluxes need to be present only along the extra dimensions or they have to fill out the 4D space-time (this can be done only by p-form fluxes having $p > 3$ while 3-form fluxes need to be confined in Y_6). Non-vanishing fluxes can arise in presence of local non-vanishing sources or in absence of sources if the cycle supporting them is non-contractible. In case of non-vanishing flux the integral of the corresponding field strength needs to satisfy Dirac quantisation conditions [38]:

$$\frac{1}{(2\pi)^2\alpha'}\int_{\sigma_3} H_3 \in \mathbb{Z}\,, \qquad \frac{1}{(2\pi\sqrt{\alpha'})^{p-1}}\int_{\Sigma_p} \hat{F}_p \in \mathbb{Z}\,. \tag{2.124}$$

In particular if we consider a CY manifold and we expand H_3 in a basis for $H^3(Y_6) = H^{(3,0)} \oplus H^{(0,3)} \oplus H^{(1,2)} \oplus H^{(2,1)}$, we can define the non trivial p-cycles that are Poincaré dual to the basis elements and we get that the electric and magnetic fluxes for H_3 are given by:

$$\frac{1}{(2\pi)^2\alpha'}\int_{A_k} H_3 = m^k_{NS}\,, \qquad \frac{1}{(2\pi)^2\alpha'}\int_{B^k} H_3 = e_{NSk}\,, \qquad k = 1, \ldots, 2h_{1,2}+2 \tag{2.125}$$

where again (α_k, β^k) is the simplectic basis of $H^3(Y_6)$ and (A_k, B^k) is its dual basis of 3-cycles. Doing the same analysis for the R-R sector F_p p-forms we get

$$\begin{aligned} &\frac{1}{(2\pi)^2\alpha'}\int_{A_k} \hat{F}_3 = m^k_{RR}\,, \qquad \frac{1}{(2\pi)^2\alpha'}\int_{B^k} \hat{F}_3 = e_{RRk}\,, \qquad k = 1, \ldots, 2h_{1,2}+2 \\ &\frac{1}{2\pi\sqrt{\alpha'}}\int_{\tilde{D}_I} \hat{F}_2 = m^I_{RR}\,, \qquad \frac{1}{(2\pi\sqrt{\alpha'})^3}\int_{D^I} \hat{F}_4 = e_{RRI}\,, \qquad I = 1, \ldots, h_{1,1} \end{aligned} \tag{2.126}$$

where D^I and $\tilde{D}_I$ are non trivial 4- and 2-cycles that are Poincaré dual to $\hat{D}_I \in H^{(1,1)}$ and $\hat{\tilde{D}}^I \in H^{(2,2)}$ respectively. The contributions coming from $\hat{F}_1$ and $\hat{F}_5$ are vanishing since we do not have non-trivial 1- and 5-cycles in a CY manifold.

Poincaré dualities follow from

$$\begin{aligned}\int_{A_k}\alpha_j = -\int_{B^j}\beta_k = \int_{Y_6}\alpha_l\wedge\beta^k = \delta^k_j\,,\\ \int_{\tilde{D}_J}\hat{D}_K = -\int_{D^K}\hat{\tilde{D}}^J = \int_{Y_6}\hat{D}_K\wedge\hat{\tilde{D}}^J = \delta^K_J\,.\end{aligned} \tag{2.127}$$

The presence of fluxes has a crucial consequence on the 10D space-time: non-vanishing background fluxes back-react on the geometry of the compact space Y_6 so that Eq. (2.71) does not represent anymore a valid decomposition of $\mathcal{M}^{10}$. Imposing surviving 4D supersymmetries in presence of fluxes translates into milder geometrical requirements on Y_6 then in the flux-less case. Having a well defined 6-dimensional spinor in case of non-vanishing fluxes implies that Y_6 has to be a SU(3)-structure manifold [39, 40, 41]. This means that a connection that satisfies $\nabla g_{_{Y_6}} = 0$ and Eq. (2.73) may show a non vanishing torsion [42, 43, 44]. A Calabi-Yau manifold is a particular SU(3)-structure manifold where this connection has a vanishing torsion. Among the possible 4D $\mathcal{N}=1$ Minkowski vacua that are compatible with flux-compactifications, we focus on models where the non-vanishing torsion on Y_6 connections causes a slight deviation from the CY space and the 10D metric takes the warped compactification form

$$ds^2 = e^{2A(y)}\eta_{\mu\nu}dx^\mu dx^\nu + e^{-2A(y)}g_{mn}dy^m dy^n\,, \tag{2.128}$$

where g_{mn} is a CY metric and $A(y)$ is called the warp factor and is a function on Y_6. These are called warped compactifications since they lead to warped (conformal) CY manifolds [45, 46, 47, 48]. This class of solutions allows for R-R 5-form, R-R 3-form and NS-NS 3-form fluxes. The relevant 3-form flux is given by G_3 that is a combination of F_3 and H_3

$$G_3 = \hat{F}_3 - SH_3 \tag{2.129}$$

that needs to satisfy the imaginary self duality condition

$$*_6\, G_3 = iG_3 \tag{2.130}$$

and $G_3^{(0,3)} = 0$. If the inverse of the warp factor can be safely neglected we can keep on using results from CY-compactifications that we developed in the previous sections. This is the case in the limit of large volume in the extra-dimension since

$$e^{2A} \sim 1 + \mathcal{O}\left(\frac{g_s N\alpha'^2}{R^4}\right) \tag{2.131}$$

where R is the typical radius of extra dimensions and N measures the units of flux of G_3.

Of course any additional object introduced in the compactification can in principle backreact on the geometry and destroy the conformal CY structure. Nevertheless it can be shown that flux sources as $D3/D7$-branes and $O3/O7$-planes preserve the same type of supersymmetry as warped compactification models. Therefore in what follows we will focus on warped compactifications in presence of $D3/D7$-branes and $O3/O7$-planes and we will perform computations in the extra-dimensions large volume regime so that we can safely neglect warping effects on the moduli space of the conformal CY manifold.

The Bianchi identities for the 10D R-R forms F_p in absence of local source, Eq. 2.123, need to be valid on the compact manifold Y_6, this implies a constraint coming from a generalisation of Gauss's law that fixes the value of the integrated version of Eq. (2.123). This is called C_4 tadpole cancellation condition and derives from computing the equations of motion for the R-R field C_4. Since the integral of dF_5 on Y_6 vanishes, this would imply that the integral of $H_3 \wedge F_3$ (which is positive definite thanks to the imaginary self-duality of G_3) should vanish as well. We conclude that in absence of local sources, C_4 tadpole cancellation implies vanishing fluxes.

In order to have flux compactification with non-vanishing background fluxes, we need to add to the theory local sources that carry D3-brane charges, such as D3/anti-D3-branes, wrapped D7-branes and O3/O7-planes. Considering the presence of D3-branes and O3-planes, Eq. (2.123) the Bianchi identity for F_5 becomes

$$dF_5 - H_3 \wedge F_3 = (2\pi\sqrt{\alpha'})^4 \rho_3^{\rm loc}\,, \qquad \rho_3^{\rm loc} = \mu_3 \sum_a \hat{\pi}_6^a + \mu_{O_3} \sum_b \hat{\tilde{\pi}}_6^a \tag{2.132}$$

where $\rho_3^{\rm loc}$ represents the dimensionless localised D3 charge source while $\hat{\pi}_6^a$ and $\hat{\tilde{\pi}}_6^a$ are 6-forms Poincaré dual to the support of the D3-branes and O3-planes respectively. The D3-brane and the O3-plane charge, μ_3 and μ_{O_3}, are given by

$$\mu_3 = \frac{1}{(2\pi)^3 \alpha'^2}\,, \qquad \mu_{O_3} = \mu_3 Q_3 = -\frac{1}{2}\mu_3 \tag{2.133}$$

and we see that O3-planes, carrying negative D3 charge allow us to satisfy tadpole cancellation in presence of non-vanishing fluxes. The schematic condition on RR-tadpole cancellation becomes

$$N_{D_3} - \frac{1}{4} N_{O_3} + \frac{1}{(2\pi)^4 \alpha'^2} \int_{Y_6} H_3 \wedge F_3 = 0 \tag{2.134}$$

where N_{D_3} is the number of D3-branes and N_{O_3} is the number of O3-planes.

Other contributions to D3-brane tadpole cancellation may come from the presence of D7-branes, O7-planes and gauge fluxes on D7-branes. The generalisation

of Eq. (2.134) is given by [49, 50, 38]:

$$N_{\text{flux}} + \sum_{D3^b, D3^{b'}} N_{D3^b} - \sum_{O3^i} \frac{N_{O3^i}}{2} + N_{\text{gauge}} - \sum_{O7^j} \frac{\chi(\Gamma_{O7^j})}{6} - \sum_{D7^a, D7^{a'}} \frac{\chi(\Gamma_{D7^a})}{24} = 0\,, \tag{2.135}$$

$$\begin{aligned} N_{\text{flux}} &= \frac{1}{(2\pi)^4 \alpha'^2} \int_{Y_6} H_3 \wedge F_3\,, \\ N_{\text{gauge}} &= -\frac{1}{(2\pi)^4 \alpha'^2} \sum_{D7^a, D7^{a'}} \int_{\Gamma_{D7^a}} c_2(\mathcal{F}^{a_+}) \end{aligned} \tag{2.136}$$

where N_{D7^a} is the number of branes that wrap the internal divisor Γ_{D7^a}, $\Gamma_{Dp^{a'}} = \Omega(-1)^{F_L}\sigma\Gamma_{Dp^a} = (-1)^{\frac{p+1}{2}}\sigma\Gamma_{Dp^a}$ is the orientifold image of the divisor Γ_{Dp^a} wrapped by the Dp-branes, $\chi(\Gamma) = \int c_2(\Gamma)$ denotes the Euler characteristic of the cycle Γ and $\mathcal{F}^a$ is the gauge invariant open string field strength. The latter is given by $\mathcal{F}^a = \iota^* B_2 + 2\pi\alpha' F^a$ where $\iota^* B_2 \in H_2(\Gamma_{Dp^a})$ is the pull-back of NS-NS 2-form from Y_6 to the holomorphic cycle wrapped by the stack of D7-branes. The form B_2 can be decomposed through orientifold involution into $B_2^+ \in H_2^+(\Gamma_{Dp^a})$ and $B_2^- \in H_2^-(\Gamma_{Dp^a})$; while B_2^- takes continuous values and appears in the G_2 form, B_2^+ is quantised and has to take discrete values due to the Freed-Witten anomaly cancellation [51, 52]. We call $\mathcal{F}^{a_+} = \iota^* B_2^+ + 2\pi\alpha' F^a$ the relevant quantised gauge flux that appears in the consistency conditions. It is important to remark that the gauge flux can be non-vanishing only inside the compact dimensions Y_6 in order to preserve 4D Poincaré invariance.

Other constraints come from the equations of motion of C_5 and C_8, these are also called D5- and D7-brane tadpole cancellation conditions. From C_5 tadpole we get

$$\sum_{D7^a} \left(c_1(\iota_* \mathcal{F}^{a_+}) \wedge [\Gamma_{D7^a}] + c_1(\iota_* \mathcal{F}^{a'_+}) \wedge [\Gamma_{D7^{a'}}] \right) \wedge \omega_I = 0 \tag{2.137}$$

where $\{\omega_I\} \in H^{1,1}(Y_6, \mathbb{Z})$, primes denote again the $\Omega(-1)^{F_L}\sigma$ image, $[\Gamma_{D_7^a}] \in H^+_{1,1}$ is the Poincaré dual to the 4-cycle Γ_{D7^a} and $\iota_* \mathcal{F}^a$ denotes the push-forward from the D7-brane to the CY manifold. Finally C_8 tadpole constraint look like

$$\sum_{D7^a} N_{D7^a} \left([\Gamma_{D7^a}] + [\Gamma_{D7^{a'}}] \right) = 8 \sum_{O7_i} [\Gamma_{O7^i}]\,. \tag{2.138}$$

If there there are no elements in $H_2^-(Y_6)$, the D5-brane tadpole cancellation condition is automatically satisfied and the contributions coming form the orientifold images in Eq. (2.135), (2.136) just give a factor two. Tadpole cancellation conditions are related to the quantisation conditions but they also constraint the local sources content of the theory.

We finally mention that, despite conserving the same kind of supersymmetry, the presence of D7-branes modifies the geometry of the 10D space-time. in this case, the extra-dimensions are not represented by a conformal CY anymore (i.e. it is not Ricci-flat) and, being magnetically charged under C_0 they backreact on the axio-dilaton that acquires a non-vanishing dependence on the Y_6 coordinates. This would require to study compactifications in the context of F-theory solutions. Moreover, in order to break supersymmetry from $\mathcal{N}=1$ to $\mathcal{N}=0$ in a controllable way, we will need to introduce non-vanishing $G_3^{(0,3)}$ component of the 3-form flux. In the following sections we then assume that introducing a limited number of D7-branes, considering small contributions to $G_3^{(0,3)}$ and working in the perturbative limit $g_s \ll 1$ will lead to extra-dimensions manifolds that can be considered as small perturbations of warped compactifications. These conditions, combined with the requirement of a large Y_6 volume may allow us to keep on using the results obtained in Sec. 2.3.5.

2.3.7 Flux-stabilisation and no-scale structure

As we saw in the previous section the presence of 3-form fluxes backreacts on the 10D metric, changing the geometry of Y_6 thus putting some constraints on 4D supersymmetry conservation and on model building. On the other hand, it allows for a non-vanishing tree-level superpotential that leads to axio-dilaton and complex structure moduli stabilisation and may spontaneously break the residual $\mathcal{N}=1$ supersymmetry. In order to show how flux-stabilisation works, let us focus for simplicity on orientifold projections having $h^-_{1,1}=0$. In presence of background fluxes, the tree level superpotential takes the Gukov-Vafa-Witten superpotential form [53]:

$$W_{\text{tree}}(S,U^a) = \int_{Y_6} \Omega \wedge G_3 \tag{2.139}$$

where the complex moduli dependence is encoded in Ω while the dependence on the axio-dilaton comes from G_3. Indeed, after performing orientifold involution, we have that G_3 can be decomposed as:

$$G_3 = m^{a_-}\alpha_{a_-} + e_{a_-}\beta^{a^-}\,, \qquad a_- = 1,\dots,h^-_{1,2} \tag{2.140}$$

where

$$m^{a_-} = \tilde{m}^{a_-}_{RR} - iS\,\tilde{m}^{a_-}_{NS}\,, \qquad e_{a_-} = \tilde{e}_{RR\,a_-} - iS\,\tilde{e}_{NS\,a_-} \tag{2.141}$$

and $(\alpha_{a_-},\beta^{a-})$ is the symplectic basis of H^-_3. In the low energy/large volume approximation, the coefficients $\tilde{e}_{RR/NS\,a_-}$ and $\tilde{m}^{a_-}_{RR/NS}$ that come from Eqs. (2.125), (2.126) appear as $2h^-_{1,2}+2$ continuous complex flux parameters which deform the low energy supergravity.

In case of non vanishing fluxes we saw that the tree-level superpotential in Eq. (2.139) does not depend on Kähler moduli. This implies that:

$$D_T = W_{\text{tree}} K_T \,, \tag{2.142}$$

where T is a generic Kähler field. Thanks to the factorisation of the moduli space of Eq. (2.122), the tree-level F-term scalar potential of Eq. (2.118) is given by

$$\begin{aligned} V_{F_{\text{tree}}} &= e^K \Big(\sum_{\alpha\beta=U_j,S} K^{\alpha\bar{\beta}} D_\alpha W D_{\bar{\beta}} \bar{W} \Big) + e^K \Big(\sum_{i=T^i} K^{i\bar{j}} K_i K_{\bar{j}} - 3 \Big) |W|^2 \\ &= e^K \Big(\sum_{\alpha=U_j,S} K^{\alpha\bar{\beta}} D_\alpha W D_{\bar{\beta}} \bar{W} \Big) \\ &= e^K \Big(\sum_{j,k=1,\dots,h^{1,2}_-} K^{U_j \bar{U}_k} D_{U_j} W D_{\bar{U}_k} \bar{W} + K^{S\bar{S}} |D_S W|^2 \Big) \geqslant 0 \end{aligned} \tag{2.143}$$

since

$$(K^{i\bar{j}} K_i K_{\bar{j}} - 3) = 0 \,. \tag{2.144}$$

The relation in Eq. (2.144) is called *no-scale structure* and comes from the structure of the tree-level Kähler potential: $K_{\text{tree}} = -2\ln(\mathcal{V})$. Since $\mathcal{V}$ is a homogeneous function of degree $3/2$ in the real part of Kähler moduli τ_i's we have that $\mathcal{V}(\lambda\tau_i) = \lambda^{3/2}\mathcal{V}(\tau_i)$ and $K_{\text{tree}}(\lambda\tau_i) = K_{\text{tree}}(\tau_i) - 3\ln(\lambda)$ that imply Eq. (2.144). The only Kähler moduli dependence of the scalar potential lies in the prefactor $e^K \propto \mathcal{V}^{-2}$ and induces a runaway in the Kähler directions as can be easily seen in the case of a single Kähler modulus where $\mathcal{V} = (T + \bar{T})^{3/2}$.

At tree-level, the no-scale structure scalar potential of Eq. (2.143) is positive definite and we can supersymmetrically stabilise the complex structure moduli and the dilaton imposing that the F-terms related to those fields vanish. Since F-terms are given by

$$F^I = e^{K/2} K^{I\bar{J}} D_{\bar{J}} \bar{W} \tag{2.145}$$

having a supersymmetric stabilisation for dilaton and complex structure moduli translates to

$$D_S W = D_{U_j} W = 0 \,. \tag{2.146}$$

This gives rise to $h^{1,2}_- + 1$ complex equations that look like

$$D_S W_{\text{tree}} = -\frac{1}{S + \bar{S}} \int_{Y_6} \Omega \wedge \bar{G}_3 = 0 \,, \tag{2.147}$$

$$D_{U^a} W_{\text{tree}} = i \int_{Y_6} \chi^a \wedge G_3 = 0 \,. \tag{2.148}$$

In Eq. (2.148) we used the relation $D_{U^a}\Omega_3 = i\chi_a$ where χ_a is a basis of $H^{(2,1)}_-(Y_6)$. The equations (2.147) and (2.148) imply that $G_3^{(0,3)} = 0$ and $G_3^{(1,2)} = 0$ respectively. Therefore we conclude that in order to have a supersymmetric minimum we need G_3 to be imaginary self-dual $*_6 G_3 = iG_3$. The same constraint applied to Kähler moduli fields is given by setting Eq. (2.142) to zero. This implies $W_{\text{treee}} = 0$ that translates into $G_3^{(3,0)} = 0$ and $G_3 \in H^{(2,1)}_-$. Thus we can immediately deduce that the class of models that allows for the stabilisation of the complex structure moduli and the dilaton at a supersymmetric global minimum is given by the warped compactifications discussed in Sec. 2.3.6.

In the following sections we assume that S and U^a are stabilised by background fluxes and can be integrated out. This is true if quantum corrections give rise to a scalar potential that induces subleading corrections to their VEVs, in which case we are allowed to set

$$W_0 = W_{\text{tree}}|_{\langle U^a\rangle,\langle S\rangle} = \left\langle \int_{Y_6} \Omega_3 \times G_3 \right\rangle \tag{2.149}$$

and

$$K_{\text{tree}} = -2\ln(\mathcal{V}) - \ln\left(\frac{2}{g_s}\right) + K_{cs}\,, \tag{2.150}$$

where

$$g_s^{-1} = \langle \text{Re}(S)\rangle\,, \qquad e^{-K_{cs}} = \left\langle -i\int_{Y_6} \Omega_3 \wedge \bar{\Omega}_3 \right\rangle\,. \tag{2.151}$$

The presence of fluxes allows the stabilisation of complex structure moduli and the axio-dilaton without breaking the four dimensional $\mathcal{N} = 1$ supersymmetry. Nevertheless, it does not provide a working mechanism for Kähler moduli stabilisation. These remain classical flat directions due to the continuous rescaling symmetry that is encoded in the no-scale structure condition of Eq. (2.144). This implies that in order to develop a potential for Kähler moduli we will need to keep all possible quantum corrections that will be introduced in the next section.

2.3.8 Kähler Moduli stabilisation

We saw that the presence of fluxes allows to stabilise complex structure moduli and the axio-dilaton, while Kähler moduli are flat directions at tree-level. Nevertheless, various quantum corrections can break the no-scale structure leading to a non-vanishing potential for Kähler moduli. In particular, Kähler potential receives corrections at every order in perturbation theory. On the other hand, the superpotential is protected against perturbative corrections, thanks to the non-renormalisation theorem, and receives only non-perturbative corrections. We can

write schematically

$$W = W_0 + W_{np}\,, \qquad K = K_{\rm tree} + K_p + K_{np} \tag{2.152}$$

where the subscripts p and np stand for perturbative and non-perturbative corrections respectively, while W_0 and $K_{\rm tree}$ are the tree level contributions given in Eqs. (2.149),(2.151) and (2.150). As we mentioned in Sec. 2.3, the 2 parameters involved in perturbation theory are g_s and α'. g_s is related to the dilaton VEV and controls the strength of string interactions while α' measures how the internal curvature of the extra dimensions is related to the string length and controls the appearance of higher dimensional operators. Both these parameters need to be small in order to treat the EFT perturbatively. Non-perturbative corrections are instead related to the presence of local sources, as D3/D7-branes. These can be due to D3-instantons or gaugino condensation on a stack of D7-branes.

All the corrections that we are going to introduce are able to develop a potential for Kähler moduli and may break 4D supersymmetry. On the other hand, from a 10D perspective, they break the warped compactification geometry. Therefore we need to give the reader some intuition about the fact that we can interpret these corrections as small perturbations of the warped geometry. In the previous section we showed that axio-dilaton and complex structure moduli can be stabilised at a supersymmetric minimum that satisfies the warped geometry constraints that we introduced around Eq. (2.130). The volume dependence of the tree-level F-term potential can be read from Eq. (2.145 and is given by $V_{F\rm tree} \sim \mathcal{V}^{-2}$. All the corrections that we are going to study can be expanded in inverse powers of the overall volume and they scale as $\sim \mathcal{V}^{-c}$ where $c > 2$. Since we are going to work in the large volume scenario, where the overall volume of extra-dimension is exponentially large, we immediately understand that additional contribution leading to Kähler moduli stabilisation can be interpreted as small perturbations around the supersymmetric background that belong to the class of warped compactifications.

Non-perturbative corrections The superpotential non-perturbative corrections can be generated by Euclidian D3-brane (ED3-brane) intantons wrapping 4-cycles in the extra dimensions manifold and by gaugino condensation on a stack of D7-branes also wrapping a 4-cycle. In both cases, the form of the superpotential looks like:

$$W = W_0 + \sum_i A_i(S, U^a, \xi^\alpha) e^{-a_i T_i} \tag{2.153}$$

where A_i correspond to threshold effects, they are functions of the complex structure moduli, the axio-dilaton and the fields ξ^α which parametrise the position of the ED3/D7-brane that wrap the 4-cycle whose volume is parametrised by $\tau_i = {\rm Re}(T_i)$. The value of the coefficient a_i depends on the physical mechanism that induces the

correction: in case of ED3-brane instantons $a_i = 2\pi$, while for gaugino condensation it is given by $a_i = 2\pi/N$ where N is the number of D7-branes in the stack. In principle, there can be other higher instanton effects but they can be safely ignored as long as $a_i\tau_i \gg 1$. The contribution of non-perturbative corrections to the scalar potential is given by

$$\begin{aligned} V_{np} \sim \; & e^{K_0} K_0^{i\bar{j}} \left[a_j a_i A_i \bar{A}_j e^{-a_i T_i + a_j \bar{T}_j} - \left(a_i A_i e^{-a_i T_i} \bar{W} \partial_{\bar{T}_j} K_0 \right.\right. \\ & \left.\left. + a_j \bar{A}_j e^{-a_j \bar{T}_j} W \partial_{T_i} K_0 \right) \right] . \end{aligned} \tag{2.154}$$

α' corrections As already mentioned, α' corrections control the presence of higher derivative terms. The leading order α' correction descends from a 10D curvature correction that is given by [54]

$$S \supset \int d^{10}X \sqrt{-G} \left[\frac{M_{P_{10}}^2}{2} R + \frac{\zeta(3)}{3 \cdot 2^5} \frac{\mathcal{R}^4}{M^6} \right] \tag{2.155}$$

where $M_{P_{10}}$ is the 10D Planck mass, R is the 10D curvature, ζ is the Riemann zeta function, $\mathcal{R}$ is a quartic invariant constructed from the Riemann tensor and $M^2 = 4/\alpha'$ is the mass of the first excited level of type II superstring. The latter represents a physical cutoff because it appears upon integrating out the massive excitation of the string. In the 4D effective theory the leading order perturbative correction takes the form [55]:

$$\begin{aligned} K = \; & -2 \ln \left(\mathcal{V} + \tfrac{\xi}{2 g_s^{3/2}} \right) = K_0 - \frac{\xi}{g_s^{3/2} \mathcal{V}} + \mathcal{O}(\mathcal{V}^{-2}) , \\ \xi \equiv \; & -\frac{\chi(Y_6) \zeta(3)}{2(2\pi)^3} . \end{aligned} \tag{2.156}$$

The Euler characteristic of the CY manifold can be expressed in terms of Hodge numbers but, in general, the presence of an O7-plane in the compactification can affect the form of the α' correction, inducing a shift in $\chi(Y_6)$ that gives rise to an effective Euler characteristic [56]:

$$\chi_{\text{eff}}(Y_6) = \chi(Y_6) + 2 \int_{Y_6} \hat{D}_{O7} \wedge \hat{D}_{O7} \wedge \hat{D}_{O7} \tag{2.157}$$

where $\hat{D}_{O7}$ is the 2-form that is Poincaré dual to the divisor wrapped by the O7-plane. In presence of O7-planes, the right form of the leading order α' correction is given by Eq. (2.156) where we replace $\chi(Y_6)$ with $\chi_{\text{eff}}(Y_6)$. From Eq. (2.156) it is easy to derive that α' expansion can be seen as an expansion in inverse powers of the overall volume. We can therefore conclude that it is well defined only if

we consider large values for $\mathcal{V}$. These corrections break the no-scale structure for Kähler moduli and, at leading order, give rise to the following contribution to the scalar potential

$$V_{\alpha'} = \frac{3\xi W_0^2}{4 g_s^{3/2} \mathcal{V}^3} \,. \tag{2.158}$$

String loop corrections These corrections come from loop effects in space-time corresponding to higher-genus string world-sheets and can be related both to the bulk strings and to those located on local objects as Dp-branes. These corrections have been explicitly computed only for $\mathcal{N} = 1$ compactifications on toroidal orientifolds with D5/D9- and D3/D7-branes [57, 58]. Nevertheless, it is possible to extend those results to more general CY compactifications, finding out the string loop corrections dependence on the dilaton and the overall volume of extra dimensions [59, 60, 61, 62]. String loop expansion is governed by the parameter g_s and shows two main types of contributions: Kaluza-Klein and winding corrections:

$$\delta K_{g_s} = \delta K_{g_s}^{KK} + \delta K_{g_s}^{W} \,. \tag{2.159}$$

- **Kaluza-Klein corrections:** these contributions come from the exchange between D3-branes (or O3-planes) and D7-branes (or O7-planes) of closed strings carrying KK momentum. These can be parametrised as

$$\delta K_{g_s}^{KK} \sim \sum_{i=1}^{h^+_{1,1}} \frac{C_i^{KK}(U,\bar{U})}{\mathrm{Re}(S)\mathcal{V}} t_i^{\perp} \,, \tag{2.160}$$

  where C_i^{KK} are unknown functions of complex structure moduli and $t_i^{\perp}$ is the linear combination of 2-cycles volumes t^j that controls the distance between D3-branes/O3-planes and D7-branes/O7-planes.

- **Winding corrections:** these corrections come from the exchange of closed strings with non-vanishing winding between intersecting stacks of D7-branes (or D7-branes and O7-planes).

$$\delta K_{g_s}^{W} \sim \sum_i \frac{C_i^{W}(U,\bar{U})}{\mathcal{V} t_i^{\cap}} \tag{2.161}$$

  where C_i^W are unknown functions of complex structure moduli and $t_i^{\cap}$ is the 2-cycle parametrising the volume where D7-branes/O7-planes intersect.

The contribution of these corrections to the scalar potential at 1-loop order for a general CY is given by

$$\delta V_{g_s} \sim \frac{W_0^2}{\mathcal{V}^2} \left(\sum_i \frac{(C_i^{KK})^2}{(\mathrm{Re}(S))^2} K_{0,ii} - 2\delta K_{g_s}^{W} \right) \,. \tag{2.162}$$

2.3.9 Large Volume Scenario

The *Large Volume Scenario* (LVS) [63] describes a way to stabilise Kähler moduli using the interplay between non-perturbative corrections to the superpotential and the leading order α' correction to the Kähler potential:

$$\begin{cases} K &= K_0 - 2\ln\left(\mathcal{V} + \frac{\hat{\xi}}{2}\right) \\ W &= W_0 + \sum_i A_i e^{-a_i T_i}\,. \end{cases} \tag{2.163}$$

where $\hat{\xi} = \frac{\xi}{g_s^{3/2}}$. In this setup both complex structure moduli and the dilaton get stabilised at tree-level as explained in Sec. 2.3.7. Peculiarities of the Large Volume Scenario (LVS) are:

- We find a non-supersymmetric anti-de Sitter minimum of the scalar potential at exponentially large volume.
- Non perturbative effects do not destabilise the flux-stabilised complex structure moduli and the dilaton.
- Supersymmetry is mostly broken by the F-terms of the Kähler moduli
- The gravitino mass is exponentially suppressed with respect to M_P, allowing to get low-energy supersymmetry in a natural way.

In addition LVS stabilisation holds if $h^+_{1,1} > 1$ and the leading order α' correction generates a positive contribution to the F-term scalar potential, i.e. if $h^-_{1,2} > h^+_{1,1}$ so that $\chi(Y_6) < 0$. In the simplest setup, the volumes of the compact space takes the so called "swiss-cheese" form:

$$\mathcal{V} = \alpha\left(\tau_b^{3/2} - \sum_{i=1}^{h^+_{1,1}-1} \lambda_i \tau_i^{3/2}\right) \tag{2.164}$$

where $\tau_b^{3/2}$ is a large 4-cycle controlling the size of the extra-dimensions, $\tau_i^{3/2}$ are local blow-up modes while α and λ_j are coefficients related to the intersection numbers of the compact space. In the simplified case of $h^+_{1,1} = 2$, $h^-_{1,1} = 0$, after complex structure and dilaton stabilisation, the leading contribution to the F-term scalar potential is given by

$$V_F \simeq \frac{8a_s^2|A_s|^2\sqrt{\tau_s}}{3\alpha\mathcal{V}\lambda_s} e^{-2a_s\tau_s} + \frac{4|W_0 A_s| a_s\tau_s}{\mathcal{V}^2} e^{-a_s\tau_s}\cos(a_s\rho_s) + \frac{3|W_0|^2\hat{\xi}}{4\mathcal{V}^3} \tag{2.165}$$

where the subscript s is referred to the single local blow-up mode whose Kähler field is defined as $T_s = \tau_s + i\rho_s$. The first step in the LVS procedure is given by ρ_s stabilisation at

$$a_s\langle\rho_s\rangle = \pi \pm 2\pi k\,, \qquad k \in \mathbb{Z}\,. \tag{2.166}$$

after which the F-term potential becomes

$$V_F \simeq \frac{8a_s^2|A_s|^2\sqrt{\tau_s}}{3\alpha\mathcal{V}\lambda_s}e^{-2a_s\tau_s} - \frac{4|W_0A_s|a_s\tau_s}{\mathcal{V}^2}e^{-a_s\tau_s} + \frac{3|W_0|^2\hat{\xi}}{4\mathcal{V}^3}\,. \tag{2.167}$$

Looking at the previous equation, we see that there is a particular limit in which this scalar potential approaches zero from below:

$$\mathcal{V} \to \infty\,, \qquad a_s\tau_s = \ln(\mathcal{V}) \tag{2.168}$$

this is called LVS limit. Imposing the previous constraint, Eq. (2.167) can be re-written as V_{LVS}:

$$V_{LVS} \simeq \frac{8a_s^{3/2}|A_s|^2\sqrt{\ln(\mathcal{V})}}{3\alpha\mathcal{V}^3\lambda_s} - \frac{4|W_0A_s|\ln(\mathcal{V})}{\mathcal{V}^3} + \frac{3|W_0|^2\hat{\xi}}{4\mathcal{V}^3}\,. \tag{2.169}$$

where we see that that the second term overcomes both the first and the third term. Therefore we have, at leading order, that the scalar potential approaches zero from below:

$$V_{LVS} \sim -\frac{\ln(\mathcal{V})}{\mathcal{V}^3}|W_0A_s| \tag{2.170}$$

Since it can be shown that, at smaller volumes (but large enough to allow α' perturbative expansion), the dominant term in the scalar potential might be either the first or the third one and they can be shown to be both positive definite, we get that the potential, approaching zero from negative values in LVS, must show a large volume anti de-Sitter minimum. The minimum of this potential is given by the value of the volume at which the second term starts dominating the other two terms, we can conclude that this occurs for large values of $\ln(V)$.

The proper LVS stabilisation sets the following values for the overall volume and the small cycle VEVs:

$$\langle\tau_s\rangle^{3/2} \simeq \frac{\hat{\xi}}{2}\left(1 + 2\epsilon_s\right)\,, \qquad e^{-a_s\langle\tau_s\rangle} = \frac{3\sqrt{\tau_s}|W_0|}{4a_s|A_s|\mathcal{V}}\frac{(1-4\epsilon_s)}{(1-\epsilon_s)}\,, \tag{2.171}$$

where

$$\epsilon_s \equiv \frac{1}{4a_s\tau_s} \sim \mathcal{O}([\ln(\mathcal{V})]^{-1}) \ll 1\,. \tag{2.172}$$

From the previous equations we see that the LVS minimum lies at exponentially large volume $\mathcal{V} \sim e^{a_s\tau_s} \gg 1$ and, contrary to the KKLT setup [64], does not require any fine-tuning on the tree-level superpotential $W_0 \sim 1 \div 100$. On the other

hand, since the value of the scalar potential in its minimum gives the value of the cosmological constant we must find a way to uplift this negative minimum to a de-Sitter vacuum. This can be done by switching on magnetic fluxes on D7-branes [64], adding anti D3-branes [65, 66, 67, 68, 69, 70, 71, 72], hidden sector T-branes [73], non-perturbative effects at singularities [74] or non-zero F-terms of the complex structure moduli [75]. If some of the Kähler moduli do not appear in the superpotential, then their axionic partners, i.e. the imaginary parts of Kähler moduli, remain unstabilised giving no contribution to the scalar potential. This is what happens for the imaginary part of the volume modulus ρ_b. We can also see that the LVS minimum must be non-supersymmetric since $V_F \sim O(1/\mathcal{V}^3)$ at the minimum while $e^K|W|^2 \sim O(1/\mathcal{V}^2) \simeq m_{3/2}^2$.

In LVS models provide a natural hierarchy between energy scales that can be parametrised by inverse powers of the overall volume; this is shown in Table 2.1. In this setup most of the moduli receive a mass of order $m_{3/2}$ except for the volume mode and its related axion ρ_b.

Reduced Planck mass	$\sim 10^{18}$ GeV
String mass	$M_s = M_P/\mathcal{V}^{1/2}$
Kaluza-Klein scale	$M_{KK} = M_P/\mathcal{V}^{2/3}$
Gravitino mass	$m_{3/2} = M_P W_0/\mathcal{V}$
Volume modulus mass	$M_{\tau_b} = M_P W_0/\mathcal{V}^{3/2}$
Volume modulus axion	$M_{\rho_b} \sim 0$

Table 2.1: Relation between energy scales in Swiss-cheese LVS models.

2.3.10 Axions and ALPs from strings

The low-energy spectrum below the compactification scale generically contains many axion-like particles which arise either as closed string axions which are the Kaluza-Klein zero modes of 10D antisymmetric tensor fields or as the phase of open string modes. While the number of closed string axions is related to the topology of the internal manifold, the number of open string axions is more model dependent since their existence relies upon the brane setup. It is essential to notice that, although string compactification suggests plenty of candidates for axion and axion-like weakly interacting particles, there are several known mechanisms by which they can be removed from the low energy spectrum.

Closed string axions

In String Theory axion like particles coming from closed string modes arise from the integration of p-forms gauge field potentials over p-cycles of the compact space [21]. In what follows we consider type IIB where axions arise as integration of the NS-NS 2-form B_2 and R-R 2-form C_2 over 2-cycles Σ_2^I or from integration of R-R 4-form C_4 over 4-cycles Σ_4^I. Another axion is given by R-R 0-form C_0. In order to understand where these axionic particles come from, we define the set of harmonic $(1,1)$-forms $\hat{D}_I$, $I = \{1, \dots, h_{1,1}\}$ that comprises the Dolbeault cohomology group $H^{1,1}(Y_6)$ and the dual basis $\hat{\tilde{D}}_I$ of $H^{2,2}(Y_6)$ that satisfy the following normalisation condition:

$$\int_{\Sigma_2^I} \hat{D}^J = \alpha' \delta_I^J; \qquad \int_{\Sigma_4^I} \hat{\tilde{D}}^J = (\alpha')^2 \delta_I^J \,. \tag{2.173}$$

The 4D axion-like fields arising in $\mathcal{N} = 2$ 4D supergravity from CY string compactifications are:

$$b_I = \frac{1}{\alpha'} \int_{\Sigma_2^I} B_2 \,; \qquad c_I = \frac{1}{\alpha'} \int_{\Sigma_2^I} C_2 \,; \qquad \rho_I = \frac{1}{(\alpha')^2} \int_{\Sigma_4^I} C_4 \,. \tag{2.174}$$

These are the scalar degrees of freedom appearing in the four-dimensional 2- and 4-forms of Eqs. (2.96), (2.97). As we saw in Sec. 2.3.5, after orientifold involution the cohomolgy group $H^{1,1}$ splits into a direct sum of orientifold even and orientifold odd 2-forms cohomology. Therefore, $\hat{D}^I$ decomposes into $\hat{D}^{i_+}$ (even) and $\hat{D}^{i_-}$ (odd) respectively, where $i_+ = 1, \dots, h^{1,1}_+$, $i_- = 1, \dots, h^{1,1}_-$ and $h^{1,1}_+ + h^{1,1}_- = h^{1,1}$. After we determine the invariant scalar degrees of freedom, we need to rearrange them into the bosonic components of chiral multiplets of $\mathcal{N} = 1$ supersymmetry. The proper coordinates of moduli are the axio-dilaton (S), the 2-form field (G^{i_-}), Kähler moduli (T_{i_+}) and complex structure moduli (U^{α_-}) that we defined in Eqs. (2.109 - 2.112), s(2.115). The axionic content of the $\mathcal{N} = 1$ EFT coming from closed string modes is then given by the fields C_0, c_{i_-}, b_{i_-}, ρ_{i_+}, whose number depends on the geometrical structure of extra dimensions.
Due to topological charge quantisation, closed string axions appear in the theory equipped with a periodicity that is equal to integer multiples of the Planck mass:

$$a \equiv a + k \qquad k \in \mathbb{Z} \,, \qquad a = \{C_0,\ c_{i_-},\ b_{i_-},\ \rho_{i_+}\} \tag{2.175}$$

and enjoy a continuous shift-symmetry. The continuous symmetry related to C_0 and b_{i_-} is broken by the presence of background fluxes or Dp-branes, while C_4 and C_2 axions are stabilised through non-perturbative effects. The decay constant of these axion fields is determined by the eigenvalues of the Kähler metric $K_{I\bar{J}}$. We will focus for simplicity on C_4 axions, but similar arguments hold for C_0, C_2 and

B_2 axions. The kinetic part of the 4D Lagrangian will contain the following terms associated to T_i

$$\mathcal{L} \supset K_{i\bar{j}} \partial_\mu T^i \partial^\mu \bar{T}^j = \frac{g_{ij}}{2} \left(\partial_\mu \tau^i \partial^\mu \tau^j + \partial_\mu \rho^i \partial^\mu \rho^j \right) \tag{2.176}$$

where $K_{i\bar{j}} = \frac{\partial^2 K}{\partial T^i \partial \bar{T}^j}$ and K is the Kähler potential of the theory. Given the periodicity of Eq. (2.175) and since in usual situations we want to interpret the axion field as an angle, first of all we have to diagonalise the Kähler metric and find the axion metric eigenvalues λ_i and eigenvectors $\tilde{\rho}_i$. These will have the same periodicity as the original coordinates. After that, we define the canonically normalised axion fields as $\phi_i = \sqrt{\lambda_i} \tilde{\rho}_i M_p$ (restoring proper powers of M_p). The rotated Lagrangian will look like [76]:

$$\mathcal{L}_{kin} \supset \frac{\lambda_i M_p^2}{2} \partial_\mu \tilde{\rho}_i \partial^\mu \tilde{\rho}_i = \frac{1}{2} \partial_\mu \phi_i \partial^\mu \phi_i \,. \tag{2.177}$$

The canonical axion periodicity is then given by:

$$\phi_i \quad \rightarrow \quad \phi_i + 2\pi f_i \qquad \text{where} \qquad f_i = k_i \sqrt{\lambda_i} \, \frac{M_p}{2\pi} \tag{2.178}$$

and f_i is the axion decay constant. The value of k_i in Eq. (2.178) is determined by considering non-perturbative corrections to the superpotential which break the continuous C_4 axion shift symmetry down to a discrete one and develop a potential proportional to $\cos(a_i \rho_i)$ where $a_i = 2\pi/N_i$, $N_i \in \mathbb{N}^+$. The periodicity is therefore given by $k_i = N_i$.

As just mentioned, closed string axions that are massless at tree-level only get a mass through non-perturbative corrections to the superpotential. Depending on the stabilisation procedure, they can be either heavy or light. For instance, working with Kähler moduli, we have that if both axion and saxion are stabilised through non-perturbative corrections to the superpotential, they will show a mass degeneracy and their mass would be of the same order as the gravitino one $m_{3/2}$. The same happens if we stabilise the axio-dilaton using type IIB three-form fluxes that break SUSY. On the other hand, in LVS models, we can find ways to stabilise saxions using perturbative corrections to the Kähler potential, thus allowing for $m_{axion} \ll m_{saxion} \sim m_{3/2}$. This last case, where we can break mass degeneracy, gives rise to a richer phenomenology and allows axion-like particles to span a wide range of masses and decay constants. This goes under the name of string Axiverse [76].

Open string axions

If we are dealing with Calabi-Yau manifolds which contain collapsed cycles carrying a $U(1)$ charge, we might work with open string axions coming from anomalous U(1)

symmetries belonging to the gauge theory located at the singularity. Indeed, the presence of these particles in the theory is not straightforward and requires several constructions that we briefly list below. We will focus on an open string complex scalar matter field $C = |C|e^{i\sigma}$ which lives on a collapsed cycle, τ_{seq}. The general form of the Kähler potential and superpotential, which describe the theory for the shrinked cycle near the singularity, are given by

$$K = -2\ln\left(\mathcal{V} + \frac{\hat{\xi}}{2}\right) + \lambda_{seq}\frac{\tau_{seq}^2}{\mathcal{V}} + K_{matter}\,, \tag{2.179}$$

$$W = W_0 + \sum_{i=1}^{h_{1,1}} A_i\, e^{-a_i T_i} + W_{matter}\,, \tag{2.180}$$

where W_{matter} and K_{matter} are related to the matter sector contributions depending on the field C. The general form of K_{matter} in presence of a single matter field is given by

$$K_{matter} = \mathcal{K}(T_i, \bar{T}_i)C\bar{C}\,, \tag{2.181}$$

where $T_i = \tau_i + i\,\rho_i$ are Kähler moduli. In order to understand the properties of the ultra light axion candidate, σ, we sum up the moduli stabilisation procedure for sequestering scenario in LVS models, [77, 78, 79]. Since we want to have an ALP, we need to find a Peccei-Quinn mechanism related to the breakdown of the $U(1)$ associated to C, such that $\langle|C|^2\rangle \neq 0$. This can be achieved through D-term scalar potential stabilisation that allows us to fix a combination of the matter field $|C|$ and τ_{seq} given by

$$|\hat{C}|^2 \sim \frac{\partial K}{\partial \tau_{seq}}\,. \tag{2.182}$$

This combination fixes the supersymmetric partner of the axion that is eaten up in the process of anomaly cancellation. For sequestered models it is possible to find that the closed string axion related to τ_{seq} is eaten up, while the open string axion σ can be still considered as a flat direction, i.e. it remains a good axion candidate. The non-vanishing VEV and the mass of $|C|$ can be found computing soft-term corrections after super-symmetry breaking, they scale as

$$\langle|\hat{C}|\rangle \sim \frac{1}{\mathcal{V}^{\alpha_2-2}}\,; \qquad \langle\tau_{seq}\rangle \sim \frac{1}{\mathcal{V}^{2\alpha_2-5}}\,, \tag{2.183}$$

where $\alpha_2 = 3, 4$ depending on whether we are considering sequestering or super-sequestering scenario respectively. We immediately see that working in LVS allows us to stabilise both fields also ensuring the validity of the sequestered hypothesis,

i.e. $\tau_{seq} \ll 1$. These axions will have decay constants which scale like

$$\begin{aligned} &f_\sigma \propto \tfrac{1}{\mathcal{V}} \quad \tau_{seq} \propto \tfrac{1}{\mathcal{V}} && \text{when } \alpha_2 = 3\,; \\ &f_\sigma \propto \tfrac{1}{\mathcal{V}^2}\,; \quad \tau_{seq} \propto \tfrac{1}{\mathcal{V}^3} && \text{when } \alpha_2 = 4\,. \end{aligned} \tag{2.184}$$

Finally, we need a mechanism to develop a small but non negligible mass to σ, this can be achieved through hidden sector strong dynamics instanton effects. The scale of strong dynamics in the hidden sector is

$$\Lambda_{hid} = \Lambda_{UV} e^{-c/g^2} \tag{2.185}$$

where, in our case, $\Lambda_{UV} = M_p$, $g^{-2} = Re(S)$ and c is an $\mathcal{O}(1)$ parameter that is fixed by 1-loop β function. These quantities fix σ mass scale to be

$$m_\sigma^2 = \Lambda_{hid}^4 / f_\sigma^2\,. \tag{2.186}$$

Open string axions are more model dependent than closed string axions since their presence relies on the possibility of having fractional D3-branes at del Pezzo singularities. Nevertheless, allowing for decay constants at intermediate scales $\mathcal{O}(10^{13})$ GeV (much smaller that those ones predicted by closed string axions), they are particularly interesting from the phenomenological point of view and are the best candidates for representing QCD axion.

2.4 Inflation from string theory

Cosmic inflation represents the most promising extension of the Standard Cosmological Model and describes the period that precedes the standard Big Bang cosmology. It provides a simple explanation for the homogeneity and the isotropy observed in the universe on very large scales. Moreover, inflation can source the temperature fluctuations observed in the Cosmic Microwave Background, as well as the the primordial perturbations that gave rise to Large Scale Structure formation.

A key ingredient for the success of inflation is the presence of a scalar field (or a combination of them) that undergoes a slow-roll motion for enough time, which is attainable if its potential is sufficiently flat.

The aim of string cosmology is to provide a compactification that, after dimensional reduction, can lead to an effective 4D theory with a viable inflationary dynamics and that can predict in the post-inflationary period (after reheating) the right abundance of dark matter and dark radiation. Moreover it should be able to reproduce the SM degrees of freedom and the standard cosmological history of the Universe that we described in Sec. 1.2. As it can be easily guessed, this is far

from being an easy task. Let us then give an overview of the major requirements that such a theory needs to satisfy in order to be constructed with the current technical and computational limitations of string theory.

The fundamental scale of string theory is the string scale $M_s = (\alpha')^{-1/2}$. At energies $E \ll M_s$ only the massless string state are exited and the theory can be described as an effective 10D supergravity theory. If $H < M_s$ we can neglect truly stringy effects while if $H > M_s$ inflation should be described in the full string theory. Moreover, the compactification of the 10D space-time comes with a new energy scale, the KK scale $M_{KK} \sim M_s/\mathcal{V}^{-1/6}$, that in the perturbative regime should satisfy $M_{KK} \ll M_s$. If we work at energies $H \ll M_{KK}$ the inflationary theory can be described as a 4D EFT that might be supersymmetric or not depending on the details of the compactification manifold and on the content of the theory. We will focus on models where $H \ll M_{KK}$ so that we can use the results that were developed in the usual EFT approach to inflation. Indeed, working with models having $H > M_{KK}$ requires to give a higher dimensional interpretation of inflation and rethink many of the fundamental answers to the main problems related to the standard Big Bang cosmology that have already been addressed in 4D. For this reason we want to restrict our study to models satisfying

$$H \ll M_{KK} \ll M_s \ll M_p \tag{2.187}$$

and we will work in the Large volume scenario that satisfies this requirement, (see Table 2.1).

In order to construct a string inflation model using a bottom-up approach we need to provide a consistent string compactification choosing a specific extra-dimension manifold and orientifold involution. We also need to introduce a set of Dp-branes and Op-planes that must be consistent with background and gauge fluxes that we turn on through each cycle. Choosing all these features in a consistent way leads to a unique 4D Lagrangian whose accuracy relies only on the current state of the art of the computations related to dimensional reduction. For instance α' and string loop corrections have been computed only to some order and for certain geometries of the extra dimensions manifold. Nevertheless, assuming that the dependence on the powers of the expansion parameters and of the overall volume can be inferred from the known results coming from toroidal orientifold $T^6/(\mathbb{Z}_2 \times \mathbb{Z}_2)$, we can find out those geometry that allow for a successful inflationary dynamics.

Given the plenitude of moduli fields that arise after string compactification it not easy to realise single field inflation in string theory. Indeed fields that have masses comparable to or smaller than H can be classically and quantum mechanically active during inflation. Therefore we should compute the full spectrum of the 4D theory and distinguish between those fields that are heavy $H \ll m$ and can

be integrated out, fields having $H \sim m$ that participate in driving inflation and light spectator fields $m \ll H$ that will be classically frozen during inflation but that can affect physical observables through their quantum fluctuations, e.g. producing isocurvature fluctuations which can be converted into density perturbations through the curvaton mechanism. In general, any field having mass $0 < m_\chi < \frac{3}{2}H^2$ will develop quantum fluctuations during inflation. These fluctuations can carry the field away from its minimum and store energy. When the energy density of the universe becomes comparable to the field mass its classical part starts to oscillate and its energy density scales as matter $\rho_\chi \sim T^{-3}$. After inflation and in particular during radiation domination the energy density of the universe scales as $\rho \sim T^{-4}$ and the relative contribution coming from the field χ increases $\rho_\chi/\rho \sim T$. Thus the field χ may quickly dominate the energy density. Therefore moduli fields can affect the thermal history of the universe. In particular, since moduli in general show gravitational couplings, if they have a mass $m_\chi \lesssim 30$ TeV, they decay during of after Big Bang Nucleosynthesis spoiling the predictions coming from the light elements abundance. This would of course be in contrast with experimental evidence. On the other hand, if moduli fields are too light their gravitational coupling tells us that they would have not been decayed at present time and may cause the overclosure of the universe or they would represent a fraction of dark matter (or dark radiation if they are relativistic) that is too high compared to the observed abundance. All these constraints go under the name of *Cosmological moduli problem (CMP)* [80, 81, 82, 83].

From an effective field theory point of view, given the high sensitivity of inflation to quantum corrections, a simple way to protect the flatness of the inflationary potential against them is to assume a symmetry that forbids any dangerous operator. Nevertheless using an EFT approach shows some limitations due to the incomplete knowledge of the UV structure and in particular of quantum gravity. It is then crucial for any effective inflationary model to be embedded in an UV complete theory, such as string theory, where we have a complete formulation of quantum gravity and in principle all the corrections to the inflationary potential can be in principle explicitly computed at any order [84, 85, 86, 87, 21]. Working with a compact space we cannot have a complete decoupling between different sectors in the geometric regime. This means that we cannot treat moduli stabilisation and the inflationary dynamics as separated problems. Integrating out massive fields which couple to two different and geometrically separated sectors can lead to higher-dimensional operators that are less than Planck-suppressed and may spoil the flatness of the inflaton potential. For instance, the couplings between spatially separated D-brane sectors will be at least gravitational (one exception is given by sequestered scenario). This kind of problems arise each time we have a moduli-stabilising energy that is generically of the same order as the inflationary

energy and goes under the name of eta (η) problem [84, 85]. In $\mathcal{N} = 1$ supergravity, Planck-suppressed corrections more often appear in Kähler potential than in the superpotential that receives only non-perturbative corrections due to its holomorphicity. Indeed the main source of relevant Planck-suppressed operators comes from α' and string loop corrections. Besides, in string theory, it is possible to *justify* the presence of symmetries that protect the flatness of the potential from a top-down perspective. In particular, two common approximate symmetries that we are going to introduce in the next sections and that have led to the construction of inflationary models in string theory are: i) non-compact symmetries associated to Kähler moduli fields, the so called *extendend no-scale structure* [88], and ii) compact symmetries associated to axion fields [89, 90].

In addition embedding inflation in a fundamental theory, like string theory, is the only way to study the reheating period. This indeed requires to know what are the relevant degrees of freedom at the inflationary epoch and what are the couplings between the inflaton field (or fields in case of multifield inflation) and the other light fields in the theory belonging both to hidden sectors and to the visible sector (standard model particles). Knowing the microscopical field dependence of such couplings (that can only be a function of the string length and of the VEVs of heavy fields) can allow us to give a precise estimate of the different branching ratios related to the inflaton decay into visible, dark matter and dark radiation particles. This would potentially restrict the allowed number of string vacua that need to be considered in order to reproduce inflation together with standard cosmology and the SM.

In the rest of this thesis we will be dealing with large field inflation models: these are models where the distance travelled by the inflaton during inflation is trans-Planckian $\Delta\phi \gg M_p$. It was first pointed out by Lyth [91] that these models are the only ones that can give rise to detectable primordial gravitational waves. Nevertheless finding a trajectory in field space that is large in Planck units and so flat that it is suitable for inflation is not an easy task [84, 85]. The simplest example that describes this problem in the context of low-energy supergravity descriptions is given by writing down all the possible corrections to the Kähler potential

$$K = K_{cl}(\Phi, \Phi^\dagger) + M_p^2 \sum_i c_i \left(\frac{\Phi\Phi^\dagger}{M_p^2}\right)^{i+1} \tag{2.188}$$

where K_{cl} is the classical Kähler potential and c_i are either constants or functions of other fields in the theory. Given that in large field inflation $\phi > M_p$, unless c_i turn out to be very small, the series is badly divergent, the theory is not really described by the classical Kähler metric and the inflationary dynamics can be destroyed. This kind of argument was used for instance to constraint the allowed field excursion in D3-brane inflation in a warped throat region [92]. Notice that

small field models, despite $\Delta\phi \ll M_p$, can still be destroyed by Planck-suppressed higher-dimensional operators. This is the famous η-problems whose solution in general requires fine-tuning. An interesting setup where it seems to be natural to look for large inflation models is the closed string sector where the field ranges correspond to distances in the space of geometric moduli. A prominent example is given by the decompactification direction that is an infinite direction in the moduli space. We saw that in 4D EFT coming from string theory the tree-level Kähler potential is a function of the overall volume, $K = -2M_p^2 \ln(\mathcal{V})$, so, defining the canonically normalised radius modulus as $R = M_p\sqrt{2}\ln(\mathcal{V})$, it is easy to see that the range of R between a fixed volume $\mathcal{V}_0$ and the decompactification limit $\mathcal{V} \to \infty$ is arbitrarily large. We will see that a viable large-field inflation model that comes from similar considerations and does not require fine-tuning is given by fibre inflation, where the inflaton field is given by a modulus measuring the volume of a $K3$ fibre.

We start the next section giving a brief review of Kähler moduli inflation, focusing in particular on Fibre inflation models that will be further analysed in Chapters 3 and 4. After that, we quickly summarise axion inflation models and their possible embedding in string theory.

2.4.1 Kähler moduli inflation

One of the first ideas related to string cosmology was that the role of the inflaton field could be played by a modulus. One of the most characteristic features of 4D EFT from strings is the presence of the overall volume modulus and of Kähler moduli in general. In addition these fields are flat at tree-level thanks to the no-scale structure that we discussed in Sec. 2.3.7 and they can get stabilised by quantum corrections whose form depends on the geometry and the field content of the compactification. This means that different compactifications give rise to different Kähler moduli potentials that may lead to both small and large field inflation models.

Historically the first proposal was *Racetrack inflation* [93]. This model considers a KKLT-like compactification with a single Kähler modulus T that represents the inflaton. As we already mentioned, the overall volume has an arbitrary field range that goes from fixed values to arbitrary large values corresponding to the decompactification limit. Therefore this setup can be a breeding ground for large field inflation. The axio-dilaton and complex structure moduli are assumed to be stabilised by background fluxes. The only difference with standard KKLT is that the non-perturbative corrections to the superpotential arise through gaugino condensation in a theory with a product gauge group as $SU(N) \times SU(M)$:

$$W = W_0 + Ae^{-aT} + Be^{-bT} \tag{2.189}$$

where $a = 2\pi/N$ and $b = 2\pi/M$ and W_0, A and B can are constants that depend on the VEVs of the flux-stabilised moduli. In addition ,in order to break supersymmetry, the model requires the presence of an anti-D3-brane in a warped throat region that lead to a scalar potential contribution of the form

$$\delta V_{\bar{D}3} = \frac{\rho}{(T+\bar{T})^2} \tag{2.190}$$

where ρ depends on the warp factor at the location of the anti-D3-brane. For suitable values of the parameters A, B, a, b, W_0, ρ the potential can develop a saddle point that can be suitable for inflation. Different models have been created such that the inflationary dynamics mainly takes place along the overall volume axion $\mathrm{Im}(T)$ or modulus $\mathrm{Re}(T)$[94, 95]. Nevertheless, some of these models require a consistent amount of fine tuning, others need large values of N and M that may be difficult to construct in explicit compactifications since D7-branes, backreacting on the the geometry of extra dimensions, may lead Y_6 away from conformal CY structure. Furthermore, the validation of this model would require to perform a full Kähler moduli stabilisation adding α' and string loop corrections to the Kähler potential. Given the high level of fine-tuning required to have a successful inflationary dynamics, these terms can in fact destabilise the Kähler modulus or spoil the flatness of the inflationary potential.

Other interesting models of Kähler moduli inflation have been constructed in the Large Volume Scenario. Given that α', KK and winding corrections to the Kähler potential scale as

$$\delta K_{g_s}^{KK} \sim \frac{t^i}{\mathcal{V}}\,, \qquad \delta K_{g_s}^{W} \sim g_s \frac{1}{t^i \mathcal{V}}\,, \qquad \delta K_{\alpha'} \sim \frac{1}{\mathcal{V}} \tag{2.191}$$

one may think that in the large volume limit KK corrections may overcome α' corrections. Actually, it has been shown that, despite KK corrections dominate over α' corrections, the former cancels to a certain degree in the scalar potential, this is known as *extended no-scale structure* [61]. We can schematically see how this happens studying the simplest example with a single Kähler modulus. We can write the Kähler potential as

$$K = -2\ln(\mathcal{V}) - \frac{\hat{\xi}}{\mathcal{V}} + \frac{\sqrt{\tau}}{\mathcal{V}}\,. \tag{2.192}$$

If we assume that the superpotential is constant W_0, we find that the scalar potential is given by

$$V = \frac{W_0^2}{\mathcal{V}^2}\left(0 + \hat{\xi} + 0\cdot\sqrt{\tau} + \frac{1}{\sqrt{\tau}} + \frac{1}{\tau^{3/2}}\right)\,. \tag{2.193}$$

The first zero in the previous expression is related to the standard no-scale structure, while the second one is a consequence of the extended no-scale structure. It is easy to see that, despite the leading order corrections in Kähler potential comes from KK modes, the higher contribution to the scalar potential is instead given by α' corrections. In LVS Kähler moduli inflation this feature partially protects the flatness of the inflaton potential. Nevertheless, it is mandatory to check whether additional contributions coming from g_s and higher order α' corrections may become dangerously large.

A concrete example that suffers form this problem is *Blow-up inflation*. This model arise from a swiss-cheese compactification in LVS where the CY threefold takes a so-called 'strong Swiss-cheese' form:

$$\mathcal{V} = \lambda_b^{3/2}\tau_b^{3/2} - \sum_{i=1}^{N_{\rm small}} \lambda_i \tau_i^{3/2} \,. \tag{2.194}$$

where τ_b controls the volume of the extra dimensions and τ_i are small blow-up cycles. Complex structure moduli and the dilaton need to be stabilised by background fluxes while the total volume $\mathcal{V}$ as well as the volumes of the $N_{\rm small}$ rigid blow-up divisors τ_i are fixed following the LVS procedure [63, 62] where the leading order α'^3 corrections to the Kähler potential [55, 56, 96] are balanced against non-perturbative contributions to the superpotential [65]. The minimal field requirement for a working model is to have at least 3 Kähler moduli fields: the volume cycle τ_b and two blow up cycles, τ_s and τ_ϕ, one of which plays the role of the inflaton

$$\mathcal{V} = \alpha\left(\tau_b^{3/2} - \lambda_\phi \tau_\phi^{3/2} - \lambda_s \tau_s^{3/2}\right) \,. \tag{2.195}$$

The superpotential has the following form

$$W = W_0 + A_i e^{-a_\phi T_\phi} + A_s e^{-a_s T_s} \,. \tag{2.196}$$

In order to drive inflation without affecting LVS stabilisation τ_ϕ needs to be displaced by its VEV and its motion should not affect $\langle\tau_b\rangle$ and $\langle\tau_s\rangle$. After LVS stabilisation τ_b and τ_s can be integrated out and, for large values of τ_ϕ, the effective inflationary potential becomes:

$$V(\phi) \sim V_0\left(1 - c_1 \mathcal{V}^{5/3}\phi^{4/3} e^{-c_2 \mathcal{V}^{2/3}\phi^{4/3}}\right) \tag{2.197}$$

where $\phi = \sqrt{4\lambda_\phi/(3\mathcal{V})}\tau_\phi^{4/3}$ is the canonically normalised inflaton, while $V_0 \sim W_0^2\hat{\xi}\mathcal{V}^{-3}$, $c_1 \sim \hat{\xi}^{-1}$ and $c_2 \sim 1$ can be considered as constant values. In order to have an exponentially flat potential we need $\mathcal{V}^{2/3}\phi^{4/3} \gg 1$ and, being τ_ϕ a blow-up cycle, we need $\tau_b \gg \tau_\phi$ which means $\phi \ll 1$. Computing string loop corrections

to the inflaton potential we have

$$\delta V_{g_s} \sim \frac{1}{\sqrt{\tau_\phi}\mathcal{V}^3} \sim \frac{1}{\phi^{2/3}\mathcal{V}^{10/3}}\,. \tag{2.198}$$

Given that the minimum of the inflationary potential is $\langle\phi\rangle \sim \ln(\mathcal{V})^{3/4}/\mathcal{V}^{1/2}$ the correction to the η parameter (computed for convenience in the minimum of the inflationary potential) looks like

$$\delta\eta \sim \left.\frac{\delta V''_{g_s}}{V_0}\right|_{\langle\phi\rangle} \sim \left.\frac{1}{\phi^{8/3}\mathcal{V}^{1/3}}\right|_{\langle\phi\rangle} \sim \frac{\mathcal{V}}{\ln(\mathcal{V})^2} \gg 1\,. \tag{2.199}$$

So we see that, despite the presence of an extended no-scale structure, leading order string loop corrections can spoil the flatness of the potential.

The last model that we want to discuss is *Fibre inflation* where the role of the inflaton is played by a large cycle. In this model quantum corrections are balanced against each other, giving rise to an exponentially flat scalar potential.

Fibre inflation models

Fibre inflation models are based on a class of type IIB orientifold flux compactifications with D3/D7-branes and O3/O7-planes where the Calabi-Yau (CY) threefold takes a so-called 'weak Swiss-cheese' form:

$$\mathcal{V} = f_{3/2}(\tau_j) - \sum_{i=1}^{N_{\rm small}} \lambda_i \tau_i^{3/2} \quad \text{with} \quad j = 1, ..., N_{\rm large}\,, \tag{2.200}$$

where $h^{1,1} = N_{\rm large} + N_{\rm small}$ and $f_{3/2}$ is a homogeneous function of degree 3/2. In these models, the stabilisation of the Kähler moduli is performed in two steps. Firstly, the total volume $\mathcal{V}$ as well as the volumes of the $N_{\rm small}$ rigid blow-up divisors τ_i are fixed following the LVS procedure. This leaves $N_{\rm flat} = N_{\rm large} - 1 = h^{1,1} - N_{\rm small} - 1$ flat directions which are natural inflaton candidates. These directions can receive a potential at subleading order by g_s corrections due to the exchange of Kaluza-Klein (KK) and winding modes [58, 60, 97, 98, 61] as well as by $(\alpha')^3$ F^4-terms [99, 100]. In the simplest fibre inflation models $h^{1,1} = 3$ and $N_{\rm small} = 1$, so that $N_{\rm flat} = 1$ and

$$\mathcal{V} = \alpha\left(\tau_b\sqrt{\tau_f} - \lambda_s\tau_s^{3/2}\right)\,, \tag{2.201}$$

whereτ_b is the base modulus, while τ_f is called fibre modulus. The latter is the leading order flat direction which parametrises the volume of a K3 surface. The total scalar potential schematically looks like [101, 102, 103, 104]:

$$V = V_{LVS}(\mathcal{V}, \tau_s) + V_{\rm dS}(\mathcal{V}) + V_{\rm inf}(\mathcal{V}, \tau_s, \tau_f)\,, \tag{2.202}$$

where $V_{\rm inf}(\mathcal{V},\tau_s,\tau_f) = V_{g_s}^{KK} + V_{g_s}^{\rm W} + V_{F^4} \ll V_{LVS}(\mathcal{V},\tau_i)$ is the inflationary potential. V_{LVS} is the leading order LVS potential which fixes $\mathcal{V}$ and τ_s, $V_{\rm dS}$ is an uplifting contribution to get a dS vacuum which can originate from anti D3-branes [65, 66, 67, 68, 69, 70, 71, 72], hidden sector T-branes [73] or non-perturbative effects at singularities [74], while $V_{g_s}^{KK}$, $V_{g_s}^{\rm W}$ and V_{F^4} are respectively KK, winding string loops and F^4 terms.

In the simplest realisation of fibre inflation the inflationary potential comes from g_s string loop corrections and has the following form

$$V_{g_s} = \frac{W_0^2}{\mathcal{V}^2}\left(A\frac{g_s^2}{\tau_f^2} - B\frac{1}{\sqrt{\tau_f}\mathcal{V}} + C\frac{g_s^2\tau_f}{\mathcal{V}}\right) \tag{2.203}$$

where A, B and C are $\sim\mathcal{O}(1)$ constants that depend on complex structure moduli VEVs. Inflation takes place when τ_f is displaced far form the minimum of its potential that is given by $\langle\tau_f\rangle \sim g_s^{4/3}\mathcal{V}^{2/3}$. Assuming that the motion of τ_f does affect the overall volume VEV, the inflationary potential for the canonically normalised inflaton $\phi = \sqrt{3}\ln(\tau_f)/2$ becomes

$$V(\phi) = V_0\left(1 - \frac{4}{3}e^{-\phi/\sqrt{3}} + \frac{1}{3}e^{-4\phi/\sqrt{3}} + \frac{R}{3}e^{2\phi/\sqrt{3}}\right), \tag{2.204}$$

where $V_0 \sim \mathcal{V}^{-10/3}$ and $R \sim g_s^4 \ll 1$. Given that reproducing the correct normalisation of the scalar power spectrum in fibre inflation models requires $\mathcal{V} \sim \mathcal{O}(10^3)$, the value of the overall volume is not exponentially large. The ratio between LVS potential and the inflationary potential scales like $\sim\mathcal{V}^{1/3}$ and it often happens that multifield inflation calculations must be performed, including τ_s and $\mathcal{V}$, in order to check the goodness of single field approximation. Nevertheless in most cases performing multi-field analysis does not really affect single-field inflation predictions.

In fibre inflation models, the underlying CY threefold is a K3 fibration over a $\mathbb{P}^1$ base which has two decompactification limits, corresponding to either the K3 fibre or the base growing large. Thus, kinematically it is expected that the fibre volume can traverse several Planck units. These LVS inflationary models present a variety of distinct features that make them very promising candidates to realise large field inflation and to discuss explicit global embeddings:

1. The de Sitter uplift is independent of the inflaton. This is contrary to a hypothetical KKLT embedding [65], where the uplift would be inflaton-dependent and, thus, large field inflation would typically destroy the KKLT minimum.

2. The back-reaction of heavy moduli is incorporated and under control, in particular, due to the fact that moduli stabilisation is done in two steps and the leading order potential is independent of the inflaton because of the

extended no-scale cancellation [61]. This is in contrast with the majority of large field models of inflation [105].

3. The possibility to achieve tensor-to-scalar ratios between $r \sim 0.01$ and $r \sim 0.001$ which can be tested by future CMB observations [106, 107].

An explicit realisation of fibre inflation not only places several constraints on the underlying CY geometry, but also on the setup of D-branes and O-planes. We further analyse this model in Chapter 3 where we list the sufficient requirements to build a viable global model which also allows for a chiral visible sector. Moreover in Chapter 4 we study the impact of the ultra-light fields that can be always found in Fibre inflation, e.g base and fibre axions, on the cosmological observables.

2.4.2 Axion inflation

Axion-like particles appear in the 4D effective theory equipped with a continuous shift symmetry to all orders in perturbation theory. Therefore, they can be interpreted as good inflaton candidates and their potential is stable against quantum corrections. In string theory this symmetry can either be broken spontaneously, through non-perturbative effects, or explicitly, through the presence of branes. We saw that the first attempt to find a viable model of axion inflation was given by natural inflation, Eq. (2.56). This model requires the axion decay constant to be $f > 10M_p$ and it has been disfavored by experiments. Nevertheless, looking for a possible embedding of natural inflation leads to an important conclusion that will be valid for all the models that we will introduce later on in this section: there is no known controlled string theory construction that allows for $f \gg M_p$ (in accordance with swampland conjecture applied to axion fields [108]). This implies that the simplest version of natural inflation model does not find neither a top-down justification in string theory, nor an empirical support and so other extensions must be found.
A possible way-out is given by considering two axion fields, with decay constants that satisfy $H < f_1\,, f_2 < M_P$, that are coupled to linear combinations of two confining non-abelian gauge groups:

$$\mathcal{L} \supset \sum_{i=1}^{2}\sum_{a=1}^{2} \frac{\phi_i}{f_i}\frac{c_{ia}}{32\pi^2} Tr\left[F^{(a)} \wedge F^{(a)}\right], \tag{2.205}$$

where c_{ia} are dimensionless coefficients and $F^{(a)}$ are the non-abelian field strengths. For certain combinations of the coefficients c_{ia}, it can happen that a linear combination of the two axion fields shows an effective trans-Planckian decay constant. This is called *axion alignment* [109, 110] and allows to have trans-Planckian field

excursions without violating the constraint on single axion decay constants. Another example that can be found in the literature is *N-flation*[111], where a large number of axions is equipped with the potential in Eq. (2.56) and there is no cross-coupling between different fields. Each axion has a sub-Planckian decay constant and it feels a force given by its own potential. On the other hand the Hubble friction contains the sum of each single axion potential. This slows down the field motion and allows to get the required amount of e-foldings with reduced field displacements: the total field displacement Δ_T must satisfy $\Delta_T = \sum_i \Delta\phi_i > M_p$ but the single field excursion is $\Delta\phi_i \sim \Delta_T/\sqrt{N} < M_p$. In order to work, this mechanism requires a number of axions of order $\mathcal{O}(10^3)$. An explicit realisation of N-flation in type IIB string theory can be found in [112], where the authors use KKLT compactification and work with C_4 axions. This model presents problems related to the renormalisation of the Planck mass that receives corrections proportional to the number of axions through the Euler characteristic of the compactification manifold. In principle, this effect can be softened if $\chi(X_6) \ll h^{1,1}$. It is important to notice that this condition is necessary but maybe not sufficient, since there are higher corrections in α' and g_s expansion that are still not known. This model may need to face another problem: if supersymmetry is spontaneously broken, saxions masses are degenerate with the axion's ones, leading to a much more involved inflationary dynamics. Therefore, it is mandatory to find ways to either break supersymmetry at energies higher than the inflationary scale, or to find perturbative ways to stabilise saxions so that mass degeneracy gets broken. This has been achieved in [113] where however the authors found that N-flation with perturbative Kähler moduli stabilisation tends to be incompatible with a 4D EFT that can be kept under control.

Axion monodromy is the last class of models that we want to mention and relies on the fact that if we explicitly break shift-symmetry, the field space opens up and allows for large field excursions. If the breaking can be made small, additional corrections to the axion potential can be neglected, the trace of the axion shift symmetry protects the structure of the potential over each fundamental domain and inflation is driven by the leading shift-symmetry-breaking term. This effect can be realised when a NS5-brane wraps a 2-cycle Σ_2 in the compact extra dimension space. In this case, the dimensional reduction of the action for the NS5-brane induces a potential for the C_2 axion that is given by:

$$V(c) = \frac{\rho}{(2\pi)^6 g_s^2 \alpha'^2}\sqrt{(2\pi)^2 l^4 + g_s^2 c^2}\,, \tag{2.206}$$

where l is the size of Σ_2 in string units and ρ encodes the warp factor dependence. In these models inflation requires to have a large field excursion and the canonically normalised inflaton shows an asymptotically linear potential. An important problem related to this model is that the remnant of the shift symmetry is not

sufficient to protect the flatness of the potential. Indeed, the presence of the NS5-brane, together with the time-varying axion VEV, alters the D3-brane charge induced on the NS5-brane. In absence of working mechanisms to cancel this induced charge, the axion field gets stuck to a fixed value by Gauss's law. One way to overcome this problem is adding to the theory an anti-NS5-brane that wraps Σ_2, but is located in a different region of the extra dimensions. Indeed, a large D3-brane charge induced on the NS5-brane leads to a significant correction to the warp factor that modifies the Euclidean D3-brane action and modifies the scalar potential, spoiling the inflationary dynamics. A concrete solution, where this effect can be made parametrically small, is to place a NS5-brane and an anti-NS5-brane in a common warped throat [114, 115].

Despite all these models received a lot of attention in the past years and many extensions of them have been studied, no explicit string embedding that is completely under control has been produced. The main problem related to these models is that one needs both trans-Plankian decay constant and field excursion. A possible concrete realisation may require to soften these two requests. In Chapter 6 we study how the coupling between the axion and a $U(1)$ gauge field can reduce the required field excursion through electro-magnetic dissipation. Performing a full numerical analysis we also found that the consequences of such a coupling on the cosmological parameters leave unmistakable imprints that can be detected by future experiments.

Part II

Applications

Chapter 3

Fibre inflation models with chiral matter

3.1 Introduction

Cosmic inflation is an early period of accelerated expansion of our universe which can provide a solution to the flatness and horizon problems of standard Big Bang cosmology. Moreover, quantum fluctuations during inflation can source primordial perturbations that caused the formation of large scale structures and the temperatures anisotropies observed in the cosmic microwave background.

From a microscopic point of view, inflation is expected to be driven by the dynamics of a scalar field undergoing a slow-roll motion along a very shallow potential that mimics a positive cosmological constant. An important feature of inflationary models is the distance travelled by the inflaton in field space during inflation since it is proportional to the amount of primordial gravitational waves which get produced [91]. From an effective field theory point of view, in small field models with a sub-Planckian inflaton excursion, dimension six operators can easily spoil the flatness of the inflationary potential. On the other hand, quantum corrections to large field models with a trans-Planckian field range lead to an infinite series of unsuppressed higher-dimensional operators which seem to bring the effective field theory approach out of control.

These dangerous operators can be argued to be absent or very suppressed only in the presence of a symmetry whose origin can only be postulated from an effective field theory perspective but can instead be derived from an underlying UV complete theory. For this reason inflationary model building in string theory has received a lot of attention [84, 85, 86, 87]. Besides the presence of additional symmetries, string compactifications naturally provide many 4D scalars which can play the rôle of the inflaton. Promising inflaton candidates are type IIB Kähler

moduli which parametrise the size of the extra dimensions and enjoy non-compact rescaling symmetries inherited from the underlying no-scale structure [88].

Identifying a natural inflaton candidate with an appropriate symmetry that protects the flatness of its potential against quantum corrections is however not sufficient to trust inflationary model building in string compactifications. In fact, three additional requirements to have a successful string inflationary model are (*i*) full moduli stabilisation, (*ii*) a global embedding into consistent Calabi-Yau orientifolds with D-branes and fluxes and (*iii*) the realisation of a chiral visible sector.

The first condition is crucial to determine all the energy scales in the model and to check the stability of the inflationary dynamics by controlling the behaviour of the scalar directions orthogonal to the inflaton one. The second condition is instead fundamental to guarantee the consistency of the inflation model from the microscopic point of view by checking the cancellation of all D-brane tadpoles and Freed-Witten anomalies and the actual generation of all the effects needed to stabilise the moduli and to develop the inflationary potential. Finally the requirement of having a model which can give rise to inflation and reproduce at the same time a chiral visible sector is crucial for two main reasons: to ensure the absence of any dangerous interplay between chirality and moduli stabilisation which can forbid the generation of D-terms or non-perturbative effects needed to fix the moduli [116], and to determine the post-inflationary evolution of our universe starting from the reheating process where the inflaton energy density gets converted into the production of visible sector degrees of freedom [117, 118, 119, 120]. Other important post-inflationary issues which can affect the predictions of important inflationary observables like the number of efoldings N_e, the scalar spectral index n_s and the tensor-to-scalar ratio r are periods of matter domination due to light moduli [121, 122, 123], the production of axionic dark radiation from moduli decays [14, 124, 125, 126], non-thermal dark matter [127, 128, 129], moduli-induced baryogenesis [130, 131] and the interplay between the inflationary and the supersymmetry breaking scale [132, 133, 134, 135].

A comprehensive global chiral model which satisfies all these conditions for models where the inflaton is a local blow-up mode [136] has been recently constructed in [137]. The chiral visible sector lives on D3-branes at an orientifolded singularity and full closed string moduli stabilisation in a dS vacuum is achieved by following the LVS procedure [63, 62]. The main limitation of this model is the emergence of an η-problem associated with the presence of large g_s corrections to the effective action which tend to spoil the flatness of the inflationary potential if their flux-dependent coefficients are not tuned small.

In this regard, fibre inflation models [101] look more promising. In these constructions, the inflaton is a fibration modulus which remains exactly massless when

only the leading order no-scale breaking effects are included. The inflationary potential is then generated only at subleading order by a combination of string loop corrections [58, 60, 97, 98] and higher derivative terms [99, 100]. This hierarchy of scales is guaranteed by the extended no-scale cancellation and provides a natural solution to the η-problem [61]. This solution can also be understood from the point of view of an effective non-compact rescaling symmetry for the Kähler moduli [88].

Different versions of fibre inflation models have been constructed so far depending on the microscopic nature of the effects which drive the inflationary dynamics: Kaluza-Klein and winding string loops [101], Kaluza-Klein loops and $\mathcal{O}(\alpha'^3)$ F^4 terms [102], and winding g_s loops combined with higher derivative terms [103]. In all cases the inflationary potential is plateau-like and takes a simple form with a constant term and negative exponentials. Additional positive exponentials show up with coefficients which are naturally very small and give rise to a rising behaviour at large field values. Ref. [104] provided a generalised description of fibre inflation models showing how they can reproduce the correct spectral index observed by Planck [138, 139] while the predicted value of the tensor-to-scalar ratio is in the range $0.001 \lesssim r \lesssim 0.01$. Such a large value of r is compatible with the fact that these are large field models where the inflaton range is around 5 Planck units. An effective supergravity description of fibre inflation models as α-attractors has also been recently given in [140].

Despite all these successes, fibre inflation models are still lacking a complete global embedding into chiral string compactifications. However a first step forward has already been made in [141] where these inflationary models have been successfully embedded in consistent type IIB orientifolds with moduli stabilisation but without a chiral visible sector. In order to have a viable inflationary and moduli stabilisation mechanism, the internal Calabi-Yau manifold has to have at least $h^{1,1} = 3$ Kähler moduli and its volume form has to feature a K3 or T^4 fibration over a $\mathbb{P}^1$ base and a rigid shrinkable blow-up mode [62, 142]. Starting from concrete Calabi-Yau threefolds with these topological properties, ref. [141] provided several different examples with an explicit choice of orientifold involution and D3/D7 brane setups which are globally consistent and can generate corrections to the 4D effective action that can fix all closed string moduli inside the Kähler cone and reproduce the form of the inflationary potential of fibre inflation models. However the case with $h^{1,1} = 3$ is too simple to allow for non-trivial D7 worldvolume fluxes which give rise to chiral matter. In fact, non-zero gauge fluxes induce moduli dependent Fayet-Iliopoulos terms which, in combination with soft term contributions for $U(1)$-charged matter fields, would lift the leading order flat direction, making the inflaton too heavy to drive inflation.

In this chapter we shall extend the results of [141] by considering more complicated Calabi-Yau threefolds with $h^{1,1} = 4$ in order to build global fibre inflation

models with a chiral visible sector. After analysing the topological conditions on the underlying compactification manifold to allow a successful chiral global embedding of fibre inflation models, we find that the simplest examples involve Calabi-Yau threefolds with 3 K3 divisors and a toroidal-like volume with a diagonal del Pezzo divisor suitable to support non-perturbative effects to freeze the moduli. The internal volume is therefore controlled by 3 Kähler moduli and can equivalently be seen as different K3 fibrations over 3 different $\mathbb{P}^1$ bases. After searching through the Kreuzer-Skarke list of Calabi-Yau manifolds embedded in toric varieties [143], we find several concrete examples which admit these topological features.

We then focus on one of them and describe several possible choices of orientifold involution, D-brane setup and gauge fluxes which satisfy global consistency conditions and generate perturbative g_s and α' corrections to the 4D Kähler potential and non-perturbative effects in the superpotential that are suitable to both stabilise the moduli and reproduce the typical potential of fibre inflation models. In particular, non-zero gauge fluxes induce chiral matter on D7-branes wrapped around smooth combinations of the four-cycles which control the overall volume.[1] Moreover, a moduli-dependent Fayet-Iliopoulos term lifts one of the Kähler moduli, so that after D-term stabilisation the effective number of Kähler moduli is reduced to 3 and the internal volume simplifies to the standard expression of fibre inflation models used in the examples of [141].

After computing all relevant loop and higher derivative effects in full detail, we analyse the resulting inflationary dynamics finding an interesting result: the Kähler cone bounds set severe constraints on the allowed inflaton field range when they are combined with other phenomenological requirements, like the generation of the correct amplitude of the power spectrum by the inflaton quantum fluctuations, and consistency conditions like the stability of the inflaton evolution against possible orthogonal runaway directions, the fact that the gravitino mass remains always smaller than any Kaluza-Klein scale in the model and finally that dangerous higher derivative effects do not spoil the flatness of the inflationary potential before achieving enough efoldings of inflation.[2] Because of this tension, we also perform a full multi-field numerical analysis of the inflationary evolution showing how an early period of accelerated expansion occurs generically. On the other hand, the inflaton quantum fluctuations can generate the right amplitude of the density perturbations only if the microscopic parameters take appropriate values.

We believe that our results make fibre inflation models more robust since they represent the first concrete models which are globally consistent and chi-

[1] We do not consider K3 fibred cases where the visible sector lives on D3 branes at singularities since they would lead to dark radiation overproduction [144].

[2] These last two consistency conditions are qualitatively similar since the superspace derivative expansion is under control if $m_{3/2} \ll M_{KK}$ [145].

ral. Nonetheless several issues still need to be investigated further. The most important ones are the inclusion of an explicit uplifting mechanism to realise a dS vacuum, a thorough derivation of the perturbative corrections to the 4D effective action and a better determination of the Calabi-Yau Kähler cone, going beyond its approximated expression inherited from the toric ambient space. We leave the study of these issues for the future.

This chapter is organised as follows. In Sec. 3.2, after presenting a basic review of fibre inflation models, we summarise the minimal requirements that are needed for the construction of a fully consistent global embedding with a chiral visible sector. In Sec. 3.3 we provide a concrete Calabi-Yau example, describing the orientifold involution, the D-brane setup, the choice of gauge fluxes and the resulting chiral spectrum, Fayet-Iliopoulos term and inflationary potential generated by g_s and α' effects. The inflationary evolution is analysed in full detail in Sec. 3.4 by focusing first on the single-field approximation and by studying then the multi-field dynamics. In Sec. 3.5 we draw our conclusions and we discuss a few open issues. App. A.1 contains additional explicit chiral global examples.

3.2 Chiral global inflationary models

Let us begin by displaying the minimal requirements for a successful chiral global embedding of fibre inflation models. A brief review related to these models has been given in Sec. 2.4.1.

3.2.1 Requirements for chiral global embedding

The simplest global embedding of fibre inflation models requires at least three Kähler moduli [141]. However, in order to incorporate also a chiral visible sector we need at least $h^{1,1} = 4$ Kähler moduli. Here we will focus on obtaining chiral matter on D7-branes wrapped around a suitable divisor with world-volume gauge fluxes turned on. In this case D7 gauge fluxes induce a D-term potential for the Kähler moduli that fixes a particular combination thereof. Thus, D-term fixing and the leading order LVS stabilisation mechanism leave just a single flat direction, in our case a K3 fibre, which will play the rôle of the inflaton. In order to obtain a viable chiral global model we require the following ingredients and consistency conditions:

1. A Calabi-Yau with $h^{1,1} = 4$ featuring three large cycles and a shrinkable rigid divisor, so that the internal volume takes the form (2.200) with $N_{\rm small} = 1$. In the explicit example described in Sec. 3.3 the volume simplifies further to:

$$\mathcal{V} = c_a \sqrt{\tau_1 \, \tau_2 \, \tau_3} - c_b \, \tau_s^{3/2} \,, \tag{3.1}$$

with $c_a > 0$ and $c_b > 0$. Each of the 3 moduli τ_1, τ_2 and τ_3 controls the volume of a K3 surface while τ_s parametrises the size of a 'diagonal' del Pezzo divisor [142]. D-term stabilisation will fix $\tau_3 \propto \tau_2$ while the standard LVS procedure will freeze the overall volume $\mathcal{V} \simeq c_a \sqrt{\tau_1 \tau_2 \tau_3}$ and the blow-up mode τ_s. The leading order flat direction can be parametrised by τ_1 which will drive inflation.

2. An orientifold involution and a D3/D7-brane setup with gauge fluxes on the visible D7-brane stacks such that tadpole cancellation is satisfied with enough room for bulk three-form fluxes to be turned on for complex structure and dilaton stabilisation. The D-brane and O-plane setup must also allow for the generation of KK- and/or winding string loop corrections which have the correct form to generate a suitable inflationary potential.

3. A choice of world-volume fluxes which cancels all Freed-Witten anomalies [51, 52] but leads, at the same time, to just a single moduli-dependent Fayet-Iliopoulos (FI) term [146, 147] in order to leave a leading order inflationary flat direction by lifting just one of the two flat directions leftover by the LVS stabilisation mechanism.

4. There should be no chiral intersection between the visible sector and the del Pezzo divisor supporting non-perturbative effects required for LVS moduli fixing as otherwise the prefactor of the non-perturbative superpotential would be vanishing [116]. The absence of these dangerous chiral intersections should be guaranteed by an appropriate choice of gauge fluxes.

5. Moduli stabilisation and inflation have to take place inside the CY Kähler cone and the effective field theory should be well under control with $\langle \mathcal{V} \rangle \gg 1$ and $g_s \ll 1$.

6. In order to trust inflationary model building within an effective field theory, the following hierarchy of scales should be satisfied from horizon exit to the end of inflation:

$$m_{\rm inf} < H < m_{3/2} < M_{KK}^{(i)} < M_s < M_p \,, \tag{3.2}$$

where $m_{\rm inf}$ is the inflaton mass, H is the Hubble constant, $m_{3/2}$ is the gravitino mass which sets the mass scale of all the heavy moduli during inflation, $M_{KK}^{(i)}$ denote various KK scales associated with bulk modes and open string excitations on D7-branes wrapped around four-cycles, M_s is the string scale and M_p is the reduced Planck mass $M_p = 2.4 \cdot 10^{18}$ GeV. Notice that, apart from M_p, all these energy scales are moduli dependent and so evolve during

inflation. After stabilising $\mathcal{V}$ and τ_s à la LVS and fixing one large modulus in terms of another large direction via setting the FI-term to zero, we find that the 'reduced' moduli space of the inflationary direction is in fact a compact interval. Therefore the field space available for inflation is kinematically finite (albeit in general trans-Planckian), a feature of the model which has so far been overlooked. We will state the precise phenomenological and consistency conditions for successful inflation in Sec. 3.4.

3.3 A chiral global example

In this section, we shall present all the topological and model-building details of the global embedding of fibre inflation models into explicit chiral CY orientifolds with $h^{1,1} = 4$.

3.3.1 Toric data

Let us consider the following toric data for a CY threefold whose volume takes the form $\mathcal{V} = c_a \sqrt{\tau_1 \tau_2 \tau_3} - c_b \tau_s^{3/2}$ discussed above:

	x_1	x_2	x_3	x_4	x_5	x_6	x_7	x_8
4	0	0	0	1	1	0	0	2
4	0	0	1	0	0	1	0	2
4	0	1	0	0	0	0	1	2
8	1	0	0	1	0	1	1	4
	dP_7	NdP_{11}	NdP_{11}	K3	NdP_{11}	K3	K3	SD

The Hodge numbers are $(h^{2,1}, h^{1,1}) = (98, 4)$, the Euler number is $\chi = -188$, while the Stanley-Reisner ideal is:

$$\text{SR1} = \{x_1x_4,\, x_1x_6,\, x_1x_7,\, x_2x_7,\, x_3x_6,\, x_4x_5x_8,\, x_2x_3x_5x_8\}\,.$$

This corresponds to the polytope ID #1206 in the CY database of Ref. [148]. A detailed divisor analysis using `cohomCalg` [149, 150] shows that the divisor D_1 is a del Pezzo dP_7 while each of the divisors $\{D_4, D_6, D_7\}$ is a K3 surface. Moreover, each of the divisors $\{D_2, D_3, D_5\}$ is a 'rigid but not del Pezzo' surface with $h^{1,1} = 12$ which we denote as NdP_{11} while D_8 is a 'special deformation' divisors with

Hodge diamond:

$$\text{SD} \equiv \begin{array}{ccccc} & & 1 & & \\ & 0 & & 0 & \\ 23 & & 160 & & 23 \\ & 0 & & 0 & \\ & & 1 & & \end{array}$$

The intersection form in the basis of smooth divisors $\{D_1, D_4, D_6, D_7\}$ can be written as:

$$I_3 = 2\, D_4\, D_6\, D_7 + 2\, D_1^3\,. \tag{3.3}$$

Writing the Kähler form in the above basis of divisors as $J = t_1\, D_1 + t_4\, D_4 + t_6\, D_6 + t_7\, D_7$ and using the intersection polynomial (3.3), the CY overall volume becomes:

$$\mathcal{V} = 2\, t_4\, t_6\, t_7 + \frac{t_1^3}{3}\,. \tag{3.4}$$

The Kähler cone conditions can be derived from the following generators of the Kähler cone:

$$K_1 = -\,D_1 + D_4 + D_6 + D_7\,, \qquad K_2 = D_7\,, \qquad K_3 = D_4\,, \qquad K_4 = D_6\,. \tag{3.5}$$

Expanding the Kähler form as $J = \sum_{i=1}^{4} r_i K_i$, the Kähler cone is defined via the following conditions on the two-cycle moduli:

$$r_1 = -\,t_1 > 0\,, \qquad r_2 = t_1 + t_7 > 0\,, \qquad r_3 = t_1 + t_4 > 0\,, \qquad r_4 = t_1 + t_6 > 0\,. \tag{3.6}$$

Notice that this expression of the CY Kähler cone is only approximate since it is inherited from the Kähler cone of the ambient toric variety.[3] However this procedure can either overcount some curves of the CY threefold, for example if they do not intersect with the CY hypersurface, or miss some of them, if they cannot be obtained as the intersection between two divisors of the ambient space and the CY hypersurface. Hence the actual CY Kähler cone can turn out to be either larger or smaller. This analysis would require a deeper investigation which is however beyond the scope of this work.[4] Here we just mention that this analysis

[3] If the same CY threefold can be realised as a hypersurface embedded in different ambient spaces, the CY Kähler cone is approximated as the intersection of the Kähler cones of the different toric varieties [148].

[4] We however expect that the CY Kähler cone cannot get smaller. In fact, if this were the case, there should exist an extra constraint from requiring the positivity of a curve of the CY which is trivial in the ambient space. But this does not seem to be possible since each CY divisor is inherited from a single toric divisor (i.e. we do not have a toric divisor which splits into two CY divisors, and so where $h^{1,1}$ of the CY is larger than $h^{1,1}$ of the ambient space). In fact, if this trivial curve existed, it should have a dual divisors, and so $h^{1,1}$ of the CY should be larger than $h^{1,1}$ of the ambient case, which is however not the case.

has been performed in detail in [151] where the CY Kähler cone turned out to be larger than the approximated version.

The four-cycle moduli, which can be computed as $\tau_i = \partial_{t_i}\mathcal{V}$, look like:

$$\tau_1 = t_1^2\,, \qquad \tau_4 = 2\,t_6\,t_7\,, \qquad \tau_6 = 2\,t_4\,t_7\,, \qquad \tau_7 = 2\,t_4\,t_6\,, \tag{3.7}$$

and so, using the Kähler cone conditions (3.6), the overall volume reduces to:

$$\mathcal{V} = t_4\tau_4 - \frac{1}{3}\,\tau_1^{3/2} = t_6\tau_6 - \frac{1}{3}\,\tau_1^{3/2} = t_7\tau_7 - \frac{1}{3}\,\tau_1^{3/2} = \frac{1}{\sqrt{2}}\,\sqrt{\tau_4\,\tau_6\,\tau_7} - \frac{1}{3}\,\tau_1^{3/2}\,, \tag{3.8}$$

which shows clearly that the CY threefold X features three K3 fibrations over different $\mathbb{P}^1$ bases. The second Chern class of X is given by:

$$c_2(X) = D_4\,D_5 + 4\,D_5^2 + 12\,D_5\,D_6 + 12\,D_5\,D_7 + 12\,D_6\,D_7\,, \tag{3.9}$$

which results in the following values of the topological quantities $\Pi_i = \int_X c_2 \wedge \hat{D}_i$:

$$\Pi_1 = 8\,, \quad \Pi_2 = \Pi_3 = 16\,, \quad \Pi_4 = 24\,, \quad \Pi_5 = 16\,, \quad \Pi_6 = \Pi_7 = 24\,, \quad \Pi_8 = 128\,. \tag{3.10}$$

The intersection curves between two coordinate divisors are given in Tab. 3.1 while their volumes are listed in Tab. 3.2.

	D_1	D_2	D_3	D_4	D_5	D_6	D_7	D_8
D_1	$\mathcal{C}_3$	$\mathbb{T}^2$	$\mathbb{T}^2$	$\varnothing$	$\mathbb{T}^2$	$\varnothing$	$\varnothing$	$\mathcal{C}_3$
D_2	$\mathbb{T}^2$	$\mathbb{P}^1 \sqcup \mathbb{P}^1$	$\mathbb{P}^1 \sqcup \mathbb{P}^1$	$\mathbb{T}^2$	$\mathbb{P}^1 \sqcup \mathbb{P}^1$	$\mathbb{T}^2$	$\varnothing$	$\mathcal{C}_3$
D_3	$\mathbb{T}^2$	$\mathbb{P}^1 \sqcup \mathbb{P}^1$	$\mathbb{P}^1 \sqcup \mathbb{P}^1$	$\mathbb{T}^2$	$\mathbb{P}^1 \sqcup \mathbb{P}^1$	$\varnothing$	$\mathbb{T}^2$	$\mathcal{C}_3$
D_4	$\varnothing$	$\mathbb{T}^2$	$\mathbb{T}^2$	$\varnothing$	$\varnothing$	$\mathbb{T}^2$	$\mathbb{T}^2$	$\mathcal{C}_9$
D_5	$\mathbb{T}^2$	$\mathbb{P}^1 \sqcup \mathbb{P}^1$	$\mathbb{P}^1 \sqcup \mathbb{P}^1$	$\varnothing$	$\mathbb{P}^1 \sqcup \mathbb{P}^1$	$\mathbb{T}^2$	$\mathbb{T}^2$	$\mathcal{C}_3$
D_6	$\varnothing$	$\mathbb{T}^2$	$\varnothing$	$\mathbb{T}^2$	$\mathbb{T}^2$	$\varnothing$	$\mathbb{T}^2$	$\mathcal{C}_9$
D_7	$\varnothing$	$\varnothing$	$\mathbb{T}^2$	$\mathbb{T}^2$	$\mathbb{T}^2$	$\mathbb{T}^2$	$\varnothing$	$\mathcal{C}_9$
D_8	$\mathcal{C}_3$	$\mathcal{C}_3$	$\mathcal{C}_3$	$\mathcal{C}_9$	$\mathcal{C}_3$	$\mathcal{C}_9$	$\mathcal{C}_9$	$\mathcal{C}_{81}$

Table 3.1: Intersection curves of two coordinate divisors. Here $\mathcal{C}_g$ denotes a curve with Hodge numbers $h^{0,0} = 1$ and $h^{1,0} = g$.

3.3.2 Orientifold involution

We focus on orientifold involutions of the form $\sigma : x_i \to -x_i$ with $i = 1, ..., 8$ which feature an O7-plane on D_i and O3-planes at the fixed points listed in Tab. 3.3. The effective non-trivial fixed point set in Tab. 3.3 has been obtained after taking care of the SR ideal symmetry. Moreover, the total number of O3-planes

	D_1	D_2	D_3	D_4	D_5	D_6	D_7	D_8
D_1	$2\,t_1$	$-2\,t_1$	$-2\,t_1$	0	$-2\,t_1$	0	0	$-4\,t_1$
D_2	$-2\,t_1$	$2\,t_1$	$2(t_1+t_4)$	$2\,t_6$	$2(t_1+t_6)$	$2\,t_4$	0	$4(t_1+t_4+t_6)$
D_3	$-2\,t_1$	$2(t_1+t_4)$	$2\,t_1$	$2\,t_7$	$2(t_1+t_7)$	0	$2\,t_4$	$4(t_1+t_4+t_7)$
D_4	0	$2\,t_6$	$2\,t_7$	0	0	$2\,t_7$	$2\,t_6$	$4(t_6+t_7)$
D_5	$-2\,t_1$	$2(t_1+t_6)$	$4(t_1+t_7)$	0	$2\,t_1$	$2\,t_7$	$2\,t_6$	$4(t_1+t_6+t_7)$
D_6	0	$2\,t_4$	0	$2\,t_7$	$2\,t_7$	0	$2\,t_4$	$4(t_4+t_7)$
D_7	0	0	$2\,t_4$	$2\,t_6$	$2\,t_6$	$2\,t_4$	0	$4(t_4+t_6)$
D_8	$-4\,t_1$	$4(t_1+t_4+t_6)$	$4(t_1+t_4+t_7)$	$4(t_6+t_7)$	$4(t_1+t_6+t_7)$	$4(t_4+t_7)$	$4(t_4+t_6)$	$8(t_1+2(t_4+t_6+t_7))$

Table 3.2: Volumes of intersection curves between two coordinate divisors.

$N_{\rm O3}$ is obtained from the triple intersections restricted to the CY hypersurface, while the effective Euler number $\chi_{\rm eff}$ has been computed as:[5]

$$\chi_{\rm eff} = \chi(X) + 2\int_X [\mathrm{O7}]\wedge[\mathrm{O7}]\wedge[\mathrm{O7}]\,. \tag{3.11}$$

In what follows we shall focus on the orientifold involution $\sigma : x_8 \to -x_8$ which features just a single O7-plane located in D_8 and no O3-plane .

σ	O7	O3	$N_{\rm O3}$	χ(O7)	$\chi_{\rm eff}$
$x_1 \to -x_1$	D_1	$\{D_2D_3D_4, D_2D_4D_6, D_2D_5D_6,$ $D_3D_4D_7, D_3D_5D_7,$ $D_4D_6D_7, D_5D_6D_7\}$	14	10	-184
$x_2 \to -x_2$	$D_2 \sqcup D_7$	$D_1D_3D_5$	2	38	-192
$x_2 \to -x_3$	$D_3 \sqcup D_6$	$D_1D_2D_5$	2	38	-192
$x_4 \to -x_4$	$D_4 \sqcup D_5$	$D_1D_2D_3$	2	38	-192
$x_5 \to -x_5$	$D_4 \sqcup D_5$	$D_1D_2D_3$	2	38	-192
$x_6 \to -x_6$	$D_3 \sqcup D_6$	$D_1D_2D_5$	2	38	-192
$x_7 \to -x_7$	$D_2 \sqcup D_7$	$D_1D_3D_5$	2	38	-192
$x_8 \to -x_8$	D_8	$\varnothing$	0	208	-28

Table 3.3: Fixed point set for the involutions which are reflections of the eight coordinates x_i with $i = 1, ..., 8$.

3.3.3 Brane setup

If the D7-tadpole cancellation condition is satisfied by placing four D7-branes on top of the O7-plane, the string loop corrections to the scalar potential can

[5]The effective Euler number controls the strength of $N = 1$ $\mathcal{O}(\alpha'^3)$ corrections due to O7-planes [56].

involve only KK effects between this D7-stack and O3-planes or D3-branes since winding contributions are absent due to the absence of any intersection between D7-branes and/or O7-planes. Thus loop effects are too simple to generate a viable inflationary plateau. They might even be completely absent in our case since there are no O3-planes and the D3-tadpole cancellation condition could be satisfied without the need to include D3-branes (i.e. just switching on appropriate background three-form fluxes). We shall therefore focus on a slightly more complicate D7-brane setup which gives rise to winding loop effects. This can be achieved by placing D7-branes not entirely on top of the O7-plane as follows:

$$8[\mathrm{O7}] \equiv 8([D_8]) = 16\,([D_2] + [D_4] + [D_6])\ . \tag{3.12}$$

This brane setup involves three stacks of D7-branes wrapped around the divisors D_2, D_4 and D_6. Moreover, the condition for D3-tadpole cancellation becomes:

$$N_{\mathrm{D3}} + \frac{N_{\mathrm{flux}}}{2} + N_{\mathrm{gauge}} = \frac{N_{\mathrm{O3}}}{4} + \frac{\chi(\mathrm{O7})}{12} + \sum_a \frac{N_a\,(\chi(D_a) + \chi(D'_a))}{48} = 38\,,$$

showing that there is space for turning on both gauge and background three-form fluxes for complex structure and dilaton stabilisation.[6] As shown in [152], three-form fluxes stabilise also D7 position moduli and open string moduli living at the intersection between two different stacks of D7-branes since they generate soft supersymmetry breaking mass terms for each of these scalars. On the other hand, there are no Wilson line moduli in our model since $h^{1,0}(D_2) = h^{1,0}(D_4) = h^{1,0}(D_6) = 0$.

Let us point out that other orientifold involutions which could allow for D7-branes not entirely on top of the O7-plane are $x_4 \to -x_4$, $x_6 \to -x_6$ or $x_7 \to -x_7$. In each of these cases, the O7-plane is located on a K3 surface. However, given that $D_4 = D_1 + D_5$, $D_6 = D_1 + D_3$ and $D_7 = D_1 + D_2$, from Tab. 3.1 and 3.2 we see that the resulting D7-brane stacks are either non-intersecting (and so no winding corrections are generated) or the volumes of the intersection curves depend just on the 'small' dP_7 divisor (and so winding loops are inflaton-independent). This is the reason why we chose the involution $x_8 \to -x_8$ where the O7-plane is located on the 'special deformation' divisor D_8 which gives more freedom for D7-brane model building.

[6] We focus on flux vacua where the dilaton is fixed in a regime where our perturbative type IIB analysis is under control.

3.3.4 Gauge fluxes

In order to obtain a chiral visible sector on the D7-brane stacks wrapping D_2, D_4 and D_6 we need to turn on worldvolume gauge fluxes of the form:

$$\mathcal{F}_i = \sum_{j=1}^{h^{1,1}} f_{ij}\hat{D}_j - \frac{1}{2}\, c_1(D_i) - \iota_{D_i}^* B \quad \text{with} \quad f_{ij} \in \mathbb{Z} \quad \text{and} \quad i = 2, 4, 6\,, \tag{3.13}$$

where the half-integer contribution is due to Freed-Witten anomaly cancellation [51, 52].

However we want to generate just one moduli-dependent Fayet-Iliopoulos term in order to fix only one Kähler modulus via D-term stabilisation. In fact, if the number of FI-terms is larger than one, there is no light Kähler modulus which can play the rôle of the inflaton. Moreover we wrap a D3-brane instanton on the rigid divisor D_1 in order to generate a non-perturbative contribution to the superpotential which is crucial for LVS moduli stabilisation. In order to cancel the Freed-Witten anomaly, the D3-instanton has to support a half-integer flux, and so the general expression of the total gauge flux on D_1 becomes (with $c_1(D_1) = -\hat{D}_1$):

$$\mathcal{F}_1 = \sum_{j=1}^{h^{1,1}} f_{1j}\hat{D}_j + \frac{1}{2}\hat{D}_1 - \iota_{D_i}^* B \quad \text{with} \quad f_{1j} \in \mathbb{Z}\,. \tag{3.14}$$

However a non-vanishing $\mathcal{F}_1$ would not be gauge invariant, and so would prevent a non-perturbative contribution to the superpotential. We need therefore to check if it is possible to perform an appropriate choice of B-field which can simultaneously set $\mathcal{F}_4 = \mathcal{F}_6 = 0$ (we choose to have a non-vanishing gauge flux only on D_2 to have just one moduli-dependent FI-term) and $\mathcal{F}_1 = 0$. Recalling that both D_4 and D_6 are K3 surfaces which are spin divisors with $c_1(D_4) = c_1(D_6) = 0$ (since the K3 is a CY two-fold), if we set:

$$B = \frac{1}{2}\,\hat{D}_1\,, \tag{3.15}$$

the condition $\mathcal{F}_1 = \mathcal{F}_4 = \mathcal{F}_6 = 0$ reduces to the requirement that the following forms are integer:

$$\iota_{D_4}^*\left(\frac{1}{2}\hat{D}_1\right) \qquad \text{and} \qquad \iota_{D_6}^*\left(\frac{1}{2}\hat{D}_1\right)\,, \tag{3.16}$$

since in this case the integer flux quanta f_{ij} can always be adjusted to yield vanishing gauge fluxes. Taking an arbitrary integer form $A \in H^2(\mathbb{Z}, X)$ which can be expanded as $A = a_j\hat{D}_j$ with $a_j \in \mathbb{Z}$, the pullbacks in (3.16) give rise to integer

forms if:

$$\begin{aligned} b_4 &\equiv \int_X \left(\frac{1}{2}\hat{D}_1\right) \wedge \hat{D}_4 \wedge A \in \mathbb{Z} \\ b_6 &\equiv \int_X \left(\frac{1}{2}\hat{D}_1\right) \wedge \hat{D}_6 \wedge A \in \mathbb{Z} \end{aligned}$$

Using the intersection polynomial (3.3) we find $b_4 = b_6 = 0$, showing how the choice of B-field in (3.15) can indeed allow for $\mathcal{F}_1 = \mathcal{F}_4 = \mathcal{F}_6 = 0$. The only non-zero gauge flux is $\mathcal{F}_2$ whose half-integer contribution can be cancelled by adding an additional term to the B-field of the form $\frac{1}{2}\hat{D}_2$. Given that all the intersection numbers are even, this new term in B does not modify our previous results on the pullbacks of the B-field on D_1, D_4 and D_6. Moreover the pullback of the B-field on D_2 will also generate an integer flux contribution. We shall therefore consider a non-vanishing gauge flux on the worldvolume of D_2 of the form:

$$\mathcal{F}_2 = \sum_{j=1}^{h^{1,1}} f_{2j}\hat{D}_j \quad \text{with} \quad f_{2j} \in \mathbb{Z}\,. \tag{3.17}$$

3.3.5 FI-term and chirality

Given that the divisor D_2 is transversely invariant under the orientifold involution and it is wrapped by eight D7-branes, it supports an $Sp(16)$ gauge group which is broken down to $U(8) = SU(8) \times U(1)$ by a non-zero flux $\mathcal{F}_2$ along the diagonal $U(1)$. This non-trivial gauge flux $\mathcal{F}_2$ induces also a $U(1)$-charge q_{i2} for the i-th Kähler modulus of the form:

$$q_{i2} = \int_X \hat{D}_i \wedge \hat{D}_2 \wedge \mathcal{F}_2\,. \tag{3.18}$$

Thus $\mathcal{F}_2 \neq 0$ yields (using $D_2 = D_7 - D_1$):

$$q_{12} = -2f_{21} \qquad q_{42} = 2f_{26} \qquad q_{62} = 2f_{24} \qquad q_{72} = 0\,, \tag{3.19}$$

together with a flux-dependent correction to the gauge kinetic function which looks like:

$$\mathrm{Re}(f_2) = \alpha_2^{-1} = \frac{4\pi}{g_2^2} = \tau_2 - h(\mathcal{F}_2)\mathrm{Re}(S)\,, \tag{3.20}$$

where:

$$h(\mathcal{F}_2) = \frac{1}{2}\int_X \hat{D}_2 \wedge \mathcal{F}_2 \wedge \mathcal{F}_2 = \frac{1}{2}\left(f_{21}q_{12} + f_{24}q_{42} + f_{26}q_{62}\right)\,. \tag{3.21}$$

Moreover a non-vanishing gauge flux $\mathcal{F}_2$ induces a moduli-dependent FI-term of the form:

$$\xi = \frac{1}{4\pi\mathcal{V}}\int_X \hat{D}_2 \wedge J \wedge \mathcal{F}_2 = \frac{1}{4\pi\mathcal{V}}\sum_{j=1}^{h^{1,1}} q_{j2}\, t_j = \frac{1}{4\pi\mathcal{V}}\left(q_{12}\, t_1 + q_{42}\, t_4 + q_{62}\, t_6\right) . \quad (3.22)$$

For vanishing open string VEVs (induced for example by non-tachyonic scalar masses), a leading-order supersymmetric stabilisation requires $\xi = 0$ which implies:

$$t_4 = -\frac{q_{12}}{q_{42}}\, t_1 - \frac{q_{62}}{q_{42}}\, t_6 . \quad (3.23)$$

This $U(1)$ factor becomes massive via the Stückelberg mechanism and develops an $\mathcal{O}(M_s)$ mass by eating up a linear combination of an open and a closed string axion which is mostly given by the open string mode.

Besides breaking the worldvolume gauge group and inducing moduli-dependent FI-terms, non-trivial gauge fluxes on D7-branes generate also 4D chiral modes. In fact, open strings stretching between the D7-branes on D_2 and the O7-planes or the image branes give rise to the following zero-modes in the symmetric and antisymmetric representations of $U(8)$:

$$I_2^{(S)} = -\frac{1}{2}\int_X \hat{D}_2 \wedge [\mathrm{O7}] \wedge \mathcal{F}_2 - \int_X \hat{D}_2 \wedge \hat{D}_2 \wedge \mathcal{F}_2 = 2q_{12} - q_{42} - q_{62}, \quad (3.24)$$

$$I_2^{(A)} = \frac{1}{2}\int_X \hat{D}_2 \wedge [\mathrm{O7}] \wedge \mathcal{F}_2 - \int_X \hat{D}_2 \wedge \hat{D}_2 \wedge \mathcal{F}_2 = q_{42} + q_{62}, \quad (3.25)$$

Due to the absence of worldvolume fluxes on the D7-branes wrapped around D_4 and D_6, both of these two D7-stacks support an $Sp(16)$ gauge group (since both D_4 and D_6 are transversely invariant) which are both unbroken. Thus open strings stretched between the D7-branes on D_2 and D_4 or D_6 (or their image branes) give rise to 4D chiral zero-modes in the bi-fundamental representation (8,16) of $U(8)$ and $Sp(16)$ whose number is:

$$I_{24} = \int_X \hat{D}_2 \wedge \hat{D}_4 \wedge \mathcal{F}_2 = q_{42} , \qquad I_{26} = \int_X \hat{D}_2 \wedge \hat{D}_6 \wedge \mathcal{F}_2 = q_{62} . \quad (3.26)$$

We need finally to check that there are no chiral intersections between the D7s on D_2 and the instanton on D_1 to make sure that the prefactor of the non-perturbative contribution to the superpotential is indeed non-zero. This is ensured if:

$$I_{21} = \int_X \hat{D}_2 \wedge \hat{D}_1 \wedge \mathcal{F}_2 = q_{12} = -2f_{21} = 0 . \quad (3.27)$$

This condition can be easily satisfied by choosing $f_{21} = 0$. In turn, this choice simplifies the D-term constraint (3.23) to:

$$t_4 = -\frac{q_{62}}{q_{42}}\, t_6 \equiv \alpha\, t_6 . \quad (3.28)$$

3.3.6 Inflationary potential

Using the D-term fixing relation (3.28), the Kähler cone conditions (3.6) simplify to $t_7 > -t_1 > 0$ together with $t_6 > -t_1 > 0$ if $\alpha \geqslant 1$ or $\alpha t_6 > -t_1 > 0$ if $\alpha \leqslant 1$. Moreover the CY volume (3.4) reduces to:

$$\mathcal{V} = 2\alpha t_7 t_6^2 + \frac{t_1^3}{3} = t_7\tau_7 - \frac{1}{3}\,\tau_1^{3/2} = \frac{1}{\sqrt{2\alpha}}\,\sqrt{\tau_7}\,\tau_6 - \frac{1}{3}\,\tau_1^{3/2}\,. \tag{3.29}$$

Given that this form is linear in t_7, the effective CY volume after D-term stabilisation looks like a single K3 fibre τ_7 over a $\mathbb{P}^1$ base t_7 and reduces to the typical form used in fibre inflation models. The blow-up mode τ_1 and the overall volume $\mathcal{V}$ are stabilised in the LVS fashion by means of a non-perturbative correction to W generated by an Euclidean D3-brane instanton wrapping D_1. This leaves the fibre modulus τ_7 as a flat direction which receives a potential at subleading order.

Let us now focus on the inflationary potential. The winding loop corrections can be written as (with $\kappa = g_s/(8\pi)$ for $e^{K_{\rm cs}} = 1$):

$$V_{g_s}^{\rm w} = -2\,\kappa\,\frac{W_0^2}{\mathcal{V}^3}\,\sum_i \frac{C_i^{\rm w}}{t_i^{\cap}}\,, \tag{3.30}$$

where $t_i^{\cap}$ are the volumes of the two-cycles where D7-branes/O7-planes intersect. Notice that if two coordinate divisors D_i and D_j are wrapped by D7-branes and/or O7-planes, the scalar potential receives $t^{\cap}$-dependent winding loop corrections only if their intersection curve contains non-contractible 1-cycles, i.e. if $h^{1,0}(D_i \cap D_j) \neq 0$. In our case, we have an O7-plane located on D_8 and three stacks of D7-branes wrapping D_2, D_4 and D_6. Using Tab. 3.1 and 3.2, we see all D7s intersect with each other and with the O7 and that winding corrections can arise from any of these intersections. Thus we end up with:

$$V_{g_s}^{\rm w} = -\,\kappa\,\frac{W_0^2}{\mathcal{V}^3}\,\left[\frac{1}{\sqrt{\tau_7}}\left(C_{\rm w} - \tilde{C}_{\rm w}(\tau_7)\right) - \frac{\tau_7}{\mathcal{V}}\left(|C_3^{\rm w}| - \hat{C}_{\rm w}(\tau_7)\right)\right], \tag{3.31}$$

where (setting $t_4 = \alpha t_6$, $C_3^{\rm w} = -|C_3^{\rm w}| < 0$ and $C_4^{\rm w} = -|C_4^{\rm w}| < 0$):

$$C_{\rm w} = \sqrt{2\alpha}\left(C_1^{\rm w} + \frac{C_2^{\rm w}}{\alpha}\right) \qquad \tilde{C}_{\rm w}(\tau_7) = \frac{|C_4^{\rm w}|}{(\alpha+1)}\sqrt{\frac{\alpha}{2}}\left(1 - \frac{\sqrt{2\,\alpha}}{(\alpha+1)}\,\sqrt{\frac{\langle\tau_1\rangle}{\tau_7}}\right)^{-1}, \tag{3.32}$$

and:

$$\hat{C}_{\rm w}(\tau_7) = \frac{C_5^{\rm w}}{2}\left(1 + \frac{1}{\sqrt{2\,\alpha}}\frac{\tau_7^{3/2}}{\mathcal{V}}\right)^{-1} + \frac{C_6^{\rm w}}{2}\left(1 + \sqrt{\frac{\alpha}{2}}\,\frac{\tau_7^{3/2}}{\mathcal{V}}\right)^{-1}. \tag{3.33}$$

Due to the absence of O3-planes (we also assume that the D3-tadpoles are cancelled without including any spacetime-filling D3-branes) and the fact that all D7s intersect with each other and with the O7-plane, there are no 1-loop corrections due to the exchange of closed strings carrying KK momentum.[7]

On the other hand, higher derivative $\alpha'^3\,F^4$ corrections to the scalar potential can be written as [99]:[8]

$$V_{F^4} = -\kappa^2\,\frac{\lambda\,W_0^4}{g_s^{3/2}\,\mathcal{V}^4}\,\sum_{i=1}^{h^{1,1}}\Pi_i\,t_i\,, \tag{3.34}$$

where λ is an unknown combinatorial factor which is expected to be of order 10^{-3} [99, 100] and the topological quantities Π_i are given in (3.10). After imposing the D-term condition (3.28), the F^4 contributions can be rewritten as (ignoring the t_1-dependent term):

$$V_{F^4} = -24\kappa^2\,\frac{\lambda\,W_0^4}{g_s^{3/2}\,\mathcal{V}^3}\,\left[\frac{(\alpha+1)}{\sqrt{2\,\alpha}}\,\frac{\sqrt{\tau_7}}{\mathcal{V}}+\frac{1}{\tau_7}\right]. \tag{3.35}$$

Therefore the total inflationary potential becomes:

$$V = V_{g_s}^{\rm W}+V_{F^4} = \kappa\,\frac{W_0^2}{\mathcal{V}^3}\,\left(\frac{A_1}{\tau_7}-\frac{A_2}{\sqrt{\tau_7}}+\frac{B_1\sqrt{\tau_7}}{\mathcal{V}}+\frac{B_2\,\tau_7}{\mathcal{V}}\right), \tag{3.36}$$

where (with $\lambda=-|\lambda|<0$):

$$A_1=\frac{3}{\pi}\frac{|\lambda|W_0^2}{\sqrt{g_s}}\quad A_2=C_{\rm W}-\tilde{C}_{\rm W}(\tau_7)\quad B_1=\frac{(\alpha+1)}{\sqrt{2\,\alpha}}\,A_1\quad B_2=|C_3^{\rm W}|-\hat{C}_{\rm W}(\tau_7)\,.$$

3.4 Inflationary dynamics

In this section we shall analyse the inflationary dynamics by studying first the single-field approximation and then by focusing on the full multi-field evolution.

[7] Strictly speaking, there might be 1-loop corrections associated with the exchange of KK modes between the Euclidean D3-instanton on D_1 and the D7-branes which do not intersect D_1. However, we expect such corrections to be exponentially suppressed and, thus, not relevant for the analysis.

[8] This expression displays merely the leading order $\mathcal{O}(\mathcal{V}^{-4})$ terms which are corrected at subleading order in inverse volume by additional corrections as discussed in [103]. Furthermore, additional higher-derivative corrections mediated by the auxiliary fields sitting in the supergravity multiplet might emerge at order $\mathcal{O}(\mathcal{V}^{-5})$ [103, 153].

3.4.1 Single-field evolution

In order to realise single-field slow-roll inflation where the potential for the inflaton τ_7 features a plateau-type region [101, 103], the overall volume has to be approximately constant during the whole inflationary dynamics. Therefore, in order to get enough efoldings before reaching the dangerous limit where the base of the fibration t_7 becomes smaller than the string scale, we need to focus on the region in field space where the inflaton minimum is of order $\langle\tau_7\rangle \ll \mathcal{V}^{2/3}$. For $g_s \lesssim \mathcal{O}(0.1)$, $|\lambda| \sim \mathcal{O}(10^{-3})$ and natural $\mathcal{O}(1)$ values of the coefficients of the string loop effects, in the vicinity of the minimum the terms in (3.36) proportional to B_1 and B_2 are therefore both negligible with respect to the terms proportional to A_1 and A_2. Numerical estimates show that we need values of order $\langle\tau_7\rangle \sim \mathcal{O}(1)$ and $\mathcal{V} \sim \mathcal{O}(10^4)$ which, in turn, imply $W_0 \sim \mathcal{O}(100)$ in order to match the observed amplitude of the density perturbations.

The scalar potential (3.36) written in terms of the canonically normalised inflaton shifted from its minimum $\phi = \langle\phi\rangle + \hat{\phi}$, where $\tau_7 = \langle\tau_7\rangle e^{k\hat{\phi}}$ with $k = 2/\sqrt{3}$, becomes:

$$V = \kappa \frac{A_2 W_0^2}{\mathcal{V}^3\sqrt{\langle\tau_7\rangle}} \left(C_{\rm dS} + c\, e^{-k\hat{\phi}} - e^{-\frac{k\hat{\phi}}{2}} + \mathcal{R}_1\, e^{\frac{k\hat{\phi}}{2}} + \mathcal{R}_2\, e^{k\hat{\phi}}\right), \tag{3.37}$$

where:

$$c = \frac{3}{\pi\left(C_{\rm W} - \tilde{C}_{\rm W}(\tau_7)\right)} \frac{|\lambda| W_0^2}{\sqrt{g_s\langle\tau_7\rangle}} \sim \mathcal{O}(1)\,,$$

while for $\langle\tau_7\rangle \sim \mathcal{O}(1) \ll \mathcal{V}^{2/3}$:

$$\mathcal{R}_1 = \frac{(\alpha+1)c}{\sqrt{2\,\alpha}} \frac{\langle\tau_7\rangle^{3/2}}{\mathcal{V}} \ll 1 \qquad \text{and} \qquad \mathcal{R}_2 = \frac{\left(|C_3^{\rm W}| - \hat{C}_{\rm W}(\tau_7)\right)}{\left(C_{\rm W} - \tilde{C}_{\rm W}(\tau_7)\right)} \frac{\langle\tau_7\rangle^{3/2}}{\mathcal{V}} \ll 1\,.$$

Notice that in (3.37) we added a constant $C_{\rm dS} = 1 - c - \mathcal{R}_1 - \mathcal{R}_2$ to obtain a Minkowski (or slightly dS) vacuum. Given that no O3-planes are present in our model, the usual uplift mechanism where an anti D3-brane is located in a resolved conifold region of the extra dimensions would require additional effort to implement. We leave the explicit embedding of the source of uplift to future research.

The two negative exponentials in (3.37) compete to give a minimum at $\langle\tau_7\rangle \sim \mathcal{O}(1)$ while the two positive exponentials cause a steepening behaviour at large $\hat{\phi}$. Thus we need to make sure that both $\mathcal{R}_1 \ll 1$ and $\mathcal{R}_2 \ll 1$ to prevent the two positive exponentials from destroying the inflationary plateau before achieving

enough efoldings of inflation.[9] The condition $\mathcal{R}_1 \ll 1$ could be satisfied for $c \ll 1$, for example for $W_0 \sim \mathcal{O}(1)$ and $\langle \tau_7 \rangle \gg 1$, in which case the minimum could be obtained by balancing the two terms in the coefficient A_2. However, as we shall see below, if $\langle \tau_7 \rangle \gg 1$, the Kähler cone bounds restrict the allowed field space so much that it becomes impossible to realise enough efoldings of inflation. Hence we shall focus the region where $\mathcal{R}_1 \ll 1$ and $\mathcal{R}_2 \ll 1$ are satisfied by $\langle \tau_7 \rangle \sim \mathcal{O}(1) \ll \mathcal{V}^{2/3}$ (and possibly by allowing some tuning of the complex structure moduli-dependent coefficients of the loop corrections or by considering $|\lambda| \ll 1$).

Turning now to the explicit numerical examples, let us formulate the necessary conditions that have to be satisfied in order to have a viable model:

1. Stringy effects can be neglected if each four-cycle in string frame has a volume larger than the string scale: $\mathrm{Vol}_s^{1/4} \gg \sqrt{\alpha'}$. Given that string and Einstein frame volumes are related as $\mathrm{Vol}_s = g_s \mathrm{Vol}_E = g_s \tau_E \ell_s$ with $\ell_s = 2\pi\sqrt{\alpha'}$, we end up with the condition:

$$\epsilon_{\tau_i} \equiv \frac{1}{g_s (2\pi)^4 \, \tau_i} \ll 1 \qquad \forall \, i \, . \tag{3.38}$$

2. The whole inflationary dynamics should take place inside the Kähler cone. This implies in particular that:

$$\begin{aligned} 2\alpha\langle\tau_1\rangle \;&<\; \tau_7 < \frac{\mathcal{V}}{\sqrt{\langle\tau_1\rangle}} \qquad \text{if} \qquad \alpha \geqslant 1 \, , \\ \frac{2}{\alpha}\langle\tau_1\rangle \;&<\; \tau_7 < \frac{\mathcal{V}}{\sqrt{\langle\tau_1\rangle}} \qquad \text{if} \qquad \alpha \leqslant 1 \, . \end{aligned} \tag{3.39}$$

Notice that these conditions guarantee the absence of any singularity in the inflationary potential (3.37) which could originate from the shrinking of a two-cycle to zero size. Rewriting these conditions in terms of the canonically normalised inflaton field, we end up with:

$$\begin{aligned} \frac{\sqrt{3}}{2} \ln\left(\frac{2\alpha\langle\tau_1\rangle}{\langle\tau_7\rangle}\right) \;&<\; \hat{\phi} < \frac{\sqrt{3}}{2} \ln\left(\frac{\mathcal{V}}{\langle\tau_7\rangle\sqrt{\langle\tau_1\rangle}}\right) \qquad \text{if} \qquad \alpha \geqslant 1 \, , \\ \frac{\sqrt{3}}{2} \ln\left(\frac{2\langle\tau_1\rangle}{\alpha\langle\tau_7\rangle}\right) \;&<\; \hat{\phi} < \frac{\sqrt{3}}{2} \ln\left(\frac{\mathcal{V}}{\langle\tau_7\rangle\sqrt{\langle\tau_1\rangle}}\right) \qquad \text{if} \qquad \alpha \leqslant 1 \, . \end{aligned} \tag{3.40}$$

In order to be able to describe within a consistent EFT, not just inflation but also the post-inflationary evolution of our model, $\hat{\phi}$ should reach its minimum before hitting the lower bounds in (3.40). Moreover the inflaton should drive enough efoldings of inflation before hitting the upper bounds in (3.40).

[9] If this is the case, these steepening terms could then be responsible for an interesting power loss at large angular scales [154].

3. Horizon exit at $\hat{\phi} = \hat{\phi}_*$ should yield the required number of efoldings:

$$N_e \simeq 57 + \frac{1}{4}\ln\left(r_*\, V_*\right) - \frac{1}{3}\ln\left(\frac{V_{\rm end}}{T_{\rm rh}}\right), \tag{3.41}$$

where the reheating temperature $T_{\rm rh}$ can be estimated in terms of the inflaton mass at the minimum $m_{\hat{\phi}}$ as:

$$T_{\rm rh} \simeq \left(\frac{90}{\pi^2 g_*(T_{\rm rh})}\right)^{1/4} \sqrt{\Gamma_{\hat{\phi}} M_p} \simeq 0.1\, m_{\hat{\phi}} \sqrt{\frac{m_{\hat{\phi}}}{M_p}}\,. \tag{3.42}$$

4. Horizon exit at $\hat{\phi} = \hat{\phi}_*$ should reproduce the observed amplitude of the density perturbations:

$$\frac{V_*^3}{V_*'^2} \simeq 2.6 \cdot 10^{-7}\,. \tag{3.43}$$

5. The α' expansion of the potential can be trusted only if:

$$\epsilon_\xi = \frac{\xi}{2 g_s^{3/2} \mathcal{V}} \ll 1\,. \tag{3.44}$$

6. The effective field theory is under control if throughout all the inflationary dynamics:

$$m_{\rm inf} < H < m_{3/2} < M_{KK}^{(i)} < M_s < M_p \qquad \forall i = \text{bulk}, 2, 4, 6\,, \tag{3.45}$$

where $m_{\rm inf}$ is the inflaton mass, $H \simeq \frac{V}{3M_p^2}$ is the Hubble scale, $m_{3/2} = e^{K/2} W_0 = \sqrt{\kappa}\,\frac{W_0}{\mathcal{V}}\, M_p$ is the gravitino mass which sets the mass scale of all complex structure moduli, the dilaton and the Kähler modulus $T_1 = \tau_1 + \mathrm{i}\int_{D_1} C_4$ and $M_{KK}^{(i)} = \frac{\sqrt{\pi}}{\sqrt{\mathcal{V}}\,\tau_i^{1/4}}\, M_p$ are the different KK scales in the model associated with bulk KK modes for $\tau_{\rm bulk}^{3/2} = \mathcal{V}$ and KK replicas of open string modes living on D7-branes wrapped around D_2, D_4 and D_6. The bulk KK scale should be below the string scale $M_s = \frac{g_s^{1/4}\sqrt{\pi}}{\sqrt{\mathcal{V}}}\, M_p$ while we do not need to impose $V^{1/4} < M_{KK}^{(i)}$ since no energy can be extracted from the vacuum during an adiabatic inflationary expansion where $H \ll M_{KK}^{(i)}$.

7. Besides the two ultra-light axions associated with the base and the fibre which develop just negligible isocurvature fluctuations during inflation if they do not contribute significantly to dark matter, only the volume mode has a mass below $m_{3/2}$. In order to trust our single field approximation, we need

therefore to check that the mass of the volume mode $m_{\mathcal{V}}$ does not become smaller than the Hubble scale H. This condition boils down to:

$$\delta = \frac{H}{m_{\mathcal{V}}} \simeq \sqrt{\frac{V_*}{3V_{\alpha'}}} \lesssim 1\,, \tag{3.46}$$

where $V_{\alpha'}$ is the leading $\mathcal{O}(\alpha'^3)$ contribution to the scalar potential and reads [55]:

$$V_{\alpha'} = \kappa \frac{3\xi W_0^2}{4 g_s^{3/2} \mathcal{V}^3} \qquad \text{with} \qquad \xi = -\frac{\zeta(3)\chi(X)}{2(2\pi)^3}\,. \tag{3.47}$$

If $\delta \simeq 1$, the inflationary energy density can either destabilise the volume direction or cause a significant shift of the volume minimum. Hence the inflationary dynamics can effectively become a multi-field evolution. However, as analysed in [101], the motion might still remain mainly along the τ_7 direction, and so the predictions for the inflationary observables could be basically unaltered apart from the fact that the number of allowed efoldings slightly increases. Notice also that in LVS models the CY Euler number together with the string coupling fixes the minimum of the blow-up mode τ_1 as: $\langle \tau_1 \rangle = (3\xi/2)^{2/3}\, g_s^{-1}$. This value is important to evaluate the Kähler cone conditions in (3.40).

We shall now focus on single-field slow-roll inflation where:

$$\epsilon(\hat{\phi}) = \frac{1}{2}\left(\frac{V'}{V}\right)^2 \ll 1 \qquad \text{and} \qquad \eta(\hat{\phi}) = \frac{V''}{V} \ll 1\,.$$

Notice that the condition $\eta \ll 1$ guarantees that the inflaton is lighter than H during inflation. In order to illustrate the main features of our inflationary model, we shall now consider two different choices of the underlying parameters characterised by different values of the coefficients ξ and λ which control the strength of the $\mathcal{O}(\alpha'^3)$ corrections to the effective action at $\mathcal{O}(F^2)$ and $\mathcal{O}(F^4)$. According to [56], $N = 1$ $\mathcal{O}(\alpha'^3)$ corrections due to O7-planes cause a shift of the CY Euler number $\chi(X)$ to $\chi_{\text{eff}}(X)$ defined in (3.11) and given in Tab. 3.3. From (3.47) this modification would give $\xi = 0.067$. Moreover the coefficient λ of higher derivative $\mathcal{O}(\alpha'^3)$ effects has been estimated to be negative and of order 10^{-3} [99, 100]. Hence the first set of parameters will be characterised by $\xi = 0.067$ and $\lambda = -0.001$. However both of these corrections still lack a full supersymmetric analysis, and so in the second case we shall focus on a situation where the CY Euler number is not modified, and so $\xi = 0.456$, and the size of the coefficient λ is much smaller: $|\lambda| \lesssim 10^{-6}$.

Case 1: $\xi = 0.067$ **and** $|\lambda| = 0.001$

Let us now provide an explicit numerical example set to demonstrate the features of our inflationary model:

$$\begin{aligned} \alpha &= 1\,, \quad C_1^{\rm W} = C_2^{\rm W} = 15\,, \quad |C_3^{\rm W}| = 0.013\,, \quad |C_4^{\rm W}| = 18\,, \quad C_5^{\rm W} = C_6^{\rm W} = -5\,, \\ g_s &= 0.114\,, \quad \mathcal{V} = 10^4\,, \quad \langle \tau_1 \rangle = 1.91\,, \quad W_0 = 80\,, \quad |\lambda| = 0.001\,, \end{aligned} \tag{3.48}$$

with $\chi(X) = \chi_{\rm eff}(X) = -28$ in (3.47) which gives $\xi = 0.067$. Notice that the tuning of the steepening term here is mild since the difference between the largest and the smallest winding coefficient is between one and two orders of magnitude. The form of the inflationary potential is plotted in Fig. 3.1 and it is characterised by:

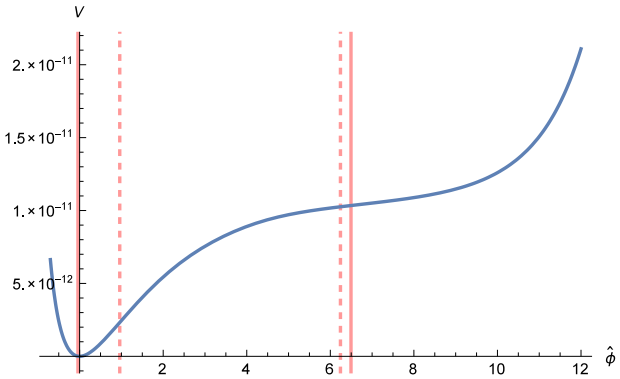

Figure 3.1: Plot of the inflationary potential for the example set (3.48). The red vertical lines correspond to the walls of the Kähler cone while the dashed vertical lines denote horizon exit and the end of inflation where $\epsilon = 1$.

- $\langle \tau_7 \rangle = 4.002$ leading to $\epsilon_{\langle \tau_7 \rangle} = 0.0014$. Moreover $2\langle \tau_1 \rangle \simeq 3.8$, and so the distance of the minimum from the lower bound of the Kähler cone is $\Delta\tau_7 \simeq 0.178$ which is still larger than the string scale since, using (3.38), we have that:

$$\epsilon_{\Delta\tau_7} = \frac{1}{g_s(2\pi)^4 \Delta\tau_7} \simeq 0.03\,. \tag{3.49}$$

- The Kähler cone bounds (3.40) in terms of the canonically normalised inflaton become $\hat{\phi}_{\rm min} \simeq -0.04 < \hat{\phi} < \hat{\phi}_{\rm max} \simeq 6.49$. Inflation ends at $\hat{\phi} = \hat{\phi}_{\rm end} \simeq 0.96$ where $\epsilon(\hat{\phi}_{\rm end}) = 1$ and $V_{\rm end} \simeq (7 \cdot 10^{15}\,{\rm GeV})^4$. Horizon exit takes place at $\hat{\phi} = \hat{\phi}_* \simeq 6.24$ where $r = 16\epsilon = 0.009$, $n_s = 1 + 2\eta_* - 6\epsilon_* = 0.983$, $V_* \simeq (1 \cdot 10^{16}\,{\rm GeV})^4$ and the amplitude normalisation (3.43) is satisfied.

Notice that such a largish value of the scalar spectral index is in perfect agreement with Planck data in the presence of dark radiation since, using $\Delta N_{\rm eff} = 0.39$ as a prior, [139] gives as best fit $n_s = 0.983 \pm 0.006$. This prior is fully justified in string models like ours where reheating is driven by the decay of the lightest modulus which naturally tends to produce extra axionic contributions to dark radiation [14, 124, 125, 126].

- Horizon exit occurs well inside the Kähler cone since from (3.39) we have:

$$\tau_7^* = e^{\kappa(\langle\phi\rangle+\hat{\phi}_*)} \simeq 5404.82 < \tau_7^{\rm max} = \frac{\mathcal{V}}{\sqrt{\langle\tau_1\rangle}} \simeq 7231.87$$
$$\Rightarrow \quad \tau_7^{\rm max} - \tau_7^* \simeq 1827.06\,.$$

- The mass of the inflaton around the minimum is $m_{\hat{\phi}} \simeq 4.25 \cdot 10^{13}$ GeV which from (3.42) implies a reheating temperature $T_{\rm rh} \simeq 1.8 \cdot 10^{10}$ GeV.

- The number of efoldings computed as:

$$N_e = \int_{\hat{\phi}_{\rm end}}^{\hat{\phi}_*} \frac{V}{V'}\, d\hat{\phi}\,, \tag{3.50}$$

gives $N_e = 52$ as required by the estimate (3.41). The maximum number of efoldings between $\hat{\phi}_{\rm end}$ and $\hat{\phi}_{\rm max}$ is $N_e^{\rm max} \simeq 60$.

- The α' expansion is under control even if in our inflationary model the inflaton travels over a trans-Planckian distance of order $\Delta\hat{\phi} = \hat{\phi}_* - \hat{\phi}_{\rm end} = 5.28$ since we have $\epsilon_\xi \sim 10^{-4}$.

- The mass of the volume mode is of order the Hubble scale during inflation since $\delta \simeq 1.6$. Hence the inflationary energy density could either cause a significant shift of the original LVS minimum or destabilise the volume direction. A definite answer to this question would require a more careful multi-field analysis. As mentioned above, a similar situation has been studied in [101], where the authors found that for $\delta \sim 1$ the minimum for the volume mode gets a large shift but the inflationary evolution still remains mostly single-field since $m_{\rm inf} \ll m_{\mathcal{V}} \sim H$. However if $\delta \sim 1$, the inflationary potential generated by string loops and $\alpha'^3\ F^4$ terms is of the same order as the $\alpha'^3\ F^2$ contribution, and so one also should carefully check if additional higher derivative corrections can be safely neglected.

- The effective field theory approximation is valid during the whole inflationary evolution since $H \simeq 2 \cdot 10^{13}\,{\rm GeV} < m_{3/2} \simeq 1 \cdot 10^{15}\,{\rm GeV} < M_{KK}^{\rm bulk} \simeq 9 \cdot 10^{15}\,{\rm GeV} < M_s \simeq 2.5 \cdot 10^{16}\,{\rm GeV}$.

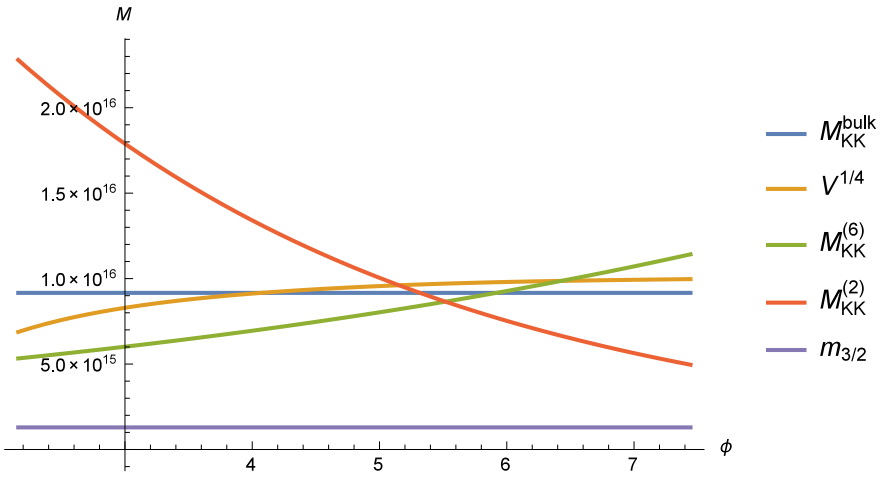

Figure 3.2: Comparison between the different KK masses, $m_{3/2}$ and the inflationary energy density $V^{1/4}$ from horizon exit to the end of inflation. Note that $M_{KK}^{(4)} = M_{KK}^{(6)}$ which is why only one of them is displayed here.

We display the evolution of the different KK masses as compared to the gravitino mass and the inflationary scale $M_{\rm inf} = V^{1/4}$ in Fig. 3.2. Notice, in particular, that at the end of inflation the inflationary scale is of order $M_{KK}^{\rm bulk}$ and, above all, mildly exceeds the KK scale $M_{KK}^{(4)}$ by a factor of roughly 1.3. As we stressed above, during an adiabatic expansion no energy can be extracted from the vacuum, and so our EFT is still valid even if some KK scales become smaller than $V^{1/4}$ since they are all always larger than $m_{3/2}$ which is, in turn, larger than H. However, since all the inflationary energy density could instead be converted into particle production at reheating, one should make sure that there is enough Hubble friction between the end of inflation and reheating to bring the inflaton energy density below the relevant KK scale. This effect can be estimated by noticing that from:

$$\rho(\phi) = \frac{1}{2}\dot{\phi}^2 + V(\phi) = 3H^2M_p^2 \qquad \Leftrightarrow \qquad \partial_t\rho(\phi) = -3H\dot{\phi}^2\,, \tag{3.51}$$

we can obtain the following relation between the energy density at the end of inflation and at reheating:

$$\rho_{\rm rh} = \rho_{\rm end} - 3\langle\dot{\phi}^2\rangle\int_{\rm end}^{\rm rh}\frac{da}{a} = \rho_{\rm end} - 3N_{\rm rh}\langle\dot{\phi}^2\rangle\,, \tag{3.52}$$

where $\langle\dot{\phi}^2\rangle$ is the time average between the end of inflation and reheating and $N_{\rm rh} = \ln(a_{\rm rh}/a_{\rm end})$ is the number of efoldings of the reheating epoch. At the end

of inflation when $\epsilon = 1$ we have:

$$\frac{1}{2}\dot{\phi}^2 = H^2 M_p^2 \qquad \Leftrightarrow \qquad \rho_{\rm end} = \frac{3}{2} V_{\rm end} \simeq 10 \left(M_{KK}^{(4)}\right)^4 . \tag{3.53}$$

On the other hand at reheating $V(\phi_{\rm rh}) \simeq 0$, and so $\rho_{\rm rh} \simeq \dot{\phi}_{\rm rh}^2/2$. If we then write the time-average kinetic energy as $\langle \dot{\phi}^2 \rangle = \dot{\phi}_{\rm rh}^2/x \simeq 2\rho_{\rm rh}/x$ with $x > 0$, we end up with the following bound:

$$\rho_{\rm rh} \simeq \frac{10}{1 + \frac{6}{x} N_{\rm rh}} \left(M_{KK}^{(4)}\right)^4 < \left(M_{KK}^{(4)}\right)^4 . \tag{3.54}$$

Using the fact that:

$$N_{\rm rh} \simeq \frac{1}{3} \ln \left(\frac{H_{\rm end}^2 M_p^2}{T_{\rm rh}^4} \right) - \frac{1}{3} \ln \left(\frac{\pi^2 g_*}{90} \right) \simeq 16 \,, \tag{3.55}$$

the bound (3.54) becomes $x < \frac{2}{3} N_{\rm rh} \simeq 10$. Our model should satisfy this bound since we expect $\dot{\phi}_{\rm end}$ to approach $\dot{\phi}_{\rm rh}$ relatively quickly due to the steepness of the potential near the end of inflation. However a definite answer would require a detailed study of the post-inflationary epoch which is beyond the scope of this work.[10]

Let us also mention that, due to the absence of KK corrections, this scenario represents a chiral global embedding of the α'-inflation models discussed in [103]. Moreover, no KK scale becomes smaller than the gravitino mass even if $r \simeq 0.01$ and $\Delta\hat{\phi} \simeq 5$ in Planck units. In fact, if we focus for example on the KK scale $M_{KK}^{(2)}$ associated with the K3 fibre (similar considerations apply to the KK scale $M_{KK}^{(6)}$ associated with the base), we have:

$$\frac{m_{3/2}}{M_{KK}^{(2)}} = \alpha_1 \, e^{\alpha_2 \phi} \simeq 0.03 \, e^{\alpha_2 \phi} \,, \tag{3.56}$$

with:

$$\alpha_1 = \sqrt{\frac{W_0}{2\pi}} \left(\frac{g_s}{2\pi}\right)^{1/4} \sqrt{\frac{m_{3/2}}{M_p}} \simeq 0.03 \qquad \text{and} \qquad \alpha_2 = \frac{1}{2\sqrt{3}} \,. \tag{3.57}$$

If we set $\phi = \phi_0 + \hat{\phi}_{\rm he} \simeq 7.44$, the ratio in (3.56) becomes $m_{3/2}/M_{KK}^{(2)} \simeq 0.26$, and so the KK scale $M_{KK}^{(2)}$ is always larger than the gravitino mass throughout all the

[10] Let us also point out that, even if $\rho_{\rm rh} \gtrsim \left(M_{KK}^{(4)}\right)^4$, our model is not necessarily ruled out but we would just need to describe reheating within a 6D EFT where the base of the fibration is much larger than the characteristic size of the fibre. It would also be interesting to find brane setups where this problem is automatically absent since there is no D7-brane wrapped around the base.

inflationary dynamics. Notice that this result seems to be in slight disagreement with the swampland conjecture of [155, 156] where the underlying parameters α_1 and α_2 were generically assumed to be of order unity.

As explained above, given that in this case $\delta \simeq 1.6$, the inflationary dynamics can be fully trusted only after determining the proper multi-field evolution. Due to the difficulty to perform a full numerical analysis, in the next section we shall instead still focus on a single-field case where $\delta \sim 0.05$ since ξ is larger, and so the volume mode mass is larger, while $|\lambda|$ is smaller, and so F^4 steepening terms can be easily neglected throughout the whole inflationary dynamics. The full three-field evolution for both of these cases will then be presented in Sec. 3.4.2.

Case 2: $\xi = 0.456$ and $|\lambda| = 10^{-7}$

According the discussion above, we shall now focus on the following different choice of the underlying parameters:

$$\begin{aligned} \alpha &= 1\,, \quad C_1^{\rm w} = C_2^{\rm w} = 0.034\,, \quad |C_3^{\rm w}| = 10^{-5}\,, \quad |C_4^{\rm w}| = 0.068\,, \\ C_5^{\rm w} &= C_6^{\rm w} = -0.024\,, \qquad g_s = 0.25\,, \quad \mathcal{V} = 4500\,, \quad \langle \tau_1 \rangle = 3.10\,, \\ W_0 &= 150\,, \quad |\lambda| = 10^{-7}\,, \end{aligned} \tag{3.58}$$

with $\chi(X) = \chi_{\rm eff}(X) = -188$ in (3.47) which gives $\xi = 0.456$. A larger value of the coefficient ξ is helpful to increase the control on the single-field approximation since, as can be seen from (3.47), the leading $\mathcal{O}(\alpha'^3)$ contribution to the scalar potential is proportional to ξ. The form of the inflationary potential is plotted in Fig. 3.3 and it is characterised by:

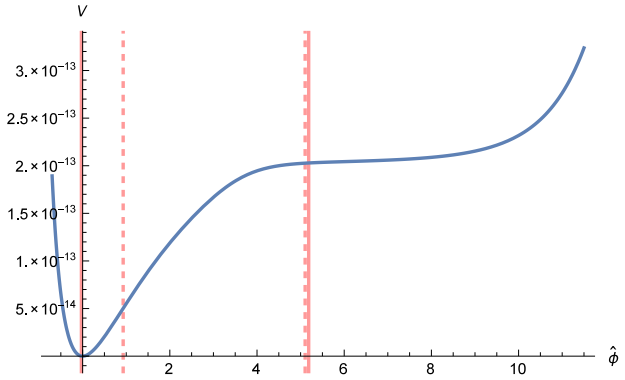

Figure 3.3: Plot of the inflationary potential for the example set (3.58). The red vertical lines correspond to the walls of the Kähler cone while the dashed vertical lines denote horizon exit and the end of inflation where $\epsilon = 1$.

- $\langle\tau_7\rangle \simeq 6.41$ leading to $\epsilon_{\langle\tau_7\rangle} \simeq 0.0004$ and $\langle\phi\rangle \simeq 1.61$. Moreover $2\langle\tau_1\rangle \simeq 6.2$, and so the minimum is located close to the walls of the Kähler cone but at a distance $\Delta\tau_7 \simeq 0.21$ which is still larger than the string scale since, using (3.38), we have that:

$$\epsilon_{\Delta\tau_7} = \frac{1}{g_s(2\pi)^4\Delta\tau_7} \simeq 0.01\,. \tag{3.59}$$

- The Kähler cone bounds (3.40) in terms of the canonically normalised inflaton become $\hat{\phi}_{\rm min} \simeq -0.028 < \hat{\phi} < \hat{\phi}_{\rm max} \simeq 5.19$. Inflation ends at $\hat{\phi} = \hat{\phi}_{\rm end} \simeq 0.93$ where $\epsilon(\hat{\phi}_{\rm end}) = 1$ and $V_{\rm end} = (4.4 \cdot 10^{15}\,{\rm GeV})^4$. Horizon exit takes place at $\hat{\phi} = \hat{\phi}_* \simeq 5.10$ where $r = 16\epsilon = 0.0014$, $n_s = 1 + 2\eta_* - 6\epsilon_* = 0.963$, $V_* = (6.2 \cdot 10^{15}\,{\rm GeV})^4$ and the amplitude normalisation (3.43) is satisfied. Notice that horizon exit occurs far away from the upper bound of the Kähler cone since from (3.39) we have:

$$\tau_7^* = e^{\kappa(\langle\phi\rangle+\hat{\phi}_*)} \simeq 2325.79 < \tau_7^{\rm max} = \frac{\mathcal{V}}{\sqrt{\langle\tau_1\rangle}} \simeq 2554.55$$
$$\Rightarrow \quad \tau_7^{\rm max} - \tau_7^* \simeq 228.76\,.$$

- The mass of the inflaton around the minimum is $m_{\hat{\phi}} \simeq 1.85 \cdot 10^{13}$ GeV which from (3.42) implies a reheating temperature $T_{\rm rh} \simeq 5.16 \cdot 10^9$ GeV.

- The number of efoldings computed as:

$$N_e = \int_{\hat{\phi}_{\rm end}}^{\hat{\phi}_*} \frac{V}{V'}\, d\hat{\phi}\,, \tag{3.60}$$

  gives $N_e = 51$ as required by the estimate (3.41). The maximum number of efoldings between $\hat{\phi}_{\rm end}$ and $\hat{\phi}_{\rm max}$ is $N_e^{\rm max} \simeq 57.5$.

- The α' expansion is under control even if in our inflationary model the inflaton travels over a trans-Planckian distance of order $\Delta\hat{\phi} = \hat{\phi}_* - \hat{\phi}_{\rm end} = 4.17$ since we have $\epsilon_\xi \simeq 0.0004$.

- The single-field approximation is under control since $\delta \simeq 0.05$.

- The effective field theory approximation is valid during the whole inflationary evolution since $H \simeq 7 \cdot 10^{12}\,{\rm GeV} < m_{3/2} \simeq 8 \cdot 10^{15}\,{\rm GeV} < M_{KK}^{\rm bulk} \simeq 1.6 \cdot 10^{16}\,{\rm GeV} < M_s \simeq 4.5 \cdot 10^{16}\,{\rm GeV}$.

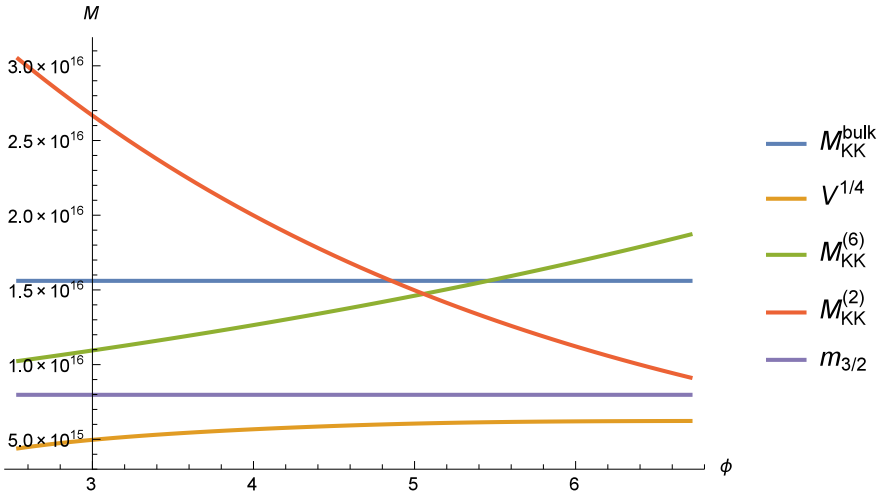

Figure 3.4: Comparison between the different KK masses, the gravitino mass $m_{3/2}$ and the inflationary energy $V^{1/4}$ from horizon exit to the end of inflation. Note that $M_{KK}^{(4)} = M_{KK}^{(6)}$ which is why only one of them is displayed here.

We display the evolution of the different KK masses as compared to the gravitino mass and the inflationary energy density $M_{\rm inf} = V^{1/4}$ in Fig. 3.4. Notice that, contrary to case 1 where $r = 0.01$, all KK scales remain above $M_{\rm inf}$ throughout all the inflationary dynamics. The reason is that in this scale the tensor-to-scalar ratio, and so also the inflationary scale, is smaller since $r = 0.001$. Moreover, as stressed above, no energy can be extracted from the vacuum during an adiabatic expansion, and so the consistency condition to be imposed during inflation is $H \ll M_{KK}^{(i)}$ which is clearly satisfied since $H = \frac{M_{\rm inf}}{\sqrt{3}} \left(\frac{M_{\rm inf}}{M_p}\right) < M_{\rm inf}$. Moreover, no KK scale becomes smaller than the gravitino mass $m_{3/2} \simeq 8 \cdot 10^{15}$ GeV. If we focus for example on the KK scale $M_{KK}^{(2)}$ associated with the K3 fibre (similar considerations apply to the KK scale $M_{KK}^{(6)}$ associated with the base of the fibration), we have:

$$\frac{m_{3/2}}{M_{KK}^{(2)}} = \alpha_1 \, e^{\alpha_2 \phi} \simeq 0.126 \, e^{\alpha_2 \phi} \,, \tag{3.61}$$

with:

$$\alpha_1 = \sqrt{\frac{W_0}{2\pi}} \left(\frac{g_s}{2\pi}\right)^{1/4} \sqrt{\frac{m_{3/2}}{M_p}} \simeq 0.126 \qquad \text{and} \qquad \alpha_2 = \frac{1}{2\sqrt{3}} \,. \tag{3.62}$$

If we set $\phi = \phi_0 + \hat{\phi}_{\rm he} \simeq 6.71$, the ratio in (3.61) becomes $m_{3/2}/M_{KK}^{(2)} \simeq 0.87$, and so the KK scale $M_{KK}^{(2)}$ is always larger than the gravitino mass throughout

all the inflationary dynamics. This result seems to be more in agreement with the swampland conjecture of [155, 156] than the one of case 1 since r is smaller, $r \simeq 0.001$, and the field range is slightly reduced, $\Delta\hat{\phi} \simeq 4$. Moreover larger values of ϕ would bring the effective field theory approach out of control.

Even if this example satisfies all consistency and phenomenological constraints and the single-field inflationary analysis is under control, in Sec. 3.4.2 we shall perform a more precise multifield analysis where the motion along the orthogonal directions enlarges the field space as well as the allowed number of efoldings.

3.4.2 Multi-field evolution

The following five consistency conditions require generically a multi-field study of the inflationary evolution (which might however still be mainly along a single direction in field space):

1. The whole inflationary dynamics takes place well inside the Kähler cone described by the conditions in (3.39);

2. The quantum fluctuations of the inflaton produce a correct amplitude of the density perturbations at horizon exit;

3. The directions orthogonal to the inflaton are not destabilised by the inflationary dynamics. This is guaranteed if inflation occurs in field space along a through which can however bend;

4. Throughout all the inflationary dynamics, no Kaluza-Klein scale becomes smaller than the gravitino mass;

5. The steepening of the inflationary potential due to F^4 corrections is negligible, so that enough efoldings can be obtained before destroying slow roll inflation.

If $\mathcal{V} \sim 10^3$ and $W_0 \sim \mathcal{O}(1)$, the last four conditions can be easily satisfied but the Kähler cone conditions (3.39) for such a small value of the volume would give an upper bound on the inflaton direction which would not allow to generate enough efoldings. In order to enlarge the inflaton field space, the value of the volume has therefore to be larger, of order $\mathcal{V} \sim 10^4$. In the large volume regime where we can trust the 4D EFT, the inflationary potential then becomes more suppressed, and so the COBE normalisation condition (2) above can be satisfied only if $W_0 \sim \mathcal{O}(100)$. However, given that the gravitino mass is proportional to W_0, for such a large value of the flux-generated superpotential, it is hard to satisfty the fourth condition above keeping $m_{3/2}$ below all KK scales during the whole inflationary evolution. Moreover, it becomes harder to suppress higher derivative

corrections (condition (5) above) unless their numerical coefficient λ turns out to be extremely small: $|\lambda| \lesssim 10^{-6}$. This is the example of case 2 above of Sec. 3.4.1.

Another option for $\mathcal{V} \sim 10^4$ could be to keep $W_0 \sim \mathcal{O}(1)$, so that the gravitino mass can remain small and the F^4 terms are still negligible, and to tune the background fluxes to increase the complex structure-dependent coefficients of the winding loop corrections. This would however make the inflaton-dependent potential of the same order of magnitude of the leading order α' correction. Hence the mass of the volume mode becomes of order the Hubble scale during inflation. This is the example of case 1 of Sec. 3.4.1 where $\delta \simeq 1.6$. This situation could either cause a considerable shift of the original LVS minimum or even a destabilisation, and so in this case one should perform a careful multi-field analysis to check that the condition (3) above is indeed satisfied.[11]

In what follows we shall therefore focus on the multifield case with $\mathcal{V} \sim 10^4$, $W_0 \sim \mathcal{O}(100)$ and $|\lambda| \lesssim 10^{-6}$. We shall also present an example with $W_0 \sim \mathcal{O}(1)$ and $|\lambda| \sim 10^{-3}$ which satisfies all conditions above except for condition (2) since the amplitude of the density perturbations turns out to be too small. The correct value could be generated by the quantum fluctuations of the two light bulk axions which could play the rôle of curvaton fields [66, 67, 68, 69, 70, 71, 72]. This study is however beyond the scope of this chapter, and so we leave it for future work.

We analyse now the full three-field cosmological evolution involving the Kähler moduli τ_7, $\mathcal{V}$ and τ_1. Their dynamics is governed by the following evolution equations for non-canonically normalised fields:

$$\begin{cases} \ddot{\phi}^i + 3H\dot{\phi}^i + \Gamma^i_{jk}\dot{\phi}^j\dot{\phi}^k + g^{ij}\frac{\partial V}{\partial \phi^j} = 0, \\ H^2 = \left(\frac{\dot{a}}{a}\right)^2 = \frac{1}{3}\left(\frac{1}{2}g_{ij}\dot{\phi}^i\dot{\phi}^j + V\right), \end{cases} \tag{3.63}$$

where the ϕ_i's represent the scalar fields τ_7, $\mathcal{V}$ and τ_1, a is the scale factor and Γ^i_{jk} are the target space Christoffel symbols using the metric g_{ij} for the set of real scalars ϕ^i such that $\frac{\partial^2 K}{\partial\Phi^I\partial\Phi^{*J}}\,\partial^\mu\Phi^I\partial_\mu\Phi^{*J} = \frac{1}{2}\,g_{ij}\partial_\mu\phi^i\partial^\mu\phi^j$.

For numerical purposes it is more convenient to express the cosmological evolution of the fields as a function of the number of efoldings N rather than time. In fact, by using $a(t) = e^N$ and $\frac{d}{dt} = H\frac{d}{dN}$, we can directly obtain $\tau_7(N)$, $\mathcal{V}(N)$ and $\tau_1(N)$ without having to solve for the scale factor. The equations of motion turn

[11] A similar situation arises in Kähler moduli inflation where however a detailed multifield analysis shows that the minimum of the volume mode is shifted during inflation without developing a runaway direction [137, 157].

out to be (with $'$ denoting a derivative with respect to N):

$$\begin{aligned}
\tau_7'' &= -(\mathcal{L}_{\rm kin}+3)\left(\tau_7'+\tau_7\mathcal{V}\frac{V_{,\mathcal{V}}}{V}+2\tau_7^2\frac{V_{,\tau_7}}{V}+2\tau_7\tau_1\frac{V_{,\tau_1}}{V}\right)+\frac{\tau_7'^2}{\tau_7} \qquad (3.64)\\
&\quad +\frac{\tau_7\tau_1'}{\mathcal{V}}\left(\frac{\tau_1'}{\sqrt{\tau_1}}-\frac{\tau_7'}{2\sqrt{\tau_7}}\right),\\
\mathcal{V}'' &= -(\mathcal{L}_{\rm kin}+3)\left(\mathcal{V}'+\frac{3\mathcal{V}^2}{2}\frac{V_{,\mathcal{V}}}{V}+\tau_7\mathcal{V}\frac{V_{,\tau_7}}{V}+\tau_1\mathcal{V}\frac{V_{,\tau_1}}{V}\right)+\frac{\mathcal{V}'^2}{\mathcal{V}}, \qquad (3.65)\\
\tau_1'' &= -(\mathcal{L}_{\rm kin}+3)\left(\tau_1'+\tau_1\mathcal{V}\frac{V_{,\mathcal{V}}}{V}+2\tau_7\tau_1\frac{V_{,\tau_7}}{V}+4\mathcal{V}\sqrt{\tau_1}\frac{V_{,\tau_1}}{V}\right)\\
&\quad +\frac{\tau_1'^2}{4\tau_1}+\frac{\tau_1\mathcal{V}'}{\mathcal{V}}\left(\frac{\tau_1'}{\tau_1}-\frac{\tau_7'}{\tau_7}\right)+\frac{\tau_1\tau_7'}{2\tau_7}\left(\frac{3\tau_7'}{2\tau_7}-\frac{\sqrt{\tau_1}}{\mathcal{V}}\tau_1'\right),
\end{aligned}$$

where the kinetic Lagrangian reads:

$$\mathcal{L}_{\rm kin}=\frac{1}{2}\left(-\frac{\mathcal{V}'^2}{\mathcal{V}^2}+\frac{\mathcal{V}'\tau_7'}{\mathcal{V}\tau_7}-\frac{3\tau_7'^2}{4\tau_7^2}+\frac{\sqrt{\tau_1}\tau_7'\tau_1'}{2\mathcal{V}\tau_7}-\frac{\tau_1'^2}{4\mathcal{V}\sqrt{\tau_1}}\right), \qquad (3.66)$$

and the full inflationary potential V is given by the sum of the standard LVS potential, the g_s loops and F^4 terms given in (3.36) and an uplifting contribution proportional to $\delta_{\rm up}$ which could come from an anti D3-brane at the tip of a warped throat:

$$\begin{aligned}
V &= \kappa\left[32A_s^2\pi^2\frac{\sqrt{\tau_1}}{\mathcal{V}}e^{-4\pi\tau_1}-8\pi A_s\frac{W_0\tau_1}{\mathcal{V}^2}e^{-2\pi\tau_1}+\frac{3\zeta}{4g_s^{3/2}}\frac{W_0^2}{\mathcal{V}^3}\right.\\
&\quad \left.+\frac{W_0^2}{\mathcal{V}^3}\left(\frac{A_1}{\tau_7}-\frac{A_2}{\sqrt{\tau_7}}+\frac{B_1\sqrt{\tau_7}}{\mathcal{V}}+\frac{B_2\,\tau_7}{\mathcal{V}}\right)+\frac{\delta_{\rm up}}{\mathcal{V}^{4/3}}\right]. \qquad (3.67)
\end{aligned}$$

$|\lambda| = 10^{-6}$ and correct amplitude of the density perturbations

Setting $\alpha = 1$ and performing the following choice of the underlying parameters:

$$\begin{aligned}
A_s &= 6\cdot 10^5 \qquad \chi=-188 \quad \Rightarrow \quad \zeta=-\frac{\zeta(3)\chi(X)}{2(2\pi)^3}=0.456 \quad W_0=50 \quad g_s=0.25\\
C_1^{\rm w} &= C_2^{\rm w}=0.05 \quad |C_3^{\rm w}|=10^{-4} \quad |C_4^{\rm w}|=0.1 \quad C_5^{\rm w}=C_6^{\rm w}=-0.05 \quad \lambda=-10^{-6},
\end{aligned}$$

the total potential (3.67) admits a Minkowski global minimum at:

$$\langle\mathcal{V}\rangle=2690.625\,, \qquad \langle\tau_7\rangle=6.503 \qquad \langle\tau_1\rangle=3.179 \quad \text{for} \quad \delta_{\rm up}=5.9598\cdot 10^{-4}\,.$$

Notice that this minimum is inside the Kähler cone since $\langle\tau_7\rangle > 2\langle\tau_1\rangle = 6.358$, which respects the lower bound in (3.39). At this level of approximation, the

closed string axions associated to $\mathcal{V}$ and τ_7 are flat directions. They receive a tiny potential from highly suppressed non-perturbative effects, and so they remain very light. Being so light, they do not affect the inflationary dynamics but would acquire isocurvature fluctuations of order H during inflation. If they do not play the rôle of dark matter, their final contribution to the amplitude of the isocurvature perturbations is negligible. On the other hand, if they are heavy enough to decay, their isocurvature fluctuations get converted into standard density perturbations, and so these bulk axions could behave as curvaton fields [66, 67, 68, 69, 70, 71, 72].

Let us now shift τ_7 away from its minimum at the initial condition $\tau_7(N = 0) = \langle\tau_7\rangle + 2030$ and recompute the new minimum for the other two directions $\langle\mathcal{V}\rangle(\tau_7)$ and $\langle\tau_1\rangle(\tau_7)$. These values would set the initial conditions for these fields, ensuring that the inflationary dynamics takes place along a stable trough in field space:

$$\mathcal{V}(0) = \langle\mathcal{V}\rangle(\tau_7(0)) = 3671.432\,, \quad \tau_7(0) = 2036.503\,, \quad \tau_1(0) = \langle\tau_1\rangle(\tau_7(0)) = 3.227\,.$$

Notice that these initial conditions are again inside the Kähler cone since $\tau_7(0) < \frac{\mathcal{V}(0)}{\sqrt{\tau_1(0)}} = 2043.7$, which satisfies the upper bound in (3.39). We shall also focus on vanishing initial velocities for all scalar fields: $\mathcal{V}'(0) = \tau_7'(0) = \tau_1'(0) = 0$.

Considering this set of initial conditions, we solved the system of equations of motion (3.65) finding the cosmological evolution of each scalar field as a function of the number of efoldings N. Inflation occurs in the region in field space where the generalised ϵ-parameter:

$$\epsilon(N) = -\frac{1}{4\mathcal{L}_{\rm kin}V^2}\left(V_{,\mathcal{V}}\,\mathcal{V}' + V_{,\tau_7}\,\tau_7' + V_{,\tau_1}\,\tau_1'\right)^2\,, \tag{3.68}$$

is much smaller than unity. As can be seen from Fig. 3.5, $\epsilon \ll 1$ during the first 57 efoldings and then quickly increases and reaches $\epsilon = 1$ at $N = 57.93$ where inflation ends.

Using the variable N to parametrise the cosmological evolution of the scalar fields and denoting by N_e the physical number of efoldings of inflation, $N_e = 52$, as estimated in Sec. 3.4.1, at $N_* = 5.93$. This is the point of horizon exit in field space where $\epsilon(N_*) = 1.456 \cdot 10^{-4}$ which yields a tensor-to-scalar ratio $r = 16\epsilon(N_*) = 0.0023$. The amplitude of the scalar power spectrum is:

$$\sqrt{P(N_*)} = \frac{1}{10\pi}\sqrt{\frac{2\,V(N_*)}{3\,\epsilon(N_*)}} = 1.035 \cdot 10^{-5}\,, \tag{3.69}$$

reproducing the reference COBE value $\sqrt{P_{\rm COBE}} \simeq 2 \cdot 10^{-5}$ with a good accuracy. Moreover the scalar spectral index is given by:

$$n_s(N_*) = 1 + \frac{d}{dN}\,\ln P(N)\Big|_{N=N_*} = 0.9701\,, \tag{3.70}$$

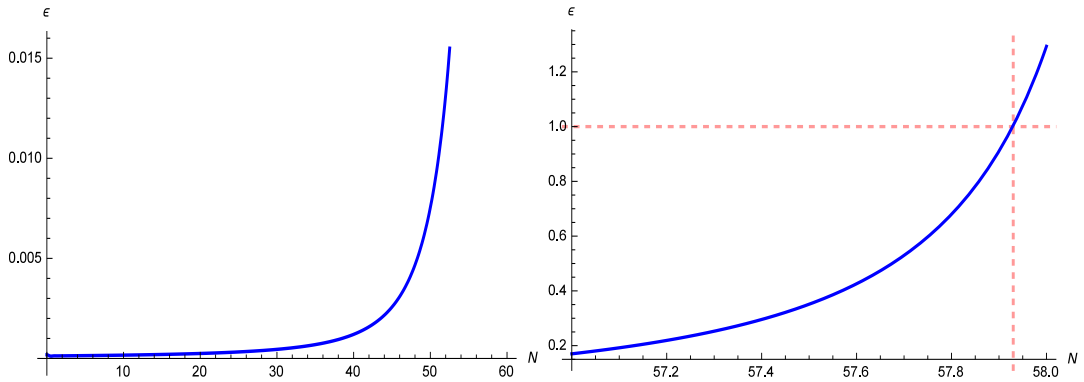

Figure 3.5: Evolution of the ϵ-parameter as a function of the number of efoldings N for (left) the entire inflationary dynamics and (right) for the last efolding.

in good agreement with Planck data [138, 139].

Fig. 3.6, 3.7 and 3.8 show the cosmological evolution of the three scalar fields τ_7, $\mathcal{V}$ and τ_1 during the whole inflationary dynamics and their final settling into the global minimum after a few oscillations. Fig. 3.9 shows instead the path of the inflationary trajectory in the $(\tau_7, \mathcal{V})$-plane (on the left) and in the (τ_7, τ_1)-plane (on the right). Clearly, as expected from the single-field analysis of Sec. 3.4.1, the inflaton travels mainly along the τ_7-direction.

Finally Fig. 3.10 presents a plot with the cosmological evolution of all KK mass scales, the inflationary scale $M_{\rm inf} = V^{1/4}$ and the gravitino mass $m_{3/2}$ from horizon exit to the final settling into the global minimum. The fact that $M_{\rm inf}$ remains always below all the KK scales, ensures that the Hubble scale during inflation $H = \frac{M_{\rm inf}}{\sqrt{3}}\left(\frac{M_{\rm inf}}{M_p}\right) < M_{\rm inf}$ is also always below each KK scale. The gravitino mass also remains always smaller than $M_{KK}^{(i)}$ $\forall i$. This guarantees that the 4D effective field theory is under control. In particular, $M_{KK}^{(2)}$, $M_{KK}^{(6)}$ and the inflationary scale evolve from $M_{KK}^{(2)}(N_*) \simeq 1.1{\cdot}10^{16}$ GeV, $M_{KK}^{(6)}(N_*) \simeq 2.1{\cdot}10^{16}$ GeV and $M_{\rm inf}(N_*) \simeq 5.3{\cdot}10^{15}$ GeV at horizon exit to $M_{KK}^{(2)}(N=60) \simeq 6.2\cdot 10^{16}$ GeV, $M_{KK}^{(6)}(N=60) \simeq 1.3\cdot 10^{16}$ GeV and $M_{\rm inf}(N=60) \simeq 9.3\cdot 10^{14}$ GeV around the final minimum. On the other hand the other scales remain approximately constant during the whole inflationary evolution around: $H \simeq 5\cdot 10^{12}\,{\rm GeV} < m_{3/2} \simeq 4\cdot 10^{15}\,{\rm GeV} < M_{KK}^{\rm bulk} \simeq 2\cdot 10^{16}\,{\rm GeV}$.

$|\lambda| = 10^{-3}$ and negligible amplitude of the density perturbations

We shall now relax the condition of generating the correct amplitude of the density perturbations from the inflaton quantum fluctuations. As explained above, the right COBE value of the amplitude of the power spectrum could instead be

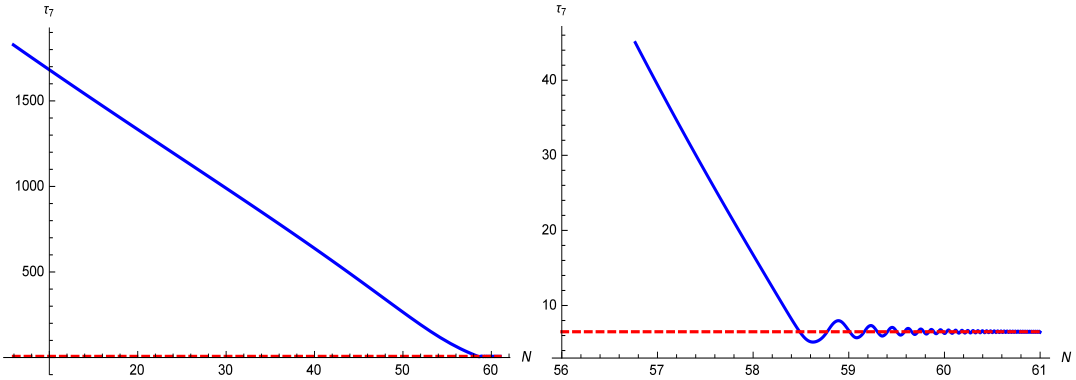

Figure 3.6: Evolution of τ_7 as a function of the number of efoldings N for (left) the entire inflationary dynamics and (right) for the last 2 efoldings. The dashed red line represents the position of the final global minimum.

reproduced in a non-standard way by a curvaton-like mechanism involving the quantum fluctuations of the two light bulk axions [66, 67, 68, 69, 70, 71, 72]. In this case we can focus on $\mathcal{V} \sim 5 \cdot 10^3$, $W_0 \sim \mathcal{O}(1)$, $\lambda \sim 10^{-3}$ and relatively small values of the coefficients of the winding loop corrections which generate the plateau, so that all the remaining four conditions listed at the beginning of Sec. 3.4.2 are fully satisfied.

We shall set $\alpha = 1$ and perform the following choice of the underlying parameters:

$$A_s = 1 \cdot 10^4 \quad \chi = -188 \quad \Rightarrow \quad \zeta = -\frac{\zeta(3)\chi(X)}{2(2\pi)^3} = 0.455 \quad W_0 = 1 \quad g_s = 0.25$$
$$C_1^{\rm w} = C_2^{\rm w} = 0.05 \quad C_3^{\rm w} = -10^{-4} \quad C_4^{\rm w} = -0.1 \quad C_5^{\rm w} = C_6^{\rm w} = -0.05 \quad \lambda = -0.001\,,$$

which yield a global Minkowski minimum inside the Kähler cone at:

$$\langle \mathcal{V} \rangle = 3220.899\,, \qquad \langle \tau_7 \rangle = 6.403 \qquad \langle \tau_1 \rangle = 3.179 \quad \text{for} \quad \delta_{\rm up} = 1.76588 \cdot 10^{-7}\,.$$

The initial conditions for the inflationary evolution are again derived in the same way: the fibre modulus τ_7 is shifted away from its minimum at $\tau_7(N = 0) = \langle \tau_7 \rangle + 2450$ and the other two directions $\langle \mathcal{V} \rangle(\tau_7)$ and $\langle \tau_1 \rangle(\tau_7)$ are set at the new minimum:

$$\mathcal{V}(0) = \langle \mathcal{V} \rangle(\tau_7(0)) = 4436.094\,, \quad \tau_7(0) = 2456.403\,, \quad \tau_1(0) = \langle \tau_1 \rangle(\tau_7(0)) = 3.228\,.$$

Notice that these initial conditions are inside the Kähler cone since $\tau_7(0) < \frac{\mathcal{V}(0)}{\sqrt{\tau_1(0)}} = 2468.95$, which satisfies the upper bound in (3.39). Focusing again on

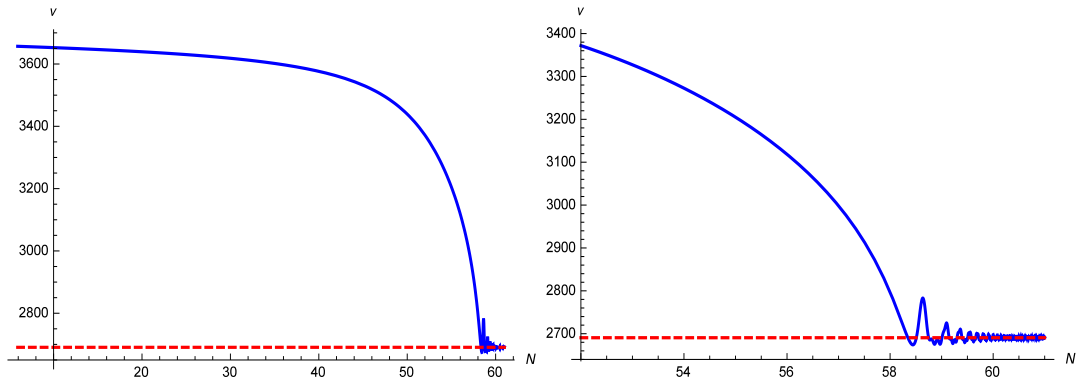

Figure 3.7: Evolution of $\mathcal{V}$ as a function of the number of efoldings N for (left) the entire inflationary dynamics and (right) for the last 6 efoldings. The dashed red line represents the position of the final global minimum.

vanishing initial velocities for all scalar fields, i.e. $\mathcal{V}'(0) = \tau_7'(0) = \tau_1'(0) = 0$, we worked out the cosmological evolution of each scalar field as a function of N by solving the system of equations of motion (3.65). Looking for a slow-roll region in field space where the generalised ϵ-parameter (3.68) is much smaller than unity, we found that $\epsilon \ll 1$ during the first 69 efoldings and then quickly increases and reaches $\epsilon = 1$ at $N = 69.15$ where inflation ends. The point of horizon exit corresponding to a physical number of efoldings of inflation $N_e = 52$ is localised at $N_* = 17.15$ where $\epsilon(N_*) = 1.36 \cdot 10^{-4}$. The main cosmological observables at horizon exit take the following values:

$$n_s(N_*) = 1 + \frac{d}{dN} \ln P(N)\Big|_{N=N_*} = 0.9676\,, \qquad r = 16\epsilon(N_*) = 0.0022\,,$$
$$\sqrt{P(N_*)} = \frac{1}{10\pi}\sqrt{\frac{2\,V(N_*)}{3\,\epsilon(N_*)}} = 1.64 \cdot 10^{-7}\,.$$

The scalar spectral index n_s and the tensor-to-scalar ratio r are in good agreement with Planck data [138, 139] while the amplitude of the scalar power spectrum, as expected, is much smaller than the reference COBE value $\sqrt{P_{\rm COBE}} \simeq 2 \cdot 10^{-5}$. As can be seen from Fig. 3.11, in this case the low-energy 4D effective field theory is fully under control since throughout all the inflationary evolution all KK scales are much higher than both the gravitino mass and the inflationary scale (and so also the Hubble scale).

In particular, $M_{KK}^{(2)}$, $M_{KK}^{(6)}$ and the inflationary scale evolve from $M_{KK}^{(2)}(N_*) \simeq 9.8 \cdot 10^{15}$ GeV, $M_{KK}^{(6)}(N_*) \simeq 1.8 \cdot 10^{16}$ GeV and $M_{\rm inf}(N_*) \simeq 6.5 \cdot 10^{14}$ GeV at horizon exit to $M_{KK}^{(2)}(N = 70) \simeq 5.5 \cdot 10^{16}$ GeV, $M_{KK}^{(6)}(N = 70) \simeq 1.2 \cdot 10^{16}$ GeV and

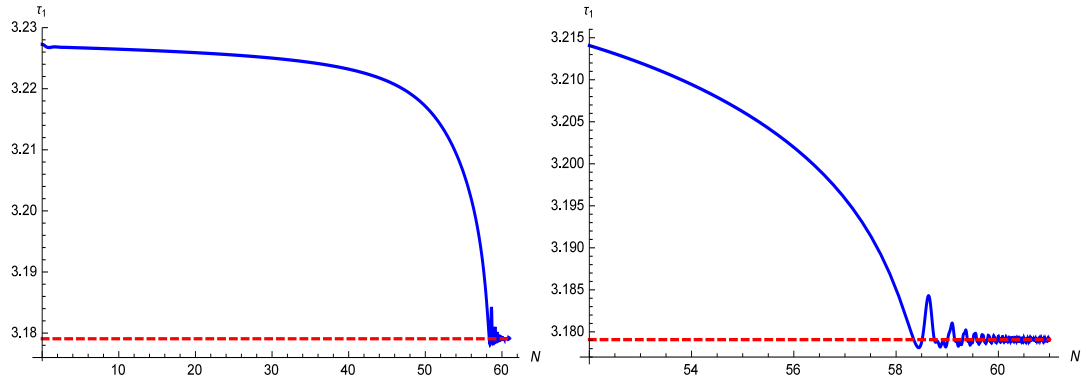

Figure 3.8: Evolution of τ_1 as a function of the number of efoldings N for (left) the entire inflationary dynamics and (right) for the last 6 efoldings. The dashed red line represents the position of the final global minimum.

$M_{\rm inf}(N=70) \simeq 1.4 \cdot 10^{14}$ GeV around the final minimum. On the other hand the other scales remain approximately constant during the whole inflationary evolution around: $H \simeq 8 \cdot 10^{11}\,{\rm GeV} < m_{3/2} \simeq 6 \cdot 10^{13}\,{\rm GeV} < M_{KK}^{\rm bulk} \simeq 2 \cdot 10^{16}\,{\rm GeV}$.

3.5 Conclusions

The study of large field inflationary models is particularly interesting from both a phenomenological and a theoretical point of view. In fact, from one side the next generation of CMB observations will be able to test values of the tensor-to-scalar ratio in the window $0.001 \lesssim r \lesssim 0.01$, while on the other hand trans-Planckian inflaton excursions need a symmetry mechanism to trust the effective field theory approach.

Natural inflaton candidates from type IIB string compactifications are Kähler moduli which enjoy non-compact shift-symmetries [88]. In particular, fibre inflation models provide promising plateau-like potentials which seem to fit Planck data rather well and lead to the prediction of observable tensor modes [101, 102, 103, 104]. These inflationary models are built within LVS moduli stabilisation scenarios and can be globally embedded in K3-fibred Calabi-Yau manifolds [141].

In this chapter we extended previous work by constructing the first explicit realisations of fibre inflation models in concrete type IIB Calabi-Yau orientifolds with consistent brane setups, full closed string moduli fixing and chiral matter on D7-branes. The underlying compactification manifold features $h^{1,1} = 4$ Kähler moduli which after D-term stabilisation get effectively reduced to the standard 3 moduli of fibre inflation models.

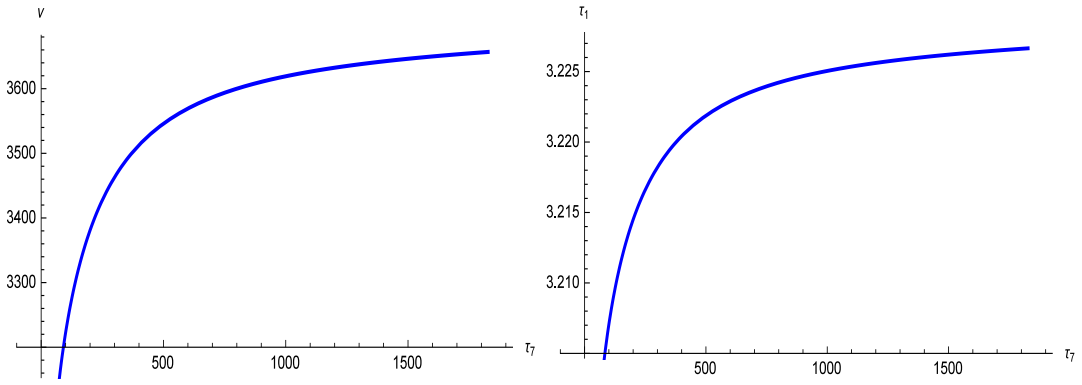

Figure 3.9: Plot of the whole inflationary evolution in the $(\tau_7, \mathcal{V})$-plane (on the left) and in the (τ_7, τ_1)-plane (on the right). Notice that the scales are different on the two axes since the inflaton travels mainly along the τ_7-direction.

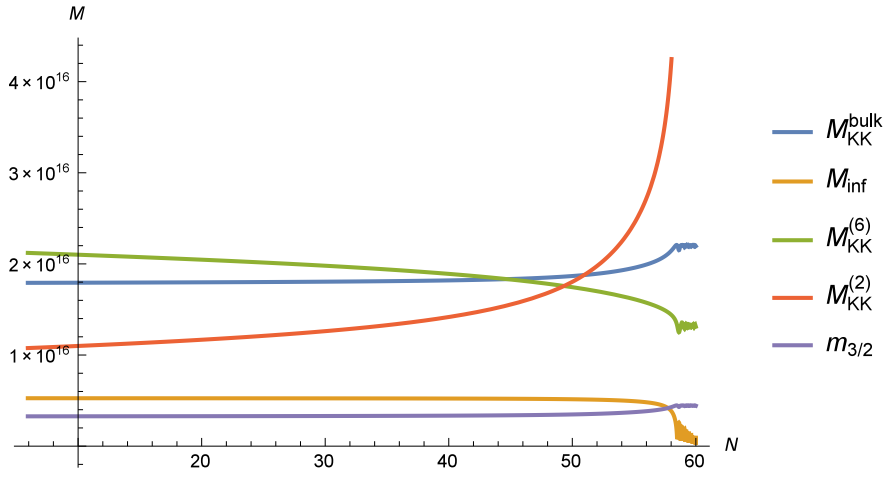

Figure 3.10: Evolution of all KK masses (with $M_{KK}^{(4)} = M_{KK}^{(2)}$), the inflationary scale $M_{\rm inf} = V^{1/4}$ and the gravitino mass $m_{3/2}$ in GeV units from horizon exit to the final settling into the global minimum.

We found that the inflationary dynamics is strongly constrained by the Kähler cone conditions which never allow for enough efoldings of inflation if the internal volume is of order $\mathcal{V} \sim 10^3$. For larger values of the Calabi-Yau volume of order $\mathcal{V} \sim 10^4$, the Kähler cone becomes large enough for the inflaton to drive $N_e \simeq 52$ efoldings, as required by an estimate of the post-inflationary evolution. However such a large value of $\mathcal{V}$ tends to suppress the amplitude of the density perturbations below the reference COBE value. This can be avoided by considering large values

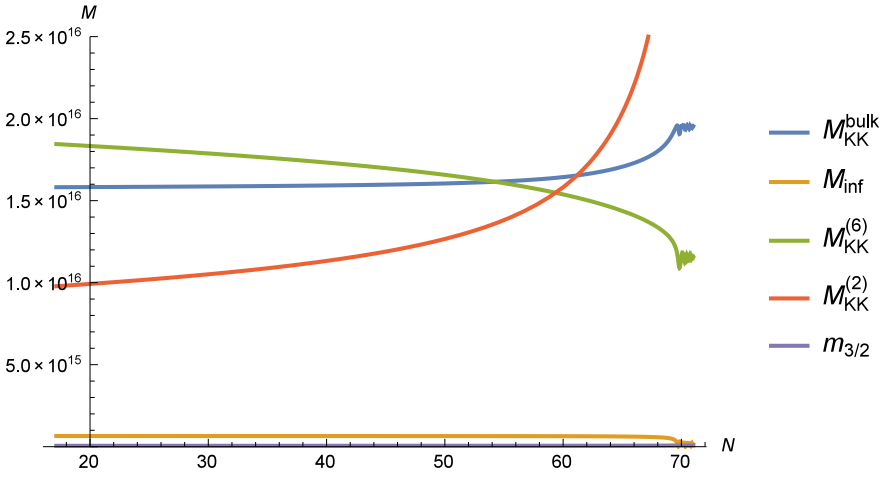

Figure 3.11: Evolution of all KK masses (with $M_{KK}^{(4)} = M_{KK}^{(2)}$), the inflationary scale $M_{\rm inf} = V^{1/4}$ and the gravitino mass $m_{3/2}$ in GeV units from horizon exit to the final settling into the global minimum.

of either the coefficients of the winding loops which generate the plateau, or the flux superpotential W_0. Let us stress that in the string landscape this choice is guaranteed to be possible by the fact that both of these microscopic parameters are flux-dependent.

However, as shown in Sec. 3.4.1, large values of the coefficients of the winding g_s corrections make the Hubble scale during inflation of the same order of magnitude of the mass of the volume mode. This could either cause a large shift of the original LVS minimum or even a problem for the stability of the inflationary direction against orthogonal runaway directions. A definite answer to this issue hence requires a proper multi-field analysis even if the two-field study of [101] revealed that the inflationary motion is still mostly single-field.

On the other hand, if the flux superpotential is of order $W_0 \sim 100$, the gravitino mass can become too close to some KK scale in the model, destroying the 4D effective field theory. Moreover, F^4 terms are proportional to $|\lambda| W_0^4$. Thus if W_0 is large, these higher derivative effects can spoil the flatness of the inflationary potential before achieving enough efoldings of inflation if $|\lambda|$ is not small enough. Hence in Sec. 3.4.1 we presented a model with $W_0 \sim 100$ and a very small value of $|\lambda|$ of order $|\lambda| = 10^{-7}$ which makes the F^4 terms harmless. The gravitino mass also turns out to be slightly smaller than any KK scale throughout the whole inflationary dynamics.

Due to the fact that in the single-field case not all our approximations are fully under control, in Sec. 3.4.2 we performed a complete numerical analysis of the

3-field cosmological evolution. For $W_0 \sim 100$ and $|\lambda| = 10^{-6}$, the multi-field analysis of Sec. 3.4.2 revealed that the accuracy of our approximations improves. In particular, the allowed number of efoldings of inflation increases due to the extra motion along the volume and blow-up directions. Hence inflation can successfully work also for smaller values of $\mathcal{V}$ which cause a smaller Kähler cone for the fibre modulus. This, in turn, requires smaller values of W_0 to match the COBE normalisation of the density perturbations, which enlarges the hierarchy between $m_{3/2}$ and the KK scales in the model.

We point out however that some of the underlying parameters are not flux-dependent, and so are not tunable in the string landscape. Two examples of this kind of parameters are the effective Euler number $\chi_{\rm eff}$ which controls the strength of $\mathcal{O}(\alpha'^3)$ corrections due to O7-planes [56] and the combinatorial factor λ which is the coefficient of $\mathcal{O}(\alpha'^3)$ higher derivatives [99]. Both of these microscopic parameters have not been computed in full detail yet, even if λ has been estimated to be of order 10^{-3} [100]. Hence in Sec. 3.4.2 we also presented a case with $|\lambda| = 0.001$ where it is hard to obtain enough efoldings inside the Kähler cone and generate, at the same time, the correct amplitude of the density perturbations in a framework where all the approximations are fully under control. Hence we chose the flux superpotential so that the contribution of the inflaton quantum fluctuations to the scalar power spectrum is negligible. In this case a viable inflationary phenomenology can therefore be achieved only in the presence of a non-standard mechanism for the generation of the density perturbations. A promising case could be the curvaton scenario where the initial isocurvature fluctuations could be produced by the quantum oscillations of the two light bulk closed string axions [158, 159, 160]. We study the impact of these ultra-light degrees of freedom on the inflationary parameters in Chapter 4. Indeed, the presence of light spectator fields in a curved field space may cause an uncontrolled growth of primordial perturbations that may quickly lead the system out of the perturbative regime.

Besides a complete computation of the exact value of both $\chi_{\rm eff}$ and λ, and the detailed derivation of a curvaton-like mechanism, there are several other important open issues for future work. A crucial one is that our chiral global models still lack an explicit implementation of a mechanism responsible for the realisation of a dS vacuum. Moreover, the study of the post-inflationary cosmological evolution of our universe is of primary importance in order to discriminate among different models that feature the same inflationary predictions of fibre inflation models. A first step forward towards understanding (p-)reheating has been taken in [161, 162]. A full understanding of this mechanism requires further investigation of the underlying microscopic dynamics.

Finally we stress that a better determination of the actual Calabi-Yau Kähler cone would be needed in order to find the actual moduli space volume. In this work

we just used an approximation inherited from the Mori cone of the ambient toric variety. Giving an answer to this question was the starting point of [163] where the authors investigate the space of flat directions of IIB Calabi-Yau orientifold models after partial moduli stabilization in an LVS vacuum. They looked at the list of Kreuzer-Skarke CY LVS-geometries showing diagonal del Pezzo divisors and scanned over all possible $h^{1,1} = 3,\ 4$. They found that CYs showing a K3 fibration generically allow for trans-Planckian field excursions.

Chapter 4

Geometrical destabilisation issues in String inflation?

4.1 Introduction

Many inflationary scenarios beyond the SM feature non-linear sigma models characterised by multiple scalar fields and a curved field manifold. In particular, these arise naturally within the framework of supergravity, string compactifications and models with non-minimal coupling. In a multi-field set-up, there are several spectator fields which can be either *heavy*, i.e. $m_{\rm h} \gg H$, or *light*, i.e. $m_{\rm l} \ll H$.

It has recently been claimed that when the field manifold is negatively curved, the effective mass of the isocurvature modes receives negative contributions which can potentially induce a geometrical instability by making them tachyonic [164]. In this case the effective mass-squared of the isocurvature fluctuations receives additional contributions from the Christoffel symbols and the Ricci scalar which can cause their exponential growth [164]. In principle this problem may be related to both heavy and light fields that are orthogonal to the inflationary trajectory. This effect could induce a *geometrical destabilisation* of the inflationary trajectory since the growth of the isocurvature perturbations quickly brings the system in the non-perturbative regime [1].

The low-energy limit of string compactifications is a 4D supergravity theory which is generically characterised by non-canonical kinetic terms so it may suffer from geometrical stabilisation problems. Indeed, a typical feature of 4D string models is the presence, at tree-level, of a plethora of massless fields, called moduli. Typically these fields acquire mass via supersymmetry breaking effects like non-

[1] This behaviour is to be distinguished from that of the recently proposed "ultra-light isocurvature scenario" [165, 166] where the isocurvature modes are effectively massless (and constant on superhorizon scales) and act as a source of curvature perturbations.

vanishing background fluxes at semi-classical level, string loops or α' corrections at perturbative level and higher-derivative contributions to the low-energy effective action.

Some of these moduli are however periodic axion-like fields which enjoy a shift symmetry that is exact at perturbative level [167, 168]. Hence they become massive only via tiny non-perturbative effects which tend to make them naturally very light, i.e. exponentially lighter than the gravitino mass which sets the mass scale of all the other non-axionic moduli [169, 76]. Being ultra-light, these axions are perfect candidates for dark radiation [14, 124] and quintessence fields [170, 171, 172, 173], and even for cold dark matter via the misalignment mechanism [174]. Another cosmological application of axion-like particles is to act as curvaton fields [175, 176]. In fact, during inflation, these ultra-light fields are expected to be much lighter than the Hubble scale. Hence they acquire isocurvature fluctuations which can be converted into standard adiabatic perturbations when the axions decay. If instead the axions are so light that they are still stable, one has to make sure that they do not contribute significantly to dark matter otherwise the amplitude of the isocurvature fluctuations would tend to be larger that the one detected in CMB observations [139]. Examples of such ultra-light axions are given by C_4 closed string axions related to large cycles (e.g. volume cycle) in the extra dimensions. Indeed, although they can get a mass through non-perturbative corrections to the superpotential, their contribution will be exponentially suppressed giving rise to sub-eV to nearly massless particles. These fields are always present in the effective field theory and their existence only relies on the topological properties of the Calabi-Yau manifold. Axionic isocurvature fluctuations are guaranteed to remain in the perturbative regime only when the field space is flat. On the other hand, when the fields live on a curved manifold we will see that an interesting dynamics can develop.

This chapter is organised as follows. In Sec.4.2 we briefly review the potential geometrical destabilisation of inflation. After that we show in Sec. 4.3 that, despite what has been claimed by other authors, heavy modes are stable when the system evolves along the attractor background trajectory, in agreement with previous results found in models with non-minimal coupling [177, 178]. In Sec. 4.4 we present our main result which is the new observation that a potential geometrical instability arises instead generically for ultra-light fields, i.e. $m_l \to 0$, when the background trajectory is geodesic. The occurrence of such instability is model dependent and a full understanding of the inflationary dynamics may require to go beyond perturbation theory. Being interested in string inflation model building, we come to the conclusion that, due to the generic presence of ultra-light axions and a curved field space, string inflationary models might be plagued by geometric destabilisation problems.

For this reason we then focus on concrete examples writing down the equations of motion for 2-field systems where we have a diagonal but non-canonical mass matrix. We first analyse a toy-model with two fields, ϕ_1 and ϕ_2, where ϕ_1 is a quintessence-like field whose potential is simply a negative exponential while ϕ_2 is massless, Sec. 4.5. We show that, despite the presence of a negatively curved field space, this system does not feature any geometrical destabilisation due to a non-zero turning rate of the underlying bending trajectory, which induces a positive contribution to the mass-squared of the isocurvature fluctuations.

In Sec. 4.6 we then focus on a type IIB inflationary model, Fibre Inflation (FI) [101, 104], which is characterised by the presence of two ultra-light axions and a curved field manifold. This model is particularly promising since it is based on an effective rescaling shift symmetry [88] and it allows for the construction of globally consistent Calabi-Yau models with inflation and chirality [141, 2] and the study of reheating [179]. Depending on which effects generate the inflationary potential (1-loop open string corrections [58, 60, 61] or higher derivative α' effects [99, 100]), slightly different FI models can arise [101, 102, 103]. However all of them feature a qualitatively similar shape of the inflationary potential characterised by a trans-Planckian plateau which resembles Starobinsky inflation [180] and supergravity α-attractors [181, 140]. The inflaton field range is around 5 in Planck units with larger values bounded by the size of the Kähler cone [163]; we saw this constraint arising in Chapter 3. In these models primordial gravity waves are at the edge of detectability since the tensor-to-scalar ratio turns out to be of order $0.005 \lesssim r \lesssim 0.01$.

We first analyse FI models in the limit where the two ultra-light axions are exactly massless and show that the quantum fluctuations of one of these entropic modes always experiences an exponential growth. We then try to avoid this geometrical destabilisation by turning on a non-zero axionic mass via non-perturbative effects. However we find that, in order to obtain a positive mass-squared of the isocurvature modes, these non-perturbative effects have to be of the same order of magnitude of the loop and higher derivative corrections which generate the inflationary potential. The inflationary model therefore changes completely since it becomes intrinsically multi-field. Hence, its dynamics should be re-analysed and the predictions for the cosmological observables should be re-derived. We therefore may be tempted to conclude that, if one requires a typical FI dynamics at leading order, there is no way to avoid a tachyonic instability for one of the two ultra-light axions.

Nevertheless at this point we need to face a paradoxical state of affairs. As previously mentioned, the tachyonic instability appears also in case of massless axion, that shows vanishing on-shell energy density. This happens despite the fact that the background trajectory is essentially single field and stable. This result is

somehow puzzling from a physical point of view and has prompted us to investigate this issue further.

In the last part of this chapter we show that the growth of isocurvature perturbations is triggered by the ill-defined coordinate system identified by the tangent and normal projectors into the inflationary trajectory. We then summarise the various definitions of entropy perturbations that are currently used in the literature, trying to understand which definition should be used in order to match the experimental result coming from isocurvature bounds. We find that the right quantity to compute is given by the standard definition of relative entropy between two scalar fluids. In the FI system these are identified by the energy density and pressure related to the inflaton field and the massless axion. The full computation of the relative entropy of the system shows that is it finite and vanishing during inflation, suggesting that FI models are presently viable both in what concerns curvature and entropy perturbations.

4.2 Geometrical destabilisation

The Lagrangian of a generic non-linear sigma model is:

$$\mathcal{L}/\sqrt{|g|} = \frac{1}{2}\gamma_{ij}(\phi_i)\partial_\mu\phi_i\partial^\mu\phi_j - V(\phi_i)\,, \tag{4.1}$$

where $\gamma_{ij}(\phi_i)$ denotes the field space metric. In such multi-field models the background trajectory defines a projection for the gauge invariant perturbations into a tangent component, the curvature perturbations, and an orthogonal component, the isocurvature perturbations. The inflationary dynamics of these models has been intensively studied over the last two decades and it has been shown to be significantly richer than that of single-field models while still being compatible with observational constraints.

The phenomenon of geometrical destabilisation follows directly from the mass matrix of gauge invariant scalar perturbations:

$$Q^i \equiv \delta\phi^i + \frac{\dot{\phi}^i}{H}\,\psi\,, \tag{4.2}$$

where $\phi^i(t,x) = \phi^i(t) + \delta\phi^i(t,x)$ and $\psi(t,x)$ denotes the scalar perturbation to the metric tensor. Let us therefore briefly review how the mass matrix arises in the context of multi-field models of inflation.

In the 2-field models we will be dealing with, it is convenient to project the gauge invariant perturbations Q^i onto normal $Q^N = N_iQ^i$ and parallel $Q^T = T_iQ^i$ components with respect to the background trajectory. N^i and T^i have unitary

2-norm with respect to the field space metric, γ_{ij}, so they satisfy the following relations:

$$N^i N^j \gamma_{ij} = 1\,, \qquad T^i N^j \gamma_{ij} = 0\,, \qquad T^i T^j \gamma_{ij} = 1\,. \tag{4.3}$$

From the second order action for the perturbations one finds the following equation of motion [182]:[2]

$$\frac{D^2 Q^i}{\partial t^2} + 3H\frac{DQ^i}{\partial t} + \frac{k^2}{a^2}\,Q^i + M^i{}_j Q^j = 0\,. \tag{4.4}$$

The covariant derivatives are defined as:

$$\frac{DQ^i}{\partial t} = \frac{\partial Q^i}{\partial t} + \Gamma^i_{jk}\dot{\phi}^j Q^k\,, \tag{4.5}$$

and the connections follow from the field space metric γ_{ij}. The mass matrix in the field basis reads:

$$M^i{}_j = V^i{}_{;j} - R^i_{klj}\dot{\phi}^k\dot{\phi}^l - \frac{1}{a^3}\frac{D}{\partial t}\left(\frac{a^3}{H}\dot{\phi}^i\dot{\phi}_i\right). \tag{4.6}$$

It is convenient to study the perturbations in the $\{T, N\}$ basis, where one finds an equation of motion of similar form to (4.4) with the covariant derivatives defined in terms of the spin connection (see e.g. [183, 184] for more details). Focusing on the equation of motion for a single orthogonal perturbation, Q^N, one finds that the mass term takes the form:

$$m^2_{\perp,\,\mathrm{eff}} = V_{;\,NN} + \epsilon\, R\, H^2 + 3\eta_\perp^2\, H^2\,, \tag{4.7}$$

where the projection of the covariant derivative is given by:

$$V_{;\,NN} = \left(V_{,ij} - \Gamma^k_{ij}V_{,k}\right) N^i N^j\,. \tag{4.8}$$

In (4.7) the first two terms depend both on the geometry of the field space and on the scalar potential, while $\eta_\perp$ is related to the inverse of the radius of curvature of the inflationary trajectory in field space and parametrises its non-geodesicity:

$$\eta_\perp = \frac{V_i N^i}{\dot{\phi}_0 H} \qquad \text{with} \qquad \dot{\phi}_0 = \sqrt{\gamma_{ij}\dot{\phi}^i\dot{\phi}^j}\,. \tag{4.9}$$

The second term in (4.7) depends on the curvature of the 2-dimensional field space R, and is the focus of this work. If negative and sufficiently large it can trigger an instability for the isocurvature perturbations by turning their mass-squared negative [185, 164]. Before delving into the stability analysis of specific models, let us see under which conditions the geometrical instability may arise.

[2] In our notation $i, j, \ldots$ denote field space directions while capital indices refer to the T and N orthonormal basis.

4.3 Geometrical stability for heavy fields

The destabilisation originally considered in [164] concerned heavy spectator fields during inflation. These are degrees of freedom with a super-Hubble mass, that naively would not play a rôle in the low energy dynamics. Given that for heavy fields $N^i N^j V_{ij} \gg H^2$ and during inflation $\epsilon \ll 1$, this can happen only if $|R| \gg 1$. Ref. [164] considered a simple model where a heavy field is coupled to the inflaton kinetic terms via a higher-order operator suppressed by M:

$$\frac{\mathcal{L}}{\sqrt{-g}} = \frac{1}{2} f^2 \left(\frac{\chi}{M}\right) \partial_\mu \phi \partial^\mu \phi + \frac{1}{2} \partial_\mu \chi \partial^\mu \chi - V(\phi) - \frac{1}{2} m_h^2 \chi^2 \,, \tag{4.10}$$

with $m_h \gg H$ and $f_{\chi\chi}/f > 0$ for a certain range of M, the mass parameter setting the scale of the field space curvature. In this case $|R| \simeq 4/M^2$, and so $M \ll 1$ can generate a large negative contribution to $m^2_{\perp\,\mathrm{eff}}$. Indeed, while the zero mode of the heavy field sits at its minimum $\dot{\chi} = \chi = 0$, causing $\eta_\perp = 0$, the mass-squared of the isocurvature perturbations:

$$m^2_{\perp,\,\mathrm{eff}} = V_{\chi\chi} - 2\frac{f_{\chi\chi}}{f}\,\epsilon H^2 \,, \tag{4.11}$$

becomes negative due to the curvature term dominating $m^2_{\perp\,\mathrm{eff}}$. This could trigger an instability characterised by a super-horizon growth of the isocurvature perturbations which signals a breakdown of perturbation theory and a potential premature end of inflation [164]. Let us point out that negatively curved field manifolds arise naturally both in supergravity and in multifield models with non-minimal couplings [186]. In fact, the simple Kähler potential $K = -3\ln(T + \bar{T})$ for the complex volume modulus T gives $R = -8/3$. However the reference scale of supergravity is the Planck mass, and so $M \simeq 1$. This implies that during inflation generically $\epsilon|\mathbb{R}|H^2 \ll H^2$, resulting in an absence of any geometric instability.

In what follows we shall however show that, even if $|R| \gg 1$, m^2_{eff} is negative only if it is computed on a repulsive trajectory, while the isocurvature modes are stable if the system evolves along the attractor trajectory. Thus the physical interpretation of $m^2_{\mathrm{eff}} < 0$ is not that quantum fluctuations grow beyond the regime of validity of perturbation theory but that the classical field trajectory is unstable under perturbations of the initial conditions.

To analyse the model we focus on the case where:

$$\gamma_{ij} = \begin{pmatrix} 1 & 0 \\ 0 & f^2(\phi_1) \end{pmatrix} \quad \text{and} \quad V = V(\phi_1) + V(\phi_2) \,. \tag{4.12}$$

Notice that we made this choice following [164] since it allows to have simple analytic formulae, but a geometrical instability can arise also for more generic

cases with non-diagonal metric and non-sum-separable potential. It can be shown that the corresponding curvature scalar can be negative since it takes the form:

$$\mathbb{R} = -2\,\frac{f_{11}}{f}\,. \tag{4.13}$$

The equations of motion from (4.1) and (4.12) for $\phi_i = \phi_i(t)$ in an expanding Universe with $\sqrt{|g|} = a^3$ read:

$$\dot{\pi}_1 = a^3\left(f f_1 \dot{\phi}_2^2 - V_1\right) \qquad \dot{\pi}_2 = -a^3\,V_2\,, \tag{4.14}$$

where the conjugate momenta are:

$$\pi_1 = a^3\dot{\phi}_1 \qquad\qquad \pi_2 = a^3 f^2 \dot{\phi}_2\,. \tag{4.15}$$

The background dynamics of the system is determined by (4.14), (4.15) and the Friedmann equation:

$$H^2 = \frac{1}{3}\left(\frac{1}{2}\gamma_{ij}\dot{\phi}^i\dot{\phi}^j + V\right). \tag{4.16}$$

4.3.1 Canonical heavy field

We first consider the case where the heavy field has canonical kinetic terms, and so identify ϕ_1 with the heavy scalar and ϕ_2 with the inflaton. We see from (4.14) that the equation for ϕ_1 admits a slow-roll solution with [187]:

$$f f_1 \dot{\phi}_2^2 \simeq V_1\,, \tag{4.17}$$

which implies that π_1 is an approximately conserved quantity. Given that during inflation $a \propto e^{Ht}$, (4.15) then gives $\dot{\phi}_1 \to 0$. In this solution the heavy field does not sit at the minimum of its potential but it is displaced from it by the inflaton's kinetic energy. Hence the motion is non-geodesic since:

$$\eta_\perp = \frac{V_1}{H f \dot{\phi}_2} = -\frac{f_1\dot{\phi}_2}{H}\,, \tag{4.18}$$

leading to an isocurvature mass:

$$m_{\rm eff}^2 = V_{11} + \left(3\eta_\perp^2 - 2\epsilon\,\frac{f_{11}}{f}\right)H^2\,. \tag{4.19}$$

Using (4.17), we can further simplify $m_{\rm eff}^2$ and show that on this generic solution it is strictly positive:

$$m_{\rm eff}^2 = 8\epsilon\left(\frac{f_1}{f}\right)^2 H^2\,, \tag{4.20}$$

even if the Ricci scalar is negative. This signals that the background trajectory is stable, regardless of the functional form of the kinetic coupling $f^2(\phi_1)$.

Notice however that, in particular cases where $V_1 = 0$ and $ff_1 = 0$ have a common root, (4.17) could also be exactly satisfied with the heavy field sitting at the bottom of its potential. In this case $\eta_\perp = 0$, and so the effective mass (4.19) reduces to:

$$m_{\rm eff}^2 = V_{11} - 2\epsilon \frac{f_{11}}{f} H^2 \,. \tag{4.21}$$

If $0 < f \ll f_{11}$ (or $f_{11} \ll f < 0$), this effective mass can become negative in regimes where the field space curvature contribution dominates [185, 164].

However we will now show that this unusual behaviour is merely a consequence of doing cosmological perturbation theory on a repulsive background trajectory since the trivial solution is unstable under perturbations of the initial conditions:

$$\phi_1 = \bar{\phi}_1 + \delta \,, \tag{4.22}$$

where $\bar{\phi}_1$ is the solution to $ff_1\dot{\phi}_2^2 = V_1 = 0$ and δ is a small homogeneous perturbation. One can then study the stability of the solution $\phi_1 = \bar{\phi}_1$ by expanding (4.14) to linear order in δ (we neglect perturbations in ϕ_2 as we are interested in getting a qualitative picture of the behaviour of the system) and solving for the time evolution of the perturbation. From (4.14) one finds:

$$\dot{\pi}_1|_{\bar{\phi}_1} + a^3 \left(V_1 - ff_1\dot{\phi}_2^2\right)\Big|_{\bar{\phi}_1} = -a^3 \left(\ddot{\delta} + 3H\dot{\delta} + \mu^2\delta\right) , \tag{4.23}$$

where the mass parameter μ is defined as:

$$\mu^2 \equiv V_{11}|_{\bar{\phi}_1} - (f_1^2 + ff_{11})|_{\bar{\phi}_1}\dot{\phi}_2^2 \,. \tag{4.24}$$

By definition of $\bar{\phi}_1$, the l.h.s. of (4.23) vanishes, and so the perturbation to the background trajectory δ obeys:

$$\ddot{\delta} + 3H\dot{\delta} + \mu^2\delta = 0 \,. \tag{4.25}$$

Evaluating (4.24) on the trivial solution $ff_1\dot{\phi}_2^2 = V_1 = 0$ with $\eta_\perp = 0$, we find:

$$\mu^2 = m_{\rm eff}^2|_{\bar{\phi}_1} \,, \tag{4.26}$$

indicating that the super-horizon growth of the isocurvature perturbations for $m_{\rm eff}^2 < 0$ is just an artifact of doing perturbation theory on an unstable background with $\mu^2 < 0$. This is not a surprise since δ can be seen as a long wavelength isocurvature perturbation. This means that the trivial solution is not an attractor

for the inflationary dynamics, and so the system will reach it only if the initial conditions are finely tuned such that at $t = 0$:

$$\phi_1 = \bar{\phi}_1 \quad \text{and} \quad \dot{\phi}_1 = \ddot{\phi}_1 = 0\,. \tag{4.27}$$

However, from a multi-field point of view, the evolution of the system will proceed initially along the steepest directions of the potential without leading to the initial conditions (4.27). Hence, in general, the system will evolve along the generic solution (4.17) which gives $\mu = 0$, indicating that perturbations get exponentially damped and this non-trivial background is indeed an attractor of the inflationary dynamics.

We illustrate this point in Figs. 4.1 and 4.2 which show the dynamics for the minimal geometry of [164]:

$$f^2(\phi_1) = 1 + 2\frac{\phi_1^2}{M^2}\,, \tag{4.28}$$

supplemented by a double quadratic potential:

$$V = \frac{1}{2}m_1^2\phi_1^2 + \frac{1}{2}m_2^2\phi_2^2\,. \tag{4.29}$$

Given the analytic arguments presented above, the qualitative features of this two-field system do not depend on this particular choice. In fact, similar results can be found with different potentials like that of [164]. In this minimal geometry:

$$\mathbb{R} = -\frac{4M^2}{\left(M^2 + 2\phi_1^2\right)^2} \simeq -\frac{4}{M^2}\,, \tag{4.30}$$

where in the last step we took $\phi_1/M \ll 1$. By tuning the mass scale M small, one can enhance the effects of the field space curvature and trigger the instability as formulated in [164]. For numerical purposes we have chosen $\{m_1, m_2, M\} = \{1, 10, 0.05\}$. In Fig. 4.1 we show the evolution of m^2_{eff} for the trivial background where it is always negative, and upon addition of a small perturbation that triggers the transition between the trivial solution $ff_1\dot{\phi}_2^2 = V_1 = 0$ and the attractor of (4.17) where $m^2_{\text{eff}} > 0$. Notice that these results are consistent with what has been previously found in models with non-minimal coupling [177, 178].

To highlight the effects of perturbations to the initial conditions (4.27), we plot in Fig. 4.2 (a subspace of) the phase space of the non-linear sigma model. It is clear that even very small perturbations of (4.27) take the trajectory away from the trivial solution and into the inflationary attractor, confirming the analytical result of (4.26).

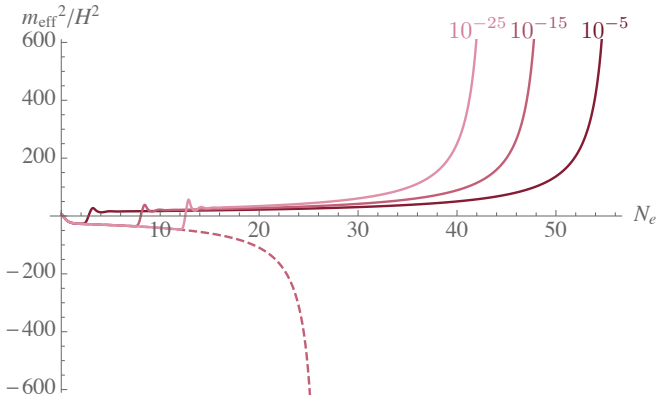

Figure 4.1: Effective mass for the isocurvature modes on the trivial background (dashed) and upon transition from this solution to the attractor (4.17) by addition of perturbations to the heavy field $\delta = \{10^{-5}, 10^{-15}, 10^{-25}\}$.

4.3.2 Canonical inflaton

We now identify the canonical field ϕ_1 with the inflaton and study if an instability can arise. The equation for the heavy field ϕ_2 in (4.14) is solved by $V_2 \simeq 0$ which from (4.15) implies that $\pi_2 = 0$ is approximately constant with $\dot{\phi}_2 \to 0$ if f does not increase exponentially during inflation. The momentum π_2 becomes exactly constant for:

$$V_2 = \dot{\phi}_2 = 0\,, \tag{4.31}$$

implying that on this trivial solution we have $\vec{T} = (\pm 1, 0)$ and $\vec{N} = (0, f^{-1})$. Notice that this solution does not constrain f_1, unlike in the case analysed in Sec. 4.3.1. One can then show that (4.31) yields $\eta_\perp = 0$ and an effective mass of the form:

$$m_{\rm eff}^2 = \frac{V_{22}}{f^2} + \frac{f_1}{f} V_1 - 2\frac{f_{11}}{f}\epsilon H^2\,. \tag{4.32}$$

Using the slow-roll approximation, the contribution to this effective mass coming from the field space Christoffel symbols can be rewritten as:

$$\frac{f_1}{f} V_1 = -3H\frac{f_1}{f}\dot{\phi}_1 = -3H^2\frac{d\ln f}{dN}\,, \tag{4.33}$$

where $N = \ln a$ denotes the number of e-foldings. Defining $g(N) \equiv \frac{d\ln f}{dN}$ one can integrate to find:

$$f(N) = f_0\, e^{\int_0^N g(N')dN'}\,. \tag{4.34}$$

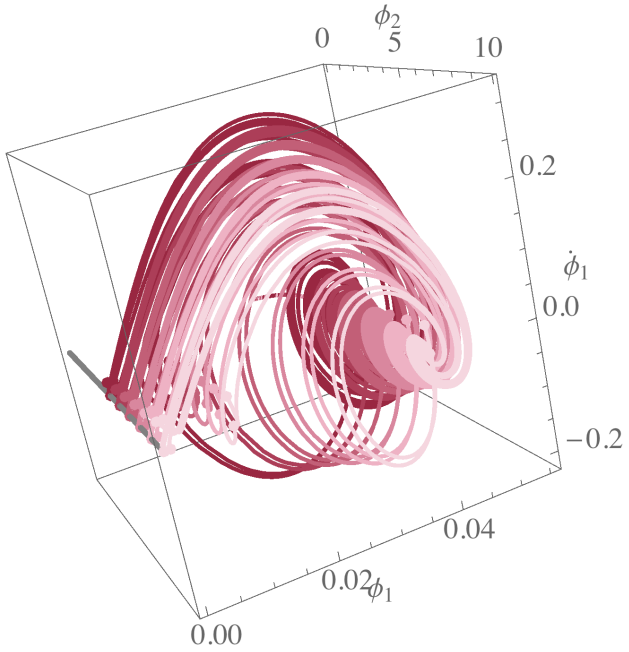

Figure 4.2: Phase space projection of the non-linear sigma model. The trivial trajectory is shown in grey. The repulsive nature of this background trajectory is evident since small perturbations of the initial conditions (4.27) take the background towards the attractor solution (4.17).

The isocurvature effective mass (4.32) can then be rewritten in terms of the function $g(N)$ as:

$$\frac{m_{\rm eff}^2}{H^2} = \frac{V_{22}}{H^2 f^2} - 3g - g^2 + g\epsilon - \frac{dg}{dN}\,, \tag{4.35}$$

which shows that an instability would be present if:

$$1 \ll \frac{V_{22}}{H^2 f^2} \ll g^2\,. \tag{4.36}$$

The sign of $g(N)$ is crucial for determining the behaviour of the system. For $g > 0$, f grows during inflation and $m_{\rm eff}^2 < 0$ coincides with the mass of ϕ_2 becoming sub-Hubble, in contradiction with our assumption that ϕ_2 is a heavy field which corresponds to the first inequality in (4.36). In this case one should not talk about an instability since the system becomes effectively a two-field model which would require a different analysis. Conversely, if $g < 0$, the contribution to $m_{\rm eff}^2$ coming from the mass of ϕ_2 increases and prevents the instability from ever taking hold. Thus we conclude that the case with a canonical inflaton does not feature any geometrical instability.

4.4 An instability for ultra-light fields?

In Sec. 4.3 we have shown that heavy fields with $m_{\rm h} \gg H$ do not suffer from any geometrical destabilisation when the effective mass of the isocurvature perturbations is computed on the attractor background solution. In this section, we shall however point out that the case of *ultra-light* fields with $m_{\rm l} \to 0$ is potentially dangerous since isocurvature fluctuations can become tachyonic when the background trajectory is geodesic. We shall again study separately the two cases where the canonical field is either the ultra-light mode or the inflaton.

4.4.1 Canonical ultra-light field

If the ultra-light field is ϕ_1, $V = V(\phi_2)$ and so $V_1 = 0$. In this case, as can be seen from (4.14), π_1 is not a conserved quantity and (4.15) shows that there is a non-zero turning rate of the background trajectory since $\dot{\phi}_1 \neq 0$. This results in tangent and normal unit vectors with generic non-zero components:

$$\vec{T} = \frac{1}{|\dot{\phi}|}\left(\dot{\phi}_1, \dot{\phi}_2\right) \qquad \vec{N} = \frac{1}{f|\dot{\phi}|}\left(-f^2\dot{\phi}_2, \dot{\phi}_1\right) , \tag{4.37}$$

leading to a non-zero $\eta_\perp$ of the form:

$$\eta_\perp = \frac{\dot{\phi}_1 V_2}{Hf|\dot{\phi}|^2} . \tag{4.38}$$

Hence the isocurvature mass (4.19) reduces to:

$$\frac{m_{\rm eff}^2}{H^2} = 3\eta_\perp^2 - 2\epsilon\,\frac{f_{11}}{f} \simeq 2\epsilon\left[\left(\frac{f_1}{f}\right)^2 - \frac{f_{11}}{f}\right] + \mathcal{O}(\epsilon^2) , \tag{4.39}$$

where in the last step we have used the slow-roll approximation. Clearly the sign of $m_{\rm eff}^2$ depends on the particular functional dependence of $f(\phi_1)$. A generic supergravity case is $f = f_0\, e^{k\phi_1^p}$ which gives $m_{\rm eff}^2 \simeq 0$ for $p = 1$ and any value of k. This limiting case has been studied in [188, 165] which showed that the isocurvature power spectrum remains constant on super-horizon scales and acts as a continuous source of curvature perturbations due to a non-zero coupling induced by $\eta_\perp \neq 0$. Different values of p and k can lead to a positive or negative $m_{\rm eff}^2$, showing that a geometrical instability can potentially arise. Notice that, in contrast with the findings of Sec. 4.3.1, this case features a genuine instability which is not simply a signal of the repulsive character of the background trajectory since (4.39) has been computed for $\dot{\pi}_1 = a^3 f f_1 \dot{\phi}_2^2$ that is the attractor of the dynamical system.

4.4.2 Canonical inflaton

We now study the case where the inflaton is ϕ_1 while the ultra-light field is ϕ_2 with $V_2 = 0$. From (4.14) we see that π_2 is exactly constant, and so in slow-roll (4.15) gives:

$$\dot{\phi}_2(t) \simeq \dot{\phi}_2(0) \left(\frac{f(0)}{f(t)}\right)^2 e^{-3Ht}\,, \tag{4.40}$$

which shows that $\dot{\phi}_2(t) = 0$ if the initial condition is $\dot{\phi}_2(0) = 0$. In this case the trajectory is exactly geodesic with $\eta_\perp = 0$ and the isocurvature mass (4.35) reduces to:

$$\frac{m_{\rm eff}^2}{H^2} = -3g - g^2 + g\epsilon - \frac{dg}{dN}\,. \tag{4.41}$$

This signals the generic appearance of a geometrical instability which could be avoided only for $-3 < g < 0$. Notice that, using (4.33), (4.41) in the slow-roll approximation can also be rewritten as:

$$\frac{m_{\rm eff}^2}{H^2} = -3\frac{f_1}{f}\frac{\dot{\phi}_1}{H} - 2\frac{f_{11}}{f}\epsilon\,, \tag{4.42}$$

showing that the sign of the inflaton velocity is crucial to determine the presence of an instability. We stress again that this would be a genuine instability since we are considering a trajectory which is a dynamical attractor.

An interesting string model where such a situation might arise is *Fibre Inflation* [101] where the rôle of ϕ_2 is played by the supersymmetric axionic partner of the inflaton and in *Kähler moduli Inflation* [136] where the rôle of ϕ_2 is played by the axion related to the volume modulus. We study the first case in more detail in Sec. 4.6.

If the initial velocity of the ultra-light field is different from zero but f does not decrease exponentially during inflation, (4.40) shows that $\dot{\phi}_2$ relaxes to zero exponentially quickly, and so the previous analysis still holds. Ref. [189] however considered the case with $V = V_0\, e^{-k_1\phi_1}$ and $f = f_0\, e^{-k_2\phi_1} = f_0\, e^{-k_1 k_2 N}$ where f can decrease exponentially with the number of e-foldings if $k_1 k_2 > 0$. In this case $\dot{\phi}_2$ can no longer be neglected and the system does not evolve along a geodesic trajectory. Hence $m_{\rm eff}^2$ receives a positive contribution proportional to:

$$\eta_\perp^2 = \left(\frac{f\dot{\phi}_2 V_1}{H}\right)^2 \frac{1}{|\dot{\phi}|^4} \neq 0\,, \tag{4.43}$$

which can prevent the instability. Notice that, when $\dot{\phi}_2(0) \neq 0$, the system can be studied by integrating out $\dot{\phi}_2$ and rewriting the first equation in (4.14) as:

$$\dot{\pi}_1 = -a^3\, V_{\rm eff,1}\,, \tag{4.44}$$

with a time-dependent effective potential, extending the definition given in [189] to curved (time varying) backgrounds:

$$V_{\rm eff} \equiv V(\phi_1) + \frac{\pi_2^2}{2a^6 f^2(\phi_1)}\,. \tag{4.45}$$

We extensively study this toy model in Sec. 4.5 where we classify all the possible behaviors of the system, depending on the values of k_1 and k_2.

In what follows we will focus on concrete examples where a canonical inflaton field ϕ_1 is kinetically coupled to an ultra-light field ϕ_2. The reason for this specific choice comes from the fact that this is the most common situation that can be found in concrete string inflation models. In particular we will consider cases where the ultra-light field is an axion and we assume that the field space metric can be written as in Eq. (4.12). This class of metrics occurs often in the closed string moduli sector, where the function f might depend explicitly on the inflaton ϕ_1 while the dependence on the other heavy moduli $\phi_{\rm h}$ is given in terms of their vacuum expectation values: $f = f(\phi_1, \langle\phi_{\rm h}\rangle)$. In the remaining part of this section we explicitly compute the main quantities that will be used in the analysis of specific examples starting from Sec. 4.5. The 2-field system is described by:

$$\begin{cases} \ddot{\phi}_1 + 3H\dot{\phi}_1 - f\, f_1 \dot{\phi}_2^2 + V_1 = 0 \\ \ddot{\phi}_2 + 3H\dot{\phi}_2 + 2\frac{f_1}{f}\dot{\phi}_2\dot{\phi}_1 + \frac{V_2}{f^2} = 0 \end{cases} \tag{4.46}$$

and:

$$T^a = \frac{1}{\dot{\phi}_0}\begin{pmatrix}\dot{\phi}_1 \\ \dot{\phi}_2\end{pmatrix} \qquad N^a = \frac{1}{\dot{\phi}_0}\begin{pmatrix}-f\,\dot{\phi}_2 \\ f^{-1}\,\dot{\phi}_1\end{pmatrix}\,. \tag{4.47}$$

The turning rate of the trajectory reduces to:

$$\eta_\perp = \frac{1}{2\epsilon H^3}\left(f^{-1}\dot{\phi}_1 V_2 - f\dot{\phi}_2 V_1\right), \tag{4.48}$$

where we used $\dot{\phi}_0^2 = 2\epsilon H^2$. This implies:

$$\begin{aligned} m^2_{\perp,\,\rm eff} \;=\; & \frac{1}{\dot{\phi}_0^2}\left[(f\dot{\phi}_2)^2\left(V_{11} + 3\frac{V_1^2}{\dot{\phi}_0^2}\right)\right. \\ & - 2\dot{\phi}_1(f\dot{\phi}_2)\left(\frac{V_{12}}{f} - \frac{f_1}{f}\frac{V_2}{f} + 3\frac{V_1 V_2}{f\dot{\phi}_0^2}\right) \\ & + \left.\dot{\phi}_1^2\left(\frac{V_{22}}{f^2} + \frac{f_1}{f}V_1 + 3\frac{V_2^2}{\dot{\phi}_0^2 f^2}\right)\right] - \dot{\phi}_0^2\frac{f_{11}}{f}\,. \end{aligned} \tag{4.49}$$

Defining the fraction of kinetic energy carried by ϕ_1 and ϕ_2 as $\alpha_1 \equiv \frac{\dot\phi_1}{\dot\phi_0}$ and $\alpha_2 \equiv \frac{f\dot\phi_2}{\dot\phi_0}$ respectively, the entropic mass-squared can be written as:

$$\begin{aligned} m^2_{\perp,\,\mathrm{eff}} &= \alpha_2^2\left(V_{11}+3\frac{V_1^2}{\dot\phi_0^2}\right)-2\alpha_1\alpha_2\left(\frac{V_{12}}{f}-\frac{f_1}{f}\frac{V_2}{f}+3\frac{V_1V_2}{f\dot\phi_0^2}\right) \\ &+ \alpha_1^2\left(\frac{V_{22}}{f^2}+\frac{f_1}{f}V_1+3\frac{V_2^2}{\dot\phi_0^2 f^2}\right)-\dot\phi_0^2\frac{f_{11}}{f}\,. \end{aligned} \tag{4.50}$$

If ϕ_2 is ultra-light, i.e. $V_2 \simeq 0$, (4.50) reduces to:

$$m^2_{\perp,\,\mathrm{eff}} = \alpha_2^2\left(V_{11}+3\frac{V_1^2}{\dot\phi_0^2}\right)+\alpha_1^2\frac{f_1}{f}V_1-\dot\phi_0^2\frac{f_{11}}{f}\,. \tag{4.51}$$

In what follows we shall be interested in models where the curvature is constant and negative:

$$R=-|R|=-2\,\frac{f_{11}}{f}=\text{constant}\,, \tag{4.52}$$

which implies:

$$f(\phi_1)=A_+\,e^{\lambda\phi_1}+A_-\,e^{-\lambda\phi_1} \qquad \text{with} \qquad \lambda=\sqrt{\frac{|R|}{2}}\,. \tag{4.53}$$

In the two special cases with respectively $A_+ = 0$ or $A_- = 0$, the equations of motion become:

$$\begin{cases} \ddot\phi_1+3H\dot\phi_1\mp\lambda A_\pm^2\,e^{\pm 2\lambda\phi_1}\dot\phi_2^2+V_1=0 \\ \ddot\phi_2+3H\dot\phi_2\pm\lambda\dot\phi_2\dot\phi_1=0 \end{cases} \tag{4.54}$$

while the effective mass-squared for the isocurvature perturbation simplifies to:

$$m^2_{\perp,\,\mathrm{eff}} = -\lambda^2\dot\phi_0^2\pm\lambda\alpha_1^2V_1+\alpha_2^2\left(\frac{3V_1^2}{\dot\phi_0^2}+V_{11}\right). \tag{4.55}$$

In the single-field approximation where ϕ_1 drives inflation while the background value of ϕ_2 is essentially frozen, i.e. $\alpha_2 \ll \alpha_1 \simeq 1$, Eq. (4.55) can be approximated as:

$$m^2_{\perp,\,\mathrm{eff}} \simeq \lambda\left(\pm V_1-\lambda\dot\phi_0^2\right). \tag{4.56}$$

The requirement of having a positive mass-squared for the isocurvature perturbation then reduces to $|V_1| > \lambda\dot\phi_0^2$ with $V_1 > 0$ for $A_- = 0$ and $V_1 < 0$ for $A_+ = 0$. Using $\dot\phi_0^2 = 2\epsilon H^2$, and the single-field slow-roll approximations $H^2 \simeq V/3$ and $2\epsilon \simeq (V_1/V)^2$, we can easily see that for $\epsilon \ll 1$ and $\lambda \sim \mathcal{O}(1)$:

$$\frac{\lambda\dot\phi_0^2}{|V_1|} \simeq \frac{\lambda}{3}\sqrt{2\epsilon} < 1\,. \tag{4.57}$$

Hence the positivity of the effective mass-squared of the isocurvature perturbation is determined just by the sign of V_1 which is the term associated with the metric connection in Eq. (4.8). Interestingly, the Fibre Inflation models which we will discuss in Sec. 4.6.1 feature two ultra-light axions, one with $A_+ = 0$ and the other with $A_- = 0$. Hence one of them has necessarily to be geometrically unstable.

Since in this context the geometrical destabilisation phenomenon is by definition model dependent, we devote the next two sections to the analysis of specific examples. We first look into a simple quintessence-like potential before turning to the string inspired case of Fibre Inflation.

4.5 Stability of quintessence-like potentials

4.5.1 Equations of motion

Exponential potentials can provide the energy density for driving the observed late time accelerated expansion of the universe. Furthermore their simplicity renders them interesting for our purposes as it allows for exact analytic results. Let us therefore focus on the following toy-model involving a quintessence-like field ϕ_1 and a massless field ϕ_2 with non-canonical kinetic terms. The metric has the same form as (4.12) with $f = f_0\, e^{-k_1\phi_1}$ while the scalar potential reads:

$$V = V_0\, e^{-k_2\phi_1}\,. \tag{4.58}$$

From (4.51) we see that the effective mass-squared of the isocurvature perturbations is:

$$m^2_{\perp,\,\text{eff}} = k_2\, V\left(\alpha_2^2 k_2\left(1+\frac{3\,V}{\dot\phi_0^2}\right)+\alpha_1^2 k_1\right) - k_1^2\dot\phi_0^2\,. \tag{4.59}$$

The equations of motion are:

$$\begin{cases} \ddot\phi_1 + 3H\dot\phi_1 + k_1\left(f\dot\phi_2\right)^2 - k_2 V = 0 \\ \ddot\phi_2 + \left(3H - 2k_1\dot\phi_1\right)\dot\phi_2 = 0 \end{cases} \tag{4.60}$$

which, after trading cosmic time for the number of efoldings $N = \ln a$, can also be rewritten as (the prime superscript denotes derivatives with respect to N):

$$\begin{cases} \phi_1'' + (3-\epsilon)\,(\phi_1' - k_2) + k_1\,(f\phi_2')^2 = 0 \\ \phi_2'' + (3 - \epsilon - 2k_1\phi_1')\,\phi_2' = 0 \end{cases} \tag{4.61}$$

The ϕ_2 equation can be integrated exactly yielding an explicit expression for the velocity of the ultra-light field:

$$\phi_2'(N) = C\, e^{-3N + 2k_1\phi_1(N) + \int_0^N \epsilon(\tilde N)\, d\tilde N}\,, \tag{4.62}$$

where $C = \phi_2'(0)\, e^{-2k_1\phi_1(0)}$. Since the kinetic terms of the massless field ϕ_2 are non-canonical, it is more appropriate to consider the quantity:

$$(f\phi_2')\,(N) = f_0 C\, e^{-3N+k_1\phi_1(N)+\int_0^N \epsilon(\tilde{N})\, d\tilde{N}}\,, \tag{4.63}$$

which enters into the inflationary ϵ parameter:

$$\epsilon = \frac{1}{2}\,\phi_1'^2 + \frac{1}{2}\,(f\phi_2')^2\,. \tag{4.64}$$

Let us now study the behaviour of the system using both an analytical and a computational approach. In the attractor regime where $\phi_1'' \simeq (f\phi_2')' \simeq 0$, the equations of motion take the form:

$$\begin{cases} (3-\epsilon)\,(\phi_1' - k_2) + k_1(f\phi_2')^2 = 0 \\ (3-\epsilon-k_1\phi_1')\,(f\phi_2') = 0 \end{cases} \tag{4.65}$$

The system admits two different solutions depending on whether ϕ_2 is frozen or not.

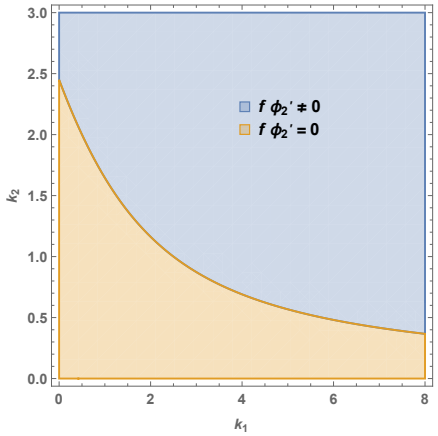

Figure 4.3: Velocity of the massless isocurvature mode in the (k_1, k_2) parameter space.

4.5.2 Case I: Non-zero turning rate

This case is characterised by a rolling massless field with $f\phi_2' \neq 0$, $\epsilon = \frac{3k_2}{(2k_1+k_2)}$ and:

$$\begin{cases} \phi_1' = \frac{3-\epsilon}{k_1} \\ (f\phi_2')^2 = \phi_1'^2\left(\frac{k_1 k_2}{3-\epsilon} - 1\right) \end{cases}. \tag{4.66}$$

For $k_1 > 0$, the conditions $\epsilon < 1$, $k_1\phi_1' > 0$ and $(f\phi_2')^2 \geqslant 0$ can be satisfied only for:

$$k_2 \geqslant \sqrt{k_1^2 + 6} - k_1 \,. \tag{4.67}$$

It is easy to realise that under this condition the effective mass-squared of the isocurvature mode remains always non-negative:

$$\frac{m_{\perp,\,\mathrm{eff}}^2}{H^2} = \frac{6k_1(k_2^2 + 2k_1k_2 - 6)}{2k_1 + k_2} \geqslant 0 \,. \tag{4.68}$$

The absence of geometrical destabilisation is due to the fact that the trajectory deviates from a simple geodesic since:

$$\eta_\perp^2 = \left[\frac{(3-\epsilon)}{2\epsilon}\frac{V_1}{V}(f\phi_2')\right]^2 = \frac{k_1}{2k_1 + k_2}\frac{m_{\perp,\,\mathrm{eff}}^2}{H^2} \neq 0 \,. \tag{4.69}$$

Notice that in the limiting case where $k_2 = -k_1 + \sqrt{k_1^2 + 6}$, the system evolves towards the attractor solution where $f\phi_2' = 0$, $\alpha_2 = 0$, $\alpha_1 = 1$, $m_{\perp,\,\mathrm{eff}}^2 = 0$ and $\eta_\perp = 0$. However, we checked that the convergence to this point is extremely slow and the turning rate of the trajectory remains non-negligible for a large number of e-foldings.

4.5.3 Case II: Geodesic motion

In this case $f\phi_2' = 0$, $\epsilon = k_2^2/2$ and the asymptotic state reached by the system is:

$$\begin{cases} \phi_1' = k_2 \\ (f\phi_2')^2 = 0 \end{cases} \tag{4.70}$$

under the requirement:

$$k_2 \leqslant \sqrt{k_1^2 + 6} - k_1 \,. \tag{4.71}$$

Fig. 4.3 shows the behaviour of the velocity of the massless field ϕ_2 for different values of the parameters k_1 and k_2. In this case the system evolves along a geodesic with $\eta_\perp = 0$ and the sign of the effective mass-squared of the entropic perturbation depends on the sign of k_2 since:

$$\frac{m_{\perp,\,\mathrm{eff}}^2}{H^2} = \frac{k_1k_2}{2}\underbrace{\left(6 - 2k_1k_2 - k_2^2\right)}_{\geqslant 0} \,. \tag{4.72}$$

Hence $m_{\perp,\,\mathrm{eff}}^2 \geqslant 0$ for $k_2 > 0$, while $m_{\perp,\,\mathrm{eff}}^2 \leqslant 0$ for $k_2 < 0$. Notice that in this case geometrical destabilisation can be avoided for $k_2 > 0$ due to the positive contribution coming from the metric connection. These results are completely independent on the initial conditions.

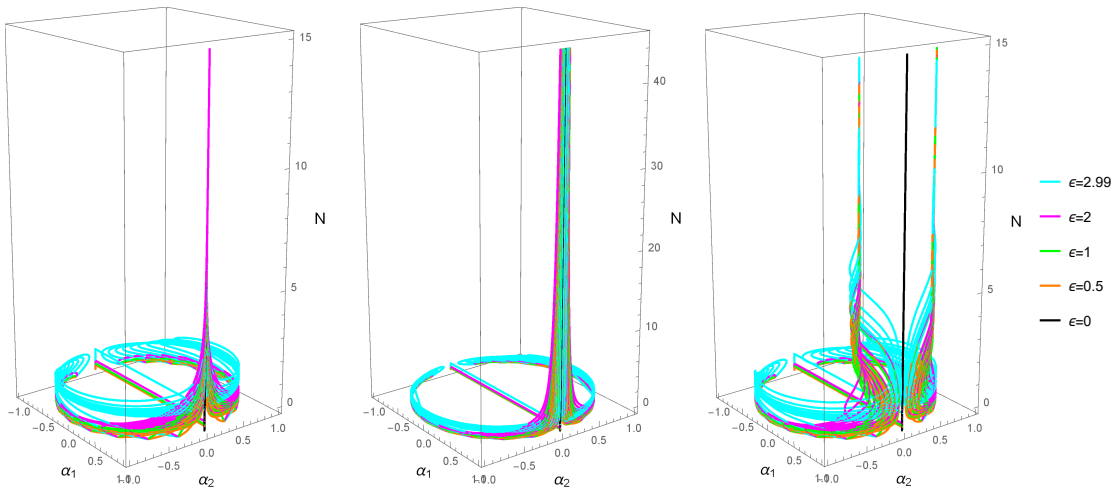

Figure 4.4: Evolution of $\alpha_1 \equiv \dot{\phi}_1/\dot{\phi}_0$ and $\alpha_2 \equiv f\dot{\phi}_2/\dot{\phi}_0$ (with $\alpha_1^2 + \alpha_2^2 = 1$) for different initial values of $\epsilon = \dot{\phi}_0^2/(2H^2)$. We set $k_2 = \beta(\sqrt{k_1^2+6} - k_1)$ with $\beta = 0.8$ (left), $\beta = 1$ (centre), $\beta = 1.2$ (right) and $k_1 = 1$.

4.5.4 Numerical analysis

In order to strengthen our analytical results, we also performed a numerical analysis using several parameter sets. We considered different values of the initial kinetic energy $\epsilon_i(0) = \{0, 0.5, 1, 2, 3\}$[3] and for each of these values we analysed 20 different types of initial conditions for the field velocities:

$$\begin{cases} \phi_1'(0)|_{(ik)} = \sqrt{2\epsilon_i(0)}\,\cos\left(\frac{k\pi}{10}\right) \\ (f\phi_2')\,(0)|_{(ik)} = \sqrt{2\epsilon_i(0)}\,\sin\left(\frac{k\pi}{10}\right) \end{cases} \qquad k = 0, \ldots, 19\,. \tag{4.73}$$

The dynamics of the system is independent on both the initial field values and the normalisation of the scalar potential and the kinetic function. Hence we set, without loss of generality, $\phi_1(0) = \phi_2(0) = 0$ and $V_0 = f_0 = 1$. We studied the 3 interesting cases with $k_2 = \beta(\sqrt{k_1^2+6} - k_1)$ and $\beta = 0.8, 1, 1.2$ for $k_1 = 1$. Our numerical results are shown in Figs. 4.4-4.6 and are in perfect agreement with our analytical analysis. In Fig. 4.4 we can clearly see that for $\beta \leqslant 1$ the system converges to a single-field behaviour with $\eta_\perp = 0$, while for $\beta > 1$ the turning rate of the trajectory is non-zero and the asymptotic behaviour of the system depends on the initial condition for the velocity of the massless field ϕ_2.

Notice that the trajectories which move away from the unit circle $\alpha_1^2 + \alpha_2^2 = 1$ correspond to cases with special initial conditions, $\phi_1'(0)$ with the same sign as V_1

[3]These values of ϵ describe initial conditions ranging from slow-roll ($\epsilon \ll 1$) to kinetic domination ($\epsilon = 3$). For kinetic domination we actually chose $\epsilon = 2.99$ in order to avoid a singularity in the equations of motion stemming from the use of N as the time variable.

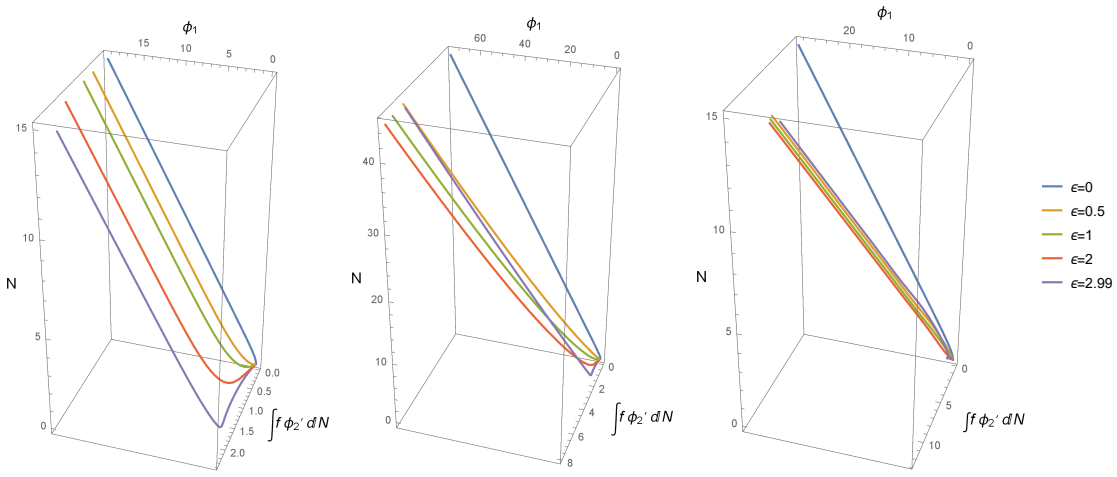

Figure 4.5: Evolution of the physical fields $\{\phi_1(N), \int_0^N f(\phi_1(\tilde{N}))\phi_2'(\tilde{N})d\tilde{N}\}$ for different values of the initial kinetic energy (setting $k = 1$ in the initial conditions (4.73) for the field velocities) and $\beta = 0.8$ (left), $\beta = 1$ (centre), $\beta = 1.2$ (right).

and $\phi_2'(0) = 0$, where ϕ_1 initially climbs up the potential and then it slows down until it stops and changes its direction. At this point $\phi_1' = \phi_2' = 0$, and so the coordinates α_1 and α_2 are ill-defined. As soon as ϕ_1 changes its direction, $\phi_1' \neq 0$, and so the system jumps to the opposite point in the unit circle.

Fig. 4.6 presents the evolution of $m^2_{\perp,\text{eff}}$ and $\eta_\perp$, showing that the numerical solutions correctly approach our analytic results for 3 different cases. Notice that in the limiting case with $\beta = 1$ all curves tend asymptotically to $m^2_{\perp,\text{eff}} = \eta_\perp = 0$, while in case I with $\beta = 1.2$, only the blue curve corresponding to $\omega = 0$ features a negative mass-squared due to the initial condition $(f\phi_2')(0) = 0$. This is the only case which could be plagued by a geometric destabilisation problem but it corresponds to a very non-generic choice of initial conditions as argued in [3]. As soon as $(f\phi_2')(0)$ or ω slightly deviates from zero, Fig. 4.6 clearly shows that the mass-squared becomes positive due to a non-vanishing $\eta_\perp$.

4.6 Geometrical destabilisation in Fibre Inflation

4.6.1 Ultra-light axions in Fibre inflation

The simplest version of Fibre Inflation involves 3 type IIB Kähler moduli $T_i = \tau_i + \mathrm{i}\theta_i$, $i = 1, 2, 3$ where the τ's control volumes of 4-cycles while the θ's are periodic axion-like fields which enjoy a perturbative shift symmetry. The Kähler

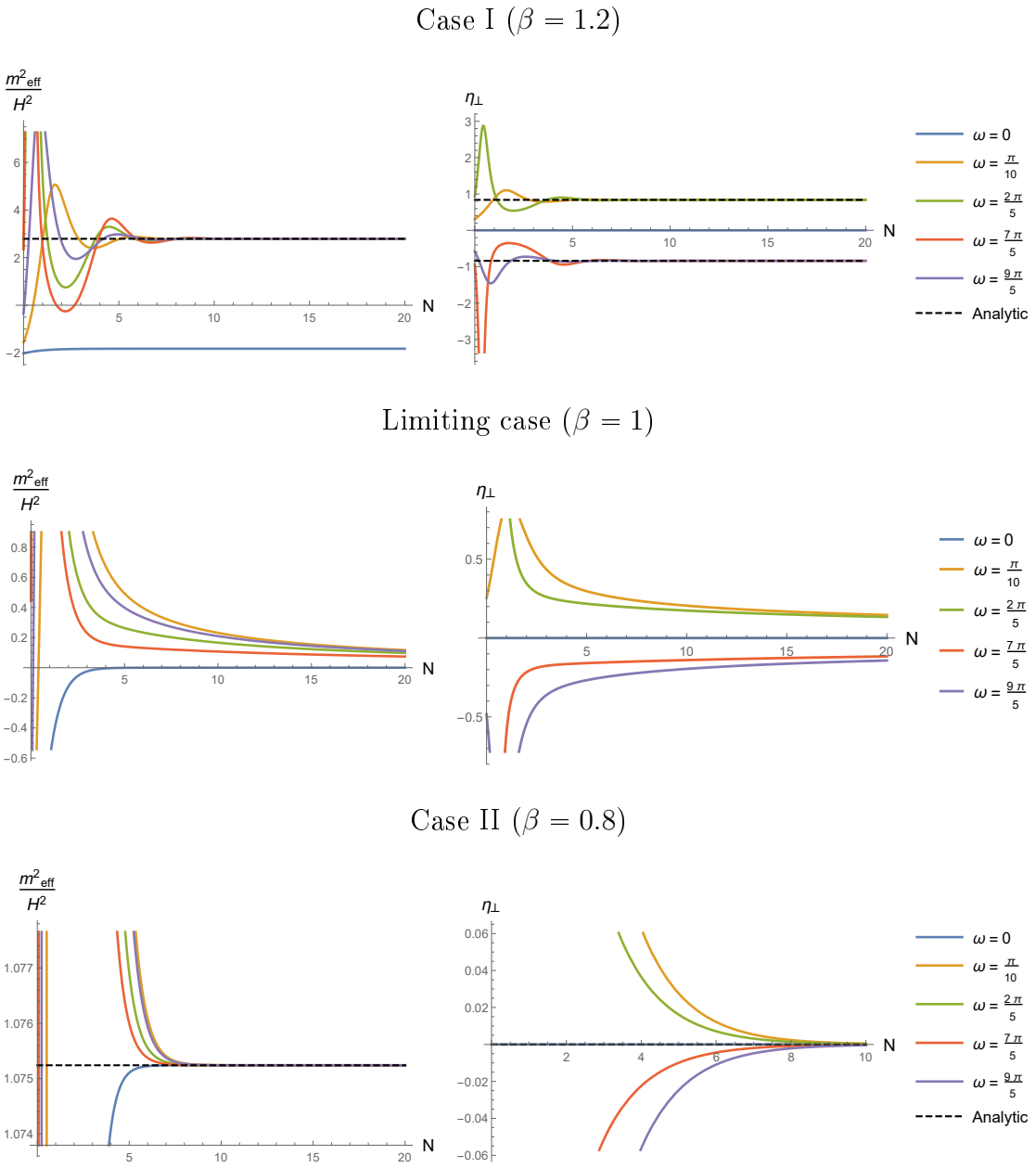

Figure 4.6: Evolution of $m^2_{\perp,\text{eff}}/H^2$ (left) and $\eta_\perp$ (right) for $\epsilon(0) = 2$ and different initial field velocities identified by $\omega_k \equiv k\pi/10$ with $\kappa = \{0, 1, 4, 14, 18\}$. The 3 different cases correspond to $\beta = \{0.8, 1, 1.2\}$.

potential reads:

$$K = -2\ln\left(\mathcal{V} + \frac{\xi}{2g_s^{3/2}}\right) + K_{g_s}\,, \tag{4.74}$$

where $\mathcal{V} = \alpha\left(\sqrt{\tau_1}\tau_2 - \lambda_3\tau_3^{3/2}\right)$ is the Calabi-Yau volume, the $\mathcal{O}(1)$ constant ξ controls the leading order α' contribution [55], while K_{g_s} denotes 1-loop open string corrections [58, 60, 61]. The superpotential is instead given by a tree-level constant W_0 and non-perturbative effects from gaugino condensation on D7-branes or ED3-instantons [190]:

$$W = W_0 + A_3\, e^{-a_3 T_3}\,. \tag{4.75}$$

If g_s loops are neglected, the Kähler potential (4.74) and the superpotential (4.75) generate a scalar potential of the LVS form [63, 62]:

$$V_{\rm LVS} = \frac{8a_3^2A_3^2\sqrt{\tau_3}}{3\alpha\lambda_3\mathcal{V}}e^{-2a_3\tau_3} + \frac{4a_3A_3\tau_3W_0\cos(a_3\theta_3)}{\mathcal{V}^2}\,e^{-a_3\tau_3} + \frac{3\xi W_0^2}{4g_s^{3/2}\mathcal{V}^3}\,, \tag{4.76}$$

which leads to the existence of AdS vacua at exponentially large volume (in string units) where $\mathcal{V}$, τ_3 and θ_3 are stabilised at:

$$\begin{aligned} a_3\langle\theta_3\rangle = \pi\,, \qquad a_3\langle\tau_3\rangle &= \left(\frac{\xi}{2\alpha\lambda_3}\right)^{2/3}\frac{1}{g_s}\,, \\ \langle\mathcal{V}\rangle &= \frac{3W_0\alpha\lambda_3}{4a_3A_3}\sqrt{\langle\tau_3\rangle}\,e^{a_3\langle\tau_3\rangle}\,. \end{aligned} \tag{4.77}$$

It is easy to see that the scalar potential (4.76) features three flat directions corresponding to τ_1 and the two axions θ_1 and θ_2. The inclusion of subleading g_s or α' corrections to the Kähler potential can lift τ_1 but not θ_1 and θ_2 which are protected by a perturbative shift symmetry. In the presence of sources of positive vacuum energy which can allow for dS vacua (see for example [65, 74, 73, 75]), the potential for τ_1 can be flat enough to drive inflation. τ_1 plays the rôle of the inflaton since, when it is shifted away from its minimum, it is naturally much lighter then the Hubble scale during inflation H whose value is set by the mass of τ_1 close to the minimum, $H^2 \simeq W_0^2/\mathcal{V}^{10/3}$ (see [101] for more details).

On the other hand, the other five spectator fields are isocurvature modes which are expected to stay around their minima during inflation. Three of them, $\mathcal{V}$, τ_3 and θ_3, are heavy fields with a mass larger than H, while θ_1 and θ_2 are ultra-light fields since they can develop a non-zero mass only via tiny non-perturbative corrections to the superpotential (4.75). In order to study the possibility of having geometrical destabilisation of any of these entropic directions, we need to focus on the field space metric which looks like:

$$\mathcal{L}_{\rm kin} = \frac{\partial^2 K}{\partial T_i\partial\bar{T}_j}\,\partial_\mu T_i\partial^\mu\bar{T}_j = \frac{\gamma_{ij}}{2}\left(\partial_\mu\tau_i\partial^\mu\tau_j + \partial_\mu\theta_i\partial^\mu\theta_j\right). \tag{4.78}$$

The field space is curved, and so the kinetic terms can be diagonalised exactly only locally. However, in LVS models, we can use the exponentially large overall volume

$\mathcal{V}$ as an excellent expansion parameter to obtain leading order results. Thus if we transform the real parts of the Kähler moduli as [160]:

$$\begin{aligned} \tau_1 &= e^{\frac{2}{\sqrt{3}}\phi_1+\sqrt{\frac{2}{3}}\phi_2+\frac{1}{2}\phi_3^2}\,, \qquad \mathcal{V} = e^{\sqrt{\frac{3}{2}}\phi_2}\,, \\ \tau_3 &= \left(\frac{3}{4\alpha\lambda_3}\right)^{2/3} e^{\sqrt{\frac{2}{3}}\phi_2}\phi_3^{4/3}\,, \end{aligned} \tag{4.79}$$

the kinetic Lagrangian (4.78) for the real parts simplifies to:

$$\begin{aligned} \mathcal{L}_{\rm kin}^{(\phi)} &= \frac{1}{2}\partial_\mu\phi_1\partial^\mu\phi_1\left(1+\frac{3}{4}\phi_3^2\right)+\frac{1}{2}\partial_\mu\phi_2\partial^\mu\phi_2 \\ &+ \frac{1}{2}\partial_\mu\phi_3\partial^\mu\phi_3\left(1-\frac{3}{4}\phi_3^2+\frac{9}{16}\phi_3^4\right)+\frac{3\sqrt{3}}{8}\phi_3^3\,\partial_\mu\phi_1\partial^\mu\phi_3\,. \end{aligned} \tag{4.80}$$

Notice that this expression is diagonal at leading order since (4.79) implies $\phi_3^2 \sim \mathcal{O}(\mathcal{V}^{-1}) \ll 1$, while subleading corrections induce a kinetic coupling between the heavy field ϕ_3 and the canonically normalised inflaton ϕ_1. However we shall show below that this field is heavy enough to prevent any geometrical destabilisation. Moreover, we point out that in the kinetic Lagrangian (4.78) there is no mixing between real and imaginary parts of the Kähler moduli. The kinetic terms for the axions read:

$$\begin{aligned} \mathcal{L}_{\rm kin}^{(\theta)} &= \frac{1}{4\tau_1^2}\partial_\mu\theta_1\partial^\mu\theta_1+\frac{\alpha^2\lambda_3\tau_3^{3/2}}{2\mathcal{V}^2\sqrt{\tau_1}}\partial_\mu\theta_1\partial^\mu\theta_2+\frac{\alpha^2\tau_1}{2\mathcal{V}^2}\partial_\mu\theta_2\partial^\mu\theta_2 \\ &- \frac{3\alpha\lambda_3\sqrt{\tau_3}}{4\tau_1\mathcal{V}}\partial_\mu\theta_1\partial^\mu\theta_3-\frac{3\alpha^2\lambda_3\sqrt{\tau_1}\sqrt{\tau_3}}{2\mathcal{V}^2}\partial_\mu\theta_2\partial^\mu\theta_3 \\ &+ \frac{3\alpha\lambda_3}{8\mathcal{V}\sqrt{\tau_3}}\partial_\mu\theta_3\partial^\mu\theta_3\,, \end{aligned} \tag{4.81}$$

where τ_1, $\mathcal{V}$ and τ_3 are given by (4.79). The kinetic Lagrangian (4.81) clearly shows that the two ultra-light axions θ_1 and θ_2 are kinetically coupled to the canonically normalised inflaton ϕ_1. It is therefore crucial to analyse the contribution to the isocurvature power spectrum of each of these two entropic modes. We shall find below that the effective mass-squared of one of these two ultra-light axions is negative during inflation while the other always remains positive. This result justifies the fact that we will study the dynamics of the system by focusing just on the 2-field subspace spanned by the inflaton ϕ_1 and the unstable isocurvature direction, as summarised in Sec. 4.2.

We shall find that which of the two axions is unstable depends on the particular realisation of Fibre Inflation. Thus we conclude this section by providing a brief description of two ways to generate the inflationary potential which are qualitatively similar but quantitatively slightly different:

- **Right-left inflation**

  Kaluza-Klein and winding 1-loop open string corrections to K [58, 60, 61] generate a potential for the inflaton shifted from its minimum, i.e. $\phi_1 = \langle\phi_1\rangle + \hat{\phi}_1$, of the form [101]:

$$V = V_0 \left(3 - 4\, e^{-\frac{\hat{\phi}_1}{\sqrt{3}}} + e^{-\frac{4\hat{\phi}_1}{\sqrt{3}}}\right), \tag{4.82}$$

  where we included an uplifting term to achieve a dS vacuum after the end of inflation and we neglected additional subleading loop effects which would lift the flatness of the inflationary plateau at very large field values. Notice that this is a case of right-left inflation where $\hat{\phi}_1$ evolves from positive and large field values to smaller ones towards the end of inflation. Hence $V_{\hat{\phi}_1} > 0$ during inflation.

- **Left-right inflation**

  The inflationary potential can receive non-negligible contributions not just from string loops but also from higher derivative α' effects which at the level of the 4-dimensional effective field theory appear as F^4 terms [99, 100]. When these effects are combined with Kaluza-Klein string loops, the inflationary potential looks like [102]:

$$V = \tilde{V}_0 \left(1 - e^{\frac{1}{\sqrt{3}}\hat{\phi}_1}\right)^2, \tag{4.83}$$

  where again we included an uplifting term and we ignored subdominant contributions which would spoil the inflationary plateau for $\hat{\phi}_1$ negative and very large in absolute value. Contrary to the previous case, this is therefore a realisation of left-right inflation where $V_{\hat{\phi}_1} < 0$ during inflation.

4.6.2 Stability of heavy fields

The leading order potential (4.76) depends just on the three fields ϕ_2, ϕ_3 and θ_3, which therefore turn out to be heavier that the inflaton ϕ_1. We shall now consider the 2-field subspaces spanned by ϕ_1 and each of these heavy fields separately, and show that all of them are heavy enough to ensure the absence of any geometrical destabilisation. The field space metric and the Ricci scalar of these 2-dimensional subspaces are listed in Tab. 4.1.

The simpler cases to analyse involve ϕ_2 and θ_3 since the metric is diagonal at this level of approximation (perturbative and non-perturbative corrections to the Kähler potential will definitely induce subdominant non-diagonal entries), and so the scalar curvature is vanishing. Moreover, we expect the heavy fields to sit

	θ_3	ϕ_2	ϕ_3
γ_{ij}	$\begin{pmatrix} 1+\frac{3}{4}\phi_3^2 & 0 \\ 0 & \frac{3\alpha\lambda_3}{4\mathcal{V}\sqrt{\tau_3}} \end{pmatrix}$	$\begin{pmatrix} 1+\frac{3}{4}\phi_3^2 & 0 \\ 0 & 1 \end{pmatrix}$	$\begin{pmatrix} 1+\frac{3}{4}\phi_3^2 & \frac{3\sqrt{3}}{8}\phi_3^3 \\ \frac{3\sqrt{3}}{8}\phi_3^3 & 1-\frac{3}{4}\phi_3^2+\frac{9}{16}\phi_3^4 \end{pmatrix}$
R	0	0	$-3/2$

Table 4.1: Field space metric and Ricci scalar for the 2-field subspaces spanned by the inflaton ϕ_1 and each of the three heavy fields.

around their minima, i.e. $V_{\phi_2} = V_{\theta_3} \simeq 0$, and inflation to be driven by ϕ_1, i.e. $\alpha_{\phi_1} \simeq 1$ while $\alpha_{\phi_2} \simeq \alpha_{\theta_3} \simeq 0$. Therefore the trajectory is geodesic in both cases (denoting the 2 heavy fields collectively as $\phi_{\rm h}$):

$$\eta_\perp \simeq \frac{1}{H\dot{\phi}_0}\left(\alpha_{\phi_1}\frac{V_{\phi_{\rm h}}}{f} - \alpha_{\phi_{\rm h}}V_{\phi_1}\right) \simeq 0\,. \tag{4.84}$$

The effective mass-squared (4.7) therefore reduces simply to:

$$m^2_{\theta_3,\,\rm eff} \simeq \frac{V_{\theta_3\theta_3}}{f^2} \simeq \frac{W_0^2}{\mathcal{V}^2} \gg m^2_{\phi_2,\,\rm eff} \simeq V_{\phi_2\phi_2} \simeq \frac{W_0^2}{\mathcal{V}^3} \gg H^2 \simeq \frac{W_0^2}{\mathcal{V}^{10/3}}\,. \tag{4.85}$$

Similar considerations apply to the subspace spanned by ϕ_1 and ϕ_3 since the field space is flat at leading order. However subleading corrections proportional to $\phi_3^2 \sim \mathcal{O}(\mathcal{V}^{-1}) \ll 1$, induce non-vanishing Christoffel symbols and Ricci scalar:

$$\Gamma^{\phi_1}_{\phi_3\phi_3} = \frac{9\sqrt{3}}{8}\phi_3^2\left(1-\frac{1}{2}\phi_3^2+\frac{3}{16}\phi_3^4\right) \sim \mathcal{O}\left(\frac{1}{\mathcal{V}}\right)\,, \qquad R = -\frac{3}{2}\,. \tag{4.86}$$

The effective mass-squared of the heavy field ϕ_3 for $V_{\phi_3} \simeq \alpha_{\phi_3} \simeq 0$ and $\alpha_{\phi_1} \simeq 1$, which imply $\eta_\perp \simeq 0$, reduces to:

$$m^2_{\phi_3,\,\rm eff} \simeq V_{\phi_3\phi_3} - \Gamma^{\phi_1}_{\phi_3\phi_3}V_{\phi_1} - \frac{3}{2}\epsilon H^2\,. \tag{4.87}$$

This quantity is clearly positive regardless of the shape of the inflationary potential since:

$$V_{\phi_3\phi_3} \simeq \frac{W_0^2}{\mathcal{V}^2} \gg \begin{cases} \Gamma^{\phi_1}_{\phi_3\phi_3}V_{\phi_1} \simeq \frac{W_0^2\sqrt{\epsilon}}{\mathcal{V}^{13/3}} \\ \frac{3}{2}\epsilon H^2 \simeq \frac{W_0^2\epsilon}{\mathcal{V}^{10/3}} \end{cases}\,. \tag{4.88}$$

We have therefore shown that, as expected, all heavy fields remain stable during Fibre Inflation.

	θ_1	θ_2
γ_{ij}	$\begin{pmatrix} 1 & 0 \\ 0 & A_-^2\, e^{-\frac{4}{\sqrt{3}}\phi_1} \end{pmatrix}$	$\begin{pmatrix} 1 & 0 \\ 0 & A_+^2\, e^{\frac{2}{\sqrt{3}}\phi_1} \end{pmatrix}$
R	$-8/3$	$-2/3$

Table 4.2: Field space metric and Ricci scalar for the 2-field subspaces spanned by the inflaton ϕ_1 and each of the two ultra-light axions.

4.6.3 Potential destabilisation of ultra-light axions

In this section we analyse the behaviour of the two ultra-light axionic modes θ_1 and θ_2. The metric of the 2-dimensional field spaces spanned by the inflaton ϕ_1 and either θ_1 or θ_2 takes the same form as (4.12) if we neglect subdominant ϕ_3-dependent corrections. Notice that the kinetic function $f(\phi_1)$ becomes ϕ_1-dependent after (4.79) is used to express τ_1 in terms of the canonically normalised fields ϕ_2 and ϕ_3 which are fixed at their minima. Given that $f(\phi_1)$ is a particular case of the more general form (4.53), the scalar curvature is constant and negative. These geometrical quantities are summarised in Tab. 4.2 where the quantities A_+ and A_- depend on the background values of the heavy fields.

In the case where θ_1 and θ_2 are exactly massless, we find that one of them is always unstable. In order to solve this potential issue, we investigate the possibility of stopping the exponential growth of the corresponding isocurvature perturbations by turning on a tiny but non-zero mass for this entropic mode. Let us therefore study these two different cases separately.

Massless case

The analysis of the possible geometrical destabilisation of θ_1 and θ_2 can be borrowed from Sec. 4.4.2 where we already discussed the case where the spectator fields are massless and ϕ_1 drives inflation in a single-field approximation. Using the result (4.56) under the condition (4.57) we therefore conclude that one of the two axions is always stable while the perturbations of the other experience a geometrical instability. In particular, it is the sign of $V_{\hat{\phi}_1}$ that determines which of the two axions is unstable. For $V_{\hat{\phi}_1} > 0$, as in the case of right-left inflation, θ_1 is unstable while θ_2 is stable. On the contrary, for $V_{\hat{\phi}_1} < 0$, as in the case of left-right inflation, θ_1 is stable while θ_2 becomes unstable.

These results have been obtained analytically in the single-field approximation where $\alpha_{\phi_1} \simeq 1$ and $\alpha_{\theta_i} \simeq 0$ with $i = 1, 2$. However they hold more generically as

we will show now via a more general semi-analytic study and a detailed numerical analysis.

As pointed out above, the metric has the same form as (4.12) with $f = f_0\, e^{-k_1\hat{\phi}_1}$, where $f_0 = A_-\, e^{-k_1\langle\phi_1\rangle}$ and $k_1 = 2/\sqrt{3}$ for θ_1, while $f_0 = A_+\, e^{-k_1\langle\phi_1\rangle}$ and $k_1 = -1/\sqrt{3}$ for θ_2. The equations of motion which govern the evolution of the system are very similar to the ones studied in Sec. 4.5.1 for the case of a quintessence-like potential. We shall therefore use the same results, translating them for the case of Fibre Inflation. In particular, the second equation in (4.61) does not depend on the inflationary potential, and so it applies exactly also to our case after identifying ϕ_2 with either θ_1 or θ_2. Its solution is given by (4.63) which in our case becomes:

$$(f\theta_i')\,(N) = (f\theta_i')\,(0)\, e^{-\lambda(N)}\,, \qquad \forall i = 1,2\,, \tag{4.89}$$

where for $\epsilon \ll 1$ the exponent $\lambda(N)$ can be approximated as:

$$\lambda(N) \simeq 3N - k_1\left(\hat{\phi}_1(N) - \hat{\phi}_1(0)\right)\,. \tag{4.90}$$

The functional dependence of the inflaton ϕ_1 on the number of e-foldings N depends on the particular form of the inflationary potential. Let us therefore consider separately the case of right-left [101] and left-right inflation [102].

- **Right-left inflation**

  For right-left inflation the scalar potential is given by (4.82) which in the inflationary plateau region can be very well approximated as:

  $$V \simeq V_0\left(3 - 4\, e^{-k_2\hat{\phi}_1}\right), \qquad \text{with} \quad k_2 = \frac{1}{\sqrt{3}}\,. \tag{4.91}$$

  The number of e-foldings N in the single-field slow-roll approximation is given by:

  $$\begin{aligned} N(\hat{\phi}_1) &= \int_{\hat{\phi}_1}^{\hat{\phi}_1(0)} \frac{V}{V_{\hat{\phi}_1}}\, d\hat{\phi}_1 \\ &= \frac{9}{4}\left(e^{k_2\hat{\phi}_1(0)} - e^{k_2\hat{\phi}_1}\right) - \sqrt{3}\left(\hat{\phi}_1(0) - \hat{\phi}_1\right)\,. \end{aligned} \tag{4.92}$$

  This expression cannot be inverted exactly but we can still express the inflaton at leading order as [179]:

  $$\hat{\phi}_1(N) - \hat{\phi}_1(0) \simeq \frac{1}{k_2}\ln\left(1 - \frac{4N}{9}\, e^{-k_2\hat{\phi}_1(0)}\right)\,, \tag{4.93}$$

  where $\hat{\phi}_1(0)$ corresponds to the value of the inflaton at CMB horizon exit. It is easy to see that $50-60$ e-foldings of inflation correspond to $\hat{\phi}_1(0) \sim \mathcal{O}(6)$.

Substituting this result into the solution for the velocity of the ultra-light axions (4.89), we find that the exponent (4.90) scales with the number of e-foldings as:

$$\lambda(N) = 3N - \frac{k_1}{k_2} \ln\left(1 - \frac{4N}{9}\, e^{-k_2\hat{\phi}_1(0)}\right) . \tag{4.94}$$

This quantity is always positive for both $k_1 = 2/\sqrt{3}$ and $k_1 = -1/\sqrt{3}$, implying that, regardless of the initial conditions, the velocity of the ultra-light axions goes very quickly to zero, and so the system relaxes rapidly to the simple case studied above with $\eta_\perp = 0$, $\alpha_{\phi_1} \simeq 1$ and $\alpha_{\theta_i} \simeq 0$ with $i = 1, 2$.

- **Left-right inflation**

  In the case of left-right inflation, the number of e-foldings derived from the inflationary potential (4.83) in the slow-roll approximation is given by:

$$\begin{aligned} N(\hat{\phi}_1) &= \frac{1}{2k_2} \int_{\hat{\phi}_1(0)}^{\hat{\phi}_1} \left(e^{-k_2\hat{\phi}_1} - 1\right) d\hat{\phi}_1 \\ &= \frac{1}{2k_2^2}\left(e^{-k_2\hat{\phi}_1(0)} - e^{-k_2\hat{\phi}_1(0)}\right) - \frac{1}{k_2}(\hat{\phi}_1 - \hat{\phi}_1(0)) . \end{aligned} \tag{4.95}$$

  Again, even if it is not possible to invert this expression exactly, we can still obtain the following leading order approximation for the inflaton field:

$$\hat{\phi}_1(N) - \hat{\phi}_1(0) = -\frac{1}{k_2} \ln\left(1 - \frac{2N}{3}\, e^{k_2\hat{\phi}_1(0)}\right) , \tag{4.96}$$

  where $\hat{\phi}_1(0) < 0$ since inflation proceeds from left to right starting from inflaton values which are negative and large in absolute value. If the result (4.96) is substituted into the expression (4.90) for the exponent of the solution (4.89) for the velocity of the isocurvature modes, we find:

$$\lambda(N) = 3N + \frac{k_1}{k_2} \ln\left(1 - \frac{2N}{3}\, e^{k_2\hat{\phi}_1(0)}\right) . \tag{4.97}$$

  It is easy to realise that this quantity is again always positive for both $k_1 = 2/\sqrt{3}$ and $k_1 = -1/\sqrt{3}$. Hence also in this case, regardless of the initial conditions, the system approaches very rapidly a geodesic trajectory with $\eta_\perp = 0$.

We have checked these conclusions by performing a full numerical solution of the equations of motion governing the evolution of the system for both right-left and left-right inflation. We present now the numerical results just for right-left

inflation since they are qualitatively very similar in the case of left-right inflation. Without loss of generality we considered $f_0 = V_0 = 1$, $\hat{\phi}_1(0) = 5.8$ and $\theta_i(0) = 0$ for $i = 1, 2$. Fig. 4.7 shows clearly that for different values of the initial kinetic energy and for several exponents of the kinetic function, $k_1 = \{-5, -2, -1, 0, 1, 2, 5\}$, the system always evolves towards a single-field behaviour.

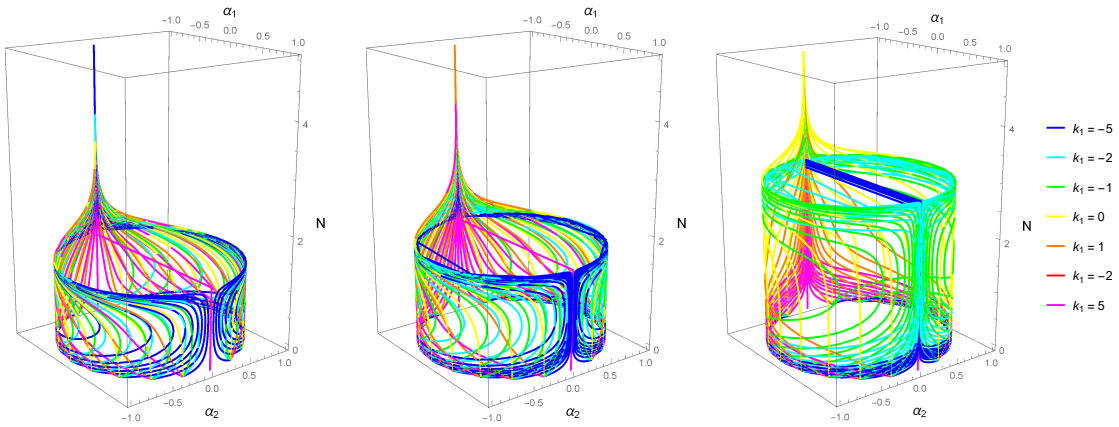

Figure 4.7: Evolution of the system for several values of k_1 and different initial kinetic energies, $\epsilon(0) = 1$ (left), $\epsilon(0) = 2$ (centre), $\epsilon(0) = 2.99$ (right).

Fig. 4.8 presents instead the trajectory of the physical fields $\hat{\phi}_1(N)$ and $\int_0^N (f\theta_i')(\tilde{N})d\tilde{N}$ for different values of k_1. Finally Fig. 4.9 shows that any value of k_1 leads to a geodesic motion with $\eta_\perp = 0$ but the effective mass-squared of the isocurvature perturbations can remain positive only for $k_1 < 0$, implying that θ_1 (with $k_1 = 2/\sqrt{3}$) is unstable, while θ_2 (with $k_1 = -1/\sqrt{3}$) does not experience any geometrical destabilisation. Notice that the situation is reversed in the case of left-right inflation.

Massive case

In Sec. 4.6.3 we have shown that in Fibre Inflation models, when the axions are considered as exactly massless, one of them always experiences geometrical destabilisation. However in a full quantum model, these entropic modes are expected to receive a tiny but non-zero mass from non-perturbative corrections to the superpotential (4.75) which break their perturbative shift symmetry. Let us investigate now if these non-perturbative effects can be large enough to avoid any geometrical destabilisation problem and, at the same time, small enough to prevent any modification of the inflationary dynamics.

As we have seen in the analysis of the massless case, the single-field approximation with $\alpha_{\phi_1} \simeq 1$ and $\alpha_{\theta_i} \simeq 0$ with $i = 1, 2$ provides a very good description of

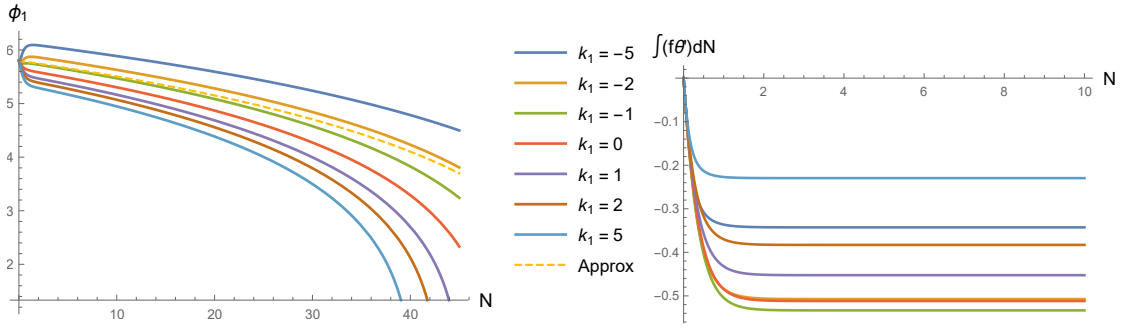

Figure 4.8: Trajectories of the physical fields $\hat{\phi}_1(N)$ and $\int_0^N f(\phi_1(\tilde{N}))\theta_i'(\tilde{N})d\tilde{N}$ for different values of k_1 and $\epsilon(0) = 1$, $\hat{\phi}_1'(0) = \sqrt{2}\cos(\omega)$, $(f\theta_i')(0) = \sqrt{2}\sin(\omega)$ with $\omega = 7\pi/5$. The dashed line represents the single-field analytical approximation with zero initial velocity.

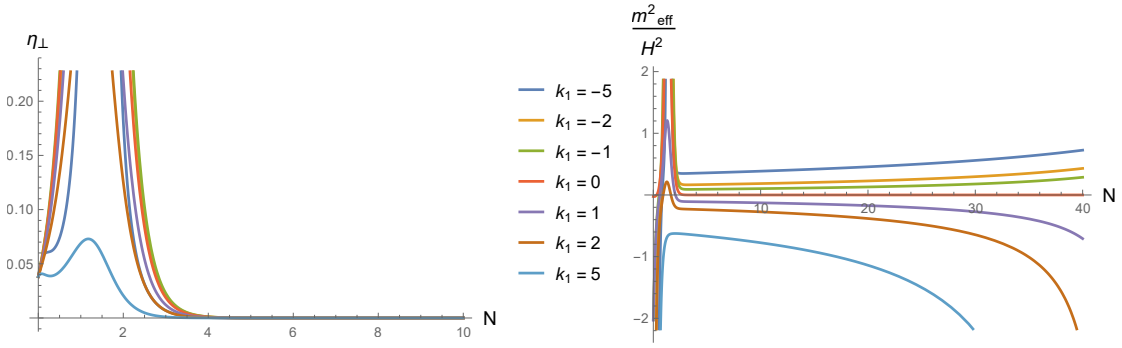

Figure 4.9: $\eta_\perp$ (left) and $m^2_{\perp,\text{eff}}/H^2$ (right) as a function of the number of e-foldings for different values of k_1, setting again $\epsilon(0) = 1$, $\hat{\phi}_1'(0) = \sqrt{2}\cos(\omega)$ and $(f\theta_i')(0) = \sqrt{2}\sin(\omega)$ with $\omega = 7\pi/5$.

the more general dynamics of the system. Hence the equation to analyse is (4.50) which after identifying ϕ_2 with θ_i and setting $\alpha_{\phi_1} \simeq 1$ and $\alpha_{\theta_i} \simeq 0$ for $i = 1, 2$, takes the form:

$$m^2_{\theta_i,\text{eff}} = \left(\frac{V_{\theta_i\theta_i}}{f^2} + \frac{f_{\hat{\phi}_1}}{f}V_{\hat{\phi}_1} + 3\frac{V^2_{\theta_i}}{\dot{\phi}_0^2 f^2}\right) - \dot{\phi}_0^2\frac{f_{\hat{\phi}_1\hat{\phi}_1}}{f}\,. \tag{4.98}$$

If we write the kinetic function as in (4.53) and we recall the slow-roll condition (4.57), the effective mass-squared (4.98) for the dangerous entropic modes simplifies to:

$$m^2_{\theta_i,\text{eff}} \simeq -\lambda\left|V_{\hat{\phi}_1}\right|\left[1 - \frac{1}{\lambda f^2\sqrt{2\epsilon}}\left(\frac{V_{\theta_i\theta_i}}{V} + \frac{9}{2\epsilon}\frac{V^2_{\theta_i}}{V^2}\right)\right]\,, \tag{4.99}$$

where we have used the slow-roll approximations $\dot{\phi}_0^2 = 2\epsilon H^2 \simeq 2\epsilon V/3$ and $\sqrt{2\epsilon} \simeq \left|V_{\hat{\phi}_1}\right|/V$.

The potential for the entropic directions is generated by T_i-dependent non-perturbative corrections to the superpotential (4.75):

$$W = W_0 + A_3\, e^{-a_3 T_3} + A_i\, e^{-a_i T_i}\,, \qquad i = 1, 2\,, \tag{4.100}$$

which induce a non-zero potential for the ultra-light axions θ_i of the form:

$$V(\theta_i) = \Lambda_i \cos(a_i \theta_i)\,, \qquad \text{with} \quad \Lambda_i = \frac{4 a_i A_i W_0 \tau_i}{\mathcal{V}^2}\, e^{-a_i \tau_i}\,, \quad i = 1, 2\,. \tag{4.101}$$

Hence we obtain:

$$V_{\theta_i}^2 = a_i^2\, \Lambda_i^2 \sin^2(a_i \theta_i) \qquad \text{and} \qquad V_{\theta_i \theta_i} = -a_i^2\, \Lambda_i \cos(a_i \theta_i)\,. \tag{4.102}$$

The effective mass-squared of the isocurvature perturbations (4.99) can therefore be rewritten as:

$$m^2_{\theta_i,\,\text{eff}} \simeq -\lambda \left|V_{\hat{\phi}_1}\right| \left[1 - \frac{a_i^2}{\lambda f^2 \sqrt{2\epsilon}} \left(\frac{9\delta^2}{2\epsilon} \sin^2(a_i \theta_i) - \delta \cos(a_i \theta_i)\right)\right]\,, \tag{4.103}$$

where δ is the ratio between the size of the axion potential and the inflationary potential:

$$\delta \equiv \frac{\Lambda_i}{V(\hat{\phi}_1)}\,. \tag{4.104}$$

Let us point out that, once τ_i with $i = 1, 2$ is written in terms of canonically normalised fields using (4.79), the axion potential (4.101) clearly depends on the inflaton $\hat{\phi}_1$ since:

$$\Lambda_i = \Lambda_i^{(0)}\, e^{-g_i(\hat{\phi}_1)}\,, \qquad \text{with} \quad \Lambda_i^{(0)} = \frac{4 a_i A_i W_0 \langle \tau_i \rangle}{\mathcal{V}^2} \quad \forall i = 1, 2\,, \tag{4.105}$$

where:

$$g_1(\hat{\phi}_1) = -2 k_2 \hat{\phi}_1 + a_1 \langle \tau_1 \rangle e^{2 k_2 \hat{\phi}_1}\,, \qquad g_2(\hat{\phi}_1) = k_2 \hat{\phi}_1 + a_2 \langle \tau_2 \rangle\, e^{-k_2 \hat{\phi}_1}\,. \tag{4.106}$$

Notice that for the case of right-left inflation, the dangerous axionic mode is θ_1 and during inflation $\hat{\phi}_1$ evolves from positive large values to smaller one. On the other hand, in left-right inflation, we need to focus on θ_2 and at the beginning of inflation $\hat{\phi}_1$ is negative and large in absolute value. Thus in both cases, the axion potential experiences a double exponential suppression, being larger close to the end of inflation and extremely suppressed in the region around CMB horizon exit.

The fact that the axion potential is $\hat{\phi}_1$-dependent implies that we cannot make the mass of θ_i as large as we would like by tuning the underlying parameters A_i and a_i since at a certain point the potential (4.101) will become of the same order of magnitude of the inflationary potential. This will induce $\mathcal{O}(1)$ corrections to the inflationary dynamics which would destroy Fibre Inflation as we know it. Hence for consistency we need to impose $\delta \ll 1$, which implies that the two terms proportional to δ in (4.103) are subdominant.

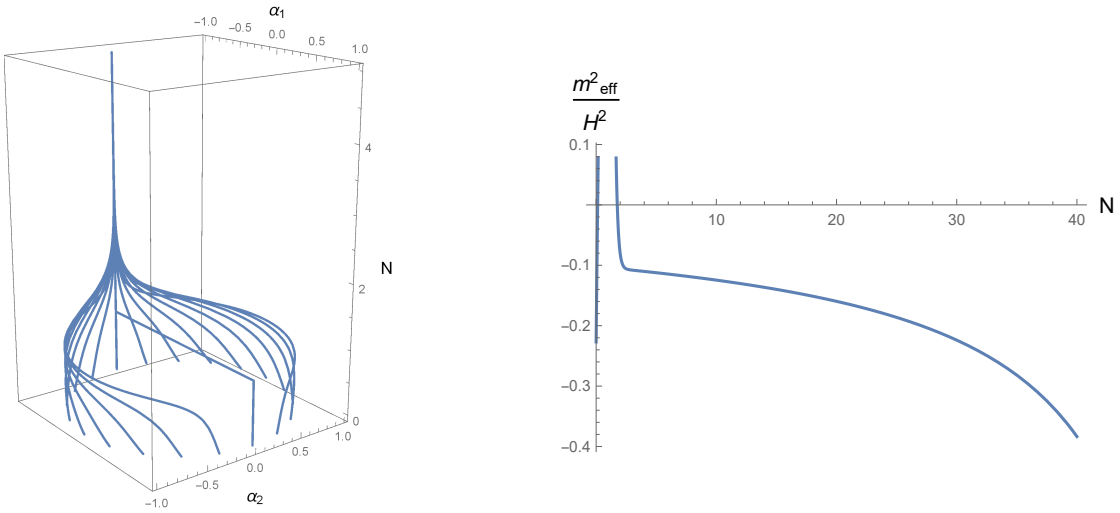

Figure 4.10: The plot on the left hand side shows the evolution of the 2-field system of right-left inflation for different initial velocities, $\hat{\phi}_1(0) = 5.8$, $a_1\theta_1(0) = 1$, initial kinetic energy $\epsilon(0) = 0.1$, $A_1 = W_0 = 1$, $a_1 = 2\pi$, $\langle\tau_1\rangle = 5.43$, $V_0 = 3.5 \times 10^{-11}$ and $\mathcal{V} = 1.8 \times 10^3$. The plot on the right hand side exhibits instead the behaviour of the effective mass-squared of θ_1 for $\hat{\phi}_1'(0) = \sqrt{2}\cos(\omega)$ and $(f\theta_1')(0) = \sqrt{2}\sin(\omega)$ with $\omega = 7\pi/5$.

Let us stress that, even if $\delta \ll 1$, one of these two terms might actually be the dominant contribution since $f \ll 1$ and $\epsilon \ll 1$, but this can occur only locally around a particular region in field space. In fact, as can be seen from (4.106), Λ_i has a double exponential suppression, and so small deviations of the inflaton $\hat{\phi}_1$ would immediately suppress these positive contributions to $m^2_{\theta_i,\,\mathrm{eff}}$. We conclude that, even in the presence of non-vanishing scalar potential contributions, the isocurvature fluctuations associated to one of the two ultra-light axions in Fibre Inflation experience an exponential growth, regardless of the particular microscopic realisation of the inflationary model.

We checked the validity of these analytic results by performing a full numerical solution of the evolution of the system in the presence of non-perturbative corrections of the form (4.100). The results for right-left inflation are shown in Fig.

4.10-4.11. In particular, Fig. 4.10 shows that the system quickly converges towards a geodesic trajectory and that the effective mass-squared of θ_1 is initially positive due to an appropriate choice of initial conditions but then rapidly settles down to negative values. On the other hand, in Fig. 4.11 we see that natural choices of the underlying parameters can keep the axion potential always subleading with respect to the inflationary potential. In this way, the inflationary dynamics is guaranteed to reproduce the one of Fibre Inflation but one of the axionic modes experiences a potential geometrical destabilisation. We finally point out that we obtained numerical results also for left-right inflation and they turn out to be qualitatively very similar.

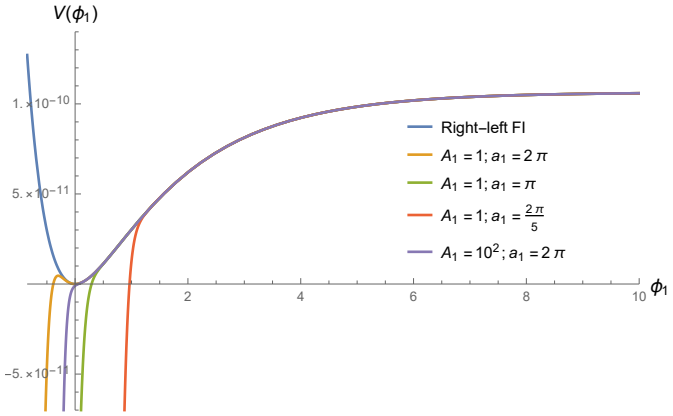

Figure 4.11: Comparison between the standard single-field and the 2-field version of right-left inflation for different values of the parameters A_1 and a_1. Notice that the axionic potential is subleading with respect to the inflationary potential until the end of inflation only for $A_1 = 1$ and $a_1 = 2\pi$.

The growth of isocurvature perturbations does not seem to be avoidable in these models, also considering small mass terms for axion fields. In the next section we point out that the coordinate system identified by the normal and tangent directions shows an anomalous behavior that may be the cause of the uncontrolled growth of isocurvature perturbations.

4.6.4 A growing projector

In this section we briefly analyse the time evolution of tangent and normal vectors in case of a massless axion kinetically coupled to the inflaton as in the right-left inflation case of section 4.6.3. The relation between the covariant derivatives of the two projectors are

$$\frac{DT^a}{dt} = -H\eta_\perp N^a\,, \qquad \frac{DN^a}{dt} = H\eta_\perp T^a. \tag{4.107}$$

Given the single field behaviour of the background system described in the previous section, we saw that on-shell $\eta_\perp = 0$. The single components of T^a and N^a are defined as

$$T^a = \left\{\alpha_1, \frac{\alpha_2}{f}\right\}, \qquad N^a = \left\{-\alpha_2, \frac{\alpha_1}{f}\right\}, \tag{4.108}$$

where, again, $\alpha_1 = \frac{\dot\phi}{\sqrt{\dot\phi^2+f^2\dot\chi^2}}$ and $\alpha_2 = \frac{f\dot\chi}{\sqrt{\dot\phi^2+f^2\dot\chi^2}}$ parametrise the fraction of kinetic energy carried by the fields. The results obtained in Sec. 4.6.3 showed that these two quantities quickly relax to $\alpha_1 \to 1$ and $\alpha_2 \to 0$ (see Fig. 4.7), implying that $T^a \to \{-1, 0\}$ and $N^a \to \{0, -1/f\}$. Knowing that $H\eta_\perp = -\alpha_2 \frac{V_\phi}{\dot\phi_0}$, we can easily find the time derivative of the projector components to be:

$$\begin{aligned}
\tfrac{dT_1}{dt} &= \alpha_2^2\left(\tfrac{f_\phi}{f^2}\dot\phi_0 - \tfrac{V_\phi}{\dot\phi_0}\right) \to 0\,,\\
\tfrac{dT_2}{dt} &= \alpha_1\alpha_2\tfrac{V_\phi f}{\dot\phi_0} \to 0\,,\\
\tfrac{dN_1}{dt} &= \alpha_1\alpha_2\left(\tfrac{f_\phi}{f}\dot\phi_0 - \tfrac{V_\phi}{\dot\phi_0}\right) \to 0\,,\\
\tfrac{dN_2}{dt} &= f_\phi\dot\phi_0 - \alpha_2^2\tfrac{V_\phi f}{\dot\phi_0} \to f_\phi\dot\phi_0 < 0\,.
\end{aligned} \tag{4.109}$$

From the previous equations, we see that the tangent vector seems to be well defined, i.e. its coordinates relax to constant values with vanishing time derivatives. On the other hand, despite the system tends to a single-field behaviour, the second component of the normal projector keeps on varying during inflation. Since N_2 starts from negative values and $\frac{dN_2}{dt}$ is negative and decreases during inflation, we see that N_2 evolves towards more and more negative values at increasing rate. The time evolution of the single components is depicted in Figure 4.12. The continuous growth of N_2 during inflation is due to the normalisation prescription of the projectors and reveals that the coordinate system is probably ill-defined.

In the next section we discuss whether and how growing isocurvature modes can affect the predictions on cosmological parameters and how experimental bounds on isocurvature perturbations can constraint inflationary models. We start by briefly reviewing how entropy perturbations can be computed during inflation.

4.6.5 Entropy perturbations during inflation

In this section we clarify the relations between the various definitions of entropy that can be found in the literature, in an effort to understand how the entropy generated during inflation is then transferred to the primordial plasma in the radiation phase.

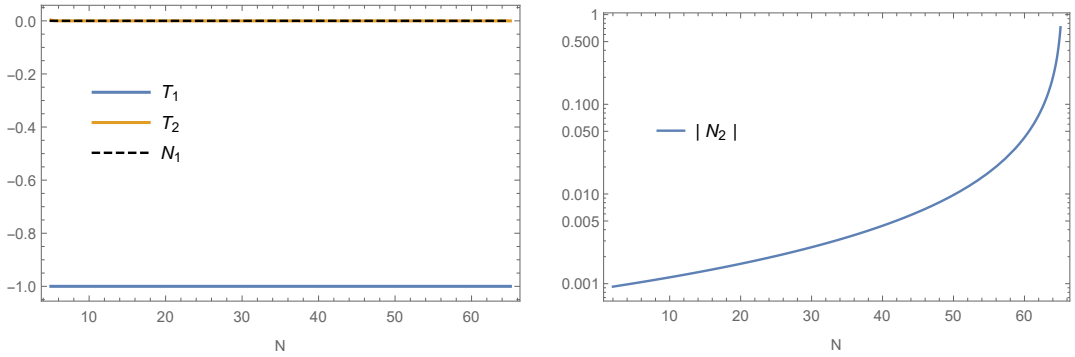

Figure 4.12: Evolution of T_a and N_a components during inflation in the system described in Sec. 4.6.3. We refer in particular to the right-left inflation case in Eq. (4.91) where the two-field system is composed by the inflaton field ϕ and the θ_1 massless axion with kinetic coupling $f = e^{-2/\sqrt{3}\phi}$.

For a generic fluid $P = P(\rho, S)$, i.e. the pressure is a function of the energy density ρ and the entropy S. Pressure perturbations can therefore be decomposed into an adiabatic and a non-adiabatic part, according to

$$\delta P = \frac{\delta P}{\delta \rho}\Big|_S \delta\rho + \frac{\delta P}{\delta S}\Big|_\rho \delta S. \tag{4.110}$$

The adiabatic pressure perturbation is $\delta P_{ad} = c_s^2 \delta\rho$, where c_s^2 is the speed of sound defined as $c_s^2 \equiv \frac{\dot{P}}{\dot{\rho}}$. The non-adiabatic pressure perturbations, denoted δP_{nad} are formally given by $\delta P_{nad} = \frac{\dot{P}}{\dot{S}}\delta S$ and are in practice computed via $\delta P_{nad} = \delta P - \delta P_{ad}$.

The total entropy can be defined in terms of the non-adiabatic pressure perturbations δP_{nad} as

$$S = \frac{H}{\dot{P}}\delta P_{nad} = \frac{H}{\dot{P}}\left(\delta P - c_s^2 \delta\rho\right) \ . \tag{4.111}$$

If the Universe is composed by multiple fluids, labelled by α, one can define the intrinsic entropy perturbation $S_{int,\alpha}$ as

$$S_{int,\alpha} = \frac{H}{\dot{P}}\left(\delta P_\alpha - c_\alpha^2 \delta\rho_\alpha\right) \ , \tag{4.112}$$

such that the total intrinsic entropy of a system with multiple components is

$$S_{int} = \sum_\alpha S_{int,\alpha}. \tag{4.113}$$

Note that $S_{int} = 0$ for fluids having equation of state $P_\alpha = P_\alpha(\rho_\alpha)$. One can also define the relative entropy as

$$S_{rel} = S - S_{int} \ . \tag{4.114}$$

Noting that $\delta P = \sum_\alpha \delta P_\alpha$ and that $\delta\rho = \sum_\alpha \delta\rho_\alpha$ and making use of Eqs. (4.111), (4.112) and (4.113) one may write [191]

$$\begin{aligned} S_{rel} =& \frac{H}{\dot{P}\dot{\rho}} \sum_{\alpha\beta} c_\alpha^2 (\dot{\rho}_\beta \delta\rho_\alpha - \dot{\rho}_\alpha \delta\rho_\beta) = \\ =& -\frac{1}{6\dot{\rho}\dot{P}} \sum_{\alpha\beta} \dot{\rho}_\alpha \dot{\rho}_\beta (c_\alpha^2 - c_\beta^2) S_{\alpha\beta} \,, \end{aligned} \tag{4.115}$$

where in the last line we introduced the standard definition of entropy perturbation between two fluids

$$S_{\alpha\beta} \equiv \zeta_\alpha - \zeta_\beta = -3H \left(\frac{\delta\rho_\alpha}{\dot{\rho}_\alpha} - \frac{\delta\rho_\beta}{\dot{\rho}_\beta} \right) , \tag{4.116}$$

as is commonly found in the context of hot big bang cosmology, and we have defined the speed of sound of each fluid as $c_\alpha^2 = \frac{\dot{P}_\alpha}{\dot{\rho}_\alpha}$. Note that, since the curvature perturbation on uniform ρ_α hypersurfaces, $\zeta_\alpha = -\psi - H\frac{\delta\rho_\alpha}{\dot{\rho}_\alpha}$, is a gauge invariant quantity (see Appendix B.1), $S_{\alpha\beta}$ is automatically gauge invariant, even in the presence of energy transfer between the fluids [192, 191].

During inflation, when scalar fields dominate the energy content of the Universe, one may write the entropies of the system in terms of $\phi_\alpha, \delta\phi_\alpha$ and their derivatives. In case of multi-field inflation in a curved field manifold we have that Eq. (4.111) reads

$$S = -\frac{H}{3H\dot{\phi}^a\dot{\phi}_a + 2\dot{\phi}^a V_a} \delta P_{\rm nad} \,, \tag{4.117}$$

where $\delta P_{\rm nad}$ is given by

$$\begin{aligned} \delta P_{nad} = \; & -2V_\alpha \delta\phi^\alpha + \tfrac{V_\alpha \dot{\phi}^\alpha \delta\phi_\beta \dot{\phi}^\beta}{3H^2} - \tfrac{2}{3H} \tfrac{V_\lambda \dot{\phi}^\lambda}{\dot{\phi}_\gamma \dot{\phi}^\gamma} \Big[\dot{\phi}_\alpha \dot{\delta\phi}^\alpha + \\ & + \tfrac{1}{2} \dot{\phi}^\alpha \dot{\phi}^\beta \partial_\sigma G_{\alpha\beta} \delta\phi^\sigma + V_\alpha \delta\phi^\alpha \Big] \end{aligned} \tag{4.118}$$

and we used the spatially flat gauge. Further details and extended computations can be found in App. B. For two minimally coupled scalars with canonical kinetic terms and sum-separable potentials one can show that [193]

$$S_{rel} = \frac{2}{3\dot{\phi}_0^2} \frac{V_N \dot{\phi}_1 \dot{\phi}_2}{3H\dot{\phi}_0 + 2V_T} S_{12} \,, \tag{4.119}$$

where we have defined $\dot{\phi}_0 \equiv \sqrt{\dot{\phi}_1^2 + \dot{\phi}_2^2}$, the projection of the scalar potential along the direction of the background trajectory $V_T = T^a V_a$ and orthogonal to it $V_N = N^a V_a$. It can be readily shown that

$$S_{12} = a^3 \frac{d}{dt} \left(\frac{\delta\phi_{12}}{a^3} \right) \tag{4.120}$$

where we have used the notation of [194] and defined the quantity

$$\delta\phi_{12} \equiv \frac{\delta\phi_1}{\dot{\phi}_1} - \frac{\delta\phi_2}{\dot{\phi}_2} \tag{4.121}$$

that in [193] is called generalised entropy and is gauge invariant by construction.

In the context of inflationary physics, entropy perturbations are often characterised in terms of the quantity

$$\delta s = N^a \delta\phi_a, \tag{4.122}$$

often called isocurvature direction/perturbation, which can be directly related to the total entropy on super-horizon scales [193]

$$S \approx \frac{-2H}{\dot{\phi}_0^2} \frac{V_N \dot{\phi}_0}{3H\dot{\phi}_0 + 2V_T} \delta s \tag{4.123}$$

and to the generalised entropy between the two scalar fields as

$$\delta s = \frac{\dot{\phi}_1 \dot{\phi}_2}{\dot{\phi}_0} \delta\phi_{12} \ . \tag{4.124}$$

Finding and solving the evolution equation for δs not only gives us an intuitive picture of the entropy perturbations but is also a more robust manner of numerically computing entropy perturbations than subtracting from the total pressure perturbation its adiabatic component [193, 195]. For these reasons it has become the preferred way of describing entropy perturbations during inflation. The relations between the different definitions of entropy perturbations are summed up in Figure 4.13. We stress in particular which of them can be only used in case of flat field space without kinetic coupling.

4.6.6 Entropy perturbations after inflation

After inflation and the subsequent reheating phase, the Universe is expected to enter a radiation dominated phase, where radiation, baryons, dark matter and neutrinos make up the primordial plasma. Neglecting velocity isocurvature perturbations, the presence of entropy at this stage leads to a difference in the number density perturbations, $\frac{\delta n_\alpha}{n_\alpha}$, between the various species. Hence, we can have non-vanishing relative entropies $S_{\gamma\,\mathrm{CDM}}$, $S_{\gamma\,\nu}$, $S_{\gamma\,\mathrm{baryons}}$.

One crucial question to ask at this point is which definition of entropy should be used to transfer the entropy mode from the scalar field system, used to describe inflation, to the primordial plasma, that consists of fluids only. We note that in

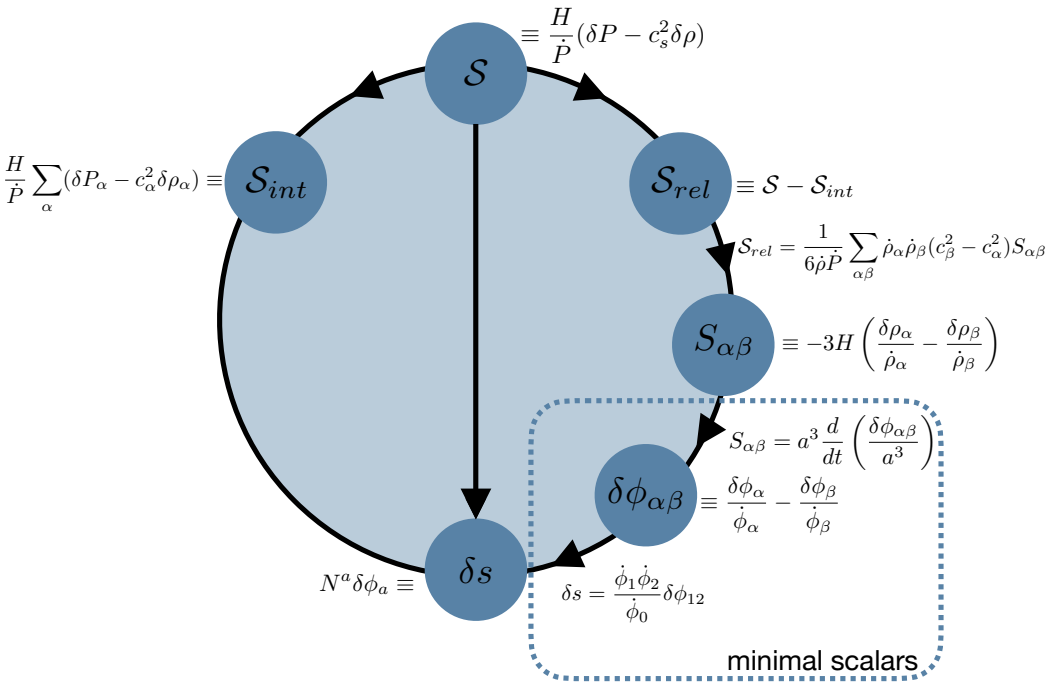

Figure 4.13: Summary of the various definitions of entropy and of the relations between them. The relations contained within the dashed rectangle hold only for what we call minimal scalar models: scalar fields with sum separable potentials and canonical kinetic terms.

previous works [196, 197, 198] the definition of entropy in Eq. (4.116) has been used. We will argue in the next sections that the use of Eq. (4.116) can lead in specific models to an instability in the entropy perturbations that is not physical but is due to a ill-definition of the curvature ζ in those models. Interestingly, it turns out that using one or the other variable does not lead to equivalent results: in some cases the difference in the resulting isocurvature power spectrum that is constrained by Planck is of several orders of magnitude [199]. It is then necessary to understand what is the proper variable to be used when matching the inflationary perturbations onto the perturbations in the primordial radiation dominated universe.

Let us try to be more explicit and review how the constraints can be enforced on a simple two-fields inflationary model following [200]. The study of cosmological perturbations generated during inflation boils down to the study of CMB anisotropies that can be characterized by their power spectra

$$(2\pi)^3\delta(\mathbf{k}+\mathbf{q})P_{IJ}(k) = \langle I(\mathbf{k})I(\mathbf{q})\rangle\,, \tag{4.125}$$

where I, J denote the curvature $\zeta = \sum_\alpha \zeta_\alpha$ and/or any isocurvature mode S. The constraints can be formulated in terms of the *primordial isocurvature fraction*[4]

$$\beta_{\rm iso}(k) = \frac{P_{\tilde{S}\tilde{S}}(k)}{P_{\zeta\zeta}(k) + P_{\tilde{S}\tilde{S}}(k)}\,, \tag{4.127}$$

where $\tilde{S}$ refers to the post-inflationary isocurvature perturbations, i.e. any of $S_{\gamma\,\rm CDM}$, $S_{\gamma\,\nu}$, $S_{\gamma\,\rm baryons}$. In general this quantity is not scale invariant, so that the Planck constraints are placed at three different reference scales. Given our illustrative purposes though, we adopt the assumption of [200] and take the spectral index for all the spectra to be zero, so that the primordial isocurvature fraction turns out to be scale-independent.

Of course the constraint on $\beta_{\rm iso}$ comes indirectly: once we have the primordial power spectra P_{IJ} at the start of the radiation dominated era (that implies that we have consistently transferred all the perturbations from the inflationary to the post-inflationary eras, as described above) we need to evolve them through the Einstein equations till the release of the CMB, and then translate them into

[4] We are not interested in this paper on the other parameter that is constrained by Planck observations, namely the *correlation fraction*

$$\cos\Delta_{IJ} = \frac{P_{IJ}}{(P_{II}P_{JJ})^{1/2}} \in (-1,1)\,, \tag{4.126}$$

which is taken to be scale-independent in Planck analyses.

observable quantities using the Boltzmann equations. Only then we are able to indirectly place constraints on $\beta_{\rm iso}$ by means of the constraints on CMB.

In the context of the hot big bang model, entropy, like curvature perturbations, appears as an undetermined initial condition for the radiation epoch. In the context of inflationary cosmology, both curvature and entropy perturbations at the onset of radiation domination are determined by the time evolution of scalars during inflation and reheating. In order to make contact between the two phases one must have a complete model, where the couplings of the inflationary scalars to the various species are known and then to evolve S_{rel} or $S_{\alpha\beta}$ up to radiation domination.

In the next section we focus again on Fibre inflation models. Indeed, despite the study of the reheating phase is far beyond the aim of the present work, we can try understand whether the growth of isocurvature perturbations, that we analysed in Sec. 4.6.3, can lead to large values of $S_{\alpha\beta}$ at the end of inflation.

4.6.7 Vanishing relative entropy from massless axions in FI

In order to provide some evidence that the geometrical instability studied in Sec. 4.6.3 is unphysical, let us compute the relative entropy during inflation, as given by S_{rel} for the two scalar fields system described in Sec. 4.6.3. We focus for simplicity on the right-left inflation case where the θ_1 massless axion induces the would-be geometrical instability of the system. This can be summed up as:

$$\mathcal{L}/\sqrt{g} = \frac{1}{2}(\partial\phi)^2 + \frac{f^2}{2}(\partial\chi)^2 - V\,, \qquad f^2 = f_0^2\, e^{-\frac{4}{\sqrt{3}}\phi_1}\,, \qquad V \simeq V_0\left(3 - 4\, e^{-\frac{\phi}{\sqrt{3}}}\right)\,,$$

where we set $\chi \equiv \theta_1$ to simplify notation. The energy momentum tensor during inflation can be factorised as

$$T^{\mu\nu} = T^{\mu\nu}_{(1)} + T^{\mu\nu}_{(2)}, \tag{4.128}$$

where the subscripts (1) and (2) refer to the scalars ϕ and χ respectively. Due to the kinetic coupling, the individual $T^{\mu\nu}_{(i)}$ are non conserved, but instead there is energy transfer between the fluids:

$$\nabla_\nu T^{\mu\nu}_{(1)} = Q^\mu \qquad \text{and} \qquad \nabla_\nu T^{\mu\nu}_{(2)} = -Q^\mu, \tag{4.129}$$

where Q^μ is the energy transfer function. Despite the fact that there is some freedom in the definition of the two fluids, it is natural to write the energy density and pressure of the two fields as

$$\rho_1 = \frac{1}{2}\dot{\phi}^2 + V(\phi)\,, \qquad\qquad \rho_2 = \frac{1}{2}f(\phi)^2\dot{\chi}^2\,, \tag{4.130}$$

$$P_1 = \frac{1}{2}\dot{\phi}^2 - V(\phi)\,, \qquad P_2 = \rho_2\,, \tag{4.131}$$

so that the energy transfer function computed on background quantities takes the form

$$Q^\mu = \begin{pmatrix} \dot{\rho}_1 + 3H(\rho_1 + P_1) \\ \vec{0} \end{pmatrix} = \begin{pmatrix} f f_\phi \dot{\phi}\,\dot{\chi}^2 \\ \vec{0} \end{pmatrix}. \tag{4.132}$$

The sound speeds of the two fluids defined in Eq. (4.130), (4.131) are

$$c_{s\,1}^2 = 1 + \frac{2V_\phi}{3H\dot{\phi} - f f_\phi\,\dot{\chi}^2}\,, \qquad c_{s\,2}^2 = 1, \tag{4.133}$$

while the overall sound speed is given by

$$c_s^2 = 1 + \frac{2}{3H}\frac{V_\alpha \dot{\phi}^\alpha}{\dot{\phi}_\gamma \dot{\phi}^\gamma}. \tag{4.134}$$

In order to compute the relative entropy between the fluids, we need to use perturbation theory at linear order. The following results are obtained using spatially flat gauge. The perturbed Einstein equations and further details can be found in App. B.2. Energy density and pressure perturbations take the form

$$\delta\rho_1 = -\Phi\dot{\phi}^2 + \dot{\phi}\dot{\delta\phi} + V_\phi\delta\phi\,, \tag{4.135}$$

$$\delta P_1 = -\Phi\dot{\phi}^2 + \dot{\phi}\dot{\delta\phi} - V_\phi\delta\phi\,, \tag{4.136}$$

$$\delta\rho_2 = \delta P_2 = -\Phi f^2\dot{\chi}^2 + f^2\dot{\chi}\dot{\delta\chi} + \frac{1}{2}\dot{\chi}^2\partial_\phi f^2\delta\phi\,, \tag{4.137}$$

where the time lapse scalar perturbation is given by

$$\Phi = \frac{1}{2H}\left(\dot{\phi}\delta\phi + f^2\dot{\chi}\delta\chi\right). \tag{4.138}$$

Since χ is a perfect fluid, the only intrinsic pressure perturbation is related to the field ϕ

$$\begin{aligned} \delta P_{intr} &= \sum_\alpha \left(\delta P_\alpha - c_{s\alpha}^2\delta\rho_\alpha\right) = \\ &= \delta P_1 - c_{s\,1}^2\delta\rho_1 \\ &= \left(-\Phi\dot{\phi}^2 + \dot{\phi}\dot{\delta\phi}\right)(1 - c_{s\,1}^2) - (1 + c_{s\,1}^2)V_\phi\delta\phi\,. \end{aligned} \tag{4.139}$$

The non-adiabatic pressure perturbation can be written as

$$\delta P_{nad} \equiv \delta P_{intr} + \delta P_{rel}\,, \tag{4.140}$$

thus it is easy to see that we can write

$$\delta P_{rel} = \sum_{\alpha} \left(c_{s\alpha}^2 - c_s^2\right) \delta\rho_\alpha \,. \tag{4.141}$$

Writing down explicitly the difference between the total sound speed and that one related to the single components (using the number of e-foldings as time variable) we get

$$\begin{aligned} c_{s\,1}^2 - c_s^2 &= (c_s^2 - 1) f^2 \chi^{'2} \left(\frac{1 + \frac{f_\phi \phi'}{3f}}{\phi'^2 - f^2 \chi'^2 \frac{f_\phi \phi'}{3f}} \right) \sim \mathcal{O}(f^2 \chi^{'2}) \,, \\ c_{s\,2}^2 - c_s^2 &= (1 - c_s^2) \,. \end{aligned} \tag{4.142}$$

It is easy to see that the inflaton contribution to δP_{rel} is suppressed by the exponentially decreasing factor $f\chi'$, that we computed in Eqs. (4.89), (4.90) and whose behaviour was also numerically checked in Sec. 4.6.3. In addition, we can recast the energy density perturbations as follows:

$$\begin{aligned} \delta\rho_\phi &= H^2 \left[\left(\tfrac{V_\phi}{H^2} - \tfrac{\phi'^3}{2} \right) \delta\phi + \phi' \delta\phi' \right] - H^2 f^2 \chi' \tfrac{\phi'^2}{2} \delta\chi \\ &= H^2 \left[\left(\tfrac{V_\phi}{H^2} - \tfrac{\phi'^3}{2} \right) \delta\phi + \phi' \delta\phi' \right] + \mathcal{O}(f\chi') \,, \end{aligned} \tag{4.143}$$

$$\begin{aligned} \delta\rho_\chi &= H^2 f \chi' \left[\tfrac{\chi' f}{2} \left(\tfrac{\partial_\phi f^2}{f^2} - \phi' \right) \delta\phi + f \delta\chi' - \tfrac{f^3 \chi'^2}{2} \delta\chi \right] \\ &\sim \mathcal{O}(f\chi') \,. \end{aligned} \tag{4.144}$$

From the previous equations we see that, during inflation, $\delta P_{rel} \sim \mathcal{O}(f\chi') \to 0$ as $f\chi' \to 0$.
We conclude that in this 2-field system we would expect the non-adiabatic pressure perturbations to be just given by the inflaton contribution to δP_{intr}. This is confirmed by the numerical analysis of the different components of the non-adiabatic entropy, $S, S_{\rm rel}$, $S_{\rm intr}$, that is shown in Figure 4.14.

We can then conclude that the presence of the ultralight axion does not seem to affect the entropy of the system and the geometrical instability of isocurvature perturbations should not be considered as a physical effect. As mentioned in the previous sections, observational bounds on isocurvature perturbations are given in terms of the relative entropies S_{rel} or $S_{\alpha\beta}$. Therefore the observed growth in δs does not rule out these models. In order to check the constraints coming from experimental observations, what one should do is to compute the relative entropy, using Eq. (4.116) and evolve it till radiation domination era.

In this particular case however S_{12} is ill-defined as the axion field has an action

$$\mathcal{L}/\sqrt{|g|} = \frac{f^2(\phi)}{2} (\partial\chi)^2 \tag{4.145}$$

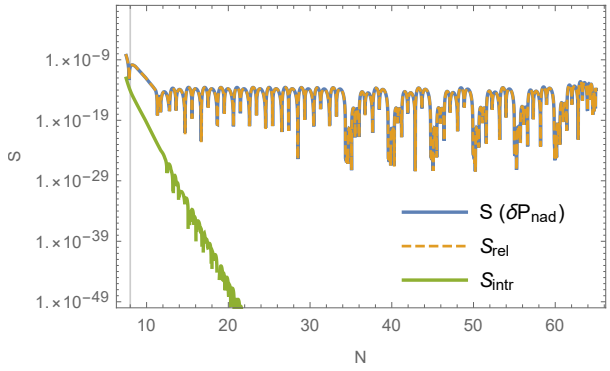

Figure 4.14: Different contributions to the entropy perturbations coming from non-adiabatic pressure in the right-left FI case described in Sec. 4.6.3. It is easy to see that $\mathcal{S}_{rel}$ goes rapidly to zero and the total entropy of the system is just given by $\mathcal{S}_{intr}$.

from which we can read that $\rho_2 = \frac{f^2(\phi)}{2}(\partial\chi)^2$ vanishes on-shell. One therefore sees that, despite the fact that S_{rel} is finite and vanishingly small, S_{12} is singular. We note that the same problem arises for canonically normalised massless scalars (which however do not suffer from a growing δs).

The fact that the growth in δs is due to a growing projector N^a and that S_{rel} is finite, allows us to argue that the instability noted in Sec. 4.6.3 is of no physical consequence and that the underlying models are presently viable both in what concerns curvature and entropy perturbations.

4.7 Conclusions

In this chapter we have studied the geometrical (in)stability in models of inflation where the field space has negative scalar curvature. These models arise naturally in the presence of non-minimal coupling, in supergravity and in string theory. We have shown that there is no instability for heavy non-inflationary scalars and that the isocurvature modes are tachyonic only in a spurious, non-attractive solution to the background dynamics. Notice that the stability of heavy fields is in agreement with results previously found in models with non-minimal coupling [177, 178]. Moreover, ref. [201] has recently shown that, even if the initial conditions are tuned such that $\dot{\chi} = \chi = 0$, the backreaction of the isocurvature fluctuations shuts off the instability before reaching the non-linear regime. Instead we have shown that the instability can be present for massless spectator fields kinetically coupled to the inflaton. The existence of large numbers of mass-

less scalars, the moduli, is a hallmark of string compactification models. For the phenomenological viability of such models it is imperative to generate a mass for the moduli fields, a research area that has seen significant progress over the last 15 years and that often involves the addition of subleading corrections, both perturbative and non-perturbative, to the effective action. Despite the sophistication of current constructions, one can sometimes end up with some remaining massless fields. These are the focus of the second part of this Chapter, in particular their rôle during inflation.

After gaining some intuition from analysing the simple case of exponential quintessence-like potentials, we studied this instability in the context of Fibre Inflation [101, 104], a type IIB string inflation model where the inflationary potential is generated by perturbative corrections to the Kähler potential. In this setup there are two axionic fields that remain massless after moduli stabilisation, θ_1 and θ_2, both of which are kinetically coupled to the inflaton. We showed that one of these fields always induces a geometrical instability. For right-left Fibre Inflation models [101], it is the fibre axion θ_1 that leads to unstable isocurvature perturbations, while in left-right realisations of Fibre Inflation [102], the instability is triggered by the base axion θ_2. In both cases we have tried to avoid the instability by giving a small mass to the axions. We found that, although a potential for these fields can be generated by non-perturbative effects, it is not possible to avoid the instability without significantly modifying the dynamics of Fibre Inflation. This would lead to a completely different inflationary model with a truly multi-field dynamics that should be carefully analysed, but this is far beyond the aim of the current work. Furthermore we have numerically probed the system and have shown that the arising of geometrical destabilisation is independent of the choice of initial conditions.

When present, this instability should make one reconsider the validity of whatever inflationary model leading to it. The simplest possibility is that perturbation theory remains valid throughout the evolution. In this case the growth of the isocurvature perturbations might lead to a tension with current observational bounds on the isocurvature fraction only if the ultra-light fields contribute considerably to dark matter [138], a possibility which we consider however unlikely given that these fields are in practice massless. We found that the entropy perturbations, as defined by δs, grow rapidly on superhorizon scales also considering kinetically coupled *massless* scalars that have vanishing on-shell energy density. This happens despite the fact that the background trajectory is essentially single field and stable. This somewhat paradoxical state of affairs has prompted us to investigate this issue further.

In the analysis of Fibre Inflation with more than one ultra-light entropic direction, in order to make use of the results in the literature concerning the effective

mass-squared of the isocurvature modes, we have reduced the field space to two dimensions by projecting out one of the ultra-light directions at a time. Following [202], we also numerically checked the full 3-field system but, since our results did not qualitatively change, we decided not to insert the analysis in this work.

Moreover we showed that the coordinate system, identified by tangent and orthogonal perturbations, is somehow ill-defined. Indeed, one of the two components of the normal projector N_a keeps on growing during inflation, causing the growth of the isocurvature mode δs.

Finally, we introduce the various definitions of entropy that can be found in the literature, pointing out the relation between them and their limits of applicability. Our aim was to understand if the growing isocurvature modes, that we found in the previous sections, can affect the predictions on cosmological parameters. The usual entropy definition that is used in the literature to transfer the entropy mode from the inflationary scalar field system to the primordial plasma [196, 197, 198] is given in Eq. (4.116). We find that in the system under study S_{12} is ill-defined as the massless axion has vanishing energy density on-shell. Nevertheless, we can estimate the relative size of the entropy perturbations generated by non-adiabatic pressure using the fluid approach. We showed that S_{rel} is finite and rapidly decays in time. Therefore, the total entropy of the system is just given by the intrinsic entropy of the inflaton field. This allows us to argue that the instability noted in Sec. 4.6.3 has no physical impact and the underlying model is presently viable.

Chapter 5

Axionic DM from String Theory: 3.55keV line

5.1 Introduction

In 4D string models, ALPs can emerge either as closed string modes arising from the dimensional reduction of 10D anti-symmetric forms or as phases of open string modes charged under anomalous $U(1)$ symmetries on stacks of D-branes [167, 168, 169, 203, 76]. Some of these modes can be removed from the low-energy spectrum by the orientifold projection which breaks $N = 2$ supersymmetry down to $N = 1$, others can be eaten up by anomalous $U(1)$'s via the Green-Schwarz mechanism for anomaly cancellation or can become as heavy as the gravitino if the corresponding saxions are stabilised by the same non-perturbative effects which give mass to the axions. However the axions enjoy a shift symmetry which is broken only at non-perturbative level. Therefore when the corresponding saxions are frozen by perturbative corrections to the effective action, the axions remain exactly massless at this level of approximation. They then develop a mass via non-perturbative effects which are however exponentially suppressed with respect to perturbative corrections. Hence whenever perturbative contributions to the effective scalar potential play a crucial rôle for moduli stabilisation, the axions are exponentially lighter than the associated saxions [204]. Notice that this case is rather generic in string compactifications for two main reasons: (i) if the background fluxes are not tuned, non-perturbative effects are naturally subleading with respect to perturbative ones; (ii) it is technically difficult to generate non-perturbative contributions to the superpotential which depend on all moduli (because of possible extra fermionic zero modes [190], chiral intersections with the visible sector [116] or non-vanishing gauge fluxes due to Freed-Witten anomaly cancellation [52]).

Despite being naturally light, these particles can play both the rôle of cold DM and dark radiation depending on their production mechanism. The oscillations of classical misaligned axion fields produce a condensate of non-relativistic axions [13], while axions produced from heavy moduli decay can free-stream without thermalising and may form today a Cosmic Axion Background (CAB) [16]. In this Chapter we focus on the possible physical explanation of the 3.55 keV line that has been recently detected from several galaxy clusters and other astrophysical objects. This line could not be identified with any other known spectral line from atomic transitions in the intra-cluster medium and may be a possible sign of BSM physics. A physical explanation that is in good accordance with experimental results is given in [17], where the authors claim that the photon line is produced by a double decay. A DM particle directly decay into extremely light ALPs that convert into photons inside the galactic magnetic field. Indeed, thanks to the existence of the following coupling between axions and photons:

$$\mathcal{L}_{a\gamma} = -\frac{a}{4M} F_{\mu\nu}\tilde{F}^{\mu\nu} = -\frac{a}{2M}\,\vec{E}\cdot\vec{B}\,, \tag{5.1}$$

an axion can convert into a photon or viceversa through Primakoff effect in a background magnetic field (see Fig. 5.1). The axion-photon conversion probability in

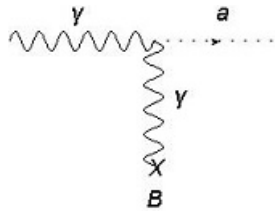

Figure 5.1: Primakoff effect.

a plasma with frequency ω_p at leading order and in the small-angle approximation is given by [17]:

$$P_{a\to\gamma} \approx \begin{cases} \frac{1}{4}\left(\frac{BL}{M}\right)^2 & \text{for } m_a < \omega_p \\ \frac{1}{4}\left(\frac{BL}{M}\right)^2\left(\frac{\omega_p}{m_a}\right)^4 = P_{a\to\gamma}[m_a<\omega_p]\left(\frac{\omega_p}{m_a}\right)^4 & \text{for } m_a \gg \omega_p \end{cases} \tag{5.2}$$

where L is the B-field coherence length and we considered a single domain of homogeneous magnetic field. We therefore realise that in order to have a large $P_{a\to\gamma}$, we need to have magnetic fields which are larger in size over huge domains. Galaxy clusters meet these requirements and usually have $\omega_p \sim 10^{-12}$ eV. Thus ALPs with masses $m_a \lesssim 10^{-12}$ eV can give rise to observable signals in the X-ray band [17].

The main goal of this Chapter is to provide a string embedding of this model [17] where we focus in particular on type IIB flux compactifications where moduli stabilisation has already been studied in depth.

This Chapter is organized as follows: in Sec. 5.2 we give an overview of the experimental observations that have been collected in recent years and in Sec. 5.3 we list the requirements on the geometry of the extra dimensions that need to be satisfied in order to successfully reproduce the appearance of the photon line. In Sec. 5.4 we first discuss the phenomenology of the dark matter to ALP to photon model for the 3.5 keV line and its observational constraints, and then we describe how these phenomenological conditions turn into precise requirements on the Calabi-Yau geometry, the brane setup and gauge fluxes. We than point out which of the 4D fields can successfully play the rôle of either the DM particle or the ultra-light ALP, we list the form of the various interactions and we present the resulting low-energy 4D supergravity. Sec. 5.5 provides a thorough discuss of moduli stabilisation showing how different sources of corrections to the effective action can fix all closed string moduli and the $U(1)$-charged open string modes. In Sec. 5.6 we first derive the expressions for the canonically normalised fields and their masses and then we use these results to work out the strength of the DM-ALP coupling. Several technical details are relegated to App. C.

5.2 The 3.55 keV line

Recently several studies have shown the appearance of a photon line at $E \sim 3.5$ keV, based on stacked X-ray data from galaxy clusters and the Andromeda galaxy [205, 206]. The line has been detected in galaxy clusters by the X-ray observatories XMM-Newton, Chandra and Suzaku [207, 208] and in Andromeda with XMM-Newton [206]. The Hitomi satellite would have been able to study the 3.5 keV line with unprecedented energy resolution. However, unfortunately Hitomi was lost after only a few weeks in operation and the limited exposure time on the Perseus cluster only allows to put upper bounds on the 3.5 keV line which are consistent with the detection of the other satellites [209]. The findings of [205, 206] have inspired further searches in other astrophysical objects such as the galactic center [210, 211, 206, 212], galaxies [213], dwarfs [214, 215, 216] and other galaxy clusters [217, 218].[1] Currently, a compelling standard astrophysical explanation, e.g. in terms of atomic lines of the (cluster) gas is lacking.[2] This gives rise to the possibility that the 3.5 keV line is a signal related to dark matter (DM) physics.

A much explored model is that of dark matter decay, e.g. a sterile neutrino with mass $m_{DM} \sim 7$ keV decaying into an active neutrino and a photon [221, 222]. In

[1] For a summary of observations and models on the 3.5 keV line see [219].

[2] See however [211, 220].

this case, the photon flux from an astrophysical object is solely determined by the lifetime of the dark matter particle and the dark matter column density. The width of the line is due to Doppler broadening. There are several observational tensions, if one wants to explain the (non-)observation of the 3.5 keV line in currently analysed astrophysical objects. Most prominently, these are:

- Non-observation of the 3.5 keV line from dwarf spheroidal galaxies [214, 215, 216]. The dark matter density of these objects is rather well known and the X-ray background is low, making dwarf spheroidals a prime target for detecting decaying dark matter.

- Non-observation of the 3.5 keV line from spiral galaxies [213], where again the X-ray background is low. According to the dark matter estimates of [213], the non-observation of a 3.5 keV signal from spiral galaxies excludes a dark matter decay origin of the 3.5 keV line very strongly at $11\,\sigma$.

- The radial profile of the 3.5 keV line in the Perseus cluster peaks on shorter scales than the dark matter profile, rather following the gas profile than the dark matter profile [205, 212]. However, the observed profile with Suzaku is only in mild tension with the dark matter profile [208].

These tensions, even though they could be potentially explained by uncertainties in the dark matter distributions in these objects [219], motivate different dark matter models than direct dark matter decay into a pair of 3.5 keV photons.

A dark matter model that is consistent with all the present (non-)observations was given in [17]. A dark matter particle with mass $m_{DM} \sim 7$ keV decays into an almost massless ($m_{ALP} \lesssim 10^{-12}$ eV) axion-like particle (ALP) with energy 3.5 keV which successively converts into 3.5 keV photons that are finally observed. Compared to direct dark matter decay into photons, the observed photon flux does not depend just on the dark matter column density, but also on the probability for ALPs to convert into photons. This is determined by the size and coherence scale of the magnetic field and the electron density in e.g. a galaxy cluster.

The 3.5 keV emission is stronger in astrophysical regions with relatively large and coherent magnetic field. This is verified by the experimental fact that cool core clusters like the Perseus cluster have stronger magnetic fields than non-cool core clusters and also a higher 3.5 keV flux is observed from such an object. Furthermore, the fact that central regions of a cool core cluster host particularly strong magnetic fields explains the radial morphology of the 3.5 keV flux from Perseus as the signal comes disproportionally from the central region of the cluster. The model has made the prediction that galaxies can only generate a non-negligible 3.5 keV photon flux if they are spiral and edge-on as for instance the Andromeda galaxy [17]. In this case, the full length of the regions with regular magnetic field

can be used efficiently for ALP to photon conversion. These predictions agree with the experimental results of non-observation of the 3.5 keV signal from generic (edge-on and face-on) spiral galaxies and dwarf galaxies [223].[3]

5.3 Model requirements

Given that the 4D low-energy limit of string compactifications generically leads to several light ALPs [167, 168, 169, 203, 76], it is natural to try to embed the model of [17] in string theory.

String compactifications where some moduli are fixed by perturbative effects are the perfect frameworks to derive models for the 3.5 keV line with light ALPs which can behave as either the 7 keV decaying DM particle or as the ultra-light ALP which converts into photons. Indeed, whenever perturbative contributions to the effective scalar potential play a crucial rôle for moduli stabilisation, axions-saxion mass degeneracy gets broken making the axions exponentially lighter than their supersymmetric counterpart. Notice that this case is rather generic in string compactifications for two main reasons: (*i*) if the background fluxes are not tuned, non-perturbative effects are naturally subleading with respect to perturbative ones; (*ii*) it is technically difficult to generate non-perturbative contributions to the superpotential which depend on all moduli (because of possible extra fermionic zero modes [190], chiral intersections with the visible sector [116] or non-vanishing gauge fluxes due to Freed-Witten anomaly cancellation [52]).

The main moduli stabilisation mechanism which exploits perturbative corrections to the Kähler potential is the LARGE Volume Scenario (LVS) [63, 225, 62]. We shall therefore present an LVS model with the following main features (see Fig. 5.2 for a pictorial view of our microscopic setup):

- The underlying Calabi-Yau (CY) manifold is characterised by $h^{1,1} = 5$ Kähler moduli $T_i = \tau_i + \mathrm{i}c_i$ where the c_i's are closed string axions while the τ_i's control the volume of 5 different divisors: a large four-cycle D_b, a rigid del Pezzo four-cycle D_s which intersects with a 'Wilson divisor' D_p ($h^{0,1}(D_p) = 1$ and $h^{0,2}(D_p) = 0$) and two non-intersecting blow-up modes D_{q_1} and D_{q_2}.

- The two blow-up modes D_{q_1} and D_{q_2} shrink down to zero size due to D-term stabilisation and support D3-branes at the resulting singularities. These constructions are rather promising to build a semi-realistic visible sector with SM-like gauge group, chiral spectrum and Yukawa couplings [226, 227]. If D_{q_1} and D_{q_2} are exchanged by the orientifold involution, the visible sector

[3] Despite the successful interpretation of all these observations, this model would not be able to explain the dip around 3.5 keV in the Perseus AGN spectrum which might arise from Chandra data [224].

features two anomalous $U(1)$ symmetries (this is always the case for any del Pezzo singularity) [151, 228, 78], while if the two blow-up modes are separately invariant, one of them supports the visible sector and the other a hidden sector [229, 137]. Each of the two sectors is characterised by a single anomalous $U(1)$ factor.

- A smooth combination of D_s and D_p is wrapped by a stack of D7-branes which give rise to string loop corrections to the Kähler potential K [58, 60, 61]. Moreover, non-vanishing world-volume fluxes generate moduli-dependent Fayet-Iliopoulos (FI) terms [146, 147]. An ED3-instanton wraps the rigid divisor D_s and generates standard T_s-dependent non-perturbative corrections to the superpotential W. A second ED3-instanton wraps the Wilson divisor D_p. Due to the presence of Wilson line modulini, this ED3-instanton contributes to the superpotential only via T_p-dependent poly-instanton effects [230, 231].

- At leading order in an inverse volume expansion, the moduli are fixed supersymmetrically by requiring vanishing D- and F-terms. These conditions fix the dilaton and the complex structure moduli in terms of three-form flux quanta together with the blow-up modes τ_{q_1} and τ_{q_2} in terms of charged open string fields, and hidden matter fields on the D7-stack in terms of τ_p.

- Quantum corrections beyond tree-level break supersymmetry and stabilise most of the remaining flat directions: α' corrections to K [55] and single non-perturbative corrections to W [65] fix τ_b, τ_s and c_s, while soft supersymmetry breaking mass terms and g_s loop corrections to K fix τ_p.

- Subdominant T_p-dependent poly-instanton corrections to W stabilise the local closed string axion c_p while a highly suppressed T_b-dependent non-perturbative superpotential fixes the bulk closed string axion c_b. Sequestered soft term contributions stabilise instead the radial component of $U(1)$-charged matter fields $C = |C|\, e^{\mathrm{i}\,\theta}$ living on the D3-brane stacks.

- Both c_b and c_p are exponentially lighter than the gravitino, and so could play the rôle of the decaying DM particle with $m_{DM} \sim 7$ keV. On the other hand the ultra-light ALP with $m_{ALP} \lesssim 10^{-12}$ eV which converts into photons is given by the open string phase θ. Notice that if D_{q_1} and D_{q_2} are identified by the orientifold involution, there are two open string phases in the visible sector: one behaves as the standard QCD axion, which is however heavier than 10^{-12} eV, and the other is the ultra-light ALP θ. If instead D_{q_1} and D_{q_2} are separately invariant under the involution, θ is an open string axion belonging to a hidden sector.

- The coupling of the closed string axions c_b and c_p to the open string ALP θ is induced by kinetic mixing due to non-perturbative corrections to the Kähler potential. However we shall show that the scale of the induced DM-ALP coupling can be compatible with observations only if the DM candidate is the local closed string axion c_p.
- If the ultra-light ALP θ belongs to the hidden sector, its coupling to ordinary photons can be induced by $U(1)$ kinetic mixing which gets naturally generated by one-loop effects [232]. Interestingly, the strength of the resulting interaction can easily satisfy the observational constraints if the open string sector on the D3-brane stack is both unsequestered and fully sequestered from the sources of supersymmetry breaking in the bulk.
- The branching ratio for the direct axion DM decay into ordinary photons is negligible by construction since it is induced by kinetic mixing between Abelian gauge boson on the D7-stack and ordinary photons on the D3-stack which gives rise to an interaction controlled by a scale which is naturally trans-Planckian.

5.4 Phenomenology and microscopic realisation

In this section we first discuss the observational constraints of the model of [17] for the 3.5 keV line, and we outline the main phenomenological features of our embedding in LVS type IIB flux compactifications. We then provide the technical details of the microscopic realisation of the DM to ALP to photon model for the 3.5 keV line. We start by illustrating the geometry of the underlying Calabi-Yau compactification manifold. We then present the brane setup and gauge fluxes, and we finally describe the main features of the resulting low-energy 4D effective field theory.

5.4.1 Observational constraints

The effective Lagrangian of the dark matter to ALP to photon model for the 3.5 keV line can be described as follows:

$$\begin{aligned}\mathcal{L} &= -\frac{1}{4}F^{\mu\nu}F_{\mu\nu} - \frac{a_{ALP}}{4M}F^{\mu\nu}\tilde{F}_{\mu\nu} + \frac{1}{2}\partial_\mu a_{ALP}\partial^\mu a_{ALP} - \frac{1}{2}m_{ALP}^2 a_{ALP}^2 \\ &+ \frac{a_{DM}}{\Lambda}\partial_\mu a_{ALP}\partial^\mu a_{ALP} + \frac{1}{2}\partial_\mu a_{DM}\partial^\mu a_{DM} - \frac{1}{2}m_{DM}^2 a_{DM}^2\,, \end{aligned} \tag{5.3}$$

where a_{ALP} is an ALP with mass m_{ALP} that converts into photons in astrophysical magnetic fields via the coupling suppressed by M. a_{DM} is a pseudoscalar which is

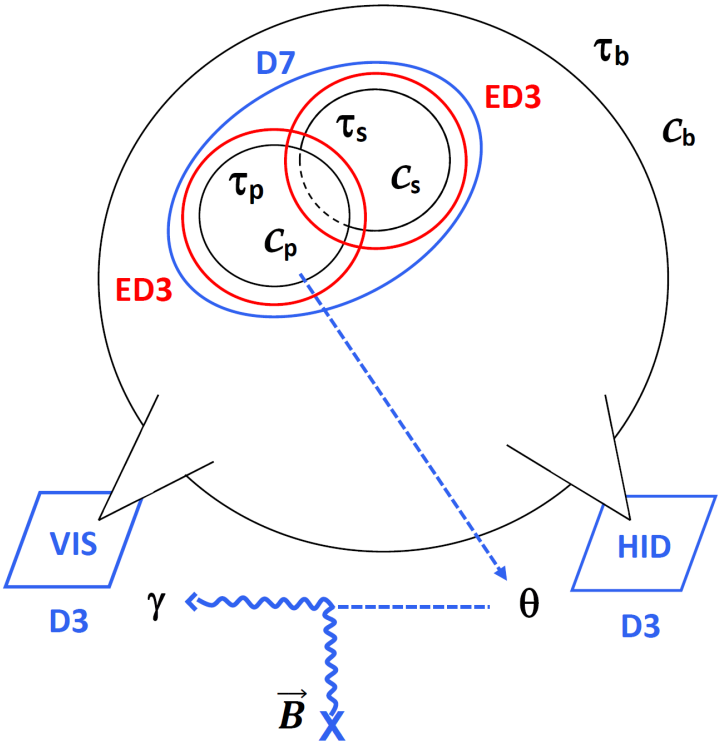

Figure 5.2: Pictorial view of our setup: a stack of D7-branes wraps the combination $\tau_s + \tau_p$, two ED3-instantons wrap respectively the rigid cycle τ_s and the Wilson divisor τ_p while two stacks of D3-branes at singularities support the visible and a hidden sector. The DM particle is the closed string axion c_p which acquires a 7 keV mass due to tiny poly-instanton effects and decays to the ultra-light open string ALP θ that gives the 3.5 keV line by converting into photons in the magnetic field of galaxy clusters.

the dark matter particle with mass $m_{DM} \sim 7$ keV. It decays via the kinetic mixing term in (5.3) with characteristic scale Λ. In order for ALP-photon conversion to be efficient in galaxy cluster magnetic field environments, we require $m_{ALP} \lesssim 10^{-12}$ eV which is the characteristic energy scale of the electron-photon plasma [17]. Otherwise, the ALP to photon conversion is suppressed by $\sim (10^{-12}\,\text{eV}/m_{ALP})^4$. Therefore a_{ALP} is too light to be the standard QCD axion but it has instead to be a stringy axion-like particle.

The observed photon flux at an X-ray detector is given by:

$$F_{DM\to a_{ALP}\to\gamma} \propto \Gamma_{a_{DM}\to a_{ALP}a_{ALP}}\, P_{a_{ALP}\to\gamma}\, \rho_{DM}\,, \tag{5.4}$$

where ρ_{DM} is the dark matter column density and:

$$\Gamma_{a_{DM}\to a_{ALP}a_{ALP}} = \frac{1}{32\pi}\frac{m_{DM}^3}{\Lambda^2}\,, \tag{5.5}$$

is the dark matter decay rate and $P_{a_{ALP}\to\gamma}$ is the ALP to photon conversion probability. It is given as $P_{a_{ALP}\to\gamma} \propto M^{-2}$ and furthermore depends on the electron density in the plasma, the energy of the ALP/photon, the coherence length and the strength of the magnetic field. Hence, $F_{DM\to a_{ALP}\to\gamma} \propto \Lambda^{-2}M^{-2}$. For the ALP to photon conversion conditions in the Perseus cluster magnetic field, the observed 3.5 keV flux then implies [17]:

$$\Lambda \cdot M \sim 7 \cdot 10^{28}\ \text{GeV}^2\,. \tag{5.6}$$

The scales M and Λ are subject to certain constraints. There is a lower bound $M \gtrsim 10^{11}$ GeV from observations of SN1987A [233, 234, 235], the thermal spectrum of galaxy clusters [236] and active galactic nuclei [237, 238, 239]. This lower bound implies an upper bound on Λ via (5.6). To get sufficiently stable dark matter, we assume that the dark matter particle has a lifetime larger than the age of the universe, i.e. $\Lambda \gtrsim 5 \cdot 10^{12}$ GeV. This implies an upper bound on M via (5.6). To summarise, the parameters M and Λ have to satisfy (5.6) together with the following phenomenological constraints:

$$10^{11}\ \text{GeV} \lesssim M \lesssim 10^{16}\ \text{GeV}\,, \qquad 5 \cdot 10^{12}\ \text{GeV} \lesssim \Lambda \lesssim 7 \cdot 10^{17}\ \text{GeV}\,. \tag{5.7}$$

Notice that ultra-light ALPs with intermediate scale couplings to photons will be within the detection reach of helioscope experiments like IAXO [240] and potentially light-shining-through-a-wall experiments like ALPS [241].

5.4.2 Phenomenological features

The phenomenological requirements for a viable explanation of the 3.5 keV line from dark matter decay to ALPs which then convert into photons, can be translated into precise conditions on the topology and the brane setup of the microscopic

realisation. We shall focus on type IIB flux compactifications where moduli stabilisation has already been studied in depth. According to (5.6) and (5.7), we shall focus on the parameter space region where the DM to ALP coupling is around the GUT/Planck scale, $\Lambda \sim 10^{16}$-10^{18} GeV, whereas the ALP to photon coupling is intermediate: $M \sim 10^{11}$-10^{13} GeV. This region is particularly interesting since an ALP with this decay constant could also explain the diffuse soft X-ray excess from galaxy cluster via axion-photon conversion in the cluster magnetic field [242]. This phenomenological requirement, together with the observation that $m_{DM} \sim 10$ keV while $m_{ALP} \lesssim 10^{-12}$ eV, sets the following model building constraints:

- **ALP as an open string axion at a singularity:** From the microscopic point of view, a_{ALP} can be either a closed or an open string axion. In the case of closed string axions, a_{ALP} could be given by the reduction of C_4 on orientifold-even four-cycles or by the reduction of C_2 on two-cycles duals to orientifold-odd four-cycles. As explained in [168, 76] and reviewed in App. C.1, since axions are the imaginary parts of moduli, $T_i = \tau_i + \mathrm{i}\, c_i$ (c_i is a canonically unnormalised axion), whose interaction with matter is gravitational, they tend to be coupled to photons with Planckian strength. However this is true only for bulk axions which have $M \simeq M_p$, while the coupling to photons of local axions, associated to blow-up modes of point-like singularities, is controlled by the string scale: $M \simeq M_s$. $M_s \sim M_p/\sqrt{\mathcal{V}}$ can be significantly lower than M_p if the volume of the extra dimensions in string units $\mathcal{V}$ is very large, and so local closed string axions could realise $M \sim M_s \sim 10^{11}$-10^{13} GeV.

  A moduli stabilisation scheme which leads to an exponentially large $\mathcal{V}$ is the LARGE Volume Scenario [63, 225, 62] whose simplest realisation requires a Calabi-Yau volume of the form:

$$\mathcal{V} = \tau_b^{3/2} - \tau_s^{3/2} \,. \tag{5.8}$$

  The moduli are fixed by the interplay of the leading order α' correction to the Kähler potential and non-perturbative effects supported on the rigid cycle τ_s. The decay constant of the axionic partner of τ_s, which we denote as c_s, is set by the string scale, $M \sim M_s$, but this mode develops a mass of order the gravitino mass $m_{c_s} \sim m_{3/2} \sim M_p/\mathcal{V}$. The large divisor τ_b is lighter than the gravitino due to the underlying no-scale structure of the 4D effective field theory, $m_{\tau_b} \sim m_{3/2}/\sqrt{\mathcal{V}}$, but it has to be heavier than about 50 TeV in order to avoid any cosmological moduli problem. Hence the local axion c_s is much heavier than 10^{-12} eV, and so cannot play the rôle of a_{ALP}. Moreover, the bulk axion c_b cannot be the desired ALP as well since, even if it is almost massless, its coupling scale to photons would be too high: $M \sim M_p$.

We are therefore forced to consider an open string axion realisation for a_{ALP}. Anomalous $U(1)$ factors appear ubiquitously in both D7-branes wrapped around four-cycles in the geometric regime and in D3-branes at singularities. In the process of anomaly cancellation, the $U(1)$ gauge boson becomes massive by eating up an axion [243]. As explained in [204], the combination of axions which gets eaten up is mostly given by an open string axion for D7-branes and by a closed string axion for D3-branes. The resulting low-energy theory below the gauge boson mass, features a global $U(1)$ which is an ideal candidate for a Peccei-Quinn like symmetry. In the case of D3-branes at singularities, the resulting D-term potential looks schematically like:

$$V_D = g^2 \left(q|\hat{C}|^2 - \xi \right)^2 , \tag{5.9}$$

where we focused just on one canonically normalised charged matter field $\hat{C} = |\hat{C}|\, e^{\mathrm{i}\,\theta}$ whose phase θ can play the rôle of an axion with decay constant set by the VEV of the radial part $|\hat{C}|$. The FI term $\xi \sim \tau_q/\mathcal{V}$ is controlled by the four-cycle τ_q which gets charged under the anomalous $U(1)$ and whose volume resolves the singularity. A leading order supersymmetric solution fixes $|\hat{C}|^2 = \xi/q$, leaving a flat direction in the $(|\hat{C}|, \tau_q)$-plane. This remaining flat direction is fixed by subdominant supersymmetry breaking contributions from background fluxes which take the form [78]:

$$V_F(|\hat{C}|) = c_2 m_0^2 |\hat{C}|^2 + c_3 A |\hat{C}|^3 + O(|\hat{C}|^4) , \tag{5.10}$$

where c_2 and c_3 are $\mathcal{O}(1)$ coefficients. If we parametrise the volume dependence of the soft scalar masses as $m_0 \sim M_p/\mathcal{V}^{\alpha_2}$ and the trilinear A-term as $A \sim M_p/\mathcal{V}^{\alpha_3}$, and we use the vanishing D-term condition to write τ_q in terms of $|\hat{C}|$ as $\tau_q \sim |\hat{C}|^2\mathcal{V}$, the matter field VEV scales as:

$$\begin{aligned} &(i)\ \text{If } c_2 > 0 \quad |\hat{C}| = 0 \quad \Leftrightarrow \quad \tau_q = 0 , \\ &(ii)\ \text{If } c_2 < 0 \quad |\hat{C}| \simeq \frac{M_p}{\mathcal{V}^{2\alpha_2 - \alpha_3}} \quad \Leftrightarrow \quad \tau_q \simeq \frac{1}{\mathcal{V}^{4\alpha_2 - 2\alpha_3 - 1}} . \end{aligned}$$

Only in case (ii) the matter field $|\hat{C}|$ becomes tachyonic and breaks the Peccei-Quinn symmetry, leading to a viable axion realisation. In the presence of flavour D7-branes intersecting the D3-brane stack at the singularity, the soft terms are unsequestered and $\alpha_2 = \alpha_3 = 1$ [244], giving $|\hat{C}| \sim M_p/\mathcal{V} \sim m_{3/2}$ and $\tau_q \simeq \mathcal{V}^{-1} \ll 1$ which ensures that τ_q is still in the singular regime. If the internal volume is of order $\mathcal{V} \sim 10^8$, the large modulus τ_b is heavy enough to avoid the cosmological moduli problem: $m_{\tau_b} \sim 100$ TeV. In turn the gravitino mass, all soft terms and the axion decay constant $f_{a_{ALP}} = |\hat{C}|$

are around 10^9 GeV. Setting $\theta = a_{ALP}/f_{a_{ALP}}$, the axion to photon coupling then takes the form:

$$\frac{g^2}{32\pi^2}\frac{a_{ALP}}{f_{a_{ALP}}}F_{\mu\nu}\tilde{F}^{\mu\nu} \quad \Leftrightarrow \quad M = \frac{32\pi^2\, f_{a_{ALP}}}{g^2} = \frac{32\pi^2\, f_{a_{ALP}}}{g_s} \sim 10^{12}\,\text{GeV}\,, \tag{5.11}$$

since for D3-branes the coupling $g^{-2} = \text{Re}(S) = g_s^{-1}$ is set by the dilaton S which controls also the size of the string coupling that we assume to be in the perturbative regime: $g_s \simeq 0.1$.

On the other hand, in the absence of flavour D7-branes the soft terms are sequestered with $\alpha_3 = 2$ and $\alpha_2 = 3/2$ or $\alpha_2 = 2$ depending on the form of the quantum corrections to the Kähler metric for matter fields and the effects responsible for achieving a dS vacuum [77, 79]. Notice that possible non-perturbative desequestering effects from couplings in the superpotential of the form $W_{\text{np}} \supset \mathcal{O}_{\text{matter}}\, e^{-a_s T_s}$ with $\mathcal{O}_{\text{matter}}$ a gauge-invariant operator composed of matter fields, cannot actually change the volume dependence of either the soft scalar masses or the A-terms [245]. Thus if $\alpha_2 = 3/2$ we have $f_{a_{ALP}} = |\hat{C}| \simeq M_p/\mathcal{V}$ and $\tau_q \sim \mathcal{V}^{-1} \ll 1$, while if $\alpha_2 = 2$ the open axion decay constant scales as $f_{a_{ALP}} = |\hat{C}| \simeq M_p/\mathcal{V}^2$ and $\tau_q \sim \mathcal{V}^{-3} \ll 1$. In both cases without flavour D7-branes the gaugino masses scale as $M_{1/2} \sim 0.1\, M_p/\mathcal{V}^2$ and lie around the TeV scale for $\mathcal{V} \sim 10^7$. Considering this value of the volume, the axion-photon coupling therefore becomes:

$$(a)\ \text{If } \alpha_2 = \frac{3}{2} \quad M = \frac{32\pi^2\, f_{a_{ALP}}}{g_s} \sim 10^3\, m_{3/2} \sim 10^{13}\,\text{GeV}\,, \tag{5.12}$$

$$(b)\ \text{If } \alpha_2 = 2 \quad M = \frac{32\pi^2\, f_{a_{ALP}}}{g_s} \sim 10^3\, \frac{m_{3/2}}{\mathcal{V}} \sim 10^6\,\text{GeV}\,. \tag{5.13}$$

- **ALP-photon coupling induced by $U(1)$ kinetic mixing**: We have shown above that, if the matter field $|\hat{C}|$ charged under the anomalous $U(1)$ develops a non-zero VEV due to a tachyonic soft scalar mass contribution, the open string axion θ can have an intermediate scale coupling to photons. However θ in general plays the rôle of the standard QCD axion which becomes much heavier than $m_{ALP} \lesssim 10^{-12}$ eV due to QCD instanton effects. Hence the simplest realisation of an ultralight ALP with the desired phenomenological features to reproduce the 3.5 keV line requires the existence of at least two open string axions. The Calabi-Yau volume (5.8) has then to be generalised to:

$$\mathcal{V} = \tau_b^{3/2} - \tau_s^{3/2} - \tau_{q_1}^{3/2} - \tau_{q_2}^{3/2}\,, \tag{5.14}$$

where τ_{q_1} and τ_{q_2} are both collapsed to a singularity via D-term fixing and support a stack of D3-branes. There are two possibilities to realise a viable a_{ALP}:

1. The two blow-up modes τ_{q_1} and τ_{q_2} are exchanged by the orientifold involution [151, 228, 78]. The resulting quiver gauge theory on the visible sector stack of D3-branes generically features two anomalous $U(1)$ symmetries. This is for example always the case for del Pezzo singularities. Hence the visible sector is characterised by the presence of two open string axions: one behaves as the QCD axion while the other can be an almost massless a_{ALP} with $M \sim 10^{11}$-10^{12} GeV as in (5.11) or (5.12). In this case the matter field $|\hat{C}|$ which develops a VEV of order the gravitino mass has to be a Standard Model gauge singlet in order not to break any visible sector gauge symmetry at a high scale.

2. The two blow-up divisors τ_{q_1} and τ_{q_2} are invariant under the orientifold involution [229, 137]. Therefore one D3-stack has to reproduce the visible sector while the other represents a hidden sector. Each of the two sectors features an anomalous $U(1)$ which gives rise to an open string axion with a coupling to the respective photons controlled by the scale M. The visible sector axion plays the rôle of the QCD axion while the hidden sector open string axion can behave as a_{ALP}. Its coupling to ordinary photons can be induced by a $U(1)$ kinetic mixing of the form [232, 246, 247]:

$$\mathcal{L} \supset -\frac{1}{4}F_{\mu\nu}F^{\mu\nu} - \frac{1}{4}G_{\mu\nu}G^{\mu\nu} + \frac{\chi}{2}F_{\mu\nu}G^{\mu\nu} - \frac{a_{QCD}}{4M_{\rm vis}}F_{\mu\nu}\tilde{F}^{\mu\nu} - \frac{a_{ALP}}{4M_{\rm hid}}G_{\mu\nu}\tilde{G}^{\mu\nu}\,, \tag{5.15}$$

where we denoted the QCD axion as a_{QCD}, the kinetic mixing parameter as χ and the visible sector Maxwell tensor as $F_{\mu\nu}$ while the hidden one as $G_{\mu\nu}$. The kinetic mixing parameter is induced at one-loop level and scales as:

$$\chi \sim \frac{g_{\rm vis}g_{\rm hid}}{16\pi^2} = \frac{g_s}{16\pi^2} \simeq 10^{-3}\,. \tag{5.16}$$

After diagonalising the gauge kinetic terms in (5.15) via $G_{\mu\nu} = G'_{\mu\nu} + \chi F_{\mu\nu}$, a_{ALP} acquires a coupling to ordinary photons of the form:

$$\mathcal{L} \supset -\frac{\chi^2\, a_{ALP}}{4M_{\rm hid}}F_{\mu\nu}\tilde{F}^{\mu\nu} \qquad \Leftrightarrow \qquad M \simeq \frac{M_{\rm hid}}{\chi^2} \gg M_{\rm hid}\,. \tag{5.17}$$

Given that $M \gg M_{\rm hid}$, a_{ALP} can be a hidden sector open string axion only in case (5.13) where the scale of the coupling to hidden photons of order $M_{\rm hid} \sim 10^6$ GeV is enhanced via $U(1)$ kinetic mixing to $M \sim 10^{12}$ GeV for the coupling to ordinary photons.

- **DM as a local closed string axion fixed by poly-instanton effects:** In order to produce a monochromatic 3.5 keV line, the DM mass has to be

around $m_{DM} \sim 7$ keV. Such a light DM particle can be a sterile neutrino realised as an open string mode belonging to either the visible or the hidden sector. However we shall focus on a more model-independent realisation of the decaying DM particle as a closed string axion. A generic feature of any 4D string model where the moduli are stabilised by perturbative effects, is the presence of very light axions whose mass is exponentially suppressed with respect to the gravitino mass [204]. Thus closed string axions are perfect candidates for ultra-light DM particles. In LVS models, there are two kinds of axions which remain light:

1. Bulk closed string axion c_b since the corresponding supersymmetric partner τ_b is fixed by α' corrections to the Kähler potential K. This axionic mode develops a tiny mass only via T_b-dependent non-perturbative contributions to the superpotential W: $m_{c_b} \sim m_{\tau_b} e^{-\pi\tau_b} \ll m_{\tau_b} \sim m_{3/2}/\sqrt{\mathcal{V}}$.

2. Local closed string axion c_p whose associated modulus τ_p is stabilised by g_s loop corrections to K. This can happen for so-called 'Wilson divisors' D_p which are rigid, i.e. $h^{2,0}(D_p) = 0$, with a Wilson line, i.e. $h^{1,0}(D_p) = 1$ [231]. Under these topological conditions, an ED3-instanton wrapping such a divisor does not lead to a standard non-perturbative contribution to W but it generates a non-perturbative correction to another ED3-instanton wrapping a different rigid divisor τ_s. This gives rise to poly-instanton corrections to W of the form [230]:

$$W_{\rm np} = A_s\, e^{-2\pi\left(T_s + A_p e^{-2\pi T_p}\right)} \simeq A_s\, e^{-2\pi T_s} - 2\pi A_s A_p\, e^{-2\pi T_s} e^{-2\pi T_p}\,. \quad (5.18)$$

   In LVS models, the blow-up mode τ_s is fixed by the dominant non-perturbative correction in (5.18) since the leading loop contribution to the scalar potential is vanishing due to the 'extended no-scale' structure [61]. Thus the corresponding axion c_s becomes too heavy to play the rôle of a_{DM} since it acquires a mass of the same order of magnitude: $m_{\tau_s} \sim m_{c_s} \sim m_{3/2}$. On the other hand, the T_p-dependent non-perturbative correction in (5.18) has a double exponential suppression, and so τ_p gets frozen by perturbative g_s effects [58, 60]. Given that c_p enjoys a shift symmetry which is broken only at non-perturbative level, this axion receives a potential only due to tiny poly-instanton contributions to W which make it much lighter than τ_p. Hence c_p is a natural candidate for a_{DM} since $m_{c_p} \sim m_{\tau_p} e^{-\pi\tau_p/2} \ll m_{\tau_p} \sim m_{3/2}$. Notice that the presence of a 'Wilson divisors' τ_p would modify the volume form (5.14) to [231]:

$$\mathcal{V} = \tau_b^{3/2} - \tau_s^{3/2} - (\tau_s + \tau_p)^{3/2} - \tau_{q_1}^{3/2} - \tau_{q_2}^{3/2}\,. \quad (5.19)$$

- **DM to ALP decay induced by non-perturbative effects in K:** A DM to ALP coupling controlled by the scale Λ of the form shown in (5.3) can arise from the kinetic mixing between a closed string DM axion and an open string ALP. Given that the kinetic terms are determined by the Kähler potential, a kinetic mixing effect can be induced by non-perturbative corrections to the Kähler metric for matter fields which we assume to take the form:[4]

$$K_{\rm np} \supset B_i\, e^{-b_i \tau_i}\, \cos(b_i c_i)\, C\bar{C}\,, \tag{5.20}$$

where $i = b$ if a_{DM} is a bulk closed string axion or $i = p$ if a_{DM} is a local closed string axion fixed by poly-instanton effects. As we shall show in Sec. 5.6.3 after performing a proper canonical normalisation of both axion fields, the resulting scale which controls the DM-ALP coupling is given by:

$$\Lambda \sim \begin{cases} \dfrac{e^{b_b \tau_b}}{B_b\, \mathcal{V}^{4/3}}\, M_p \sim \dfrac{e^{b_b \mathcal{V}^{2/3}}}{B_b\, \mathcal{V}^{4/3}}\, M_p \gg M_p \quad \text{for} \quad a_{DM} = c_b \\ \dfrac{e^{b_p \tau_p}}{B_p\, \mathcal{V}^{7/6}}\, M_p \sim \dfrac{M_p}{B_p\, \mathcal{V}^{7/6-\kappa/N}} \quad \text{for} \quad a_{DM} = c_p \end{cases} \tag{5.21}$$

where $b_p = 2\pi/N$, $\kappa = \tau_p/\tau_s$ and we have approximated $\mathcal{V} \sim \tau_b^{3/2} \sim e^{2\pi\tau_s}$. From (5.21) it is clear that Λ can be around the GUT/Planck scale only if the DM particle is a local closed string axion stabilised by tiny poly-instanton corrections to W which can give it a small mass of order $m_{DM} \sim 7$ keV.

5.4.3 Calabi-Yau threefold

As explained in Sec. 5.4.2, the minimal setup which can yield a viable microscopic realisation of the $a_{DM} \to a_{ALP} \to \gamma$ model for the 3.5 keV line of [17], is characterised by a Calabi-Yau with $h^{1,1} = 5$ Kähler moduli and a volume of the form (5.19). A concrete Calabi-Yau threefold built via toric geometry which reproduces the volume form (5.19) for $h^{1,1} = 4$ (setting either $\tau_{q_1} = 0$ or $\tau_{q_2} = 0$) is given by example C of [231]. We therefore assume the existence of a Calabi-Yau threefold X with one large divisor controlling the overall volume D_b, three del Pezzo surfaces, D_s, D_{q_1} and D_{q_2} and a 'Wilson divisor' D_p.

We expand the Kähler form J in a basis of Poincaré dual two-forms as $J = t_b \hat{D}_b - t_s \hat{D}_s - t_{q_1} \hat{D}_{q_1} - t_{q_2} \hat{D}_{q_2} - t_p \hat{D}_p$, where the t_i's are two-cycle volumes and we

[4] Similar non-perturbative corrections to K induced by ED1-instantons wrapped around two-cycles have been computed for type I vacua in [248] and for type IIB vacua in [249], while similar non-perturbative effects in K from an ED3-instanton wrapped around the K3 divisor in type I′ string theory, i.e. type IIB compactified on K3$\times T^2/\mathbb{Z}_2$, have been derived in [250].

took a minus sign for the rigid divisors so that the corresponding t_i's are positive. The Calabi-Yau volume then looks like:

$$\mathcal{V} = \frac{1}{6}\int_X J\wedge J\wedge J = \frac{1}{6}\left[k_{bbb}t_b^3 - k_{sss}\left(t_s+\lambda t_p\right)^3 - \mu t_p^3 - k_{q_1q_1q_1}t_{q_1}^3 - k_{q_2q_2q_2}t_{q_2}^3\right], \tag{5.22}$$

where the coefficients λ and μ are determined by the triple intersection numbers $k_{ijk} = \int_X \hat{D}_i\wedge\hat{D}_j\wedge\hat{D}_k$ as:

$$\lambda = \frac{k_{ssp}}{k_{sss}} = \frac{k_{spp}}{k_{ssp}} \qquad \text{and} \qquad \mu = k_{ppp} - \frac{k_{ssp}^3}{k_{sss}^2}\,.$$

The volume of the curve resulting from the intersection of the del Pezzo divisor D_s with the Wilson surface D_p is given by:

$$\mathrm{Vol}(D_s\cap D_p) = \int_X J\wedge\hat{D}_s\wedge\hat{D}_p = -\left(k_{ssp}t_s + k_{spp}t_p\right) = -k_{ssp}\left(t_s+\lambda t_p\right)\,. \tag{5.23}$$

The volume of this curve is positive and the signature of the matrix $\frac{\partial^2\mathcal{V}}{\partial t_i\partial t_j}$ is guaranteed to be $(1, h^{1,1}-1)$ (so with 1 positive and 4 negative eigenvalues) [28] if $k_{ssp}<0$ while all the other intersection numbers are positive and $t_s+\lambda t_p>0$.[5] The four-cycle moduli can be computed as:

$$\tau_i = \frac{1}{2}\int_X J\wedge J\wedge\hat{D}_i\,, \tag{5.24}$$

and so they become:

$$\begin{aligned}
\tau_b &= \frac{1}{2}k_{bbb}\,t_b^2\,, \qquad \tau_{q_1} = \frac{1}{2}k_{q_1q_1q_1}\,t_{q_1}^2\,, \qquad \tau_{q_2} = \frac{1}{2}k_{q_2q_2q_2}\,t_{q_2}^2\,,\\
\tau_s &= \frac{1}{2}\left(k_{sss}\,t_s^2 + k_{spp}\,t_p^2 + 2k_{ssp}\,t_st_p\right) = \frac{1}{2}k_{sss}\left(t_s+\lambda t_p\right)^2\,,\\
\tau_p &= \frac{1}{2}\left(k_{ppp}\,t_p^2 + k_{ssp}\,t_s^2 + 2k_{spp}\,t_st_p\right) = \frac{1}{2}k_{ssp}\left(t_s+\lambda t_p\right)^2 + \frac{1}{2}\mu t_p^2\,.
\end{aligned} \tag{5.25}$$

The overall volume (5.22) can therefore be rewritten in terms of the four-cycle moduli as:

$$\mathcal{V} = \lambda_b\tau_b^{3/2} - \lambda_s\tau_s^{3/2} - \lambda_p\left(\tau_p + x\tau_s\right)^{3/2} - \lambda_{q_1}\tau_{q_1}^{3/2} - \lambda_{q_2}\tau_{q_2}^{3/2}\,, \tag{5.26}$$

where:

$$\lambda_i = \frac{1}{3}\sqrt{\frac{2}{k_{iii}}}\,, \quad \forall\, i = b,s,q_1,q_2\,, \qquad \lambda_p = \frac{1}{3}\sqrt{\frac{2}{\mu}} \qquad \text{and} \qquad x = -\frac{k_{ssp}}{k_{sss}} > 0\,.$$

Notice that (5.26) reproduces exactly the volume form (5.19).

[5] This analysis includes example C of [231] where $k_{sss} = k_{spp} = -k_{ssp} = 9$ and $k_{ppp} = 0$.

5.4.4 Brane set-up and fluxes

As explained in Sec. 5.4.2, a_{ALP} can be realised as an open string axion belonging either to the visible sector or to a hidden sector. In the first case the two rigid divisors D_{q_1} and D_{q_2} are exchanged by a proper orientifold involution whereas in the second case they are invariant. As we shall see more in detail in Sec. 5.5.1, these two blow-up modes shrink down to zero size due to D-term stabilisation and support a stack of D3-branes at the resulting singularity.

Full moduli stabilisation requires the presence of non-perturbative corrections to the superpotential. We shall therefore consider an ED3-instanton wrapped around the 'small' rigid divisor D_s which generates a standard non-perturbative contribution to W, together with another ED3-instanton wrapped around the Wilson surface D_p which gives rise to poly-instanton effects. In order to make τ_p heavier than the DM axion c_p, we need also to include a D7-stack that generates τ_p-dependent string loop corrections to the Kähler potential. This can be achieved if a stack of D7-branes wraps the divisor D_{D7} (which we assume to be smooth and connected) given by:

$$D_{D7} = m_s\, D_s + m_p\, D_p\,, \quad \text{with} \quad m_s, m_p \in \mathbb{Z}\,. \tag{5.27}$$

In what follows we shall assume the existence of a suitable orientifold involution and O7-planes which allow the presence of such a D7-stack in a way compatible with D7-tadpole cancellation. The cancellation of Freed-Witten anomalies requires to turn on half-integer world-volume fluxes on the instantons and the D7-stack of the form [52]:

$$F_{D7} = f_s\, \hat{D}_s + f_p\, \hat{D}_p + \frac{1}{2}\, \hat{D}_{D7}\,, \qquad F_s = \frac{1}{2}\, \hat{D}_s\,, \qquad F_p = \frac{1}{2}\, \hat{D}_p\,, \tag{5.28}$$

with $f_s,\ f_p \in \mathbb{Z}$. In order to guarantee a non-vanishing contribution to W, the total flux $\mathcal{F}_j = F_j - \iota_j^* B$ (with $\iota_j^* B$ the pull-back of the NSNS B-field on D_j) on both instantons has to be zero: $\mathcal{F}_s = \mathcal{F}_p = 0$. This can be achieved if the B-field is chosen such that:

$$B = \frac{1}{2}\, \hat{D}_s + \frac{1}{2}\, \hat{D}_p\,, \tag{5.29}$$

and the pull-back of $\hat{D}_s/2$ on D_p and of $\hat{D}_p/2$ on D_s are both integer forms since in this case we can always turn on integer flux quanta to cancel their contribution to the total gauge flux. This is indeed the case if, for an arbitrary integer form $\omega = \omega_i \hat{D}_i \in H^2(\mathbb{Z}, X)$ with $\omega_i \in \mathbb{Z}$, we have that:

$$\frac{1}{2} \int_X \hat{D}_s \wedge \hat{D}_p \wedge \omega = \frac{1}{2}\, (k_{ssp}\, \omega_s + k_{spp}\, \omega_p) \in \mathbb{Z}\,. \tag{5.30}$$

This condition can be easily satisfied if both k_{ssp} and k_{spp} are even.

The total gauge flux on the D7-stack instead becomes:

$$\mathcal{F}_{D7} = f_s\,\hat{D}_s + f_p\,\hat{D}_p + \frac{1}{2}\,(m_s-1)\,\hat{D}_s + \frac{1}{2}\,(m_p-1)\,\hat{D}_p = f_s\,\hat{D}_s + f_p\,\hat{D}_p\,,$$

where without loss of generality, we have chosen $m_s = m_p = 1$ so that $\mathcal{F}_{D7}$ is an integer flux. The presence of this flux has several implications:

- The blow-up moduli T_s and T_p get charged under the diagonal $U(1)$ of the D7-stack with charges:

$$q_i = \int_X \mathcal{F}_{D7}\wedge\hat{D}_{D7}\wedge\hat{D}_i = f_s\,(k_{ssi}+k_{spi}) + f_p\,(k_{spi}+k_{ppi})\,,\quad i=s,p\,, \tag{5.31}$$

  which implies $q_p = \mu f_p - x\,q_s$.

- The coupling constant of the gauge theory living on D_{D7} acquires a flux-dependent shift of the form:

$$g_{D7}^{-2} = \tau_s + \tau_p - h(\mathcal{F}_{D7})\,\mathrm{Re}(S)\,, \tag{5.32}$$

  where $\mathrm{Re}(S) = e^{-\varphi} = g_s^{-1}$ is the real part of the axio-dilaton while the flux-dependent shift reads:

$$h(\mathcal{F}_{D7}) = \frac{1}{2}\int_X \mathcal{F}_{D7}\wedge\mathcal{F}_{D7}\wedge\hat{D}_{D7} = \frac{f_s}{2}\,q_s + \frac{f_p}{2}\,q_p\,. \tag{5.33}$$

- $\mathcal{F}_{D7}$ generates a moduli-dependent FI-term which looks like:

$$\xi_{D7} = \frac{1}{4\pi\,\mathcal{V}}\int_X J\wedge\mathcal{F}_{D7}\wedge\hat{D}_{D7} = \frac{1}{4\pi\,\mathcal{V}}\,(q_s\,t_s + q_p\,t_p)\,. \tag{5.34}$$

- A non-vanishing gauge flux on D_{D7} might induce chiral intersections between the D7 stack and the instantons on D_s and D_p. Their net number is counted by the moduli $U(1)$-charges as:

$$I_{D7\text{-}E3} = \int_X \mathcal{F}_{D7}\wedge\hat{D}_{D7}\wedge\hat{D}_s = q_s\,,\qquad I_{D7\text{-poly}} = \int_X \mathcal{F}_{D7}\wedge\hat{D}_{D7}\wedge\hat{D}_p = q_p\,. \tag{5.35}$$

The relations (5.35) imply that, whenever an instanton has a non-vanishing chiral intersection with a stack of D-branes, the four-cycle modulus $T_{\rm inst}$ wrapped by the instanton gets charged under the diagonal $U(1)$ on the D-brane stack. Therefore a non-perturbative contribution to the superpotential of the form $W_{\rm np}\supset e^{-T_{\rm inst}}$ would not be gauge invariant. Thus a proper combination of $U(1)$-charged matter

fields ϕ_i has to appear in the prefactor in order to make the whole contribution gauge invariant: $W_{\rm np} \supset \prod_i \phi_i \, e^{-T_{\rm inst}}$. If however the ϕ_i are visible sector matter fields, they have to develop a vanishing VEV in order not to break any Standard Model gauge group at high energies [116]. In our case the absence of chiral intersections between the instantons on D_s and D_p and the visible sector is guaranteed by the structure of the intersection numbers since $k_{sq_ij} = 0$ and $k_{pq_ij} = 0 \; \forall j$ for either $i = 1$ or $i = 2$.

On the other hand, as can be seen from (5.35), there are chiral intersections between the hidden D7-stack on D_{D7} and the two instantons on D_s and D_p. We could kill both of these intersections by setting $\mathcal{F}_{D7} = 0$. However this choice of the gauge flux on D_{D7} would also set to zero the FI-term in (5.34) which is instead crucial to make τ_p heavier than the DM axion c_p. We shall therefore perform a choice of the gauge flux $\mathcal{F}_{D7}$ which sets $I_{D7\text{-}E3} = q_s = 0$ but leaves $I_{D7\text{-poly}} = q_p \neq 0$ so that ξ_{D7} can develop a non-trivial dependence on τ_p. This can take place if the flux quanta f_p and f_s are chosen such that:

$$f_p = -\frac{k_{sss} + k_{ssp}}{k_{ssp} + k_{spp}} \, f_s \quad \Leftrightarrow \quad q_s = 0 \quad \text{and} \quad q_p = \mu f_p \, . \tag{5.36}$$

The FI-term in (5.34) then becomes:

$$\xi_{D7} = \frac{q_p}{4\pi} \, \frac{t_p}{\mathcal{V}} = \frac{f_p \sqrt{2\,\mu}}{4\pi} \, \frac{\sqrt{\tau_p + x\tau_s}}{\mathcal{V}} \, , \tag{5.37}$$

while the shift of the gauge coupling in (5.33) simplifies to $h(\mathcal{F}_{D7}) = \frac{\mu}{2} \, f_p^2$. Due to non-zero chiral intersections between the D7-stack and the divisor D_p, the poly-instanton contribution to the superpotential comes with a prefactor that depends on a $U(1)$-charged matter field ϕ. In Sec. 5.5.1 we will show that the interplay between D-terms and string loop effects can fix ϕ at a non-zero VEV, so that the poly-instanton correction is non-vanishing. Notice that ϕ belongs to a hidden sector, and so it can safely develop a non-zero VEV at high energies without violating any phenomenological requirement.

5.4.5 Low-energy 4D theory

Type IIB string theory compactified on an orientifold of the Calabi-Yau three-fold described in Sec. 5.4.3 with the brane setup and gauge fluxes of Sec. 5.4.4 gives rise to an $N = 1$ 4D supergravity effective field theory characterised by a Kähler potential K and a superpotential W of the form:

$$K = K_{\rm mod} + K_{\rm matter} \qquad \text{and} \qquad W = W_{\rm tree} + W_{\rm np} \, , \tag{5.38}$$

where:

- The moduli Kähler potential receives perturbative α' and g_s corrections beyond the tree-level approximation:

$$K_{\rm mod} = K_{\rm tree} + K_{\alpha'} + K_{g_s}\,, \tag{5.39}$$

with:

$$K_{\rm tree} = -2\ln\mathcal{V} + \frac{\tau_{q_1}^2}{\mathcal{V}} + \frac{\tau_{q_2}^2}{\mathcal{V}}\,, \quad K_{\alpha'} = -\frac{\zeta}{g_s^{3/2}\mathcal{V}}\,, \quad K_{g_s} = g_s\sum_i \frac{C_i^{KK}\, t_i^{\perp}}{\mathcal{V}}\,. \tag{5.40}$$

In (5.40) we neglected the tree-level Kähler potential for the dilaton $S = e^{-\varphi} - \mathrm{i}\,C_0$ and the complex structure moduli U_{a_-}, $a_- = 1, \cdots, h^{1,2}_-$ and we expanded the effective theory around the singularities obtained by collapsing the two blow-up modes τ_{q_1} and τ_{q_2} (hence the volume $\mathcal{V}$ in (5.40) should be thought of as (5.26) with $\tau_{q_1} = \tau_{q_2} = 0$). Moreover, we included only the leading order α' correction which depends on $\zeta = -\frac{\zeta(3)\chi(X)}{2(2\pi)^3}$ [55] since in the large volume limit higher derivative α' effects yield just subdominant contributions [99]. Finally in K_{g_s} we considered only string loop corrections arising from the exchange of Kaluza-Klein modes between non-intersecting stacks of D-branes and O-planes (C_i^{KK} are complex structure dependent coefficients and $t_i^{\perp}$ is the two-cycle controlling the distance between two parallel stacks of D-branes/O-planes) while we did not introduce any g_s effects coming from the exchange of winding modes since these arise only in the presence of intersections between D-branes which are however absent in our setup [61, 58, 60].

- In the matter Kähler potential we focus just on the dependence on the matter fields which will develop a non-zero VEV. These are two $U(1)$-charged matter fields: $\phi = |\phi|\, e^{\mathrm{i}\psi}$ which belongs to the hidden D7-stack on D_{D7} and $C = |C|\, e^{\mathrm{i}\theta}$ which can be either a visible sector gauge singlet (if D_{q_1} and D_{q_2} are exchanged by the orientifold involution) or a hidden sector field (if both D_{q_1} and D_{q_2} are invariant under the orientifold involution) living on a D3-brane stack [251, 252]:

$$K_{\rm matter} = \frac{\phi\bar{\phi}}{\mathrm{Re}(S)} + \tilde{K}(T_i, \bar{T}_i)\, C\bar{C}\,. \tag{5.41}$$

In (5.41) we wrote down just the tree-level Kähler metric for ϕ while we shall consider both perturbative and non-perturbative corrections to the Kähler metric for C which we assume to take the form:

$$\tilde{K}(T_i, \bar{T}_i) = \frac{f(S,U)}{\mathcal{V}^{2/3}} + \tilde{K}_{\rm pert} + B_i\, e^{-b_i\tau_i}\,\cos(b_i c_i) \qquad \text{with} \quad i = b, p\,, \tag{5.42}$$

where $f(S,U)$ is an undetermined function of the dilaton and complex structure moduli, $\tilde{K}_{\rm pert}$ represents perturbative corrections which do not depend

on the axionic fields because of their shift symmetry and the last term is a non-perturbative correction which can in principle depend on either the large or the poly-instanton cycle. This term induces a kinetic mixing between the open string axion θ and either of the two ultra-light closed string axions c_b and c_p. As we shall see in Sec. 5.5.1, the open string axion ψ gets eaten up by the anomalous $U(1)$ on the D7-stack, and so light closed string axions cannot decay to this heavy mode. This is the reason why we did not include any non-perturbative effect in the Kähler metric for ϕ.

- The tree-level superpotential $W_{\rm tree} = \int_X G_3 \wedge \Omega$, with Ω the Calabi-Yau $(3,0)$-form, is generated by turning on background three-form fluxes $G_3 = F_3 - {\rm i}\, S H_3$ and depends just on the dilaton and the U-moduli but not on the T-moduli [38].

- The non-perturbative superpotential receives a single contribution from the ED3-instanton wrapped around D_s together with poly-instanton effects from the ED3-instanton wrapped around the Wilson surface D_p and takes the same form as (5.18):

$$W_{\rm np} = A_s\, e^{-2\pi T_s} - 2\pi A_s A_p\, e^{-2\pi T_s} e^{-2\pi T_p}\,. \tag{5.43}$$

The prefactors A_s and A_p depend on S and U-moduli. Given that T_p is charged under the anomalous diagonal $U(1)$ on the D7-stack, A_p has to depend also on the charged matter field ϕ in order to make $W_{\rm np}$ gauge invariant. If we make the dependence of A_p on ϕ explicit by replacing $A_p \to A_p \phi^n$ with arbitrary n, and we use the fact that ϕ and T_p behave under a $U(1)$ transformation as:

$$\delta\phi = {\rm i}\, q_\phi\, \phi \qquad \text{and} \qquad \delta T_p = {\rm i}\, \frac{q_p}{2\pi}\,, \tag{5.44}$$

the variation of $W_{\rm np}$ under a $U(1)$ transformation becomes:

$$\delta W_{\rm np} = W_{\rm np} \left(n\, \frac{\delta\phi}{\phi} - 2\pi \delta T_p \right) = {\rm i}\, W_{\rm np}\, (n\, q_\phi - q_p)\,. \tag{5.45}$$

Hence W is gauge invariant only if $n = q_p/q_\phi$. Notice that $n > 0$ since, as we shall see in Sec. 5.5.1, a consistent D-term stabilisation can yield a non-zero VEV for ϕ only if q_ϕ and q_p have the same sign.

5.5 Moduli stabilisation

In this section we shall show how to stabilise all closed string moduli together with the two charged open string modes ϕ and C. The total $N = 1$ supergravity

scalar potential descending from the K and W described in Sec. 5.4.5, includes both F- and D-term contributions of the form:

$$V = V_F + V_D = e^K \left(K^{I\bar{J}} D_I W D_{\bar{J}} \bar{W} - 3|W|^2 \right) + \frac{g_{D7}^2}{2} D_{D7}^2 + \frac{g_{D3}^2}{2} D_{D3}^2 \,, \qquad (5.46)$$

where the Kähler covariant derivative is $D_I W = \partial_I W + W \partial_I K$, the gauge coupling of the field theory living on the D7-stack is given by (5.32) while $g_{D3}^{-2} = \mathrm{Re}(S)$ for the quiver gauge theory on the D3-stack. The two D-term contributions look like:

$$D_{D7} = q_\phi \, \phi \, \frac{\partial K}{\partial \phi} - \xi_{D7} \,, \qquad \text{and} \qquad D_{D3} = q_C \, C \, \frac{\partial K}{\partial C} - \xi_{D3} \,, \qquad (5.47)$$

where the FI-term for the D7-stack is given by (5.37) whereas the FI-term for the D3-brane stack is:

$$\xi_{D3} = q_i \, \frac{\partial K}{\partial T_{q_i}} = q_i \, \frac{\tau_{q_i}}{\mathcal{V}} \qquad \text{for either } i = 1 \text{ or } i = 2 \,. \qquad (5.48)$$

In LVS models the Calabi-Yau volume is exponentially large in string units, and so $1/\mathcal{V} \ll 1$ is a small parameter which can be used to control the relative strength of different contributions to the total scalar potential (5.46). Let us analyse each of these contributions separately.

5.5.1 Stabilisation at $\mathcal{O}(1/\mathcal{V}^2)$

As can be seen from the volume scaling of the two FI-terms (5.37) and (5.48), the total D-term potential scales as $V_D \sim M_p^4/\mathcal{V}^2 \sim M_s^4$. Therefore its leading order contribution has to be vanishing since otherwise the effective field theory would not be under control since the scalar potential would be of order the string scale. As we shall see in more detail below, this leading order supersymmetric stabilisation fixes $|\phi|$ in terms of $\tilde{\tau}_p \equiv \tau_p + x\tau_s$ and τ_{q_i} in terms of $|C|$. The open string axion ψ and the closed string axion c_{q_i} are eaten up by the two anomalous $U(1)$'s living respectively on the D7 and D3-stack. Additional $\mathcal{O}(1/\mathcal{V}^2)$ tree-level contributions to the scalar potential arise from background fluxes which stabilise the dilaton and the complex structure moduli in a supersymmetric manner at $D_S W_{\text{tree}} = D_{U_a\_} W_{\text{tree}} = 0$ [38]. At this level of approximation the Kähler moduli are still flat due to the no-scale cancellation. They can be lifted by subdominant corrections to the effective action which can be studied by assuming a constant tree-level superpotential $W_0 = \langle W_{\text{tree}} \rangle$ that is naturally of $\mathcal{O}(1)$. Summarising the total $\mathcal{O}(1/\mathcal{V}^2)$ contribution to the scalar potential looks schematically like (we show the dependence just on the scalar fields which get frozen):

$$V_{\mathcal{O}(1/\mathcal{V}^2)} = V_D(|\phi|, \tau_{q_i}) + V_F^{\text{tree}}(S, U) \,. \qquad (5.49)$$

Let us focus in particular on the dynamics of the total D-term potential which from (5.37), (5.46) and (5.48) reads:

$$V_D = \frac{g_{D7}^2}{2}\left(q_\phi \frac{|\phi|^2}{\mathrm{Re}(S)} - \frac{f_p\sqrt{2\,\mu}}{4\pi}\frac{\sqrt{\tilde{\tau}_p}}{\mathcal{V}}\right)^2 + \frac{g_{D3}^2}{2}\left(q_C\,\tilde{K}(T_i,\bar{T}_i)\,|C|^2 - q_i\,\frac{\tau_{q_i}}{\mathcal{V}}\right)^2 . \tag{5.50}$$

Supersymmetry is preserved if:

$$q_\phi \frac{|\phi|^2}{\mathrm{Re}(S)} = \frac{f_p\sqrt{2\,\mu}}{4\pi}\frac{\sqrt{\tilde{\tau}_p}}{\mathcal{V}} \qquad \text{and} \qquad q_C\,\tilde{K}(T_i,\bar{T}_i)\,|C|^2 = q_i\,\frac{\tau_{q_i}}{\mathcal{V}}\,. \tag{5.51}$$

These two relations fix one direction in the $(|\phi|,\tilde{\tau}_p)$-plane and one direction in the $(|C|,\tau_{q_i})$-plane. Each of these two directions corresponds to the supersymmetric partner of the axion which is eaten up by the relative anomalous $U(1)$ gauge boson in the process of anomaly cancellation. The axions which become the longitudinal components of the massive gauge bosons are combinations of open string axions with decay constant $f_{\rm op}$ and closed string axions with decay constant $f_{\rm cl}$. The Stückelberg mass of the anomalous $U(1)$'s scales as [253]:

$$M_{U(1)}^2 \simeq g^2\left(f_{\rm op}^2 + f_{\rm cl}^2\right)\,, \tag{5.52}$$

where:

$$\begin{aligned}
\text{D7 case:}\quad f_{\rm op}^2 &= \frac{|\phi|^2}{\mathrm{Re}(S)} = \frac{f_p\sqrt{2\mu}}{4\pi\,q_\phi}\frac{\sqrt{\tilde{\tau}_p}}{\mathcal{V}} \gg f_{\rm cl}^2 = \frac{1}{4}\frac{\partial^2 K}{\partial\tau_p^2} = \frac{1}{4\sqrt{2\mu}}\frac{1}{\mathcal{V}\sqrt{\tilde{\tau}_p}}\,,\\
\text{D3 case:}\quad f_{\rm op}^2 &= \tilde{K}(T_i,\bar{T}_i)\,|C|^2 = \frac{q_i}{q_C}\frac{\tau_{q_i}}{\mathcal{V}} \ll f_{\rm cl}^2 = \frac{1}{4}\frac{\partial^2 K}{\partial\tau_{q_i}^2} = \frac{1}{2\mathcal{V}}\,,
\end{aligned} \tag{5.53}$$

for:

$$\tilde{\tau}_p \gg z_p \equiv \frac{\pi\,q_\phi}{2\mu f_p} \qquad \text{and} \qquad \tau_{q_i} \ll z_{q_i} \equiv \frac{q_C}{2q_i}\,. \tag{5.54}$$

In Sec. 5.5.2 and 5.5.3 we shall explain how to fix the remaining flat directions, showing that the conditions in (5.54) can be satisfied dynamically. These conditions imply that for the D7 case the combination of axions eaten up is mostly given by the open string axion ψ, and so (5.51) should be read off as fixing $|\phi|$ in terms of $\tilde{\tau}_p$, while for the D3 brane case the combination of axions eaten up is mostly given by the closed string axion c_{q_i} which means that (5.51) fixes τ_{q_i} in terms of $|C|$. Notice that from (5.54) the $U(1)$ gauge bosons acquire a mass of order the string scale: $M_{U(1)} \sim M_p/\sqrt{\mathcal{V}} \sim M_s$.

5.5.2 Stabilisation at $\mathcal{O}(1/\mathcal{V}^3)$

As we shall explain more in detail below, $\mathcal{O}(1/\mathcal{V}^3)$ effects arise from both the leading α' and $\tilde{\tau}_p$-dependent g_s corrections to K in (5.40) together with the single instanton contribution in (5.43). They give rise to a scalar potential which depends on τ_s, c_s, τ_p and τ_b but not on the associated axions c_p and c_b since both T_p- and T_b-dependent non-perturbative corrections to W are much more suppressed due to the double exponential suppression of poly-instanton effects and the exponentially large value of $\tau_b \sim \mathcal{V}^{2/3}$. These $\mathcal{O}(1/\mathcal{V}^3)$ contributions alone would yield an AdS minimum which breaks supersymmetry spontaneously [63, 225, 62]. Additional contributions of the same order of magnitude can arise rather naturally from a hidden D7 T-brane stack [73] or from anti-D3 branes at the tip of a warped throat [65, 67, 70] and can be tuned to obtain a dS vacuum. The Kähler moduli develop non-zero F-terms and mediate supersymmetry breaking to each open string sector via gravitational interactions. Matter fields on the D7-stack are unsequestered, and so acquire soft masses of order $m_{3/2}$. After using the vanishing D-term condition to write $|\phi|$ in terms of $\tilde{\tau}_p$, the resulting F-term potential for the matter fields also scales as $\mathcal{O}(1/\mathcal{V}^3)$. Thus the full $\mathcal{O}(1/\mathcal{V}^3)$ scalar potential behaves as:

$$V_{\mathcal{O}(1/\mathcal{V}^3)} = V_F^{\alpha'}(\mathcal{V}) + V_F^{g_s}(\mathcal{V},\tilde{\tau}_p) + V_F^{E3}(\tau_s, c_s, \mathcal{V}) + V_F^{\rm matter}(\mathcal{V},\tilde{\tau}_p) + V_{\rm up}(\mathcal{V})\,. \quad (5.55)$$

All these $\mathcal{O}(1/\mathcal{V}^3)$ contributions take the following precise form:

$$\begin{aligned}
V_F^{\alpha'}(\mathcal{V}) &= \frac{3\,\zeta}{32\pi\,\sqrt{g_s}}\frac{W_0^2}{\mathcal{V}^3}\,, \qquad V_F^{g_s}(\mathcal{V},\tilde{\tau}_p) = \frac{3\,g_s\,\lambda_p}{64\pi}\left(g_s\,C_p^{KK}\right)^2\frac{W_0^2}{\mathcal{V}^3\sqrt{\tilde{\tau}_p}}\,,\\
V_F^{E3}(\tau_s, c_s, \mathcal{V}) &= \frac{4g_s\pi A_s^2}{3\lambda_s}\frac{\sqrt{\tau_s}\,e^{-4\pi\tau_s}}{\mathcal{V}} + g_s A_s\cos(2\pi c_s)\frac{W_0\,\tau_s\,e^{-2\pi\tau_s}}{\mathcal{V}^2}\,,\\
V_F^{\rm matter}(\mathcal{V},\tilde{\tau}_p) &= m_{3/2}^2\frac{|\phi|^2}{{\rm Re}(S)} = \frac{3\,g_s\,\lambda_p}{64\pi z_p}\frac{W_0^2\sqrt{\tilde{\tau}_p}}{\mathcal{V}^3}\,,
\end{aligned} \quad (5.56)$$

where the string loop potential includes only the leading Kaluza-Klein contribution from K_{g_s} in (5.40) which is given by [61]:

$$V_F^{g_s}(\mathcal{V},\tilde{\tau}_p) = \left(\frac{g_s}{8\pi}\right)\left(g_s\,C_p^{KK}\right)^2\frac{W_0^2}{\mathcal{V}^2}\frac{\partial^2 K}{\partial\tau_p^2}\,,$$

and in $V_F^{\rm matter}$ we substituted the relation (5.51) which expresses $|\phi|$ in terms of $\tilde{\tau}_p$. Summing up the four contributions in (5.56), the total scalar potential at $\mathcal{O}(1/\mathcal{V}^3)$ has a minimum at (for $2\pi\tau_s \gg 1$):

$$\begin{aligned}
c_s &= k + \frac{1}{2} \quad \text{with } k\in\mathbb{Z}\,, \qquad \mathcal{V} = \frac{3\lambda_s}{8\pi A_s}\,W_0\sqrt{\tau_s}\,e^{2\pi\tau_s}\,, \\
\tau_s &= \left(\frac{\zeta}{2\lambda_s}\right)^{2/3}\frac{1}{g_s}\,(1+\epsilon) \sim \frac{1}{g_s}\,, \qquad \tilde{\tau}_p = z_p\,(g_s\,C_p^{KK})^2 \sim \frac{1}{g_s}\,,
\end{aligned} \quad (5.57)$$

for $C_p^{KK} \sim g_s^{-3/2} \gg 1$ and:

$$\epsilon = \left(\frac{2\lambda_p}{3\zeta z_p}\right) g_s^{3/2} \sqrt{\tilde{\tau}_p} \sim g_s^{5/2} C_p^{KK} \sim g_s \ll 1 \,. \tag{5.58}$$

Notice that the condition $\tilde{\tau}_p \gg z_p$ in (5.54), which ensures that the closed string axion c_p is not eaten up by the anomalous $U(1)$ on the D7-stack and so can play the rôle of DM, can be easily satisfied if $C_p^{KK} \sim g_s^{-3/2} \gg 1$. We point out that the coefficients of the string loop corrections are complex structure moduli dependent, and so their values can be tuned by appropriate choices of background fluxes. Therefore for $z_p \sim \mathcal{O}(1)$, $\tilde{\tau}_p \sim \tau_s \sim \tau_p \sim g_s^{-1} \gg 1$. This behaviour justifies also the scaling of the small parameter ϵ in (5.58).

As stressed above, this minimum is AdS but can be uplifted to dS via several different positive definite contributions. Two examples which emerge rather naturally in type IIB flux compactifications are T-branes [73] or anti-D3 branes [65, 67, 70].

5.5.3 Stabilisation at $\mathcal{O}(1/\mathcal{V}^{3+p})$

Taking into account all contributions to the scalar potential up to $\mathcal{O}(1/\mathcal{V}^3)$, there are still four flat directions: the charged matter field $|C|$, the open string axion θ and the two closed string axions c_p and c_b. We shall now show how to stabilise the DM axion c_p and $|C|$ which sets the decay constant of the ALP θ and fixes τ_{q_i} from (5.51). The bulk closed string axion c_b receives scalar potential contributions only from T_b-dependent non-perturbative corrections, and so it is almost massless: $m_{c_b} \sim m_{\tau_b} e^{-\pi \mathcal{V}^{2/3}} \sim 0$.

The closed string axion c_p and the open string matter field $|C|$ receive a potential respectively via poly-instanton corrections to the effective action and soft supersymmetry breaking terms. As we shall see below, these terms scale as $\mathcal{O}(1/\mathcal{V}^{3+p})$ with $p > 0$. The only exception which leads to $p = 0$ is the case where flavour D7-branes desequester the open string sector on the D3-brane at a singularity. However, as shown in Sec. 5.4.2, these effects would not modify the VEV of $|C|$ which sets the open string axion decay constant, and so, without loss of generality, we shall consider just the sequestered case. The resulting $\mathcal{O}(1/\mathcal{V}^{3+p})$ scalar potential looks schematically as (showing again just the dependence on the fields which get stabilised at this order in the inverse volume expansion of V):

$$V_{\mathcal{O}(1/\mathcal{V}^{3+p})} = V_F^{\text{poly}}(c_s) + V_F^{\text{matter}}(|C|) \,. \tag{5.59}$$

The leading order expression of the C-dependent soft supersymmetry breaking terms is given by (5.10). A more complete expression in terms of the canonically

normalised field $\hat{C} = |\hat{C}|\, e^{i\theta} = \sqrt{\tilde{K}}\, C$ (see Sec. 5.6.1 for more details) is (the c_i's are $\mathcal{O}(1)$ coefficients) [78]:

$$V_F(|\hat{C}|) = c_2 m_0^2 |\hat{C}|^2 + c_3 A |\hat{C}|^3 + c_4 \lambda |\hat{C}|^4 + \mathcal{O}(|\hat{C}|^5) + c_5 \frac{\tau_{q_i}^2}{\mathcal{V}^3}\left[1 + \mathcal{O}\left(\frac{1}{\mathcal{V}}\right)\right], \quad (5.60)$$

where the first three terms originate from expanding the F-term potential in powers of $|\hat{C}|$ up to fourth order, whereas the last term comes from the fact that the τ_{q_i}-dependent term in (5.40) breaks the no-scale structure. Using (5.51) we can rewrite the last term in (5.60) in terms of $|\hat{C}|$ and parameterising the soft terms in Planck units as $m_0 \sim \mathcal{V}^{-\alpha_2}$, $A \sim \mathcal{V}^{-\alpha_3}$ and $\lambda \sim \mathcal{V}^{-\alpha_4}$, we obtain (up to fourth order in $|\hat{C}|$):

$$V_F(|\hat{C}|) = \frac{c_2}{\mathcal{V}^{\alpha_2}}|\hat{C}|^2 + \frac{c_3}{\mathcal{V}^{\alpha_3}}|\hat{C}|^3 + \frac{k_4}{\mathcal{V}^{\alpha_4}}|\hat{C}|^4 \qquad \text{with} \qquad k_4 = c_4\lambda + \frac{4c_5 z_{q_i}^2}{\mathcal{V}^{1-\alpha_4}}. \quad (5.61)$$

If the soft masses are non-tachyonic, the VEV of the matter field $|\hat{C}|$ is zero, and so the open string axion θ cannot play the rôle of the ALP a_{ALP} which gives the 3.5 keV line by converting into photons in astrophysical magnetic fields. On the other hand, as explained in Sec. 5.4.2, if $c_2 < 0$ $|\hat{C}|$ can develop a non-vanishing VEV. Open string modes living on D3-branes localised at singularities are geometrically sequestered from the sources of supersymmetry breaking in the bulk, resulting in $\alpha_3 = 2$, $\alpha_4 = 1$ and $\alpha_2 = 3/2$ or $\alpha_2 = 2$ depending on the exact moduli dependence of $\tilde{K}_{\rm pert}$ in (5.42) and the details of the uplifting mechanism to a dS vacuum [77, 79]. The VEVs of $|\hat{C}|$ and τ_{q_i} from (5.51) are therefore:

$$\alpha_2 = \frac{3}{2} \text{ case:} \qquad |\hat{C}| = f_{a_{ALP}} = \frac{M_p}{\mathcal{V}} \qquad \Leftrightarrow \qquad \tau_{q_i} = \frac{2\, z_{q_i}}{\mathcal{V}} \ll z_{q_i}\,, \quad (5.62)$$

$$\alpha_2 = 2 \text{ case:} \qquad |\hat{C}| = f_{a_{ALP}} = \frac{M_p}{\mathcal{V}^2} \qquad \Leftrightarrow \qquad \tau_{q_i} = \frac{2\, z_{q_i}}{\mathcal{V}^3} \ll z_{q_i}\,, \quad (5.63)$$

where we have identified the open string axion θ with the ALP $a_{ALP} = f_{a_{ALP}}\,\theta$. Notice that the ALP decay constant in (5.62) reproduces exactly the ALP coupling to gauge bosons in (5.12) while the $f_{a_{ALP}}$ in (5.63) gives the coupling in (5.13). We stress that (5.62) and (5.63) show also how the condition $\tau_{q_i} \ll z_{q_i}$ in (5.54) is easily satisfied for $1/\mathcal{V} \ll 1$. This ensures that the blow-up mode τ_{q_i} is indeed collapsed to a singularity. Let us remind the reader that i can be either $i = 2$ or $i = 3$. When τ_{q_1} and τ_{q_2} are identified by the orientifold involution, an open string axion is the standard QCD axion a_{QCD} while the other is a_{ALP} with $|\hat{C}|$ a Standard Model gauge singlet with a large VEV. On the other hand, when the two blow-up modes τ_{q_1} and τ_{q_2} are separately invariant under the involution, $\hat{C}$ belongs to a hidden sector and, as described in Sec. 5.4.2, its axion θ has a coupling to ordinary photons of the form (5.17) which is induced by $U(1)$ kinetic mixing.

The axionic partner c_p of the Kähler modulus τ_p which controls the volume of the Wilson divisor supporting poly-instanton effects, receives the following scalar potential contributions from the second term in (5.43) with $A_p \to A_p\phi^n$ and $n = q_p/q_\phi$:

$$\begin{aligned} V_F^{\rm poly}(c_p) &= -2g_s\pi A_s A_p \phi^n \left[\frac{8(1-x)\pi A_s}{3\lambda_s}\, \cos(2\pi c_p)\, \sqrt{\tau_s}\, e^{-2\pi\tau_s} \right. \\ &+ \left. W_0\, \cos[2\pi(c_s+c_p)]\, \frac{((1-x)\tau_s+\tilde{\tau}_p)}{\mathcal{V}} \right] \frac{e^{-2\pi\tau_s}\, e^{-2\pi\tau_p}}{\mathcal{V}}\,, \end{aligned}$$

which, after using the first D-term relation in (5.51) and substituting the VEVs in (5.57), reduces to (setting without loss of generality $\phi = |\phi|$ with $\psi = 0$):

$$V_F^{\rm poly}(c_p) = \frac{A}{\mathcal{V}^{3+p}}\, \cos(2\pi c_p)\,, \tag{5.64}$$

where:

$$A = \frac{3g_s\lambda_s A_p}{4} \left(\frac{3\lambda_p\, C_p^{KK}}{8\sqrt{z_p}} \right)^{n/2} \left(\frac{3\lambda_s\sqrt{\tau_s}}{8\pi A_s} \right)^{\kappa} \tilde{\tau}_p\, \sqrt{\tau_s}\, W_0^{2+\kappa}\,,$$

with:

$$\kappa \equiv \frac{\tau_p}{\tau_s} > 0 \qquad \text{and} \qquad p = \frac{n}{2} + \kappa > 0\,. \tag{5.65}$$

Therefore the DM axion c_p is stabilised at $\mathcal{O}(1/\mathcal{V}^{3+p})$ at $c_p = 1/2 + k$ with $k \in \mathbb{Z}$ and $A > 0$.

5.6 Mass spectrum and couplings

In this section we shall first determine the expressions for all canonically normalised fields and their mass spectrum, and then we will compute the strength of the coupling of the light DM axion c_p to the open string ALP θ which is induced by non-perturbative corrections to the matter Kähler metric in (5.42).

5.6.1 Canonical normalisation

Similarly to the scalar potential, also the kinetic Lagrangian derived from the Kähler potential for the moduli given by the three terms in (5.40) and for the matter fields given by (5.41), can be organised in an expansion in $1/\mathcal{V} \ll 1$. Hence the kinetic terms can be canonically normalised order by order in this inverse volume expansion. The detailed calculation is presented in App. C.2 and here we just quote the main results which are useful to work out the strength of the DM-ALP coupling. The expressions for the canonically normalised fields at leading order

look like (the moduli and the matter fields are dimensionless while canonically normalised scalar fields have standard mass dimensions):

$$\begin{aligned}
&\frac{|\hat{C}|}{M_p} = \sqrt{2\tilde{K}}|C|\,, \quad a_{ALP} = |\hat{C}|\theta = f_{a_{ALP}}\theta\,, \quad \frac{|\hat{\phi}|}{M_p} = \sqrt{\frac{2}{\mathrm{Re}(S)}}\,|\phi|\,,\\
&\frac{\phi_b}{M_p} = \sqrt{\frac{3}{2}}\,\ln\tau_b\,, \quad \frac{a_b}{M_p} = \sqrt{\frac{3}{2}}\frac{c_b}{\tau_b}\,, \quad \frac{\phi_s}{M_p} = \sqrt{\frac{4\lambda_s}{3\mathcal{V}}}\,\tau_s^{3/4}\,, \quad \frac{\phi_{q_i}}{M_p} = \frac{\tau_{q_i}}{\sqrt{\mathcal{V}}}\\
&\frac{a_s}{M_p} = \sqrt{\frac{3\lambda_s}{4\mathcal{V}\sqrt{\tau_s}}}\,c_s\,, \quad \frac{\tilde{\phi}_p}{M_p} = \sqrt{\frac{4\lambda_p}{3\mathcal{V}}}\,\tilde{\tau}_p^{3/4}\,, \quad \frac{\tilde{a}_p}{M_p} = \sqrt{\frac{3\lambda_p}{4\mathcal{V}\sqrt{\tilde{\tau}_p}}}\,\tilde{c}_p\,,
\end{aligned} \tag{5.66}$$

where we did not include the axions ψ and c_{q_i} which are eaten up by two anomalous $U(1)$'s on the D7- and D3-brane stack respectively. Notice that the Kähler modulus $T_p = \tau_p + \mathrm{i}\,c_p$ is given by the following combinations of the canonically normalised fields $\Phi_s = \phi_s + \mathrm{i}\,a_s$ and $\tilde{\Phi}_p = \tilde{\phi}_p + \mathrm{i}\,\tilde{a}_p$:

$$\tau_p = \tilde{\tau}_p - x\tau_s = \left(\frac{3\mathcal{V}}{4}\right)^{2/3}\left[\frac{1}{\lambda_p^{2/3}}\left(\frac{\tilde{\phi}_p}{M_p}\right)^{4/3} - \frac{x}{\lambda_s^{2/3}}\left(\frac{\phi_s}{M_p}\right)^{4/3}\right]\,, \tag{5.67}$$

and:

$$c_p = \tilde{c}_p - xc_s = \sqrt{\frac{4\mathcal{V}}{3}}\left(\frac{\tilde{\tau}_p^{1/4}}{\sqrt{\lambda_p}}\frac{\tilde{a}_p}{M_p} - \frac{x\tau_s^{1/4}}{\sqrt{\lambda_s}}\frac{a_s}{M_p}\right)\,. \tag{5.68}$$

5.6.2 Mass spectrum

The mass matrix around the global minimum and its eigenvalues are derived in detail in App. C.3. Here we just show the leading order volume scaling of the mass of all moduli and charged matter fields for $g_s \sim 0.1$ (in order to trust our approach based on perturbation theory) and $\mathcal{V} \sim 10^7$. As explained in Sec. 5.4.2, this choice of the internal volume leads naturally to TeV-scale soft terms for sequestered scenarios with D3-branes at singularities, while it guarantees the absence of any cosmological moduli problem for unsequestered cases with flavour D7-branes. The resulting mass spectrum looks like:

$$
\begin{aligned}
m_{c_{q_i}} &\sim m_{\tau_{q_i}} \sim m_{\psi} \sim m_{|\phi|} \sim M_s \sim g_s^{1/4}\sqrt{\pi}\,\frac{M_p}{\sqrt{\mathcal{V}}} \sim 10^{15}\ \text{GeV}\,, \\
m_{\tau_s} &\sim m_{c_s} \sim \sqrt{\frac{g_s}{8\pi}}\,\frac{M_p}{\mathcal{V}}\,\ln\mathcal{V} \sim 10^{11}\ \text{GeV}\,, \\
m_{3/2} &\sim \sqrt{\frac{g_s}{8\pi}}\,\frac{M_p}{\mathcal{V}} \sim 10^{10}\ \text{GeV}\,, \\
m_{\tilde{\tau}_p} &\sim \sqrt{\frac{g_s}{8\pi}}\,\frac{M_p}{\mathcal{V}\sqrt{\ln\mathcal{V}}} \sim 10^{9}\ \text{GeV}\,, \\
m_{\tau_b} &\sim \sqrt{\frac{g_s}{8\pi}}\,\frac{M_p}{\mathcal{V}^{3/2}\sqrt{\ln\mathcal{V}}} \sim 10^{6}\ \text{GeV}\,, \\
m_{|C|} &\sim \sqrt{\frac{g_s}{8\pi}}\,\frac{M_p}{\mathcal{V}^{2}} \sim 1\ \text{TeV}\,, \\
m_{c_p} &\sim \sqrt{\frac{g_s}{8\pi}}\,\frac{M_p}{\mathcal{V}^{1+p/2}}\,\sqrt{\ln\mathcal{V}} \sim 10\ \text{keV} \qquad \text{for} \quad p=\frac{9}{2}\,, \\
m_{\theta} &\sim \frac{\Lambda_{\rm hid}^2}{f_{a_{ALP}}} \lesssim 10^{-12}\ \text{eV}\,, \\
m_{c_b} &\sim \sqrt{\frac{g_s}{8\pi}}\,\frac{M_p}{\mathcal{V}^{2/3}}\,e^{-\pi\,\mathcal{V}^{2/3}} \sim 0\,,
\end{aligned}
\tag{5.69}
$$

where we focused on the sequestered case with $\alpha_2 = 2$ illustrated in Sec. 5.5.3 and $\Lambda_{\rm hid}$ represents the scale of strong dynamics in the hidden sector which gives mass to the open string axion $\theta = a_{ALP}/f_{a_{ALP}}$ whose decay constant is $f_{a_{ALP}} = |\hat{C}| \simeq M_p/\mathcal{V}^2$. As explained in Sec. 5.4.2, this decay constant leads to a coupling to hidden photons controlled by the scale $M_{\rm hid} \sim 10^6$ GeV that can yield a coupling to ordinary photons via $U(1)$ kinetic mixing given by (5.17) which can be naturally suppressed by an effective scale of order $M \sim 10^{12}$ GeV. Notice that the DM axion c_p can acquire a mass from poly-instanton effects of order $m_{c_p} \sim 10$ keV if $p = \frac{n}{2} + \kappa = \frac{9}{2}$, which can be obtained for any $\mathcal{O}(1)$ value of n by appropriately choosing the flux dependent underlying parameters so that $\kappa \equiv \frac{\tau_p}{\tau_s} = \frac{1}{2}\,(9-n)$.

5.6.3 DM-ALP coupling

As shown by the mass spectrum in (5.69) and by the coupling to ordinary photons in (5.17), the open string axion θ is a natural candidate for the ALP mode a_{ALP} which converts into photons in the magnetic field of galaxy clusters and generates the 3.5 keV line. However a monochromatic line requires the decay into a pair of ALP particles of a DM particle a_{DM} with mass $m_{DM} \sim 7$ keV. According to

the mass spectrum in (5.69) a_{DM} could be either the local closed string axion c_p or the bulk closed string mode c_b (if T_b-dependent non-perturbative effects do not suppress its mass too much). We shall now show that non-perturbative corrections to the matter Kähler metric in (5.41) can induce a coupling of the form $\frac{a_{DM}}{\Lambda}\,\partial_\mu a_{ALP}\partial^\mu a_{ALP}$ due to kinetic mixing between the closed string axion a_{DM} and the open string axion a_{ALP}. We shall also work out the value of the coupling Λ, finding that it can lie around the Planck/GUT scale only if the DM particle is the local axion c_p (c_b would give a trans-Planckian Λ). Finally we will explain how in our model a direct DM decay to photons induced by potential couplings of the form $\frac{a_{DM}}{4M_{DM}}\,F^{\mu\nu}\tilde{F}_{\mu\nu}$ is naturally suppressed by construction.

In order to compute the DM-ALP coupling, let us focus on contributions to the kinetic Lagrangian of the form:

$$\mathcal{L}_{\rm kin} \supset \frac{\partial^2 K}{\partial C \partial \bar{C}}\,\partial_\mu C \partial^\mu \bar{C} = \tilde{K}(T_i,\bar{T}_i)\left(\partial_\mu |C| \partial^\mu |C| + |C|^2\,\partial_\mu\theta\partial^\mu\theta\right)\,. \tag{5.70}$$

If we now expand the closed string axions c_i and the charged open string mode $C = |C|\,e^{{\rm i}\,\theta}$ around the minimum as:

$$c_i(x) \to \langle c_i\rangle + c_i(x)\,, \qquad |C|(x) \to \langle |C|\rangle + |C(x)|\,, \qquad \theta(x) \to \langle\theta\rangle + \theta(x)\,, \tag{5.71}$$

the kinetic terms (5.70) become:

$$\left[\langle\tilde{K}\rangle - B_i\,e^{-b_i\tau_i}\,\left(\cos(b_i\langle c_i\rangle)\frac{b_i}{2}\hat{c}_i^2 + \sin(b_i\langle c_i\rangle)\,b_i\hat{c}_i\right)\right]\left(\partial_\mu|C|\partial^\mu|C| + |C|^2\,\partial_\mu\theta\partial^\mu\theta\right). \tag{5.72}$$

If we now express the open string mode C in terms of the canonically normalised fields $\hat{C}$ and a_{ALP} using (5.66), (5.72) contains DM-ALP interaction terms of the form:

$$\frac{B_i}{2\langle\tilde{K}\rangle}\,e^{-b_i\langle\tau_i\rangle}\,\left(\cos(b_i\langle c_i\rangle)\frac{b_i}{2}\,\hat{c}_i^2 + \sin(b_i\langle c_i\rangle)\,b_i\,\hat{c}_i\right)\partial_\mu a_{ALP}\partial^\mu a_{ALP}\,, \tag{5.73}$$

showing that, in order to obtain a three-leg vertex which can induce a two-body DM decay into a pair of ultra-light ALPs, the VEV of c_i has to be such that $b_i\langle c_i\rangle = (2k+1)\frac{\pi}{2}$ with $k\in\mathbb{Z}$. Let us therefore focus on this case and consider separately the two options with either $i=b$ or $i=p$:

- $i=b$ **case:** Plugging in (5.73) the canonical normalisation for c_b from (5.66), we find a DM-ALP coupling of the form:

$$\frac{a_b}{\Lambda}\,\partial_\mu a_{ALP}\partial^\mu a_{ALP} \quad \text{with} \quad \Lambda = \frac{\sqrt{6}\langle\tilde{K}\rangle}{B_b b_b}\,\frac{e^{b_b\langle\tau_b\rangle}}{\langle\tau_b\rangle}\,M_p \sim \frac{e^{b_b\mathcal{V}^{2/3}}}{B_b\,\mathcal{V}^{4/3}}\,M_p \gg M_p\,, \tag{5.74}$$

which reproduces the value of Λ in (5.21) for $a_{DM} = c_b$. According to the phenomenological constraints discussed in Sec. 5.4.1, c_b cannot play the rôle of the DM particle since the scale of its ALP coupling is trans-Planckian.

- $i = p$ **case:** Writing $b_p = \frac{2\pi}{N}$ and using the fact that the minimum for c_p lies at $\langle c_p \rangle = \frac{1}{2} + k_1$ with $k_1 \in \mathbb{Z}$, the condition $b_p \langle c_p \rangle = (2k_2+1)\frac{\pi}{2}$ with $k_2 \in \mathbb{Z}$ can be satisfied if $\frac{N}{2} = \frac{(2k_1+1)}{(2k_2+1)}$. Hence in the simplest case with $k_1 = k_2 = 0$ we just need $N = 2$. Plugging in (5.73) the canonical normalisation for c_p from (5.68), the DM-ALP coupling turns out to be:

$$\frac{\tilde{a}_p}{\Lambda}\,\partial_\mu a_{ALP}\partial^\mu a_{ALP} \qquad \text{with} \qquad \Lambda = \frac{\sqrt{3\lambda_p}}{\tilde{\tau}_p^{1/4}}\,\frac{\langle \tilde{K} \rangle}{B_p b_p}\,\frac{e^{b_p\langle \tau_p \rangle}}{\sqrt{\mathcal{V}}}\,M_p \sim \frac{M_p}{B_p\,\mathcal{V}^{7/6-\kappa/N}}\,, \tag{5.75}$$

which reproduces the value of Λ in (5.21) for $a_{DM} = c_p$. This scale of the DM-ALP coupling can easily be around the Planck/GUT scale. For example if $N = 2$ and the underlying parameters are chosen such that $\kappa \equiv \tau_p/\tau_s = 2$, $\Lambda \sim M_p/\mathcal{V}^{1/6} \sim 10^{17}$ GeV for $\mathcal{V} \sim 10^7$ and $B_p \sim \mathcal{O}(1)$. Due to the poly-instanton nature of the non-perturbative effects supported by the Wilson divisor D_p, the prefactor B_p can however be exponentially small. Comparing T_p-dependent poly-instanton corrections to the superpotential in (5.43) with T_p-dependent non-perturbative corrections to the matter Kähler metric in (5.42), B_p at the minimum could scale as $B_p \sim \mathcal{O}(\mathcal{V}^{-1})$. In this case Λ can be below the Planck scale only if $\kappa \ll N$.

Let us conclude this section by showing that the branching ratio for direct DM decay into ordinary photons is negligible. Using the fact that the gauge kinetic function for the D7-stack is given by $f_{D7} = T_s + T_p$ (we neglect the flux dependent shift) and the canonical normalisation (5.68), the closed string axion $c_p = \langle c_p \rangle + \hat{c}_p$ couples to Abelian gauge bosons living on the hidden D7-stack via an interaction term of the form:

$$\frac{\hat{c}_p}{4\,(\langle \tau_s \rangle + \langle \tau_p \rangle)}\,F^{\mu\nu}_{\rm hid}\tilde{F}^{\rm hid}_{\mu\nu} \sim \frac{\tilde{a}_p}{4M_s}\,F^{\mu\nu}_{\rm hid}\tilde{F}^{\rm hid}_{\mu\nu}\,. \tag{5.76}$$

One-loop effects generate a kinetic mixing between hidden photons on the D7-stack and ordinary photons on the D3-stack which is controlled by the mixing parameter $\chi \sim 10^{-3}$ given in (5.16). Thus the DM axion c_p develops an effective coupling to visible sector photons which from (5.17) looks like:

$$\frac{\tilde{a}_p}{4\,M_{DM}}\,F_{\mu\nu}\tilde{F}^{\mu\nu} \sim \frac{\chi^2\,\tilde{a}_p}{4M_s}\,F_{\mu\nu}\tilde{F}^{\mu\nu} \qquad \Leftrightarrow \qquad M_{DM} \sim \frac{M_s}{\chi^2} \sim 10^5\,\frac{M_p}{\sqrt{\mathcal{V}}} \sim 10^{20}\ \text{GeV}\,, \tag{5.77}$$

which is naturally much larger than the scale Λ controlling the DM coupling to ALPs.

5.7 Conclusions

In this Chapter we described how to perform a successful global embedding in type IIB string compactifications of the model of [17] for the recently observed 3.5 keV line from galaxy clusters. The main feature of this model is the fact that the monochromatic 3.5 keV line is not generated by the direct decay of a 7 keV dark matter particle into a pair of photons but it originates from DM decay into ultra-light ALPs which subsequently convert into photons in the cluster magnetic field. Therefore the final signal strength does not depend just on the DM distribution but also on the magnitude of the astrophysical magnetic field and its coherence length which, together with the ALP to photon coupling, determine the probability for ALPs to convert into photons. These additional features make the model of [17] particularly interesting since it manages to explain not just the observation of a 3.5 keV line from galaxy clusters but also the morphology of the signal (e.g. the intensity of the line from Perseus seems to be picked at the centre where the magnetic field is in fact more intense) and its non-observation in dwarf spheroidal galaxies (due to the fact that their magnetic field is not very intense and has a relatively small spatial extension). These phenomenological features seem to make this model more promising than standard explanations where DM directly decays into a pair of photons.

Despite this observational success, the model of [17] for the 3.5 keV line did not have a concrete microscopic realisation. In this Chapter we filled this gap by describing how to construct an explicit type IIB Calabi-Yau compactification which can reproduce all the main phenomenological features of the DM to ALP to photon model. We focused in particular on LVS models since they generically lead to very light axions because some of the moduli are stabilised by perturbative corrections to the effective action. The DM particle is realised as a local closed string axion which develops a tiny mass due to poly-instanton corrections to the superpotential. By an appropriate choice of background and gauge fluxes, the DM mass can be around 7 keV. The ultra-light ALP is instead given by the phase of an open string mode living on D3-branes at singularities. The ALP decay constant is set by the radial part of this open string mode which is charged under an anomalous $U(1)$. Thus the radial part gets fixed in terms of a moduli-dependent FI-term. In sequestered models with low-energy supersymmetry, the resulting decay constant is naturally in the right ballpark to reproduce a coupling to ordinary photons via $U(1)$ kinetic mixing which is around the intermediate scale, in full agreement with current observations. Notice that future helioscope experiments like IAXO might be able to detect ultra-light ALPs with intermediate scale couplings to photons [240]. Moreover the DM-ALP coupling is generated by kinetic mixing induced by non-perturbative corrections to the Kähler potential. For suitable choices of the underlying flux dependent parameters, the scale which controls the associated

coupling can be around the GUT/Planck scale, again in good agreement with present observational constraints.

We discussed in full depth moduli stabilisation, the mass spectrum and the resulting strength of all relevant couplings but we just described the geometrical and topological conditions on the underlying Calabi-Yau manifold without presenting an explicit example built via toric geometry. This task is beyond the scope of our work, and so we leave it for future work. Let us however stress that the construction of a concrete Calabi-Yau example with all the desired features for a successful microscopic realisation of our model for the 3.5 keV line is crucial to have a fully trustworthy scenario. Moreover it would be very interesting to have a more concrete computation of non-perturbative corrections to the 4D $N = 1$ Kähler potential.

Another aspect which would deserve further investigation is the cosmological history of our setup from inflation to the present epoch. Here we just point out that the rôle of the inflaton could be played by a small blow-up mode like τ_s [137, 136]. On the other hand, reheating might be due to the volume mode τ_b which gets displaced from its minimum during inflation [122] and later on decays giving rise to a reheating temperature of order $T_{\rm rh} \sim 1 - 10$ GeV [128]. Such a low reheating temperature would dilute standard thermal WIMP dark matter and reproduce it non-thermally [128]. Given that in sequestered models with unified gaugino masses the WIMP is generically a Higgsino-like neutralino with an under-abundant non-thermal production in vast regions of the underlying parameter space [129, 254], an additional DM component in the form of a very light axion like c_p would be needed. Finally one should make sure that tight dark radiation bounds are satisfied since τ_b could decay both to a pair of ultra-light closed string axions c_b and to a pair of DM axions c_p which could behave as extra neutrino-like species [14, 126]. Notice however that the decay of τ_b to open string axions θ living on D3-branes at singularities is negligible since it is highly suppressed by sequestering effects [14]. The DM axions c_p are produced non-thermally at the QCD phase transition via the standard misalignment mechanism. Given that the decay constant of the local closed string axion c_p is of order the string scale which from (5.69) is rather high, i.e. $M_s \sim 10^{15}$ GeV, axion DM overproduction can be avoided only if the initial misalignment angle is very small. This might be due to a selection effect from the inflationary dynamics [255]. We finally stress that if inflation is driven by a blow-up mode like τ_s, the Hubble scale during inflation is rather low, $H \sim m_{\tau_b} \sim 10^6$ GeV, and so axion isocurvature perturbations would not be in tension with CMB data [256].

Chapter 6

Axion Inflation and electro-magnetic dissipation

6.1 Introduction

Axion-like particles are among the prime candidates for particle physics implementations of cosmic inflation. Protected by an approximate shift-symmetry, these Pseudo Nambu Goldstone Bosons naturally come with a sufficiently flat scalar potential to support slow-roll inflation and to be protected against quantum corrections. Many concrete realizations of axion inflation in field theory have been proposed beginning with Ref. [257], for axions in string theory see [258, 167].

As already seen in the previous Chapters, in the context of string theory, axion-like particles can naturally emerge as closed and open string axions. These particles may receive a mass through non-perturbative corrections due to world-sheet instantons, gaugino condensation on space-time filling D-branes and euclidian D-branes. Thanks to these corrections the classical continuous shift symmetry is broken to a discrete shift symmetry, usually involving a cosine potential. It is widely known that, in order to get a prolonged inflation with just one axion playing the rôle of the inflaton, the decay constant associated to this field should be trans-Planckian. Examples of axions showing this feature have not been found in a controlled string compactification. For instance, considering C_4 axions, the largest decay constants are related to large cycles that parametrise the overall volume. In such cases we have that the eigenvalues of the Kähler metric in Eqs. (2.176),(2.177) are given by $\lambda_i \sim \tau^{-1}$ implying that $f \sim M_p/\tau$. Having a trans-Planckian decay constant would require $\tau \ll 1$ but such small 4-cycles volumes are not consistent with the EFT approach since α' expansion is not under control. The reason why it is not easy to evade the condition $f \lesssim M_p$ is summed up in the weak gravity conjecture and its applications to axion fields [108, 259]. In the case of a single axion field it

states that $fS \lesssim M_p$, where S is the action of an instanton coupled to the axion field. Indeed, if we want a single axion field to be the inflaton, its potential needs to satisfy the constraints coming from COBE normalisation and the field mass can not become arbitrarily small; since the instanton action S is related to the axion mass, setting a bound such as $Sf \lesssim M_p$ puts severe constraints on model building. In addition, these models need a trans-Planckian field range excursion during inflation that would be in contrast with the infinite distance swampland conjecture [260]. As already mentioned in Sec. 2.4.2, a way to overcome the problem related to the magnitude of the decay constant can be considering a system of two or more axions, each with a sub-Planckian decay constant, where moduli stabilisation allows a combination of the fields to enjoy an *effective trans-Planckian* decay constant [109, 112, 110]. However we need to mention that such models may not be under control since they show problems related to dS entropy [261] and moduli stabilisation [113]. The second problem related to field space distance travelled by the inflaton can be softened through electro-magnetic dissipation, introducing a coupling with a $U(1)$ gauge field [262]. This coupling to (hidden-)photons and its phenomenological consequences are precisely what we are going to investigate in the present Chapter, focusing in particular on the quantitative analysis of the electro-magnetic backreaction effects on the inflationary trajectory. Due to the large amount of computational work, we restrict ourselves to a toy model given by a single axionic inflaton showing a quadratic potential and a trans-Planckian decay constant.

The shift-symmetry of the axion-like inflaton Φ allows for a derivative coupling to the field strength tensor $F_{\mu\nu}$ of a (dark) gauge sector,

$$\mathcal{L}_{\rm int} = -\frac{\sqrt{-g}}{4f}\Phi F_{\mu\nu}\tilde{F}^{\mu\nu}\,, \tag{6.1}$$

with f denoting the axion decay constant and for simplicity, we will consider $F_{\mu\nu}$ to describe a hidden sector abelian gauge group, i.e. a dark photon.[1] This interaction triggers a tachyonic instability of the dark photon driven by the velocity $\dot{\Phi}$ of the inflaton, leading to an exponential production of dark photons [265, 266, 267]. The resulting non-thermal gauge field distribution backreacts on the inflaton, dampening its motion. At the same time, the gauge fields act as a source of scalar and tensor perturbations [268, 269, 270, 271], in addition to the standard vacuum fluctuations amplified during cosmic inflation. These perturbations can be probed by CMB observations [268, 272], searches for primordial black holes [273, 274,

[1] If the theory contains particles charged under this $U(1)$ (as is e.g. the case for the Standard Model hypercharge), these particles must be included in the analysis if they are sufficiently light, as they will be produced via Schwinger production from the vacuum, thereby significantly damping the gauge field production. On the contrary, the impact of heavier particles is exponentially suppressed and they can be safely integrated out [263, 264].

275, 276] and gravitational wave experiments [271, 277, 278, 279], rendering axion inflation not only a theoretically well motivated but also an experimentally testable proposal for cosmic inflation [269].

In this work we have a closer look at the backreaction of the gauge field distribution on the inflaton equations of motion. Since this determines the evolution of the homogeneous inflaton field, this has a crucial impact on all potential observables of this framework and may influence the required inflationary field excursion. The interaction (6.1) results in a friction term in the background equation of motion for Φ which is proportional to $\langle F\tilde{F}\rangle$. In Fourier space, this non-linear interaction involves an integral over all relevant Fourier modes of the gauge field, leading to a integro-differential system describing the evolution of the gauge field modes and the homogeneous component of the inflaton.

In many previous works, this system is solved by assuming the inflaton velocity to be constant in the gauge field equation of motion (see e.g. [269]), motivated by the usual slow-roll approximation employed in cosmic inflation. However, since the gauge field enhancement and hence the backreaction on the inflaton are exponentially sensitive to this velocity, this approximation becomes invalid in the phenomenologically interesting regime of sizable gauge field production. Recently, several alternative approaches have been put forward. Lattice simulations [280, 281, 282], focusing mainly on the preheating phase, accurately capture the backreaction but are limited in the amount of time evolution that can be tracked. Ref. [283] proposed a gradient expansion of the generated electric and magnetic field. Self-consistent numerical solutions of the integro-differential system have been obtained in Refs. [284, 285, 286]. These latter studies noted the appearance of remarkable oscillatory features in the inflaton velocity. In this work, we reproduce these findings and quantitatively explain the occurring resonance phenomenon based on semi-analytical arguments. Since the enhancement of the gauge field modes is most sensitive to the inflaton velocity around horizon crossing whereas the backreaction is dominated by super-horizon gauge field modes, the system responds with a time delay to a change in the inflaton velocity. This time delay is logarithmically sensitive to the inflaton velocity. As the inflaton velocity increases during the course of inflation the system hits its resonance frequency, leading to strong oscillations in the amplitude of $\langle F\tilde{F}\rangle$ as a function of time. This crucially impacts both the background equation of motion as well as the generation of scalar and tensor perturbations.

The power spectrum of scalar perturbations can be obtained by solving the linearized inhomogeneous equation of motion for the inflaton field taking into account the backreaction and source terms proportional to $F\tilde{F}$. In the pioneering works [262, 268, 270, 273] this task has been solved in the weak and very strong backreaction regime. Here we extend these results to arbitrary inflaton gauge field

couplings by numerically determining the Greens function including the backreaction term. We report two important results. Firstly, for a smoothly growing $\langle F\tilde{F}\rangle$, we find that the analytical estimate in [262] significantly overestimates the backreaction compared to our full numerical results. As a result, the actual power spectrum is significantly enhanced compared to previous estimates. Consequently, a large primordial black hole (PBH) abundance can be generated, leading to an early PBH dominated phase. Requiring the transition to radiation domination to occur before the onset of big bang nucleosynthesis imposes stringent constraints on the parameter space. Secondly, for an oscillating $\langle F\tilde{F}\rangle$ as found in the numerical solution of the background equation of motion, the scalar power spectrum features prominent peaks which, for suitable parameters, may lead to a PBH population peaked at logarithmically equidistant masses, accompanied by a gravitational wave spectrum with similar features. This would be a smoking gun signature of the resonance phenomenon inherent to axion inflation.

This Chapter is organized as follows. In Sec. 6.2 we review the mechanism of axion inflation. Sec. 6.3 explains the resonance inherent to this coupled system of differential equations and provides analytical estimates for the relevant time scales, which are further refined in appendix D.1. This is numerically confirmed by our numerical results presented in Sec. 6.4 for two exemplary values of the axion decay constant. Based on these results for the background evolution, we compute the power spectrum of scalar fluctuations in Sec. 6.5 before concluding in Sec. 6.6. Details on our numerical procedure as well as on the comparison with previous works can be found in appendices D.2 and D.4, respectively.

6.2 Inflationary dynamics

We consider a pseudo-scalar Φ coupled to the field strength tensor $F_{\mu\nu}$ of an abelian gauge group through a shift-symmetric coupling (see e.g. [269] for a review),

$$\frac{\mathcal{L}}{\sqrt{-g}} = -\frac{1}{2}\partial_\mu\Phi\partial^\mu\Phi - \frac{1}{4}F_{\mu\nu}F^{\mu\nu} - V_{,\Phi} - \frac{1}{4f}\Phi F_{\mu\nu}\tilde{F}^{\mu\nu}\,. \tag{6.2}$$

Here $V(\Phi)$ is a scalar potential explicitly breaking the shift-symmetry of Φ and $\tilde{F}^{\mu\nu} = \epsilon^{\mu\nu\rho\sigma}F_{\rho\sigma}/(2\sqrt{-g})$ with $\epsilon^{0123} = 1$ is the dual field strength tensor. Working in quasi de-Sitter space we introduce the time variable

$$N = \int H dt\,, \tag{6.3}$$

where $H = \dot{a}/a$ denotes the (approximately constant) Hubble parameter. In the separate Universe picture, the number of e-folds N elapsed in a time interval $[t_1, t_2]$ between two equal-density hyper surfaces varies by δN between 'separate', locally

homogeneous universes, accounting for the inhomogeneities in our primordial Universe [287, 288, 182, 289]. Expanding[2]

$$\Phi = \Phi_{\delta N=0} + \left.\frac{\partial \Phi}{\partial N}\right|_{\delta N=0} \delta N \equiv \phi + \delta\phi \tag{6.4}$$

we obtain the equation of motion for the homogeneous part

$$\phi'' + \frac{H'}{H}\phi' + 3\phi' + \frac{V_{,\phi}}{H^2} - \frac{1}{fH^2}\langle \vec{E}\vec{B}\rangle = 0\,, \tag{6.5}$$

with $' = \partial/\partial N$ and $\langle \dots \rangle$ denoting the average over many universes, thus selecting the globally homogeneous contribution.[3]

Turning to the gauge fields, the CP-odd nature of $F_{\mu\nu}\tilde{F}^{\mu\nu}$ will be most transparent when expanding in Fourier-modes of the comoving vector potential in the chiral basis,

$$\vec{A}(\tau,\vec{x}) = \int \frac{d^2k}{(2\pi)^{3/2}} \sum_{\sigma=\pm} \left[A_\sigma(\tau,\vec{k})\hat{e}_\sigma(\hat{k})\hat{\boldsymbol{a}}(\vec{k})e^{i\vec{k}\vec{x}} + A^*_\sigma(\tau,\vec{k})\hat{e}^*_\sigma(\hat{k})\hat{\boldsymbol{a}}^\dagger(\vec{k})e^{-i\vec{k}\vec{x}}\right], \tag{6.6}$$

with the polarization tensors obeying $\hat{e}_\sigma(\hat{k})\cdot\vec{k} = 0$, $\hat{e}_\sigma(\hat{k})\cdot\hat{e}_{\sigma'}(\hat{k}) = \delta_{\sigma\sigma'}$ and $i\vec{k}\times\hat{e}_\sigma(\hat{k}) = \sigma k\hat{e}_\sigma(\hat{k})$ where $\vec{k} = |\vec{k}|\hat{k} = k\,\hat{k}$, $\hat{\boldsymbol{a}}$ ($\hat{\boldsymbol{a}}^\dagger$) denoting the annihilation (creation) operators and $d\tau = dt/a$ denoting conformal time. In this basis, the equation of motion for the Fourier coefficients $A_\sigma(\tau,\vec{k})$ is obtained as

$$\frac{d^2A_\pm(\tau,\vec{k})}{d\tau^2} + \left[k^2 \pm 2\lambda\xi kaH\right]A_\pm(\tau,\vec{k}) = 0 \qquad \text{with} \quad \xi \equiv \frac{\lambda\phi'}{2f} > 0\,, \tag{6.7}$$

where $\lambda \equiv \text{sign}(\phi')$. For a sufficiently large inflaton velocity the effective mass term in the square brackets for the helicity mode with $\sigma = -\lambda$ undergoes a tachyonic instability, leading to an exponential enhancement. These gauge fields backreact on the inflaton equation of motion. The physical electric and magnetic fields entering in (6.5) are obtained as

$$\vec{E} = -\frac{1}{a^2}\frac{d\vec{A}}{d\tau}\,, \qquad \vec{B} = \frac{1}{a^2}\vec{\nabla}\times\vec{A}\,, \tag{6.8}$$

[2]Here we are dropping terms of $\mathcal{O}(\delta N^2)$, assuming $\delta N \ll 1$. Moreover, throughout this work, we will neglect the spatial gradients of the inflaton field. As we will see later, due to the strong enhancement of the scalar power spectrum in axion inflation, this is a non-trivial limitation of our analysis. To go beyond this and include strong spatial gradients of the scalar and gauge field into the analysis would require moving beyond the δN-formalism, e.g. along the lines of the full quantum formalism of [290].

[3]Here we assume a definite sign for the initial value of ϕ'. In a CP conserving universe this corresponds to averaging over a finite subset of Hubble patches.

leading to

$$\langle \vec{E}\vec{B} \rangle = -\frac{\lambda}{a^4} \int \frac{dk}{4\pi} k^3 \frac{d}{d\tau} \left| A_{-\lambda}(\tau, \vec{k}) \right|^2 , \tag{6.9}$$

and the energy density

$$\left\langle \frac{E^2 + B^2}{2} \right\rangle = \frac{1}{a^4} \int \frac{dk}{4\pi^2} k^2 \left(\left| \frac{dA_{-\lambda}(\tau, \vec{k})}{d\tau} \right|^2 + k^2 \left| A_{-\lambda}(\tau, \vec{k}) \right|^2 \right) , \tag{6.10}$$

where we have considered only the dominant, enhanced helicity mode. In summary, Eqs. (6.5), (6.7) and (6.9), together with the Friedmann equation

$$3H^2 M_P^2 = V(\phi) + \frac{1}{2} H^2 (\phi')^2 + \left\langle \frac{E^2 + B^2}{2} \right\rangle , \tag{6.11}$$

form a closed, integro-differential system of equations describing the gauge field production induced by the motion of the inflaton, taking into account the backreaction of these gauge fields.

6.3 Resonant gauge field production

In the limit of quasi de-Sitter space-time, $\tau = -1/(aH)$, and for constant ξ, Eq. (6.7) can be solved exactly. For the enhanced mode, this yields

$$A_{-\lambda}(\tau, \vec{k}) = \frac{e^{\pi\xi/2}}{\sqrt{2k}} W_{-i\xi,1/2}(2ik\tau) . \tag{6.12}$$

Here $W_{k,m}(z)$ denotes the Whittaker function and we have imposed Bunch Davies vacuum as an initial condition for far sub-horizon modes. Inserting this into Eqs. (6.9) and (6.10) yields

$$\langle \vec{E}\vec{B} \rangle \simeq -\frac{\lambda e^{2\pi\xi}}{2^{21}\pi^2\xi^4} H^4 \int_0^{x_{\rm uv}} x^7 e^{-x} dx \simeq -2.4 \cdot 10^{-4}\, \lambda\, H^4 \frac{e^{2\pi\xi}}{\xi^4} , \tag{6.13}$$

and

$$\begin{aligned} \left\langle \frac{E^2 + B^2}{2} \right\rangle &\simeq \frac{e^{2\pi\xi}}{2^{19}\pi^2\xi^3} H^4 \left[\int_0^{x_{\rm uv}} x^6 e^{-x} dx + \frac{1}{(2^3\xi)^2} \int_0^{x_{\rm uv}} x^8 e^{-x} dx \right] \\ &\simeq 1.3 \cdot 10^{-4}\, H^4 \frac{e^{2\pi\xi}}{\xi^3} , \end{aligned} \tag{6.14}$$

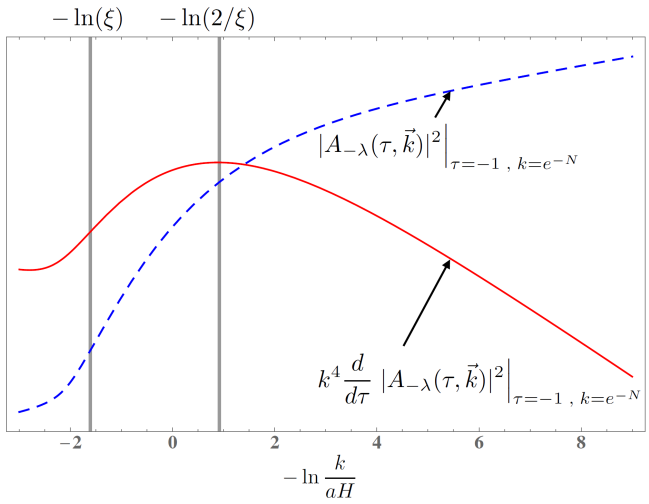

Figure 6.1: Blue dash: The square of the gauge field mode $|A_{-\lambda}(\tau,\vec{k})|^2$. Red solid: The $\langle\vec{E}\vec{B}\rangle$ integrand $k^4\frac{d}{d\tau}|A_{-\lambda}(\tau,\vec{k})|^2$. Both curves are evaluated at $\tau=-1$, and displayed as a function of wavenumber, such that $\ln\left(\frac{k}{aH}\right)=0$ corresponds to a horizon sized mode. Left vertical line: wavenumber (or number of e-folds after horizon crossing) of the maximal exponential growth of $|A_{-\lambda}(\tau,\vec{k})|^2$. Right vertical line: The $\langle\vec{E}\vec{B}\rangle$ integrand gets its dominant contribution at about ΔN_ξ later. Here we have set $\xi=5$.

with $x_{\rm uv}\simeq 2\xi$ ensuring the cut-off of the UV divergence. The last equality is valid for $\xi\gtrsim 3$, smaller values of ξ require a more careful regularization scheme [291, 292].

We shall now provide arguments that once ξ becomes time-dependent, a second time scale (besides H^{-1}) appears, characterizing a resonance phenomenon with a frequency in e-fold time of $\omega_N^{res}=2\pi/\Delta N_\xi$. This resonance drives self-excited oscillations with frequency ω_N^{res} appearing in $\langle\vec{E}\vec{B}\rangle$.

Let us start our analysis by looking again at the gauge field Fourier mode equation of motion (6.7). Rewriting this into e-fold time

$$dN=aHd\tau \quad\Rightarrow\quad \frac{d^2}{d\tau^2}=a^2H^2\left(\frac{d^2}{dN^2}+(1-\epsilon)\frac{d}{dN}\right) \quad , \tag{6.15}$$

we get

$$A''_\pm(\vec{k})+(1-\epsilon)A'_\pm(\vec{k})+\frac{k}{aH}\left(\frac{k}{aH}\pm 2\lambda\xi\right)A_\pm(\vec{k})=0 \quad . \tag{6.16}$$

In the remainder of this section, we will neglect all terms suppressed by the slow-roll parameter $\epsilon=-H'/H\ll 1$. In our numerical analysis, described in Sec. 6.4, we keep all slow-roll corrections though. We see that the mode $A_{-\lambda}$ becomes

tachyonic once $k/(aH) < 2\xi$, while it starts freezing out due to the friction term $A'_{-\lambda}$ taking over once $k/(aH) < 1/(2\xi)$. We now look at the behaviour of the mass term of the growing mode more closely. For constant ξ, the mass terms takes its maximally negative value $\hat{m}^2_{-\lambda} = -\xi^2$ at $k/(aH) = \xi$ since the quadratic function of $m^2_{-\lambda} = k/(aH)\,(k/(aH) - 2\xi)$ has zeroes at $k/(aH) = 0$ and at $k/(aH) = 2\xi$. Hence, due the behaviour of the Whittaker function governing the gauge field modes, the major part of the growth of $A_{-\lambda}$ out of the Bunch-Davies initial conditions happens while $k/(aH) \simeq \xi$.

However, the integrand of $\langle \vec{E}\vec{B} \rangle$, due to the τ-derivative and the k^4 prefactor, takes its maximum contribution at approximately $k/(aH) = 2/\xi$ (see also Appendix D.1). This implies that $\langle \vec{E}\vec{B} \rangle$ is dominated by modes whose 'knowledge' of the value of ξ governing their maximum growth period originates from about

$$\Delta N_\xi \simeq \ln \frac{\xi^2}{2} \tag{6.17}$$

e-folds earlier. This is clearly visible in Fig. 6.1, where we see that the $\langle \vec{E}\vec{B} \rangle$ integrand $k^4 \frac{d}{d\tau} |A_{-\lambda}(\tau, \vec{k})|^2$ has its peak contribution about ΔN_ξ after the time when $|A_{-\lambda}(\tau, \vec{k})|^2$ has its maximum exponential growth. Note, that in Fig. 6.1 we took $\tau = -1$ and expressed the wavenumber k as number of e-folds after horizon crossing $-\ln k/aH$. This means that the gauge modes are still sub-horizon at the time of maximal growth ($k/aH = \xi > 1$), but already super-horizon when they provide the peak contribution to the $\langle \vec{E}\vec{B} \rangle$ integrand ($k/aH = 2/\xi < 1$).

Using this information, we can ask a simple question – how does $\langle \vec{E}\vec{B} \rangle$ react if we allow for a sudden step-like change of ξ at a certain moment of time? For explicitness, let us assume that $\xi = \xi_0$ changes to $\xi_0 + \Delta\xi > \xi_0$ at $N = N_0$ suddenly. At $N = N_0$ the integral $\langle \vec{E}\vec{B} \rangle$ gets its dominant contribution from modes $A_{-\lambda}(\vec{k})$ with $k/(aH) \simeq 2/\xi$ which had their growth happening ΔN_ξ e-folds earlier. At that time $N_0 - \Delta N_\xi$ we still had $\xi = \xi_0$ and hence

$$|\langle \vec{E}\vec{B} \rangle_{N_0}| \simeq 2.4 \cdot 10^{-4} H^4 \frac{e^{2\pi\xi_0}}{\xi_0^4} \quad . \tag{6.18}$$

Conversely, modes $A_{-\lambda}(\vec{k})$ with $k/(aH) \simeq 2/\xi$ at $N = N_0$ will grow towards their plateau value and thus dominate $\langle \vec{E}\vec{B} \rangle$ only starting at time $N = N_0 + \Delta N_\xi$. These modes experience their growth for $N > N_0$ when $\xi > \xi_0$. Hence, they will approach a plateau governed by $\xi = \xi_0 + \Delta\xi$ and thus

$$|\langle \vec{E}\vec{B} \rangle_{N_0 + \Delta N_\xi}| \simeq 2.4 \cdot 10^{-4} H^4 \frac{e^{2\pi(\xi_0 + \Delta\xi)}}{(\xi_0 + \Delta\xi)^4} > |\langle \vec{E}\vec{B} \rangle_{N_0}| \quad . \tag{6.19}$$

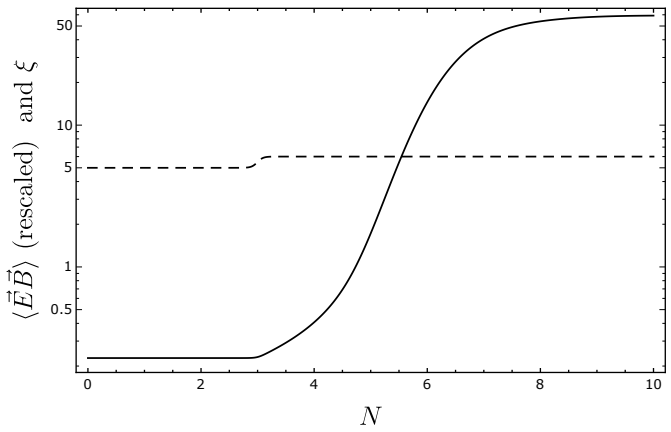

Figure 6.2: Black solid: Numerically computed, and rescaled, response of $\langle \vec{E}\vec{B} \rangle$ to the change in ξ with significant lag $\simeq \Delta N_\xi$. Black dash: Almost step function like change of ξ modeled as $\xi(N) = \xi_0 + \frac{\Delta\xi}{2}\left(1 + \tanh(\mu_\xi(N - N_0))\right)$ with the jump taking place at $N_0 = 3$ from $\xi_0 = 5$ with amplitude $\Delta\xi = 1$ and steepness $\mu_\xi = 10$ (dashed black).

The transition from the initial plateau to the final plateau happens smoothly, yet clearly the system shows 'lag': It reacts to a sudden change in ξ by changing to its new $\langle \vec{E}\vec{B} \rangle$ value only with a time lag of about ΔN_ξ. A numerical computation of $\langle \vec{E}\vec{B} \rangle$ displayed in Fig. 6.2 clearly confirms this lag.

Assume now that instead of a sudden change, we provide ξ with a periodic time dependence $\xi(N + 2\pi/\omega_N) = \xi(N)$ with constant frequency ω_N in e-fold time. Clearly, $\langle \vec{E}\vec{B} \rangle$ will now react with the same lag and thus oscillate with a phase shift

$$\Delta\alpha = \omega_N \Delta N_\xi \tag{6.20}$$

as long as this phase shift $\Delta\alpha < 2\pi$.[4] Clearly then, demanding $\Delta\alpha = \pi$ as a necessary condition for resonance (which can only occur if $\langle \vec{E}\vec{B} \rangle$ couples back to $\dot{\phi}$, this we will discuss shortly), this defines a critical frequency

$$\omega_N^\star = \frac{\pi}{\Delta N_\xi} \quad . \tag{6.21}$$

We can numerically compute the full $\langle \vec{E}\vec{B} \rangle$ responding to a harmonic perturbation of ξ around $\bar{\xi}$ with frequency ω_N. Figure 6.3 shows this for a frequency near

[4] To see this from the 'sudden approximation' argument before, break up a periodic $\xi(N)$ into small step-wise changes.

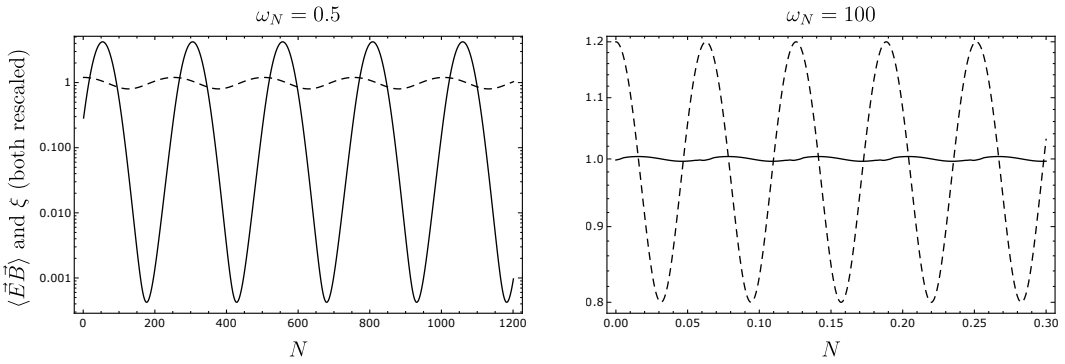

Figure 6.3: Left: Numerically computed, and rescaled, response of $\langle \vec{E}\vec{B} \rangle$ with significant lag (solid black) for a harmonic perturbation of ξ with near-critical frequency $\omega_N \sim \omega_N^\star$ (dashed black). Right: For much larger frequencies the response averages out to zero. We chose $\bar{\xi} = 5$ and the oscillation amplitude $\Delta\xi = 1$.

$\omega_N^\star$, and for a frequency much larger than $\omega_N^\star$. We see clearly, that at $\omega_N \sim \omega_N^\star$ there is strong response of $\langle \vec{E}\vec{B} \rangle$ with lag. Moreover, at $\omega_N \sim \omega_N^\star$ the lag corresponds to a significant phase shift, while for much larger frequencies the response averages out to zero.

Finally, we can numerically determine the lag ΔN_ξ occurring as a function of ξ. This is shown in Fig. 6.4 for $\omega_N = 0.2$ and clearly shows (solid red line) the scaling $\Delta N_\xi = \ln(\xi^2/2)$ derived in Eq. (6.17). The refined estimate derived in App. D.1 is depicted by the dashed red line. The oscillations visible at larger values of ξ are not captured by the estimate (6.17), which was based on determining the difference between the points of maximal growth and maximal contribution to $\langle \vec{E}\vec{B} \rangle$ for any given mode at constant ξ. For a periodically varying ξ these estimates receive corrections, which depend in particular on the shape of the pulses in the periodic function ξ.

At this point it becomes interesting to turn to our dynamically coupled system, where the ξ-parameter is determined by the scalar field equation of motion

$$\ddot{\phi} + 3H\dot{\phi} + V_{,\phi} - \frac{1}{f}\langle \vec{E}\vec{B} \rangle = 0 \quad . \tag{6.22}$$

The driving force of the scalar potential $V_{,\phi}$ is balanced by the sum of the Hubble friction (second term) and the gauge-field induced friction (contained in the last term), while the $\ddot{\phi}$ only becomes relevant in the very last stages of inflation. In our full numerical solution which clearly displays a resonance (see Sec. 6.4) we can observe that the oscillating parts of the two friction terms $3H\dot{\phi}$ and $\langle \vec{E}\vec{B} \rangle$ (sourced by the time-dependent part of ξ) cancel against each other at $N \lesssim 60$ where the

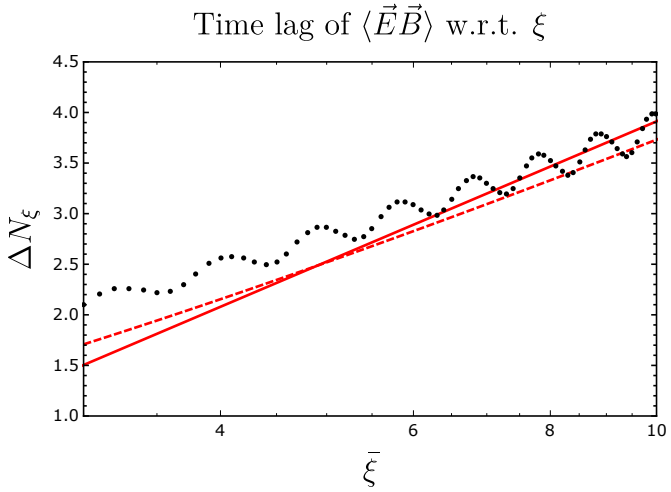

Figure 6.4: Data points: The lag ΔN_ξ for the numerically computed response of $\langle \vec{E}\vec{B} \rangle$ to a harmonic perturbation of ξ with frequency $\omega_N = 0.2$ as a function of ξ. Solid red line: our estimate $\Delta N_\xi \sim \ln(\xi^2/2)$ in Eq. (6.17). Dashed red line: refined estimate derived in App. D.1.

backreaction is not yet very strong, whereas $V_{,\phi}$, which depends only on ϕ but not on $\dot{\phi}$, evolves to good approximation monotonously. This is clearly visible in Fig. 6.5 where we plot the different parts of the scalar field equation of motion evaluated on the numerical solution for $1/f = 25$, discussed in detail in Sec. 6.4.

We now parametrize ξ as $\xi = \bar{\xi} + \Delta\xi(N)$ with the long-time average $\overline{\Delta\xi}(N) \equiv \frac{1}{N}\int dN \Delta\xi(N) = 0$, where an over-bar denotes averaging over time while all quantities are implicitly containing an average over separate universes part of the δN formalism (unless this average is written explicitly as $\langle \ldots \rangle$). Consequently, we can recast the time dependent part of $\dot{\phi}$ as $\Delta\xi(N)$ and get approximately

$$6H^2 \frac{f}{\lambda} \Delta\xi - \frac{1}{f} \Delta\langle \vec{E}\vec{B} \rangle (\Delta\xi) \simeq 0 \tag{6.23}$$

where $\langle \vec{E}\vec{B} \rangle = \overline{\langle \vec{E}\vec{B} \rangle} + \Delta\langle \vec{E}\vec{B} \rangle$.

Now we use the properties of the background $\overline{\langle \vec{E}\vec{B} \rangle}$ given in Eqs. (6.9),(6.12) to write

$$\overline{\langle \vec{E}\vec{B} \rangle} = -\lambda \mathcal{A}_{EB} \tag{6.24}$$

where $\mathcal{A}_{EB} > 0$ is a positive definite function. Assuming the oscillating part $\Delta\langle \vec{E}\vec{B} \rangle$ will not change the sign of the total $\langle \vec{E}\vec{B} \rangle$, we can then define the split of $\langle \vec{E}\vec{B} \rangle$ into background and oscillatory part with a definite phase relative to the

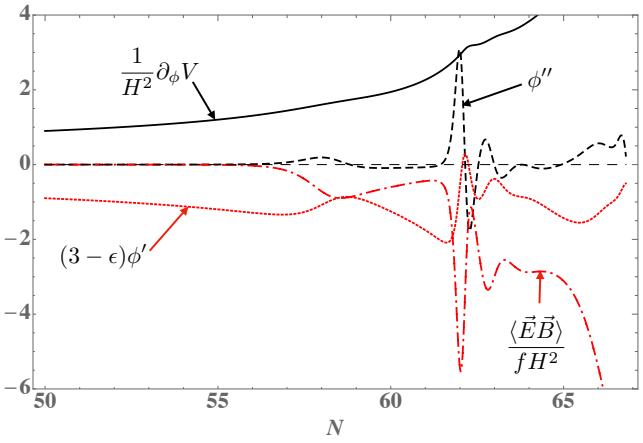

Figure 6.5: The contributions ϕ'' (black dash), $\partial_\phi V/H^2$ (black solid), $(3-\epsilon)\phi'$ (red short dash), and $\langle \vec{E}\vec{B}\rangle/(fH^2)$ (red dash-dot) to the scalar field equation of motion for $f = 1/25$ and $V(\phi) = m^2\phi^2/2$ (see Sec. 6.4) [in units of M_P]. We have conveniently expressed the derivatives $\dot{\phi}$ and $\ddot{\phi}$ in terms of e-fold time derivatives ϕ', ϕ''. Note that for $N \lesssim 60$ we find that ϕ'' is negligible, while the first long-wave oscillation has ϕ' and $\langle \vec{E}\vec{B}\rangle$ of opposite phase. Note further, that for $N \gtrsim 60$ the long-wave oscillations are superimposed by faster damped oscillations. For these, ϕ'' is no longer negligible, and the phase shift at each step of the chain $\phi'' \to \phi' \to \langle \vec{E}\vec{B}\rangle$ is about $\pi/2$.

sign of $\overline{\langle \vec{E}\vec{B}\rangle}$ by writing

$$\langle \vec{E}\vec{B}\rangle = \overline{\langle \vec{E}\vec{B}\rangle} + \Delta\langle \vec{E}\vec{B}\rangle \equiv -\lambda\left(\mathcal{A}_{EB} + \Delta\mathcal{A}_{EB}\right) \quad . \tag{6.25}$$

This allows us rewrite Eq. (6.23) as

$$\Delta\xi + \frac{1}{6f^2H^2}\Delta\mathcal{A}_{EB}(\Delta\xi) = 0 \quad \Leftrightarrow \quad \Delta\xi = -\frac{1}{6}\frac{\Delta\mathcal{A}_{EB}(\Delta\xi)}{f^2H^2} \quad . \tag{6.26}$$

Moreover, from the values of f and H we see that the factor $1/(6f^2H^2)$ rescales $\Delta\mathcal{A}_{EB}$ to be dimensionless and to have the same magnitude as $\Delta\xi$.

For this rescaled $\Delta\mathcal{A}_{EB}$, the discussion around Eq. (6.21) and the numerical observation of the time delay in Fig. 6.3 indicate the presence of a resonance at $\omega_N = \omega_N^\star$. The argument for this goes as follows: At the resonance frequency the observed time delay corresponds to a phase shift of ϕ, that is, we observe

$$\frac{\Delta\mathcal{A}_{EB}(\Delta\xi(N))}{6f^2H^2} \sim \Delta\xi\left(N - \frac{\pi}{\omega_N^\star}\right) \quad . \tag{6.27}$$

Moreover, if we assume a nearly harmonic perturbation with an approximately constant frequency for $\Delta\xi$, we have by definition

$$\Delta\xi\left(N - \frac{\pi}{\omega_N^\star}\right) \sim \Delta\xi'' \quad . \tag{6.28}$$

Therefore, in plugging eq. (6.28) into eq. (6.27), and this in turn into the right-hand side of Eq. (6.26) we find that on a harmonic perturbation the equation of motion of ξ becomes consistent with an oscillator equation.

$$\Delta\xi \sim -\Delta\xi'' \quad . \tag{6.29}$$

Next, we observe that for $N \gtrsim 60$ in Fig. 6.5 there is a secondary pattern of damped oscillations at higher frequency compared to the long-wave 'base frequency' oscillations discussed above. For this pattern the oscillating contribution of $\ddot{\phi}$ is no longer negligible. Moreover, we observe that the phase shift at each step of the chain $\phi'' \to \phi' \to \langle\vec{E}\vec{B}\rangle$ is about $\pi/2$. This implies that for this pattern the corresponding high-frequency (labeled by 'h.f.') oscillating parts $\Delta\xi^{(h.f.)}$ and $\Delta\mathcal{A}_{EB}^{(h.f.)}$, split off the full quantities the same way as we did for the base frequency parts above, satisfy

$$(\Delta\xi^{(h.f.)})' + 3\Delta\xi^{(h.f.)} + \frac{1}{2f^2H^2}\Delta\mathcal{A}_{EB}^{(h.f.)}(\Delta\xi) = 0 \quad . \tag{6.30}$$

The observed phase relation in Fig. 6.5 then states that $\Delta\mathcal{A}_{EB}^{(h.f.)}(\Delta\xi)$ has a phase shift of $\pi/2$ to the right compared to $\Delta\xi^{(h.f.)}$ and of π to the right compared to $(\Delta\xi^{(h.f.)})'$. Hence, the figure indicates that for the high-frequency oscillations

$$\Delta\xi^{(h.f.)} \sim (\Delta\mathcal{A}_{EB}^{(h.f.)})' \quad , \quad (\Delta\xi^{(h.f.)})' \sim (\Delta\mathcal{A}_{EB}^{(h.f.)})'' \quad . \tag{6.31}$$

Plugging this relation into Eq. (6.30) we get the structure of the dampened harmonic oscillator differential equation

$$(\Delta\mathcal{A}_{EB}^{(h.f.)})'' + \mathcal{O}(1)(\Delta\mathcal{A}_{EB}^{(h.f.)})' + (\omega^{(h.f.)})^2\Delta\mathcal{A}_{EB}^{(h.f.)} = 0 \quad . \tag{6.32}$$

While we cannot determine the frequency of these faster oscillations $\omega^{(h.f.)}$ at this time, we consider the fact that the equation of motion takes the dampened oscillator form to be strong evidence supporting the existence of these secondary, faster dampened oscillations in the coupled system.

It is due to this line of reasoning that we conclude the presence of resonance occurring in the strong gauge-field back-reaction regime. Neglecting the resonance phenomenon, ξ is typically a monotonically growing function of N, while the resonance frequency only scales logarithmically with ξ and thus N. Hence, the

sweep of ξ effectively scans over possible resonance frequencies. Hence we expect the increasing value of ξ to eventually trigger the resonance behaviour with approximately the predicted frequency. Some of the ideas presented here have been qualitatively previously presented in Refs. [284, 285, 286]. After formalizing these arguments, we here succeed in quantitatively explaining the observed resonance frequency. Strictly speaking, the arguments spelled out above form a necessary, but not sufficient condition to ensure a resonance. However, in our numerical solutions to this coupled system of differential equations (see next section) we always see this resonance, indicating that this is indeed a generic feature.

6.4 Numerical results

We performed a full numerical analysis taking $M_P/f = \{20, 25\}$ and $V(\phi) = m^2\phi^2/2$ with $m = 6 \times 10^{-6}\, M_P$, reproducing the observed amplitude of the scalar power spectrum at CMB scales.[5] Our final goal is to find the solution of the system of coupled integro-differential equations (6.5), (6.7) and (6.9). The first step is to solve the inflaton equation of motion using the estimate of $\langle \vec{E}\vec{B} \rangle$ given in Eq. (6.13), which is obtained by solving the equations of motion of the gauge field modes, $A_{-\lambda}(\tau, k)$, assuming a constant inflaton speed, Eq. (6.12). Then, choosing an appropriate array of k-modes, we solve Eq. (6.7) for each mode and we compute the discretized integral of equation Eq. (6.9), getting a new estimate of the backreaction. We reach the final solution by iterating this procedure until we reach the end of inflation with a self-consistent solution, see App. D.2 for details. The initial conditions for the inflaton field are chosen at CMB scales in accordance with the vacuum slow-roll solution while the A_k modes satisfy Bunch-Davies vacuum conditions; we stop the time evolution when the system reaches the end of inflation $\epsilon \simeq 1$.

The results of our analysis for $1/f = \{20, 25\}$ are shown in Fig. 6.6 where we compare the final solution for $\langle \vec{E}\vec{B} \rangle$ and $\rho_{EB} = \langle \frac{E^2+B^2}{2} \rangle$ with the analytical estimate of Eqs. (6.13) and (6.14). We also plot the ξ parameter which shows that the oscillatory behaviour of the inflaton speed becomes more apparent in case of strong backreaction.[6] We see that the numerical solution including the backreaction oscillates around the analytical estimate, with an oscillation period

[5] As expected for the discussion in Sec. 6.3, the generic features of the results discussed here are not very sensitive to the precise form of the scalar potential. In particular, we confirm similar results using a potential linear in ϕ.

[6] At the maxima of these oscillations, the value of ξ exceeds the threshold $\xi \simeq 4.7$ bounding the perturbative regime for approximately constant ξ [293, 294]. This threshold cannot be immediately applied to a strongly oscillating ξ and we will comment on perturbativity constraints in more detail in Sec. 6.5.

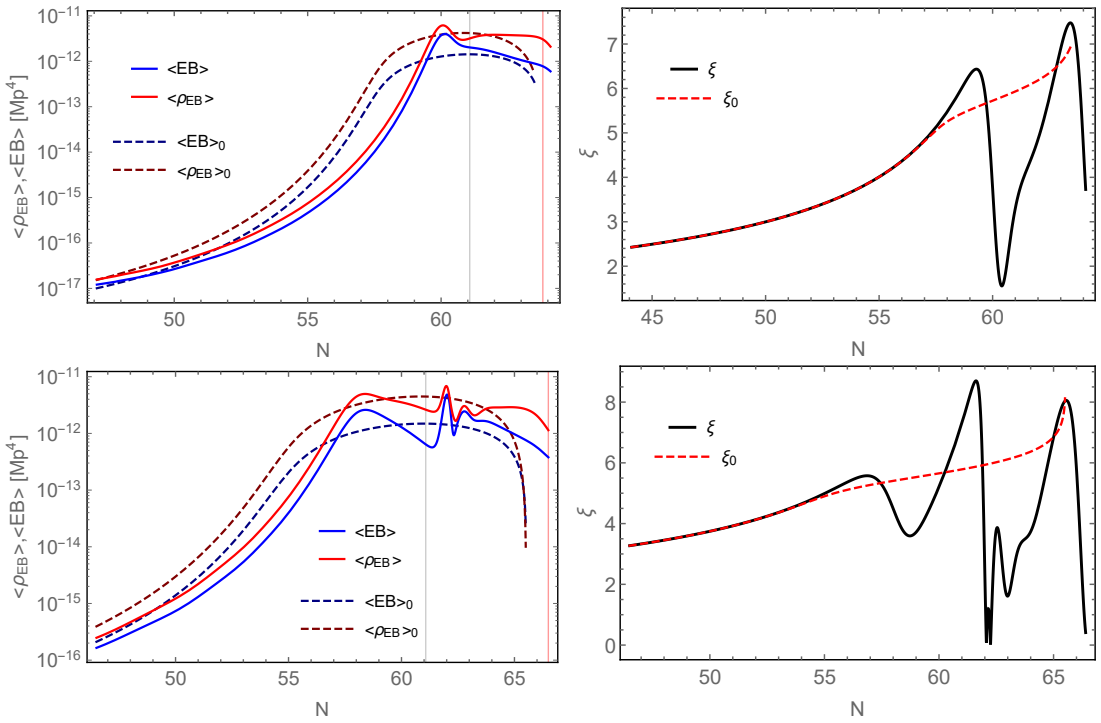

Figure 6.6: Top: $1/f = 20$. Bottom: $1/f = 25$. The left panels show the numerical results of ρ_{EB} and $\langle \vec{E}\vec{B} \rangle$ (solid lines) compared to their analytical estimate (6.13), (6.14) (dashed lines). The vertical lines refer to the end of inflation in absence of backreaction (black line) and for the full numerical analysis (red line). The right panels show the oscillatory behaviour of the ξ parameter (solid black line) compared to its analytical result coming from the solution of the inflaton equation of motion when the gauge field backreaction is given by (6.13) (dashed red line). For better visibility, we display only the last ~ 20 e-folds of inflation.

of $\Delta N_\xi \sim 3$, in accordance with our estimate in Sec. 6.3. For $f = 1/25$ the value of ϕ' temporarily changes sign (at $N \simeq 62$). The reason for this is the delay in gauge friction term discussed in Sec. 6.3. As $|\phi'|$ drops, the gauge friction drops and the opposite sign of ϕ' (encoded by λ) entails the opposite sign for the gauge friction term as one would expect of a friction term. However, since the gauge friction term is dominated by modes which are controlled by the value of ϕ' some ΔN_ξ e-folds earlier, the sign change in the gauge friction term is delayed, allowing ϕ' to temporarily change sign.

Our results are in accordance with those previously found in Refs. [284, 285, 286], which reported oscillatory features in the inflaton velocity with a period of $3-5$ e-folds. All these studies are based on fully independent codes and numerical methods, and the results observed can be nicely explained with the semi-analytical

arguments presented in Sec. 6.3.

6.5 Scalar power spectrum and primordial black holes

6.5.1 Scalar power spectrum sourced by gauge field configuration

The gauge field population does not only backreact on the dynamics of the homogeneous inflaton field but also acts as source term for the scalar inhomogeneities sourcing the density perturbations of the Universe. In the separate universe picture, curvature fluctuations on super-horizon scales are obtained as [287, 288, 182, 289] [7]

$$\zeta_c \simeq \delta N(t_*) \simeq N_{,\phi}(t_*)\, \delta\phi(t_*)\,. \tag{6.33}$$

Here $N(t_*)$ denotes the average number of e-folds elapsed between t_* and the end of inflation, whereas $\delta N(t_*)$ denotes the deviation occurring in a particular patch of the Universe induced by super-horizon scalar fluctuations. The perturbed version of Eq. (6.5) reads

$$\begin{aligned} 0 =& \phi'' + \left(3 + \frac{H'}{H}\right)\phi' + \frac{V_{,\phi}}{H^2} \\ &+ \frac{H'}{H}\delta\phi' + \phi'\frac{\partial}{\partial N}\left(\frac{H'}{H}\right)\delta N + \frac{\partial}{\partial N}\left(\frac{V_{,\phi}}{H^2}\right)\delta N + \frac{2H'}{fH^3}\langle\vec{E}\vec{B}\rangle\,\delta N \\ &+ \delta\phi'' + 3\,\delta\phi' - \frac{1}{fH^2}\vec{E}\vec{B} - \frac{1}{fH^2}\frac{\partial\langle\vec{E}\vec{B}\rangle}{\partial N}\delta N\,. \end{aligned} \tag{6.34}$$

Since we are keeping only fluctuations to first order, all occurrences of H, V and $\langle\vec{E}\vec{B}\rangle$ are here understood to be evaluated in terms of the homogeneous field ϕ. On the contrary, the factor $\vec{E}\vec{B}$ in the third term of the third line includes the inhomogeneities in the gauge fields sourced by $\delta\phi$. Using Eq. (6.5) to replace the terms in the first line, dropping the slow-roll suppressed terms in the second line

[7] This expression relies on the assumption that $\Delta N(\phi_1, \phi_2)$, the time in e-folds required for the inflaton to move from ϕ_1 to ϕ_2 does not depend on any further independent parameters, such as e.g. the inflaton velocity. For the attractor solution, this is justified even taking into account the strong, velocity-dependent friction. In the strongly oscillatory phase towards the end of inflation we expect corrections due to the break-down of the slow-roll approximation.

and inserting Eq. (6.33) this simplifies to

$$L_N[\delta\phi(N)] \equiv \delta\phi'' + 3\,\delta\phi' - \frac{N_{,\phi}}{fH^2}\frac{\partial\langle\vec{E}\vec{B}\rangle}{\partial N}\delta\phi = \frac{1}{fH^2}(\vec{E}\vec{B} - \langle\vec{E}\vec{B}\rangle) \equiv \frac{1}{fH^2}\delta_{EB}\,. \tag{6.35}$$

This inhomogeneous linear differential equation can be solved by the Greens function method, see e.g. [262, 270].[8]
For any linear operator L_N, the Greens function satisfying

$$L_N\,G(N,N') = \delta(N-N')\,, \tag{6.36}$$

can be convoluted with the source term $S(N)$,

$$\delta\phi(N) = \int G(N,N')S(N')dN'\,, \tag{6.37}$$

to obtain a solution of the inhomogeneous equation $L_N\,\delta\phi(N) = S(N)$. In Eq. (6.35) we identify $S(N) = \delta_{EB}/(fH^2)$. Moreover, for any given function $\langle\vec{E}\vec{B}\rangle(N)$ we can determine (at least numerically) the Greens function of the corresponding linear operator L_N by solving the ordinary differential equation (6.36). Since this is a second order differential equation we need to specify two boundary conditions which we take to be $G(N,N) = 0$ and $G'(N,N) = 1$.[9]

With this, the two-point function of scalar perturbations exiting the horizon at e-fold N can be computed as

$$\langle\zeta^2\rangle = \langle\delta N^2\rangle = N_{,\phi}^2\langle\delta\phi^2\rangle = N_{,\phi}^2\int dN'G(N,N')\int dN''G(N,N'')\langle S(N')S(N'')\rangle\,. \tag{6.38}$$

[8]For a comparison with these pioneering works see App. D.4. In short, we confirm the results found in the weak backreaction regime but disagree in the strong backreaction regime. We find the backreaction to be weaker than previously estimated, leading to a significant enhancement of the scalar power spectrum in this regime.

[9]For the retarded Green's function $G(N,N') = 0$ if $N' > N$. In addition we know that $G(N,N')$ must be a continuous function since $L_NG(N,N')$ does not involve generalized functions beyond $\delta(N-N')$ functions and in particular it does not contain derivatives of δ functions. Imposing continuity at equal time requires $\lim_{N'\to N_-} G(N,N') = \lim_{N'\to N_+} G(N,N') = 0$. On the other hand, integrating (6.36) over an infinitesimal neighbourhood of $N = N'$ we get $\int_{N'-\epsilon}^{N'+\epsilon} L_NG(N,N')dN = 1$. G being continuous, ∂_NG must be bounded and we immediately see that if we shrink the integration domain to zero size the only term which can give a finite contribution is $\lim_{\epsilon\to0}\int_{N'-\epsilon}^{N'+\epsilon} L_NG(N,N')dN = \lim_{\epsilon\to0}\int_{N'-\epsilon}^{N'+\epsilon}\partial_N^2G(N,N')dN = \partial_NG(N'_+,N') - \partial_NG(N'_-,N') = \partial_NG(N'_+,N') = 1$.

We parametrize the unequal time correlations by $g(N', \Delta N)$,

$$\int_{N'+\Delta N}^{\infty} dN'' \langle S(N')S(N'')\rangle = \langle S(N')^2\rangle g(N', \Delta N)\,. \tag{6.39}$$

with

$$g(N', \Delta N) = \begin{cases} \gamma & \Delta N = 0 \\ \epsilon & \Delta N > 0 \end{cases} \tag{6.40}$$

where $\gamma = \mathcal{O}(1)$ and $\epsilon \to 0$ in the limit of vanishing unequal time correlators, i.e. in the limit of white noise. If $G(N, N'')$ and $\langle S^2(N')\rangle$ do not vary significantly over the support of $g(N', \Delta N)$ we can approximate[10]

$$\begin{aligned} \int dN'' G(N, N'')\langle S(N')S(N'')\rangle &\simeq G(N, N')\langle S^2(N')\rangle g(N', 0) \\ &\simeq \frac{G(N, N')}{f^2 H^4}\langle \delta^2_{EB}(N')\rangle \\ &= \frac{G(N, N')}{f^2 H^4}\sigma^2_{EB}(N')\,, \end{aligned} \tag{6.41}$$

with $\sigma^2_{EB} \equiv (\vec{E}\vec{B} - \langle \vec{E}\vec{B}\rangle)^2$ denoting the variance of $\vec{E}\vec{B}$ at a given time. For a given set of mode functions $A_k(N)$ the variance σ^2_{EB} can be computed explicitly, see e.g. App. A of [273]. The final expression for the power spectrum then reads

$$\Delta^2_\zeta = \langle \delta\zeta^2\rangle \simeq N^2_{,\phi} \int dN' \frac{G^2(N, N')\sigma^2_{EB}(N')}{f^2 H^2(N')} + \langle \zeta^2\rangle_{\rm vac}\,, \tag{6.42}$$

where $\langle \zeta^2\rangle^{1/2}_{\rm vac} = H/(2\pi\phi')$ is the usual vacuum contribution.

The result obtained by numerically evaluating the Greens function $G(N, N')$ and the variance σ_{EB} is depicted in Fig. 6.7. The power spectrum is dramatically enhanced towards the end of inflation and inherits the resonant oscillations present in the source term. As highlighted by the gray band, the power spectrum extends above $\zeta \sim 0.3$, indicating the breakdown of the perturbative expansion used in

[10] To verify these approximations and quantify the importance of the unequal time contributions, we numerically evaluate $g(N', \Delta N)$ using the mode functions $A_k(N)$ from the numerical computation in Sec. 6.4. See App. D.3 for details. Far away from the resonance regime, we find this approximation to be unproblematic. As we approach the resonant regime, the unequal time correlators become more important while at the same time $\sigma^2_{\rm EB}$ varies more rapidly. We find values of $g(N', 0.1)/\gamma \simeq 0.9$ and $g(N', 0.5)/\gamma \simeq 0.4$, indicating that most of the support of g is focused on a small region over which $\sigma^2_{\rm EB}$ varies only moderately. We conclude that the unequal time correlators most likely lead to an $\mathcal{O}(1)$ correction to (6.42) in the resonance regime, slightly smearing out the peaks and troughs.

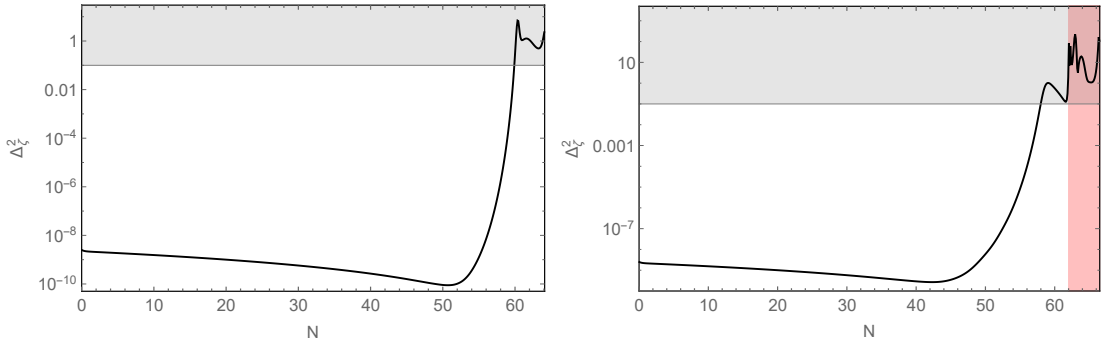

Figure 6.7: Scalar power spectrum for $1/f = 20$ (left) and $1/f = 25$ (right). The resonantly enhanced gauge field population leads to strong enhancement of the scalar power spectrum at small scales, with peaks reflecting the resonance structure. The gray and red shaded areas indicate the limitations of the δN formalism, see text for details.

our analysis. Moreover, for $f = 1/25$, the inflaton speed temporarily changes sign (see Fig. 6.6), implying that ϕ is not monotonously increasing. Strictly speaking, this requires to go beyond the standard δN formalism (see footnote 7). In practice, since this only happens for a very short period of time, we expect the δN formalism (with the inflaton speed regularized to some small value round $N \simeq 62$) to nevertheless give a good estimate. The corresponding problematic region is highlighted in red in the right panel of Fig. 6.7. Due to these caveats, we cannot make a prediction about the precise amplitude of the scalar power spectrum at small scales. However, we can conclude that power spectrum reaches values of $\Delta^2_\zeta \gtrsim 0.01$ in the last e-folds of inflation, exceeding the threshold for primordial black hole formation (see below).

The very large values for the scalar perturbations at small scales, indicating an inhomogeneous field configuration with large gradient energy, may trigger a premature end of inflation. This would relax the bounds from primordial black hole formation and consequently the bound on the coupling $1/f$ (see below). However, recent findings [295, 296, 297, 298] indicate that high-scale inflation is quite robust against large gradient energies. How much of this stability against large gradients remains on the $\simeq 2..3\, M_{\rm P}$ of field range corresponding to the last about 5 e-folds of inflation in a quadratic potential is an open question which we leave for future work. We hope that our findings will trigger a more detailed non-perturbative analysis of this last stage of inflation.

Even discarding the peaks arising from the resonant enhancement, the amplitude of the power spectrum in Fig. 6.7 at small scales is significantly larger than expected from previous estimates [262, 273]. We provide a detailed comparison and discussion in Appendix D.4. In summary, we conclude that previous ana-

lytical analyses have overestimated the amount of backreaction in Eq. (6.35) and have hence underestimated the amplitude of the power spectrum in the strong backreaction regime. Consequently, the amplitude of the scalar power spectrum we report is in particular significantly larger than found in [284], which accounted for the oscillating inflaton velocity but used the estimate for the power spectrum derived in [273].

6.5.2 Primordial black hole formation and phenomenology

If the scalar perturbations at a given scale exceed a critical threshold $\zeta_c \sim 0.5$ they collapse into a primordial black hole upon horizon re-entry [299]. The mass of the corresponding black hole is determined by the energy contained in a Hubble volume at the time of horizon re-entry,

$$M_{PBH}(N) \simeq \gamma \frac{4\pi}{3} \left(e^{-jN} H_{\rm inf}\right)^{-3} \times 3 \left(e^{-jN} H_{\rm inf}\right)^2 M_P^2 \simeq 55 \text{ g} \, \gamma \left(\frac{10^{-6} M_P}{H_{\rm inf}}\right) e^{jN} \,, \tag{6.43}$$

with N counting the number of e-folds from the horizon exit of the respective fluctuation until the end of inflation, $H_{\rm inf}$ denoting the Hubble parameter at this time, $j = 2$ ($j = 3$) for radiation (matter) domination after inflation and $\gamma \simeq 0.4$ parametrizes the efficiency of the gravitational collapse [300, 301].

Once formed, the PBHs can slowly decay by emitting Hawking radiation. In particular, PBHs with $M_{PBH} \lesssim 10^{11}$ kg decay into thermal radiation before the onset of big bang nucleosynthesis and their abundance can thus be very large [302, 303]. On the other hand, PBHs with 10^{11} kg $\lesssim M_{PBH} \lesssim 10^{14}$ kg have a life-time comparable with the age of the universe and their abundance is highly constrained by the non-observation of their Hawking radiation. Heavier black holes are stable and contribute to dark matter, their abundance is constrained by the observed dark matter abundance as well as by direct searches, see e.g. Refs. [299, 304] for an overview.

For a given amplitude of the scalar power spectrum, the probability of forming PBHs depends on the statistical properties of the scalar fluctuations, since typically PBH formation is a rare event occurring in the tail of the distribution function. For a gaussian distribution any power spectrum generating stable black holes with $\langle \zeta^2 \rangle \gtrsim 10^{-2}$ leads to an overclosure of the universe [305]. For a positive χ^2-distribution, as expected for the sourced scalar perturbations in axion inflation, this value is lowered to $\langle \zeta^2 \rangle \gtrsim 10^{-3}$ [273]. The amplitude of the power spectrum in Fig. 6.7 clearly exceeds these values towards the end of inflation. Thus requiring $M_{PBH}(N) < 10^{11}$ kg to avoid these overclosure bounds restricts the enhancement of the scalar power spectrum to the last ~ 10 e-folds, see Eq. (6.43). Here we have set $j = 3$ since the expected large abundance of PBHs generated right after

inflation will lead to an early matter dominated phase.

Consequently, the power spectrum depicted in Fig. 6.7 which is only enhanced in the last ~ 5 (9) e-folds for $f = 1/20$ (1/25), is (marginally) compatible with bounds from PBH formation. Significantly larger values of $1/f$ will lead to overproduction of stable PBHs, though the precise bound will depend on the details of the last stages of inflation, see discussion below Eq. (6.42). On the contrary, a large abundance of metastable black holes as found for $1/f \lesssim 25$ entails several interesting phenomenological consequences. Firstly, an early PBH dominated phase, eventually releasing its energy into thermal Hawking radiation, provides a remarkable reheating mechanism. Any radiation released during preheating or in the inflaton decay is strongly red-shifted during the PBH dominated era, and hot big cosmology is re-ignited once the PBHs decay. Among others, this poses interesting challenges for baryogenesis. Secondly, there are three significant sources of gravitational waves (GWs): (i) GWs sourced by the gauge field population during inflation [271], (ii) GWs sourced (at second order) from the large scalar perturbations [306, 307, 308] and (iii) GWs sourced as a component of the Hawking radiation of the decaying PBHs [302, 309]. All of these sources result in high frequency ($\sim$ MHz and beyond) GWs, beyond the scope of current experiments but suggesting a potential target for potential future high frequency experiments. We expect that the characteristic oscillating features of the source $\langle \vec{E}\vec{B} \rangle$ will also be visible in the GW spectrum. Note that any GWs which are sub-horizon during the PBH dominated phase will be strongly diluted, leading to an interesting interplay between the GW and PBH spectrum. This applies in particular to GWs generated during preheating right after inflation [282].

6.6 Conclusions

Axion inflation is generically accompanied by an explosive gauge field production, triggered by a tachyonic instability of roughly horizon sized gauge field modes, which is in turn sourced by the inflaton velocity. The energy budget of this gauge field configuration is drained from the kinetic motion of the inflation, which can be described as a backreaction of the classical gauge fields on the homogeneous inflaton equation of motion. In this chapter we study the resulting coupled system of differential equations numerically, pointing out several new aspects which point to a more complex dynamics than previously anticipated.

The tachyonic instability is most effective on slightly sub-horizon scales, and hence the amplitude of any gauge field mode is set by the value of the inflaton velocity just before this mode crosses the horizon. On the other hand, the nonlinear backreaction term is dominated by super-horizon gauge field modes, and hence reacts with a time lag to any change in the inflaton velocity. As the average

speed of the inflaton increases over the course of inflation this system eventually hits a resonance frequency, where this time-lag corresponds to a phase shift of π. This leads to oscillations with increasing amplitude and fixed frequency in e-fold time, clearly visible in the inflaton velocity, the backreaction term and the gauge field energy density. This drastically changes the dynamics of axion inflation in the strong backreaction regime.

An example of an observable which is significantly impacted by this change in the inflaton dynamics is the scalar power spectrum. At very early times, when the scales relevant for the CMB exited the horizon, the backreaction is irrelevant and the spectrum closely resembles the usual spectrum of vacuum fluctuations. On smaller scales, corresponding to later stages of inflation, the scalar power spectrum receives an additional contribution sourced by the inhomogeneous part of the gauge field distribution, leading to an enhancement by many orders of magnitude. In this work we re-visit the equation of motion for the scalar perturbations, reproducing results found previously in the weak backreaction regime but finding a significant larger amplitude for the scalar power spectrum in the strong backreaction regime. This result holds even when working with a time-averaged backreaction, i.e. discarding the resonance discussed above. Including the resonance leads to additional oscillatory features in the power spectrum at small scales. However, our results also indicate that the strong backreaction regime entails such large scalar perturbations (invoking in particular significant spatial gradients in the inflaton field) that the perturbative description fails. The formation of (metastable) primordial black holes seems unavoidable, entailing interesting phenomenological consequences. Despite electro-magnetic dissipation reduces the required field excursion compared to axion inflation models in absence of gauge couplings, we saw in Sec. 6.4 that the full numerical treatment does not show significant differences in terms of initial field displacement. Nevertheless, the breakdown of perturbation theory suggests that all predictions related to the last e-foldings should be revisited. Unfortunately, any more quantitative analysis requires a non-perturbative description of this system, which is beyond the scope of the present work.

In this context, it is interesting to note the recent progress made in simulating the preheating phase of this model on the lattice [280, 281, 282] (see also [310] for related work). The challenges induced by the growing separation of scales in an expanding Universe limits the amount of e-folds which can be tracked, but the characteristic time scale $\Delta N_\xi \simeq \ln(\xi^2/2)$ of the resonance seems to be within reach of such analyses. The preheating phase, and in particular its gravitational wave production, can impose stringent bounds on the axion to photon coupling, down to $1/f \lesssim 10$ [282]. However, an early PBH dominated phase, triggered by the drastically enhanced scalar power spectrum, would significantly dilute the energy density in gravitational wave radiation which redshifts faster than the PBH

component. This could re-open the parameter space of larger couplings. We leave a more detailed study of this question to future work.

The observed resonance phenomenon will not only affect the scalar power spectrum but also the tensor power spectrum, since it too receives a contribution sourced by the gauge field population. Moreover, we expect that similar resonance phenomena can occur in other cosmological systems which feature a tachyonic instability of gauge fields modes driven by a non-vanishing axion velocity. This includes models of baryogenesis driven by the motion of axion-like particle [291, 311] and models of cosmological relaxation of the electroweak scale utilizing gauge field friction [312, 313, 314, 315, 316, 317]. We leave these questions to future work.

Chapter 7

Conclusions and Outlook

We conclude this work by providing a brief summary of the contents and the results reported in this thesis.

In Chap. 1 we give an overview of the current knowledge of high energy physics for what concerns both particle physics and cosmology. We briefly review the main achievements and limitations of the Standard Model of particle physics and ΛCDM model. These models fail to address several issues like the hierarchy problem for the Higgs mass, gauge coupling unification and the strong CP problem. Moreover, they are not able to explain the origin of DM, baryogenesis and dark energy.

In order to overcome the experimental and theoretical problems related to the current state of the art, several theories have been proposed for fundamental physics beyond current understanding. In this work we focus in particular on inflation and axions and their possible embedding in string theory. Inflation, that is presented in section 2.1, provides a dynamical way to overcome the initial condition problems of standard Big Bang cosmology, leading to successful large structure formation. The existence of axions was firstly theorised to solve the strong CP problem. Axions and ALPs are introduced in section 2.2, where we explain how, depending on their production mechanism, their mass and coupling to other particles, these fields can represent both DM and dark radiation, or can play the role of the inflaton field. Finally, we present a brief introduction on string theory which is at present the best candidate for a unified theory of all interactions, which describes also gravity at the quantum level in a consistent way. In section 2.3 we focus in particular on type IIB string theory. We explain how to construct low energy 4D theories that can reproduce the basic ingredients of SM physics, such as chiral matter, gauge theories and Yukawa couplings. We presented an overview of the generic tools needed for the study of string compactifications. We showed which class of extra dimensions manifold allows us to get an $\mathcal{N} = 1$ supersymmetric effective field theory starting from the 10D action for massless string states. Such 4D EFTs suffer from the presence of many massless scalar fields,

named moduli, that may lead to the presence of undetected fifth-forces and other phenomenological problems. For these reasons we review the current mechanisms that are used to provide a potential for these fields. This goes under the name of moduli stabilisation. In this thesis we use a bottom-up approach, analysing 4D string vacua equipped with sets of local sources as Dp-branes and Op-planes. This method may be more efficient in trying to identify promising string vacua which can reproduce all the features of the SM together with inflation. We work in the large volume scenario that allows us to work with CY manifolds also in presence of background fluxes and induces an hierarchy between different energy scales that is suitable for safely building a 4D EFT description of inflation.

The second part of this thesis contains the results, related to the aforementioned topics, that I achieved during my PhD.

In Chapter 3 we construct the first explicit realisations of Fibre Inflation models in concrete type IIB Calabi-Yau orientifolds with consistent brane setups, full closed string moduli fixing and chiral matter on D7-branes. We perform a consistent choice of orientifold involution, brane setup and gauge fluxes which leads to chiral matter and a moduli-dependent Fayet-Iliopoulos term. Using LVS we are able to perform moduli stabilisation step by step. The underlying compactification manifold features $h^{1,1} = 4$ Kähler moduli and is reduced to the standard 3 moduli of Fibre Inflation models after D-term stabilisation. The inflationary potential is generated by string loop corrections and higher derivative $\alpha'^3 F^4$ corrections. We found that the inflationary dynamics is strongly constrained by the Kähler cone conditions which never allow for enough efoldings of inflation if we consider natural values of the internal volume ($\mathcal{V} \sim 10^3$). For larger values of the Calabi-Yau volume of order $\mathcal{V} \sim 10^4$, the Kähler cone becomes large enough and allows to have enough e-foldings. However, such a large value of $\mathcal{V}$ tends to suppress the amplitude of the density perturbations below the reference COBE value. The tension between getting the right number of e-foldings and matching the right normalisation of curvature perturbations can be softened choosing background fluxes that allow for large values of the winding loop coefficients or W_0. However, some parameters as χ_{eff}, which controls the strength of $\mathcal{O}(\alpha'^3)$ corrections due to presence of O7-planes, and λ which is the combinatorial factor in $\mathcal{O}(\alpha'^3)$ higher derivative term, are not flux dependent and have not been computed in full detail yet. A better determination of these parameters may influence the required field range during inflation. On the other hand, if the current estimates of χ_{eff} and λ turn out to be right, other possible ways of producing the correct amplitude of the scalar power spectrum should be found. An interesting option may be given by the curvaton scenario that can be realised by the presence of ultra-light closed string axions associated to large bulk cycles that are always present in FI models. The last open issue for future work is that, despite there are several known mechanisms

responsible for the realisation of a dS vacuum (switching on magnetic fluxes on D7-branes [64], adding anti D3-branes [65, 66, 67, 68, 69, 70, 71, 72], hidden sector T-branes [73], non-perturbative effects at singularities [74] or non-zero F-terms of the complex structure moduli [75]), our chiral global models still lack an explicit dS construction.

In Chapter 4 we study geometrical destabilisation [164] and its application to some 4D EFTs coming from string theory. It has recently been claimed that when the field manifold is negatively curved, the effective mass-squared of the isocurvature modes receives negative contributions from the Christoffel symbols and the Ricci scalar which can potentially induce a geometrical instability by making them tachyonic [164]. In principle this problem may be related to both heavy and light fields that are orthogonal to the inflationary trajectory. The low-energy EFTs coming from string theory are generally characterised by non-canonical kinetic terms and can therefore be plagued by geometrical destabilisation problems. We first analyse generic 2-field models with negative curvature and we conclude that there is no instability for heavy non-inflationary scalars. The background analysis shows that the isocurvature modes may become tachyonic only for a short time period and on spurious non-attractive solutions with extremely fine-tuned initial conditions. On the other hand, the analysis of 2-field systems with an ultra-light scalar shows that the tachyonic instability of isocurvature modes can arise also along stable background trajectories and is model dependent. We then move to the analysis of concrete examples. We first study the simple case of quintessence-like potentials and then we moved to the analysis of Fibre Inflation models where the inflationary potential is generated by perturbative corrections to the Kähler potential. In this setup there are two axionic fields that remain massless after moduli stabilisation. These are the two bulk closed string axions which are both kinetically coupled to the inflaton. The inflationary dynamics of these systems shows that, despite the background trajectory is stable against a wide range of initial conditions, one of the two massless axions develops exponentially growing isocurvature perturbations. We try to avoid this geometrical destabilisation by turning on a non-zero axionic mass via non-perturbative effects. However we find that, in order to obtain a positive mass-squared of the isocurvature modes, these non-perturbative effects have to be of the same order of magnitude of the loop corrections which generate the inflationary potential, completely changing the inflationary dynamics. In the last part of this chapter, we show however that the geometrical destabilisation of these systems is just a spurious instability. We first uncover the origin of the growth of the isocurvature perturbations in the ill-defined kinematic basis. After that, we point out which definition of entropy should be used in order to check the observational bounds on isocurvature perturbations. This comes from the definition of the relative entropy between the fluids, iden-

tified with the inflaton and the kinetically coupled massless field. The standard definition of entropy perturbation between two fluids cannot be applied in this context, being the energy density of the massless axion vanishing on-shell. Nevertheless we show that the relative entropy perturbation between the two scalars is finite and vanishingly small during inflation. This allows us to argue that the instability of Fibre Inflation systems has no physical impact and the underlying models are presently viable. In the future it would be interesting to study which definition of entropy should be used in these models (also considering small axion masses) to transfer the entropy mode from the scalar field system used to describe inflation to the primordial plasma. Indeed, this cannot be done in a canonical way [196, 197, 198] being the curvature associated to the axion field ill-defined. Another important goal would be to extend the fluid approach in the estimate of entropy perturbations [191, 318] to inflationary systems with curved field space.

In Chapter 5 we study an example of axionic DM particle coming from type IIB string compactifications. We focus on explaining the origin of the 3.5 keV line that has been recently detected from galaxy clusters and other astrophysical objects. In particular we describe how to perform a successful global embedding in type IIB string compactifications of the model of [17]. In this model, the line is generated by a double decay: a 7 keV dark matter particle decays into ultra-light ALPs which are converted into photons in the cluster magnetic field. This process is particularly interesting since it can explain the morphology of the signal and other experimental evidences, namely its non-observation in dwarf spheroidal galaxies. In this chapter we give a concrete microscopic realisation of [17], listing the required properties for the explicit type IIB Calabi-Yau compactification. We focus on LVS models since they generically lead to very light axions, especially when some of the moduli are stabilised by perturbative corrections to the effective action. The 7 keV DM particle is given by a closed string axion that receives a mass through poly-instanton effects to the superpotential. A hidden sector, hosting the ultra-light ALP, and the visible sector come from two non-intersecting blow-up modes that shrink down to zero size due to D-term stabilisation and support D3-branes at singularities. The two divisors are invariant under the orientifold involutions and the coupling between the ALP and ordinary photons is induced by $U(1)$ kinetic mixing. The ultra-light ALP is related to the phase of the hidden sector open string mode which is charged under an anomalous $U(1)$. Its radial part gets fixed in terms of a moduli-dependent FI-term and represents the ALP decay constant. In sequestered models with low-energy supersymmetry the radial part can develop a non-vanishing VEV due to a tachyonic soft scalar mass contribution leading to an intermediate scale coupling between photons and ALPs which is in full agreement with current observations. The DM-ALP coupling is generated by kinetic mixing induced by non-perturbative corrections to the Kähler potential.

Despite we discuss the required features needed to get a successful embedding of [17], performing full moduli stabilisation and also computing the mass spectrum and all relevant couplings, we do not present an explicit construction built via toric geometry, leaving it as a future task. Another important open question for future work would be to embed inflation in this setup, trying also to reproduce the cosmological history of the universe to the present epoch.

In Chapter 6 we analyse electro-magnetic dissipation in axion inflation. Indeed, these particles are naturally good inflaton candidates since they appear in the theory equipped with an approximate shift symmetry that can protect the inflationary potential against dangerous quantum corrections. We study how the coupling to a hidden sector $U(1)$ gauge field can affect the inflationary dynamics and if it may lead to well recognisable imprints on the cosmological parameters. This coupling causes a massive gauge field production, triggered by a tachyonic instability of roughly horizon size gauge modes, that is sourced by the inflaton velocity. This system has been widely studied in the literature using a semi-analytical approach. It was shown that the electro-magnetic dissipation slows down the inflaton motion and it can allow for inflation also on steep potentials [262]. Moreover, from the phenomenological point of view, it usually causes an enhancement of scalar and tensor perturbations at small scales that is sourced classically by inhomogeneities in the electromagnetic field [268, 269, 270, 271]. In this work we perform a full numerical analysis of axion inflation with a trans-Planckian decay constant and a quadratic potential, bringing to light a new resonant behaviour that has not been seen before. We found that the time lag between the tachyonic instability, that is most effective on slightly sub-horizon scales where it sets the amplitude of each gauge mode exiting the horizon, and the non-linear backreaction term, that is dominated by superhorizon gauge modes, causes an oscillatory behaviour in both the inflaton velocity and the gauge field production. In case of strong backreaction regime, the system hits a resonance frequency that leads to oscillations with increasing amplitude and constant frequency. Studying the impact of the resonant behaviour on the scalar power spectrum, we find that at early times the backreaction is negligible and the scalar power spectrum matches the usual vacuum fluctuations result. On the other hand, at smaller scales, the relevant contribution to the scalar power spectrum comes from the inhomogeneous part of the gauge field distribution. For strong backreactions, the power spectrum shows a resonant behaviour at small scales and it grows to the point that the perturbative description fails. This can have interesting phenomenological consequences, as the production of a large amount of primordial black-holes and gravitational waves. In order to give a quantitative description of these phenomena we should develop a non-perturbative description of this system. This may be done in future works, following the evolution of the system at least for few e-folding, using lattice

simulations or full numerical GR tools. Another important goal would be to give an embedding of this model in string theory. Since it is well known that single axion inflation models usually require a trans-Planckian decay constant that has not be found in controlled string compactifications, we should focus on those constructions where the inflaton field is given by a combination of axions that enjoy an *effective trans-Planckian* decay constant [109, 112, 110].

Let me conclude by stressing that the major aim of string cosmology (and of high energy physics in general) is to provide a class of string compactifications (or models) that can predict a viable inflationary dynamics with the right couplings between different sectors, so that it can successfully reproduce standard Big Bang cosmology, and therefore the SM degrees of freedom, at low energy. This problem could be faced in different ways, also using the EFT approach, and leads to many different models that share some features (in order to match the experimental constraints coming from inflation), but rely on different constructions. Indeed, the lack of new experimental results in high energy physics, together with the end of LHC run 2 without supersymmetric particles detection, leaves a lot of freedom in model building. Fortunately, new experimental constraints will come from cosmological observations. Indeed, the large-scale structure and the evolution of the universe has in the last few years entered a qualitatively new phase, driven by a host of experimental results. In particular, results from CMB studies, collected by COBE [319], WMAP [320] and the Planck Collaboration [10, 8], and gravitational wave data, collected by ground-based interferometers, e.g. LIGO and VIRGO [321], will be combined in the next years with results coming from future precision experiment, e.g. LISA interferometer [279] and Euclid satellite [322]. These experiments together will be able to span a wide range of redshift data, constraining the nature of dark energy, dark matter, probing also the electroweak scale and providing severe constraints on inflationary models [323, 324]. I therefore think that, precisely because there are many different paths to follow, theoretical efforts must be made in order to give experimentalists clear and precise predictions coming from different models. As a theorist I believe that whatever effective field theory of primordial cosmology should have a UV embedding in order to be considered complete. This is the reason why, during my PhD, I focused my research on effective theories coming from strings.

Appendix A

Another example of global embedding with chiral matter

A.1 Another chiral global example

A.1.1 Toric data

Let us consider the following toric data for a CY threefold with $h^{1,1} = 4$ which is a K3-fibration over a $\mathbb{P}^1$ base along with a so-called 'small' divisor:

	x_1	x_2	x_3	x_4	x_5	x_6	x_7	x_8
8	0	0	0	1	1	1	1	4
6	0	0	1	0	1	0	1	3
6	0	1	0	0	0	1	1	3
4	1	0	0	0	0	0	1	2
	dP_5	NdP_{11}	NdP_{11}	dP_7	K3	K3	SD1	SD2

with Hodge numbers $(h^{2,1}, h^{1,1}) = (106, 4)$ and Euler number $\chi = -204$. The Stanley-Reisner ideal is:

$$\mathrm{SR} = \{x_1x_4,\, x_1x_7, x_3x_5,\, x_4x_5,\, x_2x_3x_7,\, x_2x_6x_8,\, x_4x_6x_8\}\,.$$

This corresponds to the CY threefold used in [325] to build global models with chiral matter on D7-branes and Kähler moduli stabilisation but without any inflationary dynamics. A detailed divisor analysis using `cohomCalg` [149, 150] shows that the divisor D_4 is a del Pezzo dP_7 which we find to be shrinkable after investigating the CY volume form. Further, each of the divisors $\{D_2,\, D_3\}$ are non-diagonal del Pezzo surfaces and $\{D_5,\, D_6\}$ are two K3 surfaces while the divisors

$\{D_7,\, D_8\}$ are two 'special deformation' divisors with Hodge diamond:

$$\text{SD1} \equiv \begin{array}{ccccc} & & 1 & & \\ & 0 & & 0 & \\ 3 & & 38 & & 3 \\ & 0 & & 0 & \\ & & 1 & & \end{array} \qquad \text{and} \qquad \text{SD2} \equiv \begin{array}{ccccc} & & 1 & & \\ & 0 & & 0 & \\ 25 & & 172 & & 25 \\ & 0 & & 0 & \\ & & 1 & & \end{array}$$

The intersection form in the basis of smooth divisors $\{D_1, D_4, D_5, D_6\}$ can be written as:

$$I_3 = 2\, D_1\, D_5\, D_6 - 2\, D_1^2\, D_5 - 2\, D_1^2\, D_6 + 2\, D_4^3 + 4\, D_1^3\,. \tag{A.1}$$

Writing the Kähler form in the above basis of divisors as $J = t_1\, D_1 + t_4\, D_4 + t_5\, D_5 + t_6\, D_6$ and using the intersection polynomial (A.1), the CY overall volume takes the form:

$$\mathcal{V} = 2\, t_1\, t_5\, t_6 - t_1^2\, t_5 - t_1^2\, t_6 + \frac{t_4^3}{3} + \frac{2}{3}\, t_1^3\,. \tag{A.2}$$

In order to express $\mathcal{V}$ in terms of four-cycle moduli, we need to know the Kähler cone conditions which can be determined from the following Kähler cone generators:

$$K_1 = D_1 + D_5 + D_6, \quad K_2 = D_1 - D_4 + D_5 + D_6, \quad K_3 = D_5, \quad K_4 = D_6\,. \tag{A.3}$$

Expanding the Kähler form J in these Kähler cone generators as $J = \sum_{i=1}^{4} r_i\, K_i$ results in the following conditions for the two-cycle moduli:

$$r_1 = t_1 + t_4 > 0\,, \qquad r_2 = -t_4 > 0\,, \qquad r_3 = t_5 - t_1 > 0\,, \qquad r_4 = t_6 - t_1 > 0\,. \tag{A.4}$$

Using the four-cycle moduli, $\tau_i = \partial_{t_i}\mathcal{V}$, given by:

$$\tau_1 = 2\,(t_5 - t_1)(t_6 - t_1), \quad \tau_4 = t_4^2, \quad \tau_5 = t_1(2\,t_6 - t_1), \quad \tau_6 = t_1(2\,t_5 - t_1)\,, \tag{A.5}$$

the overall volume can be rewritten as:

$$\mathcal{V} = \frac{1}{3}\left(t_1\tau_1 + t_5\tau_5 + t_6\tau_6 - \tau_4^{3/2}\right)\,. \tag{A.6}$$

The second Chern class of the CY threefold X is instead given by:

$$c_2(X) = 2\, D_6\, D_8 + 8\, D_7\, D_8 - 2\, D_6^2 - 4\, D_6\, D_7 - 12\, D_7^2\,, \tag{A.7}$$

which results in the following values of the topological quantities Π_i's:

$$\Pi_1 = 4, \quad \Pi_2 = \Pi_3 = 16, \quad \Pi_4 = 8, \quad \Pi_5 = \Pi_6 = 24, \quad \Pi_7 = 44, \quad \Pi_8 = 136\,.$$

The intersection curves between two coordinate divisors are given in Tab. A.1 while their volumes are listed in Tab. A.2.

	D_1	D_2	D_3	D_4	D_5	D_6	D_7	D_8
D_1	$\mathcal{C}_5$	$\mathbb{P}^1$	$\mathbb{P}^1$	$\varnothing$	$\mathbb{P}^1$	$\mathbb{P}^1$	$\varnothing$	$\mathbb{T}^2$
D_2	$\mathbb{P}^1$	$\mathbb{P}^1 \sqcup \mathbb{P}^1$	$\mathbb{P}^1 \sqcup \mathbb{P}^1$	$\mathbb{T}^2$	$\mathbb{T}^2$	$\varnothing$	$\mathbb{P}^1$	$\mathcal{C}_3$
D_3	$\mathbb{P}^1$	$\mathbb{P}^1 \sqcup \mathbb{P}^1$	$\mathbb{P}^1 \sqcup \mathbb{P}^1$	$\mathbb{T}^2$	$\varnothing$	$\mathbb{T}^2$	$\mathbb{P}^1$	$\mathcal{C}_3$
D_4	$\varnothing$	$\mathbb{T}^2$	$\mathbb{T}^2$	$\mathcal{C}_3$	$\varnothing$	$\varnothing$	$\mathbb{T}^2$	$\mathcal{C}_3$
D_5	$\mathbb{P}^1$	$\mathbb{T}^2$	$\varnothing$	$\varnothing$	$\varnothing$	$\mathbb{T}^2$	$\mathcal{C}_2$	$\mathcal{C}_9$
D_6	$\mathbb{P}^1$	$\varnothing$	$\mathbb{T}^2$	$\varnothing$	$\mathbb{T}^2$	$\varnothing$	$\mathcal{C}_2$	$\mathcal{C}_9$
D_7	$\varnothing$	$\mathbb{P}^1$	$\mathbb{P}^1$	$\mathbb{T}^2$	$\mathcal{C}_2$	$\mathcal{C}_2$	$\mathcal{C}_3$	$\mathcal{C}_{19}$
D_8	$\mathbb{T}^2$	$\mathcal{C}_3$	$\mathcal{C}_3$	$\mathcal{C}_3$	$\mathcal{C}_9$	$\mathcal{C}_9$	$\mathcal{C}_{19}$	$\mathcal{C}_{89}$

Table A.1: Intersection curves of two coordinate divisors. Here $\mathcal{C}_g$ denotes a curve with Hodge numbers $h^{0,0} = 1$ and $h^{1,0} = g$.

	D_1	D_2	D_3	D_4	D_5	D_6	D_7	D_8
D_1	$4t_1 - 2(t_5 + t_6)$	$2(t_5 - t_1)$	$2(t_6 - t_1)$	0	$2(t_6 - t_1)$	$2(t_5 - t_1)$	0	$2(t_5 + t_6) - 4t_1$
D_2	$2(t_5 - t_1)$	$2t_4$	$2(t_1 + t_4)$	$-2t_4$	$2t_1$	0	$2(t_5 + t_4)$	$2(t_1 + 2t_4 + 2t_5)$
D_3	$2(t_6 - t_1)$	$2(t_1 + t_4)$	$2t_4$	$-2t_4$	0	$2t_1$	$2(t_6 + t_4)$	$2(t_1 + 2t_4 + 2t_6)$
D_4	0	$-2t_4$	$-2t_4$	$2t_4$	0	0	$-2t_4$	$-4t_4$
D_5	$2(t_6 - t_1)$	$2t_1$	0	0	0	$2t_1$	$2t_6$	$2(2t_6 + t_1)$
D_6	$2(t_5 - t_1)$	0	$2t_1$	0	$2t_1$	0	$2t_5$	$2(2t_5 + t_1)$
D_7	0	$2(t_5 + t_4)$	$2(t_6 + t_4)$	$-2t_4$	$2t_6$	$2t_5$	$2(t_4 + t_5 + t_6)$	$4t_4 + 6(t_5 + t_6)$
D_8	$2(t_5 + t_6) - 4t_1$	$2(t_1 + 2t_4 + 2t_5)$	$2(t_1 + 2t_4 + 2t_6)$	$-4t_4$	$2(2t_6 + t_1)$	$2(2t_5 + t_1)$	$4t_4 + 6(t_5 + t_6)$	$4[t_1 + 2t_4 + 4(t_5 + t_6)]$

Table A.2: Volumes of intersection curves between two coordinate divisors.

A.1.2 Orientifold involution

We focus on orientifold involutions of the form $\sigma : x_i \to -x_i$ with $i = 1, ..., 8$ which feature an O7-plane on D_i and O3-planes at the fixed points listed in Tab. A.3. The effective non-trivial fixed point set in Tab. A.3 has been obtained after taking care of the SR ideal symmetry. Moreover, the total number of O3-planes $N_{\rm O3}$ is obtained from the triple intersections restricted to the CY hypersurface, while the effective Euler number $\chi_{\rm eff}$ has been computed as:

$$\chi_{\rm eff} = \chi(X) + 2\int_X [\mathrm{O7}] \wedge [\mathrm{O7}] \wedge [\mathrm{O7}]\,. \tag{A.8}$$

In what follows we shall focus on the orientifold involution $\sigma : x_7 \to -x_7$ which features two non-intersecting O7-planes located in D_1 and D_7 and two O3-planes at $\{D_2 D_3 D_4\}$.

σ	O7	O3	$N_{\rm O3}$	χ(O7)	$\chi_{\rm eff}$
$x_1 \to -x_1$	$D_1 \sqcup D_7$	$\{D_2D_3D_4\}$	2	54	-192
$x_2 \to -x_2$	D_2	$\{D_1D_6D_8, D_3D_4D_7, D_6D_7D_8\}$	{2, 2, 6}	14	-208
$x_3 \to -x_3$	D_3	$\{D_1D_5D_8, D_2D_4D_7, D_5D_7D_8\}$	{2, 2, 6}	14	-208
$x_4 \to -x_4$	D_4	$\{D_1D_2D_3, D_1D_5D_6,$ $D_2D_5D_8, D_3D_6D_8, D_5D_6D_7\}$	{2, 2, 4, 4, 2 }	10	-200
$x_5 \to -x_5$	D_5	$\{D_1D_3D_8, D_3D_7D_8, D_2D_4D_8\}$	{2, 2, 4}	24	-204
$x_6 \to -x_6$	D_6	$\{D_1D_2D_8, D_2D_7D_8, D_3D_4D_8\}$	{2, 2, 4}	24	-204
$x_7 \to -x_7$	$D_1 \sqcup D_7$	$\{D_2D_3D_4\}$	2	54	-192
$x_8 \to -x_8$	D_8	$\varnothing$	0	224	-28

Table A.3: Fixed point set for the involutions which are reflections of the eight coordinates x_i with $i = 1, ..., 8$.

A.1.3 Brane setup

If the D7-tadpole cancellation condition is satisfied by placing four D7-branes on top of the O7-plane, the string loop corrections to the scalar potential involve only KK effects since winding contributions are absent due to the absence of any intersection between D7-branes and/or O7-planes. Thus loop effects are too simple to generate a viable inflationary plateau. We shall therefore focus on a slightly more complicate D7-brane setup which gives rise also to winding loop effects. This can be achieved by placing D7-branes not entirely on top of the O7-plane as follows:

$$8[\text{O7}] \equiv 8([D_1] + [D_7]) = 8\,(2[D_1] + [D_2] + [D_5])\,. \tag{A.9}$$

This brane setup involves three stacks of D7-branes wrapped around the divisors D_1, D_2 and D_5. Moreover, the condition for D3-tadpole cancellation becomes:

$$N_{\rm D3} + \frac{N_{\rm flux}}{2} + N_{\rm gauge} = \frac{N_{\rm O3}}{4} + \frac{\chi(\text{O7})}{12} + \sum_a \frac{N_a\,(\chi(D_a) + \chi(D'_a))}{48} = 14\,,$$

showing that there is space for turning on both gauge and background three-form fluxes for complex structure and dilaton stabilisation.

A.1.4 Gauge fluxes

In order to obtain a chiral visible sector on the D7-brane stacks wrapping D_1, D_2 and D_5 we need to turn on worldvolume gauge fluxes of the form:

$$\mathcal{F}_i = \sum_{j=1}^{h^{1,1}} f_{ij}\hat{D}_j + \frac{1}{2}\hat{D}_i - \iota_{D_i}^* B \quad \text{with} \quad f_{ij} \in \mathbb{Z} \quad \text{and} \quad i = 1, 2, 5\,, \tag{A.10}$$

where the half-integer contribution is due to Freed-Witten anomaly cancellation [51, 52].

However we want to generate just one moduli-dependent Fayet-Iliopoulos term in order to fix only one Kähler modulus via D-term stabilisation. In fact, if the number of FI-terms is larger than one, there is no light Kähler modulus which can play the rôle of the inflaton. Moreover we wrap a D3-brane instanton on the rigid divisor D_4 in order to generate a non-perturbative contribution to the superpotential which is crucial for LVS moduli stabilisation. In order to cancel the Freed-Witten anomaly, the D3-instanton has to support a half-integer flux, and so the general expression of the total gauge flux on D_4 becomes:

$$\mathcal{F}_4 = \sum_{j=1}^{h^{1,1}} f_{4j}\hat{D}_j + \frac{1}{2}\hat{D}_4 - \iota_{D_i}^* B \quad \text{with} \quad f_{4j} \in \mathbb{Z}\,. \tag{A.11}$$

However a non-vanishing $\mathcal{F}_4$ would not be gauge invariant, and so would prevent a non-perturbative contribution to the superpotential. We need therefore to check if it is possible to perform an appropriate choice of B-field which can simultaneously set $\mathcal{F}_1 = \mathcal{F}_2 = 0$ (we choose to have a non-vanishing gauge flux only on D_5 to have just one moduli-dependent FI-term) and $\mathcal{F}_4 = 0$. If we set:

$$B = \frac{1}{2}\hat{D}_1 + \frac{1}{2}\hat{D}_2 + \frac{1}{2}\hat{D}_4\,, \tag{A.12}$$

the condition $\mathcal{F}_1 = \mathcal{F}_2 = \mathcal{F}_4 = 0$ reduces to the requirement that the following forms are integer:

$$\iota_{D_1}^*\left(\frac{1}{2}\hat{D}_2 + \frac{1}{2}\hat{D}_4\right) \qquad \iota_{D_2}^*\left(\frac{1}{2}\hat{D}_1 + \frac{1}{2}\hat{D}_4\right) \qquad \iota_{D_4}^*\left(\frac{1}{2}\hat{D}_1 + \frac{1}{2}\hat{D}_2\right)\,, \tag{A.13}$$

since in this case the integer flux quanta f_{ij} can always be adjusted to yield vanishing gauge fluxes. Taking an arbitrary integer form $A \in H^2(\mathbb{Z}, X)$ which can be expanded as $A = a_j\hat{D}_j$ with $a_j \in \mathbb{Z}$, the pullbacks in (A.13) give rise to integer

forms if:

$$\begin{aligned} b_1 &\equiv \int_X \left(\frac{1}{2}\hat{D}_2 + \frac{1}{2}\hat{D}_4\right) \wedge \hat{D}_1 \wedge A \in \mathbb{Z} \\ b_2 &\equiv \int_X \left(\frac{1}{2}\hat{D}_1 + \frac{1}{2}\hat{D}_4\right) \wedge \hat{D}_2 \wedge A \in \mathbb{Z} \\ b_4 &\equiv \int_X \left(\frac{1}{2}\hat{D}_1 + \frac{1}{2}\hat{D}_2\right) \wedge \hat{D}_4 \wedge A \in \mathbb{Z} \end{aligned}$$

Using the intersection polynomial (A.1) we find $b_1 = a_5 - a_1 \in \mathbb{Z}$, $b_2 = b_1 - a_4 \in \mathbb{Z}$ and $b_4 = -a_4 \in \mathbb{Z}$, showing how the choice of B-field in (A.12) can indeed allow for $\mathcal{F}_1 = \mathcal{F}_2 = \mathcal{F}_4 = 0$. The only non-zero gauge flux is $\mathcal{F}_5$ which does not feature any half-integer contribution since $c_1(D_5) = 0$ given that D_5 is a K3 surface. Given that all the intersection numbers are even, the pullback of the B-field on D_5 does also not generate an half-integer flux. We shall therefore consider a non-vanishing gauge flux on the worldvolume of D_5 of the form:

$$\mathcal{F}_5 = \sum_{j=1}^{h^{1,1}} f_{5j}\hat{D}_j \quad \text{with} \quad f_{5j} \in \mathbb{Z}\,. \tag{A.14}$$

A.1.5 FI-term and chirality

Given that the divisor D_5 is transversely invariant under the orientifold involution and it is wrapped by four D7-branes, it supports an $Sp(8)$ gauge group which is broken down to $U(4) = SU(4) \times U(1)$ by a non-zero flux $\mathcal{F}_5$ along the diagonal $U(1)$. This non-trivial gauge flux $\mathcal{F}_5$ induces also a $U(1)$-charge q_{i5} for the i-th Kähler modulus of the form:

$$q_{i5} = \int_X \hat{D}_i \wedge \hat{D}_5 \wedge \mathcal{F}_5\,. \tag{A.15}$$

Thus $\mathcal{F}_5 \neq 0$ yields:

$$q_{15} = 2(f_{56} - f_{51}) \qquad q_{45} = q_{55} = 0 \qquad q_{65} = 2f_{51}\,, \tag{A.16}$$

together with a flux-dependent correction to the gauge kinetic function which looks like:

$$\mathrm{Re}(f_5) = \alpha_5^{-1} = \frac{4\pi}{g_5^2} = \tau_5 - h(\mathcal{F}_5)\mathrm{Re}(S)\,, \tag{A.17}$$

where:

$$h(\mathcal{F}_5) = \frac{1}{2}\int_X \hat{D}_5 \wedge \mathcal{F}_5 \wedge \mathcal{F}_5 = \frac{1}{2}\left(f_{51}q_{15} + f_{56}q_{65}\right)\,. \tag{A.18}$$

Moreover a non-vanishing gauge flux $\mathcal{F}_5$ induces a moduli-dependent FI-term of the form:

$$\xi = \frac{1}{4\pi\mathcal{V}}\int_X \hat{D}_5 \wedge J \wedge \mathcal{F}_5 = \frac{1}{4\pi\mathcal{V}}\sum_{j=1}^{h^{1,1}} q_{j5}\, t_j = \frac{1}{4\pi\mathcal{V}}\left(q_{15}\, t_1 + q_{65}\, t_6\right) . \tag{A.19}$$

For vanishing open string VEVs (induced for example by non-tachyonic scalar masses), a leading-order supersymmetric stabilisation requires $\xi = 0$ which implies:

$$t_6 = -\frac{q_{15}}{q_{65}}\, t_1 = \left(1 - \frac{f_{56}}{f_{51}}\right) t_1 \equiv \alpha\, t_1 . \tag{A.20}$$

This $U(1)$ factor becomes massive via the Stückelberg mechanism and develops an $\mathcal{O}(M_s)$ mass by eating up a linear combination of an open and a closed string axion which is mostly given by the open string mode.

Besides breaking the worldvolume gauge group and inducing moduli-dependent FI-terms, non-trivial gauge fluxes on D7-branes generate also 4D chiral modes. In fact, open strings stretching between the D7-branes on D_5 and the O7-planes or the image branes give rise to the following zero-modes in the symmetric and antisymmetric representations of $U(4)$:

$$I_5^{(S)} = -\frac{1}{2}\int_X \hat{D}_5 \wedge [\mathrm{O7}] \wedge \mathcal{F}_5 - \int_X \hat{D}_5 \wedge \hat{D}_5 \wedge \mathcal{F}_5 = -\left(q_{15} + \frac{q_{65}}{2}\right), \tag{A.21}$$

$$I_5^{(A)} = \frac{1}{2}\int_X \hat{D}_5 \wedge [\mathrm{O7}] \wedge \mathcal{F}_5 - \int_X \hat{D}_5 \wedge \hat{D}_5 \wedge \mathcal{F}_5 = -I_5^{(S)} . \tag{A.22}$$

Due to the absence of worldvolume fluxes on the D7-branes wrapped around D_1 and D_2, the gauge groups supported by these two D7-stacks are respectively $SO(16)$ (since D_1 is an O7-locus) and $Sp(8)$ (since D_2 is transversely invariant) which are both unbroken. Thus open strings stretched between the D7-branes on D_5 and D_1 (or its image brane) give rise to chiral zero-modes in the bi-fundamental representation (4,16) of $U(4)$ and $SO(16)$ whose number is:

$$I_{51} = \int_X \hat{D}_5 \wedge \hat{D}_1 \wedge \mathcal{F}_5 = q_{15} . \tag{A.23}$$

On the other hand, the number of 4D chiral zero-modes in the bi-fundamental representation (4,8) of $U(4)$ and $Sp(8)$ (corresponding to open strings stretching between the D7s on D_5 and D_2) is:

$$I_{52} = \int_X \hat{D}_5 \wedge \hat{D}_2 \wedge \mathcal{F}_5 = q_{65} . \tag{A.24}$$

We need finally to check that there are no chiral intersections between the D7s on D_5 and the instanton on D_4 to make sure that the prefactor of the non-perturbative contribution to the superpotential is indeed non-zero. This is ensured by the fact that:

$$I_{54} = \int_X \hat{D}_5 \wedge \hat{D}_4 \wedge \mathcal{F}_5 = 0\,. \tag{A.25}$$

A.1.6 Inflationary potential

Using the D-term fixing relation (A.20), the Kähler cone conditions (A.4) simplify to $t_5 > t_1 > -t_4 > 0$ and $\alpha > 1$. Moreover the CY volume (A.6) reduces to:

$$\mathcal{V} = (2\alpha - 1)\, t_5 t_1^2 - \left(\alpha - \frac{2}{3}\right) t_1^3 + \frac{t_4^3}{3} = t_b \tau_f - \frac{1}{3}\,\tau_4^{3/2}\,. \tag{A.26}$$

Given that this form is linear in t_5, the effective CY volume after D-term stabilisation looks like a K3 fibre τ_f over a $\mathbb{P}^1$ base t_b whose volumes are given by:

$$\tau_f = \tau_5 = (2\alpha - 1)\, t_1^2 \qquad \text{and} \qquad t_b = t_5 - \frac{\left(\alpha - \frac{2}{3}\right)}{(2\alpha - 1)}\, t_1\,. \tag{A.27}$$

Notice that the Kähler cone condition $t_5 > t_1$ can be rewritten as:

$$\tau_f < \sigma(\alpha)\, \mathcal{V}^{2/3}\,, \tag{A.28}$$

where:

$$\sigma(\alpha) \equiv (2\alpha - 1) \left(\frac{3}{3\alpha - 1}\right)^{2/3} \quad \text{with} \quad \alpha > 1\,. \tag{A.29}$$

In terms of the canonically normalised inflaton shifted from its minimum, the condition (A.28) reads:

$$\tau_f = \langle \tau_f \rangle\, e^{2\hat{\phi}/\sqrt{3}} < \sigma\, \mathcal{V}^{2/3} \qquad \Leftrightarrow \qquad \hat{\phi} < \frac{\sqrt{3}}{2} \ln\left(\frac{\sigma}{\langle \tau_f \rangle}\, \mathcal{V}^{2/3}\right). \tag{A.30}$$

Let us now focus on the inflationary potential. The winding loop corrections look like (with $\kappa = g_s/(8\pi)$ for $e^{K_{\rm cs}} = 1$):

$$V_{g_s}^{\rm W} = -\kappa \frac{W_0^2}{\mathcal{V}^3} \frac{C_{\rm W}}{\sqrt{\tau_f}}\,, \tag{A.31}$$

where:

$$C_{\rm W} = \sqrt{2\alpha - 1} \left(C_1^{\rm W} + \frac{C_2^{\rm W}}{\alpha}\right). \tag{A.32}$$

On the other hand, the KK loop corrections read (neglecting τ_4-dependent terms which yield subdominant contributions):

$$V_{g_s}^{KK} = \kappa g_s^2 \frac{W_0^2}{\mathcal{V}^2} \sum_{i,j=1,5,6} C_i^{KK} C_j^{KK} K_{ij} \,. \tag{A.33}$$

After substituting $t_6 = \alpha t_1$, we obtain:

$$Z\mathcal{V}^2 \sum_{i,j} C_i^{KK} C_j^{KK} K_{ij} = a t_1^2 + C_5^2 t_5 \left(t_5 - t_1\right) - (1-Z)\left(b t_1^2 + c t_1 t_5 + \frac{C_5^2}{2} t_5^2\right),$$

where:

$$\begin{aligned} a &= C_1\left(C_1 + C_5 + C_6\right) + C_5\left(C_6 + \frac{C_5}{2}\right) + C_6^2\left(\alpha^2 - \alpha + \frac{1}{2}\right) \\ b &= \alpha C_1 C_6 + \frac{\alpha^2}{2} C_6^2 + \frac{C_1^2}{2} \qquad\qquad c = C_5\left(C_1 + \alpha C_6\right), \end{aligned}$$

and:

$$Z = 1 - \frac{2}{3\alpha - 1}\left(\frac{\tau_f}{\sigma\,\mathcal{V}^{2/3}}\right)^{3/2}.$$

Notice that the Kähler cone conditions $\tau_f < \sigma\,\mathcal{V}^{2/3}$ and $\alpha > 1$ imply $0 < Z < 1$. This guarantees the absence of any singularity in the Kähler metric. Expressing the scalar potential in terms of the 4-cycle moduli, we end up with:

$$V_{g_s}^{KK} = \kappa g_s^2 \frac{W_0^2}{Z\mathcal{V}^2}\left[\frac{C_5^2}{\tau_f^2} - \frac{2}{3\left(2\alpha-1\right)^{3/2}} \frac{C_5^2}{\mathcal{V}\sqrt{\tau_f}} + d\,\frac{\tau_f}{\mathcal{V}^2}\left(1 - h\,\frac{\tau_f^{3/2}}{\mathcal{V}}\right)\right], \tag{A.34}$$

where $h = u/d$ with:

$$\begin{aligned} d &= \frac{a}{(2\alpha-1)} - \frac{2}{3}\frac{c}{(2\alpha-1)^2} - \frac{C_5^2}{(2\alpha-1)^3}\left(\alpha^2 - \frac{\alpha}{3} - \frac{2}{9}\right) \\ u &= \frac{2\,b}{3\,(2\alpha-1)^{5/2}} + \frac{2\,c}{3}\,\frac{\left(\alpha - \frac{2}{3}\right)}{(2\alpha-1)^{7/2}} + \frac{C_5^2}{3}\,\frac{\left(\alpha - \frac{2}{3}\right)^2}{(2\alpha-1)^{9/2}}\,. \end{aligned}$$

If all the coefficients of the KK corrections take natural $\mathcal{O}(1)$ values, the term in (A.34) proportional to h is suppressed by $h \ll 1$, and so it can be safely neglected.

On the other hand, higher derivative $\alpha'^3\,F^4$ corrections take the form (neglecting the t_4-dependent term and setting $t_6 = \alpha t_1$):

$$V_{F^4} = -4\kappa^2 \frac{\lambda W_0^4}{g_s^{3/2}\mathcal{V}^4}\left[(6\alpha+1)t_1 + 6t_5\right], \tag{A.35}$$

which in terms of four-cycle moduli looks like:

$$V_{F^4} = -4\kappa^2 \frac{\lambda W_0^4}{g_s^{3/2}\mathcal{V}^4}\left[\frac{12\alpha^2+2\alpha-5}{(2\alpha-1)^{3/2}}\sqrt{\tau_f}+6\frac{\mathcal{V}}{\tau_f}\right]. \tag{A.36}$$

Therefore the total inflationary potential becomes:

$$V = V_{g_s}^{\rm W} + V_{g_s}^{KK} + V_{F^4} = \kappa\frac{W_0^2}{\mathcal{V}^2}\left(\frac{A_1}{\tau_f^2}+\frac{A_2}{\mathcal{V}\tau_f}-\frac{A_3}{\mathcal{V}\sqrt{\tau_f}}+\frac{B_1\sqrt{\tau_f}}{\mathcal{V}^2}+\frac{B_2\,\tau_f}{\mathcal{V}^2}\right), \tag{A.37}$$

where (with $\lambda = -|\lambda| < 0$):

$$A_1 = \frac{g_s^2}{Z}C_5^2 \qquad A_2 = \frac{3}{\pi}\frac{|\lambda|W_0^2}{\sqrt{g_s}} \qquad A_3 = C_{\rm W} + \frac{g_s^2}{Z}\frac{2\,C_5^2}{3\,(2\alpha-1)^{3/2}} \simeq C_{\rm W} \tag{A.38}$$

and:

$$B_1 = \frac{12\alpha^2+2\alpha-5}{6(2\alpha-1)^{3/2}}A_2 \qquad B_2 = \frac{g_s^2\,d}{Z}. \tag{A.39}$$

The potential (A.37) could support single-field slow-roll inflation driven by τ_f [101, 103]. In order to get enough efoldings before hitting the walls of the Kähler cone given in (A.30), we need to focus on the region in field space where the inflaton minimum is of order $\langle\tau_f\rangle \ll \mathcal{V}^{2/3}$. Numerical estimates show that we need values of order $\langle\tau_f\rangle \sim \mathcal{O}(1)$ and $\mathcal{V} \sim \mathcal{O}(10^4)$ which, in turn, imply $W_0 \sim \mathcal{O}(100)$ in order to match the observed amplitude of the density perturbations. For $g_s \lesssim \mathcal{O}(0.1)$, $|\lambda| \sim \mathcal{O}(10^{-3})$ and natural $\mathcal{O}(1)$ values of the coefficients of the string loop effects, the terms in (A.37) proportional to B_1 and B_2 are both negligible with respect to the first three terms in the vicinity of the minimum where $\tau_f \sim \mathcal{O}(1) \ll \mathcal{V}^{2/3}$.

The scalar potential (A.37) written in terms of the canonically normalised inflaton $\phi = \langle\phi\rangle + \hat{\phi}$ looks like (with $k = 2/\sqrt{3}$):

$$V = \kappa\,\frac{A_1 W_0^2}{\langle\tau_f\rangle^2\mathcal{V}^2}\left(C_{\rm dS} + e^{-2k\hat{\phi}} + \lambda_1 Z\,e^{-k\hat{\phi}} - \lambda_2 Z\,e^{-\frac{k\hat{\phi}}{2}} + \mathcal{R}_1 Z\,e^{\frac{k\hat{\phi}}{2}} + \mathcal{R}_2\,e^{k\hat{\phi}}\right), \tag{A.40}$$

where we added a constant $C_{\rm dS} = \lambda_2 Z - \lambda_1 Z - 1 - \mathcal{R}_1 Z - \mathcal{R}_2$ to obtain a Minkowski (or slightly dS) vacuum and:

$$\lambda_1 = \frac{3\langle\tau_f\rangle}{\pi C_5^2}\frac{|\lambda|W_0^2}{g_s^{5/2}\,\mathcal{V}} \sim \mathcal{O}(1-10) \qquad \lambda_2 \simeq \frac{\langle\tau_f\rangle^{3/2}}{C_5^2}\frac{C_{\rm W}}{g_s^2\,\mathcal{V}} \sim \mathcal{O}(1-10),$$

while:

$$\mathcal{R}_1 = \frac{12\alpha^2+2\alpha-5}{6(2\alpha-1)^{3/2}}\frac{\lambda_1\langle\tau_f\rangle^{3/2}}{\mathcal{V}} \ll 1 \qquad \mathcal{R}_2 = \frac{\langle\tau_f\rangle^3}{C_5^2}\frac{d}{\mathcal{V}^2} \ll 1.$$

The three negative exponentials in (A.40) compete to give a minimum at $\langle \tau_f \rangle \sim \mathcal{O}(1)$ while the two positive exponentials cause a steepening behaviour at large $\hat{\phi}$.

In this section we shall not present a detailed quantitative analysis of inflation. We however point out that, if the approximated expression (A.30) is correct, in this case the Kähler cone bounds seem to be more constraining than in the case discussed in the main text since the inflaton direction τ_f is bounded by $\mathcal{V}^{2/3}$ instead of $\mathcal{V}/\sqrt{\tau_s}$. Thus a viable inflationary dynamics in this case would require a more severe tuning of the underlying parameters and a better understanding of the validity of our effective field theory approach.

Appendix B

Cosmological perturbations in curved field space

B.1 Note on first order gauge invariance for non trivial scalar manifolds

The Lagrangian of a generic non-linear sigma model is:

$$\mathcal{L}/\sqrt{|g|} = \frac{1}{2} G_{ij}(\varphi_k)\partial_\mu\varphi_i\partial^\mu\varphi_j - V(\varphi_k)\,, \tag{B.1}$$

Here we choose a diagonal metric in the N-dimensional field space $G_{ij}(\varphi_k) = G_i(\varphi_k)\delta_{ij}$. Let us also arbitrarily decompose the potential $V(\varphi_k) = \sum_i V^{(i)}(\varphi_k)$. Let us split the fields in background and fluctuation components $\varphi_i(x^\mu) = \phi_i(x^0) + \delta\phi_i(x^\mu)$.

The background evolution in a FLRW space-time with scale factor a such that $H = \dot{a}/a$ is given by (not using the covariant description in field space)

$$G_i\ddot{\phi}_i + 3HG_i\dot{\phi}_i + \sum_j G_{i,j}\dot{\phi}_i\dot{\phi}_j - \frac{1}{2}\sum_j G_{j,i}\dot{\phi}_j^2 + \sum_j V_{,i}^{(j)} = 0\,. \tag{B.2}$$

Let us define the background density and pressure components of the system as

$$\begin{aligned} \rho_{0i} &= \frac{1}{2}G_i\dot{\phi}_i^2 + V^{(i)}\,, \\ P_{0i} &= \frac{1}{2}G_i\dot{\phi}_i^2 - V^{(i)}\,, \end{aligned} \tag{B.3}$$

which sum up to the total quantities $\rho_0 = \sum_i \rho_{0i}$ and $P_0 = \sum_i P_{0i}$.

Using the EOM (B.2) one finds

$$\begin{aligned}\dot{\rho}_{0i} &= \frac{1}{2}\sum_j G_{i,j}\dot{\phi}_j\dot{\phi}_i^2 + G_i\dot{\phi}_i\ddot{\phi}_i + \sum_j V_{,j}^{(i)}\dot{\phi}_j \\ &= -3HG_i\dot{\phi}_i^2 - \frac{1}{2}\sum_j G_{i,j}\dot{\phi}_j\dot{\phi}_i^2 + \frac{1}{2}\sum_j G_{j,i}\dot{\phi}_j^2\dot{\phi}_i + \sum_j\left(V_{,j}^{(i)}\dot{\phi}_j - V_{,i}^{(j)}\dot{\phi}_i\right) \quad \text{(B.4)}\end{aligned}$$

Then one can trivially verify

$$\dot{\rho}_0 = \sum_i \dot{\rho}_{0i} = -3HG_i\dot{\phi}_i^2 = -3H(\rho_0 + P_0) \quad \text{(B.5)}$$

Moving to the density fluctuations we can write

$$\delta\rho_i = -\Phi G_i\dot{\phi}_i^2 + \frac{1}{2}\sum_j G_{i,j}\dot{\phi}_i^2\delta\phi^j + G_i\dot{\phi}_i\delta\dot{\phi}_i + \sum_j V_{,j}^{(i)}\delta\phi_j\,. \quad \text{(B.6)}$$

Let us consider a gauge transformation, induced by a change of reference frame $x^\mu \to \tilde{x}^\mu = x^\mu + \xi^\mu$. A change in the time component gives at linear order

$$\delta\tilde{\phi}_i = \delta\phi_i - \dot{\phi}_i\xi^0, \quad \tilde{\Phi} = \Phi - \dot{\xi}^0, \quad \tilde{\Psi} = \Psi + H\xi^0\,, \quad \text{(B.7)}$$

where Φ and Ψ are the two metric scalar fluctuations with no derivatives in g_{00} and g_{ii}, respectively.

The change in the density fluctuations goes as follow

$$\begin{aligned}\delta\tilde{\rho}_i &= -\tilde{\Phi}G_i\dot{\phi}_i^2 + \frac{1}{2}\sum_j G_{i,j}\dot{\phi}_i^2\delta\tilde{\phi}^j + G_i\dot{\phi}_i\delta\dot{\tilde{\phi}}_i + \sum_j V_{,j}^{(i)}\delta\tilde{\phi}_j \\ &= -(\Phi - \dot{\xi}^0)G_i\dot{\phi}_i^2 + \frac{1}{2}\sum_j G_{i,j}\dot{\phi}_i^2(\delta\phi_j - \dot{\phi}_j\xi^0) + G_i\dot{\phi}_i(\delta\dot{\phi}_i - \dot{\phi}_i\dot{\xi}^0 - \ddot{\phi}_i\xi^0) \quad \text{(B.8)} \\ &\quad + \sum_j V_{,j}^{(i)}(\delta\phi_j - \dot{\phi}_j\xi^0) \\ &= \delta\rho_i - \xi^0\dot{\rho}_{0i}\,, \quad \text{(B.9)}\end{aligned}$$

where again the EOM (B.2) have been used.

Therefore one can construct N distinct gauge invariant variables

$$\zeta_i = -\Psi - H\frac{\delta\rho_i}{\dot{\rho}_{0i}} \quad \text{(B.10)}$$

as well as $\frac{N(N-1)}{2}$ relative entropy gauge invariant perturbations

$$S_{ij} = 3(\zeta_i - \zeta_j) = -3H\left(\frac{\delta\rho_i}{\dot{\rho}_{0i}} - \frac{\delta\rho_j}{\dot{\rho}_{0j}}\right)\,. \quad \text{(B.11)}$$

B.2 Perturbation theory in curved field space

Let us start by considering the most generic perturbed line element

$$ds^2 = -(1+2\Phi)dt^2 + 2aB_i dt dx^i + a^2\left[(1-2\Psi)\delta_{ij} + E_{ij}\right]dx^i dx^j\,. \tag{B.12}$$

Combining metric perturbations with scalar fields perturbations

$$\phi^\alpha = \bar{\phi}^\alpha + \delta\phi^\alpha \tag{B.13}$$

we can compute the perturbed Einstein equations as (using natural units, i.e. $M_p = 1$):

$$\delta G^\nu_\mu = \delta T^\nu_\mu\,. \tag{B.14}$$

Considering a curved field space, we list the resulting equations in the following lines. In order to simplify the notation we will refer to background quantities $\bar{\phi}$ simply as ϕ. The $(0,0)$ component of Eq. (B.14) gives

$$\begin{aligned}\left(6H\partial_t - 2\frac{\partial_{kk}}{a^2}\right)\Psi + 2H\frac{\partial_{kk}B}{a} + \left(6H^2 - \dot{\phi}_A\dot{\phi}^A\right)\Phi - \frac{1}{2a^2}\partial_{ki}E_{ki} + \\ + V_A\delta\phi^A + \dot{\phi}^A G_{AB}\dot{\delta\phi}^B + \frac{1}{2}\dot{\phi}^A\dot{\phi}^B G_{AB,C}\delta\phi^C = 0\,.\end{aligned} \tag{B.15}$$

From component $(i,0)$ we get

$$2\partial_i\dot{\Psi} + 2H\partial_i\Phi + \frac{1}{2}\partial_j\dot{E}_{ij} - \dot{\phi}^A G_{AB}\partial_i\delta\phi^B = 0\,. \tag{B.16}$$

The spatial components (i,j) in case of $i \neq j$ give rise to

$$\begin{aligned}\frac{\partial_i\partial_j\Psi}{a^2} - \frac{\partial_i\partial_j\Phi}{a^2} + \left(\frac{\partial_{tt}}{2} + \frac{3}{2}H\partial_t - \frac{\partial_{kk}}{2a^2}\right)E_{ij} + \frac{\partial_{ik}E_{jk}}{2a^2} + \\ + \frac{\partial_{jk}E_{ik}}{2a^2} - \frac{1}{a}\left(\partial_t + 2H\right)\partial_{ij}B = 0\,,\end{aligned} \tag{B.17}$$

while if $i = j$ we find

$$\begin{aligned}\left(6\partial_{tt} - 2\frac{\partial_{ii}}{a^2} + 18H\partial_t\right)\Psi + \frac{2}{a}\left(\partial_t + 2H\right)\partial_{kk}B + \\ \left(2\frac{\partial_{ii}}{a^2} + 6H\partial_t + 6H^2 + 12\frac{\ddot{a}}{a} + 3\dot{\phi}^A\dot{\phi}_A\right)\Phi - \frac{1}{2}\frac{\partial_{ki}E_{ik}}{a^2} + \\ + 3\left(V_A\delta\phi^A - \dot{\delta\phi}^A\dot{\phi}^B G_{AB} - \dot{\phi}^A\dot{\phi}^B G_{AB,C}\delta\phi^C\right) = 0\,.\end{aligned} \tag{B.18}$$

In what follows we use the spatially flat gauge, $E = \Psi = 0$, that represents the more convenient setup for computing inflationary perturbations.

After two spatial integrations and fixing arbitrary integration functions of time to zero, the component (i, j) with $i \neq j$ reduces to

$$\Phi + 2\dot{a}B + a\dot{B} = 0\,. \tag{B.19}$$

After one spatial integration, component $(0, i)$ becomes

$$H\Phi = \frac{1}{2}\dot{\phi}_\alpha \delta\phi^\alpha\,. \tag{B.20}$$

Finally, the component $(0, 0)$ is given by

$$6\Phi\left(\tfrac{\dot{a}}{a}\right)^2 + 2\tfrac{\dot{a}}{a^2}B_{ii} \;\; = \Phi\dot{\phi}_\alpha\dot{\phi}^\alpha - \dot{\phi}_\alpha\dot{\delta\phi}^\alpha - \tfrac{1}{2}\dot{\phi}^\alpha\dot{\phi}^\beta\partial_\sigma G_{\alpha\beta}\delta\phi^\sigma - V_\alpha\delta\phi^\alpha \tag{B.21}$$

and, making use of the previous equations, becomes:

$$\tfrac{\partial_i\partial_i B}{a} = \;\; \tfrac{1}{2H}\left[\tfrac{(\dot{\phi})^2}{2H}\dot{\phi}_\beta - 3H\dot{\phi}_\beta - \tfrac{1}{2}G_{\rho\sigma,\beta}\dot{\phi}^\rho\dot{\phi}^\sigma - V_\beta\right]\delta\phi^\beta - \tfrac{1}{2H}\dot{\phi}_\beta\dot{\delta\phi}^\beta \quad . \tag{B.22}$$

Working in the spatially flat gauge, the Mukhanov-Sasaki variables coincide with field perturbations:

$$Q^\alpha \equiv \delta\phi^\alpha - \frac{\dot{\phi}^\alpha}{H}\Psi \equiv \delta\phi^\alpha \tag{B.23}$$

and the Klein-Gordon equation for perturbations is given by

$$\begin{aligned} &D_t D_t Q^\omega - \tfrac{\partial_i\partial_i}{a^2}Q^\omega + 3H D_t Q^\omega + \Big[R^\omega_{\rho\alpha\sigma}\dot{\phi}^\rho\dot{\phi}^\sigma + G^{\omega\lambda}V_{;\lambda\alpha} \\ &+\tfrac{1}{H}\left(\dot{\phi}_\alpha V^\omega + V_\alpha\dot{\phi}^\omega\right) + \dot{\phi}_\alpha\dot{\phi}^\omega\left(3 - \tfrac{(\dot{\phi})^2}{2H^2}\right)\Big]Q^\alpha = 0 \end{aligned} \tag{B.24}$$

where $D_t X^a = \partial_t X^a + \Gamma^a_{bc}X^b\dot{\phi}^c$ and $V_{;\lambda\alpha} = V_{\lambda\alpha} - \Gamma^\beta_{\lambda\alpha}V_\beta$ are referred to covariant derivatives and $R^\omega_{\rho\alpha\sigma}$ is the Riemann tensor related to the field space. This is the well-known gauge invariant equation for field perturbations [182].

B.2.1 Two inequivalent quantisations

We then move to the quantisation of the perturbation modes. Given that neither the mass matrix, nor the kinetic terms of Eq. (B.24) are diagonal, we need to find a way to perform canonical quantisation. Two different approaches are widely spread in the literature but they do not lead to the same results. We call them field basis method (see e.g. [195]) and kinetic basis method (see e.g. [193]), since the main difference between these two approaches is the moment in which perturbations are projected into normal and tangent components to the background inflationary trajectory. Another important difference is given by the normalisation conditions, i.e. the choice of field perturbations that should be initialised to a BD vacuum.

Field basis method To use this method we first need to define an independent set of canonical creation-annihilation operators $\hat{a}_\alpha$ that satisfies

$$[\hat{a}_\alpha(\mathbf{k}), \hat{a}_{\beta\dagger}(\mathbf{p})] = (2\pi)^3 \delta_{\alpha\beta}\delta(\mathbf{k}-\mathbf{p})\,, \qquad \alpha = 1, \ldots, N\,. \tag{B.25}$$

The number of operators is equal to the dimensionality of the field space. After that we expand each mode $\hat{Q}^\alpha$ on this basis:

$$\begin{aligned} \hat{Q}^\alpha(\mathbf{k}, t) &= \tilde{Q}^{\alpha\beta}(\mathbf{k}, t)\, \hat{a}_\beta(\mathbf{k})\,, \\ \hat{Q}^{\alpha\dagger}(\mathbf{k}, t) &= \tilde{Q}^{\alpha\beta *}(\mathbf{k}, t)\, \hat{a}^\dagger_\beta(\mathbf{k})\,. \end{aligned} \tag{B.26}$$

The equations of motion for the new modes $\tilde{Q}^{\omega\gamma}$ are given by:

$$\begin{aligned} &D_t D_t \tilde{Q}^{\omega\gamma} - \tfrac{\partial_i \partial_i}{a^2}\tilde{Q}^{\omega\gamma} + 3H D_t \tilde{Q}^{\omega\gamma} + \Big[R^\omega_{\rho\alpha\sigma}\dot{\phi}^\rho \dot{\phi}^\sigma + G^{\omega\lambda} V_{;\lambda\alpha} \\ &+ \tfrac{1}{H}\left(\dot{\phi}_\alpha V^\omega + V_\alpha \dot{\phi}^\omega\right) + \dot{\phi}_\alpha \dot{\phi}^\omega \left(3 - \tfrac{(\dot{\phi})^2}{2H^2}\right)\Big] \tilde{Q}^{\alpha\gamma} = 0\,. \end{aligned} \tag{B.27}$$

Rephrasing the previous equations in terms of

$$v^{\omega\gamma} = a\tilde{Q}^{\omega\gamma} \tag{B.28}$$

we get

$$D_\tau D_\tau v^{\omega\gamma} + \left(k^2 - \frac{a''}{a}\right) v^{\omega\gamma} + M^\omega_\alpha v^{\alpha\gamma} = 0\,, \tag{B.29}$$

where τ denotes conformal time, i.e. $d\tau \equiv a dt$, and

$$\begin{aligned} M^\omega_\alpha = a^2 \;\; &\big[2H^2 \epsilon R^\omega_{\rho\alpha\sigma} T^\rho T^\sigma + G^{\omega\lambda} V_{;\lambda\alpha} + \sqrt{2\epsilon}(T_\alpha V^\omega + V_\alpha T^\omega) \\ &+ 2\epsilon H^2 (3-\epsilon) T_\alpha T^\omega\big]\,. \end{aligned} \tag{B.30}$$

Finding the perturbation spectrum requires to set the initial conditions in Eq.(B.30). We set BD conditions for $\tilde{Q}^{\omega\gamma}$ in the far past. This implies that we need to choose the basis such that $\tilde{Q}^{\omega\gamma}$ are originally diagonal in the far past and the mode matrix satisfies

$$\frac{d^2 v^{\omega\gamma}}{d\tau^2} + k^2 v^{\omega\gamma} = 0\,. \tag{B.31}$$

We can then safely set

$$\lim_{\tau\to-\infty} v^{\omega\gamma}(k,\tau) = \frac{\delta_{\omega\gamma}}{\sqrt{2k}} e^{-ik\tau}\,. \tag{B.32}$$

Finding a solution for field perturbations allows us to compute the power spectrum tensor as

$$\mathcal{P}^{\alpha\beta} = \frac{k^3}{2\pi^2 a^2} v^{\alpha\gamma}(k, N) v^{*\beta\gamma}(k, N)\,. \tag{B.33}$$

In order to define the comoving curvature and isocurvature power spectra, we need to define a set of tangent and normal projectors onto the background trajectory. In a two-field system we get

$$T^\alpha = \frac{1}{|\dot\phi|}\dot\phi^\alpha\,, \qquad N_\alpha T^\alpha = 0\,, \qquad N_\alpha N^\alpha = 1\,, \tag{B.34}$$

where $|\dot\phi| = \sqrt{G_{\alpha\beta}\dot\phi^\alpha\dot\phi^\beta}$. Since we are considering a 2-dimensional field space, these projectors are related to the field space metric as follows

$$G^{\alpha\beta} = T^\alpha T^\beta + N^\alpha N^\beta\,. \tag{B.35}$$

The curvature perturbation on comoving hypersurfaces $\mathcal{R}$ and the isocurvature perturbations $\mathcal{S}$ are related to the field perturbations as

$$\mathcal{R} = \frac{H}{|\dot\phi|}T_\alpha\hat Q^\alpha\,, \qquad \mathcal{S} = \frac{H}{|\dot\phi|}N_\alpha\hat Q^\alpha\,. \tag{B.36}$$

Then, the adiabatic curvature power spectrum $\mathcal{P}_\mathcal{R}$ can be found projectiong $\mathcal{P}^{\alpha\beta}$ along the tangent vector T_α as

$$\mathcal{P}_\mathcal{R} = \frac{1}{2\epsilon}T_\alpha T_\beta\mathcal{P}^{\alpha\beta}\,. \tag{B.37}$$

On the other hand, the isocurvature power spectrum $\mathcal{P}_\mathcal{S}$ arises from the projection of $\mathcal{P}^{\alpha\beta}$ along the normal direction to the inflationary background trajectory, N_α, as

$$\mathcal{P}_\mathcal{S} = \frac{1}{2\epsilon}N_\alpha N_\beta\mathcal{P}^{\alpha\beta}\,. \tag{B.38}$$

Kinetic basis method An alternative way to treat perturbations in multi-field inflationary models is to perform from the very beginning a field rotation into an adiabatic field, σ and isocurvature fields s_i. In case of a 2-field system, these are defined as

$$\delta\sigma = T_\alpha\delta\phi^\alpha\,, \qquad \delta s = N_\alpha\delta\phi^\alpha\,. \tag{B.39}$$

The relation between the covariant derivatives of T^α and N^α is given by

$$\frac{DT^\alpha}{dt} = -H\eta_\perp N^\alpha\,, \qquad \frac{DN^\alpha}{dt} = H\eta_\perp T^\alpha \tag{B.40}$$

where $DX^\alpha/dt = d/dt + \Gamma^\alpha_{\beta\gamma}X^\beta\dot\phi^\gamma$ and $\eta_\perp = \frac{N^\alpha V_\alpha}{\dot\phi_0 H}$. Starting form Eq. (B.24) and using the previous relations, we can easily find the equations of motion for $\delta\sigma$ and

δs. We write these equations in terms of $v^I = aQ^I = \{v^\sigma,\, v^s\}$ where $Q^I = \{\delta\sigma, \delta s\}$ and $i = 1, 2$:

$$\begin{aligned} &v^{\sigma''} + 2\zeta v^{s'} - \zeta^2 v^\sigma + \zeta' v^s + \Omega_{\sigma s} v^s + (\Omega_{\sigma\sigma} + k^2) v^\sigma = 0\,, \\ &v^{s''} - 2\zeta v^{\sigma'} - \zeta^2 v^s - \zeta' v^\sigma + \Omega_{\sigma s} v^\sigma + (k^2 + \Omega_{ss}) v^s = 0\,, \end{aligned} \tag{B.41}$$

where $' = d/d\tau$ and

$$\begin{aligned} \Omega_{\sigma\sigma} &= -a^2H^2(2 + 2\epsilon - 3\eta_\parallel + \eta_\parallel\xi_\parallel - 4\epsilon\eta_\parallel + 2\epsilon^2 - \eta_\perp^2)\,, \\ \Omega_{ss} &= -a^2H^2(2 - \epsilon) + a^2(V_{;ss} + H^2\epsilon R)\,, \\ \Omega_{\sigma s} &= a^2H^2\eta_\perp(3 + \epsilon - 2\eta_\parallel - \xi_\perp)\,. \end{aligned} \tag{B.42}$$

Again, we need to define a normal set of creation and annihilation operators such that

$$[\hat{a}_\alpha(\mathbf{k}), \hat{a}^\dagger_\beta(\mathbf{p})] = (2\pi)^3\delta_{\alpha\beta}\delta(\mathbf{k} - \mathbf{p})\,, \qquad \alpha, \beta = 1, 2 \tag{B.43}$$

so that we can expand density and isocurvature perturbations as:

$$\hat{v^I}(\mathbf{k}, \tau) = \tilde{v}^{I\alpha}(\mathbf{k}, \tau)\, \hat{a}_\alpha(\mathbf{k}) \tag{B.44}$$

where $\tilde{v}^{I\alpha} = \{(v^\sigma)^\alpha\,,\, (v^s)^\alpha\}$. We set the BD initial conditions as

$$\lim_{\tau\to-\infty} v^{I\alpha}(\mathbf{k}, \tau) = \frac{\delta_{I\alpha}}{\sqrt{2k}} e^{-ik\tau}\,. \tag{B.45}$$

The power spectrum related to tangent and normal perturbations is then given by

$$\mathcal{P}^{IJ} = \frac{k^3}{2\pi^2 a^2}\tilde{v}^{I\gamma}(k, N)\tilde{v}^{*J\gamma}(k, N)\,. \tag{B.46}$$

Given that the renormalised curvature and entropy perturbations are

$$\mathcal{R}_k = \frac{H}{|\dot{\phi}|}\delta\sigma \qquad \mathcal{S}_k = \frac{H}{|\dot{\phi}|}\delta s\,, \tag{B.47}$$

the comoving density and the isocurvature power spectra can be written as

$$\mathcal{P}_\mathcal{R}(\mathbf{k}, \tau) = \frac{1}{2\epsilon}\mathcal{P}^{\sigma\sigma}(\mathbf{k}, \tau)\,, \qquad \mathcal{P}_\mathcal{S}(\mathbf{k}, \tau) = \frac{1}{2\epsilon}\mathcal{P}^{ss}(\mathbf{k}, \tau)\,. \tag{B.48}$$

Different Normalisations We can easily compare the BD normalisation procedure used in the two methods. The relation between the perturbation variables is given by

$$v^{\alpha} = T^{\alpha} v^{\sigma} + N^{\alpha} v^{s} \,, \tag{B.49}$$

from which we can conclude that

$$|v|^2 = v_{\alpha} v^{\alpha *} = (v^{\sigma})^2 + (v^{s})^2, \,. \tag{B.50}$$

Nevertheless, expanding the two basis on the same set of orthogonal creation and annihilation operators we get:

$$v^{\alpha\beta} = T^{\alpha} v^{\sigma\beta} + N^{\alpha} v^{s\beta} \,. \tag{B.51}$$

The first approach requires that

$$\lim_{\tau\to-\infty} |v^{\alpha\beta}(k,\tau)| = \frac{\delta_{\alpha\beta}}{\sqrt{2k}} \quad \rightarrow \quad \lim_{\tau\to-\infty} |v^{11}(k,\tau)| = \lim_{\tau\to-\infty} |v^{22}(k,\tau)| = \frac{1}{\sqrt{2k}} \,, \tag{B.52}$$

while the second approach implies

$$\lim_{\tau\to-\infty} |v^{I\beta}(k,\tau)| = \frac{\delta_{I\beta}}{\sqrt{2k}} \quad \rightarrow \quad \lim_{\tau\to-\infty} |(v^{\sigma})^1(k,\tau)| = \lim_{\tau\to-\infty} |(v^{s})^2(k,\tau)| = \frac{1}{\sqrt{2k}} \,. \tag{B.53}$$

The discrepancy between the different normalisation prescriptions becomes apparent when the tangent and normal vector components become dynamically ill-defined, i.e. they tend to zero or explode to infinity. This is precisely what happens in the 2-field system that we analyse in Sec. 4.6.3. Here We focus for simplicity on the right-left fibre inflation case where the θ_1 massless axion induces the geometrical instability of the system. in this case the tangent and normal vector asymptotically behave as

$$T^a = \left\{ \alpha_1, \frac{\alpha_2}{f} \right\} \rightarrow \{1, 0\} \,, \qquad N^a = \left\{ -\alpha_2, \frac{\alpha_1}{f} \right\} \rightarrow \left\{ 0, \frac{1}{f} \right\} \tag{B.54}$$

so that we find the following relation between perturbations in the two different schemes

$$v^{\sigma} \rightarrow v^{1} \,, \qquad v^{s} \rightarrow \frac{1}{f} v^{2} \,. \tag{B.55}$$

It is immediate to find out that the two approaches are not equivalent as

$$|v^{22}| \neq |(v^{s})^2| = \left| \frac{v^{22}}{f} \right| \,. \tag{B.56}$$

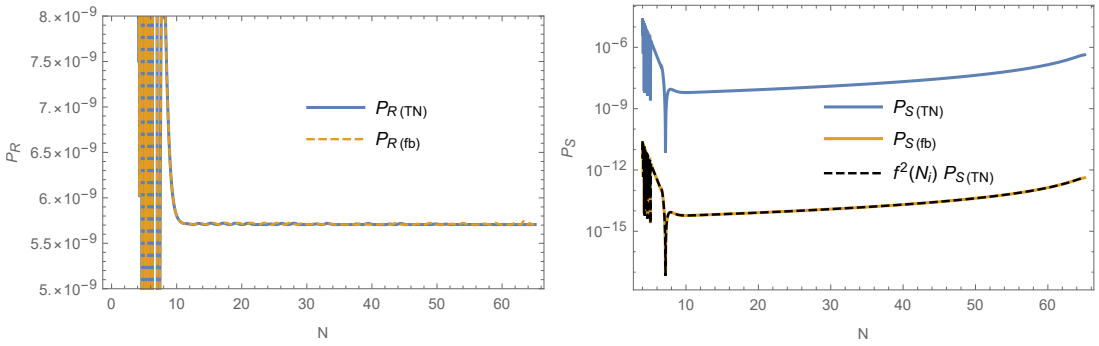

Figure B.1: Power spectra behaviour of the right-left Fibre inflation model presented in Sec. 4.6.3 in case of massless θ_1 axion. We compare the results coming from the two methods presented in this appendix. Left plot is referred to the power spectrum of density perturbations, right plot contains the results of the isocurvature power spectrum. Orange lines are related to the field basis (fb) method while blue lines come from the kinetic basis (TN) method. We also numerically checked the relation in Eq. (B.56): $P_{S\,(fb)} = f^2(N_i)P_{S\,(TN)}$ where N_i is the initial simulation time where we set Bunch-Davies conditions.

Indeed, studying perturbations using the two methods in case of FI leads to the results presented in Figure B.1 where we see that, while the results on $P_{\mathcal{R}}$ coincide, those ones related to $P_{\mathcal{S}}$ differ by many orders of magnitude. Indeed, despite the evolution of the isocurvature power spectrum is very similar in the two approaches, the different choice of initial conditions leads to very huge discrepancies in case of "ill-defined" tangent and normal projectors.

Entropy from non-adiabatic pressure

Considering the system described by Eq. (B.1), we can write down the total background energy and pressure as

$$\rho = \frac{1}{2}\dot{\phi}_\alpha\dot{\phi}^\alpha + V(\phi)\,, \tag{B.57}$$

$$P = \frac{1}{2}\dot{\phi}_\alpha\dot{\phi}^\alpha - V(\phi)\,. \tag{B.58}$$

Computing cosmological perturbations as described in Appendix B.2 and using the spatially flat gauge, $E = \Psi = 0$, we can write down energy density and pressure perturbations

$$\delta\rho = -\delta T^0_0 = -\Phi\dot{\phi}_\alpha\dot{\phi}^\alpha + \dot{\phi}_\alpha\delta\dot{\phi}^\alpha + \frac{1}{2}\dot{\phi}^\alpha\dot{\phi}^\beta\partial_\sigma G_{\alpha\beta}\delta\phi^\sigma + V_\alpha\delta\phi^\alpha\,, \tag{B.59}$$

$$\delta P = \delta T^i_i = -\Phi\dot{\phi}_\alpha\dot{\phi}^\alpha + \dot{\phi}_\alpha\dot{\delta\phi}^\alpha + \frac{1}{2}\dot{\phi}^\alpha\dot{\phi}^\beta\partial_\sigma G_{\alpha\beta}\delta\phi^\sigma - V_\alpha\delta\phi^\alpha\,. \tag{B.60}$$

The adiabatic sound speed, given by $c_s^2 = \frac{\dot{P}}{\dot{\rho}}$, takes the following form:

$$c_s^2 = 1 + \frac{2}{3H}\frac{V_\alpha\dot{\phi}^\alpha}{\dot{\phi}_\gamma\dot{\phi}^\gamma} \tag{B.61}$$

and the non-adiabatic pressure, $\delta P_{\rm nad} = \delta P - c_s^2\delta\rho$, is given by

$$\delta P_{\rm nad} = \ -2V_\alpha\delta\phi^\alpha + \tfrac{2}{3H}\tfrac{V_\lambda\dot{\phi}^\lambda}{\dot{\phi}_\gamma\dot{\phi}^\gamma}\left[\Phi\dot{\phi}_\alpha\dot{\phi}^\alpha - \dot{\phi}_\alpha\dot{\delta\phi}^\alpha - \tfrac{1}{2}\dot{\phi}^\alpha\dot{\phi}^\beta\partial_\sigma G_{\alpha\beta}\delta\phi^\sigma - V_\alpha\delta\phi^\alpha\right]. \tag{B.62}$$

Using Eq. (B.20) and considering the number of e-foldings as time variable, the previous equation can be written as:

$$\delta P_{\rm nad} = \ f_\alpha(\phi,\phi')\delta\phi^\alpha + g_\alpha(\phi,\phi')\delta\phi'^\alpha\,, \tag{B.63}$$

where $' = d/dN$ and

$$\begin{aligned} f_\alpha(\phi,\phi') &= \left[-2V_\alpha + \tfrac{V_\beta\phi'^\beta}{3\epsilon}\left(\epsilon\phi'_\alpha - \tfrac{1}{2}\phi'^\rho\phi'^\sigma\partial_\alpha G_{\rho\sigma} - \tfrac{V_\alpha}{H^2}\right)\right], \\ g_\alpha(\phi,\phi') &= -\tfrac{V_\lambda\phi'^\lambda}{3\epsilon}\phi'_\alpha\,. \end{aligned} \tag{B.64}$$

The entropy perturbation coming from non-adiabatic pressure is defined to be:

$$\mathcal{S}_{nad} = \frac{1}{P'}\delta P_{nad} \tag{B.65}$$

where the pressure time derivative of the system is given by

$$P' = -\left(3H^2 G_{\alpha\beta}\phi'^\alpha\phi'^\beta + 2V_\beta\phi'^\beta\right). \tag{B.66}$$

We can finally compute the power spectrum of non-adiabatic entropy perturbations as

$$\mathcal{P}_{\mathcal{S}_{nad}} = \frac{k^2}{2\pi^2(P')^2}\left(f_\alpha\tilde{Q}^{\alpha\beta} + g_\alpha\tilde{Q}'^{\alpha\beta}\right)\left(f_\gamma\tilde{Q}^{*\gamma\beta} + g_\gamma\tilde{Q}'^{*\gamma\beta}\right), \tag{B.67}$$

where we made use of Eq. (B.26).

Moreover, giving the following equations that link field perturbations with the tangent and normal projectors

$$\begin{aligned} Q^\alpha &= T^\alpha\delta\sigma + N^\alpha\delta s\,, \\ Q^{\alpha'} &= \tfrac{dT^\alpha}{dN}\delta\sigma + T^\alpha\delta\sigma' + \tfrac{dN^\alpha}{dN}\delta s + N^\alpha\delta s'\,, \\ \tfrac{dT^\alpha}{dN} &= -\tfrac{V_N N^\alpha}{\phi'_0 H} - \phi'_0\Gamma^\alpha_{\beta\gamma}T^\beta T^\gamma\,, \\ \tfrac{dN^\alpha}{dN} &= +\tfrac{V_N T^\alpha}{\phi'_0 H} - \phi'_0\Gamma^\alpha_{\beta\gamma}N^\beta T^\gamma\,, \end{aligned} \tag{B.68}$$

we can write $\mathcal{S}_{nad}$ as a function of perturbations in the kinetic basis

$$\mathcal{S}_{nad} = \frac{1}{\left(3H^2\epsilon+\phi_0' V_T\right)}\left[V_T\left(1+\frac{V_T}{3\phi_0' H^2}-\frac{\epsilon}{3}\right)\delta\sigma+\frac{V_T}{3}\delta\sigma'\right]+\frac{V_N\delta s}{3H^2\epsilon}\,, \tag{B.69}$$

where $V_T = V_\alpha T^\alpha$ and $V_N = V_\alpha N^\alpha$.

Appendix C

Detailed computations on 3.55 keV line

C.1 Closed string axion decay constants

In type IIB string compactifications on Calabi-Yau orientifolds axion-like particles emerge in the low-energy $N = 1$ effective field theory from the dimensional reduction of the Ramond-Ramond forms C_p with $p = 2, 4$. The Kaluza-Klein decomposition under the orientifold projection of these forms is given by [35]:

$$C_2 = c^{i_-}(x)\,\hat{D}_{i_-} \quad \text{and} \quad C_4 = c_{i_+}(x)\tilde{D}^{i_+} + Q_2^{i_+}(x)\wedge\hat{D}_{i_+} + V^{a_+}(x)\wedge\alpha_{a_+} - \tilde{V}_{a_+}(x)\wedge\beta^{a_+}\,,$$

where $i_\pm = 1, ..., h^{1,1}_\pm$, $a_+ = 1, ..., h^{1,2}_+$, $\tilde{D}^{i_+}$ is a basis of $H^{2,2}_+$ dual to the $(1,1)$-forms $\hat{D}_{i_+}$ and $(\alpha_{a_+}, \beta^{a_+})$ is a real, symplectic basis of $H^3_+ = H^{1,2}_+ \oplus H^{2,1}_+$.

As explained in Sec. 5.5.1, in our model the orientifold-odd axions c_{i_-}, if present, are eaten up by anomalous $U(1)$'s in the process of anomaly cancellation. We shall therefore focus on the case with $h^{1,1}_- = 0$ where the Kähler moduli take the simple expression $T_i = \tau_i + \mathrm{i}\,c_i$ with $i = 1, ..., h^{1,1}_+ = h^{1,1}$.

The coupling of orientifold-even closed string axions to $F \wedge F$ can be derived from the Kaluza-Klein reduction of the Chern-Simons term of the D-brane action. Moreover, the periods of the canonically unnormalised axions c_i are integer multiples of M_p and their kinetic terms read [76]:

$$\mathcal{L}_{\text{kin}} = K_{ij}\partial_\mu c_i \partial^\mu c_j = \frac{1}{8}\,\eta_i\,\partial_\mu c_i' \partial^\mu c_i'\,, \tag{C.1}$$

where the c_i''s are the axions which diagonalise the Kähler metric K_{ij} and η_i are its eigenvalues. A proper canonical normalisation of the kinetic terms can then be easily obtained by defining:

$$\frac{1}{8}\,\eta_i \partial_\mu c_i' \partial^\mu c_i' \equiv \frac{1}{2}\,\partial_\mu a_i \partial^\mu a_i \qquad \text{with} \qquad a_i = \frac{1}{2}\,\sqrt{\eta_i}\,c_i'\,, \tag{C.2}$$

which shows that the canonically normalised axions a_i acquire periods of the form:

$$\frac{2}{\sqrt{\eta_i}}\, a_i = \frac{2}{\sqrt{\eta_i}}\, a_i + M_p \qquad \Rightarrow \qquad a_i = a_i + \frac{\sqrt{\eta_i}}{2}\, M_p\,. \tag{C.3}$$

We can then set the conventional axionic period as:

$$a_i = a_i + 2\pi f_{a_i} \qquad \text{with} \qquad f_{a_i} = \frac{\sqrt{\eta_i}\, M_p}{4\pi}\,, \tag{C.4}$$

where f_{a_i} is the standard axion decay constant. Closed string axions which propagate in the bulk of the extra dimensions have a decay constant of order the Kaluza-Klein scale $M_{KK} \sim M_p/\mathcal{V}^{2/3}$, whereas the decay constant of closed string axions whose corresponding saxion parameterises the volume of localised blow-up modes is controlled by the string scale $M_s \sim M_p/\sqrt{\mathcal{V}}$:

$$f_{a_i} \simeq \begin{cases} M_p/\tau_i \sim M_{KK} & \text{bulk axion} \\ M_p/\sqrt{\mathcal{V}} \sim M_s & \text{local axion} \end{cases} \tag{C.5}$$

Notice however that the axion coupling to the Abelian gauge bosons living on the D-brane wrapping the four-cycle whose volume is controlled by the associated saxion τ_i, is given by:

$$\frac{g_i^2}{32\pi^2}\, \frac{a_i}{f_{a_i}}\, F^{(i)}_{\mu\nu} \tilde{F}^{\mu\nu}_{(i)} = \frac{1}{32\pi^2}\, \frac{a_i}{\tau_i f_{a_i}}\, F^{(i)}_{\mu\nu} \tilde{F}^{\mu\nu}_{(i)}\,, \tag{C.6}$$

since the gauge coupling is set by the saxion as $g_i^2 = \tau_i$. Hence combining (C.5) with (C.6) we realise that that the coupling of bulk closed string axions to gauge bosons is controlled by $M \sim \tau_i f_{a_i} \sim M_p$, in agreement with the fact that moduli couple to ordinary matter with gravitational strength. On the other hand the coupling of local closed string axions to gauge bosons is set by the string scale M_s which in LVS models with exponentially large volume can be considerably smaller than the Planck scale.

C.2 Canonical normalisation

The kinetic terms for all Kähler moduli and the charged open string modes ϕ and C can be derived from the total Kähler potential $K = K_{\rm mod} + K_{\rm matter}$, where $K_{\rm mod}$ is given by the three contributions in (5.40) and $K_{\rm matter}$ is shown in (5.41) and (5.42), as follows:

$$\mathcal{L}_{\rm kin} = \frac{\partial^2 K}{\partial\chi_i \partial\bar{\chi}_{\bar{j}}}\, \partial_\mu \chi_i \partial^\mu \bar{\chi}_{\bar{j}}\,, \tag{C.7}$$

where χ_i denotes an arbitrary scalar field of our model. As can be seen from (5.41), the D7 open string mode ϕ mixes only with the dilaton S, and so can be easily written in terms of the corresponding canonically normalised field $\hat{\phi}$ as:

$$\frac{\hat{\phi}}{M_p} = \sqrt{\frac{2}{\mathrm{Re}(S)}}\,\phi\,. \tag{C.8}$$

From the first term in (5.40) we also realise that cross-terms between the blow-up mode τ_{q_i} and any of the other Kähler moduli are highly suppressed when evaluated at the minimum for $\tau_{q_i} \simeq 0$ (more precisely, as discussed in Sec. 5.5.3, depending on the level of sequestering of soft masses, we can have either $\tau_{q_i} \sim \mathcal{V}^{-1} \ll 1$ or $\tau_{q_i} \sim \mathcal{V}^{-3} \ll 1$). Hence it is straightforward to write also τ_{q_i} in terms of the corresponding canonically normalised field ϕ_{q_i} as:

$$\frac{\phi_{q_i}}{M_p} = \frac{\tau_{q_i}}{\sqrt{\mathcal{V}}} \qquad \text{for} \quad i = 1, 2\,. \tag{C.9}$$

The remaining fields T_b, T_s, T_p and C mix with each other, leading to a non-trivial Kähler metric whose components take the following leading order expressions for $\mathcal{V} \simeq \lambda_b \tau_b^{3/2} \gg 1$:

$$\begin{aligned}
K_{T_i\bar{T}_{\bar{j}}} &\simeq \frac{3}{8\mathcal{V}} \begin{pmatrix} \frac{2\lambda_b}{\sqrt{\tau_b}} & -\frac{3}{\tau_b}\left(\lambda_s\sqrt{\tau_s} + x\lambda_p\sqrt{\tilde{\tau}_p}\right) & -\frac{3}{\tau_b}\,\lambda_p\sqrt{\tilde{\tau}_p} \\ -\frac{3}{\tau_b}\left(\lambda_s\sqrt{\tau_s} + x\lambda_p\sqrt{\tilde{\tau}_p}\right) & \frac{\lambda_s}{\sqrt{\tau_s}} + \frac{x^2\lambda_p}{\sqrt{\tilde{\tau}_p}} & \frac{x\lambda_p}{\sqrt{\tilde{\tau}_p}} \\ -\frac{3}{\tau_b}\,\lambda_p\sqrt{\tilde{\tau}_p} & \frac{x\lambda_p}{\sqrt{\tilde{\tau}_p}} & \frac{\lambda_p}{\sqrt{\tilde{\tau}_p}} \end{pmatrix} \\
K_{T_b\bar{C}} &\simeq -\frac{\tilde{K}}{2\,\tau_b}\,C\,, \qquad K_{T_s\bar{C}} \simeq \frac{\tilde{K}}{2\mathcal{V}}\left(\lambda_s\sqrt{\tau_s} + x\lambda_p\sqrt{\tilde{\tau}_p}\right)C\,, \\
K_{T_p\bar{C}} &\simeq \frac{\tilde{K}}{2\mathcal{V}}\,\lambda_p\sqrt{\tilde{\tau}_p}\,C\,, \qquad K_{C\bar{C}} = \tilde{K}\,.
\end{aligned}$$

In the large volume limit, different contributions to the kinetic Lagrangian can be organised in an expansion in $1/\mathcal{V} \ll 1$ as follows:

$$\mathcal{L}_{\rm kin} = \mathcal{L}_{\rm kin}^{\mathcal{O}(1)} + \mathcal{L}_{\rm kin}^{\mathcal{O}(\mathcal{V}^{-1})} + \mathcal{L}_{\rm kin}^{\mathcal{O}(\mathcal{V}^{-4/3})}\,,$$

where, trading T_p for $\tilde{T}_p = T_p + xT_s$, we have:

$$\begin{aligned}
\mathcal{L}_{\rm kin}^{\mathcal{O}(1)} &= \frac{3}{4\,\tau_b^2}\,\partial_\mu\tau_b\partial^\mu\tau_b\,,\\
\mathcal{L}_{\rm kin}^{\mathcal{O}(\mathcal{V}^{-1})} &= \frac{3}{8\mathcal{V}}\left[\frac{\lambda_s}{\sqrt{\tau_s}}\left(\partial_\mu\tau_s\partial^\mu\tau_s+\partial_\mu c_s\partial^\mu c_s\right)+\frac{\lambda_p}{\sqrt{\tilde{\tau}_p}}\left(\partial_\mu\tilde{\tau}_p\partial^\mu\tilde{\tau}_p+\partial_\mu\tilde{c}_p\partial^\mu\tilde{c}_p\right)\right]\\
&- \frac{9}{4\mathcal{V}}\frac{\partial_\mu\tau_b}{\tau_b}\left(\lambda_s\sqrt{\tau_s}\,\partial^\mu\tau_s+\lambda_p\sqrt{\tilde{\tau}_p}\,\partial^\mu\tilde{\tau}_p\right)\,,\\
\mathcal{L}_{\rm kin}^{\mathcal{O}(\mathcal{V}^{-4/3})} &= \frac{3}{4\,\tau_b^2}\,\partial_\mu c_b\partial^\mu c_b\,.
\end{aligned}$$

At leading order the kinetic terms become canonical if τ_b is replaced by ϕ_b defined as:

$$\frac{\phi_b}{M_p} = \sqrt{\frac{3}{2}}\,\ln\tau_b\,, \tag{C.10}$$

whereas $\mathcal{L}_{\rm kin}^{\mathcal{O}(\mathcal{V}^{-1})}$ becomes diagonal if the small modulus T_s and the Wilson modulus $\tilde{T}_p$ are substituted by:

$$\begin{aligned}
\frac{\phi_s}{M_p} &= \sqrt{\frac{4\lambda_s}{3\mathcal{V}}}\,\tau_s^{3/4}\,, \qquad \frac{a_s}{M_p} = \sqrt{\frac{3\lambda_s}{4\mathcal{V}\sqrt{\tau_s}}}\,c_s\,,\\
\frac{\tilde{\phi}_p}{M_p} &= \sqrt{\frac{4\lambda_p}{3\mathcal{V}}}\,\tilde{\tau}_p^{3/4}\,, \qquad \frac{\tilde{a}_p}{M_p} = \sqrt{\frac{3\lambda_p}{4\mathcal{V}\sqrt{\tilde{\tau}_p}}}\,\tilde{c}_p\,,
\end{aligned} \tag{C.11}$$

and the canonical normalisation (C.10) for τ_b gets modified by the inclusion of a subleading mixing with τ_s and $\tilde{\tau}_p$ of the form:

$$\frac{\phi_b}{M_p} = \sqrt{\frac{3}{2}}\,\ln\tau_b - \sqrt{\frac{2}{3}}\,\frac{1}{\mathcal{V}}\left(\lambda_s\tau_s^{3/2}+\lambda_p\tilde{\tau}_p^{3/2}\right)\,. \tag{C.12}$$

Finally the kinetic term in $\mathcal{L}_{\rm kin}^{\mathcal{O}(\mathcal{V}^{-4/3})}$ are canonically normalised if the bulk axion c_b gets redefined as:

$$\frac{a_b}{M_p} = \sqrt{\frac{3}{2}}\frac{c_b}{\tau_b}\,. \tag{C.13}$$

The $U(1)$-charged open string mode C appears in the kinetic Lagrangian only at $\mathcal{O}(|C|^2\mathcal{V}^{-2/3})$ which according to (5.62) and (5.63) can scale as either $\mathcal{V}^{-8/3}$ or $\mathcal{V}^{-14/3}$. This part of the kinetic Lagrangian looks like:

$$\mathcal{L}_{\rm kin} \supset \tilde{K}\,|C|^2\left(\frac{\partial_\mu|C|}{|C|}\frac{\partial^\mu|C|}{|C|}+\partial_\mu\theta\partial^\mu\theta-\frac{\partial_\mu\tau_b}{\tau_b}\frac{\partial^\mu|C|}{|C|}\right)\,, \tag{C.14}$$

and becomes diagonal by redefining:

$$\frac{|\hat{C}|}{M_p} = \sqrt{2\tilde{K}}|C| \qquad \text{and} \qquad a_{ALP} = |\hat{C}|\theta = f_{a_{ALP}}\theta\,.$$

C.3 Mass matrix

As described in Sec. 5.5.1, the moduli stabilised at tree-level are τ_{q_i} and $|\phi|$ while the corresponding axions are eaten up by two anomalous $U(1)$'s. Given that they fixed at $\mathcal{O}(1/\mathcal{V}^2)$, all these modes develop a mass of order the string scale:

$$m_{\tau_{q_i}} \sim m_{c_{q_i}} \sim m_{|\phi|} \sim m_{\psi} \sim M_s = g_s^{1/4}\sqrt{\pi}\,\frac{M_p}{\sqrt{\mathcal{V}}}\,. \tag{C.15}$$

On the other hand, τ_b, τ_s, $\tilde{\tau}_p$ and the closed string axion c_s are stabilised at $\mathcal{O}(1/\mathcal{V}^3)$. The masses of the corresponding canonically normalised fields derived in App. C.2 are given by the eigenvalues of the mass matrix evaluated at the minimum of the $\mathcal{O}(1/\mathcal{V}^3)$ scalar potential. The leading order contributions of all the elements of this 4×4 matrix read:

$$\begin{aligned}
\frac{\partial^2 V}{\partial\phi_b\partial\phi_b} &= \left(\frac{g_s}{8\pi}\right)\frac{9\,\lambda_s\,\tau_s^{3/2}}{2}\frac{W_0^2}{\mathcal{V}^3}\,,\\
\frac{\partial^2 V}{\partial\phi_b\partial\phi_s} &= \left(\frac{g_s}{8\pi}\right)\frac{3\sqrt{2\lambda_s}\,\tau_s^{3/4}}{\sqrt{\mathcal{V}}}\left(\frac{W_0}{\mathcal{V}}\right)^2(2\pi\tau_s)\,,\\
\frac{\partial^2 V}{\partial\phi_s\partial\phi_s} &= \frac{\partial^2 V}{\partial a_s\partial a_s} = 4\left(\frac{g_s}{8\pi}\right)\left(\frac{W_0}{\mathcal{V}}\right)^2(2\pi\tau_s)^2\,,\\
\frac{\partial^2 V}{\partial\tilde{\phi}_p\partial\tilde{\phi}_p} &= \left(\frac{g_s}{8\pi}\right)\frac{1}{4z_p\tilde{\tau}_p}\left(\frac{W_0}{\mathcal{V}}\right)^2,\\
\frac{\partial^2 V}{\partial\phi_b\partial\tilde{\phi}_p} &= \frac{\partial^2 V}{\partial\phi_b\partial a_s} = \frac{\partial^2 V}{\partial\phi_s\partial\tilde{\phi}_p} = \frac{\partial^2 V}{\partial\phi_s\partial a_s} = \frac{\partial^2 V}{\partial\tilde{\phi}_p\partial a_s} = 0\,,
\end{aligned}$$

The eigenvalues of this mass matrix turn out to be:

$$\begin{aligned}
m_{\phi_s}^2 &= m_{a_s}^2 = 4\left(\frac{g_s}{8\pi}\right)\left(\frac{W_0}{\mathcal{V}}\right)^2(2\pi\tau_s)^2 \simeq m_{3/2}^2\,(\ln\mathcal{V})^2\,,\\
m_{\tilde{\phi}_p}^2 &= \left(\frac{g_s}{8\pi}\right)\frac{\pi}{2z_p}\left(\frac{W_0}{\mathcal{V}}\right)^2\frac{1}{2\pi\tilde{\tau}_p} \simeq \frac{m_{3/2}^2}{\ln\mathcal{V}} \qquad \text{and} \qquad m_{\phi_b}^2 = 0\,,
\end{aligned} \tag{C.16}$$

where the gravitino mass is given by:

$$m_{3/2}^2 = e^K\,|W|^2 \simeq \left(\frac{g_s}{8\pi}\right)\left(\frac{W_0}{\mathcal{V}}\right)^2. \tag{C.17}$$

The mass of the canonically normalised large modulus ϕ_b becomes non-zero once we include subleading $1/(2\pi\tau_s) \sim 1/\ln\mathcal{V} \ll 1$ corrections to the elements of the mass matrix, and scales as (with c an $\mathcal{O}(1)$ numerical coefficient):

$$m_{\phi_b}^2 = c\,\lambda_s \tau_s^{3/2} \left(\frac{g_s}{8\pi}\right) \frac{W_0^2}{\mathcal{V}^3} \frac{1}{2\pi\tau_s} \simeq \frac{m_{3/2}^2}{\mathcal{V}\ln\mathcal{V}}\,. \tag{C.18}$$

As explained in Sec. 5.5.3, the charged matter field $|C|$ is fixed by soft supersymmetry breaking contributions to the scalar potential and can acquire a mass of order $m_{3/2}/\sqrt{\mathcal{V}}$ or $m_{3/2}/\mathcal{V}$ depending on the level of sequestering. The corresponding phase $\theta = a_{ALP}/f_{a_{ALP}}$ behaves as an open string ALP which develops a mass of order:

$$m_{a_{ALP}} \sim \frac{\Lambda_{\rm hid}^2}{f_{a_{ALP}}} \sim \frac{\Lambda_{\rm hid}^2}{|\hat{C}|}\,, \tag{C.19}$$

where $\Lambda_{\rm hid}$ is the scale of strong dynamics effects in the hidden sector. In order to obtain a phenomenologically viable value $m_{a_{ALP}} \lesssim 10^{-12}$ eV, we need to have $\Lambda_{\rm hid} \lesssim 10^4$ eV if $f_{a_{ALP}} \sim m_{3/2} \sim 10^{10}$ GeV or $\Lambda_{\rm hid} \lesssim 1$ eV if $f_{a_{ALP}} \sim m_{3/2}/\mathcal{V} \sim 1$ TeV.

The DM axion c_p is stabilised by tiny poly-instanton corrections at $\mathcal{O}(1/\mathcal{V}^{3+p})$. Using the fact that $K^{-1}_{T_p\bar{T}_p} \sim \mathcal{V}\sqrt{\tilde{\tau}_p}$ and the expression (5.64) for the scalar potential for c_p, its mass can be easily estimated as:

$$m_{\tilde{a}_p}^2 \sim K^{-1}_{T_p\bar{T}_p} \frac{\partial^2 V_F^{\rm poly}(c_p)}{\partial c_p^2} \sim \left(\frac{g_s}{8\pi}\right) \frac{W_0^2}{\mathcal{V}^{2+p}}\, 2\pi\tilde{\tau}_p \sim \frac{m_{3/2}^2}{\mathcal{V}^p}\,\ln\mathcal{V}\,. \tag{C.20}$$

If the volume is of order $\mathcal{V} \sim 10^7$, this mass can be around 10 keV if $p = 9/2$. As explained in Sec. 5.6.2 this value of p can be accommodated by an appropriate choice of underlying flux parameters. Finally the axion c_b of the large modulus $T_b = \tau_b + \mathrm{i}\,c_b$ can receive a potential only from highly suppressed non-perturbative contributions to the superpotential of the form $W_{\rm np} \supset A_b\, e^{-2\pi T_b}$ which can be shown to lead to a mass for the axion c_b that scales as:

$$m_{a_b}^2 \sim \left(\frac{g_s}{8\pi}\right) \frac{M_p^2}{\mathcal{V}^{4/3}}\, e^{-\frac{2\pi}{\lambda_b^{2/3}}\mathcal{V}^{2/3}} \sim 0\,. \tag{C.21}$$

Appendix D

Extended calculations on Axion inflation with electro-magnetic backreaction

D.1 Phase shift

In this appendix we derive in a slightly different manner the value of the characteristic time scale ΔN_ξ that denotes the lag between $\langle \vec{E}\vec{B} \rangle(N)$ and $\xi(N)$, given in Eq. (6.17).

First, we notice that in the case of constant ξ we can define a self-similar function $\tilde{A}(N)$ that captures the growth of the gauge modes for any large enough value of ξ. If we evaluate the enhanced gauge modes $A_{-\lambda}(N,k)$ at the time $N + \ln 2\xi$ and additionally rescale their amplitude with $\sqrt{\frac{2\pi k\xi}{e^{\pi\xi}\sinh(\pi\xi)}}$ (such that they asymptote to unity) their equation of motion in e-folds reads

$$\tilde{A}_k'' + \tilde{A}_k' + \frac{k}{aH}\left(\frac{k}{4aH\xi^2} - 1\right)\tilde{A}_k = 0 \ . \tag{D.1}$$

Therefore, plugging in the constant ξ solution for the gauge modes given in Eq. (6.12), we find that

$$\tilde{A}_k = \sqrt{\frac{\pi\xi}{\sinh(\pi\xi)}} W_{-i\xi,1/2}\left(-i\frac{k}{aH\xi}\right) \tag{D.2}$$

is a 'self-similar' solution that only depends on N (and on a trivial way on k) as long as the $k/4aH\xi^2$ correction can be neglected in Eq. (D.1). Numerically,

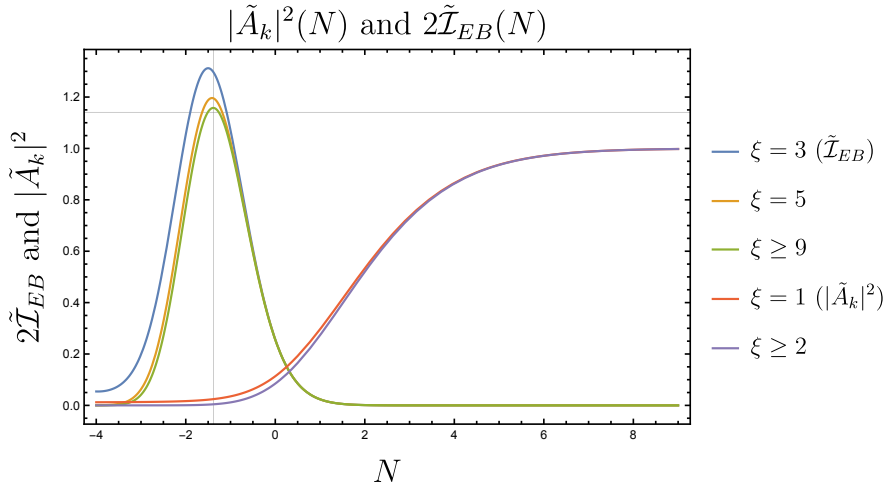

Figure D.1: Evolution of $\left|\tilde{A}_k\right|^2(N)$ evaluated at $N_k = 0$ (red and purple lines) and support of $2\tilde{\mathcal{I}}_{EB}(N)$ (blue, orange and green lines) for various values of constant ξ.

we find indeed that the ξ-dependence drops out for $\xi \gtrsim 2$. See Figure D.1. The original gauge mode A_k can then be expressed in terms of $\tilde{A}_k$ as

$$A_k(\xi, N) = \sqrt{\frac{\sinh(\pi\xi)}{2\pi k\xi}} e^{\pi\xi/2} \tilde{A}_k(N - \ln 2\xi) \ . \tag{D.3}$$

Similarly, using Eq. (6.9), we define a self-similar function for the integrand of $\langle \vec{E}\vec{B} \rangle$

$$\tilde{\mathcal{I}}_{E\cdot B}(N) = \frac{\pi\xi e^{-3N}}{\sinh(\pi\xi)} \partial_N |W_{-i\xi,1/2}\left(-2ie^{-N-\ln 2\xi}\right)|^2, \tag{D.4}$$

such that the integrand of $\langle \vec{E}\vec{B} \rangle$ (in $d\ln k$) is given by

$$\mathcal{I}_{E\cdot B}(k, \xi, N) = \frac{H^4 \sinh(\pi\xi) e^{\pi\xi}}{64\pi^3\xi^4 a_0^3} \tilde{\mathcal{I}}_{E\cdot B}(N - \ln 2\xi - N_k) \ , \tag{D.5}$$

where N_k is the time that the mode k crosses the horizon. The self-similar integrand (D.4) indeed becomes independent of ξ, but only for $\xi \gtrsim 4$. This is because of the additional e^{-3N} that shifts the peak almost 3 e-foldings to sub-horizon scales. We find that $\tilde{\mathcal{I}}_{E\cdot B}$ peaks at $N \approx -1.38 \approx \ln(1/4)$ with amplitude $\tilde{\mathcal{I}} \approx 0.57$ and has most of its support ± 1.5 e-foldings around it. See Figure D.1. The integrand therefore peaks approximately at the wavenumber that crosses the horizon at $N_{\rm peak} = N - \ln\xi/2$.

Second, when ξ is time-dependent, the gauge mode function A_k grows to a plateau value, corresponding to the value reached for some constant $\xi_{\rm eff}$, $A_k(\xi(\tau); k\tau \ll 1) = A_k(\xi_{\rm eff}; k\tau \ll 1)$. If ξ is slowly varying in time, we expect $\xi_{\rm eff}$ to track ξ adiabatically with some time delay. Indeed, we find that a good fit is given by

$$\xi_{\rm eff}(N_k) = \xi(N_*) \quad \text{with} \quad N_* = N_k - \log(\xi(N_*)/a), \tag{D.6}$$

where N_* is implicitly defined and $a \approx 1.2 - 2.0$. This refines the argument given in Sec. 6.3 that the value of ξ at $k/aH \simeq \xi$ determines the growth of A_k. If we deviate from adiabatic tracking, however, the effective ξ averages out to some degree. This makes sense, as the growth of the gauge modes will start to feel a range of values of ξ. As we can see from Fig. 6.2, the effective ξ that $\langle \vec{E}\vec{B} \rangle$ feels is not exactly the value of ξ evaluated at a particular instance of time, but rather an average over a range of values. We can imagine a smoothing window of width $\sim \ln 4\xi^2$ going over the dashed curve as time proceeds. Only if the smoothing window has completely passed the jump at N_0, then $\langle \vec{E}\vec{B} \rangle$ will have reached its final plateau value. Therefore, we expect that Eq. (D.6) needs to be refined if ξ changes considerably over the coarse of $\sim \ln 4\xi^2$ e-folds.

At this point we make an ansatz: the integrand of $\langle \vec{E}\vec{B} \rangle$ is given by $\mathcal{I}_{E\cdot B}(k, \xi_{\rm eff}(N_k), N)$. This indeed seems to be a good approximation for slowly varying ξ, see Figure D.2, where we take $a = 1.45$. The above considerations allow us to find a semi-analytical estimate for ΔN_ξ. Let us focus on the harmonic

$$\xi(N) = \bar{\xi} + A\cos(\omega_\xi N) \; . \tag{D.7}$$

The first maximum of $\xi_{\rm eff}$ reflecting the maximum of ξ at $N_* = 0$ will be at

$$0 = N_{\rm max} - \ln\big((\bar{\xi} + A)/a\big) \quad \longrightarrow \quad N_{\rm max} = \ln\big((\bar{\xi} + A)/a\big) \; . \tag{D.8}$$

Meanwhile, the integrand of $\langle \vec{E}\vec{B} \rangle(N)$ peaks at $N_p = N - \ln(\xi_{\rm eff}(N_p)/2)$ and will take the maximal value at $N = \Delta N_\xi$ when $N_{\rm peak} = N_{\rm max}$, hence

$$N_{\rm max} = \Delta N_\xi - \ln\big((\bar{\xi} + A)/2\big) \quad \longrightarrow \quad \Delta N_\xi = \ln\big((\bar{\xi} + A)^2/2a\big) \; . \tag{D.9}$$

We find that a good fit is given for $a \approx 1.45$ and is shown in Figure 6.4 together with the original estimate $\Delta N_\xi = \ln(\xi^2/2)$ that was argued for in the main text.

D.2 Details on the numerics

In order to obtain our numerical results we use an iterative procedure whose starting point is given by the analytical estimate of the mode function A_k assuming constant inflaton speed $\phi'(N)$, Eq. (6.12):

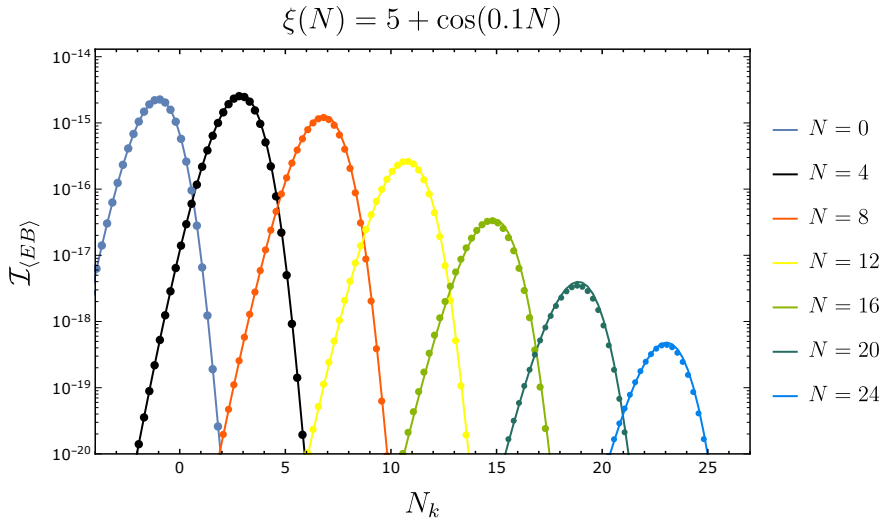

Figure D.2: Comparison of the integrand of $\langle \vec{E}\vec{B}\rangle$ (discrete points) with $\mathcal{I}_{EB}(N_k, \xi_{\rm eff}(N_k), N)$ (solid lines) for an oscillating $\xi = 5 + \cos(0.1N)$ evaluated at various times N.

$$\langle \vec{E}\vec{B}\rangle_{(0)} = \tfrac{1}{2^{21}\pi^2}\tfrac{H_0^4}{\xi^4}e^{2\pi\xi}\int_0^{8\xi} x^7 e^{-x}dx\,, \tag{D.10}$$

$$\langle \rho_{_{EB}}\rangle_{(0)} = \langle \tfrac{E^2+B^2}{2}\rangle_{(0)} = \tfrac{6!}{2^{19}\pi^2}\tfrac{H_0^4}{\xi^3}e^{2\pi\xi}\,, \tag{D.11}$$

where H_0 is given by the Hubble parameter in absence of any backreaction, $H_0^2 = \frac{V(\phi)}{3-\frac{1}{2}\phi'^2}$. Denoting the j-th order iteration quantities with the subscript j, our first step is to find the solution of the following differential equation for a given $\langle \vec{E}\vec{B}\rangle_{(j-1)}$ obtained in the previous iteration:

$$\phi''_{(j)} + (3-\epsilon_{(j)})\phi'_{(j)} + \frac{1}{H^2_{(j)}}\left(V_\phi(\phi_{(j)}) + \frac{\alpha}{\Lambda}\langle \vec{E}\vec{B}\rangle_{(j-1)}\right) = 0\,, \tag{D.12}$$

where

$$H^2_{(j)} = \frac{V(\phi_{(j)}) + \langle \rho_{_{EB}}\rangle_{(j-1)}}{3-\frac{\phi'^2_{(j)}}{2}}\,; \qquad \epsilon_{(j)} = \frac{1}{2}\phi'^2_{(j)} + \frac{2}{3H^2_{(j)}}\langle \rho_{_{EB}}\rangle_{(j-1)}\,. \tag{D.13}$$

Once we get the solution of this equation, $\phi_{(j)}(N)$, we plug the derived quantities $H_{(j)}(N)$, $\epsilon_{(j)}(N)$ and $\xi_{(j)}(N)$ inside the gauge mode equations

$$A''_{k,\pm} + (1-\epsilon_{(j)})A'_{k,\pm} + \frac{k}{aH_{(j)}}\left(\frac{k}{aH_{(j)}} \mp 2\,\xi_{(j)}(N)\right)A_{k,\pm} = 0\,. \tag{D.14}$$

Then, choosing an array of k-modes with an exponential spacing, we estimate the discretized version of $\langle \rho_{EB} \rangle_{(j)}$ and $\langle \vec{E}\vec{B} \rangle_{(j)}$

$$\langle \rho_{EB} \rangle_{(j)} = \frac{1}{4\pi^2 a^4} \sum_{i=1}^{M} d\ln k_i \left(k_i^3 a^2 H_{(j)}^2 |A_{k_i}^{\prime\sigma}|^2 + k_i^5 |A_{k_i}^{\sigma}|^2 - k_i^4 \right) \theta\left(N - N_i\right) , \quad \text{(D.15)}$$

$$\langle \vec{E}\vec{B} \rangle_{(j)} = \sigma \frac{H_{(j)}}{4\pi^2 a^3} \sum_{i=1}^{M} d\ln k_i \, k_i^3 \frac{\partial}{\partial N} |A_{k_i}^{\sigma}|^2 \theta\left(N - N_i\right) , \quad \text{(D.16)}$$

where σ is the polarization which experiences the tachyonic behaviour and the third term in Eq. (D.15) accounts for the subtraction of the Bunch-Davies contributions. With $N_i = \min_N \{2aH\xi - k_i < 0\}$ the Heaviside θ function is introduced to take into account only those modes that have already become tachyonic.

The array of k-modes is defined as $k_p = k_{in} e^{\sum_{i=1}^{p-1} \Delta_i}$ where $p = 2 \ldots M$, $k_1 = k_{in}$ is the lowest momentum taken into account and $\Delta_i = \{0.1, 0.02\}$. The value we choose for Δ_i depends on the oscillatory behaviour of the solution: the stronger the backreaction, the thinner the momentum grid. Given this choice, we can write down the integration step as $dk = k\, d\ln k$. The weight related to the contribution of a single mode to the integral is evaluated using the trapezoidal rule, i.e. $d\ln k_p = \frac{1}{2}\log\left(\frac{k_{p+1}}{k_{p-1}}\right) = \Delta_p$ and $d\ln k_1 = \frac{1}{2}\log\left(\frac{k_2}{k_1}\right) = \frac{\Delta_1}{2}$, $d\ln k_M = \frac{1}{2}\log\left(\frac{k_M}{k_{M-1}}\right) = \frac{\Delta_{M-1}}{2}$.

Once we have evaluated the integrals (D.15) and (D.16) in this way we are able to define next iteration quantities $\epsilon_{(j+1)}$, $H_{(j+1)}$ and the new approximated equation of motion that the inflaton field needs to satisfy. Iterating this procedure allows us to find better approximations of the real solution of the system. We stop the calculations when there is no appreciable difference between the consecutive iterations. We do not prove here that this procedure always converges at a reasonable rate. But if convergence is reached (as is the case in our explicit numerical examples), this procedure ensures a self-consistent solution of the integro-differential system (6.5), (6.7) and (6.9).

During the algorithm we check that the contributions coming from the non-tachyonic polarizations is completely negligible.

D.3 Estimate of non-equal time correlation function

D.3.1 Analytical estimate

Far away from the resonance region the parameter ξ varies only slowly and we can estimate the importance of the non-equal time contributions to Eq. (6.38) by

looking at the result Eqs. (A3) and (A4) from [262]. These expressions are based on parametrizing the gauge field mode functions with Whittaker functions, see Eq. (6.12). Massaging the expressions a little bit, we get for the correlator

$$\int d^3x\, e^{i\vec{p}\vec{x}} \langle 0|\delta_{EB}(N',0)\delta_{EB}(N'',x)|0\rangle \sim \frac{H'H''}{a'^3a''^3}\frac{e^{2\pi(\xi'+\xi'')}}{(\sqrt{\rho'}+\sqrt{\rho''})^{10}}C(\kappa) \quad , \tag{D.17}$$

$$\begin{aligned} C(\kappa) =& \kappa^5 \int_0^\infty dq q^3 \int_{-1}^{1} d\alpha \sqrt{1+q^2+2q\alpha}\, e^{-\sqrt{\kappa}(q+\sqrt{1+q^2+2q\alpha})} \\ & \times \left(1+\frac{\sqrt{q}}{(1+q^2+2q\alpha)^{1/4}}\right) \int_0^{2\pi} d\phi |\epsilon_+(-\hat{q})\cdot\epsilon_+(\hat{q}+\hat{e}_z)|^2 \quad . \end{aligned}$$

Here, we define $\rho \equiv 2\xi/(aH)$, $\vec{q} \equiv \vec{k}/|p|$, $\vec{p} \equiv |p|\hat{e}_z$ and $\kappa \equiv 4|p|(\sqrt{\rho'}+\sqrt{\rho''})^2$. In this appendix only, for notational brevity the superscripts $()'$ and $()''$ denote the given quantity at time N' and N'', respectively. We now see, firstly, that the κ^5 factor inside $C(\kappa)$ and the factor $1/(\sqrt{\rho'}+\sqrt{\rho''})^{10}$ multiplying $C(\kappa)$ cancel each other. Secondly, we recognize that the correlator is bounded from above by its value on far super-horizon scales $\kappa \to 0$, and that the correlator depends only polynomially on a' and a'' in this limit. Hence we find that the correlator at late times scales as

$$\int d^3x\, e^{i\vec{p}\vec{x}} \langle 0|\delta_{EB}(N',0)\delta_{EB}(N'',x)|0\rangle \sim \frac{1}{a'^3a''^3} \sim e^{-3(N'+N'')} = e^{-6N'}e^{-3\Delta N}\,, \tag{D.18}$$

assuming $N'' > N'$ with loss of generality. By comparison, we conclude that the argument of $g(N,\Delta N)$ scales as $e^{-3\Delta N}$. For a functional form $f(\Delta N) = \exp(-c\,\Delta N)$ the integral

$$g(N',0) = \int_{N'}^{\infty} dN'' \exp(-c\,\Delta N) = \frac{1}{c} \tag{D.19}$$

is of $\mathcal{O}(1)$ for $\mathcal{O}(1)$ values of c. Since in our case we have $c = 3$, the inclusion of unequal time correlations does not significantly alter our result. This can also be confirmed by a comparison of our results with previous analysis [262, 270] which included this unequal time correlator, see App. D.4.

D.3.2 Numerical evaluation

In the resonant regime the Whittaker functions used in App. D.3.1 are no longer a good approximation to the full mode functions. In this region, we evaluate the

non-equal time correlator numerically, based on the mode functions obtained in Sec. 6.4.

In order to compute the shape of the non-equal time correlation function, we define symmetrized version of δ_{EB} (see Eq. (6.35)), analogous to the symmetrized $\langle \vec{E}\vec{B}\rangle$ introduced in Eq. (6.9) (see also [291]),

$$\begin{aligned}\delta_{EB}(\tau,x)_S &= \left(E^i(\tau,x)B^i(\tau,x)\right)_S - \langle \vec{E}\vec{B}\rangle_S(\tau') \\ &= \frac{1}{2}\left(E^i(\tau,x)B^i(\tau,x) + B^i(\tau,x)E^i(\tau,x)\right) - \langle \vec{E}\vec{B}\rangle_S(\tau)\,, \end{aligned} \tag{D.20}$$

and consequently

$$\begin{aligned}&\langle 0|\left[\delta_{EB}(\tau',x)_S\ \delta_{EB}(\tau'',0)_S\right]_S|0\rangle \\ &\qquad = \frac{1}{2}\langle 0|\delta_{EB}(\tau',x)_S\delta_{EB}(\tau'',0)_S + \delta_{EB}(\tau'',0)_S\delta_{EB}(\tau',x)_S\rangle|0\rangle\,. \end{aligned} \tag{D.21}$$

If we consider only positive helicity modes, $\lambda = +$, and we use the following short notation

$$\begin{aligned} &E_1^i = E^i(k,\tau'',\vec{x},+)\,, \quad B_1^i = B^i(k,\tau'',\vec{x},+)\,, \quad E_2^j = E^j(k,\tau',0,+)\,, \\ &B_2^j = B^j(k,\tau',0,+)\,, \quad B_2^j = B^j(k,\tau',0,+)\,, \quad A_+(\tau,\vec{k}) = A(\tau,\vec{k}) \end{aligned} \tag{D.22}$$

we end up with

$$\begin{aligned} &\int d^3\vec{x}e^{i\vec{q}\cdot\vec{x}}\langle 0|\left[\delta_{EB}(\tau',x)_S\delta_{EB}(\tau'',0)_S\right]_S|0\rangle = \\ &= \frac{1}{2}\int d^3\vec{x}e^{i\vec{q}\cdot\vec{x}}\left[\langle E_1^iE_2^j\rangle\langle B_1^iB_2^j\rangle + \langle E_1^iB_2^j\rangle\langle B_1^iE_2^j\rangle + \right. \\ &\qquad\qquad \left. + \langle E_2^jE_1^i\rangle\langle B_2^jB_1^i\rangle + \langle E_2^jB_1^i\rangle\langle B_2^jE_1^i\rangle\right] \\ &= \frac{1}{2a'^4a''^4}\int\frac{d^3\vec{k}}{(2\pi)^3}|\vec{k}|^2\left|\vec{\epsilon}_+(\vec{k})\cdot\vec{\epsilon}_+(-\vec{k}-\vec{q})\right|^2\times \\ &\quad\times\left\{\partial_\tau A(\tau',-\vec{k}-\vec{q})\partial_\tau A^*(\tau'',-\vec{k}-\vec{q})A(\tau',\vec{k})A^*(\tau'',\vec{k}) + \right. \\ &\qquad + 2\frac{|-\vec{k}-\vec{q}|}{|\vec{k}|}Re\left[\partial_\tau A(\tau',-\vec{k}-\vec{q})A^*(\tau'',-\vec{k}-\vec{q})A(\tau',\vec{k})\partial_\tau A^*(\tau'',\vec{k})\right] + \\ &\qquad \left. + \frac{|-\vec{k}-\vec{q}|^2}{|\vec{k}|^2}A(\tau'',-\vec{k}-\vec{q})A^*(\tau',-\vec{k}-\vec{q})\partial_\tau A(\tau'',\vec{k})\partial_\tau A^*(\tau',\vec{k})\right\} \end{aligned} \tag{D.23}$$

where in this appendix only, $a' \equiv a(\tau')$ and $a'' \equiv a(\tau'')$. Given that the positive polarization vector can written as

$$\epsilon_+(\vec{k}) = \frac{\hat{k}\cdot\hat{e}_x + i\left(\hat{k}(\hat{k}\cdot\hat{e}_x) - \hat{e}_x\right)}{\sqrt{2}|\hat{k}\cdot\hat{e}_x|}, \tag{D.24}$$

if we assume that $\vec{q} = \{0, 0, q\}$, we can see that using polar coordinates and setting $\cos(\theta) = \alpha$, the polarization dependent factor inside Eq. (D.23) becomes

$$\begin{aligned}\left|\epsilon_+(\vec{k})\cdot\epsilon_+(-\vec{q}-\vec{k})\right|^2 =& \frac{2k^2 + 4kq\alpha + q^2(1+\alpha^2)}{4k^2\left(1 + 2\alpha\frac{q}{k} + \frac{q^2}{k^2}\right)} + \\ &+ \frac{k^3 + 3k^2q\alpha + q^3\alpha + kq^2(1+2\alpha^2)}{2k^3\left(1 + 2\alpha\frac{q}{k} + \frac{q^2}{k^2}\right)^{3/2}}.\end{aligned} \tag{D.25}$$

In order to have a more compact notation we also define

$$\begin{aligned}C_1(k,q,\alpha) &= \left|\epsilon_+(\vec{k})\cdot\epsilon_+(-\vec{q}-\vec{k})\right|^2, \\ C_2(k,q,\alpha) &= C_1(k,q,\alpha)\sqrt{1 + 2\alpha\frac{q}{k} + \frac{q^2}{k^2}},\end{aligned} \tag{D.26}$$

and since the gauge mode equation of motion depends just on the magnitude of the k-vector, we can write

$$\begin{aligned}&A(N,\vec{k}) = A(N,k); \\ &A(N,-\vec{k}-\vec{q}) = A(N,k\sqrt{1 + 2\alpha\frac{q}{k} + \frac{q^2}{k^2}}) \equiv A(N,k,q,\alpha).\end{aligned} \tag{D.27}$$

Rearranging Eq. D.23 and using the number e-foldings as time variable we get

$$\begin{aligned}&\int d^3\vec{x}e^{i\vec{q}\cdot\vec{x}}\langle 0|\left[\delta_{EB}(N',x)_S\delta_{EB}(N'',0)_S\right]_S|0\rangle = \frac{H'H''}{a'^3a''^3}\int_0^\infty\frac{dk}{(4\pi^2)}k^4\int_{-1}^1 d\alpha\times \\ &\{C_1(k,q,\alpha)Re\left[\partial_N A(N',k,q,\alpha)\partial_N A^*(N'',k,q,\alpha)A(N',k)A^*(N'',k)\right] \\ &+C_2(k,q,\alpha)Re\left[\partial_N A(N',k,q,\alpha)A^*(N'',k,q,\alpha)A(N',k)\partial_N A^*(N'',k)\right]\}\end{aligned} \tag{D.28}$$

where in this appendix only, $H' \equiv H(N')$ and $H'' \equiv H(N'')$. It is easy to see that the final result has the desired properties: it is real and symmetric under $N' \leftrightarrow N''$ and $\vec{x} \leftrightarrow -\vec{x}$.

As in App. D.3.1 we focus on far super-horizon scales $q \to 0$,

$$\begin{aligned}\langle \delta_{EB}(N')\delta_{EB}(N'')\rangle =& \lim_{q\to 0}\int d^3\vec{x}e^{i\vec{q}\cdot\vec{x}}\langle 0|\left[\delta_{EB}(N',x)_S\delta_{EB}(N'',0)_S\right]_S|0\rangle \\ =& \frac{H'H''}{a'^3a''^3}\int_0^\infty \frac{dk}{(2\pi^2)}k^4\times \\ & \{Re\left[\partial_N A(N',k)\partial_N A^*(N'',k)A(N',k)A^*(N'',k)\right] + \\ & +Re\left[\partial_N A(N',k)A^*(N'',k)A(N',k)\partial_N A^*(N'',k)\right]\}.\end{aligned} \tag{D.29}$$

For numerical purposes we discretize the integral as follows

$$\begin{aligned}\langle \delta_{EB}(N')\delta_{EB}(N'')\rangle =& \frac{H'H''}{(2\pi^2)a'^3a''^3}\sum_{k_i} d\ln k_i\, k_i^5 \sum_j \Delta\alpha\ \times \\ & \{Re\left[\partial_N A(N',k_i)\partial_N A^*(N'',k_i)A(N',k_i)A^*(N'',k_i)\right] + \\ & +Re\left[\partial_N A(N',k_i)A^*(N'',k_i)A(N',k_i)\partial_N A^*(N'',k_i)\right]\}.\end{aligned} \tag{D.30}$$

the discretization scheme is the same as in App. (D.2).

We can now compute a numerical estimate of the normalized non-equal time correlation function that was introduced in Eq. (6.39),

$$g(N',\Delta N) = \langle \delta^2_{EB}(N')\rangle^{-1}\int_{N'+\Delta N}^\infty dN''\langle \delta_{EB}(N')\delta_{EB}(N'')\rangle. \tag{D.31}$$

Fig. D.3 shows the integrand of $g(N',\Delta N)$ at five distinct times deep in the resonance regime. As in our analytical estimate in App. D.3.1, the integrand of $g(N',\Delta N)$ drops exponentially as $\exp(-c\Delta N)$ with $c = \mathcal{O}(1)$. For small values of ΔN the behaviour deviates from the exponential decay. Numerically performing the integral for some representative choices of ΔN yields

- $N' = 60$, $\Delta N = \{1, 0.5, 0.1\}$, $g(N',\Delta N)/\gamma = \{0.19, 0.46, 0.86\}$
- $N' = 61.4$, $\Delta N = \{1, 0.5, 0.1\}$, $g(N',\Delta N)/\gamma = \{6.6\times 10^{-2}, 0.31, 0.82\}$
- $N' = 61.8$, $\Delta N = \{1, 0.5, 0.1\}$, $g(N',\Delta N)/\gamma = \{6.4\times 10^{-2}, 0.24, 0.76\}$
- $N' = 62$, $\Delta N = \{1, 0.5, 0.1\}$, $g(N',\Delta N)/\gamma = \{0.13, 0.31, 0.76\}$
- $N' = 62.2$, $\Delta N = \{1, 0.5, 0.1\}$, $g(N',\Delta N)/\gamma = \{0.15, 0.34, 0.79\}$

We conclude that the support of $g(N',\Delta N)$ is mainly focused at small values of ΔN, i.e. that unequal time correlations are mainly relevant on time scales over which $\langle \delta^2(EB)\rangle$ does not change too drastically. However, the contributions from

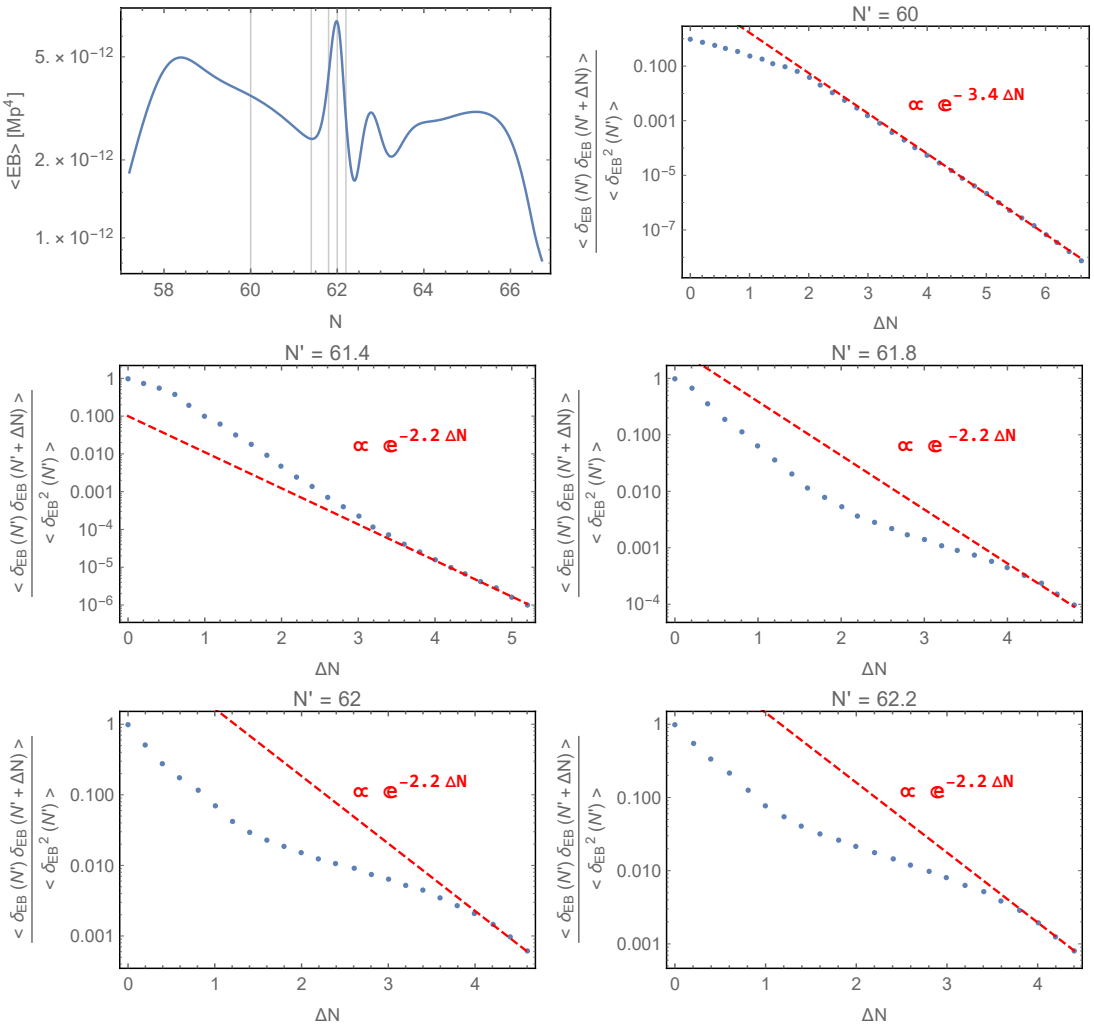

Figure D.3: Integrand of $g(N', \Delta N)$, for various values of N' for $1/f = 25$. The top left panel corresponds to the bottom left panel of Fig. 6.6 and serves as an orientation to identify the position of the maxima and minima. All other panels show the integrand of $g(N', \Delta N)$ for local minima ($N' = 61.4$), local maxima ($N' = 62$) and steep regions ($N' = \{60, 61.8, 62.2\}$) of $\langle \vec{E}\vec{B} \rangle$. The red lines give the best fit for the exponentially decreasing tail of the distributions.

more distant times are not fully negligible, and hence we expect $\mathcal{O}(1)$ corrections to the power spectrum in the resonance regime. These will tend to slightly smooth the maxima and minima of the power spectrum in this regime. However, since the minima are unobservable and the maxima violate perturbativity (see discussion in Sec. 6.5) this does not significantly impact our discussion in the main text.

D.4 Scalar power spectrum: comparison with earlier work

The scalar power spectrum generated during axion inflation has been previously estimated in Refs. [262, 268, 270, 273] based on the analytical estimate for $\langle \vec{E}\vec{B}\rangle$ given in Eq. (6.13). In this appendix we briefly review these derivations and their limitations. Of particular interest to us are Refs. [262, 270] which are based on the Greens function method. Generalizing this approach leads to the results for the power spectrum reported in the main text.

We start from the equation of motion for the scalar perturbations, Eq. (6.35),

$$\delta\phi'' + 3\,\delta\phi' - \frac{N_{,\phi}}{fH^2}\frac{\partial\langle \vec{E}\vec{B}\rangle}{\partial N}\delta\phi = \frac{1}{fH^2}\delta_{EB}\,. \tag{D.32}$$

Ref. [270] focuses on the regime of weak or mild backreaction (wb) where the $\partial\langle \vec{E}\vec{B}\rangle/\partial N$ term can be neglected,[1]

$$L_N^{(wb)}[\delta\phi(N)] \equiv \delta\phi'' + 3\,\delta\phi' \simeq \frac{1}{fH^2}\delta_{EB}\,. \tag{D.33}$$

Following the steps in Eq. (6.35) to (6.42) of the main text yields

$$\langle \delta N^2\rangle^{(wb)} \simeq N_{,\phi}^2 \int dN' \frac{G_{wb}^2(N,N')\sigma_{EB}^2(N')}{f^2H^2(N')}\,, \tag{D.34}$$

with $G_{wb}(N,N')$ denoting the Greens function of the linear operator $L_N^{(wb)}$.

Ref. [262] focuses on the opposite limit of strong backreaction. In this case, the the backreaction term in Eq. (D.32) can be approximated as

$$\frac{N_{,\phi}}{fH^2}\frac{\partial\langle \vec{E}\vec{B}\rangle}{\partial N}\delta\phi \simeq \frac{1}{2f^2H^2}\frac{\partial\langle \vec{E}\vec{B}\rangle}{\partial \xi}\delta\phi' \simeq \frac{1}{2f^2H^2}\left(2\pi\langle \vec{E}\vec{B}\rangle\right)\delta\phi' \simeq \frac{2\pi}{2fH^2}V_{,\phi}\delta\phi'\,. \tag{D.35}$$

[1] We note that Eq. [270] includes the slow-roll suppressed mass term for $\delta\phi$ and (working in Fourier space) the unequal time correlations in $\langle\delta_{EB}(N)\delta_{EB}(N')\rangle$. However, as the very good agreement in Fig. D.4 shows, these do not significantly change the result.

In the first step, we have Taylor expanded $\langle \vec{E}\vec{B} \rangle$ in terms of ξ instead of N. This is valid if $\langle \vec{E}\vec{B} \rangle$ can be expressed as a function of ξ only and if ξ is strictly monotonic, implying that the evolution of ξ can serve as a well-defined 'clock' during inflation. As long as the fluctuations are small, $\delta N, \delta\xi \ll 1$, both descriptions are then equivalent. In the full system studied in the main text where ξ becomes an oscillating function, this procedure can not be applied. The second step relies on the explicit form of $\langle \vec{E}\vec{B} \rangle$ in Eq. (6.13) with the additional assumption of H being approximately constant. The final step uses the background equation of motion in the strong backreaction regime where the $\dot{\phi}$-term can be neglected.[2] Based on this, Eq. (D.32) can be expressed as

$$L_N^{(sb)}[\delta\phi(N)] \equiv \delta\phi'' + 3\delta\phi' - \frac{\pi}{fH^2} V_{,\phi}\delta\phi' \simeq \frac{1}{fH^2}\delta_{EB}\,, \tag{D.36}$$

and correspondingly

$$\langle \delta N^2 \rangle^{(sb)} \simeq N_{,\phi}^2 \int dN' \frac{G_{sb}^2(N,N')\sigma_{EB}^2(N')}{f^2H^2(N')}\,, \tag{D.37}$$

with $G_{sb}(N,N')$ denoting the Greens function of the linear operator $L_N^{(sb)}$.

Fig. D.4 compares our formalism (black curve) with the approximations performed in Ref. [270] (blue curves) and Ref. [262] (orange curve). In all cases, for the purpose of the comparison with previous results, we assume in this appendix $\langle \vec{E}\vec{B} \rangle$ to be given by Eq. (6.13) and correspondingly $\sigma_{EB}^2 \simeq \langle \vec{E}\vec{B} \rangle$ (see e.g. Ref. [273]). The black solid curve indicates our result based on (6.42), i.e. including the gauge field backreaction in the $\delta\phi$ equation of motion, with the gray dashed curve displaying for reference the vacuum contribution. The dashed blue curve (essentially coinciding with the black curve) is the result obtain based on the linear operator (D.33) in the weak backreaction regime, the dashed orange curve is correspondingly based on the linear operator (D.36) in the strong backreaction regime[3]. The dotted blue and orange curves are the results derived in Refs. [270] and [262] for the weak and strong backreaction regime, respectively, demonstrating our ability to reproduce these results when using the same approximations. Finally, in the gray shaded region $\zeta \geqslant 0.3$, indicating that we cannot trust the perturbative analysis underlying our computations.

The excellent agreement between our full result (black) and the weak backreaction approximation (blue) indicates that the backreaction term in the $\delta\phi$ equation

[2] In our numerical evolution of this system of $1/f = 35$ we find all three terms of the background eom to be of similar size towards the end of inflation. This approximation thus induces an $\mathcal{O}(5)$ error in the Greens function, which is squared in the power spectrum and essentially accounts for the discrepancy between the black and dashed orange curve.

[3] Note that the strong backreaction approximation can only be expected to be valid at large values of ξ, towards the end of inflation.

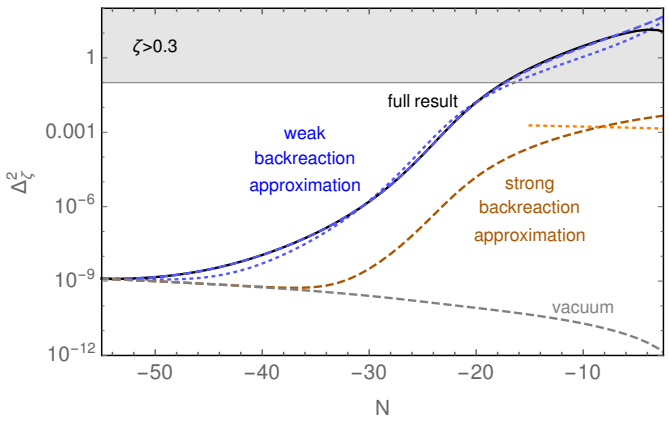

Figure D.4: Scalar power spectrum sourced by Eq. (6.13) for $1/f = 35$. The black curve is our full result, the dashed blue and orange curves implement the weak and strong backreaction approximation of Refs. [270] and [262], respectively. The corresponding dotted curves indicate the very good agreement with the final expressions for the power spectrum derived in these references. In this appendix we use the convention that inflation ends at $N = 0$.

of motion is essentially irrelevant for the parameters discussed here. This conclusion is in contradiction to the conclusion drawn in [262, 273], which would indicate that backreaction dominates roughly above the dotted orange horizontal line in Fig. D.4, consequently suppressing the resulting power spectrum. We can track this difference down to the approximations performed in Eq. (D.35), in particular in the last step thereof. We conclude that the sourced scalar power spectrum is two to three orders of magnitude larger than previously estimated. Nevertheless, our procedure also entails approximations which need to be scrutinized, most notably the omission of the gradients $\nabla\Phi$ and the dropping the unequal time contribution of the δ_{EB} two-point correlator. Given the importance of this result for the production of primordial black holes, this clearly calls for further investigation.

Finally, Ref. [273] presents a simplified derivation of the results obtained in Refs. [262, 270]. In the strong backreaction regime this relies on the same approximations as [262], hence it is not surprising that Ref. [273] also finds a strong suppression of the power spectrum in the strong backreaction regime.

Bibliography

[1] M. Cicoli, V. A. Diaz, V. Guidetti, and M. Rummel, *The 3.5 keV Line from Stringy Axions*, JHEP **10** (2017) 192, [arXiv:1707.02987].

[2] M. Cicoli, D. Ciupke, V. A. Diaz, V. Guidetti, F. Muia, and P. Shukla, *Chiral Global Embedding of Fibre Inflation Models*, JHEP **11** (2017) 207, [arXiv:1709.01518].

[3] M. Cicoli, V. Guidetti, F. G. Pedro, and G. P. Vacca, *A geometrical instability for ultra-light fields during inflation?*, JCAP **12** (2018) 037, [arXiv:1807.03818].

[4] M. Cicoli, V. Guidetti, and F. G. Pedro, *Geometrical Destabilisation of Ultra-Light Axions in String Inflation*, JCAP **05** (2019) 046, [arXiv:1903.01497].

[5] V. Domcke, V. Guidetti, Y. Welling, and A. Westphal, *Resonant backreaction in axion inflation*, JCAP **09** (2020) 009, [arXiv:2002.02952].

[6] C. Quigg, Gauge Theories of the Strong, Weak, and Electromagnetic Interactions: Second Edition. Princeton University Press, USA, 9, 2013.

[7] W. Porter, *Naturalness, the autonomy of scales, and the 125 GeV Higgs*, Studies in History and Philosophy of Science Part B: Studies in History and Philosophy of Modern Physics **51** (2015) 82–96.

[8] **Planck** Collaboration, N. Aghanim et al., *Planck 2018 results. VI. Cosmological parameters*, Astron. Astrophys. **641** (2020) A6, [arXiv:1807.06209].

[9] A. G. Riess, S. Casertano, W. Yuan, L. M. Macri, and D. Scolnic, *Large Magellanic Cloud Cepheid Standards Provide a 1% Foundation for the Determination of the Hubble Constant and Stronger Evidence for Physics beyond ΛCDM*, Astrophys. J. **876** (2019), no. 1 85, [arXiv:1903.07603].

[10] **Planck** Collaboration, Y. Akrami et al., *Planck 2018 results. X. Constraints on inflation*, arXiv:1807.06211.

[11] S. Dodelson, *Coherent phase argument for inflation*, AIP Conf. Proc. **689** (2003), no. 1 184–196, [hep-ph/0309057].

[12] R. Peccei, *The Strong CP problem and axions*, Lect. Notes Phys. **741** (2008) 3–17, [hep-ph/0607268].

[13] S. Davidson, *Axions: Bose Einstein Condensate or Classical Field?*, Astropart. Phys. **65** (2015) 101–107, [arXiv:1405.1139].

[14] M. Cicoli, J. P. Conlon, and F. Quevedo, *Dark radiation in LARGE volume models*, Phys. Rev. D **87** (2013), no. 4 043520, [arXiv:1208.3562].

[15] A. G. Riess, L. Macri, H. L. Stefano Casertano, H. C. Ferguson, A. V. Filippenko, S. W. Jha, W. Li, and R. Chornock, *A 3% Solution: Determination of the Hubble Constant with the Hubble Space Telescope and Wide Field Camera 3*, Astrophys.J. **730** (2011) id. 119, [arXiv:1103.2976].

[16] S. Angus, J. P. Conlon, M. C. D. Marsh, A. J. Powell, and L. T. Witkowski, *Soft X-ray Excess in the Coma Cluster from a Cosmic Axion Background*, JCAP **09** (2014) 026, [arXiv:1312.3947].

[17] M. Cicoli, J. P. Conlon, M. C. D. Marsh, and M. Rummel, *3.55 keV photon line and its morphology from a 3.55 keV axionlike particle line*, Phys. Rev. D **90** (2014) 023540, [arXiv:1403.2370].

[18] J. Polchinski, String theory. Vol. 1: An introduction to the bosonic string. Cambridge Monographs on Mathematical Physics. Cambridge University Press, 12, 2007.

[19] M. B. Green, J. Schwarz, and E. Witten, SUPERSTRING THEORY. VOL. 1: INTRODUCTION. Cambridge Monographs on Mathematical Physics. 7, 1988.

[20] L. E. Ibanez and A. M. Uranga, String theory and particle physics: An introduction to string phenomenology. Cambridge University Press, 2, 2012.

[21] D. Baumann and L. McAllister, Inflation and String Theory. Cambridge Monographs on Mathematical Physics. Cambridge University Press, 5, 2015.

[22] K. Becker, M. Becker, and J. Schwarz, String theory and M-theory: A modern introduction. Cambridge University Press, 12, 2006.

[23] B. S. Acharya, G. L. Kane, and P. Kumar, *Perspectives On String Phenomenology (Advanced Directions in High Energy Physics Vol.22)*, .

[24] J. Polchinski, *Dirichlet Branes and Ramond-Ramond charges*, Phys. Rev. Lett. **75** (1995) 4724–4727, [hep-th/9510017].

[25] M. Grana, T. W. Grimm, H. Jockers, and J. Louis, *Soft supersymmetry breaking in Calabi-Yau orientifolds with D-branes and fluxes*, Nucl. Phys. B **690** (2004) 21–61, [hep-th/0312232].

[26] H. Jockers and J. Louis, *The Effective action of D7-branes in N = 1 Calabi-Yau orientifolds*, Nucl. Phys. B **705** (2005) 167–211, [hep-th/0409098].

[27] B. R. Greene and M. Plesser, *Duality in Calabi-Yau Moduli Space*, Nucl. Phys. B **338** (1990) 15–37.

[28] P. Candelas and X. de la Ossa, *Moduli Space of {Calabi-Yau} Manifolds*, Nucl. Phys. B **355** (1991) 455–481.

[29] J. Louis and A. Micu, *Type 2 theories compactified on Calabi-Yau threefolds in the presence of background fluxes*, Nucl. Phys. B **635** (2002) 395–431, [hep-th/0202168].

[30] J. Michelson, *Compactifications of type IIB strings to four-dimensions with nontrivial classical potential*, Nucl. Phys. B **495** (1997) 127–148, [hep-th/9610151].

[31] G. Dall'Agata, *Type IIB supergravity compactified on a Calabi-Yau manifold with H fluxes*, JHEP **11** (2001) 005, [hep-th/0107264].

[32] G. Pradisi and A. Sagnotti, *Open String Orbifolds*, Phys. Lett. B **216** (1989) 59–67.

[33] B. S. Acharya, M. Aganagic, K. Hori, and C. Vafa, *Orientifolds, mirror symmetry and superpotentials*, hep-th/0202208.

[34] I. Brunner and K. Hori, *Orientifolds and mirror symmetry*, JHEP **11** (2004) 005, [hep-th/0303135].

[35] T. W. Grimm and J. Louis, *The Effective action of N = 1 Calabi-Yau orientifolds*, Nucl. Phys. B **699** (2004) 387–426, [hep-th/0403067].

[36] G. Dall'Agata, *On supersymmetric solutions of type IIB supergravity with general fluxes*, Nucl. Phys. B **695** (2004) 243–266, [hep-th/0403220].

[37] M. Grana, *Flux compactifications in string theory: A Comprehensive review*, Phys. Rept. **423** (2006) 91–158, [hep-th/0509003].

[38] S. B. Giddings, S. Kachru, and J. Polchinski, *Hierarchies from fluxes in string compactifications*, Phys. Rev. D **66** (2002) 106006, [hep-th/0105097].

[39] P. Kaste, R. Minasian, M. Petrini, and A. Tomasiello, *Nontrivial RR two form field strength and SU(3) structure*, Fortsch. Phys. **51** (2003) 764–768, [hep-th/0301063].

[40] A. R. Frey, *Notes on SU(3) structures in type IIB supergravity*, JHEP **06** (2004) 027, [hep-th/0404107].

[41] K. Behrndt, M. Cvetic, and P. Gao, *General type IIB fluxes with SU(3) structures*, Nucl. Phys. B **721** (2005) 287–308, [hep-th/0502154].

[42] G. Lopes Cardoso, G. Curio, G. Dall'Agata, D. Lust, P. Manousselis, and G. Zoupanos, *NonKahler string backgrounds and their five torsion classes*, Nucl. Phys. B **652** (2003) 5–34, [hep-th/0211118].

[43] J. P. Gauntlett, D. Martelli, and D. Waldram, *Superstrings with intrinsic torsion*, Phys. Rev. D **69** (2004) 086002, [hep-th/0302158].

[44] M. Grana, R. Minasian, M. Petrini, and A. Tomasiello, *Type II strings and generalized Calabi-Yau manifolds*, Comptes Rendus Physique **5** (2004) 979–986, [hep-th/0409176].

[45] A. R. Frey, *Warped strings: Selfdual flux and contemporary compactifications*, other thesis, 8, 2003.

[46] S. B. Giddings and A. Maharana, *Dynamics of warped compactifications and the shape of the warped landscape*, Phys. Rev. D **73** (2006) 126003, [hep-th/0507158].

[47] O. DeWolfe and S. B. Giddings, *Scales and hierarchies in warped compactifications and brane worlds*, Phys. Rev. D **67** (2003) 066008, [hep-th/0208123].

[48] M. Grana and J. Polchinski, *Supersymmetric three form flux perturbations on AdS(5)*, Phys. Rev. D **63** (2001) 026001, [hep-th/0009211].

[49] R. Blumenhagen, V. Braun, T. W. Grimm, and T. Weigand, *GUTs in Type IIB Orientifold Compactifications*, Nucl. Phys. B **815** (2009) 1–94, [arXiv:0811.2936].

[50] P. Betzler and E. Plauschinn, *Type IIB flux vacua and tadpole cancellation*, Fortsch. Phys. **67** (2019), no. 11 1900065, [arXiv:1905.08823].

[51] R. Minasian and G. W. Moore, *K theory and Ramond-Ramond charge*, JHEP **11** (1997) 002, [hep-th/9710230].

[52] D. S. Freed and E. Witten, *Anomalies in string theory with D-branes*, Asian J. Math. **3** (1999) 819, [hep-th/9907189].

[53] S. Gukov, C. Vafa, and E. Witten, *CFT's from Calabi-Yau four folds*, Nucl. Phys. B **584** (2000) 69–108, [hep-th/9906070]. [Erratum: Nucl.Phys.B 608, 477–478 (2001)].

[54] D. J. Gross and E. Witten, *Superstring Modifications of Einstein's Equations*, Nucl. Phys. B **277** (1986) 1.

[55] K. Becker, M. Becker, M. Haack, and J. Louis, *Supersymmetry breaking and alpha-prime corrections to flux induced potentials*, JHEP **06** (2002) 060, [hep-th/0204254].

[56] R. Minasian, T. G. Pugh, and R. Savelli, *F-theory at order α'^3*, JHEP **10** (2015) 050, [arXiv:1506.06756].

[57] M. Berg, M. Haack, and B. Kors, *Loop corrections to volume moduli and inflation in string theory*, Phys. Rev. D **71** (2005) 026005, [hep-th/0404087].

[58] M. Berg, M. Haack, and B. Kors, *String loop corrections to Kahler potentials in orientifolds*, JHEP **11** (2005) 030, [hep-th/0508043].

[59] G. von Gersdorff and A. Hebecker, *Kahler corrections for the volume modulus of flux compactifications*, Phys. Lett. B **624** (2005) 270–274, [hep-th/0507131].

[60] M. Berg, M. Haack, and E. Pajer, *Jumping Through Loops: On Soft Terms from Large Volume Compactifications*, JHEP **09** (2007) 031, [arXiv:0704.0737].

[61] M. Cicoli, J. P. Conlon, and F. Quevedo, *Systematics of String Loop Corrections in Type IIB Calabi-Yau Flux Compactifications*, JHEP **01** (2008) 052, [arXiv:0708.1873].

[62] M. Cicoli, J. P. Conlon, and F. Quevedo, *General Analysis of LARGE Volume Scenarios with String Loop Moduli Stabilisation*, JHEP **10** (2008) 105, [arXiv:0805.1029].

[63] V. Balasubramanian, P. Berglund, J. P. Conlon, and F. Quevedo, *Systematics of moduli stabilisation in Calabi-Yau flux compactifications*, JHEP **03** (2005) 007, [hep-th/0502058].

[64] C. Burgess, R. Kallosh, and F. Quevedo, *De Sitter string vacua from supersymmetric D terms*, JHEP **10** (2003) 056, [hep-th/0309187].

[65] S. Kachru, R. Kallosh, A. D. Linde, and S. P. Trivedi, *De Sitter vacua in string theory*, Phys. Rev. D **68** (2003) 046005, [hep-th/0301240].

[66] R. Kallosh and T. Wrase, *Emergence of Spontaneously Broken Supersymmetry on an Anti-D3-Brane in KKLT dS Vacua*, JHEP **12** (2014) 117, [arXiv:1411.1121].

[67] E. A. Bergshoeff, K. Dasgupta, R. Kallosh, A. Van Proeyen, and T. Wrase, *D3 and dS*, JHEP **05** (2015) 058, [arXiv:1502.07627].

[68] R. Kallosh, F. Quevedo, and A. M. Uranga, *String Theory Realizations of the Nilpotent Goldstino*, JHEP **12** (2015) 039, [arXiv:1507.07556].

[69] L. Aparicio, F. Quevedo, and R. Valandro, *Moduli Stabilisation with Nilpotent Goldstino: Vacuum Structure and SUSY Breaking*, JHEP **03** (2016) 036, [arXiv:1511.08105].

[70] I. García-Etxebarria, F. Quevedo, and R. Valandro, *Global String Embeddings for the Nilpotent Goldstino*, JHEP **02** (2016) 148, [arXiv:1512.06926].

[71] M. P. Garcia del Moral, S. Parameswaran, N. Quiroz, and I. Zavala, *Anti-D3 branes and moduli in non-linear supergravity*, JHEP **10** (2017) 185, [arXiv:1707.07059].

[72] J. Moritz, A. Retolaza, and A. Westphal, *Toward de Sitter space from ten dimensions*, Phys. Rev. D **97** (2018), no. 4 046010, [arXiv:1707.08678].

[73] M. Cicoli, F. Quevedo, and R. Valandro, *De Sitter from T-branes*, JHEP **03** (2016) 141, [arXiv:1512.04558].

[74] M. Cicoli, A. Maharana, F. Quevedo, and C. Burgess, *De Sitter String Vacua from Dilaton-dependent Non-perturbative Effects*, JHEP **06** (2012) 011, [arXiv:1203.1750].

[75] D. Gallego, M. C. D. Marsh, B. Vercnocke, and T. Wrase, *A New Class of de Sitter Vacua in Type IIB Large Volume Compactifications*, JHEP **10** (2017) 193, [arXiv:1707.01095].

[76] M. Cicoli, M. Goodsell, and A. Ringwald, *The type IIB string axiverse and its low-energy phenomenology*, JHEP **10** (2012) 146, [arXiv:1206.0819].

[77] R. Blumenhagen, J. Conlon, S. Krippendorf, S. Moster, and F. Quevedo, *SUSY Breaking in Local String/F-Theory Models*, JHEP **09** (2009) 007, [arXiv:0906.3297].

[78] M. Cicoli, D. Klevers, S. Krippendorf, C. Mayrhofer, F. Quevedo, and R. Valandro, *Explicit de Sitter Flux Vacua for Global String Models with Chiral Matter*, JHEP **05** (2014) 001, [arXiv:1312.0014].

[79] L. Aparicio, M. Cicoli, S. Krippendorf, A. Maharana, F. Muia, and F. Quevedo, *Sequestered de Sitter String Scenarios: Soft-terms*, JHEP **11** (2014) 071, [arXiv:1409.1931].

[80] T. Banks, M. Berkooz, and P. Steinhardt, *The Cosmological moduli problem, supersymmetry breaking, and stability in postinflationary cosmology*, Phys. Rev. D **52** (1995) 705–716, [hep-th/9501053].

[81] B. de Carlos, J. Casas, F. Quevedo, and E. Roulet, *Model independent properties and cosmological implications of the dilaton and moduli sectors of 4-d strings*, Phys. Lett. B **318** (1993) 447–456, [hep-ph/9308325].

[82] G. Coughlan, W. Fischler, E. W. Kolb, S. Raby, and G. G. Ross, *Cosmological Problems for the Polonyi Potential*, Phys. Lett. B **131** (1983) 59–64.

[83] M. Khlopov and A. D. Linde, *Is It Easy to Save the Gravitino?*, Phys. Lett. B **138** (1984) 265–268.

[84] L. McAllister and E. Silverstein, *String Cosmology: A Review*, Gen. Rel. Grav. **40** (2008) 565–605, [arXiv:0710.2951].

[85] D. Baumann and L. McAllister, *Advances in Inflation in String Theory*, Ann. Rev. Nucl. Part. Sci. **59** (2009) 67–94, [arXiv:0901.0265].

[86] M. Cicoli and F. Quevedo, *String moduli inflation: An overview*, Class. Quant. Grav. **28** (2011) 204001, [arXiv:1108.2659].

[87] C. Burgess, M. Cicoli, and F. Quevedo, *String Inflation After Planck 2013*, JCAP **11** (2013) 003, [arXiv:1306.3512].

[88] C. Burgess, M. Cicoli, F. Quevedo, and M. Williams, *Inflating with Large Effective Fields*, JCAP **11** (2014) 045, [arXiv:1404.6236].

[89] E. Pajer and M. Peloso, *A review of Axion Inflation in the era of Planck*, Class. Quant. Grav. **30** (2013) 214002, [arXiv:1305.3557].

[90] A. Westphal, *String cosmology — Large-field inflation in string theory*, Int. J. Mod. Phys. A **30** (2015), no. 09 1530024, [arXiv:1409.5350].

[91] D. H. Lyth, *What would we learn by detecting a gravitational wave signal in the cosmic microwave background anisotropy?*, Phys. Rev. Lett. **78** (1997) 1861–1863, [hep-ph/9606387].

[92] D. Baumann and L. McAllister, *A Microscopic Limit on Gravitational Waves from D-brane Inflation*, Phys. Rev. D **75** (2007) 123508, [hep-th/0610285].

[93] J. Blanco-Pillado, C. Burgess, J. M. Cline, C. Escoda, M. Gomez-Reino, R. Kallosh, A. D. Linde, and F. Quevedo, *Racetrack inflation*, JHEP **11** (2004) 063, [hep-th/0406230].

[94] R. Kallosh and A. D. Linde, *Landscape, the scale of SUSY breaking, and inflation*, JHEP **12** (2004) 004, [hep-th/0411011].

[95] A. D. Linde and A. Westphal, *Accidental Inflation in String Theory*, JCAP **03** (2008) 005, [arXiv:0712.1610].

[96] F. Bonetti and M. Weissenbacher, *The Euler characteristic correction to the Kähler potential — revisited*, JHEP **01** (2017) 003, [arXiv:1608.01300].

[97] M. Berg, M. Haack, J. U. Kang, and S. Sjörs, *Towards the one-loop Kähler metric of Calabi-Yau orientifolds*, JHEP **12** (2014) 077, [arXiv:1407.0027].

[98] M. Haack and J. U. Kang, *One-loop Einstein-Hilbert term in minimally supersymmetric type IIB orientifolds*, JHEP **02** (2016) 160, [arXiv:1511.03957].

[99] D. Ciupke, J. Louis, and A. Westphal, *Higher-Derivative Supergravity and Moduli Stabilization*, JHEP **10** (2015) 094, [arXiv:1505.03092].

[100] T. W. Grimm, K. Mayer, and M. Weissenbacher, *Higher derivatives in Type II and M-theory on Calabi-Yau threefolds*, JHEP **02** (2018) 127, [arXiv:1702.08404].

[101] M. Cicoli, C. Burgess, and F. Quevedo, *Fibre Inflation: Observable Gravity Waves from IIB String Compactifications*, JCAP **03** (2009) 013, [arXiv:0808.0691].

[102] B. J. Broy, D. Ciupke, F. G. Pedro, and A. Westphal, *Starobinsky-Type Inflation from α'-Corrections*, JCAP **01** (2016) 001, [arXiv:1509.00024].

[103] M. Cicoli, D. Ciupke, S. de Alwis, and F. Muia, *α' Inflation: moduli stabilisation and observable tensors from higher derivatives*, JHEP **09** (2016) 026, [arXiv:1607.01395].

[104] C. Burgess, M. Cicoli, S. de Alwis, and F. Quevedo, *Robust Inflation from Fibrous Strings*, JCAP **05** (2016) 032, [arXiv:1603.06789].

[105] A. Westphal, *String Cosmology — Large-Field Inflation in String Theory*, .

[106] M. Remazeilles, C. Dickinson, H. Eriksen, and I. Wehus, *Sensitivity and foreground modelling for large-scale cosmic microwave background B-mode polarization satellite missions*, Mon. Not. Roy. Astron. Soc. **458** (2016), no. 2 2032–2050, [arXiv:1509.04714].

[107] M. Remazeilles, C. Dickinson, H. Eriksen, and I. Wehus, *Joint Bayesian estimation of tensor and lensing B-modes in the power spectrum of CMB polarization data*, Mon. Not. Roy. Astron. Soc. **474** (2018), no. 3 3889–3897, [arXiv:1707.02981].

[108] N. Arkani-Hamed, L. Motl, A. Nicolis, and C. Vafa, *The String landscape, black holes and gravity as the weakest force*, JHEP **06** (2007) 060, [hep-th/0601001].

[109] J. E. Kim, H. P. Nilles, and M. Peloso, *Completing natural inflation*, JCAP **01** (2005) 005, [hep-ph/0409138].

[110] I. Ben-Dayan, F. G. Pedro, and A. Westphal, *Hierarchical Axion Inflation*, Phys. Rev. Lett. **113** (2014) 261301, [arXiv:1404.7773].

[111] S. Dimopoulos, S. Kachru, J. McGreevy, and J. G. Wacker, *N-flation*, JCAP **08** (2008) 003, [hep-th/0507205].

[112] R. Easther and L. McAllister, *Random matrices and the spectrum of N-flation*, JCAP **05** (2006) 018, [hep-th/0512102].

[113] M. Cicoli, K. Dutta, and A. Maharana, *N-flation with Hierarchically Light Axions in String Compactifications*, JCAP **08** (2014) 012, [arXiv:1401.2579].

[114] E. Silverstein and A. Westphal, *Monodromy in the CMB: Gravity Waves and String Inflation*, Phys. Rev. D **78** (2008) 106003, [arXiv:0803.3085].

[115] L. McAllister, E. Silverstein, and A. Westphal, *Gravity Waves and Linear Inflation from Axion Monodromy*, Phys. Rev. D **82** (2010) 046003, [arXiv:0808.0706].

[116] R. Blumenhagen, S. Moster, and E. Plauschinn, *Moduli Stabilisation versus Chirality for MSSM like Type IIB Orientifolds*, JHEP **01** (2008) 058, [arXiv:0711.3389].

[117] D. R. Green, *Reheating Closed String Inflation*, Phys. Rev. D **76** (2007) 103504, [arXiv:0707.3832].

[118] R. H. Brandenberger, A. Knauf, and L. C. Lorenz, *Reheating in a Brane Monodromy Inflation Model*, JHEP **10** (2008) 110, [arXiv:0808.3936].

[119] N. Barnaby, J. Bond, Z. Huang, and L. Kofman, *Preheating After Modular Inflation*, JCAP **12** (2009) 021, [arXiv:0909.0503].

[120] M. Cicoli and A. Mazumdar, *Reheating for Closed String Inflation*, JCAP **09** (2010) 025, [arXiv:1005.5076].

[121] K. Dutta and A. Maharana, *Inflationary constraints on modulus dominated cosmology*, Phys. Rev. D **91** (2015), no. 4 043503, [arXiv:1409.7037].

[122] M. Cicoli, K. Dutta, A. Maharana, and F. Quevedo, *Moduli Vacuum Misalignment and Precise Predictions in String Inflation*, JCAP **08** (2016) 006, [arXiv:1604.08512].

[123] S. Bhattacharya, K. Dutta, and A. Maharana, *Constraints on Kähler moduli inflation from reheating*, Phys. Rev. D **96** (2017), no. 8 083522, [arXiv:1707.07924]. [Addendum: Phys.Rev.D 96, 109901 (2017)].

[124] T. Higaki and F. Takahashi, *Dark Radiation and Dark Matter in Large Volume Compactifications*, JHEP **11** (2012) 125, [arXiv:1208.3563].

[125] A. Hebecker, P. Mangat, F. Rompineve, and L. T. Witkowski, *Dark Radiation predictions from general Large Volume Scenarios*, JHEP **09** (2014) 140, [arXiv:1403.6810].

[126] M. Cicoli and F. Muia, *General Analysis of Dark Radiation in Sequestered String Models*, JHEP **12** (2015) 152, [arXiv:1511.05447].

[127] B. S. Acharya, P. Kumar, K. Bobkov, G. Kane, J. Shao, and S. Watson, *Non-thermal Dark Matter and the Moduli Problem in String Frameworks*, JHEP **06** (2008) 064, [arXiv:0804.0863].

[128] R. Allahverdi, M. Cicoli, B. Dutta, and K. Sinha, *Nonthermal dark matter in string compactifications*, Phys. Rev. D **88** (2013), no. 9 095015, [arXiv:1307.5086].

[129] L. Aparicio, M. Cicoli, B. Dutta, S. Krippendorf, A. Maharana, F. Muia, and F. Quevedo, *Non-thermal CMSSM with a 125 GeV Higgs*, JHEP **05** (2015) 098, [arXiv:1502.05672].

[130] G. Kane, J. Shao, S. Watson, and H.-B. Yu, *The Baryon-Dark Matter Ratio Via Moduli Decay After Affleck-Dine Baryogenesis*, JCAP **11** (2011) 012, [arXiv:1108.5178].

[131] R. Allahverdi, M. Cicoli, and F. Muia, *Affleck-Dine Baryogenesis in Type IIB String Models*, JHEP **06** (2016) 153, [arXiv:1604.03120].

[132] J. P. Conlon, R. Kallosh, A. D. Linde, and F. Quevedo, *Volume Modulus Inflation and the Gravitino Mass Problem*, JCAP **09** (2008) 011, [arXiv:0806.0809].

[133] T. He, S. Kachru, and A. Westphal, *Gravity waves and the LHC: Towards high-scale inflation with low-energy SUSY*, JHEP **06** (2010) 065, [arXiv:1003.4265].

[134] S. Antusch, K. Dutta, and S. Halter, *Combining High-scale Inflation with Low-energy SUSY*, JHEP **03** (2012) 105, [arXiv:1112.4488].

[135] W. Buchmuller, E. Dudas, L. Heurtier, and C. Wieck, *Large-Field Inflation and Supersymmetry Breaking*, JHEP **09** (2014) 053, [arXiv:1407.0253].

[136] J. P. Conlon and F. Quevedo, *Kahler moduli inflation*, JHEP **01** (2006) 146, [hep-th/0509012].

[137] M. Cicoli, I. Garcìa-Etxebarria, C. Mayrhofer, F. Quevedo, P. Shukla, and R. Valandro, *Global Orientifolded Quivers with Inflation*, JHEP **11** (2017) 134, [arXiv:1706.06128].

[138] **Planck** Collaboration, P. Ade et al., *Planck 2015 results. XX. Constraints on inflation*, Astron. Astrophys. **594** (2016) A20, [arXiv:1502.02114].

[139] **Planck** Collaboration, P. Ade et al., *Planck 2015 results. XIII. Cosmological parameters*, Astron. Astrophys. **594** (2016) A13, [arXiv:1502.01589].

[140] R. Kallosh, A. Linde, D. Roest, A. Westphal, and Y. Yamada, *Fibre Inflation and α-attractors*, JHEP **02** (2018) 117, [arXiv:1707.05830].

[141] M. Cicoli, F. Muia, and P. Shukla, *Global Embedding of Fibre Inflation Models*, JHEP **11** (2016) 182, [arXiv:1611.04612].

[142] M. Cicoli, M. Kreuzer, and C. Mayrhofer, *Toric K3-Fibred Calabi-Yau Manifolds with del Pezzo Divisors for String Compactifications*, JHEP **02** (2012) 002, [arXiv:1107.0383].

[143] M. Kreuzer and H. Skarke, *Complete classification of reflexive polyhedra in four-dimensions*, Adv. Theor. Math. Phys. **4** (2002) 1209–1230, [hep-th/0002240].

[144] S. Angus, *Dark Radiation in Anisotropic LARGE Volume Compactifications*, JHEP **10** (2014) 184, [arXiv:1403.6473].

[145] M. Cicoli, J. P. Conlon, A. Maharana, and F. Quevedo, *A Note on the Magnitude of the Flux Superpotential*, JHEP **01** (2014) 027, [arXiv:1310.6694].

[146] M. Dine, N. Seiberg, and E. Witten, *Fayet-Iliopoulos Terms in String Theory*, Nucl. Phys. B **289** (1987) 589–598.

[147] M. Dine, I. Ichinose, and N. Seiberg, *F Terms and d Terms in String Theory*, Nucl. Phys. B **293** (1987) 253–265.

[148] R. Altman, J. Gray, Y.-H. He, V. Jejjala, and B. D. Nelson, *A Calabi-Yau Database: Threefolds Constructed from the Kreuzer-Skarke List*, JHEP **02** (2015) 158, [arXiv:1411.1418].

[149] R. Blumenhagen, B. Jurke, T. Rahn, and H. Roschy, *Cohomology of Line Bundles: A Computational Algorithm*, J. Math. Phys. **51** (2010) 103525, [arXiv:1003.5217].

[150] R. Blumenhagen, B. Jurke, and T. Rahn, *Computational Tools for Cohomology of Toric Varieties*, Adv. High Energy Phys. **2011** (2011) 152749, [arXiv:1104.1187].

[151] M. Cicoli, S. Krippendorf, C. Mayrhofer, F. Quevedo, and R. Valandro, *D-Branes at del Pezzo Singularities: Global Embedding and Moduli Stabilisation*, JHEP **09** (2012) 019, [arXiv:1206.5237].

[152] P. G. Camara, L. Ibanez, and A. Uranga, *Flux-induced SUSY-breaking soft terms on D7-D3 brane systems*, Nucl. Phys. B **708** (2005) 268–316, [hep-th/0408036].

[153] D. Ciupke, *Scalar Potential from Higher Derivative $\mathcal{N} = 1$ Superspace*, arXiv:1605.00651.

[154] M. Cicoli, S. Downes, and B. Dutta, *Power Suppression at Large Scales in String Inflation*, JCAP **12** (2013) 007, [arXiv:1309.3412].

[155] D. Klaewer and E. Palti, *Super-Planckian Spatial Field Variations and Quantum Gravity*, JHEP **01** (2017) 088, [arXiv:1610.00010].

[156] R. Blumenhagen, I. Valenzuela, and F. Wolf, *The Swampland Conjecture and F-term Axion Monodromy Inflation*, JHEP **07** (2017) 145, [arXiv:1703.05776].

[157] J. J. Blanco-Pillado, D. Buck, E. J. Copeland, M. Gomez-Reino, and N. J. Nunes, *Kahler Moduli Inflation Revisited*, JHEP **01** (2010) 081, [arXiv:0906.3711].

[158] D. H. Lyth and D. Wands, *Generating the curvature perturbation without an inflaton*, Phys. Lett. B **524** (2002) 5–14, [hep-ph/0110002].

[159] T. Moroi and T. Takahashi, *Effects of cosmological moduli fields on cosmic microwave background*, Phys. Lett. B **522** (2001) 215–221, [hep-ph/0110096]. [Erratum: Phys.Lett.B 539, 303–303 (2002)].

[160] C. Burgess, M. Cicoli, M. Gomez-Reino, F. Quevedo, G. Tasinato, and I. Zavala, *Non-standard primordial fluctuations and nongaussianity in string inflation*, JHEP **08** (2010) 045, [arXiv:1005.4840].

[161] P. Cabella, A. Di Marco, and G. Pradisi, *Fiber inflation and reheating*, Phys. Rev. D **95** (2017), no. 12 123528, [arXiv:1704.03209].

[162] S. Antusch, F. Cefala, S. Krippendorf, F. Muia, S. Orani, and F. Quevedo, *Oscillons from String Moduli*, JHEP **01** (2018) 083, [arXiv:1708.08922].

[163] M. Cicoli, D. Ciupke, C. Mayrhofer, and P. Shukla, *A Geometrical Upper Bound on the Inflaton Range*, JHEP **05** (2018) 001, [arXiv:1801.05434].

[164] S. Renaux-Petel and K. Turzyński, *Geometrical Destabilization of Inflation*, Phys. Rev. Lett. **117** (2016), no. 14 141301, [arXiv:1510.01281].

[165] A. Achúcarro, V. Atal, C. Germani, and G. A. Palma, *Cumulative effects in inflation with ultra-light entropy modes*, JCAP **02** (2017) 013, [arXiv:1607.08609].

[166] A. Achúcarro, E. J. Copeland, O. Iarygina, G. A. Palma, D.-G. Wang, and Y. Welling, *Shift-Symmetric Orbital Inflation: single field or multi-field?*, arXiv:1901.03657.

[167] P. Svrcek and E. Witten, *Axions In String Theory*, JHEP **06** (2006) 051, [hep-th/0605206].

[168] J. P. Conlon, *The QCD axion and moduli stabilisation*, JHEP **05** (2006) 078, [hep-th/0602233].

[169] A. Arvanitaki, S. Dimopoulos, S. Dubovsky, N. Kaloper, and J. March-Russell, *String Axiverse*, Phys. Rev. D **81** (2010) 123530, [arXiv:0905.4720].

[170] N. Kaloper and L. Sorbo, *Where in the String Landscape is Quintessence*, Phys. Rev. D **79** (2009) 043528, [arXiv:0810.5346].

[171] S. Panda, Y. Sumitomo, and S. P. Trivedi, *Axions as Quintessence in String Theory*, Phys. Rev. D **83** (2011) 083506, [arXiv:1011.5877].

[172] K. Choi, *String or M theory axion as a quintessence*, Phys. Rev. D **62** (2000) 043509, [hep-ph/9902292].

[173] M. Cicoli, S. De Alwis, A. Maharana, F. Muia, and F. Quevedo, *De Sitter vs Quintessence in String Theory*, Fortsch. Phys. **67** (2019), no. 1-2 1800079, [arXiv:1808.08967].

[174] L. Hui, J. P. Ostriker, S. Tremaine, and E. Witten, *Ultralight scalars as cosmological dark matter*, Phys. Rev. D **95** (2017), no. 4 043541, [arXiv:1610.08297].

[175] E. J. Chun, K. Dimopoulos, and D. Lyth, *Curvaton and QCD axion in supersymmetric theories*, Phys. Rev. D **70** (2004) 103510, [hep-ph/0402059].

[176] K. Dimopoulos and G. Lazarides, *Modular inflation and the orthogonal axion as curvaton*, Phys. Rev. D **73** (2006) 023525, [hep-ph/0511310].

[177] D. I. Kaiser, E. A. Mazenc, and E. I. Sfakianakis, *Primordial Bispectrum from Multifield Inflation with Nonminimal Couplings*, Phys. Rev. D **87** (2013) 064004, [arXiv:1210.7487].

[178] K. Schutz, E. I. Sfakianakis, and D. I. Kaiser, *Multifield Inflation after Planck: Isocurvature Modes from Nonminimal Couplings*, Phys. Rev. D **89** (2014), no. 6 064044, [arXiv:1310.8285].

[179] M. Cicoli and G. A. Piovano, *Reheating and Dark Radiation after Fibre Inflation*, JCAP **02** (2019) 048, [arXiv:1809.01159].

[180] A. A. Starobinsky, *A New Type of Isotropic Cosmological Models Without Singularity*, Adv. Ser. Astrophys. Cosmol. **3** (1987) 130–133.

[181] R. Kallosh and A. Linde, *Non-minimal Inflationary Attractors*, JCAP **10** (2013) 033, [arXiv:1307.7938].

[182] M. Sasaki and E. D. Stewart, *A General analytic formula for the spectral index of the density perturbations produced during inflation*, Prog. Theor. Phys. **95** (1996) 71–78, [astro-ph/9507001].

[183] S. Groot Nibbelink and B. van Tent, *Scalar perturbations during multiple field slow-roll inflation*, Class. Quant. Grav. **19** (2002) 613–640, [hep-ph/0107272].

[184] A. Achucarro, J.-O. Gong, S. Hardeman, G. A. Palma, and S. P. Patil, *Features of heavy physics in the CMB power spectrum*, JCAP **01** (2011) 030, [arXiv:1010.3693].

[185] J.-O. Gong and T. Tanaka, *A covariant approach to general field space metric in multi-field inflation*, JCAP **03** (2011) 015, [arXiv:1101.4809]. [Erratum: JCAP 02, E01 (2012)].

[186] D. I. Kaiser, *Conformal Transformations with Multiple Scalar Fields*, Phys. Rev. D **81** (2010) 084044, [arXiv:1003.1159].

[187] S. Garcia-Saenz, S. Renaux-Petel, and J. Ronayne, *Primordial fluctuations and non-Gaussianities in sidetracked inflation*, JCAP **07** (2018) 057, [arXiv:1804.11279].

[188] S. Cremonini, Z. Lalak, and K. Turzynski, *On Non-Canonical Kinetic Terms and the Tilt of the Power Spectrum*, Phys. Rev. D **82** (2010) 047301, [arXiv:1005.4347].

[189] S. Krippendorf, F. Muia, and F. Quevedo, *Moduli Stars*, JHEP **08** (2018) 070, [arXiv:1806.04690].

[190] R. Blumenhagen, M. Cvetic, S. Kachru, and T. Weigand, *D-Brane Instantons in Type II Orientifolds*, Ann. Rev. Nucl. Part. Sci. **59** (2009) 269–296, [arXiv:0902.3251].

[191] K. A. Malik and D. Wands, *Adiabatic and entropy perturbations with interacting fluids and fields*, JCAP **02** (2005) 007, [astro-ph/0411703].

[192] K. A. Malik, D. Wands, and C. Ungarelli, *Large scale curvature and entropy perturbations for multiple interacting fluids*, Phys. Rev. D **67** (2003) 063516, [astro-ph/0211602].

[193] C. Gordon, D. Wands, B. A. Bassett, and R. Maartens, *Adiabatic and entropy perturbations from inflation*, Phys. Rev. D **63** (2000) 023506, [astro-ph/0009131].

[194] J.-c. Hwang and H. Noh, *Cosmological perturbations with multiple scalar fields*, Phys. Lett. B **495** (2000) 277–283, [astro-ph/0009268].

[195] L. C. Price, J. Frazer, J. Xu, H. V. Peiris, and R. Easther, *MultiModeCode: An efficient numerical solver for multifield inflation*, JCAP **03** (2015) 005, [arXiv:1410.0685].

[196] D. Polarski and A. A. Starobinsky, *Isocurvature perturbations in multiple inflationary models*, Phys. Rev. D **50** (1994) 6123–6129, [astro-ph/9404061].

[197] D. Langlois, *Correlated adiabatic and isocurvature perturbations from double inflation*, Phys. Rev. D **59** (1999) 123512, [astro-ph/9906080].

[198] N. Bartolo, S. Matarrese, and A. Riotto, *Adiabatic and isocurvature perturbations from inflation: Power spectra and consistency relations*, Phys. Rev. D **64** (2001) 123504, [astro-ph/0107502].

[199] I. Huston and A. J. Christopherson, *Isocurvature Perturbations and Reheating in Multi-Field Inflation*, arXiv:1302.4298.

[200] T. Montandon, G. Patanchon, and B. van Tent, *Isocurvature modes: joint analysis of the CMB power spectrum and bispectrum*, arXiv:2007.05457.

[201] O. Grocholski, M. Kalinowski, M. Kolanowski, S. Renaux-Petel, K. Turzyński, and V. Vennin, *On backreaction effects in geometrical destabilisation of inflation*, JCAP **05** (2019) 008, [arXiv:1901.10468].

[202] M. Dias, J. Frazer, and D. Seery, *Computing observables in curved multifield models of inflation—A guide (with code) to the transport method*, JCAP **12** (2015) 030, [arXiv:1502.03125].

[203] B. S. Acharya, K. Bobkov, and P. Kumar, *An M Theory Solution to the Strong CP Problem and Constraints on the Axiverse*, JHEP **11** (2010) 105, [arXiv:1004.5138].

[204] R. Allahverdi, M. Cicoli, B. Dutta, and K. Sinha, *Correlation between Dark Matter and Dark Radiation in String Compactifications*, JCAP **10** (2014) 002, [arXiv:1401.4364].

[205] E. Bulbul, M. Markevitch, A. Foster, R. K. Smith, M. Loewenstein, and S. W. Randall, *Detection of An Unidentified Emission Line in the Stacked X-ray spectrum of Galaxy Clusters*, Astrophys. J. **789** (2014) 13, [arXiv:1402.2301].

[206] A. Boyarsky, J. Franse, D. Iakubovskyi, and O. Ruchayskiy, *Checking the Dark Matter Origin of a 3.53 keV Line with the Milky Way Center*, Phys. Rev. Lett. **115** (2015) 161301, [arXiv:1408.2503].

[207] O. Urban, N. Werner, S. Allen, A. Simionescu, J. Kaastra, and L. Strigari, *A Suzaku Search for Dark Matter Emission Lines in the X-ray Brightest Galaxy Clusters*, Mon. Not. Roy. Astron. Soc. **451** (2015), no. 3 2447–2461, [arXiv:1411.0050].

[208] J. Franse et al., *Radial Profile of the 3.55 keV line out to R_{200} in the Perseus Cluster*, Astrophys. J. **829** (2016), no. 2 124, [arXiv:1604.01759].

[209] **Hitomi** Collaboration, F. Aharonian et al., *Hitomi constraints on the 3.5 keV line in the Perseus galaxy cluster*, Astrophys. J. Lett. **837** (2017), no. 1 L15, [arXiv:1607.07420].

[210] S. Riemer-Sørensen, *Constraints on the presence of a 3.5 keV dark matter emission line from Chandra observations of the Galactic centre*, Astron. Astrophys. **590** (2016) A71, [arXiv:1405.7943].

[211] T. E. Jeltema and S. Profumo, *Discovery of a 3.5 keV line in the Galactic Centre and a critical look at the origin of the line across astronomical targets*, Mon. Not. Roy. Astron. Soc. **450** (2015), no. 2 2143–2152, [arXiv:1408.1699].

[212] E. Carlson, T. Jeltema, and S. Profumo, *Where do the 3.5 keV photons come from? A morphological study of the Galactic Center and of Perseus*, JCAP **02** (2015) 009, [arXiv:1411.1758].

[213] M. E. Anderson, E. Churazov, and J. N. Bregman, *Non-Detection of X-Ray Emission From Sterile Neutrinos in Stacked Galaxy Spectra*, Mon. Not. Roy. Astron. Soc. **452** (2015), no. 4 3905–3923, [arXiv:1408.4115].

[214] D. Malyshev, A. Neronov, and D. Eckert, *Constraints on 3.55 keV line emission from stacked observations of dwarf spheroidal galaxies*, Phys. Rev. D **90** (2014) 103506, [arXiv:1408.3531].

[215] T. E. Jeltema and S. Profumo, *Deep XMM Observations of Draco rule out at the 99% Confidence Level a Dark Matter Decay Origin for the 3.5 keV Line*, Mon. Not. Roy. Astron. Soc. **458** (2016), no. 4 3592–3596, [arXiv:1512.01239].

[216] O. Ruchayskiy, A. Boyarsky, D. Iakubovskyi, E. Bulbul, D. Eckert, J. Franse, D. Malyshev, M. Markevitch, and A. Neronov, *Searching for decaying dark matter in deep XMM–Newton observation of the Draco dwarf spheroidal*, Mon. Not. Roy. Astron. Soc. **460** (2016), no. 2 1390–1398, [arXiv:1512.07217].

[217] D. Iakubovskyi, E. Bulbul, A. R. Foster, D. Savchenko, and V. Sadova, *Testing the origin of ~3.55 keV line in individual galaxy clusters observed with XMM-Newton*, arXiv:1508.05186.

[218] F. Hofmann, J. Sanders, K. Nandra, N. Clerc, and M. Gaspari, *7.1 keV sterile neutrino constraints from X-ray observations of 33 clusters of galaxies with Chandra ACIS*, Astron. Astrophys. **592** (2016) A112, [arXiv:1606.04091].

[219] D. Iakubovskyi, *Observation of the new emission line at ~3.5 keV in X-ray spectra of galaxies and galaxy clusters*, Adv. Astron. Space Phys. **6** (2016), no. 1 3–15, [arXiv:1510.00358].

[220] L. Gu, J. Kaastra, A. Raassen, P. Mullen, R. Cumbee, D. Lyons, and P. Stancil, *A novel scenario for the possible X-ray line feature at ~3.5 keV: Charge exchange with bare sulfur ions*, Astron. Astrophys. **584** (2015) L11, [arXiv:1511.06557].

[221] S. Dodelson and L. M. Widrow, *Sterile-neutrinos as dark matter*, Phys. Rev. Lett. **72** (1994) 17–20, [hep-ph/9303287].

[222] T. Asaka and M. Shaposhnikov, *The νMSM, dark matter and baryon asymmetry of the universe*, Phys. Lett. B **620** (2005) 17–26, [hep-ph/0505013].

[223] P. D. Alvarez, J. P. Conlon, F. V. Day, M. C. D. Marsh, and M. Rummel, *Observational consistency and future predictions for a 3.5 keV ALP to photon line*, JCAP **04** (2015) 013, [arXiv:1410.1867].

[224] J. P. Conlon, F. Day, N. Jennings, S. Krippendorf, and M. Rummel, *Consistency of Hitomi, XMM-Newton, and Chandra 3.5 keV data from Perseus*, Phys. Rev. D **96** (2017), no. 12 123009, [arXiv:1608.01684].

[225] J. P. Conlon, F. Quevedo, and K. Suruliz, *Large-volume flux compactifications: Moduli spectrum and D3/D7 soft supersymmetry breaking*, JHEP **08** (2005) 007, [hep-th/0505076].

[226] G. Aldazabal, L. E. Ibanez, F. Quevedo, and A. Uranga, *D-branes at singularities: A Bottom up approach to the string embedding of the standard model*, JHEP **08** (2000) 002, [hep-th/0005067].

[227] J. P. Conlon, A. Maharana, and F. Quevedo, *Towards Realistic String Vacua*, JHEP **05** (2009) 109, [arXiv:0810.5660].

[228] M. Cicoli, S. Krippendorf, C. Mayrhofer, F. Quevedo, and R. Valandro, *D3/D7 Branes at Singularities: Constraints from Global Embedding and Moduli Stabilisation*, JHEP **07** (2013) 150, [arXiv:1304.0022].

[229] M. Wijnholt, *Geometry of Particle Physics*, Adv. Theor. Math. Phys. **13** (2009), no. 4 947–990, [hep-th/0703047].

[230] R. Blumenhagen and M. Schmidt-Sommerfeld, *Power Towers of String Instantons for N=1 Vacua*, JHEP **07** (2008) 027, [arXiv:0803.1562].

[231] R. Blumenhagen, X. Gao, T. Rahn, and P. Shukla, *A Note on Poly-Instanton Effects in Type IIB Orientifolds on Calabi-Yau Threefolds*, JHEP **06** (2012) 162, [arXiv:1205.2485].

[232] S. Abel, M. Goodsell, J. Jaeckel, V. Khoze, and A. Ringwald, *Kinetic Mixing of the Photon with Hidden U(1)s in String Phenomenology*, JHEP **07** (2008) 124, [arXiv:0803.1449].

[233] J. W. Brockway, E. D. Carlson, and G. G. Raffelt, *SN1987A gamma-ray limits on the conversion of pseudoscalars*, Phys. Lett. B **383** (1996) 439–443, [astro-ph/9605197].

[234] J. Grifols, E. Masso, and R. Toldra, *Gamma-rays from SN1987A due to pseudoscalar conversion*, Phys. Rev. Lett. **77** (1996) 2372–2375, [astro-ph/9606028].

[235] A. Payez, C. Evoli, T. Fischer, M. Giannotti, A. Mirizzi, and A. Ringwald, *Revisiting the SN1987A gamma-ray limit on ultralight axion-like particles*, JCAP **02** (2015) 006, [arXiv:1410.3747].

[236] J. P. Conlon, M. D. Marsh, and A. J. Powell, *Galaxy cluster thermal x-ray spectra constrain axionlike particles*, Phys. Rev. D **93** (2016), no. 12 123526, [arXiv:1509.06748].

[237] M. Berg, J. P. Conlon, F. Day, N. Jennings, S. Krippendorf, A. J. Powell, and M. Rummel, *Constraints on Axion-Like Particles from X-ray Observations of NGC1275*, Astrophys. J. **847** (2017), no. 2 101, [arXiv:1605.01043].

[238] M. D. Marsh, H. R. Russell, A. C. Fabian, B. P. McNamara, P. Nulsen, and C. S. Reynolds, *A New Bound on Axion-Like Particles*, JCAP **12** (2017) 036, [arXiv:1703.07354].

[239] J. P. Conlon, F. Day, N. Jennings, S. Krippendorf, and M. Rummel, *Constraints on Axion-Like Particles from Non-Observation of Spectral Modulations for X-ray Point Sources*, JCAP **07** (2017) 005, [arXiv:1704.05256].

[240] **IAXO** Collaboration, I. Irastorza et al., *The International Axion Observatory IAXO. Letter of Intent to the CERN SPS committee*, .

[241] **ALPS** Collaboration, A. Spector, *ALPS II technical overview and status report*, in 12th Patras Workshop on Axions, WIMPs and WISPs, pp. 133–136, 2017. arXiv:1611.05863.

[242] J. P. Conlon and M. D. Marsh, *Excess Astrophysical Photons from a 0.1–1 keV Cosmic Axion Background*, Phys. Rev. Lett. **111** (2013), no. 15 151301, [arXiv:1305.3603].

[243] M. B. Green and J. H. Schwarz, *Anomaly Cancellation in Supersymmetric D=10 Gauge Theory and Superstring Theory*, Phys. Lett. B **149** (1984) 117–122.

[244] J. P. Conlon and F. G. Pedro, *Moduli Redefinitions and Moduli Stabilisation*, JHEP **06** (2010) 082, [arXiv:1003.0388].

[245] M. Berg, D. Marsh, L. McAllister, and E. Pajer, *Sequestering in String Compactifications*, JHEP **06** (2011) 134, [arXiv:1012.1858].

[246] M. Goodsell, J. Jaeckel, J. Redondo, and A. Ringwald, *Naturally Light Hidden Photons in LARGE Volume String Compactifications*, JHEP **11** (2009) 027, [arXiv:0909.0515].

[247] M. Cicoli, M. Goodsell, J. Jaeckel, and A. Ringwald, *Testing String Vacua in the Lab: From a Hidden CMB to Dark Forces in Flux Compactifications*, JHEP **07** (2011) 114, [arXiv:1103.3705].

[248] P. G. Camara and E. Dudas, *Multi-instanton and string loop corrections in toroidal orbifold models*, JHEP **08** (2008) 069, [arXiv:0806.3102].

[249] D. Robles-Llana, M. Rocek, F. Saueressig, U. Theis, and S. Vandoren, *Nonperturbative corrections to 4D string theory effective actions from SL(2,Z) duality and supersymmetry*, Phys. Rev. Lett. **98** (2007) 211602, [hep-th/0612027].

[250] P. Berglund and P. Mayr, *Non-perturbative superpotentials in F-theory and string duality*, JHEP **01** (2013) 114, [hep-th/0504058].

[251] L. Aparicio, D. Cerdeno, and L. Ibanez, *Modulus-dominated SUSY-breaking soft terms in F-theory and their test at LHC*, JHEP **07** (2008) 099, [arXiv:0805.2943].

[252] J. P. Conlon, D. Cremades, and F. Quevedo, *Kahler potentials of chiral matter fields for Calabi-Yau string compactifications*, JHEP **01** (2007) 022, [hep-th/0609180].

[253] N. Arkani-Hamed, M. Dine, and S. P. Martin, *Dynamical supersymmetry breaking in models with a Green-Schwarz mechanism*, Phys. Lett. B **431** (1998) 329–338, [hep-ph/9803432].

[254] L. Aparicio, M. Cicoli, B. Dutta, F. Muia, and F. Quevedo, *Light Higgsino Dark Matter from Non-thermal Cosmology*, JHEP **11** (2016) 038, [arXiv:1607.00004].

[255] A. D. Linde, *Axions in inflationary cosmology*, Phys. Lett. B **259** (1991) 38–47.

[256] P. Fox, A. Pierce, and S. D. Thomas, *Probing a QCD string axion with precision cosmological measurements*, hep-th/0409059.

[257] K. Freese, J. A. Frieman, and A. V. Olinto, *Natural inflation with pseudo - Nambu-Goldstone bosons*, Phys. Rev. Lett. **65** (1990) 3233–3236.

[258] T. Banks, M. Dine, P. J. Fox, and E. Gorbatov, *On the possibility of large axion decay constants*, JCAP **0306** (2003) 001, [hep-th/0303252].

[259] T. W. Grimm and D. Van De Heisteeg, *Infinite Distances and the Axion Weak Gravity Conjecture*, JHEP **03** (2020) 020, [arXiv:1905.00901].

[260] H. Ooguri and C. Vafa, *On the Geometry of the String Landscape and the Swampland*, Nucl. Phys. B **766** (2007) 21–33, [hep-th/0605264].

[261] J. P. Conlon, *Quantum Gravity Constraints on Inflation*, JCAP **09** (2012) 019, [arXiv:1203.5476].

[262] M. M. Anber and L. Sorbo, *Naturally inflating on steep potentials through electromagnetic dissipation*, Phys. Rev. **D81** (2010) 043534, [arXiv:0908.4089].

[263] V. Domcke and K. Mukaida, *Gauge Field and Fermion Production during Axion Inflation*, JCAP **1811** (2018), no. 11 020, [arXiv:1806.08769].

[264] V. Domcke, Y. Ema, and K. Mukaida, *Chiral Anomaly, Schwinger Effect, Euler-Heisenberg Lagrangian, and application to axion inflation*, arXiv:1910.01205.

[265] M. S. Turner and L. M. Widrow, *Gravitational Production of Scalar Particles in Inflationary Universe Models*, Phys. Rev. **D37** (1988) 3428.

[266] W. D. Garretson, G. B. Field, and S. M. Carroll, *Primordial magnetic fields from pseudoGoldstone bosons*, Phys. Rev. **D46** (1992) 5346–5351, [hep-ph/9209238].

[267] M. M. Anber and L. Sorbo, *N-flationary magnetic fields*, JCAP **0610** (2006) 018, [astro-ph/0606534].

[268] N. Barnaby and M. Peloso, *Large Nongaussianity in Axion Inflation*, Phys. Rev. Lett. **106** (2011) 181301, [arXiv:1011.1500].

[269] N. Barnaby, E. Pajer, and M. Peloso, *Gauge Field Production in Axion Inflation: Consequences for Monodromy, non-Gaussianity in the CMB, and Gravitational Waves at Interferometers*, Phys. Rev. **D85** (2012) 023525, [arXiv:1110.3327].

[270] N. Barnaby, R. Namba, and M. Peloso, *Phenomenology of a Pseudo-Scalar Inflaton: Naturally Large Nongaussianity*, JCAP **1104** (2011) 009, [arXiv:1102.4333].

[271] J. L. Cook and L. Sorbo, *Particle production during inflation and gravitational waves detectable by ground-based interferometers*, Phys. Rev. **D85** (2012) 023534, [arXiv:1109.0022]. [Erratum: Phys. Rev.D86,069901(2012)].

[272] P. D. Meerburg and E. Pajer, *Observational Constraints on Gauge Field Production in Axion Inflation*, JCAP **1302** (2013) 017, [arXiv:1203.6076].

[273] A. Linde, S. Mooij, and E. Pajer, *Gauge field production in supergravity inflation: Local non-Gaussianity and primordial black holes*, arXiv:1212.1693.

[274] J. Garcia-Bellido, M. Peloso, and C. Unal, *Gravitational waves at interferometer scales and primordial black holes in axion inflation*, JCAP **1612** (2016), no. 12 031, [arXiv:1610.03763].

[275] V. Domcke, F. Muia, M. Pieroni, and L. T. Witkowski, *PBH dark matter from axion inflation*, JCAP **1707** (2017) 048, [arXiv:1704.03464].

[276] S.-L. Cheng, W. Lee, and K.-W. Ng, *Primordial black holes and associated gravitational waves in axion monodromy inflation*, JCAP **1807** (2018), no. 07 001, [arXiv:1801.09050].

[277] M. M. Anber and L. Sorbo, *Non-Gaussianities and chiral gravitational waves in natural steep inflation*, Phys. Rev. **D85** (2012) 123537, [arXiv:1203.5849].

[278] V. Domcke, M. Pieroni, and P. Binétruy, *Primordial gravitational waves for universality classes of pseudoscalar inflation*, JCAP **1606** (2016) 031, [arXiv:1603.01287].

[279] N. Bartolo et al., *Science with the space-based interferometer LISA. IV: Probing inflation with gravitational waves*, JCAP **1612** (2016) 026, [arXiv:1610.06481].

[280] P. Adshead, J. T. Giblin, T. R. Scully, and E. I. Sfakianakis, *Gauge-preheating and the end of axion inflation*, JCAP **1512** (2015), no. 12 034, [arXiv:1502.06506].

[281] J. R. C. Cuissa and D. G. Figueroa, *Lattice formulation of axion inflation. Application to preheating*, JCAP **1906** (2019), no. 06 002, [arXiv:1812.03132].

[282] P. Adshead, J. T. Giblin, M. Pieroni, and Z. J. Weiner, *Constraining axion inflation with gravitational waves from preheating*, arXiv:1909.12842.

[283] O. O. Sobol, E. V. Gorbar, and S. I. Vilchinskii, *Backreaction of electromagnetic fields and the Schwinger effect in pseudoscalar inflation magnetogenesis*, Phys. Rev. **D100** (2019), no. 6 063523, [arXiv:1907.10443].

[284] S.-L. Cheng, W. Lee, and K.-W. Ng, *Numerical study of pseudoscalar inflation with an axion-gauge field coupling*, Phys. Rev. **D93** (2016), no. 6 063510, [arXiv:1508.00251].

[285] A. Notari and K. Tywoniuk, *Dissipative Axial Inflation*, JCAP **1612** (2016) 038, [arXiv:1608.06223].

[286] G. Dall'Agata, S. González-Martín, A. Papageorgiou, and M. Peloso, *Warm dark energy*, arXiv:1912.09950.

[287] A. A. Starobinsky, *Multicomponent de Sitter (Inflationary) Stages and the Generation of Perturbations*, JETP Lett. **42** (1985) 152–155. [Pisma Zh. Eksp. Teor. Fiz.42,124(1985)].

[288] D. S. Salopek and J. R. Bond, *Nonlinear evolution of long wavelength metric fluctuations in inflationary models*, Phys. Rev. **D42** (1990) 3936–3962.

[289] S. Yokoyama, T. Suyama, and T. Tanaka, *Primordial Non-Gaussianity in Multi-Scalar Slow-Roll Inflation*, JCAP **0707** (2007) 013, [arXiv:0705.3178].

[290] V. Gorbenko and L. Senatore, $\lambda\phi^4$ *in dS*, arXiv:1911.00022.

[291] D. Jiménez, K. Kamada, K. Schmitz, and X.-J. Xu, *Baryon asymmetry and gravitational waves from pseudoscalar inflation*, JCAP **1712** (2017), no. 12 011, [arXiv:1707.07943].

[292] M. Ballardini, M. Braglia, F. Finelli, G. Marozzi, and A. A. Starobinsky, *Energy-momentum tensor and helicity for gauge fields coupled to a pseudoscalar inflaton*, Phys. Rev. **D100** (2019), no. 12 123542, [arXiv:1910.13448].

[293] R. Z. Ferreira, J. Ganc, J. Noreña, and M. S. Sloth, *On the validity of the perturbative description of axions during inflation*, JCAP **1604** (2016), no. 04 039, [arXiv:1512.06116]. [Erratum: JCAP1610,no.10,E01(2016)].

[294] M. Peloso, L. Sorbo, and C. Unal, *Rolling axions during inflation: perturbativity and signatures*, JCAP **1609** (2016), no. 09 001, [arXiv:1606.00459].

[295] M. Kleban and L. Senatore, *Inhomogeneous Anisotropic Cosmology*, JCAP **1610** (2016), no. 10 022, [arXiv:1602.03520].

[296] K. Clough, E. A. Lim, B. S. DiNunno, W. Fischler, R. Flauger, and S. Paban, *Robustness of Inflation to Inhomogeneous Initial Conditions*, JCAP **1709** (2017), no. 09 025, [arXiv:1608.04408].

[297] K. Clough, R. Flauger, and E. A. Lim, *Robustness of Inflation to Large Tensor Perturbations*, JCAP **1805** (2018), no. 05 065, [arXiv:1712.07352].

[298] J. C. Aurrekoetxea, K. Clough, R. Flauger, and E. A. Lim, *The Effects of Potential Shape on Inhomogenous Inflation*, arXiv:1910.12547.

[299] B. J. Carr, K. Kohri, Y. Sendouda, and J. Yokoyama, *New cosmological constraints on primordial black holes*, Phys. Rev. **D81** (2010) 104019, [arXiv:0912.5297].

[300] A. M. Green, A. R. Liddle, K. A. Malik, and M. Sasaki, *A New calculation of the mass fraction of primordial black holes*, Phys. Rev. **D70** (2004) 041502, [astro-ph/0403181].

[301] B. Carr, F. Kuhnel, and M. Sandstad, *Primordial Black Holes as Dark Matter*, Phys. Rev. **D94** (2016), no. 8 083504, [arXiv:1607.06077].

[302] R. Anantua, R. Easther, and J. T. Giblin, *GUT-Scale Primordial Black Holes: Consequences and Constraints*, Phys. Rev. Lett. **103** (2009) 111303, [arXiv:0812.0825].

[303] D. Hooper, G. Krnjaic, and S. D. McDermott, *Dark Radiation and Superheavy Dark Matter from Black Hole Domination*, JHEP **08** (2019) 001, [arXiv:1905.01301].

[304] K. Inomata, M. Kawasaki, K. Mukaida, Y. Tada, and T. T. Yanagida, *Inflationary Primordial Black Holes as All Dark Matter*, Phys. Rev. **D96** (2017), no. 4 043504, [arXiv:1701.02544].

[305] A. Kalaja, N. Bellomo, N. Bartolo, D. Bertacca, S. Matarrese, I. Musco, A. Raccanelli, and L. Verde, *From Primordial Black Holes Abundance to Primordial Curvature Power Spectrum (and back)*, JCAP **1910** (2019), no. 10 031, [arXiv:1908.03596].

[306] S. Mollerach, D. Harari, and S. Matarrese, *CMB polarization from secondary vector and tensor modes*, Phys. Rev. **D69** (2004) 063002, [astro-ph/0310711].

[307] K. N. Ananda, C. Clarkson, and D. Wands, *The Cosmological gravitational wave background from primordial density perturbations*, Phys. Rev. **D75** (2007) 123518, [gr-qc/0612013].

[308] D. Baumann, P. J. Steinhardt, K. Takahashi, and K. Ichiki, *Gravitational Wave Spectrum Induced by Primordial Scalar Perturbations*, Phys. Rev. **D76** (2007) 084019, [hep-th/0703290].

[309] R. Dong, W. H. Kinney, and D. Stojkovic, *Gravitational wave production by Hawking radiation from rotating primordial black holes*, JCAP **1610** (2016), no. 10 034, [arXiv:1511.05642].

[310] P. Agrawal, N. Kitajima, M. Reece, T. Sekiguchi, and F. Takahashi, *Relic Abundance of Dark Photon Dark Matter*, Phys. Lett. **B801** (2020) 135136, [arXiv:1810.07188].

[311] V. Domcke, B. von Harling, E. Morgante, and K. Mukaida, *Baryogenesis from axion inflation*, JCAP **1910** (2019), no. 10 032, [arXiv:1905.13318].

[312] A. Hook and G. Marques-Tavares, *Relaxation from particle production*, JHEP **12** (2016) 101, [arXiv:1607.01786].

[313] K. Choi, H. Kim, and T. Sekiguchi, *Dynamics of the cosmological relaxation after reheating*, Phys. Rev. **D95** (2017), no. 7 075008, [arXiv:1611.08569].

[314] W. Tangarife, K. Tobioka, L. Ubaldi, and T. Volansky, *Relaxed Inflation*, arXiv:1706.00438.

[315] W. Tangarife, K. Tobioka, L. Ubaldi, and T. Volansky, *Dynamics of Relaxed Inflation*, JHEP **02** (2018) 084, [arXiv:1706.03072].

[316] N. Fonseca, E. Morgante, and G. Servant, *Higgs relaxation after inflation*, JHEP **10** (2018) 020, [arXiv:1805.04543].

[317] N. Fonseca, E. Morgante, R. Sato, and G. Servant, *Relaxion Fluctuations (Self-stopping Relaxion) and Overview of Relaxion Stopping Mechanisms*, arXiv:1911.08473.

[318] K. A. Malik and D. Wands, *Cosmological perturbations*, Phys. Rept. **475** (2009) 1–51, [arXiv:0809.4944].

[319] C. Bennett, A. Banday, K. Gorski, G. Hinshaw, P. Jackson, P. Keegstra, A. Kogut, G. F. Smoot, D. Wilkinson, and E. Wright, *Four year COBE DMR cosmic microwave background observations: Maps and basic results*, Astrophys. J. Lett. **464** (1996) L1–L4, [astro-ph/9601067].

[320] G. Hinshaw, D. Larson, E. Komatsu, D. N. Spergel, C. L. Bennett, J. Dunkley, M. R. Nolta, M. Halpern, R. S. Hill, N. Odegard, and et al., *Nine-year wilkinson microwave anisotropy probe (wmap) observations: Cosmological parameter results*, The Astrophysical Journal Supplement Series **208** (Sep, 2013) 19.

[321] **LIGO Scientific, Virgo, 1M2H, Dark Energy Camera GW-E, DES, DLT40, Las Cumbres Observatory, VINROUGE, MASTER** Collaboration, B. Abbott et al., *A gravitational-wave standard siren measurement of the Hubble constant*, Nature **551** (2017), no. 7678 85–88, [arXiv:1710.05835].

[322] G. D. Racca, R. Laureijs, L. Stagnaro, J.-C. Salvignol, J. Lorenzo Alvarez, G. Saavedra Criado, L. Gaspar Venancio, A. Short, P. Strada, T. Bönke, and et al., *The euclid mission design*, Space Telescopes and Instrumentation 2016: Optical, Infrared, and Millimeter Wave (Jul, 2016).

[323] I. Debono, D. K. Hazra, A. Shafieloo, G. F. Smoot, and A. A. Starobinsky, *Constraints on features in the inflationary potential from future Euclid data*, Mon. Not. Roy. Astron. Soc. **496** (2020), no. 3 3448–3468, [arXiv:2003.05262].

[324] G. Congedo and A. Taylor, *Joint cosmological inference of standard sirens and gravitational wave weak lensing*, Phys. Rev. D **99** (2019), no. 8 083526, [arXiv:1812.02730].

[325] M. Cicoli, C. Mayrhofer, and R. Valandro, *Moduli Stabilisation for Chiral Global Models*, JHEP **02** (2012) 062, [arXiv:1110.3333].